FORUM GEOMETRICORUM

A Journal on Classical Euclidean Geometry and Related Areas

published by

Department of Mathematical Sciences
Florida Atlantic University

Volume 12
2012

http://forumgeom.fau.edu

ISSN 1534-1178

Editorial Board

Table of Contents

Forum Geometricorum
Volume 12 (2012) 1–11.

FORUM GEOM
ISSN 1534-1178

Generalization and Extension of the Wallace Theorem

Gotthard Weise

Abstract. In the Wallace theorem we replace the projection directions (altitudes of the reference triangle) by all permutations of a general direction triple, and regard simultaneously the projections of a point P to each sideline. Introducing a pair of *Wallace points* and a pair of *Wallace triangles*, we present their properties and some connections to the Steiner ellipses.

1. Introduction

Most people interested in triangle geometry know the Wallace-Simson Theorem (see [2], [3] or [4]):

> In the euclidean plane be ABC a triangle and P a point not on the sidelines. Then the feet of the perpendiculars from P to the sidelines are collinear (*Wallace-Simson line*), if and only if P is a point on the circumcircle of ABC.

This theorem is one of the gems of triangle geometry. For more than two centuries mathematicians are fascinated about its simplicity and beauty, and they reflected on generalizations or extensions up to the present time.

O. Giering [1] showed that not only the collinearity of the three pedals, but also the collinearities of other intersections of the projection lines (in direction of the altitudes) with the sidelines of the triangle are interesting in this respect.

In a paper of M. de Guzmán [2] it is shown that one can take instead altitude directions a general triple $(\alpha,\ \beta,\ \gamma)$ of projection directions which are assigned to the oriented side triple (a, b, c). One gets instead the circumcircle a circumconic for which it is easy to construct three points (apart from A, B, C) and the center.

In this paper we aim at continuing some ideas of the above publications. We consider the permutations of a triple of projection directions simultaneously, and the concepts *Wallace points* and *Wallace triangles* yield new interesting insights.

2. Notations

First of all, we recall some concepts and connections of the euclidean triangle geometry. Detailed information can be found, for instance, in the books of R. A. Johnson [4] and P. Yiu [7], or in papers of S. Sigur [5].

Publication Date: January 31, 2012. Communicating Editor: Paul Yiu.

Let $\Delta = ABC$ be a triangle with the vertices A, B, C, the sides a, b, c, and the centroid G. For the representation of geometric elements we use homogeneous barycentric coordinates.

Suppose $P = (u : v : w)$ is a general point. Reflecting the traces $P_a,\ P_b,\ P_c$ of P in the midpoints $G_a,\ G_b,\ G_c$ of the sides, respectively, then the points of reflection $P_a^\bullet,\ P_b^\bullet,\ P_c^\bullet$ are the traces of the (*isotomic*) *conjugate* $P^\bullet = (\frac{1}{u} : \frac{1}{v} : \frac{1}{w})$ of P.

The line $[\frac{1}{u} : \frac{1}{v} : \frac{1}{w}]$ is the *trilinear polar (tripolar)* $\frac{x}{u} + \frac{y}{v} + \frac{z}{w} = 0$ of P, the line $[u : v : w]$ is the *dual* (the tripolar of the conjugate) of P and $\mathcal{C}_P : \frac{u}{x} + \frac{v}{y} + \frac{w}{z} = 0$ is a circumconic of Δ with *perspector* P (P*-circumconic*). A perspector of a circumconic $\mathcal{C}$ is the perspective center of Δ and the triangle formed by the tangents of $\mathcal{C}$ at A, B, C. The center M_P of $\mathcal{C}_P$ has coordinates

$$(u(v + w - u) : v(w + u - v) : w(u + v - w)). \tag{1}$$

The point by point conjugation of $\mathcal{C}_P$ yields the dual line of P. The duals of all points of $\mathcal{C}_P$ form a family of lines whose envelope is the inconic associated to the circumconic $\mathcal{C}_P$.

The points of the infinite line l_∞ satisfy the equation $x + y + z = 0$.

The *medial* operation m and the *dilated (antimedial)* operation d carry a point P to the images $\mathsf{m}P = (v + w : w + u : u + v)$ and $\mathsf{d}P = (v + w - u : w + u - v : u + v - w)$, respectively, which both lie on the line GP:

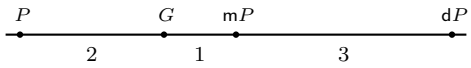

Figure 1. Medial and dilated operation

The point $(u : v : w)$ forms together with the points $(v : w : u)$ and $(w : u : v)$ a *Brocardian triple* [6]; every two of these points are the right-right Brocardian and the left-left Brocardian, respectively, of the third point.

The *Steiner circumellipse* $\mathcal{C}_G$ of Δ has the equation

$$yz + zx + xy = 0, \tag{2}$$

and the *Steiner inellipse* is described by

$$x^2 + y^2 + z^2 - 2yz - 2zx - 2xy = 0. \tag{3}$$

The *Kiepert hyperbola* is the (rectangular) circumconic of Δ through G and the orthocenter H.

3. Direction Stars, Projection Triples and their Normalized Representation

Let us call a *direction star* a set $\{\alpha,\ \beta,\ \gamma\}$ of three pairwise different directions $\alpha,\ \beta,\ \gamma$ not parallel to the sides of Δ. It is described by three points

$$\alpha = (\alpha_1 : \alpha_2 : \alpha_3), \quad \beta = (\beta_1 : \beta_2 : \beta_3), \quad \gamma = (\gamma_1 : \gamma_2 : \gamma_3)$$

on the infinite line. Their barycentrics (different from zero) form a singular matrix

$$D = \begin{pmatrix} \alpha_1 & \alpha_2 & \alpha_3 \\ \beta_1 & \beta_2 & \beta_3 \\ \gamma_1 & \gamma_2 & \gamma_3 \end{pmatrix}$$

of rank 2. Since the coordinates of each point are defined except for a non-zero factor, we can adjust by suitable factors so that all cofactors of D are equal to unity. We call such representation of a direction star its *normalized representation*. In this case not only the row sums of D vanish, but also the column sums, and

$$\beta_2 - \gamma_3 = \gamma_1 - \alpha_2 = \alpha_3 - \beta_1 =: \lambda_1, \tag{4}$$
$$\gamma_3 - \alpha_1 = \alpha_2 - \beta_3 = \beta_1 - \gamma_2 =: \lambda_2, \tag{5}$$
$$\alpha_1 - \beta_2 = \beta_3 - \gamma_1 = \gamma_2 - \alpha_3 =: \lambda_3 \tag{6}$$

and

$$\beta_3 - \gamma_2 = \gamma_1 - \alpha_3 = \alpha_2 - \beta_1 =: \mu_1, \tag{7}$$
$$\gamma_2 - \alpha_1 = \alpha_3 - \beta_2 = \beta_1 - \gamma_3 =: \mu_2, \tag{8}$$
$$\alpha_1 - \beta_3 = \beta_2 - \gamma_1 = \gamma_3 - \alpha_2 =: \mu_3. \tag{9}$$

Here is an example of a normalized representation of a direction star:

$$D = \begin{pmatrix} 1 & 2 & -3 \\ 1 & 3 & -4 \\ -2 & -5 & 7 \end{pmatrix}.$$

We will see below that two other matrices with the same elements as in D (but in other arrangements) are also involved. The rows of $D_\rightarrow$ ($D_\leftarrow$) consist of the elements of the main (skew) diagonal and their parallels:

$$D_\rightarrow := \begin{pmatrix} \alpha_1 & \beta_2 & \gamma_3 \\ \beta_1 & \gamma_2 & \alpha_3 \\ \gamma_1 & \alpha_2 & \beta_3 \end{pmatrix}, \qquad D_\leftarrow := \begin{pmatrix} \alpha_1 & \gamma_2 & \beta_3 \\ \beta_1 & \alpha_2 & \gamma_3 \\ \gamma_1 & \beta_2 & \alpha_3 \end{pmatrix}.$$

From a direction star we form $3! = 6$ ordered direction triples (permutations of the directions), which we can interpret as projection directions on the sidelines $a,\ b,\ c$ (in this order). We denote these *projection triples* by

$$\alpha_\rightarrow := (\alpha,\ \beta,\ \gamma), \qquad \alpha_\leftarrow := (\alpha,\ \gamma,\ \beta);$$
$$\beta_\rightarrow := (\beta,\ \gamma,\ \alpha), \qquad \beta_\leftarrow := (\beta,\ \alpha,\ \gamma);$$
$$\gamma_\rightarrow := (\gamma,\ \alpha,\ \beta), \qquad \gamma_\leftarrow := (\gamma,\ \beta,\ \alpha).$$

The arrows indicate whether the permutation is even or odd. Interpreting as a map, for instance $\alpha_\leftarrow(P)$ is a triple $(P_{\alpha a},\ P_{\gamma b},\ P_{\beta c})$ of feet in which the first index indicates the projection direction, and the second one refers to the side on which P is projected.

The square matrices $D,\ D_\rightarrow$ and $D_\leftarrow$ all have rank 2. Their kernels represent geometrically some points in the plane of Δ. The kernel of D is obviously $G =$

$(1,1,1)$. For $\ker D_{\rightarrow} =: (p_{\rightarrow} : q_{\rightarrow} : r_{\rightarrow})$ and $\ker D_{\leftarrow} =: (p_{\leftarrow} : q_{\leftarrow} : r_{\leftarrow})$ we find

$$p_{\rightarrow} = \alpha_2\alpha_3 - \beta_3\gamma_2 = \beta_2\beta_3 - \gamma_3\alpha_2 = \gamma_2\gamma_3 - \alpha_3\beta_2, \tag{10}$$
$$q_{\rightarrow} = \alpha_3\alpha_1 - \beta_1\gamma_3 = \beta_3\beta_1 - \gamma_1\alpha_3 = \gamma_3\gamma_1 - \alpha_1\beta_3, \tag{11}$$
$$r_{\rightarrow} = \alpha_1\alpha_2 - \beta_2\gamma_1 = \beta_1\beta_2 - \gamma_2\alpha_1 = \gamma_1\gamma_2 - \alpha_2\beta_1, \tag{12}$$

and

$$p_{\leftarrow} = \alpha_2\alpha_3 - \beta_2\gamma_3 = \beta_2\beta_3 - \gamma_2\alpha_3 = \gamma_2\gamma_3 - \alpha_2\beta_3, \tag{13}$$
$$q_{\leftarrow} = \alpha_3\alpha_1 - \beta_3\gamma_1 = \beta_3\beta_1 - \gamma_3\alpha_1 = \gamma_3\gamma_1 - \alpha_3\beta_1, \tag{14}$$
$$r_{\leftarrow} = \alpha_1\alpha_2 - \beta_1\gamma_2 = \beta_1\beta_2 - \gamma_1\alpha_2 = \gamma_1\gamma_2 - \alpha_1\beta_2. \tag{15}$$

These satisfy

$$p_{\rightarrow} - p_{\leftarrow} = q_{\rightarrow} - q_{\leftarrow} = r_{\rightarrow} - r_{\leftarrow} = 1, \tag{16}$$
$$p_{\rightarrow}q_{\rightarrow} + q_{\rightarrow}r_{\rightarrow} + r_{\rightarrow}p_{\rightarrow} - p_{\rightarrow} - q_{\rightarrow} - r_{\rightarrow} = 0, \tag{17}$$
$$p_{\leftarrow}q_{\leftarrow} + q_{\leftarrow}r_{\leftarrow} + r_{\leftarrow}p_{\leftarrow} + p_{\leftarrow} + q_{\leftarrow} + r_{\leftarrow} = 0. \tag{18}$$

Let us denote by ℓ_{Qq} the line with direction q through a point Q. Then the direction stars localized at the vertices A, B, C are described by the following lines:

$$\ell_{A\alpha} = [0 : \alpha_3 : -\alpha_2], \quad \ell_{B\alpha} = [-\alpha_3 : 0 : \alpha_1], \quad \ell_{C\alpha} = [\alpha_2 : -\alpha_1 : 0];$$
$$\ell_{A\beta} = [0 : \beta_3 : -\beta_2], \quad \ell_{B\beta} = [-\beta_3 : 0 : \beta_1], \quad \ell_{C\beta} = [\beta_2 : -\beta_1 : 0];$$
$$\ell_{A\gamma} = [0 : \gamma_3 : -\gamma_2], \quad \ell_{B\gamma} = [-\gamma_3 : 0 : \gamma_1], \quad \ell_{C\gamma}, = [\gamma_2 : -\gamma_1 : 0].$$

Next we want to assign each projection triple to a specific line. We begin with the construction of such a line $\ell_{\alpha\rightarrow}$ for the projection triple $\alpha_{\rightarrow}$. Let

$$P_1 := \ell_{B\gamma} \cap \ell_{C\beta} = (\beta_1\gamma_1 : \beta_2\gamma_1 : \beta_1\gamma_3), \tag{19}$$
$$P_2 := \ell_{C\alpha} \cap \ell_{A\gamma} = (\gamma_2\alpha_1 : \gamma_2\alpha_2 : \gamma_3\alpha_2), \tag{20}$$
$$P_3 := \ell_{A\beta} \cap \ell_{B\alpha} = (\alpha_1\beta_3 : \alpha_3\beta_2 : \alpha_3\beta_3). \tag{21}$$

Their conjugates are

$$\begin{aligned} P_1^{\bullet} &= (\beta_2\gamma_3 : \beta_1\gamma_3 : \beta_2\gamma_1), \\ P_2^{\bullet} &= (\gamma_3\alpha_2 : \gamma_3\alpha_1 : \gamma_2\alpha_1), \\ P_3^{\bullet} &= (\alpha_3\beta_2 : \alpha_1\beta_3 : \alpha_1\beta_2). \end{aligned} \tag{22}$$

In view of (4), (5), (6) it is clear that $det(P_1^{\bullet},\ P_2^{\bullet},\ P_3^{\bullet}) = 0$. Hence, these points are collinear and lie on the line

$$\ell_{\alpha\rightarrow} := [\alpha_1 : \beta_2 : \gamma_3], \tag{23}$$

which intersects the infinite line in $(\lambda_1 : \lambda_2 : \lambda_3)$. By cyclic interchange of $\alpha,\ \beta,\ \gamma$ we find

$$\ell_{\beta\rightarrow} := [\beta_1 : \gamma_2 : \alpha_3], \qquad \ell_{\gamma\rightarrow} := [\gamma_1 : \alpha_2 : \beta_3], \tag{24}$$

and the intersections $(\lambda_3 : \lambda_1 : \lambda_2)$ and $(\lambda_2 : \lambda_3 : \lambda_1)$ with the infinite line, respectively. The barycentrics of these three lines form the rows of the matrix $D_{\rightarrow}$. In a similar fashion we find the lines

$$\ell_{\alpha\leftarrow} = [\alpha_1 : \gamma_2 : \beta_3], \qquad \ell_{\beta\leftarrow} = [\beta_1 : \alpha_2 : \gamma_3], \qquad \ell_{\gamma\leftarrow} = [\gamma_1 : \beta_2 : \alpha_3] \quad (25)$$

whose coordinates form the rows of $D_{\leftarrow}$. From these we have the theorem below.

Theorem 1. *The lines $\ell_{\alpha\rightarrow}$, $\ell_{\beta\rightarrow}$, $\ell_{\gamma\rightarrow}$ are concurrent at the point*

$$W_{\rightarrow}^{\bullet} = (p_{\rightarrow} : q_{\rightarrow} : r_{\rightarrow}).$$

Likewise, the lines $\ell_{\alpha\leftarrow}$, $\ell_{\beta\leftarrow}$, $\ell_{\gamma\leftarrow}$ are concurrent at

$$W_{\leftarrow}^{\bullet} = (p_{\leftarrow} : q_{\leftarrow} : r_{\leftarrow}).$$

Recall that the conjugates of the points of a line lie on a circumconic of Δ. Hence the conjugates of the six lines in (23) - (25) are the circumconics

$$\mathcal{C}_{\alpha\rightarrow} : \frac{\alpha_1}{x} + \frac{\beta_2}{y} + \frac{\gamma_3}{z} = 0, \quad \mathcal{C}_{\beta\rightarrow} : \frac{\beta_1}{x} + \frac{\gamma_2}{y} + \frac{\alpha_3}{z} = 0, \quad \mathcal{C}_{\gamma\rightarrow} : \frac{\gamma_1}{x} + \frac{\alpha_2}{y} + \frac{\beta_3}{z} = 0\ ; \quad (26)$$

$$\mathcal{C}_{\alpha\leftarrow} : \frac{\alpha_1}{x} + \frac{\gamma_2}{y} + \frac{\beta_3}{z} = 0, \quad \mathcal{C}_{\beta\leftarrow} : \frac{\beta_1}{x} + \frac{\alpha_2}{y} + \frac{\gamma_3}{z} = 0, \quad \mathcal{C}_{\gamma\leftarrow} : \frac{\gamma_1}{x} + \frac{\beta_2}{y} + \frac{\alpha_3}{z} = 0. \quad (27)$$

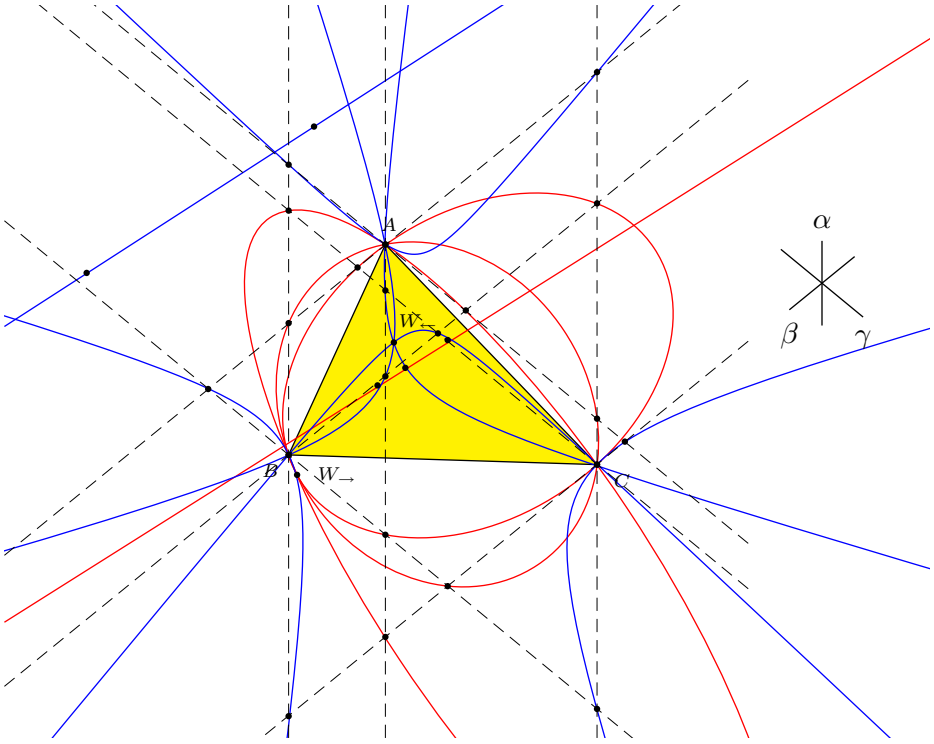

Figure 2.

Theorem 2 below follows easily from Theorem 1.

Theorem 2. *The circumconics* $\mathcal{C}_{\alpha\rightarrow},\ \mathcal{C}_{\beta\rightarrow},\ \mathcal{C}_{\gamma\rightarrow}$ (red in Figure 2) *have the common point*

$$W_{\rightarrow} = \left(\frac{1}{p_{\rightarrow}} : \frac{1}{q_{\rightarrow}} : \frac{1}{r_{\rightarrow}}\right),$$

the circumconics $\mathcal{C}_{\alpha\leftarrow},\ \mathcal{C}_{\beta\leftarrow},\ \mathcal{C}_{\gamma\leftarrow}$ (blue in Figure 2) *have the common point*

$$W_{\leftarrow} = \left(\frac{1}{p_{\leftarrow}} : \frac{1}{q_{\leftarrow}} : \frac{1}{r_{\leftarrow}}\right).$$

Hence, their perspectors are collinear on the tripolars of $W_{\rightarrow}$ *and of* $W_{\leftarrow}$*, respectively. These lines are parallel and they intersect the infinite line at the point*

$$W_{\infty} = (q_{\rightarrow} - r_{\rightarrow} : r_{\rightarrow} - p_{\rightarrow} : p_{\rightarrow} - q_{\rightarrow})$$

and define a direction δ*.*

In the special case of altitudes is $W_{\rightarrow}$ the Tarry point and $W_{\leftarrow}$ the orthocenter of Δ. The circumconic $\mathcal{C}_{\alpha\rightarrow}$ is the circumcircle. In [1], $\mathcal{C}_{\beta\rightarrow}$ and $\mathcal{C}_{\gamma\rightarrow}$ are called the right- and left-conics respectively.

4. Wallace Points

In [2] it is shown that in the case of three directions $\alpha,\ \beta,\ \gamma$ the points $P_1,\ P_2,\ P_3$ constructed for the projection triple $\alpha_{\rightarrow}$ lie on a circumconic with the property that for a point P on this circumconic the feet of the projections of P to a, b, c in direction α, β, γ, respectively, are collinear. Now we want to look at this generalization of the theorem of Wallace *simultaneously* for all 6 projection triples belonging to the direction star $\{\alpha,\ \beta,\ \gamma\}$.

Theorem 3. *The respective three feet of the three projection triples* $\alpha_{\rightarrow}(W_{\rightarrow}),\ \beta_{\rightarrow}(W_{\rightarrow})$ *and* $\gamma_{\rightarrow}(W_{\rightarrow})$ *localized at* $W_{\rightarrow}$ *are collinear on the Wallace lines* $w_{\alpha\rightarrow},\ w_{\beta\rightarrow},\ w_{\gamma\rightarrow}$*, respectively; there is analogy for the feet of* $\alpha_{\leftarrow}(W_{\leftarrow}),\ \beta_{\leftarrow}(W_{\leftarrow}),\ \gamma_{\leftarrow}(W_{\leftarrow})$*. We shall call the points* $W_{\rightarrow}$ *and* $W_{\leftarrow}$ *the Wallace-right- and Wallace-left-points respectively of the direction star* $\{\alpha,\ \beta,\ \gamma\}$*.*

Proof. Let $g_{\alpha\rightarrow},\ g_{\beta\rightarrow},\ g_{\gamma\rightarrow}$ be the lines through $W_{\rightarrow}$ in direction $\alpha,\ \beta,\ \gamma$, respectively. To simplify the equations we make use of the quantities

$$\begin{aligned}
X_1 &:= \alpha_2 q_{\rightarrow} - \alpha_3 r_{\rightarrow} = \gamma_3 r_{\rightarrow} - \gamma_1 p_{\rightarrow} = \beta_1 p_{\rightarrow} - \beta_2 q_{\rightarrow} \\
X_2 &:= \beta_2 q_{\rightarrow} - \beta_3 r_{\rightarrow} = \alpha_3 r_{\rightarrow} - \alpha_1 p_{\rightarrow} = \gamma_1 p_{\rightarrow} - \gamma_2 q_{\rightarrow} \\
X_3 &:= \gamma_2 q_{\rightarrow} - \gamma_3 r_{\rightarrow} = \beta_3 r_{\rightarrow} - \beta_1 p_{\rightarrow} = \alpha_1 p_{\rightarrow} - \alpha_2 q_{\rightarrow}.
\end{aligned}$$

These satisfy

$$X_1^2 - X_2 X_3 = X_2^2 - X_3 X_1 = X_3^2 - X_1 X_2, \tag{28}$$

and yield the equations of the lines

$$g_{\alpha\rightarrow} = [p_\rightarrow X_1 : q_\rightarrow X_2 : r_\rightarrow X_3]$$
$$g_{\beta\rightarrow} = [p_\rightarrow X_2 : q_\rightarrow X_3 : r_\rightarrow X_1]$$
$$g_{\gamma\rightarrow} = [p_\rightarrow X_3 : q_\rightarrow X_1 : r_\rightarrow X_2].$$

These projection lines intersect the sidelines in the points

$$\begin{array}{lll} Q_{\alpha a} = (0 : r_\rightarrow X_3 : -q_\rightarrow X_2), & Q_{\beta a} = (0 : r_\rightarrow X_1 : -q_\rightarrow X_3), & Q_{\gamma a} = (0 : r_\rightarrow X_2 : -q_\rightarrow X_1); \\ Q_{\alpha b} = (-r_\rightarrow X_3 : 0 : p_\rightarrow X_1), & Q_{\beta b} = (-r_\rightarrow X_1 : 0 : p_\rightarrow X_2), & Q_{\gamma b} = (-r_\rightarrow X_2 : 0 : p_\rightarrow X_3); \\ Q_{\alpha c} = (q_\rightarrow X_2 : -p_\rightarrow X_1 : 0), & Q_{\beta c} = (q_\rightarrow X_3 : -p_\rightarrow X_2 : 0), & Q_{\gamma c} = (q_\rightarrow X_1 : -p_\rightarrow X_3 : 0). \end{array}$$

The feet $Q_{\alpha a},\ Q_{\beta b},\ Q_{\gamma c}$ of the projection triple $\alpha_\rightarrow$ are collinear because their linear dependent coordinates. They yield a Wallace line

$$w_{\alpha\rightarrow} = Q_{\alpha a}Q_{\beta b} = [p_\rightarrow X_2X_3 : q_\rightarrow X_1X_2 : r_\rightarrow X_3X_1].$$

Analogously it follows from the collinearity of $Q_{\alpha b},\ Q_{\beta c},\ Q_{\gamma a}$ resp. $Q_{\alpha c},\ Q_{\beta a},\ Q_{\gamma b}$

$$w_{\beta\rightarrow} = [p_\rightarrow X_1X_2 : q_\rightarrow X_3X_1 : r_\rightarrow X_2X_3], \qquad w_{\gamma\rightarrow} = [p_\rightarrow X_3X_1 : q_\rightarrow X_2X_3 : r_\rightarrow X_1X_2].$$

The proof for the other Wallace point is analogous. □

5. Some circumconics generated by the Wallace points

The Wallace points generate some circumconics with notable properties:

- $W^\bullet_\rightarrow$-circumconic $\quad \mathcal{C}_{W^\bullet_\rightarrow} : \dfrac{p_\rightarrow}{x} + \dfrac{q_\rightarrow}{y} + \dfrac{r_\rightarrow}{z} = 0,$ (29)
- $W^\bullet_\leftarrow$-circumconic $\quad \mathcal{C}_{W^\bullet_\leftarrow} : \dfrac{p_\leftarrow}{x} + \dfrac{q_\leftarrow}{y} + \dfrac{r_\leftarrow}{z} = 0,$ (30)
- $W_\rightarrow$-circumconic $\quad \mathcal{C}_{W\rightarrow} : \dfrac{1}{p_\rightarrow x} + \dfrac{1}{q_\rightarrow y} + \dfrac{1}{r_\rightarrow z} = 0,$ (31)
- $W_\leftarrow$-circumconic $\quad \mathcal{C}_{W\leftarrow} : \dfrac{1}{p_\leftarrow x} + \dfrac{1}{q_\leftarrow y} + \dfrac{1}{r_\leftarrow z} = 0,$ (32)
- circumconic through $W_\rightarrow$ and $W_\leftarrow$,
- circumconics with the centers $\mathsf{m}W_\rightarrow$ resp. $\mathsf{m}W_\leftarrow$,
- circumconics of the medial triangle of ABC with the centers $\mathsf{m}^2W_\rightarrow$ and $\mathsf{m}^2W_\leftarrow$ respectively.

Theorem 4. (a) *The circumconics $\mathcal{C}_{W^\bullet_\rightarrow}$ and $\mathcal{C}_{W^\bullet_\leftarrow}$ intersect at the point $S_\delta := W^\bullet_\infty$ on the Steiner circumellipse.*
(b) *The circumconic through $W_\rightarrow$ and $W_\leftarrow$ has perspector W_∞. Hence it is the circumconic $\mathcal{C}_{W_\infty}$*

$$\frac{q_\rightarrow - r_\rightarrow}{x} + \frac{r_\rightarrow - p_\rightarrow}{y} + \frac{p_\rightarrow - q_\rightarrow}{z} = 0 \tag{33}$$

passing through G. Its center M_∞ lies on the Steiner inellipse. The Wallace points are antipodes.

Proof. (a) The conjugates of the circumconics $\mathcal{C}_{W\bullet_\rightarrow}$ and $\mathcal{C}_{W\bullet_\leftarrow}$, that are the lines $[p_\rightarrow : q_\rightarrow : r_\rightarrow]$ and $[p_\leftarrow : q_\leftarrow : r_\leftarrow]$, respectively, intersect on the infinite line at the point W_∞. Hence its conjugate lies on the Steiner circumellipse.

(b) The line through the conjugates of the Wallace points is

$$[q_\rightarrow - r_\rightarrow : r_\rightarrow - p_\rightarrow : p_\rightarrow - q_\rightarrow].$$

Its conjugate (a circumconic) has the perspector W_∞. The point $G = (1 : 1 : 1)$ obviously satisfies the circumconic equation (33). The center of the W_∞ - circumconic according to (1) is

$$M_\infty = ((q_\rightarrow - r_\rightarrow)^2 : (r_\rightarrow - p_\rightarrow)^2 : (p_\rightarrow - q_\rightarrow)^2). \tag{34}$$

It satisfies equation (3) of the Steiner inellipse and is - how one finds out by a longer computation in accordance with (17) - collinear with the two Wallace points, hence they must be antipodes. □

In the special case of the altitude directions the point S_δ is the Steiner point of ABC and $\mathcal{C}_{W_\infty}$ is the Kiepert hyperbola.

An interesting property of (31) and (32) is presented in Theorem 7 below.

The following theorem involves circumconics that are in connection with the 6 centers of the circumconics (26), (27).

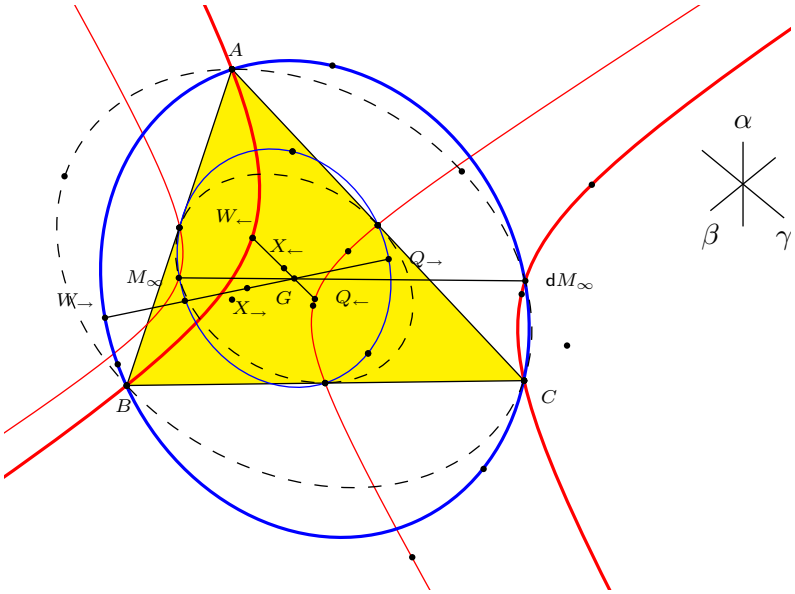

Figure 3.

Theorem 5. (a) *Suppose the Wallace point $W_\rightarrow$ (respectively $W_\leftarrow$) is reflected in the centers of the three circumconics in (26) (respectively (27)). Then the three reflection points lie on a circumconic through $W_\leftarrow$ (respectively $W_\rightarrow$). Its center is $Q_\rightarrow = \mathsf{m}W_\rightarrow$ (respectitvely $Q_\leftarrow = \mathsf{m}W_\leftarrow$). These two circumconics* (thick red and blue respectively in Figure 3) *intersect the Steiner circumellipse at point* $\mathsf{d}M_\infty$.

(b) *The centers of the three circumconics in (26) (respectively (27)) lie on a circumconic of the medial triangle through $Q_\leftarrow$ (respectively $Q_\rightarrow$) with center $X_\rightarrow = \mathsf{m}^2 W_\rightarrow$ (respectively $X_\leftarrow = \mathsf{m}^2 W_\leftarrow$). Both circumconics* (red and green respectively in Figure 3) *intersect on the Steiner inellipse at point M_∞.*

6. Wallace Triangles

The Wallace lines $w_{\alpha\rightarrow},\ w_{\beta\rightarrow},\ w_{\gamma\rightarrow}$ belonging to $W_\rightarrow$ form a triangle $\Delta_\rightarrow$ (*Wallace-right-triangle*) and the Wallace lines $w_{\alpha\leftarrow},\ w_{\beta\leftarrow},\ w_{\gamma\leftarrow}$ belonging to $W_\leftarrow$ form a triangle $\Delta_\leftarrow$ (*Wallace-left-triangle*).

Theorem 6. *Each of the Wallace triangles and Δ are triply perspective.*
(a) *The 3 centers of perspective of $(\Delta, \Delta_\rightarrow)$ are collinear on the tripolar of $W_\rightarrow$.*
(b) *The 3 centers of perspective of $(\Delta, \Delta_\leftarrow)$ are collinear on the tripolar of $W_\leftarrow$.*

Proof. With (28), the vertices of the Wallace-right-triangle $\Delta_\rightarrow$ are

$$A_\rightarrow := \left(\frac{1}{p_\rightarrow X_1} : \frac{1}{q_\rightarrow X_3} : \frac{1}{r_\rightarrow X_2}\right), \tag{35}$$

$$B_\rightarrow := \left(\frac{1}{p_\rightarrow X_3} : \frac{1}{q_\rightarrow X_2} : \frac{1}{r_\rightarrow X_1}\right), \tag{36}$$

$$C_\rightarrow := \left(\frac{1}{p_\rightarrow X_2} : \frac{1}{q_\rightarrow X_1} : \frac{1}{r_\rightarrow X_3}\right). \tag{37}$$

The triple perspectivity of Δ and $\Delta_\rightarrow$ follows from the concurrency of the lines

$$\begin{aligned}
&AA_\rightarrow, \quad BB_\rightarrow, \quad CC_\rightarrow \quad \text{at} \quad \left(\frac{X_1}{p_\rightarrow} : \frac{X_2}{q_\rightarrow} : \frac{X_3}{r_\rightarrow}\right) \quad =: \quad P_{A\rightarrow} \\
&AB_\rightarrow, \quad BC_\rightarrow, \quad CA_\rightarrow \quad \text{at} \quad \left(\frac{X_3}{p_\rightarrow} : \frac{X_1}{q_\rightarrow} : \frac{X_2}{r_\rightarrow}\right) \quad =: \quad P_{B\rightarrow} \\
&AC_\rightarrow, \quad BA_\rightarrow, \quad CB_\rightarrow \quad \text{at} \quad \left(\frac{X_2}{p_\rightarrow} : \frac{X_3}{q_\rightarrow} : \frac{X_1}{r_\rightarrow}\right) \quad =: \quad P_{C\rightarrow}.
\end{aligned}$$

These three centers of perspectivity are obviously collinear on the line $[p_\rightarrow : q_\rightarrow : r_\rightarrow]$, which is the tripolar of $\left(\frac{1}{p_\rightarrow} : \frac{1}{q_\rightarrow} : \frac{1}{r_\rightarrow}\right) = W_\rightarrow$.

The proof for $\Delta_\leftarrow$ is analogous. □

Theorem 7. *The vertices of $\Delta_\rightarrow$ and $\Delta_\leftarrow$ lie on the $W_\rightarrow$ - circumconic and on the $W_\leftarrow$ - circumconic, respectively.*

Proof. Easy verification. □

7. Direction Star and Steiner Circumellipse

Each of the 6 circumconics in (26) and (27) assigned to a direction star has a fourth common point ($S_{\alpha\rightarrow}, \ldots, S_{\gamma\leftarrow}$) with the Steiner circumellipse. These points

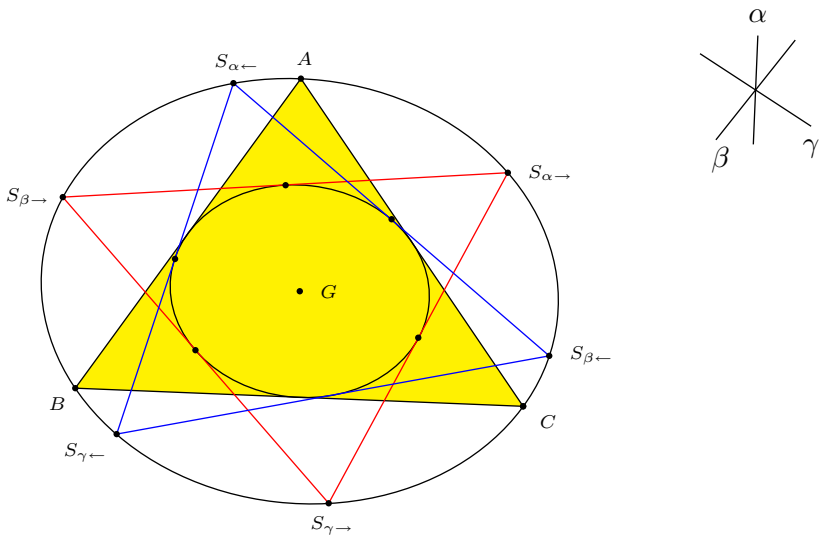

Figure 4. The triangles $\Delta S_{\rightarrow}$ and $\Delta S_{\leftarrow}$

form two triangles $\Delta S_{\rightarrow}$ and $\Delta S_{\leftarrow}$ (Figure 4). The point $S_{\alpha\rightarrow}$ is the conjugate of the intersection of $\ell_{\alpha\rightarrow}$ with the infinite line, thus according to (4) - (6) follows

$$S_{\alpha\rightarrow} = \left(\frac{1}{\beta_2-\gamma_3} : \frac{1}{\gamma_3-\alpha_1} : \frac{1}{\alpha_1-\beta_2}\right) = \left(\frac{1}{\lambda_1} : \frac{1}{\lambda_2} : \frac{1}{\lambda_3}\right), \tag{38}$$

for the other vertices of the triangle $\Delta S_{\rightarrow}$ we find

$$S_{\beta\rightarrow} = \left(\frac{1}{\gamma_2-\alpha_3} : \frac{1}{\alpha_3-\beta_1} : \frac{1}{\beta_1-\gamma_2}\right) = \left(\frac{1}{\lambda_3} : \frac{1}{\lambda_1} : \frac{1}{\lambda_2}\right), \tag{39}$$

$$S_{\gamma\rightarrow} = \left(\frac{1}{\alpha_2-\beta_3} : \frac{1}{\beta_3-\gamma_1} : \frac{1}{\gamma_1-\alpha_2}\right) = \left(\frac{1}{\lambda_2} : \frac{1}{\lambda_3} : \frac{1}{\lambda_1}\right). \tag{40}$$

The coordinates of these points are connected by cyclic interchange. Hence they form a Brocardian triple [6]. The same is valid for the triangle $\Delta S_{\leftarrow}$.

Theorem 8. (a) *The triangles $\Delta S_{\rightarrow}$ and $\Delta S_{\leftarrow}$ have the centroid G.*
(b) *The 6 sidelines of these triangles are the duals of the respective opposite vertices and hence tangents at the Steiner inellipse. The points of contact are the midpoints of the sides of these triangles.*
(c) *The triangles $\Delta S_{\rightarrow}$ and $\Delta S_{\leftarrow}$ have the same area like ABC, because each Brocardian triple with vertices on the Steiner circumellipse has this property.*

Theorem 9. *The triangles Δ, $\Delta S_{\rightarrow}$ and $\Delta S_{\leftarrow}$ are pairwise triply perspective. The 9 centers of perspective lie on the infinite line, and the 9 axes of perspective pass through G.*

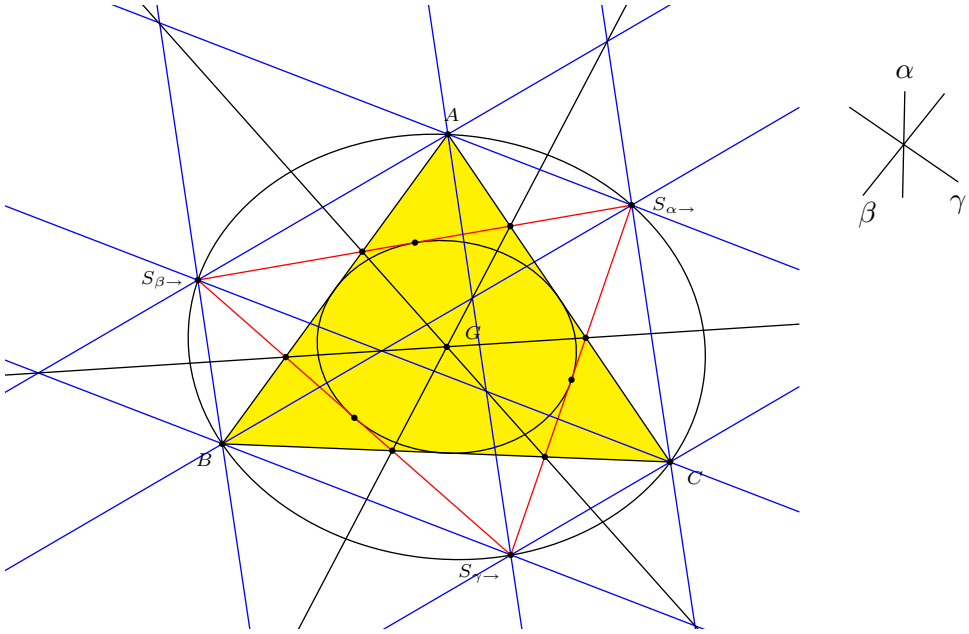

Figure 5. Triple perspectivity of Δ and $\Delta S_{\rightarrow}$

We omit the elementary but long computational proof. Figure 5 illustrates the triple perspectivity of Δ and $\Delta S_{\rightarrow}$.

References

[1] O. Giering, *Seitenstücke der Wallace-Geraden*, Sitzungsber. Österr. Akad. Wiss. Math.-nat. Kl., Abt.II (1998) 207, 199-211.
[2] M. de Guzmán, An extension of the Wallace-Simson theorem: Projecting in arbitrary directions, *Amer. Math. Monthly*, 106(1999) 574–580.
[3] R. Honsberger, *Episodes of 19th and 20th Century Euclidean Geometry*, Math. Assoc. America, 1995.
[4] R. A. Johnson, *Advanced Euclidean Geometry*, 1929, Dover reprint 2007.
[5] S. Sigur, Affine Theory of Triangle Conics, available at `http://www.paideiaschool.org/Teacherpages/Steve_Sigur/resources/conic-types-web/conic.htm`.
[6] G. Weise, Iterates of Brocardian points and lines, *Forum Geom.*, 10 (2010) 109–118.
[7] P. Yiu, *Introduction to the Geometry of the Triangle*, Florida Atlantic University Lecture Notes, 2001.

Gotthard Weise: Buchloer Str. 23, D-81475 München, Germany.
E-mail address: `gotthard.weise@tele2.de`

Forum Geometricorum
Volume 12 (2012) 13–25.

FORUM GEOM
ISSN 1534-1178

Characterizations of Orthodiagonal Quadrilaterals

Martin Josefsson

Abstract. We prove ten necessary and sufficient conditions for a convex quadrilateral to have perpendicular diagonals. One of these is a quite new eight point circle theorem and three of them are metric conditions concerning the nonoverlapping triangles formed by the diagonals.

1. A well known characterization

An *orthodiagonal quadrilateral* is a convex quadrilateral with perpendicular diagonals. The most well known and in problem solving useful characterization of orthodiagonal quadrilaterals is the following theorem. Five other different proofs of it was given in [19, pp.158–159], [11], [15], [2, p.136] and [4, p.91], using respectively the law of cosines, vectors, an indirect proof, a geometric locus and complex numbers. We will give a sixth proof using the Pythagorean theorem.

Theorem 1. *A convex quadrilateral $ABCD$ is orthodiagonal if and only if*

$$AB^2 + CD^2 = BC^2 + DA^2.$$

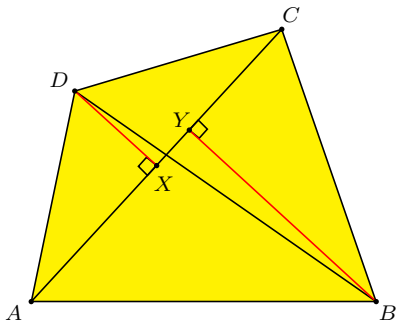

Figure 1. Normals to diagonal AC

Proof. Let X and Y be the feet of the normals from D and B respectively to diagonal AC in a convex quadrilateral $ABCD$, see Figure 1. By the Pythagorean theorem we have $BY^2+AY^2 = AB^2$, $BY^2+CY^2 = BC^2$, $DX^2+CX^2 = CD^2$

Publication Date: February 22, 2012. Communicating Editor: Paul Yiu.

and $AX^2 + DX^2 = DA^2$. Thus

$$\begin{aligned} & AB^2 + CD^2 - BC^2 - DA^2 \\ = \ & AY^2 - AX^2 + CX^2 - CY^2 \\ = \ & (AY + AX)(AY - AX) + (CX + CY)(CX - CY) \\ = \ & (AY + AX)XY + (CX + CY)XY \\ = \ & (AX + CX + AY + CY)XY \\ = \ & 2AC \cdot XY. \end{aligned}$$

Hence we have

$$AC \perp BD \qquad \Leftrightarrow \qquad XY = 0 \qquad \Leftrightarrow \qquad AB^2 + CD^2 = BC^2 + DA^2$$

since $AC > 0$. □

Another short proof is the following. The area of a convex quadrilateral with sides a, b, c and d is given by the two formulas

$$K = \tfrac{1}{2}pq\sin\theta = \tfrac{1}{4}\sqrt{4p^2q^2 - (a^2 - b^2 + c^2 - d^2)^2}$$

where θ is the angle between the diagonals p and q.[1] Hence we directly get

$$\theta = \frac{\pi}{2} \qquad \Leftrightarrow \qquad a^2 + c^2 = b^2 + d^2$$

completing this seventh proof.[2]

A different interpretation of the condition in Theorem 1 is the following. If four squares of the same sides as those of a convex quadrilateral are erected on the sides of that quadrilateral, then it is orthodiagonal if and only if the sum of the areas of two opposite squares is equal to the sum of the areas of the other two squares.

2. Two eight point circles

Another necessary and sufficient condition is that a convex quadrilateral is orthodiagonal if and only if the midpoints of the sides are the vertices of a rectangle ($EFGH$ in Figure 2). The direct theorem was proved by Louis Brand in the proof of the theorem about the *eight point circle* in [5], but was surely discovered much earlier since this is a special case of the Varignon parallelogram theorem.[3] The converse is an easy angle chase, as noted by "shobber" in post no 8 at [1]. In fact, the converse to the theorem about the eight point circle is also true, so we have the following condition as well. *A convex quadrilateral has perpendicular diagonals if and only if the midpoints of the sides and the feet of the maltitudes are*

[1] The first of these formulas yields a quite trivial characterization of orthodiagonal quadrilaterals: the diagonals are perpendicular if and only if the area of the quadrilateral is one half the product of the diagonals.

[2] This proof may be short, but the derivations of the two area formulas are a bit longer; see [17, pp.212–214] or [7] and [8].

[3] The midpoints of the sides in any quadrilateral form a parallelogram named after the French mathematician Pierre Varignon (1654-1722). The diagonals in this parallelogram are the bimedians of the quadrilateral and they intersect at the centroid of the quadrilateral.

eight concyclic points,[4] see Figure 2. The center of the circle is the centroid of the quadrilateral (the intersection of EG and FH in Figure 2). This was formulated slightly different and proved as Corollary 2 in [10].[5]

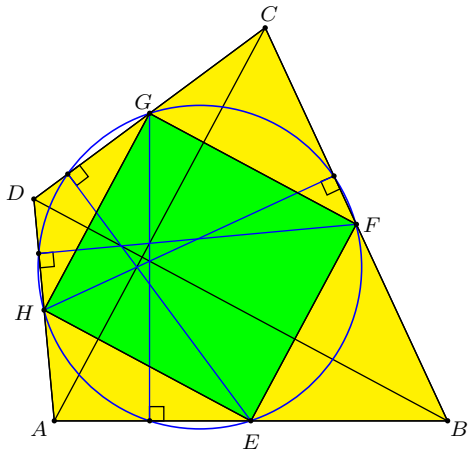

Figure 2. Brand's eight point circle and rectangle $EFGH$

There is also a second eight point circle characterization. Before we state and prove this theorem we will prove two other necessary and sufficient condition for the diagonals of a convex quadrilateral to be perpendicular, which are related to the second eight point circle.

Theorem 2. *A convex quadrilateral $ABCD$ is orthodiagonal if and only if*

$$\angle PAB + \angle PBA + \angle PCD + \angle PDC = \pi$$

where P is the point where the diagonals intersect.

Proof. By the sum of angles in triangles ABP and CDP (see Figure 3) we have

$$\angle PAB + \angle PBA + \angle PCD + \angle PDC = 2\pi - 2\theta,$$

where θ is the angle between the diagonals. Hence $\theta = \frac{\pi}{2}$ if and only if the equation in the theorem is satisfied. □

Problem 6.17 in [14, p.139] is about proving that if the diagonals of a convex quadrilateral are perpendicular, then the projections of the point where the diagonals intersect onto the sides are the vertices of a cyclic quadrilateral.[6] The solution given by Prasolov in [14, p.149] used Theorem 2 and is, although not stated as such, also a proof of the converse. Our proof is basically the same.

[4] A maltitude is a line segment in a quadrilateral from the midpoint of a side perpendicular to the opposite side.

[5] The quadrilateral formed by the feet of the maltitudes is called the principal orthic quadrilateral in [10].

[6] In [14] this is called an inscribed quadrilateral, but that is another name for a cyclic quadrilateral.

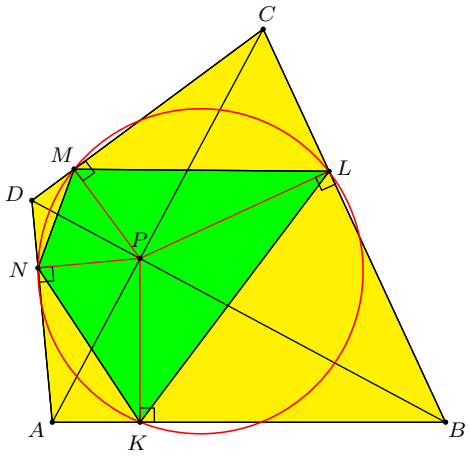

Figure 3. $ABCD$ is orthodiagonal iff $KLMN$ is cyclic

Theorem 3. *A convex quadrilateral is orthodiagonal if and only if the projections of the diagonal intersection onto the sides are the vertices of a cyclic quadrilateral.*

Proof. If the diagonals intersect in P, and the projection points on AB, BC, CD and DA are K, L, M and N respectively, then $AKPN$, $BLPK$, $CMPL$ and $DNPM$ are cyclic quadrilaterals since they all have two opposite right angles (see Figure 3). Then $\angle PAN = \angle PKN$, $\angle PBL = \angle PKL$, $\angle PCL = \angle PML$ and $\angle PDN = \angle PMN$. Quadrilateral $ABCD$ is by Theorem 2 orthodiagonal if and only if

$$\begin{aligned} & \angle PAN + \angle PBL + \angle PCL + \angle PDN = \pi \\ \Leftrightarrow \quad & \angle PKN + \angle PKL + \angle PML + \angle PMN = \pi \\ \Leftrightarrow \quad & \angle LKN + \angle LMN = \pi \end{aligned}$$

where the third equality is a well known necessary and sufficient condition for $KLMN$ to be a cyclic quadrilateral. □

Now we are ready to prove the second eight point circle theorem.

Theorem 4. *In a convex quadrilateral $ABCD$ where the diagonals intersect at P, let K, L, M and N be the projections of P onto the sides, and let R, S, T and U be the points where the lines KP, LP, MP and NP intersect the opposite sides. Then the quadrilateral $ABCD$ is orthodiagonal if and only if the eight points K, L, M, N, R, S, T and U are concyclic.*

Proof. ($\Rightarrow$) If $ABCD$ is orthodiagonal, then K, L, M and N are concyclic by Theorem 3. We start by proving that $KTMN$ has the same circumcircle as $KLMN$. To do this, we will prove that $\angle MNK + \angle MTK = \pi$, which is equivalent to proving that $\angle MTK = \angle ANK + \angle DNM$ since $\angle AND = \pi$ (see Figure 4). In cyclic quadrilaterals $ANPK$ and $DNPM$, we have $\angle ANK = \angle APK = \angle TPC$ and $\angle DNM = \angle MPD$. By the exterior angle theorem $\angle MTP = \angle TPC + \angle TCP$.

In addition $\angle MPD = \angle TCP$ since CPD is a right triangle with altitude MP. Hence

$$\angle MTK = \angle TPC + \angle TCP = \angle ANK + \angle MPD = \angle ANK + \angle DNM$$

which proves that T lies on the circumcircle of $KLMN$, since K, M and N uniquely determine a circle. In the same way it can be proved that R, S and U lies on this circle.

($\Leftarrow$) If K, L, M, N, R, S, T and U are concyclic, then $NMTK$ is a cyclic quadrilateral. By using some of the angle relations from the first part, we get

$$\begin{aligned} & \angle MTK = \pi - \angle MNK \\ \Rightarrow \quad & \angle MTP = \angle ANK + \angle DNM \\ \Rightarrow \quad & \angle TPC + \angle TCP = \angle APK + \angle MPD \\ \Rightarrow \quad & \angle TCP = \angle MPD. \end{aligned}$$

Thus triangles MPC and MDP are similar since angle MDP is common. Then

$$\angle CPD = \angle PMD = \tfrac{\pi}{2}$$

so $AC \perp BD$. □

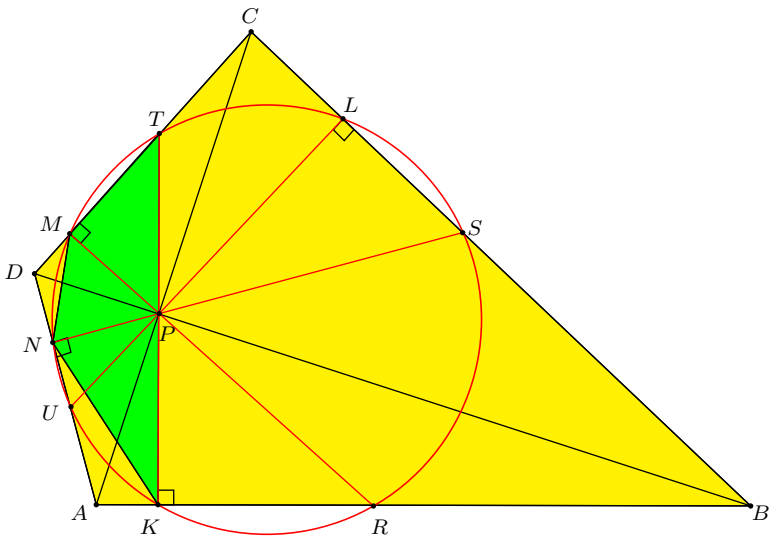

Figure 4. The second eight point circle

In the next theorem we prove that quadrilateral $RSTU$ in Figure 4 is a rectangle if and only if $ABCD$ is an orthodiagonal quadrilateral.

Theorem 5. *If the normals to the sides of a convex quadrilateral $ABCD$ through the diagonal intersection intersect the opposite sides in R, S, T and U, then $ABCD$ is orthodiagonal if and only if $RSTU$ is a rectangle whose sides are parallel to the diagonals of $ABCD$.*

Proof. ($\Rightarrow$) If $ABCD$ is orthodiagonal, then $UTMN$ is a cyclic quadrilateral according to Theorem 4 (see Figure 5). Thus

$$\angle MTU = \angle DNM = \angle MPD = \angle TCP,$$

so $UT \parallel AC$. In the same way it can be proved that $RS \parallel AC$, $UR \parallel DB$ and $TS \parallel DB$. Hence $RSTU$ is a parallelogram with sides parallel to the perpendicular lines AC and BD, so it is a rectangle.

($\Leftarrow$) If $RSTU$ is a rectangle with sides parallel to the diagonals AC and BD of a convex quadrilateral, then

$$\angle DPC = \angle UTS = \tfrac{\pi}{2}.$$

Hence $AC \perp BD$. □

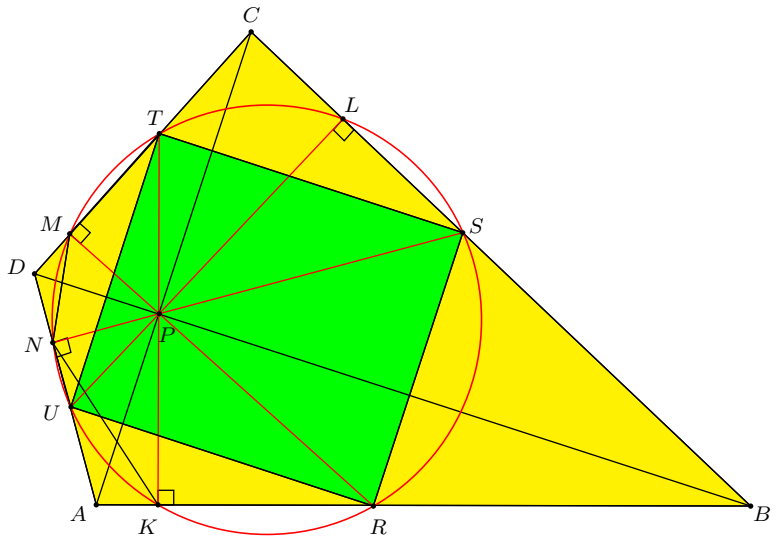

Figure 5. $ABCD$ is orthodiagonal iff $RSTU$ is a rectangle

Remark. Shortly after we had proved Theorems 4 and 5 we found out that the direct parts of these two theorems was proved in 1998 [20]. Thus, in [20] Zaslavsky proved that in an orthodiagonal quadrilateral, the eight points K, L, M, N, R, S, T and U are concyclic, and that $RSTU$ is a rectangle with sides parallel to the diagonals. We want to thank Vladimir Dubrovsky for the help with the translation of the theorems in [20].

Let's call the eight point circle due to Louis Brand the *first eight point circle* and the one in Theorem 4 the *second eight point circle*. Since $RSTU$ is a rectangle, the center of the second eight point circle is the point where the diagonals in $RSTU$ intersect.

Theorem 6. *The first and second eight point circle of an orthodiagonal quadrilateral coincide if and only if the quadrilateral is also cyclic.*

Proof. Since the second eight point circle is constructed from line segments through the diagonal intersection, the two eight point circles coincide if and only if the four maltitudes are concurrent at the diagonal intersection. The maltitudes of a convex quadrilateral are concurrent if and only if the quadrilateral is cyclic according to [12, p.19]. □

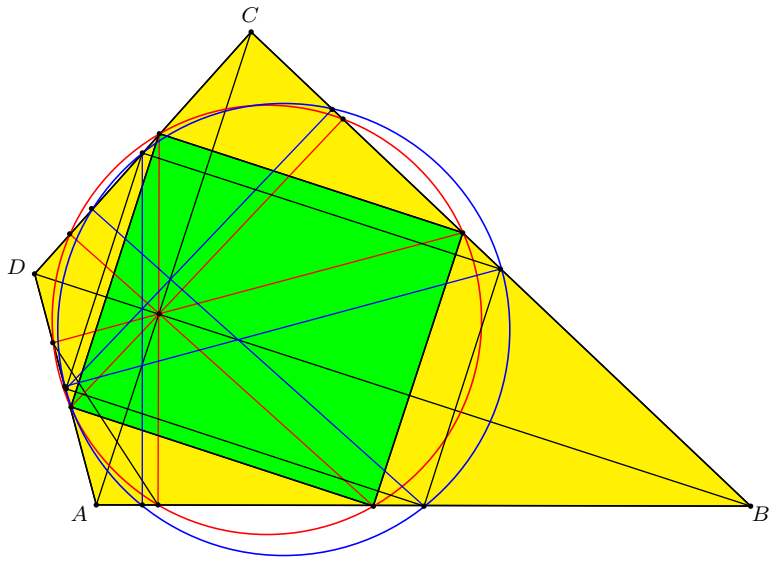

Figure 6. The two eight point circles

That the point where the maltitudes intersect (the anticenter) in a cyclic orthodiagonal quadrilateral coincide with the diagonal intersection was proved in another way in [2, p.137].

3. A duality between the bimedians and the diagonals

The next theorem gives an interesting sort of dual connection between the bimedians and the diagonals of a convex quadrilateral. The first part is a characterization of orthodiagonal quadrilaterals. Another proof of (i) using vectors was given in [6, p.293].

Theorem 7. *In a convex quadrilateral we have the following conditions:*
(i) *The bimedians are congruent if and only if the diagonals are perpendicular.*
(ii) *The bimedians are perpendicular if and only if the diagonals are congruent.*

Proof. (i) According to the proof of Theorem 7 in [9], the bimedians m and n in a convex quadrilateral satisfy

$$4(m^2 - n^2) = -2(a^2 - b^2 + c^2 - d^2)$$

where a, b, c and d are the sides of the quadrilateral. Hence

$$m = n \qquad \Leftrightarrow \qquad a^2 + c^2 = b^2 + d^2$$

which proves the condition according to Theorem 1.

(ii) Consider the Varignon parallelogram of a convex quadrilateral (see Figure 7). Its diagonals are the bimedians m and n of the quadrilateral. It is well known that the length of the sides in the Varignon parallelogram are one half the length of the diagonals p and q in the quadrilateral. Applying Theorem 1 to the Varignon parallelogram yields

$$m \perp n \qquad \Leftrightarrow \qquad 2\left(\frac{p}{2}\right)^2 = 2\left(\frac{q}{2}\right)^2 \qquad \Leftrightarrow \qquad p = q$$

since opposite sides in a parallelogram are congruent. □

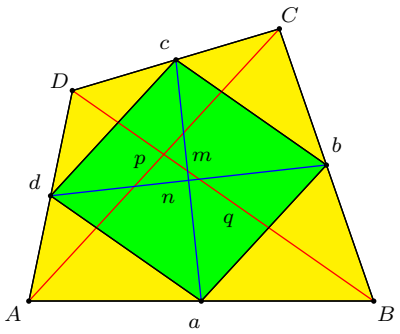

Figure 7. The Varignon parallelogram

4. Three metric conditions in the four subtriangles

Now we will use Theorem 1 to prove two more characterizations resembling it.

Theorem 8. *A convex quadrilateral $ABCD$ is orthodiagonal if and only if*

$$m_1^2 + m_3^2 = m_2^2 + m_4^2$$

where m_1, m_2, m_3 and m_4 are the medians in the triangles ABP, BCP, CDP and DAP from the intersection P of the diagonals to the sides AB, BC, CD and DA respectively.

Proof. Let P divide the diagonals in parts w, x and y, z (see Figure 8). By applying Apollonius' theorem in triangles ABP, CDP, BCP and DAP we get

$$\begin{aligned}
& m_1^2 + m_3^2 = m_2^2 + m_4^2 \\
\Leftrightarrow\ & 4m_1^2 + 4m_3^2 = 4m_2^2 + 4m_4^2 \\
\Leftrightarrow\ & 2(w^2 + y^2) - a^2 + 2(x^2 + z^2) - c^2 = 2(y^2 + x^2) - b^2 + 2(z^2 + w^2) - d^2 \\
\Leftrightarrow\ & a^2 + c^2 = b^2 + d^2
\end{aligned}$$

which by Theorem 1 completes the proof. □

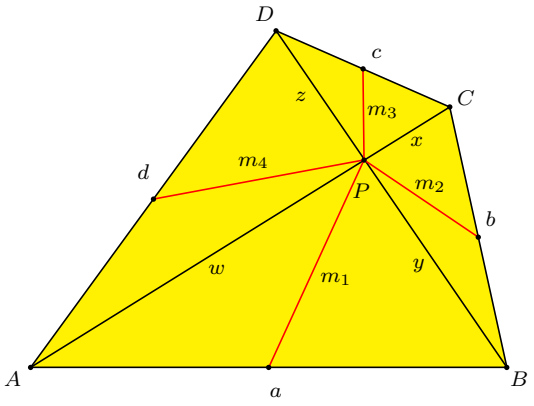

Figure 8. The subtriangle medians m_1, m_2, m_3 and m_4

Theorem 9. *A convex quadrilateral $ABCD$ is orthodiagonal if and only if*

$$R_1^2 + R_3^2 = R_2^2 + R_4^2$$

where R_1, R_2, R_3 and R_4 are the circumradii in the triangles ABP, BCP, CDP and DAP respectively and P is the intersection of the diagonals.

Proof. According to the extended law of sines applied in the four subtriangles, $a = 2R_1 \sin\theta$, $b = 2R_2 \sin(\pi - \theta)$, $c = 2R_3 \sin\theta$ and $d = 2R_4 \sin(\pi - \theta)$, see Figure 9. We get

$$a^2 + c^2 - b^2 - d^2 = 4\sin^2\theta \left(R_1^2 + R_3^2 - R_2^2 - R_4^2\right)$$

where we used that $\sin(\pi - \theta) = \sin\theta$. Hence

$$a^2 + c^2 = b^2 + d^2 \qquad \Leftrightarrow \qquad R_1^2 + R_3^2 = R_2^2 + R_4^2$$

since $\sin\theta > 0$ for $0 < \theta < \pi$. □

When studying Figure 9 it is easy to realize the following result, which gives a connection between the previous two theorems.

Theorem 10. *A convex quadrilateral $ABCD$ is orthodiagonal if and only if the circumcenters of the triangles ABP, BCP, CDP and DAP are the midpoints of the sides of the quadrilateral, where P is the intersection of its diagonals.*

Proof. The quadrilateral $ABCD$ is orthodiagonal if and only if one of the triangles ABP, BCP, CDP and DAP have a right angle at P; then all of them have it. Hence we only need to prove that the circumcenter of one triangle is the midpoint of a side if and only if the opposite angle is a right angle. But this is an immediate consequence of Thales' theorem and its converse, see [18]. □

The next theorem is our main result and concerns the altitudes in the four nonoverlapping subtriangles formed by the diagonals.

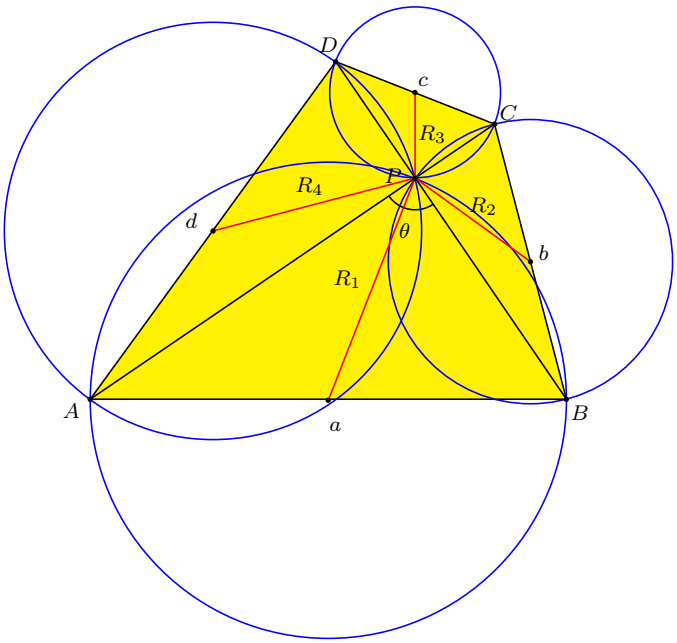

Figure 9. The circumradii R_1, R_2, R_3 and R_4

Theorem 11. *A convex quadrilateral $ABCD$ is orthodiagonal if and only if*

$$\frac{1}{h_1^2}+\frac{1}{h_3^2}=\frac{1}{h_2^2}+\frac{1}{h_4^2}$$

where h_1, h_2, h_3 and h_4 are the altitudes in the triangles ABP, BCP, CDP and DAP from the intersection P of the diagonals to the sides AB, BC, CD and DA respectively.

Proof. Let P divide the diagonals in parts w, x and y, z. From expressing twice the area of triangle ABP in two different ways we get (see Figure 10)

$$ah_1 = wy\sin\theta$$

where θ is the angle between the diagonals. Thus

$$\frac{1}{h_1^2}=\frac{a^2}{w^2y^2\sin^2\theta}=\frac{w^2+y^2-2wy\cos\theta}{w^2y^2\sin^2\theta}=\left(\frac{1}{y^2}+\frac{1}{w^2}\right)\frac{1}{\sin^2\theta}-\frac{2\cos\theta}{wy\sin^2\theta}$$

where we used the law of cosines in triangle ABP in the second equality. The same resoning in triangle CDP yields

$$\frac{1}{h_3^2}=\left(\frac{1}{x^2}+\frac{1}{z^2}\right)\frac{1}{\sin^2\theta}-\frac{2\cos\theta}{xz\sin^2\theta}.$$

In triangles BCP and DAP we have respectively

$$\frac{1}{h_2^2}=\left(\frac{1}{x^2}+\frac{1}{y^2}\right)\frac{1}{\sin^2\theta}+\frac{2\cos\theta}{yx\sin^2\theta}$$

and

$$\frac{1}{h_4^2} = \left(\frac{1}{w^2} + \frac{1}{z^2}\right)\frac{1}{\sin^2\theta} + \frac{2\cos\theta}{zw\sin^2\theta}$$

since $\cos(\pi - \theta) = -\cos\theta$. From the last four equations we get

$$\frac{1}{h_1^2} + \frac{1}{h_3^2} - \frac{1}{h_2^2} - \frac{1}{h_4^2} = -\frac{2\cos\theta}{\sin^2\theta}\left(\frac{1}{wy} + \frac{1}{yx} + \frac{1}{xz} + \frac{1}{zw}\right).$$

Hence

$$\frac{1}{h_1^2} + \frac{1}{h_3^2} = \frac{1}{h_2^2} + \frac{1}{h_4^2} \qquad \Leftrightarrow \qquad \cos\theta = 0 \qquad \Leftrightarrow \qquad \theta = \frac{\pi}{2}$$

since $(\sin\theta)^{-2} \neq 0$ and the expression in the parenthesis is positive. □

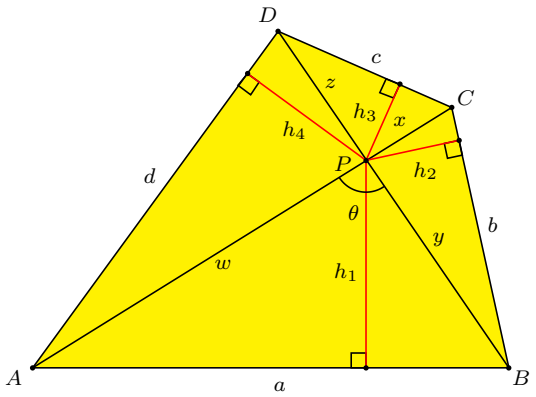

Figure 10. The subtriangle altitudes h_1, h_2, h_3 and h_4

5. Similar metric conditions in tangential and orthodiagonal quadrilaterals

A tangential quadrilateral is a quadrilateral with an incircle. A convex quadrilateral with the sides a, b, c and d is tangential if and only if

$$a + c = b + d$$

according to the well known Pitot theorem [3, pp.65–67]. In Theorem 1 we proved the well known condition that a convex quadrilateral with the sides a, b, c and d is orthodiagonal if and only if

$$a^2 + c^2 = b^2 + d^2.$$

Here all terms are squared compared to the Pitot theorem.

From the extended law of sines (see the proof of Theorem 9) we have that

$$a + c - b - d = 2\sin\theta(R_1 + R_3 - R_2 - R_4)$$

where R_1, R_2, R_3 and R_4 are the circumradii in the triangles ABP, BCP, CDP and DAP respectively, P is the intersection of the diagonals and θ is the angle between them. Hence

$$a + c = b + d \quad \Leftrightarrow \quad R_1 + R_3 = R_2 + R_4$$

since $\sin\theta > 0$, so a convex quadrilateral is tangential if and only if

$$R_1 + R_3 = R_2 + R_4.$$

In Theorem 9 we proved that the quadrilateral is orthodiagonal if and only if

$$R_1^2 + R_3^2 = R_2^2 + R_4^2.$$

All terms in this condition are squared compared to the tangential condition.

In [16] and [13] it is proved that a convex quadrilateral is tangential if and only if

$$\frac{1}{h_1} + \frac{1}{h_3} = \frac{1}{h_2} + \frac{1}{h_4}$$

where h_1, h_2, h_3 and h_4 are the same altitudes as in Figure 10. We have just proved in Theorem 11 that a convex quadrilateral is orthodiagonal if and only if

$$\frac{1}{h_1^2} + \frac{1}{h_3^2} = \frac{1}{h_2^2} + \frac{1}{h_4^2},$$

that is, all terms in the orthodiagonal condition are squared compared to the tangential condition. We find these similarities between these two types of quadrilaterals very interesting and remarkable.

References

[1] 4everwise and shobber (usernames), Quadrilateral, *Art of Problem Solving*, 2005, `http://www.artofproblemsolving.com/Forum/viewtopic.php?t=48225`

[2] N. Altshiller-Court, *College Geometry*, Dover reprint, 2007.

[3] T. Andreescu and B. Enescu, *Mathematical Olympiad Treasures*, Birkhäuser, Boston, 2004.

[4] T. Andreescu and D. Andrica, *Complex Numbers from A to... Z*, Birkhäuser, 2006.

[5] L. Brand, The Eight-Point Circle and the Nine-Point Circle, *Amer. Math. Monthly*, 51 (1944) 84–85.

[6] A. Engel, *Problem-Solving Strategies*, Springer, New York, 1998.

[7] J. Harries, Area of a Quadrilateral, *The Mathematical Gazette*, 86 (2002) 310–311.

[8] V. F. Ivanoff, C. F. Pinzka and J. Lipman, Problem E1376: Bretschneider's Formula, *Amer. Math. Monthly*, 67 (1960) 291.

[9] M. Josefsson, The area of a bicentric quadrilateral, *Forum Geom.*, 11 (2011) 155–164.

[10] M. F. Mammana, B. Micale and M. Pennisi, The Droz-Farny circles of a convex quadrilateral, *Forum Geom.*, 11 (2011) 109–119.

[11] P. Maynard and G. Leversha, Pythagoras' Theorem for Quadrilaterals, *The Mathematical Gazette*, 88 (2004) 128–130.

[12] B. Micale and M. Pennisi, On the altitudes of quadrilaterals, *Int. J. Math. Educ. Sci. Technol.* 36 (2005) 15–24.

[13] N. Minculete, Characterizations of a tangential quadrilateral, *Forum Geom.* 9 (2009) 113–118.

[14] V. Prasolov (translated and edited by D. Leites), *Problems in Plane and Solid Geometry*, 2005, available at `http://students.imsa.edu/~liu/Math/planegeo.pdf`

[15] K. R. S. Sastry and L. Hoehn, Problem 227: Orthodiagonal quadrilaterals, *The College Mathematics Journal*, 15 (1984) 165–166.

[16] I. Vaynshtejn, N. Vasilyev and V. Senderov, Problem M1495, *Kvant* (in Russian) no 6, 1995 pp. 27–28, available at http://kvant.mirror1.mccme.ru/1995/06/resheniya_zadachnika_kvanta_ma.htm
[17] J. A. Vince, *Geometry for Computer Graphics. Formulae, Examples and Proofs*, Springer, 2005.
[18] *Wikipedia*, Thales' theorem, http://en.wikipedia.org/wiki/Thales%27_theorem, accessed October 5, 2011.
[19] P. Yiu, *Notes on Euclidean Geometry*, Florida Atlantic University Lecture Notes, 1998.
[20] A. A. Zaslavsky, The Orthodiagonal Mapping of Quadrilaterals, *Kvant* (in Russian) no 4, 1998 pp. 43–44, available at http://kvant.mirror1.mccme.ru/pdf/1998/04/kv0498zaslavsky.pdf

Martin Josefsson: Västergatan 25d, 285 37 Markaryd, Sweden
E-mail address: martin.markaryd@hotmail.com

Forum Geometricorum
Volume 12 (2012) 27–28.

FORUM GEOM
ISSN 1534-1178

More Integer Triangles with $R/r = N$

John F. Goehl, Jr.

Abstract. Given an integer-sided triangle with an integer ratio of the radii of the circumcircle and incircle, a simple method is presented for finding another triangle with the same ratio.

In a recent paper, MacLeod [1] discusses the problem of finding integer-sided triangles with an integer ratio of the radii of the circumcircle and incircle. He finds sixteen examples of integer triangles for values of this ratio between 1 and 999. It will be shown that, with one exception, another triangle with the same ratio can be found for each.

Macleod shows that the ratio, N, for a triangle with sides a, b, and c is given by

$$\frac{2abc}{(a+b-c)(a+c-b)(b+c-a)} = N. \tag{1}$$

Define $\alpha = a+b-c$, $\beta = a+c-b$, and $\gamma = b+c-a$. Then

$$\frac{(\alpha+\beta)(\beta+\gamma)(\gamma+\alpha)}{4\alpha\beta\gamma} = N. \tag{2}$$

Let α' and β' be found from any one of MacLeod's triangles. Then (2) may be used to find γ'. But notice that (2) is then a quadratic equation for γ:

$$(\alpha'+\beta')(\alpha'+\gamma)(\beta'+\gamma) = 4N\alpha'\beta'\gamma. \tag{3}$$

One root is the known value, γ', while the other root gives a new triangle with the same value for N. Note that the sum of the two roots is $-\alpha' - \beta' + \frac{4N\alpha'\beta'}{\alpha'+\beta'}$. Since one root is γ', the other is given by

$$\gamma = -\alpha' - \beta' - \gamma' + \frac{4N\alpha'\beta'}{\alpha'+\beta'}.$$

For $N = 2$, $a = b = c = 1$; so $\alpha' = \beta' = \gamma' = 1$ and $\gamma = 1$. No new triangle results.

For $N = 26$, $a = 11$, $b = 39$, $c = 49$; so $\alpha' = 1$, $\beta' = 21$, $\gamma' = 77$ and $\gamma = \frac{3}{11}$. Scaling by a factor of 11 gives $\alpha' = 11$, $\beta' = 231$, and $\gamma' = 3$. The sides of the resulting triangle are $a' = 121$, $b' = 7$, and $c' = 117$.

Publication Date: March 1, 2012. Communicating Editor: Paul Yiu.

The first few values and the last value of N given by Macleod along with the original triangles and the new ones are shown in the table below.

N	a	b	c	a'	b'	c'
1	1	1	1	1	1	1
26	11	39	49	7	117	121
74	259	475	729	27	1805	1813
218	115	5239	5341	763	12493	13225
250	97	10051	10125	1125	8303	9409
866	3025	5629	8649	93	73177	73205

Table 1. Macleod triangles and the corresponding new ones (sides arranged in ascending order).

Reference

[1] A. J. MacLeod, Integer triangles with $R/r = N$, *Forum Geom.*, 10 (2010) 149–155.

John F. Goehl, Jr.: Department of Physical Sciences, Barry University, 11300 NE Second Avenue, Miami Shores, Florida 33161, USA

E-mail address: jgoehl@mail.barry.edu

Forum Geometricorum
Volume 12 (2012) 29–38.

FORUM GEOM
ISSN 1534-1178

The Isosceles Trapezoid and its Dissecting Similar Triangles

Larry Hoehn

Abstract. Isosceles trapezoids are dissected into three similar triangles and rearranged to form two additional isosceles trapezoids. Moreover, triangle centers, one from each similar triangle, form the vertices of a centric triangle which has special properties. For example, the centroidal triangles are congruent to each other and have an area one-ninth of the area of the trapezoids; whereas, the circumcentric triangles are not congruent, but still have equal areas.

1. Introduction

If you were asked whether an isosceles trapezoid can be dissected into three similar triangles by a point on the longer base, you would probably reply initially that it is not possible. However, it is sometimes possible and the search for such a point was the gateway to some other very interesting results.

Theorem 1. *If the longer base of an isosceles trapezoid is greater than the sum of the two isosceles sides, then there exists a point on the longer base of the trapezoid which when joined to the endpoints of the shorter base divides the trapezoid into three similar triangles.*

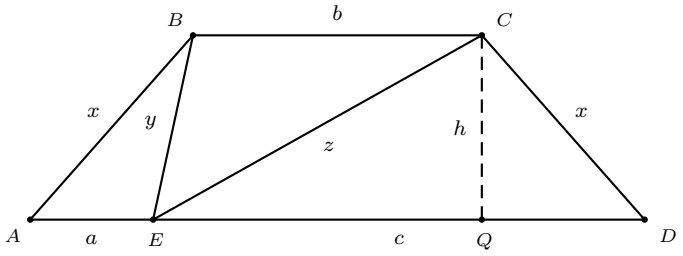

Figure 1.

Proof. To begin our construction we consider isosceles trapezoid $ABCD$ with longer base AD and congruent sides AB and CD as shown in Figure 1. Additionally we let $x = AB = CD$, $b = BC$, $e = AD$, $y = BE$, and $z = CE$.

We propose that the point E can be located on AD by letting

$$AE = \ a = \frac{e}{2} - \sqrt{\left(\frac{e}{2}\right)^2 - x^2},$$

$$ED = \ c = \frac{e}{2} + \sqrt{\left(\frac{e}{2}\right)^2 - x^2}.$$

Publication Date: March 14, 2012. Communicating Editor: Paul Yiu.

Then,

$$\frac{AE}{ED} = \frac{a}{c} = \frac{ac}{c^2} = \frac{x^2}{c^2}.$$

Therefore, $\frac{a}{x} = \frac{x}{c}$ or $\frac{AE}{AB} = \frac{CD}{ED}$. Since $\angle BAE$ and $\angle CDE$ are base angles of the isosceles trapezoid, then triangle BAE is similar to triangle EDC.

Next we consider triangles CQE and CQD where Q is the intersection of a perpendicular dropped from C to base AD. If $CQ = h$, then $QD = \frac{e-b}{2} = \frac{a+c-b}{2}$ so that $EQ = ED - QD = \frac{c-a+b}{2}$. By the Pythagorean Theorem for triangles CQE and CQD respectively, we have $z^2 = h^2 + \left(\frac{c-a+b}{2}\right)^2$ and $x^2 = h^2 + \left(\frac{a+c-b}{2}\right)^2$. By subtracting these equations we obtain

$$z^2 - x^2 = \left(\frac{c-a+b}{2}\right)^2 - \left(\frac{a+c-b}{2}\right)^2 = bc - ac.$$

Since $\frac{a}{x} = \frac{x}{c}$ (see above), we add $x^2 = ac$ to $z^2 - x^2 = bc - ac$ to obtain $z^2 = bc$. Rewriting this as $\frac{z}{b} = \frac{c}{z}$, or equivalently $\frac{EC}{CB} = \frac{DE}{EC}$, and noting that $\angle ECB$ and $\angle DEC$ are alternate interior angles of parallel lines, we have that triangles ECB and DEC are similar. By transitivity, or by repeating the method above, we get that all three triangles are similar to each other. This proves Theorem 1. □

There are some excellent books on dissection, but most involve dissecting a polygon and rearranging the pieces into one or more other polygons. However, none of these references consider isosceles trapezoids and similar triangles. See [1] and [4].

Theorem 2. *Using the notation introduced above we have the following equalities:*
(i) $y^2 = ab$, $x^2 = ac$, $z^2 = bc$;
(ii) $a = \frac{xy}{z}$, $b = \frac{yz}{x}$, $c = \frac{xz}{y}$;
(iii) $xyz = abc$, *and*
(iv) *the area of* $ABCD = \frac{1}{2}h(a+b+c)$.

Proof. The first three follow immediately from the similar dissecting triangles, and (iv) follows directly from the formula for the area of a trapezoid. □

Theorem 3. *Using the notation introduced above, the length of a diagonal,* d*, is given by*

$$d = \sqrt{ac + ab + bc} = \sqrt{x^2 + y^2 + z^2}.$$

Proof. By the law of cosines for triangles ABC and CDA, respectively, in Figure 1, we have

$$\begin{aligned} d^2 &= AC^2 = x^2 + b^2 - 2xb\cos ABC \\ &= x^2 + (a+c)^2 - 2x(a+c)\cos(180^\circ - ABC) \\ &= x^2 + (a+c)^2 + 2x(a+c)\cos ABC. \end{aligned}$$

Therefore,

$$\cos ABC = \frac{x^2 + b^2 - d^2}{2xb} = \frac{x^2 + (a+c)^2 - d^2}{-2x(a+c)}.$$

After some simplification and Theorem 2(i) this becomes

$$d^2 = x^2 + ab + bc = ac + ab + bc = x^2 + y^2 + z^2.$$

□

Theorem 4 (Generalization of the Pythagorean Theorem)**.** *Using the notation introduced above,* $y^2 + z^2 = b(a + c)$.

Proof. Since the triangles are similar, the angles BEC, BAE and CDE are congruent. By Theorem 2(i),

$$y^2 + z^2 = ab + bc = b(a + c) = b^2,$$

where the last equality holds whenever $\angle BAE = 90°$. □

This result appeared previously in [2].

Next we consider triangles whose vertices are specific triangle centers for each of the three dissecting triangles of Figure 1. Since there are over a thousand identified triangle centers, we restrict our discussion to two of the most well-known; namely, the centroid and circumcenter. We will refer to these new triangles as centroidal and circumcentric, respectively.

2. The Centroidal Triangle

It is well-known that the centroid of a triangle is the intersection of the three medians of a triangle and that the centroid is the center of gravity for the triangle. We denote the centroids of our three similar triangles as G_a, G_b, and G_c as shown in Figure 2.

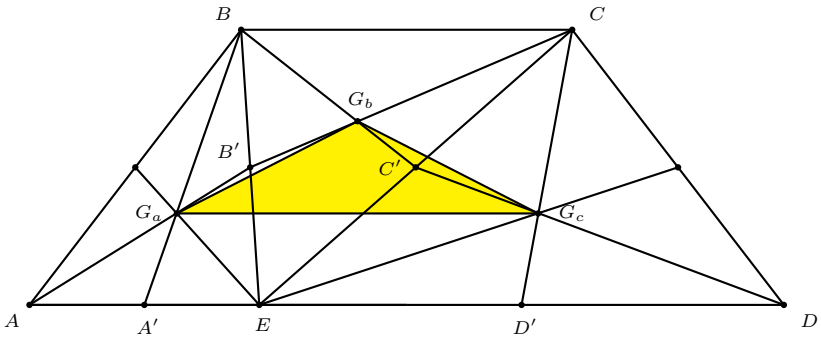

Figure 2. The centroidal triangle

Theorem 5. *Using the notation already introduced,*
(i) *Triangle* $G_aG_bG_c$ *is isosceles with* $G_aG_b = G_cG_b = \frac{1}{3}\sqrt{ab + bc + ca}$,
(ii) *the base of* G_aG_c *of triangle* $G_aG_bG_c$ *is parallel to* AD *and its length is* $G_aG_c = \frac{1}{3}(a + b + c)$, *and*
(iii) *the area of triangle* $G_aG_bG_c$ *is* $\frac{1}{9}$ *of the area of trapezoid* $ABCD$.

Proof. We consider triangle $G_aG_bG_c$ whose vertices are the respective centroids G_a, G_b, and G_c of triangles BAE, CEB and DEC. Let A', B', C', and D' be the respective midpoints of AE, BE, CE, and DE. By the midsegment, or midline theorem, *the line segment joining the midpoints of two sides of a triangle is parallel to and half the length of the third side*. Therefore, quadrilateral $A'B'C'D'$ has sides parallel to and one-half the corresponding sides of quadrilateral $ABCD$, and the quadrilaterals are similar. In particular, quadrilateral $A'B'C'D'$ is isosceles.

Since the centroid of a triangle divides each median in a ratio of $2:3$ of the median from the vertex and $1:3$ from the midpoint of the corresponding side, $G_aG_b = \frac{2}{3}A'C'$ for triangle $BA'C'$ and $G_cG_b = \frac{2}{3}B'D'$ for triangle $CB'D'$. Since trapezoid $A'B'C'D'$ has a similarity ratio of $\frac{1}{2}$ with isosceles trapezoid $ABCD$, $G_aG_b = \frac{2}{3}A'C' = \frac{2}{3}\cdot\frac{1}{2}AC = \frac{1}{3}AC$. In the same manner $G_cG_b = \frac{1}{3}BD$. Since diagonals AC and BD are congruent, $G_aG_b = G_cG_b$ and triangle $G_aG_bG_c$ is isosceles. Note that $G_aG_b = G_cG_b = \frac{1}{3}\sqrt{ab+bc+ca}$, which is one-third of the length of the diagonal of the trapezoid.

The base G_aG_c of triangle $G_aG_bG_c$ is parallel to AD and its length is $G_aG_c = \frac{2}{3}A'D' + \frac{1}{3}BC$ in trapezoid $BCD'A'$ so that

$$G_aG_c = \frac{2}{3}\left(\frac{a}{2}+\frac{c}{2}\right)+\frac{1}{3}b = \frac{1}{3}(a+b+c).$$

Finally, the area of triangle $G_aG_bG_c = \frac{1}{2}\times$ base $\times$ height $= \frac{1}{2}\cdot\frac{1}{3}(a+b+c)\cdot\frac{h}{3} = \frac{1}{9}\cdot\frac{1}{2}h(a+b+c) = \frac{1}{9}\times$ area of trapezoid $ABCD$. □

3. The Circumcentric Triangle

Next we consider the circumcenters of each of the three dissecting triangles of Figure 1. A circumcenter is the intersection of the three perpendicular bisectors of the sides of any triangle. The circumradius is the radius of the circumcircle which passes through the three vertices of the particular triangle. For our example in Figure 3, triangle ABE has circumcenter O_a and circumradius $R_a (= AO_a = BO_a = CO_a)$. Similar statements hold for O_b, O_c, R_b, and R_c.

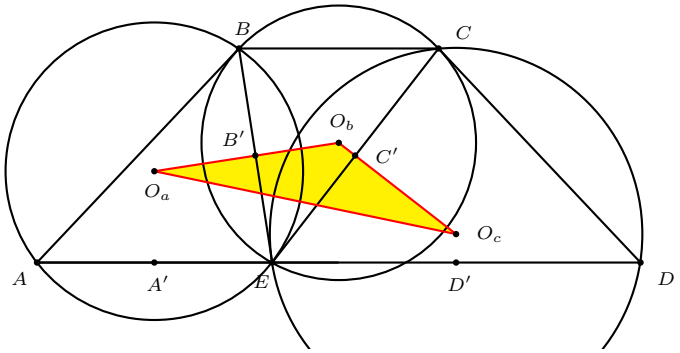

Figure 3. The circumcentric triangle

Theorem 6. *Using the notation already introduced for triangle $O_aO_bO_c$,*
(i) $O_aOb = R_c$ *and* $O_cO_b = R_a$,
(ii) $O_aO_c = \sqrt{2R_a^2 + 2R_c^2 - R_b^2}$, *and*
(iii) *the area of triangle* $O_aO_bO_c = \frac{xyz}{8h} = \frac{abc}{8h}$.

Proof. Let A' and B' be the feet of the perpendicular bisectors of two sides of triangle ABE. Since triangle AO_aE is isosceles, AO_aA' and EO_aA' are congruent right triangles. Note that O_a is the vertex of three isosceles subtriangles in triangle ABE, and also a vertex of six right triangles which are congruent in pairs. For convenience we label the angles away from center O_a numerically (see Figure 4) as

$$\begin{aligned} \angle BAE = \ \gamma &= \angle 1 + \angle 2, \\ \angle BEA = \ \alpha &= \angle 2 + \angle 3, \\ \angle ABE = \ \beta &= \angle 1 + \angle 3. \end{aligned}$$

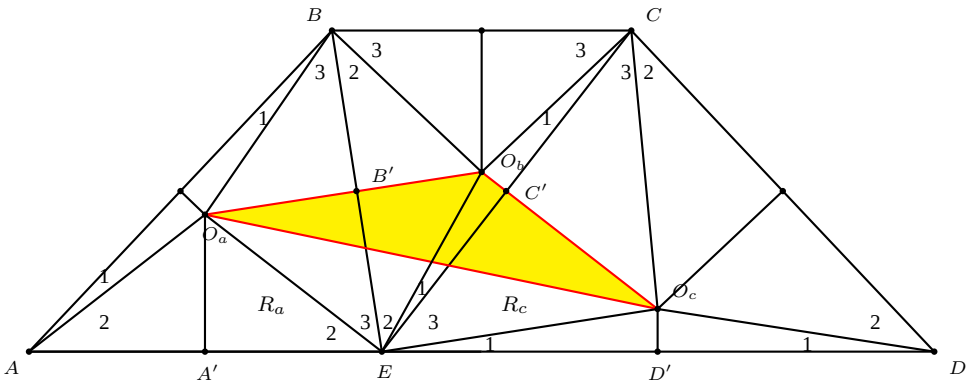

Figure 4. Numbered angles of isosceles and similar triangles

In the same manner corresponding congruent angles are denoted in Figure 4 for the similar triangles CBE and DEC.

In particular, we note that in quadrilateral $B'EC'O_b$ which has two right angles, we have

$$\angle B'O_bC' = 360^\circ - 90^\circ - 90^\circ - \angle 2 - \angle 1 = 180^\circ - \gamma = \alpha + \beta.$$

Also,

$$\angle O_aEO_c = \angle 3 + (\angle 2 + \angle 1) + \angle 3 = (\angle 3 + \angle 2) + (\angle 1 + \angle 3) = \alpha + \beta.$$

Therefore, one pair of opposite angles of quadrilateral $O_aO_bO_cE$ are congruent. Since

$$\begin{aligned} \angle EO_aO_b = \ \angle EO_aB' &= 90^\circ - \angle 3, \\ \angle EO_cO_b = \ \angle EO_cC' &= 90^\circ - \angle 3, \end{aligned}$$

the other pair of opposite angles of quadrilateral $O_aO_bO_cE$ are congruent. Hence quadrilateral $O_aO_bO_cE$ is a parallelogram. Therefore, $O_aO_b = EO_c = R_c$ and $O_cO_b = EO_a = R_a$. This proves (i).

Since the sum of the squares of the diagonals of a parallelogram is equal to the sum of the squares of the four sides, we have

$$O_aO_c^2 + O_bE^2 = O_aO_b^2 + O_bO_c^2 + O_cE^2 + EO_a^2 = 2R_c^2 + 2R_a^2.$$

Therefore, $O_aO_c^2 = 2R_c^2 + 2R_a^2 - R_b^2$. From this (ii) follows.

If we use the formula $R = \frac{abc}{4\cdot\text{Area}}$ for the circumradius of a triangle with sides of lengths a, b, c (see [3] and [4]), then for triangle ABE

$$R_a^2 = \left(\frac{axy}{4\cdot\frac{1}{2}ah}\right)^2 = \frac{x^2y^2}{4h^2} = \frac{ac\cdot ab}{4h^2} = \frac{a^2bc}{4h^2},$$

with similar results for R_b^2 and R_c^2. Therefore,

$$\begin{aligned} O_aO_c^2 &= 2R_c^2 + 2R_a^2 - R_b^2 = \frac{2a^2bc}{4h^2} + \frac{2abc^2}{4h^2} - \frac{ab^2c}{4h^2}, \\ O_aO_C &= \frac{\sqrt{abc(2a+2c-b)}}{2h}. \end{aligned}$$

Since the opposite sides of a parallelogram are parallel,

$$\begin{aligned} \angle EO_bO_c &= \angle O_bEO_a = \angle 3 + \angle 2 = \alpha, \\ \angle O_bEO_c &= \angle 1 + \angle 3 = \beta. \end{aligned}$$

This implies that $\angle O_bO_cE = \gamma$. Therefore, triangle EO_bO_c is similar to the original three similar dissecting triangles. Since EO_b is a diagonal of parallelogram $O_aO_bO_cE$, similar statements hold for triangle O_aO_bE. Finally,

$$\text{area } O_aO_bO_c = \frac{1}{2}\cdot \text{area of parallelogram } O_aO_bO_cE = \text{area of } EO_bO_c.$$

Using the basic formula for the area of a triangle we have

$$\begin{aligned} \text{area of } O_aO_bO_cE &= \text{area of } O_aO_bE + \text{area of } EO_bO_c \\ &= \frac{1}{2}\cdot\frac{y}{2}\cdot O_aO_b + \frac{1}{2}\cdot\frac{z}{2}\cdot O_bO_c \\ &= \frac{1}{4}\cdot yR_c + \frac{1}{4}\cdot zR_a. \end{aligned}$$

Recalling the formula $R = \frac{abc}{4\cdot\text{Area}}$ from above, we have

$$\begin{aligned}\text{area of } O_aO_bO_c &= \frac{1}{8}(yR_c + zR_a)\\ &= \frac{1}{8}\left(y\cdot\frac{czx}{4\cdot\frac{ch}{2}} + z\cdot\frac{axy}{4\cdot\frac{ah}{2}}\right)\\ &= \frac{1}{8}\left(\frac{xyz}{2h} + \frac{xyz}{2h}\right)\\ &= \frac{xyz}{8h} = \frac{abc}{8h}.\end{aligned}$$

□

Corollary 7. *If the dissecting triangles are right triangles, then*
(i) $c = a + b$, *and*
(ii) *the area of triangle $O_aO_bO_c$ is one-eighth the area of trapezoid $ABCD$.*

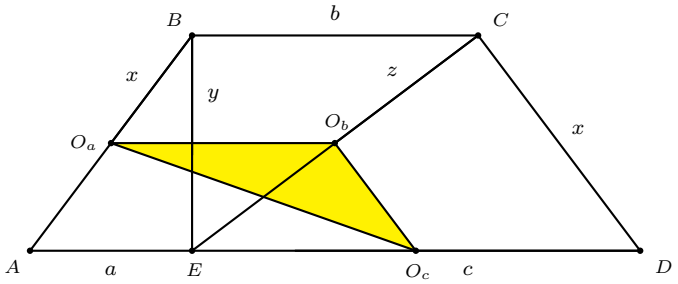

Figure 5. Circumcentric triangle with similar right triangles

Proof. For a right triangle the circumcenter is the midpoint of the hypotenuse of the right triangle. Therefore, $c^2 = x^2 + z^2$ in triangle BEC in Figure 5. Substituting $x^2 = ac$ and $z^2 = bc$ yields $c^2 = ac + bc$. From this the first result follows. Note that

$$\begin{aligned}\text{area of } O_aO_bO_c &= \text{ area of } EO_bO_c = \frac{1}{4}\cdot\text{ area of } ECD\\ &= \frac{1}{4}\cdot\frac{1}{2}\cdot hc = \frac{1}{4}\cdot\frac{1}{2}h(a+b) = \frac{1}{4}\cdot\text{ area of } ABCE.\end{aligned}$$

It also follows that EC separates the trapezoid into two parts with equal area. □

4. The Three IsoscelesTrapezoids

We return to the dissection of §1. Since we started with a dissection problem it surely occurred to the reader that we might be able to rearrange the dissected trapezoid into another configuration. That is indeed the case. The three similar triangles can be rearranged as follows:

Theorem 8. *If the isosceles trapezoid is literally cut apart, then the similar triangles can be rearranged to form two additional isosceles trapezoids which meet the same dissection criteria, have the same area, and have the same diagonal lengths as the original trapezoid.*

Proof. With the trapezoid cut apart and reassembled we get the three cases shown in Figure 6 below. The triangles are numbered #1, #2, and #3 for clarity.

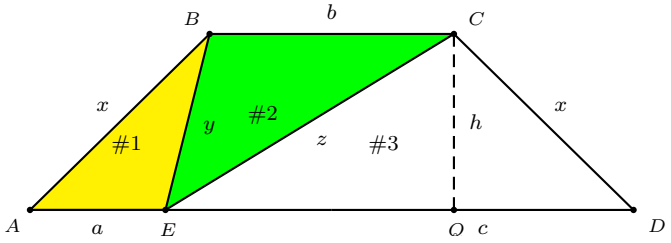

Figure 6(i) Original trapezoid with similar triangles

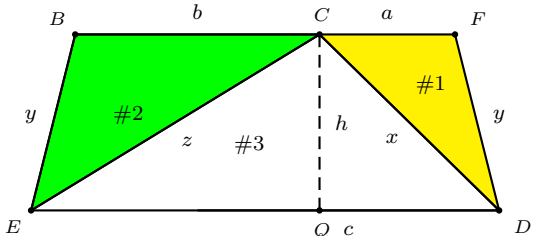

Figure 6(ii) Trapezoid with rearranged triangles

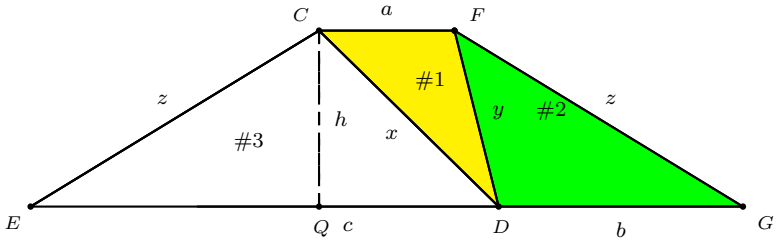

Figure 6(iii) Trapezoid with rearranged triangles

Note that the area of each of the three trapezoids is $\frac{1}{2}h(a+b+c)$ regardless of shape. In Theorem 3 the length of the diagonals for the first trapezoid was

given by the formula $d = \sqrt{ab + bc + ca} = \sqrt{x^2 + y^2 + z^2}$. Since the formula is symmetric in the variables, the formulas hold for the latter two cases as well. This can also be seen as a proof without words in Figure 7 where the dotted segments are the diagonals of the three respective trapezoids. Since the diagonals of an isosceles trapezoid are congruent, we have

$$AC = BD, \quad BD = EF, \quad EF = CG.$$

Hence all are equal in length.

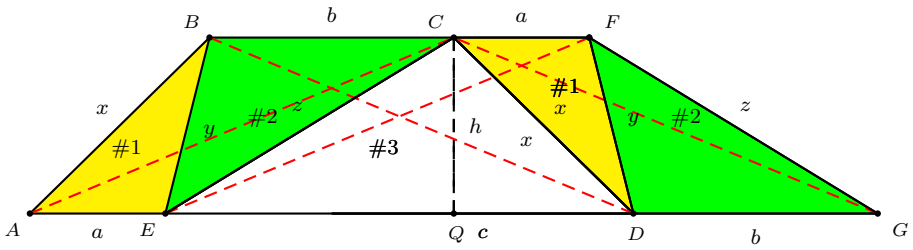

Figure 7. Proof without words: Congruent diagonals

Since many of the formulas derived in the theorems above are symmetric in variables a, b, c, x, y, and z, these particular properties also hold for the two additional trapezoidal arrangements of similar triangles. For example, since two sides of the centroidal triangle of the original trapezoid are given by $\frac{1}{3}\sqrt{ab + bc + ca}$ and the third side by $\frac{1}{3}(a + b + c)$, the three centroidal triangles of all three trapezoids are also isosceles and congruent. Additionally the areas of each of these triangles is one-ninth of the areas of the trapezoids.

Since the sides of the circumcentric triangle of the original trapezoid are given by circumradii R_a, R_c, and $\sqrt{2R_a^2 + 2R_c^2 - R_b^2}$, the circumcentric triangles of the other two trapezoids are not isosceles and are not congruent for the three trapezoidal arrangements. However, the areas of the three circumcentric triangles are the same and are given by $\frac{xyz}{8h} = \frac{abc}{8h}$.

There are some excellent books on dissection, but most involve dissecting a polygon and rearranging the pieces into one or more other polygons. For example, see [1] and [5]. However, none of these references consider isosceles trapezoids and similar triangles as presented in this paper. □

5. More Study

There are some additional questions that might be worth pursuing such as: What properties follow from other centric triangles such as incenters, orthocenters, etc.? Under what conditions are the three Euler lines of the dissecting triangles concurrent or parallel? Under what conditions are the three triangle centers for the dissecting triangles collinear? Will any of the centric triangles be similar to the dissecting triangles? Do comparable properties hold when isosceles trapezoid is

replaced by isosceles quadrilateral? Finally, is there a 3-dimensional analog for these properties?

References

[1] G. N. Frederickson, *Dissections: Plane & Fancy*, Cambridge University Press, Cambridge, United Kingdom, 1997.
[2] L. Hoehn, A generalisation of Pythagoras' theorem, *Math. Gazette*, 92 (2008) 316–317.
[3] I. M. Isaacs, *Geometry for College Students*, Brooks/Cole, 2001, Pacific Grove, CA, p.69.
[4] D. C. Kay, *College Geometry: A Discovery Approach*, 2nd edition, Addison Wesley Longman, Inc., Boston, 2001, Appendix A-9.
[5] H. Lindgren, *Recreational Problems in Geometric Dissections and How to Solve Them*, Dover Publications, Inc., New York, 1972.

Larry Hoehn: Austin Peay State University, Clarksville, Tennessee 37044, USA
E-mail address: hoehnl@apsu.edu

Forum Geometricorum
Volume 12 (2012) 39–46.

FORUM GEOM
ISSN 1534-1178

Synthetic Proofs of Two Theorems Related to the Feuerbach Point

Nguyen Minh Ha and Nguyen Pham Dat

Abstract. We give synthetic proofs of two theorems on the Feuerbach point of a triangle, one of Paul Yiu, and another of Lev Emelyanov and Tatiana Emelyanova theorem.

1. Introduction

If S is a point belonging to the circumcircle of triangle ABC, then the images of S through the reflections with axes BC, CA and AB respectively lie on the same line that passes through the orthocenter of ABC. This line is called the Steiner line of S with respect to triangle ABC.

If a line $\mathcal{L}$ passes through the orthocenter of ABC, then the images of $\mathcal{L}$ through the reflections with axes BC, CA and AB are concurrent at one point on the circumcircle of ABC. This point is named the anti-Steiner point of $\mathcal{L}$ with respect to ABC. Of course, $\mathcal{L}$ is Steiner line of S with respect to ABC if and only if S is the anti-Steiner point of $\mathcal{L}$ with respect to ABC. In 2005, using homogenous barycentric coordinates, Paul Yiu [5] established an interesting theorem related to the Feuerbach point of a triangle; see also [3, Theorem 5].

Theorem 1. *The Feuerbach point of triangle ABC is the anti-Steiner point of the Euler line of the intouch triangle of ABC with respect to the same triangle.* [1]

In 2009, J. Vonk [4] introduced a geometrically synthetic proof of Theorem 1. In 2001, by calculation, Lev Emelyanov and Tatiana Emelyanova [1] established a theorem that is also very interesting and also related to the Feuerbach point of a triangle.

Theorem 2. *The circle through the feet of the internal bisectors of triangle ABC passes through the Feuerbach point of the triangle.*

In this article, we present a synthetic proof of Theorem 1, which is different from Vonk's proof, and one for Theorem 2. We use (O), $I(r)$, (XYZ) to denote respectively the circle with center O, the circle with center I and radius r, and the circumcircle of triangle XYZ. As in [2, p.12], the directed angle from the line

Publication Date: March 22, 2012. Communicating Editor: J. Chris Fisher.
The authors thank Professor Chris Fisher for his valuable comments and suggestions.

[1] The anti-Steiner point of the Euler line is called the Euler reflection point in [3].

a to the line b denoted by (a, b). It measures the angle through which a must be rotated in the positive direction in order to become parallel to, or to coincide with, b. Therefore,
(i) $-90^\circ \leq (\mathsf{a},\ \mathsf{b}) \leq 90^\circ$,
(ii) $(\mathsf{a},\ \mathsf{b}) = (\mathsf{a},\ \mathsf{c}) + (\mathsf{c},\ \mathsf{b})$,
(iii) If a' and b' are the images of a and b respectively under a reflection, then $(\mathsf{a},\ \mathsf{b}) = (\mathsf{b}',\ \mathsf{a}')$,
(iv) Four noncollinear points A, B, C, D are concyclic if and only if $(AC, AD) = (BC, BD)$.

2. Preliminary results

Lemma 3. *Let ABC be a triangle inscribed in a circle (O), and $\mathcal{L}$ an arbitrary line. Let the parallels of $\mathcal{L}$ through A, B, C intersect the circle at D, E, F respectively. The lines $\mathcal{L}_a$, $\mathcal{L}_b$, $\mathcal{L}_c$ are the perpendiculars to BC, CA, AB through D, E, F respectively.*
(a) *The lines $\mathcal{L}_a$, $\mathcal{L}_b$, $\mathcal{L}_c$ are concurrent at a point S on the circle (O),*
(b) *The Steiner line of S with respect to ABC is parallel to $\mathcal{L}$.*

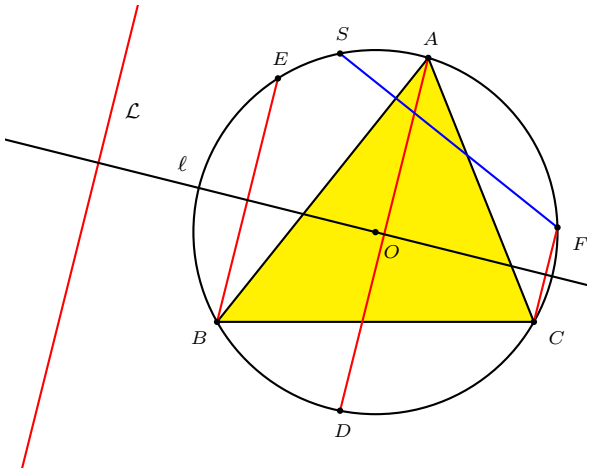

Figure 1.

Proof. Let S be the intersection of $\mathcal{L}_a$ and (O). Let ℓ be the line through O perpendicular to $\mathcal{L}$ (see Figure 1).

(a) Because A, B, and C are the images of D, E, and F through the reflections with axis $\mathcal{L}$ respectively,

$$(FE, FD) = (CA, CB). \tag{1}$$

Therefore, we have

$$\begin{aligned}(SE, AC) &= (SE, SD) + (SD, BC) + (BC, AC) \\ &= (FE, FD) + 90^\circ + (BC, AC) && (F \in (SDE), SD \perp BC) \\ &= (CA, CB) + 90^\circ + (BC, AC) \\ &= 90^\circ.\end{aligned}$$

Therefore, SE coincides $\mathcal{L}_b$, *i.e.*, S lies on $\mathcal{L}_b$. Similarly, S also lies on $\mathcal{L}_c$, and the three lines $\mathcal{L}_a$, $\mathcal{L}_b$, $\mathcal{L}_c$ are concurrent at S on the circle (O).

(b) Let B_1, C_1 respectively be the images of S through the reflections with axes CA, AB. Let B_2, C_2 respectively be the intersection points of SB_1, SC_1 with AC, AB (see Figure 2). Obviously, B_2, C_2 are the midpoints of SB_1, SC_1 respectively. Thus,

$$B_2C_2 // B_1C_1. \tag{2}$$

Since SB_2, SC_2 are respectively perpendicular to AC, AB,

$$S \in (AB_2C_2). \tag{3}$$

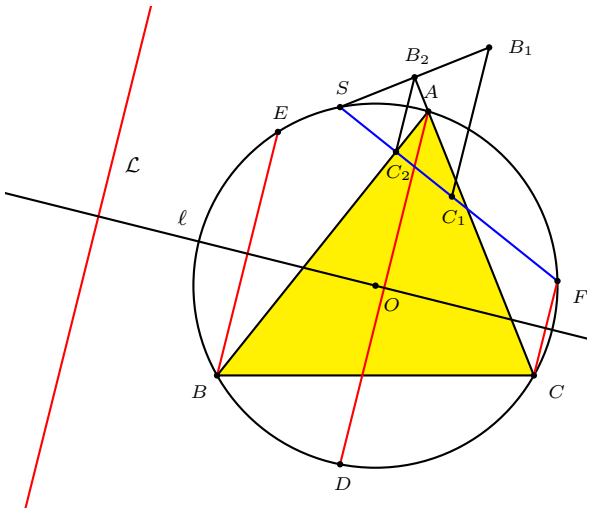

Figure 2.

Therefore, we have

$$\begin{aligned}(B_1C_1, \mathcal{L}) &= (B_1C_1, AD) && (\mathcal{L} // AD) \\ &= (B_2C_2, AD) && \text{(by (2))} \\ &= (B_2C_2, AC_2) + (AB, AD) && (B \in AC_2) \\ &= (B_2S, AS) + (AB, AD) && \text{(by (3))} \\ &= (ES, AS) + (AB, AD) && (E \in B_2S) \\ &= (ED, AD) + (DA, DE) && (D \in (SEA)) \\ &= 0^\circ.\end{aligned}$$

Therefore, $B_1C_1//\mathcal{L}$. This means that the Steiner line of S with respect to triangle ABC is parallel to $\mathcal{L}$. □

Before we go on to Lemma 4, we review a very interesting concept in plane geometry called the orthopole. Let triangle ABC and the line $\mathcal{L}$. A', B', C' are the feet of the perpendiculars from A, B, C to $\mathcal{L}$ respectively. The lines $\mathcal{L}_a$, $\mathcal{L}_b$, $\mathcal{L}_c$ pass through A', B', C' and are perpendicular to BC, CA, AB respectively. Then $\mathcal{L}_a$, $\mathcal{L}_b$, $\mathcal{L}_c$ are concurrent at one point called the orthopole of the line $\mathcal{L}$ with respect to triangle ABC. The following result is one of the most important results related to the concept of the orthopole. This result is often attributed to Griffiths, whose proof can be found in [2, pp.246–247].

Lemma 4. *Let ABC be a triangle inscribed in the circle (O), and P be an arbitrary point other than O. The orthopole of the line OP with respect to triangle ABC belongs to the circumcircle of the pedal triangle of P with respect to ABC.*

Lemma 5. *Let ABC be a triangle inscribed in (O). A_1, B_1, C_1 are the images of A, B, C respectively through the symmetry with center O. A_2, B_2, C_2 are the images of O through the reflections with axes BC, CA, AB respectively. A_3, B_3, C_3 are the feet of the perpendiculars from A, B, C to the lines OA_2, OB_2, OC_2 respectively. Then,*
(a) *The circles (OA_1A_2), (OB_1B_2), (OC_1C_2) all pass through the anti-Steiner point of the Euler line of triangle ABC with respect to the same triangle.*
(b) *The circle $(A_3B_3C_3)$ also passes through the same anti-Steiner point.*

Proof. (a) Let H be the orthocenter of ABC. Take the points D, S belonging to (O) such that $AD//OH$ and $DS \perp BC$ (see Figure 3).

According to Lemma 3, the Steiner line of S with respect to ABC is parallel to AD. On the other hand, the Steiner line of S with respect to ABC passes through H. Hence, OH is the Steiner line of S with respect to ABC. In other words,

$$S \text{ is the anti-Steiner point of the Euler line of } ABC \text{ with respect to the same triangle.} \tag{4}$$

Let S_a be the intersection of SD and OH. By (4), S_a is the images of S through the reflection with axis BC. From this, note that A_2 is the image of O through the reflection with axis BC, we have:

$$OA_2SS_a \text{ is an isosceles trapezium with } OA_2//S_a. \tag{5}$$

Therefore, we have

$$\begin{aligned}
(A_2O, A_2S) &= (S_aO, S_aS) && \text{(by (5))}\\
&= (DA, DS) && (DA//S_aO \text{ and } D \in S_aS)\\
&= (A_1A, A_1S) && (A_1 \in (DAS))\\
&= (A_1O, A_1S) && (O \in A_1A).
\end{aligned}$$

It follows that $S \in (OA_1A_2)$. Similarly, $S \in (OB_1B_2)$ and $S \in (OC_1C_2)$. Therefore,

$$\text{the circles } (OA_1A_2), (OB_1B_2), (OC_1C_2) \text{ all pass through } S. \tag{6}$$

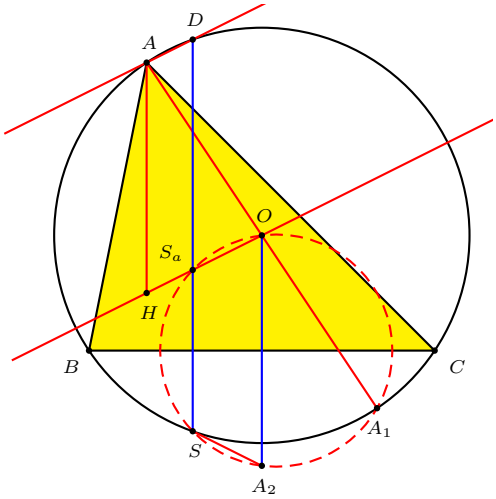

Figure 3.

From (4) and (6), we can deduce that (OA_1A_2), (OB_1B_2), (OC_1C_2) all pass through the anti-Steiner point of the Euler line of triangle ABC with respect to ABC.

(b) Take the points A_0, B_0, C_0 such that A, B, C are the midpoints of B_0C_0, C_0A_0, A_0B_0 respectively. Let M be the mid-point of BC (see Figure 4). Since $AB//CA_0$ and $AC//BA_0$, ABA_0C is a parallelogram. On the other hand, noting that $HB \perp AC$ and $CA_1 \perp AC$, $HC \perp AB$, and $BA_1 \perp AB$, we have $HB//CA_1$, $HC//BA_1$. This means that HBA_1C is a parallelogram. Thus, A_0, A_1 are the images of A, H respectively through the symmetry with center M. Therefore, the vectors $\mathbf{A_1A_0}$ and $\mathbf{AH}$ are equal.

On the other hand, since AHS_aD is a parallelogram, the vectors $\mathbf{DS_a}$ and $\mathbf{AH}$ are equal.

Hence, under the translation by the vector $\mathbf{AH}$, the points A_1, D are transformed into the points A_0, S_a respectively. This means that $A_0S_a//A_1D$.

From this, noting that $AD \perp A_1D$ and $AD//OH$, we deduce that

$$A_0S_a \perp OH. \tag{7}$$

On the other hand, because $SS_a \perp BC$ and $BC//B_0C_0$, we have

$$SS_a \perp B_0C_0. \tag{8}$$

From (7) and (8), we see that the orthopole of OH with respect to triangle $A_0B_0C_0$ lies on the line SS_a. Similarly, the orthopole of OH with respect to $A_0B_0C_0$ also lies on SS_b and SS_c, where S_b, S_c are defined in the same way with S_a. Thus,

$$S \text{ is the orthopole of } OH \text{ with respect to triangle } A_0B_0C_0. \tag{9}$$

It is also clear that H is the center of the circle $(A_0B_0C_0)$ and

$$A_3B_3C_3 \text{ is the pedal triangle of } O \text{ with respect to triangle } A_0B_0C_0. \tag{10}$$

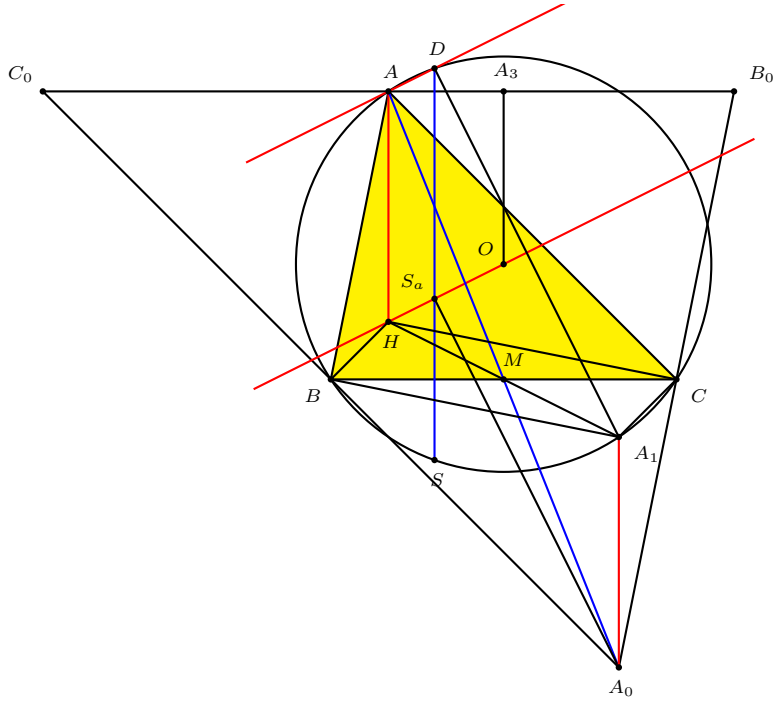

Figure 4.

From (9) and (10), and by Lemma 4, we have $S \in (A_3B_3C_3)$. □

Lemma 6. *If any of the three points in A, B, C, D are not collinear, then the nine-point circles of triangles BCD, CDA, DAB, ABC all pass through one point.*

Lemma 6 is familiar and its simple proof can be found in [2, p.242].

3. Main results

3.1. *A synthetic proof of Theorem 1.* Assume that the circle $I(r)$ inscribed in ABC touches BC, CA, AB at A_0, B_0, C_0 respectively. Let A_1, B_1, C_1 be the images of A_0, B_0, C_0 respectively through the symmetry with center I. Let A_2, B_2, C_2 be the images of I through the reflections with axes B_0C_0, C_0A_0, A_0B_0 respectively. Let A_3, B_3, C_3 be the mid-points of AI, BI, CI respectively (see Figure 5).

Under the inversion in $I(r)$, the points A_2, B_2, C_2 are transformed into the points A_3, B_3, C_3 respectively. As a result, the circles (IA_1A_2), (IB_1B_2), (IC_1C_2) are transformed into the lines A_1A_3, B_1B_3, C_1C_3 respectively. According to Lemma 5(a),

the circles (IA_1A_2), (IB_1B_2), (IC_1C_2) all pass through one point lying on the circle (I), the anti-Steiner point of the Euler line of triangle $A_0B_0C_0$ with respect to the same triangle. We call this point F. (11)

Hence, A_1A_3, B_1B_3, C_1C_3 are also concurrent at F. (12)

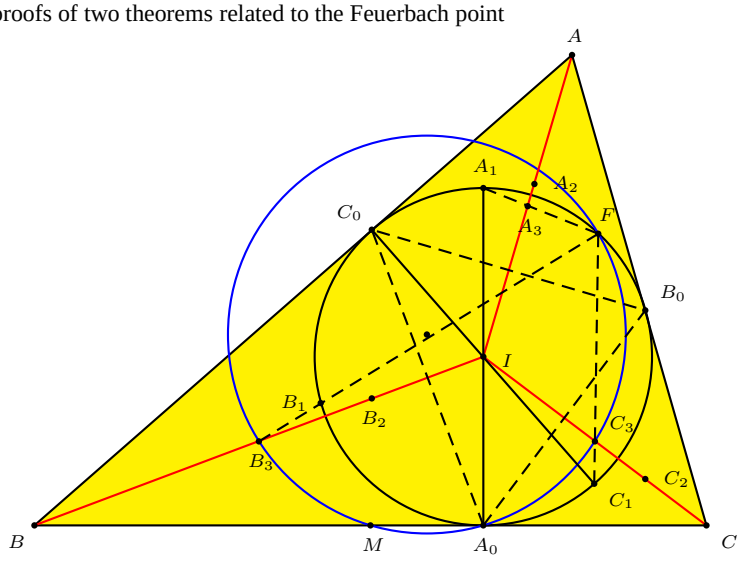

Figure 5.

Because A_1, B_1, C_1 be the images of A_0, B_0, C_0 respectively through the symmetry with center I, A_1B_1, A_1C_1 are parallel to A_0B_0, A_0C_0 respectively.

From this, noting that A_0B_0, A_0C_0 are perpendicular to IC, IB respectively, we deduce that

$$A_1B_1, A_1C_1 \text{ are perpendicular to } IC, IB. \tag{13}$$

Let M be the mid-point of BC. Noting that B_3, C_3 are the mid-points of BI, CI respectively, we have

$$IC//MB_3 \quad \text{and} \quad IB//MC_3. \tag{14}$$

Therefore, we have

$$\begin{aligned}
(FB_3, FC_3) &= (FB_1, FC_1) && \text{(by (12))} \\
&= (A_1B_1, A_1C_1) && (A_1 \in (FB_1C_1)) \\
&= (IC, IB) && \text{(by (13))} \\
&= (MB_3, MC_3) && \text{(by (14))}.
\end{aligned}$$

From this, $F \in (MB_3C_3)$, the nine-point circle of triangle IBC.

Similarly, F also belongs to the nine-point circles of triangles ICA, IAB.

Thus, from Lemma 6, F belongs to the nine-point circle of triangle ABC. This means that

$$F \text{ is the Feuerbach point of triangle } ABC. \tag{15}$$

From (11) and (15), F is not only the anti-Steiner point of the Euler line of $A_0B_0C_0$ with respect to $A_0B_0C_0$, but also the Feuerbach point of ABC.

Thus, we can conclude that the Feuerbach point of ABC is the anti-Steiner point of the Euler line of $A_0B_0C_0$.

3.2. *A synthetic proof of Theorem 2.* Suppose that the inscribed circle $I(r)$ of triangle ABC touches BC, CA, AB at A_0, B_0, C_0 respectively. Let A', B', C' be the intersections of AI, BI, CI with BC, CA, AB respectively; A'', B'', C'' be the feet of the perpendiculars from A_0, B_0, C_0 to AI, BI, CI respectively and F be the Feuerbach point of ABC (see Figure 6).

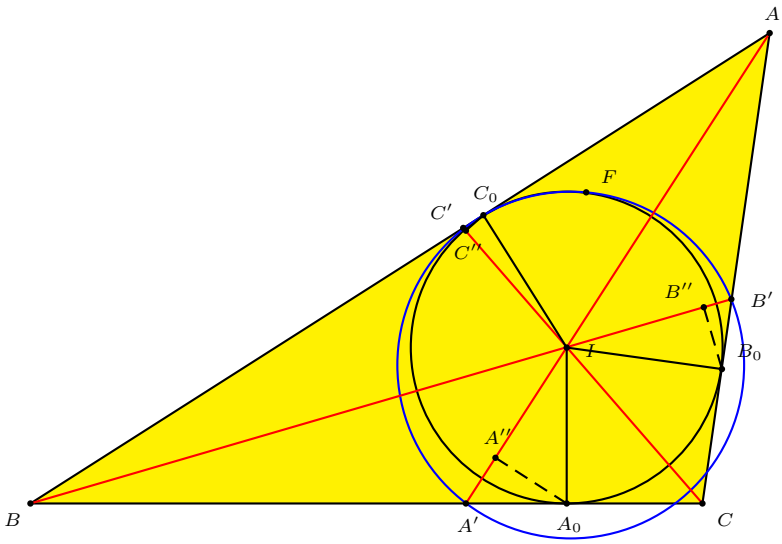

Figure 6.

From Lemma 5(b) and Theorem 1, $F \in (A''B''C'')$. (16)

On the other hand, under inversion in the incircle $I(r)$, F, A'', B'', C'' are transformed into F, A', B', C' respectively. (17)

From (16) and (17), we can conclude that In conclusion, the circumcircle of $A'B'C'$ passes through the Feuerbach point F of ABC.

References

[1] L. Emelyanov and T. Emelyanov, A note on the Feuerbach point, *Forum Geom.*, 1 (2001) 121–124.
[2] R. A. Johnson, *Advanced Euclidean Geometry*, 1929, Dover reprint 2007.
[3] B. D. Suceavă and P. Yiu, The Feuerbach point and Euler lines, *Forum Geom*, 6 (2006) 191–197.
[4] J. Vonk, The Feuerbach point and reflections of the Euler line, *Forum Geom*, 9 (2009) 47–55.
[5] P. Yiu, Hyacinthos message 11652, October 18, 2005.

Nguyen Minh Ha: Hanoi University of Education, Hanoi, Vietnam.
E-mail address: minhha27255@yahoo.com

Nguyen Pham Dat: Hanoi University of Education, Hanoi, Vietnam.
E-mail address: datpn@chuyensphn.com

Forum Geometricorum
Volume 12 (2012) 47–61.

FORUM GEOM
ISSN 1534-1178

Properties of Valtitudes and Vaxes of a Convex Quadrilateral

Maria Flavia Mammana, Biagio Micale, and Mario Pennisi

Abstract. We introduce the vaxes relative to a v-parallelogram and determine several properties of valtitudes and of vaxes. In particular, we study the quadrilateral detected by the valtitudes and the one detected by the vaxes.

Given a convex quadrilateral $\mathbf{Q}$, we call maltitude of $\mathbf{Q}$ the perpendicular line through the midpoint of a side to the opposite side. Maltitudes have been investigated in several papers (see, for example, [2, 7, 8]). In particular in [7] it has been proved that they are concurrent in a point, called anticenter in [9], if and only if $\mathbf{Q}$ is cyclic. Valtitudes relative to a v-parallelogram of a convex quadrilateral $\mathbf{Q}$ were defined in [7]. This definition generalizes the one of maltitudes. Moreover the problem of concurrency of valtitudes relative to a v-parallelogram of a convex quadrilateral $\mathbf{Q}$ was investigated. In this paper we introduce the notion of vaxis relative to a v-parallelogram and we determine several properties of valtitudes and vaxes. In particular, we study the quadrilateral detected by the valtitudes and those detected by the vaxes.

1. v-parallelograms

Let $A_1A_2A_3A_4$ be a convex quadrilateral, that we denote by $\mathbf{Q}$. A v-parallelogram of $\mathbf{Q}$ is any parallelogram with vertices on the sides of $\mathbf{Q}$ and sides parallel to the diagonals of $\mathbf{Q}$.

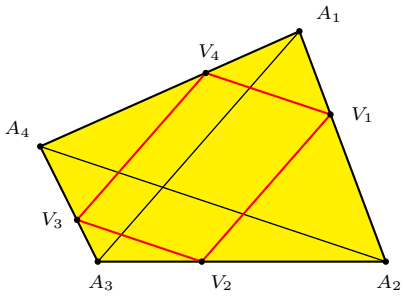

Figure 1.

To obtain a v-parallelogram of $\mathbf{Q}$ we can use the following construction. Fix an arbitrary point V_1 on the segment A_1A_2. Draw from V_1 the parallel to the diagonal A_1A_3 and let V_2 be the intersection point of this line with the side A_2A_3. Draw

Publication Date: March 28, 2012. Communicating Editor: Paul Yiu.

from V_2 the parallel to the diagonal A_2A_4 and let V_3 be the intersection point of this line with the side A_3A_4. Finally, draw from V_3 the parallel to the diagonal A_1A_3 and let V_4 be the intersection point of this line with the segment A_4A_1. The quadrilateral $V_1V_2V_3V_4$ is a v-parallelogram [7] and, by moving V_1 on the segment A_1A_2, we obtain all possible v-parallelograms of $\mathbf{Q}$ (see Figure 1).

In the following we will denote by $\mathbf{V}$ a v-parallelogram of $\mathbf{Q}$, with V_i ($i = 1, 2, 3, 4$), vertex of $\mathbf{V}$ on the side A_iA_{i+1} (with indices taken modulo 4) and with G' the common point to the diagonals of $\mathbf{V}$. Observe that $\mathbf{V}$ is orthodiagonal. The v-parallelogram $M_1M_2M_3M_4$, with M_i midpoint of the side A_iA_{i+1}, is the Varignon parallelogram of $\mathbf{Q}$. In this particular case G' is the centroid G of $\mathbf{Q}$. We recall that if M_5 and M_6 are the midpoints of the diagonals A_1A_3 and A_2A_4 of $\mathbf{Q}$ respectively, the segment M_5M_6, that we call the *third bimedian* of $\mathbf{Q}$, passes through G that bisects this segment ([1, 5]).

Theorem 1. *The locus described by the common point of the diagonals of a v-parallelogram* $\mathbf{V}$ *of* $\mathbf{Q}$ *by varying* $\mathbf{V}$ *is the third bimedian of* $\mathbf{Q}$.

Proof. Let $\mathbf{V}$ be any v-parallelogram of $\mathbf{Q}$ and let $N_1N_2N_3N_4$ be the Varignon parallelogram of $\mathbf{V}$, with midpoint N_i of V_iV_{i+1} (see Figure 2).

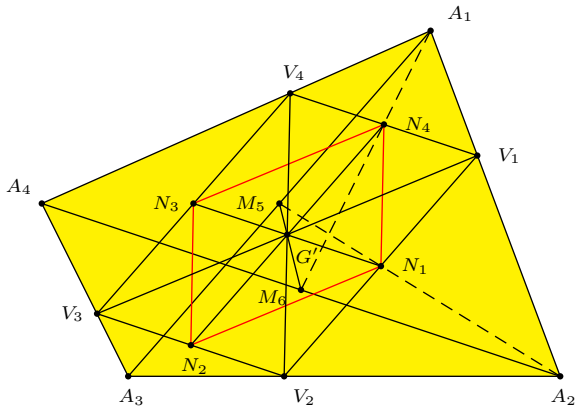

Figure 2.

The triangles $A_1A_2A_3$ and $V_1A_2V_2$ are correspondent in a homothetic transformation with center A_2. It follows that

$$\frac{A_1V_1}{A_1A_2} = \frac{A_3V_2}{A_2A_3}. \tag{1}$$

Moreover, M_5 and N_1 are collinear with A_2. Analogously, M_6 and N_4 are collinear with A_1.

Let G'_1 and G'_2 be the common points of the line M_5M_6 with N_1N_3 and N_2N_4, respectively. Because the triangles $M_5G'_1N_1$ and $M_5M_6A_2$ are similar, as are $V_2A_2N_1$ and $A_3A_2M_5$, we have

$$\frac{M_5G'_1}{M_5M_6} = \frac{M_5N_1}{M_5A_2} = \frac{A_3V_2}{A_2A_3}. \tag{2}$$

Analogously, because the triangles $M_6G_2'N_4$ and $M_5M_6A_1$ are similar, as are $A_1V_1N_4$ and $A_1A_2M_6$, we have

$$\frac{M_5G_2'}{M_5M_6} = \frac{A_1N_4}{A_1M_6} = \frac{A_1V_1}{A_1A_2}. \tag{3}$$

From (1), (2) and (3), it follows that $\frac{M_5G_1'}{M_5M_6} = \frac{M_5G_2'}{M_5M_6}$. Hence, $G_1' = G_2' = G'$, and G' lies on the bimedian M_5M_6.

Conversely, fix a point P on the bimedian M_5M_6. Let N_1 be the common point to the line A_2M_5 with the parallel line to A_2A_4 passing through P. Let V_1 be the common point to the line A_1A_2 with the parallel line to A_1A_3 passing through N_1. V_1 detectS a v-parallelogram $\mathbf{V}$ that has P as common point of its diagonals. □

2. Valtitudes

Let $\mathbf{V}$ be a v-parallelogram of $\mathbf{Q}$ and H_i be the foot of the perpendicular to $A_{i+2}A_{i+3}$ from V_i. The quadrilateral $H_1H_2H_3H_4$ is called the *orthic quadrilateral* of $\mathbf{Q}$ [6], and we will denote it by $\mathbf{H}$. The lines V_iH_i are called the *valtitudes* of $\mathbf{Q}$ with respect to $\mathbf{V}$ (see Figure 3).

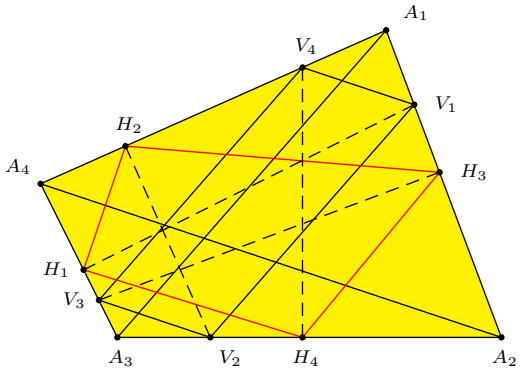

Figure 3.

In the following the valtitude V_iH_i will be denoted by h_i. Observe that $\mathbf{H}$ can be a convex, concave, or crossed quadrilateral. If $\mathbf{V}$ is the Varignon parallelogram, the quadrilateral $\mathbf{H}$ is called the *principal orthic quadrilateral* of $\mathbf{Q}$ and the lines M_iH_i are the maltitudes of $\mathbf{Q}$.

Given a v-parallelogram $\mathbf{V}$, *if the valtitudes of* $\mathbf{Q}$ *with respect to* $\mathbf{V}$ *are concurrent, then* $\mathbf{Q}$ *is cyclic or orthodiagonal* [7]. Moreover, *if* $\mathbf{Q}$ *is cyclic or orthodiagonal, there is only one v-parallelogram* $\mathbf{V}^*$ *with respect to which the valtitudes are concurrent*. Precisely,

(a) If $\mathbf{Q}$ is cyclic, $\mathbf{V}^*$ is the Varignon parallelogram of $\mathbf{Q}$ and then the valtitudes that are concurrent are the maltitudes of $\mathbf{Q}$; moreover the concurrency point of the maltitudes is the anticenter H of $\mathbf{Q}$; H is the symmetric of the circumcenter O with respect to the centroid G of $\mathbf{Q}$ and the line containing the three points H, O and G is the Euler line of $\mathbf{Q}$ (see Figure 4).

The line through the midpoint M_5 of the diagonal A_1A_3 of $\mathbf{Q}$ perpendicular to the diagonal A_2A_4 and the line through the midpoint M_6 of A_2A_4 perpendicular

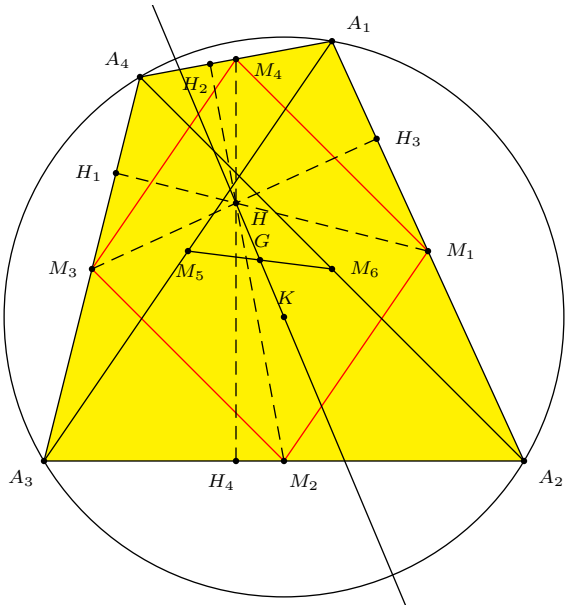

Figure 4.

to A_1A_3 are concurrent in H [6]. Observe that G is the midpoint of the segments OH and M_5M_6, then the quadrilateral OM_5HM_6 is a parallelogram with G as the common point to the diagonals.

(b) If $\mathbf{Q}$ is orthodiagonal, $\mathbf{V}^*$ is the v-parallelogram detected from the perpendiculars to the sides of $\mathbf{Q}$ through the common point K of the diagonals of $\mathbf{Q}$, that is then the concurrency point of the valtitudes (see Figure 5).

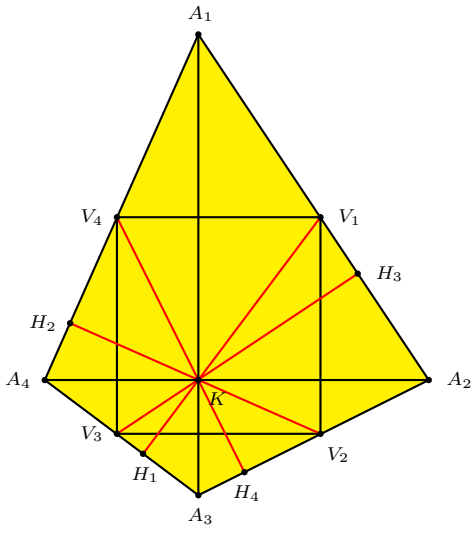

Figure 5.

3. Vaxes

Let $\mathbf{Q}$ be a convex quadrilateral and $\mathbf{V}$ a v-parallelogram of $\mathbf{Q}$.

We call the *vaxis* relative to the side A_iA_{i+1} the perpendicular to A_iA_{i+1} through V_i and denote it by k_i.

Theorem 2. *If $\mathbf{V}$ is a v-parallelogram of $\mathbf{Q}$ and G' is the common point of the diagonals of $\mathbf{V}$, in the symmetry with center G' the valtitudes relative to $\mathbf{V}$ correspond with the vaxes relative to $\mathbf{V}$.*

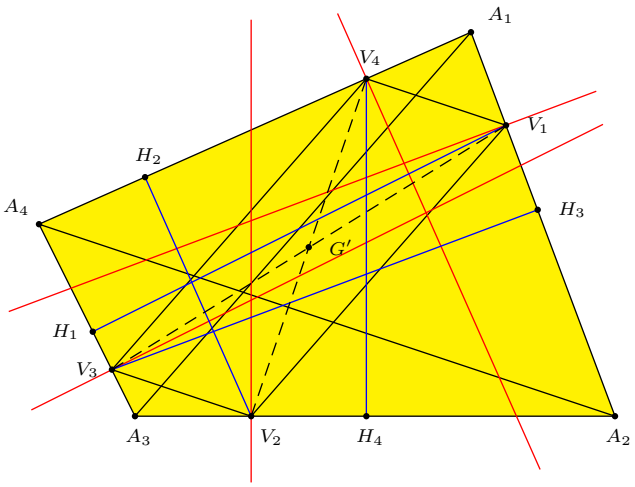

Figure 6.

Proof. In fact, V_i and V_{i+2} are symmetric with respect to G' (see Figure 6). Then the vaxis k_i and the line parallel to it passing through V_{i+2}, *i.e.*, the valtitude h_{i+2}, are correspondent in the symmetry with center G'. □

From Theorem 2 it follows that given a v-parallelogram $\mathbf{V}$, *the vaxes of $\mathbf{Q}$ relative to $\mathbf{V}$ are concurrent if and only if the valtitudes of $\mathbf{Q}$ relative to $\mathbf{V}$ are concurrent*.

Then, from the concurrency properties of valtitudes, it follows that *if the vaxes are concurrent, then $\mathbf{Q}$ is cyclic or orthodiagonal*. Moreover, *if $\mathbf{Q}$ is cyclic or orthodiagonal, there is only one v-parallelogram $\mathbf{V}^*$ such that the valtitudes relative to it are concurrent*. Precisely,

(a) If $\mathbf{Q}$ is cyclic, $\mathbf{V}^*$ is the Varignon parallelogram of $\mathbf{Q}$, and the vaxes that are concurrent are the axes of $\mathbf{Q}$ and the concurrency point is the circumcenter O of $\mathbf{Q}$.

(b) If $\mathbf{Q}$ is orthodiagonal, $\mathbf{V}^*$ is the v-parallelogram detected by the perpendiculars to the sides of $\mathbf{Q}$ through the common point K of the diagonals of $\mathbf{Q}$ and the concurrency point of the vaxes is the point K' symmetric of K with respect to G' (see Figure 7).

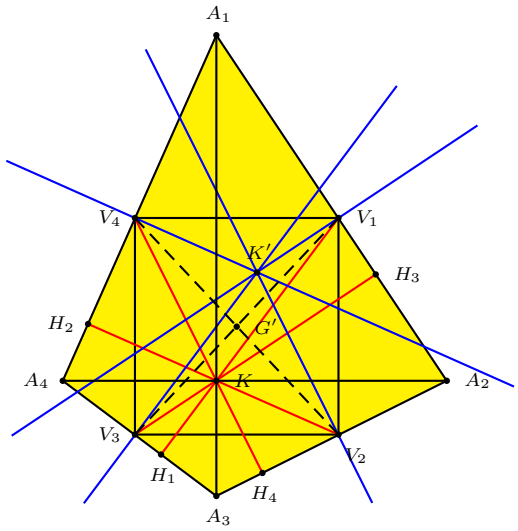

Figure 7.

4. The quadrilateral of valtitudes and the quadrilateral of vaxes

Let $\mathbf{Q}$ be a convex quadrilateral and $\mathbf{V}$ a v-parallelogram of $\mathbf{Q}$.

Let B_i be the common point to the valtitudes h_i and h_{i+1}. We call $B_1B_2B_3B_4$ the *quadrilateral of the valtitudes* and denote it by $\mathbf{Q}_h$.

Let C_i be the common point of the vaxes k_i and k_{i+1}. We call $C_1C_2C_3C_4$ the *quadrilateral of the vaxes* and denote it by $\mathbf{Q}_k$ (see Figure 8).

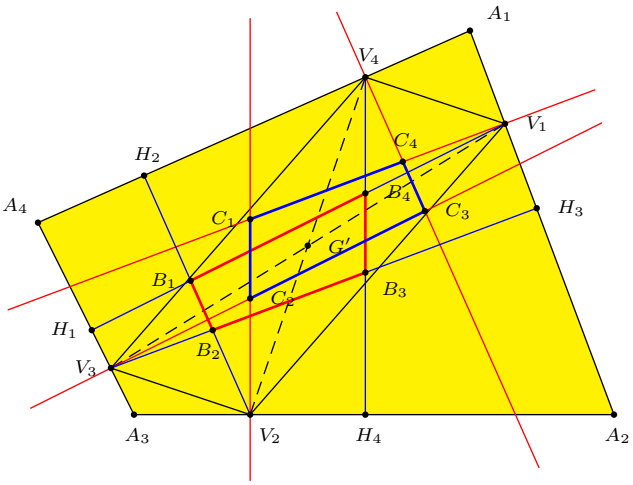

Figure 8.

If $\mathbf{V}$ is the Varignon parallelogram, the lines h_i are the maltitudes and $\mathbf{Q}_h$ is called the *quadrilateral of the maltitudes* of $\mathbf{Q}$ [4]. The lines k_i are the axes of $\mathbf{Q}$, C_i is the circumcenter of the triangle $A_iA_{i+1}A_{i+2}$ and $\mathbf{Q}_k$ is called the *quadrilateral of the circumcenters* of $\mathbf{Q}$ [4]. Observe that when $\mathbf{V}$ is the Varignon parallelogram, if $\mathbf{Q}$ is cyclic, then $\mathbf{Q}_h$ and $\mathbf{Q}_k$ are reduced to a point.

The theorem below follows from Theorem 2.

Theorem 3. *If* $\mathbf{V}$ *is a v-parallelogram of* $\mathbf{Q}$ *and* G' *is the common point of the diagonals of* $\mathbf{V}$*, the quadrilateral of the vaxes and the quadrilateral of the valtitudes are symmetric with respect to* G'*.*

Proof. In fact, the valtitude h_{i+2} is the correspondent of the vaxis k_i in the symmetry with center G', and the point B_{i+2} is the correspondent of the point C_i. □

Corollary 4 ([4, p.474])**.** *If* $\mathbf{V}$ *is the Varignon parallelogram of* $\mathbf{Q}$*, the quadrilateral of the circumcenters and the quadrilateral of the maltitudes are symmetric with respect to the centroid* G *of* $\mathbf{Q}$*.*

Let K and K' be the common points of the diagonals of $\mathbf{Q}$ and of $\mathbf{Q}_k$ respectively.

Lemma 5. *If* $\mathbf{Q}$ *is orthodiagonal, the triangles* $A_iA_{i+1}K$ *and* $C_iC_{i+3}K'$*,* $(i = 1, 2, 3, 4)$ *are similar.*

Proof. Since $\mathbf{Q}$ is orthodiagonal, the vertices B_i of $\mathbf{Q}_h$ lie on the diagonals of $\mathbf{Q}$ [6]. The diagonals of $\mathbf{Q}_h$ and those of $\mathbf{Q}$ lie on the same lines (see Figure 9). It follows that $\mathbf{Q}_h$ is orthodiagonal. Then, by Theorem 3, $\mathbf{Q}_k$ is orthodiagonal as well, and the diagonals of $\mathbf{Q}_k$ are parallel to those of $\mathbf{Q}$. Then, the lines C_1C_3 and C_2C_4 are perpendicular to the lines A_1A_3 and A_2A_4 respectively. Moreover, the line C_1C_4 is perpendicular to A_1A_2. Therefore, the triangles A_1A_2K and C_1C_4K' are similar, because they have equal angles. Analogously, the similarlity of each of the pairs A_2A_3K, C_2C_1K'; A_3A_4K, C_3C_2K'; and A_4A_1K, C_4C_3K' can be established. □

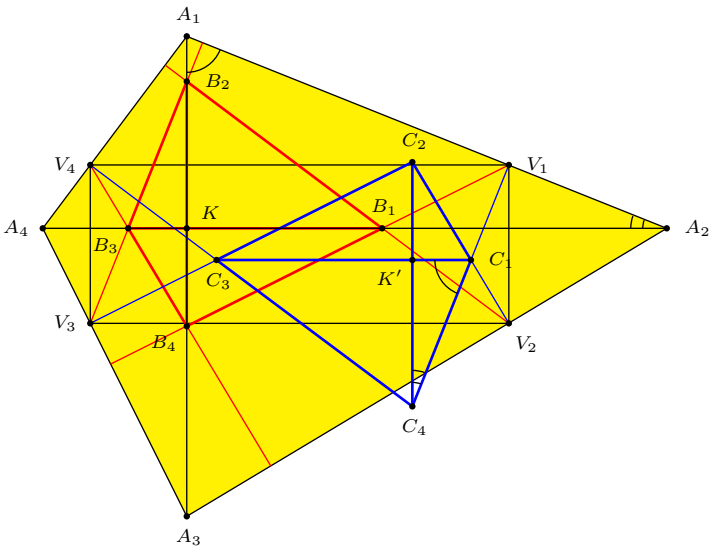

Figure 9.

Let us make some preliminary remarks.

For the two ratios $\frac{A_1K}{KA_3}$ and $\frac{A_3K}{KA_1}$ let r be the one not greater than 1. Also, for the two ratios $\frac{A_2K}{KA_4}$ and $\frac{A_4K}{KA_2}$, let r' be the one not greater than 1. The pair $\{r, r'\}$ is called the characteristic of $\mathbf{Q}$. In [3] it was proved that two quadrilaterals are affine if and only if they have the same characteristic.

Theorem 6. *If* $\mathbf{Q}$ *is orthodiagonal and* $\mathbf{V}$ *is a v-parallelogram of* $\mathbf{Q}$*, the quadrilateral of the vaxes and the quadrilateral of the valtitudes are affine to* $\mathbf{Q}$*.*

Proof. From Lemma 5, we have

$$\frac{A_1K}{A_2K} = \frac{C_1K'}{C_4K'}, \tag{4}$$

$$\frac{A_2K}{A_3K} = \frac{C_2K'}{C_1K'}, \tag{5}$$

$$\frac{A_3K}{A_4K} = \frac{C_3K'}{C_2K'}. \tag{6}$$

By multiplying (4) and (5), and also (5) and (6), we obtain:

$$\frac{A_1K}{A_3K} = \frac{C_2K'}{C_4K'},$$

$$\frac{A_2K}{A_4K} = \frac{C_3K'}{C_1K'}.$$

Thus the quadrilaterals $\mathbf{Q}$ and $\mathbf{Q}_k$ have the same characteristic, and therefore are affine. From theorem 3, also $\mathbf{Q}_h$ is affine to $\mathbf{Q}$. □

Lemma 7. *If* $\mathbf{Q}$ *is cyclic, the angles of* $\mathbf{Q}_k$ *are equal to those of* $\mathbf{Q}$*. Precisely,* $\angle C_iC_{i+1}C_{i+2} = \angle A_{i-1}A_iA_{i+1}$ *(i=1,2,3,4).*

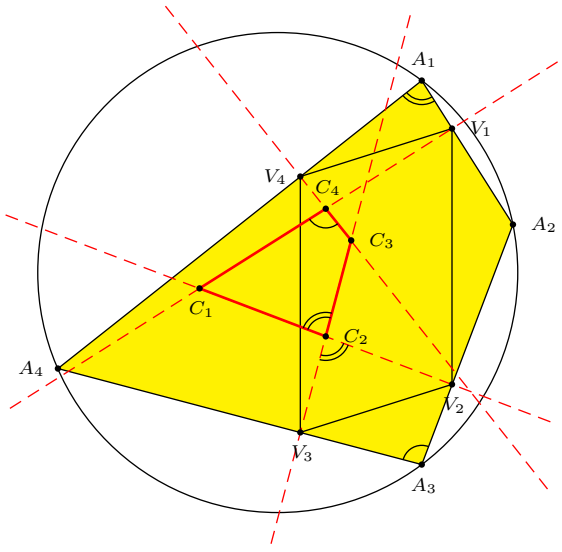

Figure 10.

Proof. Let us prove that $\angle C_1C_2C_3 = \angle A_4A_1A_2$ (see Figure 10). The other cases can be established analogously. Since $\mathbf{Q}$ is cyclic, $\angle A_4A_1A_2$ and $\angle A_2A_3A_4$ are supplementary angles. Moreover, the angles at V_2 and V_4 of the quadrilateral $V_3C_2V_2A_3$ are right angles. Therefore, $\angle C_1C_2C_3$ and $\angle A_2A_3A_4$ are supplementary angles. It follows that $\angle C_1C_2C_3 = \angle A_4A_1A_2$. □

Theorem 8. *If* $\mathbf{Q}$ *is cyclic, then the quadrilateral of the vaxes and the quadrilateral of the valtitudes are cyclic.*

Proof. Since $\mathbf{Q}$ is cyclic, $\angle A_4A_1A_2$ and $\angle A_2A_3A_4$ are supplementary angles. Therefore, from Lemma 7, $\angle C_1C_2C_3$ and $\angle C_1C_4C_2$ are supplementary angles. Then, $\mathbf{Q}_k$ is cyclic and, from Theorem 3, $\mathbf{Q}_h$ is cyclic as well. □

Theorem 9. *If* $\mathbf{Q}$ *is cyclic and orthodiagonal and* $\mathbf{V}$ *is a v-parallelogram of* $\mathbf{Q}$*, the quadrilateral of the vaxes and the quadrilateral of the valtitudes are similar to* $\mathbf{Q}$*.*

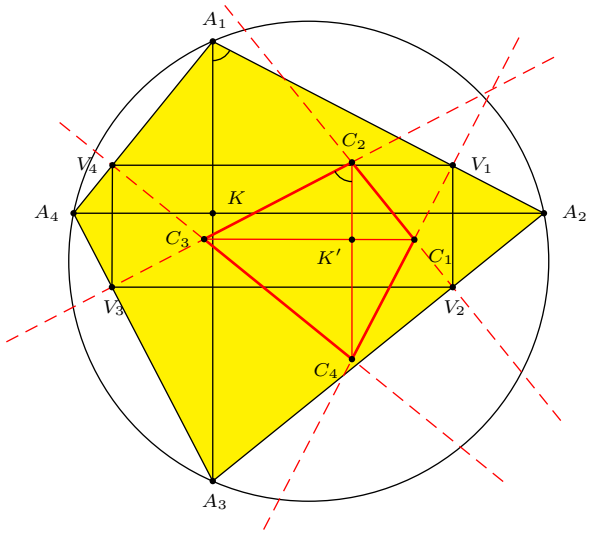

Figure 11.

Proof. From Lemma 7, $\mathbf{Q}$ and $\mathbf{Q}_k$ have equal angles. Let us prove now that the sides of $\mathbf{Q}$ are proportional to those of $\mathbf{Q}_k$. Consider the triangles $A_1A_2A_3$ and $C_2C_3C_4$ (see Figure 11). From Lemma 5 the triangles A_1A_2K and C_2C_3K' are similar, and $\angle KA_1A_2 = \angle K'C_2C_3$. Since, from Lemma 7, $\angle A_1A_2A_3 = \angle C_2C_3C_4$, the triangles $A_1A_2A_3$ and $C_2C_3C_4$ are similar.

Analogously, the similarity of each of the following pairs of triangles can be established: $A_2A_3A_4$, $C_3C_4C_1$; $A_3A_4A_1$, $C_4C_1C_2$; and $A_4A_1A_2$, $C_1C_2C_3$. It follows that

$$\frac{A_1A_2}{C_2C_3} = \frac{A_2A_3}{C_3C_4} = \frac{A_3A_4}{C_4C_1} = \frac{A_4A_1}{C_1C_2},$$

and the sides of $\mathbf{Q}$ are proportional to those of $\mathbf{Q}_k$.

Therefore, $\mathbf{Q}_k$ is similar to $\mathbf{Q}$, and from Theorem 3, $\mathbf{Q}_h$ is also similar to $\mathbf{Q}$. □

Lemma 10. *If* $\mathbf{V}$ *is a v-parallelogram of* $\mathbf{Q}$ *and* M_i *is the midpoint of the side* A_iA_{i+1} *of* $\mathbf{Q}$ $(i = 1, 2, 3, 4)$*, then*

$$\frac{A_1V_1}{A_1M_1} = \frac{A_1V_4}{A_1M_4} = \frac{A_3V_2}{A_3M_2} = \frac{A_3V_3}{A_3M_3}, \tag{7}$$

$$\frac{A_2V_1}{A_2M_1} = \frac{A_2V_2}{A_2M_2} = \frac{A_4V_3}{A_4M_3} = \frac{A_4V_4}{A_4M_4}. \tag{8}$$

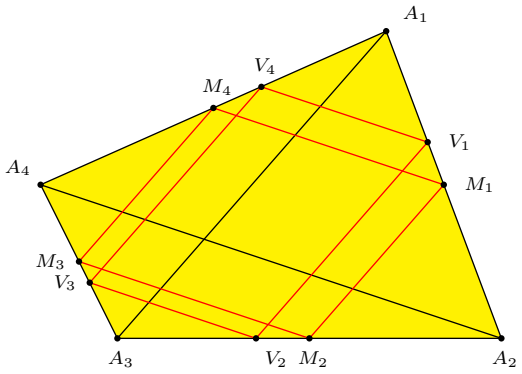

Figure 12.

Proof. In fact, since the triangles $A_1V_1V_4$ and $A_1M_1M_4$ are similar, as are triangles $A_3V_2V_3$ and $A_3M_2M_3$ (see Figure 12), we have

$$\frac{A_1V_1}{A_1M_1} = \frac{A_1V_4}{A_1M_4} = \frac{V_1V_4}{M_1M_4}, \qquad \frac{A_3V_2}{A_3M_2} = \frac{A_3V_3}{A_3M_3} = \frac{V_2V_3}{M_2M_3}.$$

Since $V_1V_4 = V_2V_3$ and $M_1M_4 = M_2M_3$, (7) holds.

Analogously, since the triangles $A_2V_1V_2$ and $A_2M_1M_2$ are similar, as are $A_4V_3V_4$ and $A_4M_3M_4$, (8) also holds. □

Theorem 11. *If* $\mathbf{Q}$ *is cyclic, the diagonals of the quadrilateral of the vaxes and those of the quadrilateral of the valtitudes are parallel to the diagonals of* $\mathbf{Q}$.

Proof. Let O be the circumcenter of $\mathbf{Q}$ (see Figure 13). Let C_4' and C_4'' be the common points of the line A_1O with the vaxes k_1 and k_4 respectively. Since the triangles $A_1V_1C_4'$ and A_1M_1O are similar, as are triangles $A_1V_4C_4''$ and A_1M_4O, we have

$$\frac{A_1V_1}{A_1M_1} = \frac{A_1C_4'}{A_1O}, \qquad \frac{A_1V_4}{A_1M_4} = \frac{A_1C_4''}{A_1O}.$$

From (7), we have $\frac{A_1C_4'}{A_1O} = \frac{A_1C_4''}{A_1O}$. Therefore, $C_4'' = C_4' = C_4$, and C_4 lies on the line A_1O. Moreover,

$$\frac{A_1C_4}{A_1O} = \frac{A_1V_1}{A_1M_1} = \frac{A_1V_4}{A_1M_4}. \tag{9}$$

Analogously, it is possible to prove that C_2 lies on the line A_3O and

$$\frac{A_3C_2}{A_3O} = \frac{A_3V_2}{A_3M_2} = \frac{A_3V_3}{A_3M_3}. \tag{10}$$

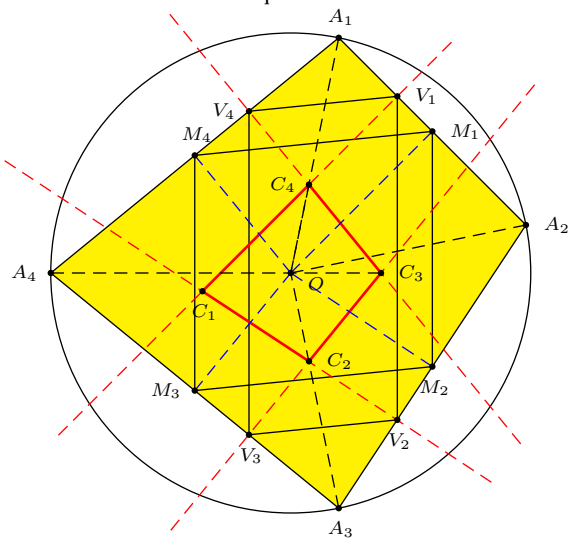

Figure 13.

From (9), (7) and (10), it follows that

$$\frac{A_1C_4}{A_1O} = \frac{A_3C_2}{A_3O}.$$

Thus, the triangles OC_2C_4 and OA_1A_3 are similar, and the diagonal C_2C_4 of $\mathbf{Q}_k$ is parallel to the diagonal A_1A_3 of $\mathbf{Q}$.

Analogously, by using (8), it is possible to prove that the triangles OC_1C_3 and OA_2A_4 are similar, and the diagonal C_1C_3 of $\mathbf{Q}_k$ is parallel to the diagonal A_2A_4 of $\mathbf{Q}$. Since, from Theorem 3, $\mathbf{Q}_k$ and $\mathbf{Q}_h$ are symmetric with respect to a point, the diagonals of $\mathbf{Q}_h$ are parallel to the diagonals of $\mathbf{Q}_k$ and thus they are parallel to the diagonals of $\mathbf{Q}$. □

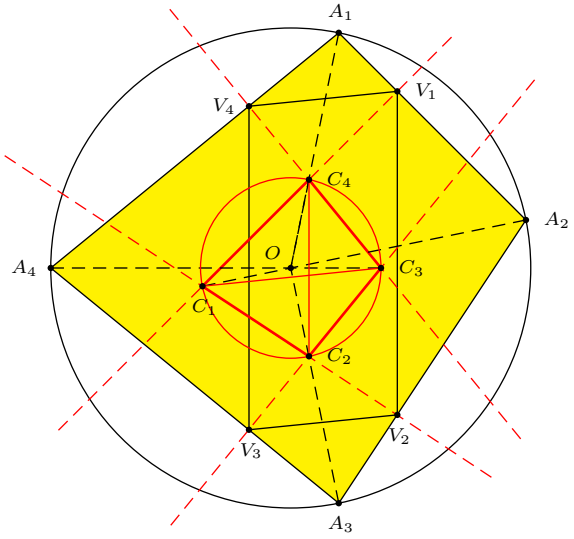

Figure 14.

Theorem 12. *If* $\mathbf{Q}$ *is cyclic and* $\mathbf{V}$ *is a v-parallelogram of* $\mathbf{Q}$*, the quadrilateral of the vaxes relative to* $\mathbf{V}$ *has the same circumcenter of* $\mathbf{Q}$*.*

Proof. From Theorem 8, $\mathbf{Q}_k$ is cyclic. The axes of segments C_2C_4 and C_1C_3 meet at the circumcenter of $\mathbf{Q}_k$. The triangles OC_2C_4 and OA_1A_3 are correspondent in a homothetic transformation with center the circumcenter O of $\mathbf{Q}$, because, from theorem 11, the lines C_2C_4 and A_1A_3 are parallel (see Figure 14). It follows that the axes of segments C_2C_4 and A_1A_3 coincide. Analogously, the axes of segments C_1C_3 and A_2A_4 coincide. Then it follows that O is the circumcenter of $\mathbf{Q}_k$. □

Theorem 13. *If* $\mathbf{Q}$ *is cyclic, all the quadrilaterals of the vaxes of* $\mathbf{Q}$ *have the same Euler line.*

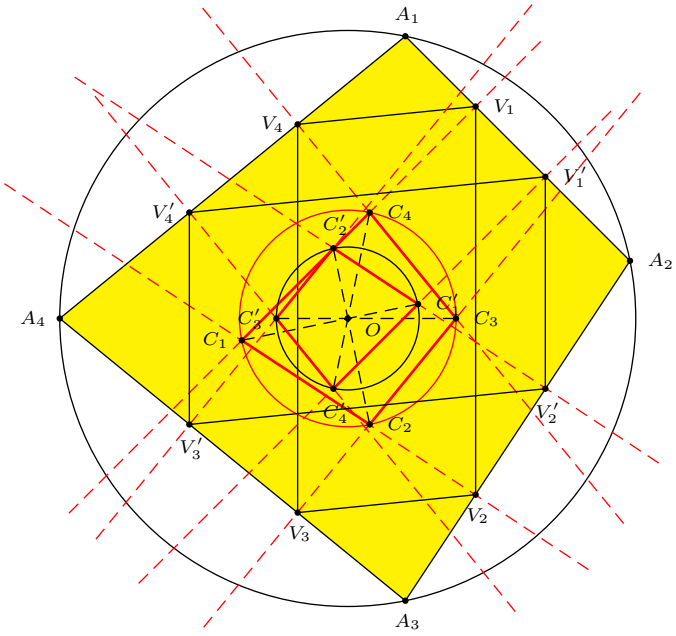

Figure 15.

Proof. Consider two v-parallelograms $\mathbf{V}$ and $\mathbf{V}'$ and their quadrilaterals of the vaxes $\mathbf{Q}_k$ and $\mathbf{Q}_k'$ respectively (see Figure 15). The vertices C_i and C_i' of $\mathbf{Q}_k$ and $\mathbf{Q}_k'$ respectively lie on the line OA_{i+1}, and the ratio between OC_i and OC_i' is equal to the ratio between the circumradii of $\mathbf{Q}_k$ and $\mathbf{Q}_k'$. Then, $\mathbf{Q}_k$ and $\mathbf{Q}_k'$ are correspondent in a homothetic transformation with center O. From Theorem 12, the Euler line of $\mathbf{Q}_k$ passes through O, therefore it is fixed in the homothetic transformation. It follows that $\mathbf{Q}_k$ and $\mathbf{Q}_k'$ have the same Euler line. □

We call the *k-line* of $\mathbf{Q}$ (cyclic) the Euler line of all the quadrilaterals of the vaxes of $\mathbf{Q}$.

Theorem 14. *If* $\mathbf{Q}$ *is cyclic and* $\mathbf{V}$ *is a v-parallelogram of* $\mathbf{Q}$*, the quadrilateral of the valtitudes relative to* $\mathbf{V}$ *has the same anticenter of* $\mathbf{Q}$*.*

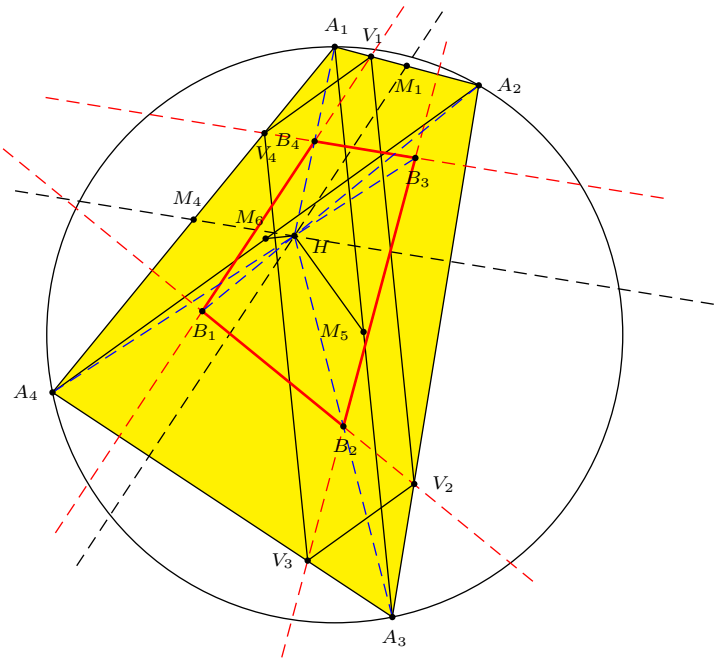

Figure 16.

Proof. Let H be the anticenter of $\mathbf{Q}$. Let B_4' and B_4'' be the common points of the line A_1H with the valtitudes h_1 and h_4, respectively (see Figure 16).

Since the triangles $A_1V_1B_4'$ and A_1M_1H are similar, as are $A_1V_4B_4''$ and A_1M_4H, we have

$$\frac{A_1V_1}{A_1M_1} = \frac{A_1B_4'}{A_1H}, \qquad \frac{A_1V_4}{A_1M_4} = \frac{A_1B_4''}{A_1H}.$$

From (7) it follows that

$$\frac{A_1B_4'}{A_1H} = \frac{A_1B_4''}{A_1H}.$$

Therefore, $B_4' = B_4'' = B_4$ and B_4 lies on the line A_1H. Analogously it is possible to prove that B_2 lies on the line A_3H.

Now consider the third bimedian M_5M_6 of $\mathbf{Q}$, with M_5 and M_6 the midpoints of the diagonals A_1A_3 and A_2A_4 of $\mathbf{Q}$ respectively. Let h_5 be the perpendicular to the line A_2A_4 through the point M_5 and let h_6 be the perpendicular to the line A_1A_3 through M_6. The lines h_5 and h_6 pass through H (see §2). The triangles HB_2B_4 and HA_1A_3 are correspondent in a homothetic transformation with center H, because, from Theorem 11, B_2B_4 and A_1A_3 are parallel. It follows that h_5 passes through the midpoint of B_2B_4 and it is perpendicular to B_1B_3, then it passes through the anticenter of $\mathbf{Q}_h$. Analogously, h_6 passes through the anticenter of $\mathbf{Q}_h$ as well, then H is the anticenter of $\mathbf{Q}_h$. □

Theorem 15. *If* $\mathbf{Q}$ *is cyclic, all the quadrilaterals of the valtitudes of* $\mathbf{Q}$ *have the same Euler line.*

Proof. Given a v-parallelogram $\mathbf{V}$ and the quadrilaterals $\mathbf{Q}_k$ and $\mathbf{Q}_h$ relative to it, from Theorem 3, the Euler line of $\mathbf{Q}_h$ is the symmetric of the Euler line of $\mathbf{Q}_k$ with respect to the point G', common point to the diagonals of $\mathbf{V}$. Then, the theorem follows from Theorem 13. □

We call the *h-line* of $\mathbf{Q}$ (cyclic) the Euler line of all the quadrilaterals of the valtitudes of $\mathbf{Q}$.

Theorem 16. *If* $\mathbf{Q}$ *is cyclic, the h-line and the k-line of* $\mathbf{Q}$ *are parallel and are symmetric with respect to the line containing the third bimedian of* $\mathbf{Q}$.

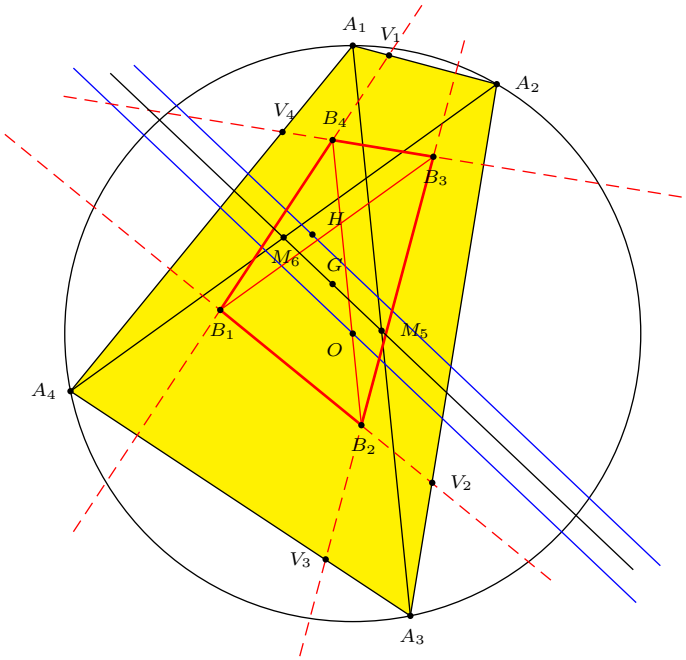

Figure 17.

Proof. From Theorems 3, 13 and 15 it follows that the h-line and the k-line of $\mathbf{Q}$ are symmetric with respect to G', common point of the diagonals of any v-parallelogram of $\mathbf{Q}$. Therefore, in particular, they are parallel. Moreover, from Theorem 1, the points G' lie on the third bimedian of $\mathbf{Q}$, then the h-line and the k-line of $\mathbf{Q}$ are symmetric with respect to the line containing the third bimedian of $\mathbf{Q}$ (see Figure 17). □

References

[1] H. S. M. Coxeter and S. L. Greitzer, *Geometry Revisited*, Washington, DC: Math. Assoc., 1967.
[2] R. Honsbergher, *Episodes in Nineteenth and Twentieth Century Euclidean Geometry*, Washington, DC: Math. Assoc. Amer., 1995.
[3] C. Mammana and B. Micale, Una classificazione affine dei quadrilateri, *La Matematica e la sua Didattica*, 3 (1999) 323–328.
[4] M. F. Mammana and B. Micale, Quadrilaterals of triangle centres, *Math. Gazette*, 92 (2008) 466-475.

[5] M. F. Mammana, B. Micale, and M. Pennisi, Quadrilaterals and tetrahedra, *Int. J. Math. Educ. Sci. Technol.*, 40 (2009) 818–828.
[6] M. F. Mammana, B. Micale, and M. Pennisi, Orthic quadrilaterals of a convex quadrilateral, *Forum Geom.*, 10 (2010) 79–91.
[7] B. Micale and M. Pennisi, On the Altitudes of Quadrilaterals, *Int. J. Math. Educ. Sci. Technol.*, 36 (2005) 15–24.
[8] M. De Villiers, Generalizations involving maltitudes, *Int. J. Math. Educ. Sci. Technol.*, 30 (1999) 541–548.
[9] P. Yiu, Notes on Euclidean Geometry, Florida Atlantic University Lecture Notes, 1998; available at `http:www.math.fau.edu/Yiu/EuclideanGeometryNotes.pdf`.

Maria Flavia Mammana: Department of Mathematics and Computer Science, University of Catania, Viale A. Doria 6, 95125, Catania, Italy
E-mail address: `fmammana@dmi.unict.it`

Biagio Micale: Department of Mathematics and Computer Science, University of Catania, Viale A. Doria 6, 95125, Catania, Italy
E-mail address: `micale@dmi.unict.it`

Mario Pennisi: Department of Mathematics and Computer Science, University of Catania, Viale A. Doria 6, 95125, Catania, Italy
E-mail address: `pennisi@dmi.unict.it`

Forum Geometricorum
Volume 12 (2012) 63–77.

FORUM GEOM
ISSN 1534-1178

Similar Metric Characterizations of Tangential and Extangential Quadrilaterals

Martin Josefsson

Abstract. We prove five necessary and sufficient conditions for a convex quadrilateral to have an excircle and compare them to similar conditions for a quadrilateral to have an incircle.

1. Introduction

There are a lot of more or less well known characterizations of tangential quadrilaterals,[1] that is, convex quadrilaterals with an incircle. This circle is tangent at the inside of the quadrilateral to all four sides. Many of these necessary and sufficient conditions were either proved or reviewed in [8]. In this paper we shall see that there are a few very similar looking characterizations for a convex quadrilateral to have an *excircle*. This is a circle that is tangent at the outside of the quadrilateral to the extensions of all four sides. Such a quadrilateral is called an *extangential quadrilateral* in [13, p.44],[2] see Figure 1.

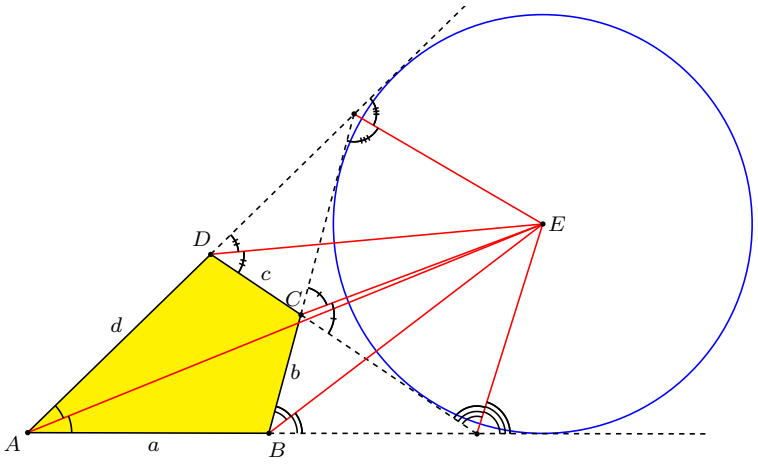

Figure 1. An extangential quadrilateral and its excircle

We start by reviewing and commenting on the known characterizations of extangential quadrilaterals and the similar ones for tangential quadrilaterals. It is well known that a convex quadrilateral is tangential if and only if the four internal angle

Publication Date: April 4, 2012. Communicating Editor: Paul Yiu.
[1]Another common name for these is circumscribed quadrilateral.
[2]Alexander Bogomolny calls them exscriptible quadrilateral at [2].

bisectors to the vertex angles are concurrent. Their common point is the incenter, that is, the center of the incircle. A convex quadrilateral is extangential if and only if six angles bisectors are concurrent, which are the internal angle bisectors at two opposite vertex angles, the external angle bisectors at the other two vertex angles, and the external angle bisectors at the angles formed where the extensions of opposite sides intersect. Their common point is the excenter (E in Figure 1).

The most well known and useful characterization of tangential quadrilaterals is the Pitot theorem, that a convex quadrilateral with sides a, b, c, d has an incircle if and only if opposite sides have equal sums,

$$a + c = b + d.$$

For the existence of an excircle, the similar characterization states that the adjacent sides shall have equal sums. This is possible in two different ways. There can only be one excircle to a quadrilateral, and the characterization depends on which pair of opposite vertices the excircle is outside of. It is easy to realize that it must be outside the vertex (of the two considered) with the biggest angle.[3] A convex quadrilateral $ABCD$ has an excircle outside one of the vertices A or C if and only if

$$a + b = c + d \tag{1}$$

according to [2] and [10, p.69]. This was proved by the Swiss mathematician Jakob Steiner (1796–1863) in 1846 (see [3, p.318]). By symmetry ($b \leftrightarrow d$), there is an excircle outside one of the vertices B or D if and only if

$$a + d = b + c. \tag{2}$$

From (1) and (2), we have that a convex quadrilateral with sides a, b, c, d has an excircle if and only if

$$|a - c| = |b - d|$$

which resembles the Pitot theorem. There is however one exception to these characterizations. The existence of an excircle is dependent on the fact that the extensions of opposite sides in the quadrilateral intersect, otherwise the circle can never be tangent to all four extensions. Therefore there is no excircle to either of a trapezoid, a parallelogram, a rhombus, a rectangle or a square even though (1) or (2) is satisfied in many of them, since they have at least one pair of opposite parallel sides.[4]

In [8, p.66] we reviewed two characterizations of tangential quadrilaterals regarding the extensions of the four sides. Let us take another look at them here. If $ABCD$ is a convex quadrilateral where opposite sides AB and CD intersect at E, and the sides AD and BC intersect at F (see Figure 2), then $ABCD$ is a tangential quadrilateral if and only if either of the following conditions holds:

$$AE + CF = AF + CE, \tag{3}$$

$$BE + BF = DE + DF. \tag{4}$$

[3] Otherwise the circle can never be tangent to all four extensions.

[4] The last four of these quadrilaterals can be considered to be extangential quadrilaterals with infinite exradius, see Theorem 8.

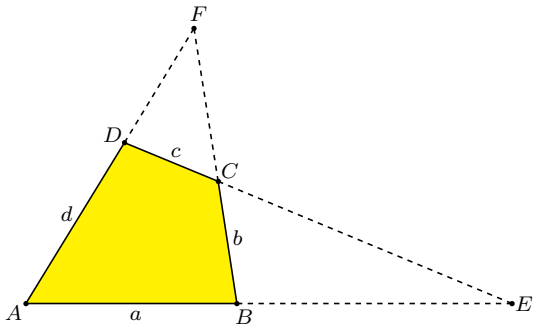

Figure 2. The extensions of the sides

The history of these conditions are discussed in [14] together with the corresponding conditions for extangential quadrilaterals. In our notations, $ABCD$ has an excircle outside one of the vertices A or C if and only if either of the following conditions holds:

$$AE + CE = AF + CF, \tag{5}$$

$$BE + DE = BF + DF. \tag{6}$$

These conditions were stated somewhat differently in [14] with other notations. Also, there it was not stated that the excircle can be outside A instead of C, but that is simply a matter of making the change $A \leftrightarrow C$ in (5) to see that the condition is unchanged. How about an excircle outside of B or D? By making the changes $A \leftrightarrow D$ and $B \leftrightarrow C$ (to preserve that AB and CD intersect at E) we find that the conditions (5) and (6) are still the same. According to [14], conditions (3) and (5) were proved by Jakob Steiner in 1846. In 1973, Howard Grossman (see [5]) contributed with the two additional conditions (4) and (6).

From a different point of view, (3) and (5) can be considered to be necessary and sufficient conditions for when a *concave* quadrilateral $AECF$ has an "incircle" (a circle tangent to two adjacent sides and the extensions of the other two) or an excircle respectively. Then (4) and (6) are necessary and sufficient conditions for a *complex* quadrilateral $BEDF$ to have an excircle.[5]

Another related theorem is due to the Australian mathematician M. L. Urquhart (1902–1966). He considered it to be "the most elementary theorem of Euclidean geometry". It was originally stated using only four intersecting lines. We restate it in the framework of a convex quadrilateral $ABCD$, where opposite sides intersect at E and F, see Figure 2. Urquhart's theorem states that if $AB+BC = AD+DC$, then $AE + EC = AF + FC$. In 1976 Dan Pedoe wrote about this theorem (see [12]), where he concluded that the proof by purely geometrical methods is not elementary and that he had been trying to find such a proof that did not involve a circle (the excircle to the quadrilateral). Later that year, Dan Sokolowsky took up

[5]Equations (4) and (6) can then be merged into one as $|BE - DF| = |BF - DE|$.

that challenge and gave an elementary "no-circle" proof in [15]. In 2006, Mowaffaq Hajja gave a simple trigonometric proof (see [6]) that the two equations in Urquhart's theorem are equivalent. According to (1) and (5), they are both characterizations of an extangential quadrilateral $ABCD$.

2. Characterizations with subtriangle circumradii

In [9, pp.23–24] we proved that if the diagonals in a convex quadrilateral $ABCD$ intersect at P, then it has an incircle if and only if

$$R_1 + R_3 = R_2 + R_4$$

where R_1, R_2, R_3 and R_4 are the circumradii in the triangles ABP, BCP, CDP and DAP respectively, see Figure 3.

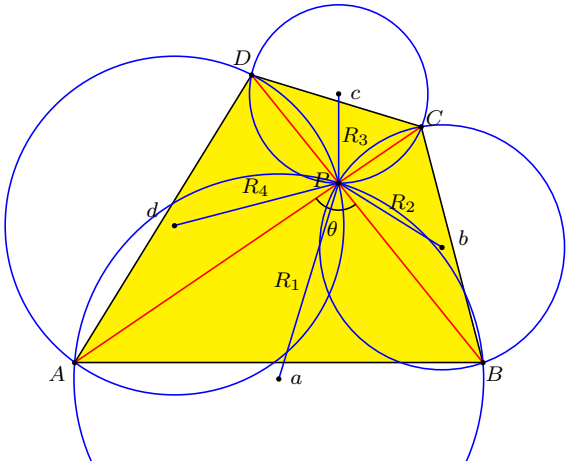

Figure 3. The subtriangle circumcircles

There are the following similar conditions for a quadrilateral to have an excircle.

Theorem 1. *Let R_1, R_2, R_3, R_4 be the circumradii in the triangles ABP, BCP, CDP, DAP respectively in a convex quadrilateral $ABCD$ where the diagonals intersect at P. It has an excircle outside one of the vertices A or C if and only if*

$$R_1 + R_2 = R_3 + R_4$$

and an excircle outside one of the vertices B or D if and only if

$$R_1 + R_4 = R_2 + R_3.$$

Proof. According to the extended law of sines, the sides satisfies $a = 2R_1 \sin\theta$, $b = 2R_2 \sin\theta$, $c = 2R_3 \sin\theta$ and $d = 2R_4 \sin\theta$, where θ is the angle between the diagonals,[6] see Figure 3. Thus

$$a + b - c - d = 2\sin\theta(R_1 + R_2 - R_3 - R_4)$$

[6]We used that $\sin(\pi - \theta) = \sin\theta$ to get two of the formulas.

and

$$a + d - b - c = 2 \sin\theta(R_1 + R_4 - R_2 - R_3).$$

From these we directly get that

$$a + b = c + d \quad \Leftrightarrow \quad R_1 + R_2 = R_3 + R_4$$

and

$$a + d = b + c \quad \Leftrightarrow \quad R_1 + R_4 = R_2 + R_3$$

since $\sin\theta \neq 0$. By (1) and (2) the conclusions follow. □

3. Characterizations concerning the diagonal parts

In [7] Larry Hoehn made a few calculations with the law of cosines to prove that in a convex quadrilateral $ABCD$ with sides a, b, c, d,

$$efgh(a+c+b+d)(a+c-b-d) = (agh+cef+beh+dfg)(agh+cef-beh-dfg)$$

where e, f, g, h are the distances from the vertices A, B, C, D respectively to the diagonal intersection (see Figure 4). Using the Pitot theorem $a + c = b + d$, we get that the quadrilateral is tangential if and only if

$$agh + cef = beh + dfg. \tag{7}$$

Now we shall prove that there are similar characterizations for the quadrilateral to have an excircle.

Theorem 2. *Let e, f, g, h be the distances from the vertices A, B, C, D respectively to the diagonal intersection in a convex quadrilateral $ABCD$ with sides a, b, c, d. It has an excircle outside one of the vertices A or C if and only if*

$$agh + beh = cef + dfg$$

and an excircle outside one of the vertices B or D if and only if

$$agh + dfg = beh + cef.$$

Proof. In [7] Hoehn proved that in a convex quadrilateral,

$$efgh\left(a^2 + c^2 - b^2 - d^2\right) = a^2g^2h^2 + c^2e^2f^2 - b^2e^2h^2 - d^2f^2g^2.$$

Now adding $efgh(-2ac + 2bd)$ to both sides, this is equivalent to

$$efgh\left((a - c)^2 - (b - d)^2\right) = (agh - cef)^2 - (beh - dfg)^2$$

which is factored as

$$efgh(a-c+b-d)(a-c-b+d) = (agh-cef+beh-dfg)(agh-cef-beh+dfg).$$

The left hand side is zero if and only if $a+b = c+d$ or $a+d = b+c$ and the right hand side is zero if and only if $agh+beh = cef+dfg$ or $agh+dfg = beh+cef$.

To show that the first equality from both sides are connected and that the second equality from both sides are also connected, we study a special case. In a kite where $a = d$ and $b = c$ and also $f = h$, the two equalities $a + b = c + d$ and $agh + beh = cef + dfg$ are satisfied, but none of the others. This proves that they

are connected. In the same way, using another kite, the other two are connected and we have that

$$a+b=c+d \quad \Leftrightarrow \quad agh+beh=cef+dfg$$

and

$$a+d=b+c \quad \Leftrightarrow \quad agh+dfg=beh+cef.$$

This completes the proof according to (1) and (2). □

Remark. The characterization (7) had been proved at least three different times before Hoehn did it. It appears as part of a proof of an inverse inradii characterization of tangential quadrilaterals in [16] and [17]. It was also proved in [11, Proposition 2 (e)]. All of the four known proofs used different notations.

4. Characterizations with subtriangle altitudes

In 2009, Nicuşor Minculete gave two different proofs (see [11]) that a convex quadrilateral $ABCD$ has an incircle if and only if the altitudes h_1, h_2, h_3, h_4 from the diagonal intersection P to the sides AB, BC, CD, DA in triangles ABP, BCP, CDP, DAP respectively satisfy

$$\frac{1}{h_1}+\frac{1}{h_3}=\frac{1}{h_2}+\frac{1}{h_4}. \tag{8}$$

This characterization of tangential quadrilaterals had been proved as early as 1995 in Russian by Vasilyev and Senderov [16]. Another Russian proof was given in 2004 by Zaslavsky [18]. To prove that (8) holds in a tangential quadrilateral (i.e. not the converse) was a problem at the 2009 mathematics Olympiad in Germany [1]. All of these but the 1995 proof used other notations.

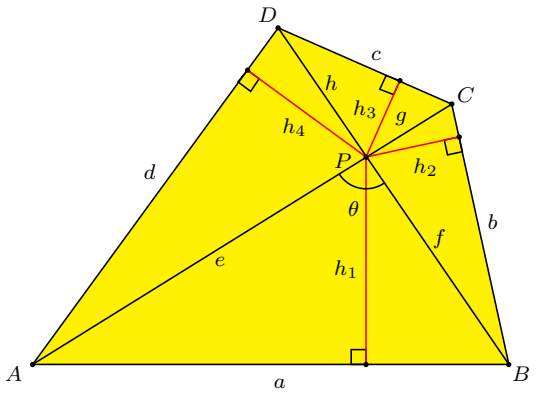

Figure 4. The subtriangle altitudes h_1, h_2, h_3 and h_4

Here we will give a short fifth proof that (8) is a necessary and sufficient condition for a convex quadrilateral to have an incircle using the characterization (7).

By expressing twice the area of ABP, BCP, CDP, DAP in two different ways, we have the equalities (see Figure 4)

$$\begin{aligned} ah_1 &= ef\sin\theta, \\ bh_2 &= fg\sin\theta, \\ ch_3 &= gh\sin\theta, \\ dh_4 &= he\sin\theta \end{aligned} \tag{9}$$

where θ is the angle between the diagonals.[7] Hence

$$\left(\frac{1}{h_1}+\frac{1}{h_3}-\frac{1}{h_2}-\frac{1}{h_4}\right)\sin\theta = \frac{a}{ef}+\frac{c}{gh}-\frac{b}{fg}-\frac{d}{he} = \frac{agh+cef-beh-dfg}{efgh}.$$

Since $\sin\theta \neq 0$, we have that

$$\frac{1}{h_1}+\frac{1}{h_3}=\frac{1}{h_2}+\frac{1}{h_4} \quad \Leftrightarrow \quad agh+cef=beh+dfg$$

which by (7) proves that (8) is a characterization of tangential quadrilaterals.

Now we prove the similar characterizations of extangential quadrilaterals.

Theorem 3. *Let h_1, h_2, h_3, h_4 be the altitudes from the diagonal intersection P to the sides AB, BC, CD, DA in the triangles ABP, BCP, CDP, DAP respectively in a convex quadrilateral $ABCD$. It has an excircle outside one of the vertices A or C if and only if*

$$\frac{1}{h_1}+\frac{1}{h_2}=\frac{1}{h_3}+\frac{1}{h_4}$$

and an excircle outside one of the vertices B or D if and only if

$$\frac{1}{h_1}+\frac{1}{h_4}=\frac{1}{h_2}+\frac{1}{h_3}.$$

Proof. The four equations (9) yields

$$\left(\frac{1}{h_1}+\frac{1}{h_2}-\frac{1}{h_3}-\frac{1}{h_4}\right)\sin\theta = \frac{a}{ef}+\frac{b}{fg}-\frac{c}{gh}-\frac{d}{he} = \frac{agh+beh-cef-dfg}{efgh}.$$

Since $\sin\theta \neq 0$, we have that

$$\frac{1}{h_1}+\frac{1}{h_2}=\frac{1}{h_3}+\frac{1}{h_4} \quad \Leftrightarrow \quad agh+beh=cef+dfg$$

which by Theorem 2 proves the first condition in the theorem. The second is proved in the same way. □

[7] Here we have used that $\sin(\pi-\theta)=\sin\theta$ in two of the equalities.

5. Iosifescu's characterization for excircles

According to [11, p.113], Marius Iosifescu proved in 1954 that a convex quadrilateral $ABCD$ has an incircle if and only if

$$\tan\frac{x}{2}\tan\frac{z}{2}=\tan\frac{y}{2}\tan\frac{w}{2}$$

where $x=\angle ABD$, $y=\angle ADB$, $z=\angle BDC$ and $w=\angle DBC$, see Figure 5. That proof was given in Romanian, but an English one was given in [8, pp.75–77].

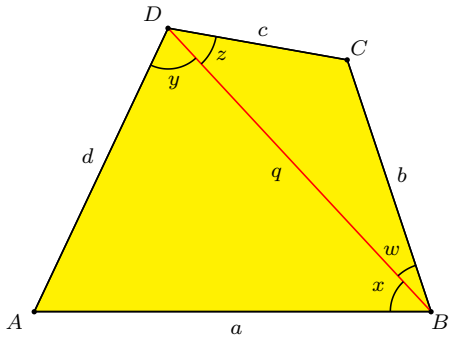

Figure 5. Angles in Iosifescu's characterization

There are similar characterizations for a quadrilateral to have an excircle, which we shall prove in the next theorem.

Theorem 4. *Let $x=\angle ABD$, $y=\angle ADB$, $z=\angle BDC$ and $w=\angle DBC$ in a convex quadrilateral $ABCD$. It has an excircle outside one of the vertices A or C if and only if*

$$\tan\frac{x}{2}\tan\frac{w}{2}=\tan\frac{y}{2}\tan\frac{z}{2}$$

and an excircle outside one of the vertices B or D if and only if

$$\tan\frac{x}{2}\tan\frac{y}{2}=\tan\frac{z}{2}\tan\frac{w}{2}.$$

Proof. In [8], Theorem 7, we proved by using the law of cosines that

$$1-\cos x=\frac{(d+a-q)(d-a+q)}{2aq},\quad 1+\cos x=\frac{(a+q+d)(a+q-d)}{2aq},$$
$$1-\cos y=\frac{(a+d-q)(a-d+q)}{2dq},\quad 1+\cos y=\frac{(d+q+a)(d+q-a)}{2dq},$$
$$1-\cos z=\frac{(b+c-q)(b-c+q)}{2cq},\quad 1+\cos z=\frac{(c+q+b)(c+q-b)}{2cq},$$
$$1-\cos w=\frac{(c+b-q)(c-b+q)}{2bq},\quad 1+\cos w=\frac{(b+q+c)(b+q-c)}{2bq},$$

where $a = AB$, $b = BC$, $c = CD$, $d = DA$ and $q = BD$ in quadrilateral $ABCD$. Using these and the trigonometric identity

$$\tan^2 \frac{u}{2} = \frac{1 - \cos u}{1 + \cos u},$$

the second equality in the theorem is equivalent to

$$\frac{(d+a-q)^2(d-a+q)(a-d+q)(c+q+b)^2(c+q-b)(b+q-c)}{16abcdq^4}$$
$$= \frac{(b+c-q)^2(b-c+q)(c-b+q)(a+q+d)^2(a+q-d)(d+q-a)}{16abcdq^4}.$$

This is factored as

$$4qQ_1(a+d-b-c)\left((a+d)(b+c)-q^2\right) = 0 \tag{10}$$

where

$$Q_1 = \frac{(a-d+q)(d-a+q)(b-c+q)(c-b+q)}{16abcdq^4}$$

is a positive expression according to the triangle inequality. We also have that $a + d > q$ and $b + c > q$, so $(a + d)(b + c) > q^2$. Hence we have proved that

$$\tan\frac{x}{2}\tan\frac{y}{2} = \tan\frac{z}{2}\tan\frac{w}{2} \quad \Leftrightarrow \quad a + d = b + c$$

which according to (2) shows that the second equality in the theorem is a necessary and sufficient condition for an excircle outside of B or D.

The same kind of reasoning for the first equality in the theorem yields

$$4qQ_2(a+b-c-d)\left((a+b)(c+d)-q^2\right) = 0 \tag{11}$$

where $(a + b)(c + d) > q^2$ and

$$Q_2 = \frac{(a-b+q)(b-a+q)(d-c+q)(c-d+q)}{16abcdq^4} > 0.$$

Hence

$$\tan\frac{x}{2}\tan\frac{w}{2} = \tan\frac{y}{2}\tan\frac{z}{2} \quad \Leftrightarrow \quad a + b = c + d$$

which according to (1) shows that the first equality in the theorem is a necessary and sufficient condition for an excircle outside of A or C. □

6. Characterizations with escribed circles

All convex quadrilaterals $ABCD$ have four circles, each of which is tangent to one side and the extensions of the two adjacent sides. In a triangle they are called the excircles, but for quadrilaterals we have reserved that name for a circle tangent to the extensions of all four sides. For this reason we will call a circle tangent to one side of a quadrilateral and the extensions of the two adjacent sides an *escribed circle*.[8] The four of them have the interesting property that their centers form a cyclic quadrilateral. If $ABCD$ has an incircle, then its center is also the intersection of the diagonals in that cyclic quadrilateral [4, pp.1–2, 5].

[8] In triangle geometry the two names excircle and escribed circle are synonyms.

First we will prove a new characterization for when a convex quadrilateral has an incircle that concerns the escribed circles.

Theorem 5. *A convex quadrilateral with consecutive escribed circles of radii R_a, R_b, R_c and R_d is tangential if and only if*

$$R_a R_c = R_b R_d.$$

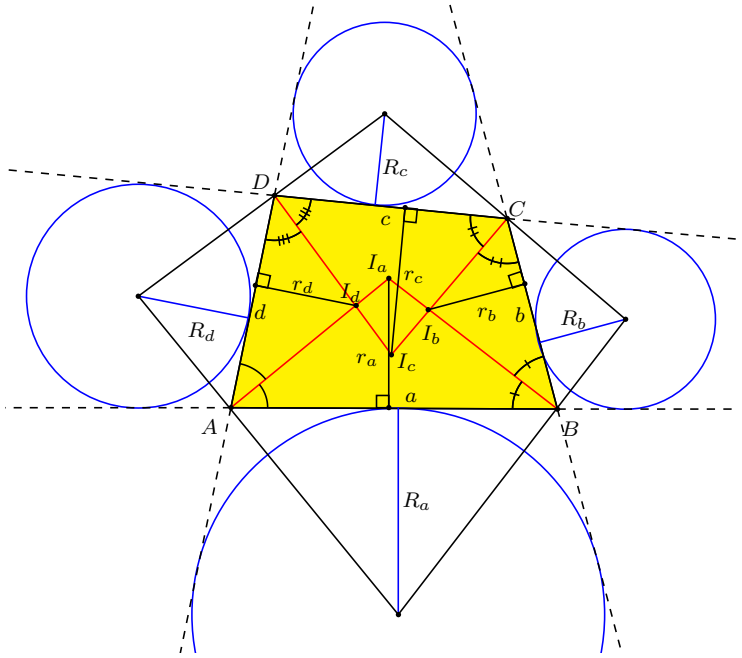

Figure 6. The four escribed circles

Proof. We consider a convex quadrilateral $ABCD$ where the angle bisectors intersect at I_a, I_b, I_c and I_d. Let the distances from these four intersections to the sides of the quadrilateral be r_a, r_b, r_c and r_d, see Figure 6. Then we have

$$\begin{aligned}
r_a\left(\cot\frac{A}{2}+\cot\frac{B}{2}\right) &= a = R_a\left(\tan\frac{A}{2}+\tan\frac{B}{2}\right),\\
r_b\left(\cot\frac{B}{2}+\cot\frac{C}{2}\right) &= b = R_b\left(\tan\frac{B}{2}+\tan\frac{C}{2}\right),\\
r_c\left(\cot\frac{C}{2}+\cot\frac{D}{2}\right) &= c = R_c\left(\tan\frac{C}{2}+\tan\frac{D}{2}\right),\\
r_d\left(\cot\frac{D}{2}+\cot\frac{A}{2}\right) &= d = R_d\left(\tan\frac{D}{2}+\tan\frac{A}{2}\right).
\end{aligned}$$

From two of these we get

$$r_b r_d \left(\cot\frac{B}{2}+\cot\frac{C}{2}\right)\left(\cot\frac{A}{2}+\cot\frac{D}{2}\right) = R_b R_d \left(\tan\frac{B}{2}+\tan\frac{C}{2}\right)\left(\tan\frac{A}{2}+\tan\frac{D}{2}\right),$$

whence

$$r_b r_d \left(\frac{\cos\frac{A}{2}\sin\frac{D}{2}+\sin\frac{A}{2}\cos\frac{D}{2}}{\sin\frac{A}{2}\sin\frac{D}{2}}\right)\left(\frac{\cos\frac{B}{2}\sin\frac{C}{2}+\sin\frac{B}{2}\cos\frac{C}{2}}{\sin\frac{B}{2}\sin\frac{C}{2}}\right) = R_b R_d \left(\frac{\sin\frac{B}{2}\cos\frac{C}{2}+\cos\frac{B}{2}\sin\frac{C}{2}}{\cos\frac{B}{2}\cos\frac{C}{2}}\right)\left(\frac{\sin\frac{A}{2}\cos\frac{D}{2}+\cos\frac{A}{2}\sin\frac{D}{2}}{\cos\frac{A}{2}\cos\frac{D}{2}}\right).$$

This is equivalent to

$$\frac{r_b r_d}{R_b R_d} = \tan\frac{A}{2}\tan\frac{B}{2}\tan\frac{C}{2}\tan\frac{D}{2}. \tag{12}$$

By symmetry we also have

$$\frac{r_a r_c}{R_a R_c} = \tan\frac{A}{2}\tan\frac{B}{2}\tan\frac{C}{2}\tan\frac{D}{2}; \tag{13}$$

so

$$\frac{r_a r_c}{R_a R_c} = \frac{r_b r_d}{R_b R_d}. \tag{14}$$

The quadrilateral is tangential if and only if the angle bisectors are concurrent, which is equivalent to $I_a \equiv I_b \equiv I_c \equiv I_d$. This in turn is equivalent to that $r_a = r_b = r_c = r_d$. Hence by (14) the quadrilateral is tangential if and only if $R_a R_c = R_b R_d$. □

We also have the following formulas. They are not new, and can easily be derived in a different way using only similarity of triangles.

Corollary 6. *In a bicentric quadrilateral* [9] *and a tangential trapezoid with consecutive escribed circles of radii R_a, R_b, R_c and R_d, the incircle has the radius*

$$r = \sqrt{R_a R_c} = \sqrt{R_b R_d}.$$

Proof. In these quadrilaterals, $A + C = \pi = B + D$ or $A + D = \pi = B + C$ (if we assume that $AB \parallel DC$). Thus

$$\tan\frac{A}{2}\tan\frac{C}{2} = \tan\frac{B}{2}\tan\frac{D}{2} = 1$$

or

$$\tan\frac{A}{2}\tan\frac{D}{2} = \tan\frac{B}{2}\tan\frac{C}{2} = 1.$$

In either case the formulas for the inradius follows directly from (13) and (12), since $r = r_a = r_b = r_c = r_d$ when the quadrilateral has an incircle. □

[9] This is a quadrilateral that has both an incircle and a circumcircle.

In comparison to Theorem 5 we have the following characterizations for an extangential quadrilateral.

Theorem 7. *Let a convex quadrilateral $ABCD$ have consecutive escribed circles of radii R_a, R_b, R_c and R_d. The quadrilateral has an excircle outside one of the vertices A or C if and only if*

$$R_aR_b = R_cR_d$$

and an excircle outside one of the vertices B or D if and only if

$$R_aR_d = R_bR_c.$$

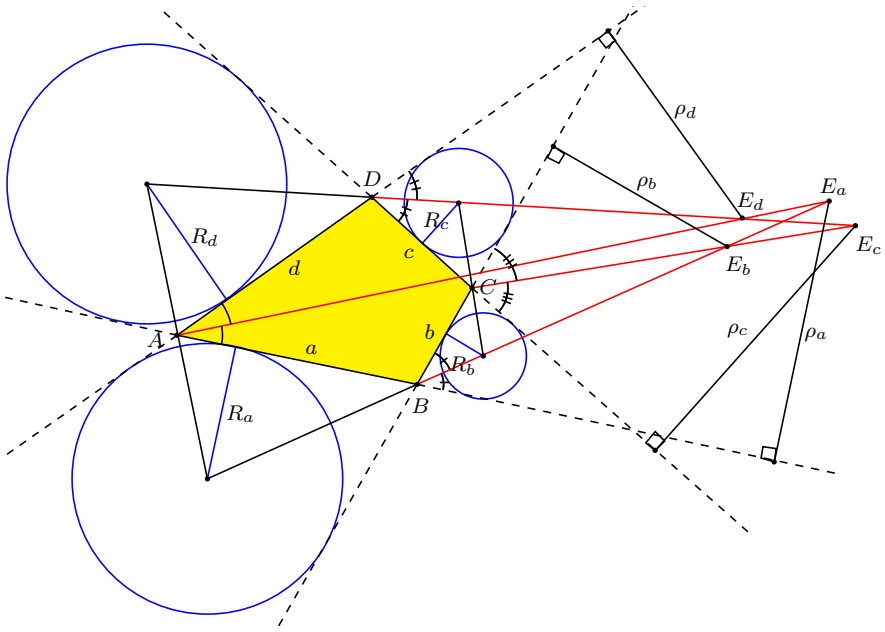

Figure 7. Intersections of four angle bisectors

Proof. We consider a convex quadrilateral $ABCD$ where two opposite internal and two opposite external angle bisectors intersect at E_a, E_c, E_b and E_d. Let the distances from these four intersections to the sides of the quadrilateral be ρ_a, ρ_c, ρ_b and ρ_d respectively, see Figure 7. Then we have

$$\rho_a\left(\cot\frac{A}{2}-\tan\frac{B}{2}\right)=a=R_a\left(\tan\frac{A}{2}+\tan\frac{B}{2}\right),$$
$$\rho_b\left(\tan\frac{B}{2}-\cot\frac{C}{2}\right)=b=R_b\left(\tan\frac{B}{2}+\tan\frac{C}{2}\right),$$
$$\rho_c\left(\tan\frac{D}{2}-\cot\frac{C}{2}\right)=c=R_c\left(\tan\frac{C}{2}+\tan\frac{D}{2}\right),$$
$$\rho_d\left(\cot\frac{A}{2}-\tan\frac{D}{2}\right)=d=R_d\left(\tan\frac{D}{2}+\tan\frac{A}{2}\right).$$

Using the first two of these, we get

$$\rho_a\rho_b\left(\cot\frac{A}{2}-\tan\frac{B}{2}\right)\left(\tan\frac{B}{2}-\cot\frac{C}{2}\right)$$
$$=R_aR_b\left(\tan\frac{A}{2}+\tan\frac{B}{2}\right)\left(\tan\frac{B}{2}+\tan\frac{C}{2}\right),$$

whence

$$\rho_a\rho_b\left(\frac{\cos\frac{A}{2}\cos\frac{B}{2}-\sin\frac{A}{2}\sin\frac{B}{2}}{\sin\frac{A}{2}\cos\frac{B}{2}}\right)\left(\frac{\sin\frac{B}{2}\sin\frac{C}{2}-\cos\frac{B}{2}\cos\frac{C}{2}}{\cos\frac{B}{2}\sin\frac{C}{2}}\right)$$
$$=R_aR_b\left(\frac{\sin\frac{A}{2}\cos\frac{B}{2}+\cos\frac{A}{2}\sin\frac{B}{2}}{\cos\frac{A}{2}\cos\frac{B}{2}}\right)\left(\frac{\sin\frac{B}{2}\cos\frac{C}{2}+\cos\frac{B}{2}\sin\frac{C}{2}}{\cos\frac{B}{2}\cos\frac{C}{2}}\right).$$

This is equivalent to

$$\rho_a\rho_b\frac{\cos\frac{A+B}{2}\left(-\cos\frac{B+C}{2}\right)}{\sin\frac{A}{2}\cos^2\frac{B}{2}\sin\frac{C}{2}}=R_aR_b\frac{\sin\frac{A+B}{2}\sin\frac{B+C}{2}}{\cos\frac{A}{2}\cos^2\frac{B}{2}\cos\frac{C}{2}},$$

which in turn is equivalent to

$$\frac{\rho_a\rho_b}{R_aR_b}=-\tan\frac{A+B}{2}\tan\frac{B+C}{2}\tan\frac{A}{2}\tan\frac{C}{2}. \tag{15}$$

By symmetry ($B\leftrightarrow D$), we also have

$$\frac{\rho_c\rho_d}{R_cR_d}=-\tan\frac{A+D}{2}\tan\frac{D+C}{2}\tan\frac{A}{2}\tan\frac{C}{2}. \tag{16}$$

Now using the sum of angles in a quadrilateral,

$$\tan\frac{A+B}{2}=-\tan\frac{D+C}{2}$$

and

$$\tan\frac{B+C}{2}=-\tan\frac{A+D}{2}.$$

Hence

$$\tan\frac{A+B}{2}\tan\frac{B+C}{2}=\tan\frac{A+D}{2}\tan\frac{D+C}{2}$$

so by (15) and (16) we have

$$\frac{\rho_a\rho_b}{R_aR_b}=\frac{\rho_c\rho_d}{R_cR_d}. \tag{17}$$

The quadrilateral is extangential if and only if the internal angle bisectors at A and C, and the external angle bisectors at B and D are concurrent, which is equivalent to $E_a\equiv E_b\equiv E_c\equiv E_d$. This in turn is equivalent to that $\rho_a=\rho_b=\rho_c=\rho_d$. Hence by (17) the quadrilateral is extangential if and only if $R_aR_b=R_cR_d$.

The second condition $R_aR_d=R_bR_c$ is proved in the same way. □

We have not found a way to express the exradius (the radius in the excircle) in terms of the escribed radii in comparison to Corollary 6. Instead we have the following formulas, which although they are simple, we cannot find a reference for. They resemble the well known formulas $r = \frac{K}{a+c} = \frac{K}{b+d}$ for the inradius in a tangential quadrilateral with sides a, b, c, d and area K.

Theorem 8. *An extangential quadrilateral with sides a, b, c and d has the exradius*

$$\rho = \frac{K}{|a-c|} = \frac{K}{|b-d|}$$

where K is the area of the quadrilateral.

Proof. We prove the formulas in the case that is shown i Figure 8. The area of the extangential quadrilateral $ABCD$ is equal to the areas of the triangles ABE and ADE subtracted by the areas of BCE and CDE. Thus

$$K = \tfrac{1}{2}a\rho + \tfrac{1}{2}d\rho - \tfrac{1}{2}b\rho - \tfrac{1}{2}c\rho = \tfrac{1}{2}\rho(a+d-b-c)$$

where the exradius ρ is the altitude in all four triangles. Hence

$$\rho = \frac{2K}{a-c+d-b} = \frac{K}{a-c} = \frac{K}{d-b}$$

since here we have $a+b = c+d$ (the excircle is outside of C), that is $a-c = d-b$. To cover all cases we put absolute values in the denominators. □

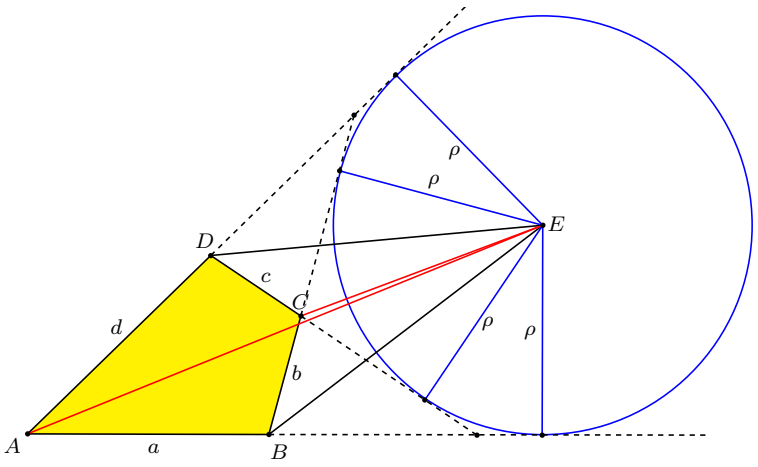

Figure 8. Calculating the area of $ABCD$ with four triangles

This theorem indicates that the exradii in all parallelograms (and hence also in all rhombi, rectangles and squares) are infinite, since in all of them $a = c$ and $b = d$.

References

[1] 48. Mathematik-Olympiade, 4. Stufe, Klasse 12-13 (in German), 2009, available at http://www.mathematik-olympiaden.de/aufgaben/48/4/A48134a.pdf

[2] A. Bogomolny, Inscriptible and exscriptible quadrilaterals, *Interactive Mathematics Miscellany and Puzzles*, http://www.cut-the-knot.org/Curriculum/Geometry/Pitot.shtml

[3] F. G.-M., *Exercices de Géométrie*, Cinquième édition (in French), Éditions Jaques Gabay, 1912.

[4] D. Grinberg, A tour around Quadrilateral Geometry, available at http://www.cip.ifi.lmu.de/~grinberg/TourQuadriPDF.zip

[5] H. Grossman, Urquhart's quadrilateral theorem, *The Mathematics Teacher*, 66 (1973) 643–644.

[6] M. Hajja, A very short and simple proof of "The most elementary theorem" of Euclidean geometry, *Forum Geom.*, 6 (2006) 167–169.

[7] L. Hoehn, A new formula concerning the diagonals and sides of a quadrilateral, *Forum Geom.*, 11 (2011) 211–212.

[8] M. Josefsson, More characterizations of tangential quadrilaterals, *Forum Geom.*, 11 (2011) 65–82.

[9] M. Josefsson, Characterizations of orthodiagonal quadrilaterals, *Forum Geom.*, 12 (2012) 13–25.

[10] K. S. Kedlaya, *Geometry Unbound*, 2006, available at http://math.mit.edu/~kedlaya/geometryunbound/

[11] N. Minculete, Characterizations of a tangential quadrilateral, *Forum Geom.*, 9 (2009) 113–118.

[12] D. Pedoe, The Most "Elementary Theorem" of Euclidean Geometry, *Math. Mag.*, 4 (1976) 40–42.

[13] M. Radić, Z. Kaliman and V. Kadum, A condition that a tangential quadrilateral is also a chordal one, *Mathematical Communications*, 12 (2007) 33–52.

[14] L. Sauvé, On circumscribable quadrilaterals, *Crux Math.*, 2 (1976) 63–67.

[15] D. Sokolowsky, A "No-circle" proof of Urquhart's theorem, *Crux Math.*, 2 (1976) 133–134.

[16] I. Vaynshtejn, N. Vasilyev and V. Senderov, Problem M1495, *Kvant* (in Russian) no. 6, 1995, pp. 27–28, available at http://kvant.mirror1.mccme.ru/djvu/1995_06.djvu

[17] W. C. Wu and P. Simeonov, Problem 10698, *Amer. Math. Monthly*, 105 (1998) 995; solution, ibid., 107 (2000) 657–658.

[18] A. Zaslavsky, Problem M1887, *Kvant* (in Russian) no. 3, 2004 p. 19, available at http://kvant.mirror1.mccme.ru/djvu/2004_03.djvu

Martin Josefsson: Västergatan 25d, 285 37 Markaryd, Sweden
E-mail address: martin.markaryd@hotmail.com

Forum Geometricorum
Volume 12 (2012) 79–82.

FORUM GEOM
ISSN 1534-1178

A New Proof of Yun's Inequality for Bicentric Quadrilaterals

Martin Josefsson

Abstract. We give a new proof of a recent inequality for bicentric quadrilaterals that is an extension of the Euler-like inequality $R \geq \sqrt{2}r$.

A *bicentric quadrilateral* $ABCD$ is a convex quadrilateral that has both an incircle and a circumcircle. In [6], Zhang Yun called these "double circle quadrilaterals" and proved that

$$\frac{r\sqrt{2}}{R} \leq \frac{1}{2}\left(\sin\frac{A}{2}\cos\frac{B}{2}+\sin\frac{B}{2}\cos\frac{C}{2}+\sin\frac{C}{2}\cos\frac{D}{2}+\sin\frac{D}{2}\cos\frac{A}{2}\right) \leq 1$$

where r and R are the inradius and circumradius respectively. While his proof mainly focused on the angles of the quadrilateral and how they are related to the two radii, our proof is based on calculations with the sides.

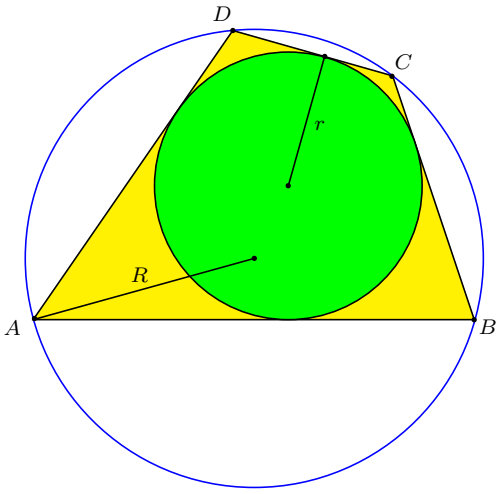

Figure 1. A bicentric quadrilateral with its inradius and circumradius

Publication Date: April 4, 2012. Communicating Editor: Paul Yiu.

In [4, p.156] we proved that the half angles of tangent in a bicentric quadrilateral $ABCD$ with sides a, b, c, d are given by

$$\tan\frac{A}{2} = \sqrt{\frac{bc}{ad}} = \cot\frac{C}{2},$$
$$\tan\frac{B}{2} = \sqrt{\frac{cd}{ab}} = \cot\frac{D}{2}.$$

We need to convert these into half angle formulas of sine and cosine. The trigonometric identities

$$\sin\frac{x}{2} = \frac{\tan\frac{x}{2}}{\sqrt{\tan^2\frac{x}{2}+1}},$$
$$\cos\frac{x}{2} = \frac{1}{\sqrt{\tan^2\frac{x}{2}+1}}$$

yields

$$\sin\frac{A}{2} = \sqrt{\frac{bc}{ad+bc}} = \cos\frac{C}{2}, \tag{1}$$
$$\cos\frac{A}{2} = \sqrt{\frac{ad}{ad+bc}} = \sin\frac{C}{2} \tag{2}$$

and

$$\sin\frac{B}{2} = \sqrt{\frac{cd}{ab+cd}} = \cos\frac{D}{2}, \tag{3}$$
$$\cos\frac{B}{2} = \sqrt{\frac{ab}{ab+cd}} = \sin\frac{D}{2}. \tag{4}$$

From the formulas for the inradius and circumradius in a bicentric quadrilateral (these where also used by Yun, but in another way)

$$r = \frac{2\sqrt{abcd}}{a+b+c+d},$$
$$R = \frac{1}{4}\sqrt{\frac{(ab+cd)(ac+bd)(ad+bc)}{abcd}}$$

we have

$$\begin{aligned}\frac{r\sqrt{2}}{R} &= \frac{8\sqrt{2}abcd}{(a+b+c+d)\sqrt{(ab+cd)(ac+bd)(ad+bc)}}\\ &\leq \frac{8\sqrt{2}abcd}{4\sqrt[4]{abcd}\sqrt{(ab+cd)(ad+bc)}\sqrt{2\sqrt{acbd}}}\\ &= \frac{2\sqrt{abcd}}{\sqrt{(ab+cd)(ad+bc)}}\end{aligned}$$

where we used the AM-GM inequality twice.

Let us for the sake of brevity denote the trigonometric expression in the parenthesis in Yun's inequality by Σ. Thus

$$\Sigma = \sin\frac{A}{2}\cos\frac{B}{2} + \sin\frac{B}{2}\cos\frac{C}{2} + \sin\frac{C}{2}\cos\frac{D}{2} + \sin\frac{D}{2}\cos\frac{A}{2}$$

and the half angle formulas (1), (2), (3) and (4) yields

$$\Sigma = \frac{\sqrt{ab^2c} + \sqrt{bc^2d} + \sqrt{acd^2} + \sqrt{a^2bd}}{\sqrt{(ab+cd)(ad+bc)}} = \frac{(\sqrt{ab}+\sqrt{cd})(\sqrt{ad}+\sqrt{bc})}{\sqrt{(ab+cd)(ad+bc)}}.$$

Using the AM-GM inequality again,

$$(\sqrt{ab}+\sqrt{cd})(\sqrt{ad}+\sqrt{bc}) \geq 2\sqrt{\sqrt{ab}\sqrt{cd}}\cdot 2\sqrt{\sqrt{ad}\sqrt{bc}} = 4\sqrt{abcd}.$$

Hence

$$\frac{r\sqrt{2}}{R} \leq \frac{2\sqrt{abcd}}{\sqrt{(ab+cd)(ad+bc)}} \leq \frac{1}{2}\Sigma.$$

This proves the left hand side of Yun's inequality.

For the right hand side we need to prove that

$$\frac{(\sqrt{ab}+\sqrt{cd})(\sqrt{ad}+\sqrt{bc})}{\sqrt{(ab+cd)(ad+bc)}} \leq 2.$$

By symmetry it is enough to prove the inequality

$$\frac{\sqrt{ab}+\sqrt{cd}}{\sqrt{ab+cd}} \leq \sqrt{2}.$$

Since both sides are positive, we can rewrite this as

$$(\sqrt{ab}+\sqrt{cd})^2 \leq 2(ab+cd) \quad \Leftrightarrow \quad 2\sqrt{abcd} \leq ab+cd$$

which is true according to the AM-GM inequality.

This completes our proof of Yun's inequality for bicentric quadrilaterals. From the calculations with the AM-GM inequality we see that there is equality on the left hand side only when all the sides are equal since we used $a+b+c+d \geq 4\sqrt[4]{abcd}$, with equality only if $a=b=c=d$. On the right hand side we have equality only if $ab=cd$ and $ad=bc$, which is equivalent to $a=c$ and $b=d$. Since it is a bicentric quadrilateral, we have equality on either side if and only if it is a square.

It can be noted that since opposite angles in a bicentric quadrilateral are supplementary angles, Yun's inequality can also (after rearranging the terms) be stated as either

$$\frac{r\sqrt{2}}{R} \leq \frac{1}{2}\left(\sin\frac{A}{2}\sin\frac{B}{2} + \sin\frac{B}{2}\sin\frac{C}{2} + \sin\frac{C}{2}\sin\frac{D}{2} + \sin\frac{D}{2}\sin\frac{A}{2}\right) \leq 1$$

or

$$\frac{r\sqrt{2}}{R} \leq \frac{1}{2}\left(\cos\frac{A}{2}\cos\frac{B}{2} + \cos\frac{B}{2}\cos\frac{C}{2} + \cos\frac{C}{2}\cos\frac{D}{2} + \cos\frac{D}{2}\cos\frac{A}{2}\right) \leq 1.$$

We conclude this note by a few comments on the simpler inequality $R \geq \sqrt{2}r$. According to [2, p.132] it was proved by Gerasimov and Kotii in 1964. The next

year, the American mathematician Carlitz published a paper [3] where he derived a generalization of Euler's triangle formula to a bicentric quadrilateral. His formula gave $R \geq \sqrt{2}r$ as a special case. Another proof can be based on Fuss' theorem, see [5]. The inequality also directly follows from the fact that the area K of a bicentric quadrilateral satisfies $2R^2 \geq K \geq 4r^2$, which was proved in [1].

References

[1] C. Alsina and R. B. Nelsen, *When Less is More. Visualizing Basic Inequalities*, Math. Assoc. Amer., 2009, p.64.
[2] O. Bottema, *Geometric Inequalities*, Wolters-Noordhoff, Groningen, 1969.
[3] L. Carlitz, A Note on Circumscriptible Cyclic Quadrilaterals, *Math. Mag.*, 38 (1965) 33–35.
[4] M. Josefsson, The area of a bicentric quadrilateral, *Forum Geom.*, 11 (2011) 155–164.
[5] nttu (username), R, r [prove $R \geq \sqrt{(2)}r$ in bicentric quadrilateral], *Art of Problem Solving*, 2004,
`http://www.artofproblemsolving.com/Forum/viewtopic.php?t=18914`
[6] Z. Yun, Euler's Inequality Revisited, *Mathematical Spectrum*, 40 (2008) 119–121.

Martin Josefsson: Västergatan 25d, 285 37 Markaryd, Sweden
E-mail address: `martin.markaryd@hotmail.com`

Forum Geometricorum
Volume 12 (2012) 83–128.

FORUM GEOM
ISSN 1534-1178

Reflection Triangles and Their Iterates

Grégoire Nicollier

Abstract. By reflecting each vertex of a triangle in the opposite side one obtains the vertices of the reflection triangle of the given triangle. We analyze the forward and backward orbit of any base triangle under this reflection process and give a complete description of the underlying discrete dynamical system with fractal structure.

1. Introduction

We consider *finite* triangles as well as *infinite* triangles with a finite side, a vertex at infinity and two semi–infinite parallel sides. By reflecting each vertex of a triangle in the opposite side one obtains the vertices of the *reflection triangle* of the given triangle. A degenerate triangle is thus its own reflection triangle – including by convention triangles with two or three coincident vertices. The reverse construction of an antireflection triangle is in general not possible with compass and ruler only [2]. By using interactive geometry software one sees how erratic the behavior of a, say, four times reflected triangle can be with respect to the base triangle (Figure 1).

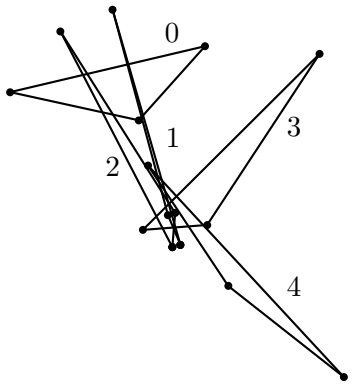

Figure 1

We give a complete description of the dynamical system generated by this reflection process and we reduce the part concerning the non-acute triangles to a symbolic system. Each *proper* triangle (*i.e.*, each finite nondegenerate triangle) is the reflection triangle of 5, 6 or 7 differently placed triangles – 7 when the triangle is equilateral or nearly equilateral (Figure 2). Each degenerate triangle with three

Publication Date: April 13, 2012. Communicating Editor: J. Chris Fisher.
The author thanks the Communicating Editor for his many helpful suggestions.

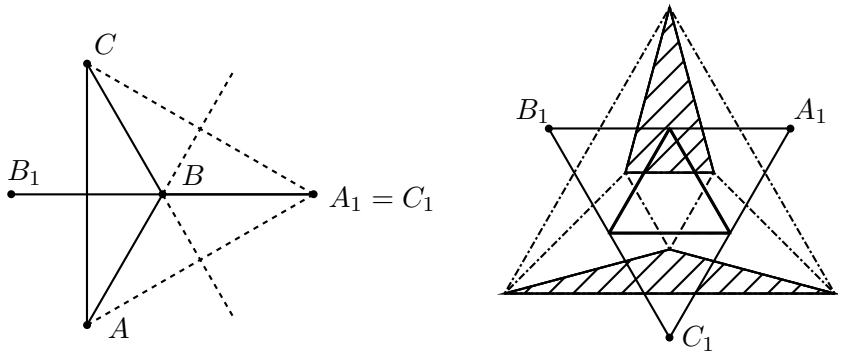

Figure 2. Isosceles triangle with equal 30°–angles and degenerate reflection triangle; the 7 triangles with the same equilateral reflection triangle

distinct vertices is the reflection triangle of exactly 5 triangles. Each nondegenerate infinite triangle is the reflection triangle of exactly 3 infinite triangles. We prove that all finite acute and right–angled triangles tend to an equilateral limit if one iterates this reflection map, and we describe the fractal structure of the triangles having an equilateral or degenerate limit. If one represents the set of triangles up to similarity by the set $\left\{(\alpha,\beta) \mid 0^\circ \leq \beta \leq \alpha \leq 90^\circ - \frac{\beta}{2}\right\}$ in the Euclidean plane, the triangles with equilateral limit form a dense open subset; the triangles with degenerate limit form a countable union of maximal path–connected subsets with empty interior; the triangles without equilateral or degenerate limit form an uncountable totally path–disconnected subset; any neighborhood of a triangle without equilateral limit contains uncountably many triangles with equilateral limit, with degenerate limit, and with neither equilateral nor degenerate limit. We show that there are up to angle similarity four finite and two infinite triangles similar to their reflection triangle (among them the degenerate and equilateral triangles, the *heptagonal triangle* with angles $\frac{\pi}{7}$, $\frac{2\pi}{7}$ and $\frac{4\pi}{7}$, and the rectangular infinite triangle). We exhibit the ten 2–cycles – three of them for infinite triangles – and the forty 3–cycles – eight of them for infinite triangles. If one identifies similar triangles, the set of non-acute triangles contains (finitely many) cycles of any fixed finite length – they are always repelling – and uncountably many disjoint divergent forward orbits for both finite and infinite triangles. We exhibit some explicit examples and describe symbolically the periodic and divergent forward orbits. It is possible to design divergent forward orbits with almost any behavior: such an orbit can for example approximate any periodic orbit of non-acute, nondegenerate triangles during any finite number of consecutive reflection steps before leaving this cycle, or it can even be dense in the space of triangles without equilateral limit. If one identifies similar triangles, infinite triangles having a degenerate limit are countably dense in the set of infinite triangles; this is also the case for the backward orbit of any nondegenerate infinite triangle; the backward orbit of a finite triangle without equilateral limit (and not reduced to a single point) is dense in the set of all triangles without equilateral limit.

Properties of finite reflection triangles can be found in [12, 5, 6] and [3, pp. 77–80]. The reflection triangle of a proper triangle Δ is homothetic – in ratio 4 with respect to the centroid of Δ – to the pedal triangle of the nine–point center N [5], *i.e.*, to the triangle with vertices on each side of Δ halfway between the side's midpoint and the altitude's foot. By the Wallace–Simson Theorem [10, p. 137] the reflection triangle of a proper triangle Δ – being similar to the pedal triangle of N – is degenerate if and only if N lies on the circumcircle of Δ: this is the case if and only if the sides a, b, c of Δ satisfy $a^2 + b^2 + c^2 = 5R^2$, R being the circumradius. Thus, by the sine law, the reflection triangle of a proper triangle with angles α, β, γ is degenerate if and only if

$$\sin^2\alpha + \sin^2\beta + \sin^2\gamma = \tfrac{5}{4}. \tag{1}$$

We mainly use a method developed by van IJzeren [9] for solving the problem of finding all triangles with a given finite reflection triangle. We reformulate, extend and fully exploit van IJzeren's results and prove them because the original proof (in Dutch) is partly incomplete and sometimes approximate. The key paper [9] was preceded by another van IJzeren's paper [8] and by publications of Dutch mathematicians on the same subject [2, 11].

2. Van IJzeren coordinates of a triangle

We identify triangles that have the same angles α, β, γ to get the set $\mathcal{T}$ of similarity classes. We then speak of a *(triangle) class* of $\mathcal{T}$ and write $\Delta \in \mathcal{T}$ or $\{\alpha, \beta, \gamma\} \in \mathcal{T}$. It is both natural and convenient to assign angles 0, 0, π to all degenerate triangles (*i.e.*, to triangles with collinear vertices) and to lump them together into a single class $\mathcal{O}$ of $\mathcal{T}$. The classes of infinite triangles are $\Pi_\alpha = \{\alpha, \pi - \alpha, 0\}$, $0 < \alpha < \pi$; these are the classes of triangles having as vertices one point at infinity and two different finite points, and as sides one line segment and two half–lines (which are parallel). Note that $\Pi_\alpha = \Pi_{\pi-\alpha}$ and that $\Pi_{\pi/2}$ contains the infinite rectangular triangles. We denote by I_α the isosceles class of the finite triangles with angles $\{\alpha, \alpha, \pi - 2\alpha\}$, $0 < \alpha < \frac{\pi}{2}$. We often identify $\mathcal{T}$ with $\left\{(\alpha, \beta) \mid 0^\circ \le \beta \le \alpha \le 90^\circ - \frac{\beta}{2}\right\}$ (Figure 4).

For both the class $\Delta = \{\alpha, \beta, \gamma\} \in \mathcal{T}$ and a triangle Δ with these angles, we define the sum $s(\Delta) = \sin^2\alpha + \sin^2\beta + \sin^2\gamma$, the product $p(\Delta) = \sin^2\alpha \cdot \sin^2\beta \cdot \sin^2\gamma$ and the *van IJzeren map*

$$V(\Delta) = \Delta^* = (s(\Delta), p(\Delta))$$

giving the *van IJzeren coordinates* of Δ. $s(\Delta)$ runs from 0 for a degenerate triangle to $\frac{9}{4}$ for an equilateral triangle; $s(\Delta)$ is > 2, $= 2$ or < 2 if Δ is acute, right–angled or obtuse, respectively. $p(\Delta)$ runs from 0 for a degenerate or infinite triangle to $\frac{27}{64}$ for an equilateral triangle. A given $s(\Delta)$ or $p(\Delta)$ determines the curve of admissible values (α, β) for two acute angles of Δ (Figure 3).

Lemma 1. *The polynomial $u^3 - su^2 + du - p$ has roots $u_1 = \sin^2\alpha$, $u_2 = \sin^2\beta$, $u_3 = \sin^2\gamma$ for some $\{\alpha, \beta, \gamma\} \in \mathcal{T}$ if and only if $s, p \in \mathbf{R}$, $p \ge 0$, $d = \frac{s^2}{4} + p$ and*

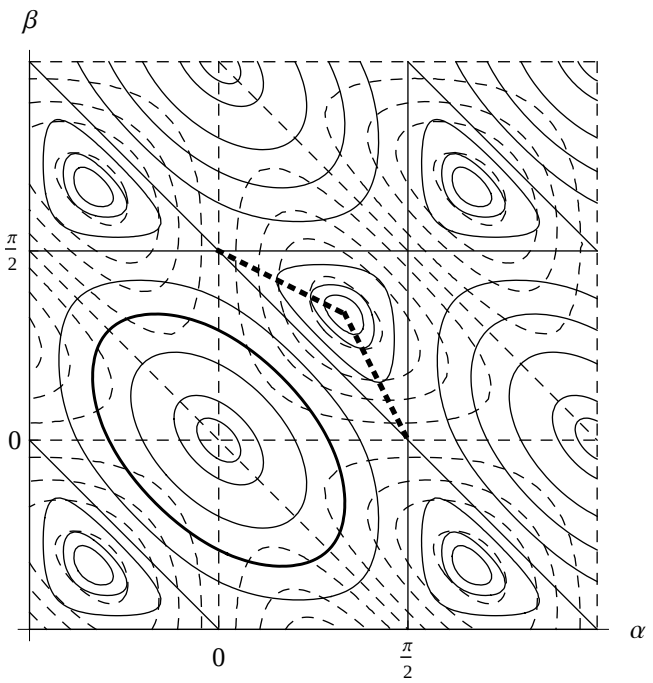

Figure 3. Level curves $\sin^2\alpha+\sin^2\beta+\sin^2(\alpha+\beta)=s$ (plain, thick for $s=\frac{5}{4}$) and $\sin^2\alpha\cdot\sin^2\beta\cdot\sin^2(\alpha+\beta)=p$ (dashed). Points (α,β) corresponding to the two smallest angles α,β of a triangle lie in the square $0\le\alpha,\beta\le\frac{\pi}{2}$ south–west of or on the thick dotted line.

$D(s,p)=(9-4s)^3-(8p+2s^2-18s+27)^2\ge 0$. *$\{\alpha,\beta,\gamma\}$ is then unique and* $s\ge 0$.

Proof. If $d=\frac{s^2}{4}+p$, $\frac{p}{16}D(s,p)$ is the polynomial's discriminant: for $s\in\mathbf{R}$ and $p>0$ one has then $D(s,p)\ge 0$ if and only if the roots are real; for $s\in\mathbf{R}$ and $p=0$ the roots are then 0 and $\frac{s}{2}$ (double) and $D(s,0)=4s^3(2-s)$ is ≥ 0 if and only if $s\in[0,2]$.

($\Rightarrow$) s, d and p are the roots' sum, the sum of products of two roots and the roots' product, respectively. Hence $s,p\in\mathbf{R}$, $p\ge 0$, and $D(s,p)\ge 0$ if $d=\frac{s^2}{4}+p$. We have to prove that $d=\frac{s^2}{4}+p$. If no angle is 0, divide the cosine law by the squared circumdiameter to get

$$2\sin\alpha\sin\beta\cos\gamma=\sin^2\alpha+\sin^2\beta-\sin^2\gamma. \tag{2}$$

If the triangle is degenerate or infinite, (2) becomes $0=0$ and is true also. Square (2) to get $4u_1u_2(1-u_3)=(s-2u_3)^2$, *i.e.*,

$$4u_1u_2-4p=s^2-4su_3+4u_3^2=s^2-4u_1u_3-4u_2u_3,\ \textit{i.e.},\ 4d-4p=s^2.$$

($\Leftarrow$) The polynomial's roots u_1, u_2, u_3 are real. Since $d=\frac{s^2}{4}+p$, one has $u^3-su^2+du-p=u(u-\frac{s}{2})^2+p(u-1)$: no root can be >1 or <0 if $p>0$; if $p=0$, the roots are 0 and $\frac{s}{2}\in[0,1]$ since $D(s,p)\ge 0$. One can thus write

$u_1 = \sin^2\alpha_1$, $u_2 = \sin^2\beta_1$, $u_3 = \sin^2\gamma_1$ for some $\alpha_1, \beta_1, \gamma_1 \in \left[0, \frac{\pi}{2}\right]$. As above, $4d - 4p = s^2$ if and only if $4u_1u_2(1-u_3) = (s-2u_3)^2 = (u_1+u_2-u_3)^2$, *i.e.*, if and only if $4u_1u_2 - 4u_1u_2u_3 = u_3^2 - 2(u_1+u_2)u_3 + (u_1+u_2)^2$, *i.e.*, if and only if

$$u_3^2 - 2(u_1+u_2-2u_1u_2)u_3 + (u_1-u_2)^2 = 0. \tag{3}$$

Since $u_1+u_2-2u_1u_2 = u_1(1-u_2) + (1-u_1)u_2$ and $u_1 - u_2 = u_1(1-u_2) - (1-u_1)u_2$, (3) is equivalent to $\big(u_3 - (u_1(1-u_2) + (1-u_1)u_2)\big)^2 = 4u_1(1-u_2)(1-u_1)u_2$, *i.e.*,

$$u_3 = \sin^2\alpha_1\cos^2\beta_1 + \cos^2\alpha_1\sin^2\beta_1 \pm 2\sin\alpha_1\cos\beta_1\cos\alpha_1\sin\beta_1,$$

which is $\sin^2\gamma_1 = \sin^2(\alpha_1 \pm \beta_1)$. If $\sin^2\gamma_1 = \sin^2(\alpha_1+\beta_1)$, take $\alpha = \alpha_1$, $\beta = \beta_1$, $\gamma = \pi - \alpha - \beta$. If $\sin^2\gamma_1 = \sin^2(\alpha_1 - \beta_1)$, suppose $\alpha_1 \geq \beta_1$ without restricting the generality and choose $\gamma = \alpha_1 - \beta_1$, $\beta = \beta_1$ and $\alpha = \pi - \beta - \gamma = \pi - \alpha_1$.

$D(s,p) = -64p^2 + p\left(-32s^2 + 288s - 432\right) - 4s^4 + 8s^3$ shows that $D(s,p) < 0$ for $p \geq 0, s < 0$. Two triangle classes with the same s and the same p have necessarily the same $d = \frac{s^2}{4} + p$ and are equal since they correspond to the same roots $\sin^2\alpha$, $\sin^2\beta$, $\sin^2\gamma$. □

Theorem 2. *The van IJzeren map is a bijection from $\mathcal{T}$ to*

$$\mathcal{T}^* = \left\{(s,p) \mid D(s,p) = (9-4s)^3 - (8p + 2s^2 - 18s + 27)^2 \geq 0, s \geq 0, p \geq 0\right\}$$

with inverse $V^{-1}\colon \mathcal{T}^* \to \mathcal{T}$ given by

$$(s,p) \mapsto \left\{\arcsin\sqrt{u_1}\,, \arcsin\sqrt{u_2}\,, \pi - \arcsin\sqrt{u_1} - \arcsin\sqrt{u_2}\,\right\}$$

where $u_1 \leq u_2 \leq u_3$ are the solutions of $u^3 - su^2 + (\frac{1}{4}s^2 + p)u - p = 0$.

For $(s,p) \in \mathcal{T}^*$ the discriminant $\frac{p}{16}D(s,p)$ of the above polynomial in u is 0 if and only if there are multiple roots among $\sin^2\alpha$, $\sin^2\beta$ and $\sin^2\gamma$, *i.e.*, if and only if $(s,p) = \Pi^*_\alpha$ for $p = 0$ or $(s,p) = I^*_\alpha$ for $D(s,p) = 0$ – in addition to $(s,p) = \mathcal{O}^*$ or $\Pi^*_{\pi/2}$ in both cases.

The curve $D(s,p) = 0$, $s \geq 0$, $p \geq 0$, is the *roof* Λ of T^* (Figure 4) and is constituted by $\mathcal{O}^*$, $\Pi^*_{\pi/2}$ and the images of the isosceles classes: the point $\{\alpha, \alpha, \pi - 2\alpha\}^*$, $0 \leq \alpha \leq \frac{\pi}{2}$, or

$$\Lambda(t) = \big(2t(3-2t), 4t^3(1-t)\big),\ 0 \leq t = \sin^2\alpha \leq 1, \tag{4}$$

travels along Λ from the origin $\mathcal{O}^*$ to $\Pi^*_{\pi/2} = (2,0)$.

The points $\Lambda(t)$ given by $t = 0, \frac{2-\sqrt{3}}{4}, \frac{1}{4}, \frac{1}{2}, \frac{3}{4}, \frac{2+\sqrt{3}}{4}$ and 1 are $\mathcal{O}^* = (0,0)$, $I^*_{\pi/12} = (\frac{5-2\sqrt{3}}{4}, \frac{7-4\sqrt{3}}{64}) \approx (0.384, 0.001)$, $I^*_{\pi/6} = (\frac{5}{4}, \frac{3}{64})$, $I^*_{\pi/4} = (2, \frac{1}{4})$, the roof top $I^*_{\pi/3} = (\frac{9}{4}, \frac{27}{64}) = (2.25, 0.421875)$, $I^*_{5\pi/12} = (\frac{5+2\sqrt{3}}{4}, \frac{7+4\sqrt{3}}{64}) \approx (2.116, 0.218)$ and $\Pi^*_{\pi/2} = (2,0)$, respectively.

For $\frac{1}{2} \leq t \leq \frac{3}{4}$ the points $\Lambda(t)$ of the left roof section and $\Lambda(\frac{3}{2} - t)$ of the right roof section have the same abscissa.

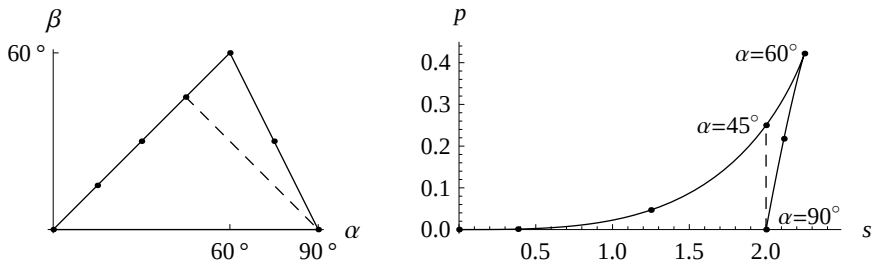

Figure 4. $\mathcal{T}$ as $\{(\alpha,\beta) \mid 0^\circ \le \beta \le \alpha \le 90^\circ - \frac{\beta}{2}\}$ and roof of $\mathcal{T}^*$ with points corresponding to $\mathcal{O}$, to the isosceles classes I_α for $\alpha = 15^\circ, 30^\circ, 45^\circ, 60^\circ$ (the maximal value of β and of p), 75°, and to Π_{90°

$\mathcal{O}^*$ and the images of the classes of infinite triangles $\{\alpha, 0, \pi - \alpha\}$, $0 < \alpha \le \frac{\pi}{2}$, form the *ground* Γ of $\mathcal{T}^*$ on the s–axis represented by the curve $(s,p) = (2t, 0), 0 \le t = \sin^2\alpha \le 1$.

The vertical segment in Figure 4 between $I^*_{\pi/4}$ and $\Pi^*_{\pi/2}$ corresponds to the curve

$$(s,p) = (2, t(1-t)),\ \tfrac{1}{2} \le t = \sin^2\alpha \le 1,$$

constituted by the images of the right–angled classes $\{\alpha, \frac{\pi}{2} - \alpha, \frac{\pi}{2}\}$, $\frac{\pi}{4} \le \alpha \le \frac{\pi}{2}$. The images of the obtuse triangle classes are to the left of this segment, the images of the acute classes to the right.

3. Coordinates of the reflection triangle

Since the elementary symmetric polynomials $s = u_1 + u_2 + u_3$, $d = u_1u_2 + u_2u_3 + u_3u_1$, $p = u_1u_2u_3$ have by Lemma 1 the property $d = \frac{s^2}{4} + p$ if $u_1 = \sin^2\alpha$, $u_2 = \sin^2\beta$ and $u_3 = \sin^2\gamma$ for some $\{\alpha,\beta,\gamma\} \in \mathcal{T}$, every symmetric polynomial in u_1, u_2, u_3 can then be expressed with s and p only:

$$\begin{aligned}
\{\alpha,\beta,\gamma\} \in \mathcal{T} \Rightarrow \sum_{\text{cyclic}} \sin^2\alpha \sin^2\beta &= d = \tfrac{s^2}{4} + p,\\
\sum_{\text{cyclic}} \sin^4\alpha &= s^2 - 2d = \tfrac{s^2}{2} - 2p,\\
\sum_{\text{cyclic}} \sin^4\alpha \sin^4\beta &= d^2 - 2sp = \left(\tfrac{s^2}{4} + p\right)^2 - 2sp,\\
\sum_{\text{cyclic}} \sin^2\alpha \sin^2\beta\left(\sin^2\alpha + \sin^2\beta\right) &= sd - 3p = \tfrac{s^3}{4} + sp - 3p.
\end{aligned} \tag{5}$$

Theorem 3. *If $r(\Delta)$ denotes the reflection triangle (class) of Δ, the map*

$$\rho\colon \mathcal{T}^* \to \mathcal{T}^*,\ (s,p) = \Delta^* \mapsto r(\Delta)^*$$

induced by r is given by $\rho(I^*_{\pi/6}) = (0,0)$ and by

$$\rho(s,p) = \big(\rho_1(s,p), \rho_2(s,p)\big) = \left(\tfrac{(s+16p)(4s-5)^2}{4s+1+64p(4s-7)}, \tfrac{p(4s-5)^6}{(4s+1+64p(4s-7))^2}\right) \text{ otherwise.} \tag{6}$$

Further,

$$D(\rho(s,p)) = D(s,p)\tfrac{(4s-5)^6(4s-1+64p(4s-9))^2}{(4s+1+64p(4s-7))^4} \tag{7}$$

if $\rho(s,p)$ is defined, i.e., *for all $(s,p) \in \mathbf{R^2}$ not lying on the hyperbola $p = -\frac{4s+1}{64(4s-7)}$. This hyperbola is tangent to the roof at $I^*_{\pi/6}$ and is otherwise exterior to $\mathcal{T}^*$.*

Proof. Consider the proper triangle $\Delta = ABC$ with angles α, β, γ and opposite sides a, b, c and reflect Δ in all its sides to get the reflection triangle $\Delta_1 = A_1B_1C_1$. Let (s,p) and (S,P) be the van IJzeren coordinates of Δ and Δ_1, respectively. Suppose first that Δ_1 is proper and consider the triangle A_1B_1C with angle $\min(3\gamma, |2\pi - 3\gamma|)$ at C. The cosine law, the formula $\cos\gamma - \cos 3\gamma = 4\sin^2\gamma\cos\gamma$ and the sine law give

$$c_1^2 = c^2 + 2ab(\cos\gamma - \cos 3\gamma) = c^2(1 + 8\sin\alpha\sin\beta\cos\gamma) \text{ and thus by (2)}$$

$$R_1^2\sin^2\gamma_1 = R^2\sin^2\gamma(1 + 4s - 8\sin^2\gamma), \text{ where } R, R_1 \text{ are the circumradii.} \tag{8}$$

The cyclic sum of (8) gives with (5)

$$R_1^2 S = R^2(s(1+4s) - 4(s^2 - 4p)) = R^2(s + 16p). \tag{9}$$

Multiplying $\sum_{\text{cyclic}} \sin^2\alpha_1 \sin^2\beta_1 = \frac{S^2}{4} + P$ by R_1^4 and using (8) for each angle of Δ_1, (5) and (9), one gets

$$\begin{aligned} R_1^4 P = {} & R^4 \sum_{\text{cyclic}} \sin^2\alpha\sin^2\beta(1+4s-8\sin^2\alpha)(1+4s-8\sin^2\beta) - R_1^4\tfrac{S^2}{4} \\ = {} & R^4 p(4s-5)^2. \end{aligned} \tag{10}$$

Note that (10) proves once again (see (1)) that all proper triangles with $s = \frac{5}{4}$ have a degenerate reflection triangle.

The product of the three formulas (8) gives together with (5)

$$\begin{aligned} R_1^6 P &= R^6 p(1+4s-8\sin^2\alpha)(1+4s-8\sin^2\beta)(1+4s-8\sin^2\gamma) \\ &= R^6 p\big((1+4s)^3 - 8(1+4s)^2 + 64(1+4s)(\tfrac{s^2}{4}+p) - 512p\big) \\ &= R^6 p\left(4s+1+64p(4s-7)\right). \end{aligned} \tag{11}$$

Use now the relations

$$R_1^2 S \cdot R_1^4 P = S \cdot R_1^6 P \text{ and } \big(R_1^4 P\big)^3 = P \cdot \big(R_1^6 P\big)^2$$

between the left sides of (9)–(11) to combine their right sides in the same way, simplify the powers of R and get $(S,P) = \rho(s,p)$ when Δ and Δ_1 are proper triangles. Since $\rho(0,0) = (0,0)$, the formula is also correct when Δ is degenerate. Theorem 4 will prove the formula when Δ_1 is degenerate and Δ proper. A limit argument establishes the validity of the formula for the infinite case $\Pi_\alpha =$

$\lim_{\varepsilon\to 0+}\{\alpha-\varepsilon, \pi-\alpha-\varepsilon, 2\varepsilon\}$. Theorem 7 gives $r(\Pi_\alpha)$ explicitly and computes its coordinates directly. The proof of (7) follows from (6) by brute computation. □

We denote by ρ^m and r^m, $m \in \mathbf{Z}$, the mth iterate of ρ and r, respectively, and speak of descendants (child, grandchild, ...) or ancestors (parents, grandparents, ...) of a point (s,p) or of a triangle (class). By (7) $(S,P) \in \mathcal{T}^* \setminus \Lambda$ has no parents $(s,p) \in \mathbf{R^2}$ outside $\mathcal{T}^*$ since $D(S,P) > 0$ and $D(s,p) < 0$ are incompatible. Note also that by (7) a non-isosceles parent of I_α (or a parent of $\mathcal{O}^*$, $\Pi^*_{\pi/2}$ that is not on the roof) has coordinates (s,p) with $s = \frac{5}{4}$ (see Theorem 4) or $p = \frac{1-4s}{64(4s-9)}$ (see Theorems 8 and 11).

Several angles play a special role in our story. We denote them by ω indexed by the rounded angle measure in degrees:

$$\omega_{12} = \arcsin\sqrt{\tfrac{3-\sqrt{7}}{8}} \approx 12.148^\circ \qquad \omega_{58} = \arcsin\sqrt{\tfrac{29-6\sqrt{6}}{20}} \approx 57.7435^\circ$$
$$\omega_{21} = \arcsin\sqrt{\tfrac{1}{8}} \approx 20.705^\circ \qquad \omega_{62} = \arcsin\sqrt{\tfrac{1+6\sqrt{6}}{20}} \approx 62.364^\circ$$
$$\omega_{38} = \arcsin\sqrt{\tfrac{3}{8}} \approx 37.761^\circ \qquad \omega_{66} = \arcsin(\sqrt{2}-\tfrac{1}{2}) \approx 66.09^\circ$$
$$\omega_{49} = \arcsin\tfrac{3}{4} \approx 48.59^\circ \qquad \omega_{68} = \arcsin\tfrac{\sqrt{1+\sqrt{6}}}{2} \approx 68.2238^\circ$$
$$\omega_{50} = \arcsin\tfrac{\sqrt{1+\sqrt{2}}}{2} \approx 50.976^\circ \qquad \omega_{71} = \arcsin\sqrt{\tfrac{3+\sqrt{17}}{8}} \approx 70.666^\circ$$
$$\omega_{51} = \arcsin\tfrac{\sqrt{17}-1}{4} \approx 51.332^\circ \qquad \omega_{72} = \arcsin\tfrac{3}{\sqrt{10}} \approx 71.565^\circ$$
$$\omega_{52} = \arcsin\sqrt{\tfrac{5}{8}} = 90^\circ - \omega_{38} \approx 52.2388^\circ$$

4. Degenerate reflection triangles

We provide here some of the details behind (1).

Theorem 4. *The reflection triangle of a nondegenerate triangle Δ is degenerate if and only if $s(\Delta) = \frac{5}{4}$,* i.e.*, if and only if the point (α,β) formed by the two smallest angles of Δ lies on the oval $\sin^2\alpha + \sin^2\beta + \sin^2(\alpha+\beta) = \frac{5}{4}$ through $(\frac{\pi}{6}, \frac{\pi}{6})$ cutting the positive axes at ω_{52}* (Figure 3)*. Triangle Δ is then obtuse with obtuse angle between $\frac{2\pi}{3}$ (for $\alpha = \beta = \frac{\pi}{6}$) and $\pi - \omega_{52}$* (infinite triangle)*.*

Proof. Let first ABC be a proper triangle with opposite sides a, b, c, circumcenter O, circumradius R, nine–point center N, centroid G and medians m_a, m_b, m_c, and let X be a point (not necessarily coplanar with ABC). [10, p. 174] proves

$$XA^2 + XB^2 + XC^2 = GA^2 + GB^2 + GC^2 + 3XG^2. \tag{12}$$

By using $m_a^2 + m_b^2 + m_c^2 = \frac{3}{4}(a^2+b^2+c^2)$ (an immediate consequence of the median theorem [10, p. 68]), taking $X = O$ and using $ON = \frac{3}{2}OG$, (12) becomes

$$3R^2 = \tfrac{1}{3}(a^2+b^2+c^2) + \tfrac{4}{3}ON^2. \tag{13}$$

The homothety $\mathsf{h}(G, \frac{1}{4})$ with center G and ratio $\frac{1}{4}$ transforms $r(ABC)$ into the pedal triangle of N [5]. By the Wallace–Simson Theorem [10, p. 137] $r(ABC)$ is thus degenerate if and only if N lies on the circumcircle, *i.e.*, if and only if (13)

becomes $a^2 + b^2 + c^2 = 5R^2$, *i.e.*, if and only if $s(ABC) = \frac{5}{4}$ by the sine law. Theorem 7 proves the result for infinite triangles. □

Here is an even shorter proof using an idea of [3, p. 78] (the proof there is flawed): when Δ is a proper triangle, the trilinear vertex matrix of $r(\Delta)$ is

$$\begin{bmatrix} -1 & 2\cos\gamma & 2\cos\beta \\ 2\cos\gamma & -1 & 2\cos\alpha \\ 2\cos\beta & 2\cos\alpha & -1 \end{bmatrix};$$

its determinant is 0 if and only if $r(\Delta)$ is degenerate; the determinant can be written as $4s(\Delta) - 5$ since one gets $s(\Delta) = 2 + 2\cos\alpha\cos\beta\cos\gamma$ by expanding $\cos\gamma = -\cos(\alpha + \beta)$.

Theorem 3 tells us that in $\mathbf{R^2}$ the parents $\rho^{-1}(\mathcal{O}^*)$ of $\mathcal{O}^* = (0, 0)$ are the origin itself and all the points $(\frac{5}{4}, p)$, $p \in \mathbf{R}$: only the origin and the points $(\frac{5}{4}, p)$, $0 \le p \le \frac{3}{64}$, lie in $\mathcal{T}^*$.

Consider a proper triangle Δ with coordinates (s, p) and its reflection triangle $\Delta_1 = A_1B_1C_1$ with sides a_1, b_1, c_1 and coordinates (S, P). (8), (9) and (11) are then also true when Δ_1 is degenerate if one replaces their left side by c_1^2, $a_1^2 + b_1^2 + c_1^2$ and $a_1^2b_1^2c_1^2$, respectively: thus $a_1^2 + b_1^2 + c_1^2 \neq 0$ and $\frac{a_1^2b_1^2c_1^2}{(a_1^2+b_1^2+c_1^2)^3} = \frac{p(64p(4s-7)+4s+1)}{(16p+s)^3}$. Suppose now that Δ_1 is degenerate, *i.e.*, $s = \frac{5}{4}$, with $c_1 = a_1 + b_1 \neq 0$ and let $x = a_1/c_1 \in [0, 1]$: then $\frac{a_1^2b_1^2c_1^2}{(a_1^2+b_1^2+c_1^2)^3} = \frac{128p(3-64p)}{(64p+5)^3} = \frac{(x-x^2)^2}{8(x^2-x+1)^3}$ is given as a function of p or x by Figure 5 with maximum $\frac{1}{54}$ for $p = \frac{1}{64}$ and for $x = \frac{1}{2}$, *i.e.*, for a parent with angles $\left\{\frac{\pi}{4}, \arcsin\sqrt{\frac{3-\sqrt{7}}{8}}, \pi - \arcsin\sqrt{\frac{3+\sqrt{7}}{8}}\right\} = \{45^\circ, \omega_{12}, 135^\circ - \omega_{12}\}$, and with minimum 0 for $I_{\pi/6}$. The following theorem is proven.

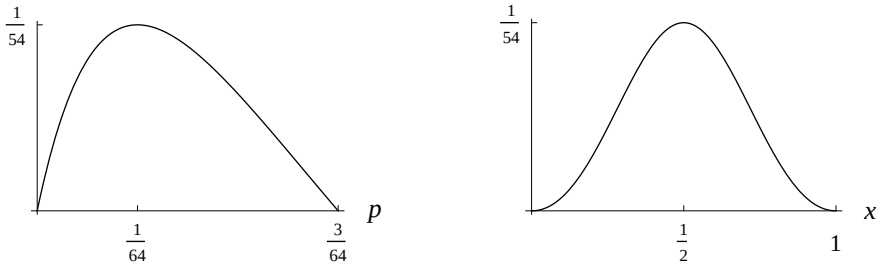

Figure 5. Graphs of $\frac{128p(3-64p)}{(64p+5)^3}$ and $\frac{(x-x^2)^2}{8(x^2-x+1)^3}$

Theorem 5. *A finite degenerate triangle Δ_1 with three different vertices is the reflection triangle of exactly 5 triangles. If the midpoint of the longest side is not a vertex, these 5 triangles are the degenerate triangle itself, a pair of non-similar non-isosceles triangles and their mirror images in the line of Δ_1. If the midpoint*

of the longest side is the third vertex, these 5 *triangles are the degenerate triangle itself, a non-isosceles triangle with angles* $\{45^\circ, \omega_{12}, 135^\circ - \omega_{12}\}$*, its mirror image in the line of* Δ_1 *and their reflections in the midpoint of the longest side. The corresponding coordinates* (s, p) *of the nondegenerate parents are given by* $s = \frac{5}{4}$ *and by the two (possibly equal) solutions* $p \in \left]0, \frac{3}{64}\right[$ *of* $\frac{128p(3-64p)}{(64p+5)^3} = \frac{(x-x^2)^2}{8(x^2-x+1)^3}$*, where* x *is the ratio of the shortest side of* Δ_1 *to the longest side* (Figure 5).

A finite degenerate triangle with only two different vertices is the reflection triangle of exactly 2 *triangles: itself by convention and an isosceles triangle with equal angles* $\frac{\pi}{6}$*. A point is the reflection triangle of itself only.*

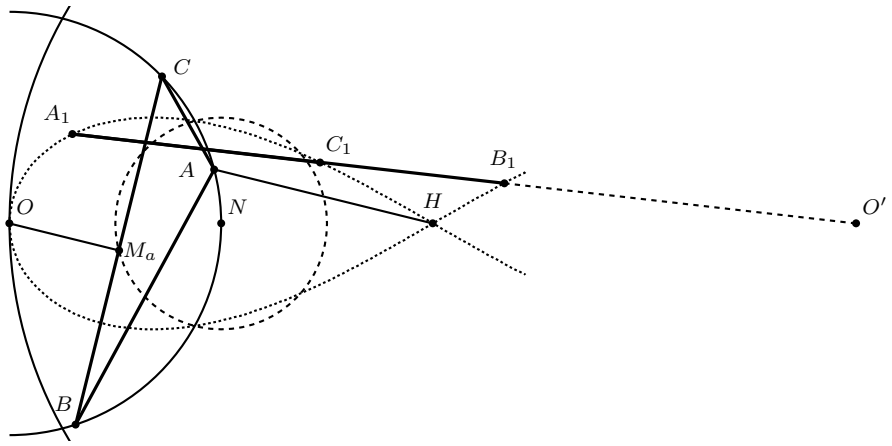

Figure 6. Construction of an inscribed triangle ABC with degenerate reflection triangle $A_1B_1C_1$. The dotted curve is the locus $\mathcal{L}$ of A_1 as function of A.

Here is a construction of all $\Delta \in \mathcal{T}$ with $s = \frac{5}{4}$ that is simpler than the corresponding construction of [5]. Take a point O and a circle $O(R)$ of radius R centered at O (Figure 6). Choose $N \in O(R)$ and reflect O in N to get the orthocenter H. We search for $A, B, C \in O(R)$ with $\overrightarrow{OH} = \overrightarrow{OA} + \overrightarrow{OB} + \overrightarrow{OC}$. Choose any $A \in O(R)$ with $HA \leq 2R$, take M_a given by $\overrightarrow{OM_a} = \frac{1}{2}\overrightarrow{AH}$ and construct the chord $a = BC$ with midpoint M_a to get – if not degenerate – a triangle ABC with $s = \frac{5}{4}$. $N\left(\frac{R}{2}\right)$ is then the nine–point circle of ABC. In the four cases where ABC degenerates into a chord (see below), one gets an infinite triangle with angle ω_{52} at the double vertex of ABC by taking a triangle's semi–infinite side along ABC and a finite side on the tangent to $O(R)$. Whether ABC is degenerate or not, one has then also $\overrightarrow{OM_b} = \frac{1}{2}\overrightarrow{BH}$ and $\overrightarrow{OM_c} = \frac{1}{2}\overrightarrow{CH}$.

There is an even simpler determination of M_a: construct the centroid G given by $\overrightarrow{OG} = \frac{2}{3}\overrightarrow{ON}$ and get M_a as the intersection of AG and $N\left(\frac{R}{2}\right)$ on the other side of G.

Let $A_1B_1C_1$ be the degenerate reflection triangle. The line $A_1B_1C_1$ goes through the reflection O' of O in H [5, without proof]: we give here a demonstration by the author, D. Grinberg (personal communication). The Simson line of any point X

of the circumcircle bisects XH [7, p. 46], hence the Simson line of N goes in our case through the midpoint M_{NH} of NH; the homothety $\mathsf{h}(G,4)$ that transforms the pedal triangle of N into the reflection triangle sends thus M_{NH} to a point of the line $A_1B_1C_1$; but this point is on the line ON at distance $\frac{2}{3}R+4\big(\frac{3}{2}R-\frac{2}{3}R\big)=4R$ from O and is thus O'.

Let $\mathcal{L}$ be the locus of A_1 as function of A. The side midpoints of ABC lie on the nine–point circle $N\big(\frac{R}{2}\big)$ inside $O(R)$, and this arc is the locus of M_a as function of A. As A moves on the portion of $O(R)$ inside $H(2R)$, $\Pi_{\omega_{52}}$ is represented at the arc's extremities $E_\pm$ with $\angle NOE_\pm=\pm\arccos\frac{1}{4}\approx\pm75.523^\circ$ and at $L_\pm$ given by $O(R)\cap N\big(\frac{R}{2}\big)\cap\mathcal{L}$ with $\angle NOL_\pm=\pm2\arcsin\frac{1}{4}\approx\pm28.955^\circ$. $I_{\pi/6}$ is represented at $\angle NOA=0^\circ,\pm60^\circ$. Any other $\Delta\in\mathcal{T}$ with $s=\frac{5}{4}$ is represented six times (once in each of the intervals delimited by the seven angles above) by a triply covered triangle (with each vertex in turn getting the label A) and its triply covered image under reflection in the line ON. The corresponding six degenerate reflection triangles $A_1B_1C_1$ occupy only two positions symmetrically to the line ON and each vertex in turn is A_1; the situation is similar for the infinite triangle and for the isosceles case: $\mathcal{L}$ contains thus also B_1 and C_1 (on the corresponding altitudes of ABC).

Place the isosceles triangle $\Delta=ABC$ of Figure 2 with equal 30°–angles and its degenerate reflection triangle $A_1B_1C_1$ into Figure 6, with B at N; let then A and B glide towards L_- (and C towards E_+) on the nine–point circle of Figure 6 in such a way that the reflection triangle $A_1B_1C_1$ remains degenerate: the angle α at A grows from 30° to ω_{52}, the coordinates (s,p) of Δ travel on the line $s=\frac{5}{4}$ from $(\frac{5}{4},\frac{3}{64})=I^*_{30^\circ}$ on the roof to $(\frac{5}{4},0)=\Pi^*_{\omega_{52}}$ on the ground and the ratio $x=A_1C_1:B_1C_1$ runs from 0 to 1 in Figure 5.

The homothety $\mathsf{h}(G,-2)$ sends $N\big(\frac{R}{2}\big)$ to $O(R)$ and thus $L_\pm$ to $E_\mp$ (hence $\{G\}=E_+L_-\cap E_-L_+$). By considering a degenerate triangle ABC with vertices E_+,L_- or E_-,L_+ (infinite triangle's case), one sees that the antipode L'_- of L_- on $N\big(\frac{R}{2}\big)$, being at distance R from H, is the midpoint of HE_+: L_- lies on the circle $L'_-(R)$ with diameter HE_+. The tangents to $\mathcal{L}$ at H form a 60°–angle because they are the tangents to $O(R)$ corresponding to the isosceles ABC representing $I_{\pi/6}$.

In a cartesian coordinate system with origin O and $N=(R,0)$, the locus $\mathcal{L}$ of A_1 as function of $A=(R\cos\varphi,R\sin\varphi)$ is the curve

$$A_1=\left(\frac{2R(7-2\cos\varphi)(1-\cos\varphi)}{5-4\cos\varphi},\frac{2R\sin\varphi(2\cos\varphi-1)}{5-4\cos\varphi}\right),\ |\varphi|\le\arccos\frac{1}{4}. \tag{14}$$

(14) gives also B_1 and C_1 from the polar coordinates of B and C, respectively. The range of the polar angle of B and C is smaller than for A: when A goes from E_- to E_+, B and C start at L_+, go to $E_\pm$ in opposite directions and come back to L_-.

The end points of $\mathcal{L}$ are the midpoints of the segments $O'L_\pm$. Indeed, since A_1 is the upper end point U of $\mathcal{L}$ for the infinite triangle's case $A=E_-$, $B=C=B_1=C_1=L_+=\big(\frac{7}{8}R,\frac{\sqrt{15}}{8}R\big)$, one has $U=\big(\frac{39}{16}R,\frac{\sqrt{15}}{16}R\big)$ by (14). The line

UL_+ is tangent to $\mathcal{L}$ at L_+ since it would be the line of the degenerate reflection triangle in the infinite triangle's case.

Theorem 6. *Let Δ be an proper triangle with degenerate reflection triangle Δ_1. The following properties are equivalent.*
(1) *Δ_1 has two equal sides and three different vertices,* i.e.*, Δ has angles 45° and ω_{12}.*
(2) *The middle vertex of Δ_1 is halfway between the corresponding vertex of Δ and the orthocenter of Δ,* i.e.*, on the nine–point circle of Δ but not on its circumcircle.*

Proof. (2)⇒(1): (14) shows that the upper part of $\mathcal{L}$ cuts $N\left(\frac{R}{2}\right)$ at C_1 if and only if the polar angle of C is $\arccos\frac{7}{8}$ (infinite triangle's case) or $\arccos\frac{3}{4}$: in this second case, $C_1 = \left(\frac{11}{8}R, \frac{\sqrt{7}}{8}R\right)$ is the midpoint of HC. By computing then with (14) the intersections of the line $O'C_1$ and of $\mathcal{L}$, one gets the polar angles $\arccos\frac{5+\sqrt{7}}{8} \approx 17.114^\circ$ for A (say) and $-\arccos\frac{5-\sqrt{7}}{8} \approx -72.886^\circ$ for B, hence $\angle AOB = 90^\circ$ and $\angle COA = \arccos\frac{1+\sqrt{7}}{4}$, thus $\angle ACB = 45^\circ$ and $\angle ABC = \omega_{12}$ by the inscribed angle theorem. C_1 is the midpoint of A_1B_1 by Theorem 5.

(1)⇒(2): there is only one position on the upper part of $\mathcal{L}$ where both shorter sides of Δ_1 are equal. □

5. Infinite reflection triangles

Theorem 7. *The action of r on a class of infinite triangles is given by $r(\Pi_\alpha) = \Pi_{(2\alpha+\arctan(3\tan\alpha)) \bmod \pi}$* (Figure 8) *and $r(\Pi_\alpha)^* = \left(\frac{s(4s-5)^2}{4s+1}, 0\right)$ for $0 < \alpha \le \frac{\pi}{2}$, where $s = s(\Pi_\alpha) = 2\sin^2\alpha$.*

Proof. The theorem is true for $\alpha = \frac{\pi}{2}$. Take an acute angle α, consider a triangle with an angle 2α between sides of length 1 and 2 and define δ as the acute or right angle formed by the bisector of 2α and the opposite side. Using the angle bisector theorem and setting $s = 2\sin^2\alpha$ one gets $\sin^2\delta = \frac{9s}{8s+2}$ and thus $\tan\delta = 3\tan\alpha$, *i.e.*, $\delta = \arctan(3\tan\alpha)$. A figure shows that the formula for $r(\Pi_\alpha)$ is exact. Developing $r(\Pi_\alpha)^* = \left(2\sin^2(2\alpha+\delta), 0\right)$ leads to the expression in s. □

Note that $r(\Pi_{\pi/6}) = \Pi_{\pi/3}$. When restricted to the s–axis, ρ is given by $\rho(s,0) = \left(\frac{s(4s-5)^2}{4s+1}, 0\right)$: the fixed points are $(0,0)$, $(\frac{3}{4},0) = \Pi^*_{\omega_{38}}$ and $(2,0)$, they lie on the ground Γ and are repelling in $\mathbf{R^2}$. Since an infinite triangle has an infinite reflection triangle, ρ maps Γ to Γ (Figures 7 and 8): $\rho|_\Gamma$ is a triple covering of Γ. Since no point of $\Gamma \setminus \{(0,0)\}$ has parents outside Γ by the formula for ρ and by (7), the backward and forward orbit under ρ of $(s,0)$, $s \in]0,2]$, remains in Γ. $\rho^n|_\Gamma$ is a 3^n–fold covering of Γ with 3^n fixed points for every integer $n \ge 1$ (Figure 7). Since $3^n > 3 + 3^2 + \cdots + 3^{n-1}$ for $n > 1$, $\rho|_\Gamma$ has n–cycles for all $n \ge 1$, *i.e.*, cycles of *minimal* period n. The length of the longest monotonicity interval of the first coordinate of $\rho^n|_\Gamma$ tends to 0 for $n \to \infty$. Each periodic or infinite forward orbit has a countable backward orbit. The following theorem is proven.

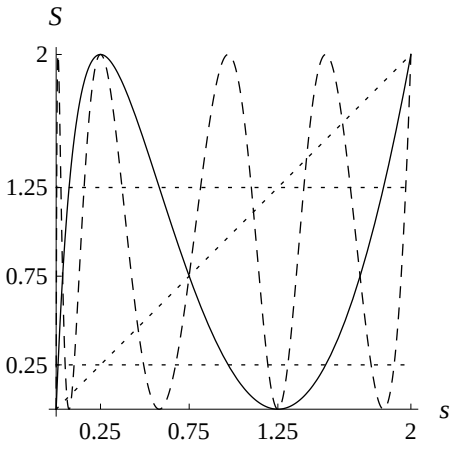

Figure 7. First coordinate of $\rho|_\Gamma$ (plain) and of $\rho^2|_\Gamma$ (dashed)

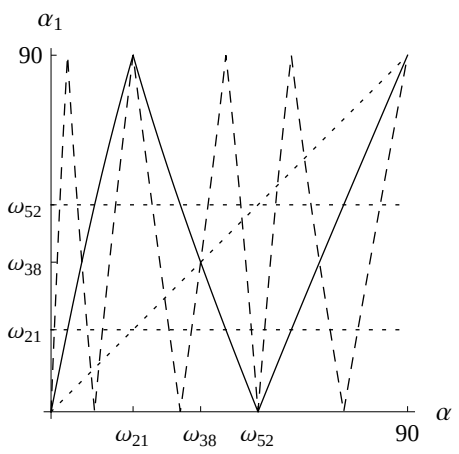

Figure 8. $\alpha_1 = \alpha_1(\alpha)$ given by $\Pi_{\alpha_1} = r(\Pi_\alpha)$ and its iterate (in $^\circ$)

Theorem 8. (1) *The two or three parents (in* $\mathbf{R^2}$*) of any* $\Pi^*_\alpha = (S, 0)$, $0 < S \le 2$, *all lie on* $\Gamma \setminus \{(0,0)\}$ *and their abscissae are the solutions of* $\frac{s(4s-5)^2}{4s+1} = S$. *The parents of* $\Pi^*_{\pi/2} = (2,0)$ *are thus itself and* $(\frac{1}{4}, 0) = \Pi^*_{\omega_{21}}$. $\Pi^*_{\omega_{52}} = (\frac{5}{4}, 0)$ *and* $(0,0)$ *are the only parents of* $(0,0)$ *on the* s*–axis and their abscissae are the solutions of* $\frac{s(4s-5)^2}{4s+1} = S = 0$.
(2) *The backward orbit of any* Π^*_α *under* ρ *lies in* Γ *and is countably dense in* Γ.
(3) $\rho|_\Gamma$ *has a nonzero finite number of* n*–periodic points for all integers* $n \ge 1$.
(4) *There are uncountably many disjoint infinite forward orbits of* $\rho|_\Gamma$.
(5) *Every nondegenerate infinite triangle has exactly* 3 *parents since* $\Pi_{\omega_{21}}$ *generates two inversely similar parents of a given rectangular infinite triangle.*

Figure 7 shows that $\rho|_\Gamma$ has three 2–cycles. Since the abscissa of $\rho^2(s,0) - (s,0)$ is

$$\frac{8s(s-2)(4s-3)(8s^2-12s+1)(256s^4-832s^3+832s^2-260s+13)}{(4s+1)^2(64s^3-160s^2+104s+1)},$$

the points $(\frac{3\pm\sqrt{7}}{4}, 0)$, which are $\Pi^*_{\omega_{12}}$ and $\Pi^*_{45^\circ+\omega_{12}}$, are exchanged by ρ, as are the points $\left(\frac{1}{16}\left(13-\sqrt{13}\pm\sqrt{78-2\sqrt{13}}\right),0\right)$, *i.e.*, $\Pi^*_{10.08\ldots^\circ}$ and $\Pi^*_{48.24\ldots^\circ}$, and $\left(\frac{1}{16}\left(13+\sqrt{13}\pm\sqrt{78+2\sqrt{13}}\right),0\right)$, *i.e.*, $\Pi^*_{28.68\ldots^\circ}$ and $\Pi^*_{63.96\ldots^\circ}$; these 2–cycles are repelling in $\mathbf{R^2}$. Notice that ω_{12} already appeared in Theorem 5. The infinite triangle and its grandchild are directly similar when corresponding to the first 2–cycle and inversely similar in the two other 2–cycles. $\rho|_\Gamma$ has eight 3–cycles, they are all repelling in $\mathbf{R^2}$. Four 3–cycles are given by the roots of $16777216s^{12} - 167772160s^{11} + 720371712s^{10} - 1735131136s^9 + 2569863168s^8 - 2413019136s^7 + 1429815296s^6 - 516909056s^5 + 106880256s^4 - 11406272s^3 +$

$543312s^2 - 8820s + 21$, approximately

$$\begin{array}{lll} 0.00285317 & 0.0702027 & 1.22068 \\ 0.0254111 & 0.553455 & 1.33684 \\ 0.145175 & 1.7937 & 1.03778 \\ 0.336812 & 1.91456 & 1.56253 \end{array}$$

and the four other 3–cycles consist of the roots of $16777216s^{12} - 163577856s^{11} + 686817280s^{10} - 1625292800s^9 + 2381971456s^8 - 2236841984s^7 + 1345982464s^6 - 504474624s^5 + 110822912s^4 - 12847168s^3 + 670592s^2 - 12028s + 31$, approximately

$$\begin{array}{lll} 0.00307391 & 0.0755414 & 1.28031 \\ 0.028553 & 0.61172 & 1.15683 \\ 0.172455 & 1.89595 & 1.47455 \\ 0.409917 & 1.75352 & 0.887586. \end{array}$$

There are no other fixed points or 2– or 3–cycles on the s–axis if one allows $s \in \mathbf{C}$.

6. Fixed points and 2–cycles of ρ

Since

$$\rho(s,p) - (s,p) = \Big(\tfrac{4(-48ps+100p+4s^3-11s^2+6s)}{256ps-448p+4s+1}, -\tfrac{8p(4s-7)(32p-8s^2+16s-9)(64ps-112p+16s^3-60s^2+76s-31)}{(256ps-448p+4s+1)^2}\Big), \quad (15)$$

the 7 fixed points of ρ in $\mathbf{C^2}$ are $\mathcal{O}^*$, $I^*_{\pi/3}$, $\Pi^*_{\pi/2}$, $\{\frac{\pi}{7}, \frac{2\pi}{7}, \frac{4\pi}{7}\}^* = (\frac{7}{4}, \frac{7}{64})$, $\Pi^*_{\omega_{38}} = (\frac{3}{4}, 0)$, $\big(\frac{6-\sqrt{5}}{4}, \frac{8\sqrt{5}-17}{64}\big) \approx \{0.297, 0.561, 2.284\}^* \approx \{17.027^\circ, 32.132^\circ, 130.84^\circ\}^*$ in $\mathcal{T}^*$ and $\big(\frac{6+\sqrt{5}}{4}, \frac{-17-8\sqrt{5}}{64}\big) \in \mathbf{R^2} \setminus \mathcal{T}^*$. The eigenvalues of the Jacobian matrix of ρ at the fixed points show that $I^*_{\pi/3}$ is attracting in $\mathbf{R^2}$ and that all other fixed points are repelling. The critical points of ρ form the line $s = \frac{5}{4}$ and their image is the origin. A triangle Δ and its reflection triangle are directly similar when Δ is degenerate, equilateral, infinite rectangular or heptagonal, and they are inversely similar when Δ^* is $\Pi^*_{\omega_{38}}$ or $\big(\frac{6-\sqrt{5}}{4}, \frac{8\sqrt{5}-17}{64}\big)$. $\big(\frac{6-\sqrt{5}}{4}, \frac{8\sqrt{5}-17}{64}\big)$ seems to correspond to a new special triangle, whose angles are probably not rational multiples of π. Note that $s\big(\{\frac{\pi}{15}, \frac{\pi}{5}, \frac{11\pi}{15}\}\big)$ is also $\frac{6-\sqrt{5}}{4}$.

Due to the location of the fixed points and to the shape of $\mathcal{T}^*$, which is closed, every forward orbit with both rightward and upward direction right from $s = \frac{7}{4}$ is forced to converge to $I^*_{\pi/3}$: as we will show, this is the case when the class of the base triangle lies in a dense open subset of $\mathcal{T}$ containing among others the classes of acute and right-angled triangles as well as the obtuse isosceles classes that are not $I_{\pi/6}$ or one of its ancestors.

There are 24 2–cycles of ρ in $\mathbf{C^2}$: three have already been described and lie in Γ, seven lie in $\mathcal{T}^* \setminus \Gamma$; the others are extraneous with three in $\mathbf{R^2} \setminus \mathcal{T}^*$ and eleven outside $\mathbf{R^2}$. The seven 2–cycles in $\mathcal{T}^* \setminus \Gamma$ all correspond to 2–cycles of obtuse triangles in $\mathcal{T}$, whose acute angles are approximately

$$\begin{array}{lll}
\{8.0763^\circ, 3.79275^\circ\} & \text{and} & \{38.5099^\circ, 17.99879^\circ\} \\
\{31.70115^\circ, 9.19698^\circ\} & \text{and} & \{32.64671^\circ, 21.218476^\circ\} \\
\{38.47736^\circ, 31.19757^\circ\} & \text{and} & \{65.27712^\circ, 13.75689^\circ\} \\
\{8.92974^\circ, 4.0548^\circ\} & \text{and} & \{42.23276^\circ, 19.04471^\circ\} \\
\{28.3017^\circ, 21.20007^\circ\} & \text{and} & \{53.85134^\circ, 16.98919^\circ\} \\
\{28.56877^\circ, 8.60948^\circ\} & \text{and} & \{41.35919^\circ, 23.72889^\circ\} \\
\{28.43994^\circ, 23.62517^\circ\} & \text{and} & \{60.10737^\circ, 12.60168^\circ\}
\end{array}$$

A triangle is directly similar to its grandchild in the first and in the last two 2–cycles, and inversely similar in the other ones. All these seven 2–cycles are repelling since all eigenvalues of the product $D\rho(s_1, p_1) \cdot D\rho(s_2, p_2)$ of the Jacobian matrices have, for each cycle, a modulus > 1. These 2–cycles are found by factoring the resultants of the two polynomial equations $\rho^2(s, p) = (s, p)$. The first 2–cycle above is given by the real roots s of $65536s^8 - 557056s^7 + 1957888s^6 - 3655680s^5 + 3872768s^4 - 2305408s^3 + 724768s^2 - 108760s + 4631$. The two following 2–cycles and a 2–cycle of $\mathbf{R^2} \setminus \mathcal{T}^*$ are given by the real roots s of $1048576s^{10} - 13107200s^9 + 70713344s^8 - 215482368s^7 + 406921216s^6 - 490459136s^5 + 373159424s^4 - 169643008s^3 + 40513488s^2 - 3790120s + 124099$. For all these four cycles,

$$\begin{aligned}
p = {} & (1/337368791278296246393273057280) \cdot \\
& (569737838757513187116449932928614 4s^{21} - 154889486440160171050477250146205696s^{20} \\
& + 196981555615894467829077018253302169 6s^{19} - 155664456710682800898723927916554485 76s^{18} \\
& + 856314627144876256787835950004489420 80s^{17} - 348112463554334373128224482745250742272s^{16} \\
& + 108350734588874886978138748463167307776 0s^{15} - 263951709209923803704038658735747996057 6s^{14} \\
& + 510111041140536292090774321305741583974 4s^{13} - 787959868256849082489150009826496374374 4s^{12} \\
& + 975501092015866666509543355929071714304 0s^{11} - 966512339039690096528929885529149800448 0s^{10} \\
& + 762172376510086419788583062308698456064 0s^9 - 473693261600146140405367041940343737548 8s^8 \\
& + 228611765030602679588457172054289049190 4s^7 - 838913081019577908008862079371766857728s^6 \\
& + 227315320515680762946527159936618376192s^5 - 436538007212937413379450471669442931 20s^4 \\
& + 560270257133815609539380747902469913 6s^3 - 441294571999478960624696851928272768s^2 \\
& + 190053879695790975456428651547484 04s - 340848826010088138830599778323827).
\end{aligned}$$

The two following 2–cycles and a 2–cycle of $\mathbf{R^2} \setminus \mathcal{T}^*$ are given by the real roots s of $1048576s^{10} - 12582912s^9 + 65470464s^8 - 193789952s^7 + 359325696s^6 - 432427008s^5 + 337883648s^4 - 166321920s^3 + 48099088s^2 - 7029296s + 326343$. The last two 2–cycles and the last 2–cycle of $\mathbf{R^2} \setminus \mathcal{T}^*$ are given by the real roots of $1048576s^{10} - 12058624s^9 + 59965440s^8 - 168624128s^7 + 293994496s^6 - 327127040s^5 + 229654528s^4 - 96299264s^3 + 21257456s^2 - 1867864s + 56317$. For all these six cycles,

$$\begin{aligned}
p = {} & (1/456742818834136280978930342445235125302067 2) \cdot \\
& (-366989312382456495272333625478786932593498521 60s^{23} \\
& + 984810666870471120012672280485882885859228778496s^{22} \\
& - 124704377587394217766523377718140868506315684577 28s^{21} \\
& + 991051704988365587160426345383537044930854482083 84s^{20} \\
& - 554556689733191355308583432652149828431320367235072s^{19} \\
& + 232334000082876148494384889254825107547791309563494 4s^{18}
\end{aligned}$$

$$
\begin{aligned}
&- 75649601126342172266492745100839877278756287713116 16 s^{17}\\
&+ 19612556761550162606749159530083584049909501234511872 s^{16}\\
&- 41140288987466333778005801486897731005916908693225472 s^{15}\\
&+ 70558385413803161958940236549368891637028689744494592 s^{14}\\
&- 99560699194220260609319527114212812701788113291182080 s^{13}\\
&+ 11589935616857067400676806343729575114476765830551961 6 s^{12}\\
&- 11126423723841509264289535056918622777839126723113779 2 s^{11}\\
&+ 87779176155017883059837850878398210925269779119865856 s^{10}\\
&- 56523554163594762683354338049606423057525776982736896 s^{9}\\
&+ 29393921592752966963028643161504310305801154828042240 s^{8}\\
&- 12157286006804762121004498275570505776082534409453568 s^{7}\\
&+ 39145923003886730525275404552483531816888842032619 52 s^{6}\\
&- 95255589942240640963730923953260807788249598179225 6 s^{5}\\
&+ 16799078312236410969454041587284439897936411646540 8 s^{4}\\
&- 20227383407106448892530229235014104156364912461632 s^{3}\\
&+ 15263940554200662713054688145220076786455771125 28 s^{2}\\
&- 63861725292150155008281030050782500647383181532 s\\
&+ 11229716715665162890067074314783780614924425 87).
\end{aligned}
$$

When p is replaced by one of the given polynomials, the corresponding polynomials for s can be indeed factored out in both coordinates of $\rho^2(s,p)-(s,p)$. Two of the 2–cycles of ρ outside $\mathbf{R^2}$ are the cycle

$$(s_\pm, p_\mp) = \left(\tfrac{5+i\pm\sqrt{-1-8i}}{4}, \tfrac{-19-22i\mp\sqrt{-56+202i}}{64}\right)$$

and its complex conjugate cycle; the remaining nine such 2–cycles are given by the non-real roots of the above polynomials in s with the corresponding above formulas for p.

In Section 10 we will prove that there are cycles of any finite length in $\mathcal{T}^* \setminus \Gamma$.

7. Isosceles triangles

Since the reflection triangle of an isosceles triangle is isosceles, ρ maps the roof Λ of Figure 4 to itself. Plug the parametric representation (4) of Λ into formula (6) to obtain $\rho(\Lambda(t))$. An investigation of this function (Figure 9) and its derivative proves that, as I^*_α travels on Λ from the origin to $(2,0)$, $\rho(I^*_\alpha)$ moves continuously as follows: start at the origin, left roof section up for $0 < \alpha \le \frac{\pi}{12}$, right roof section down for $\frac{\pi}{12} \le \alpha \le \frac{\pi}{6}$, right roof section up for $\frac{\pi}{6} \le \alpha \le \frac{\pi}{3}$, a very short down and up round trip on the left roof section near the top for $\frac{\pi}{3} \le \alpha \le \frac{5}{12}\pi$ – with turning (deepest) point

$$I^*_{\omega_{58}} = \left(\tfrac{168\sqrt{6}-187}{100}, \tfrac{3\left(135664\sqrt{6}-326751\right)}{40000}\right) \approx (2.245, 0.417)$$

for $\alpha = \omega_{68}$ – and final descent of the right roof section for $\frac{5}{12}\pi \le \alpha < \frac{\pi}{2}$ with arrival at the bottom $\Pi^*_{\pi/2}$. Not to forget: $\rho(I^*_{\pi/6})$ has been instantly catapulted from $(2,0)$ to the origin!

It is now easy to count the isosceles parents of the isosceles class I_α, $0 < \alpha < \frac{\pi}{2}$ (Figure 10): one if $0 < \alpha < \omega_{58}$, two if $\alpha = \omega_{58}$ and three otherwise. The three isosceles parents of $I_{\pi/3}$, for example, are $I_{\pi/3}$, $I_{\pi/12}$ and $I_{5\pi/12}$ (Figure 2).

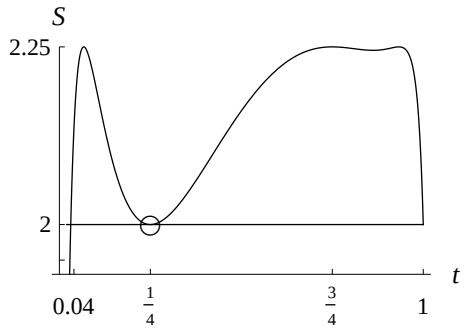

Figure 9. Abscissa $S(t)$ of $\rho(\Lambda(t))$ as a function of $t = \sin^2\alpha$: $S(0) = S(\frac{1}{4}) = 0$, $S(0.04) > 2$ and $S'(t) > 10$ on $[0, 0.04]$. The ordinate of $\rho(\Lambda(t))$ increases and decreases with $S(t)$.

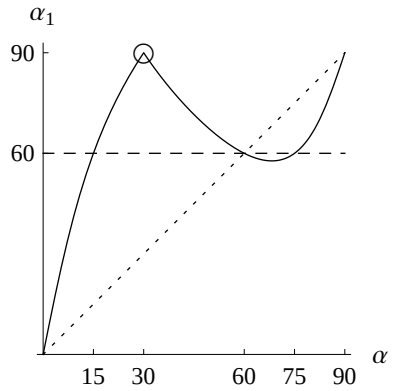

Figure 10. $\alpha_1 = \alpha_1(\alpha)$ given by $I_{\alpha_1} = r(I_\alpha)$ (in $^\circ$)

If the abscissa of I^*_α is $> \frac{7}{4}$, *i.e.*, if $\alpha > \arcsin\frac{\sqrt{3-\sqrt{2}}}{2} \approx 39.024^\circ$, and if α is different from $\frac{\pi}{3}$, $\rho(I^*_\alpha)$ lies on the roof strictly right from and above I^*_α – as an investigation of $\rho(\Lambda(t)) - \Lambda(t)$ shows (Figure 11). The forward orbit of I^*_α converges then to a fixed point that *must* be the roof top. But an I^*_α with smaller abscissa > 0 will also be stretched over $s = \frac{7}{4}$ by some iterate ρ^n of ρ (Figure 9): the orbit will thus also converge to the top unless $\rho^n(I^*_\alpha)$ transits through $\Pi^*_{\pi/2}$ with immediate transfer to the origin. The latter configuration is only possible if I^*_α belongs to the backward orbit of $I^*_{\pi/6}$: when limited to Λ, this orbit has no bifurcations and is thus an infinite sequence $I^*_{\pi/6}, I^*_{\alpha_{-1}} \approx I^*_{6.33^\circ}, I^*_{\alpha_{-2}} \approx I^*_{1.269^\circ}, \ldots$ with $\frac{\pi}{6} > \alpha_{-1} > \alpha_{-2} > \cdots$ tending to 0. The following theorem is proven.

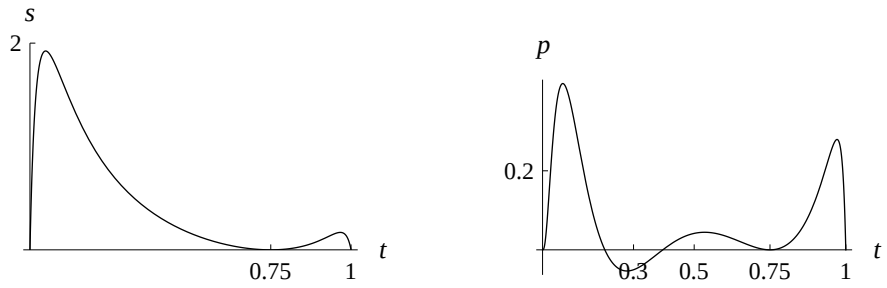

Figure 11. Abscissa s and ordinate p of $\rho(\Lambda(t)) - \Lambda(t)$ as functions of t with non-negative ordinate for $\frac{3-\sqrt{2}}{4} \le t \le 1$

Theorem 9. *The iterated reflection class of an isosceles base triangle class I_α converges to an equilateral limit unless I_α belongs to the backward orbit of $I_{\pi/6}$ and converges thus to a degenerate limit in a finite number of steps,* i.e., *unless $I_\alpha = I_{\pi/6}$, $I_{6.33...^\circ}$, $I_{1.269...^\circ}$, ..., where $I_{\pi/6} = r(I_{6.33...^\circ}), \ldots$*

See [4] for another proof, which iterates the formula

$$\cos^2 \alpha_1 = \frac{\cos^2 \alpha (4\cos^2 \alpha - 3)^2}{1 + 16\cos^2 \alpha - 16\cos^4 \alpha}$$

for a nondegenerate $r(I_\alpha) = I_{\alpha_1}$ and shows that $\lim_{n\to\infty} \cos \alpha_n = \frac{1}{2}$ unless some α_n is $\frac{\pi}{6}$.

8. Parents

ρ maps the point $(\frac{7}{4}, p)$ of the vertical line $s = \frac{7}{4}$ horizontally to the point $(8p + \frac{7}{8}, p)$ of the oblique line $s = 8p + \frac{7}{8}$.

ρ maps the vertical segment $s = 1 + \frac{\sqrt{17}}{4} \approx 2.031$, $\frac{-105+28\sqrt{17}-16\sqrt{95-23\sqrt{17}}}{64} \le p \le \frac{-105+28\sqrt{17}+16\sqrt{95-23\sqrt{17}}}{64}$, delimited by the roof onto the vertical segment $s = \frac{5+3\sqrt{17}}{8} \approx 2.171$, $\frac{19+5\sqrt{17}}{128} \le p \le \frac{181\sqrt{17}-701}{128}$, delimited by the roof between $I^*_{\omega_{71}}$ and $I^*_{\omega_{51}}$. As p grows on the first segment,

$$\rho\big(1 + \tfrac{\sqrt{17}}{4}, p\big) = \left(\tfrac{5+3\sqrt{17}}{8}, P = \frac{(\sqrt{17}-1)^6 p}{\left(64(\sqrt{17}-3)p + \sqrt{17} + 5\right)^2}\right) \tag{16}$$

travels on the second segment from the bottom up and back, reaching the left roof section for $p = \frac{4+\sqrt{17}}{64}$ (Figure 12). This gives two acute isosceles parents of $I_{\omega_{71}}$ and one acute non-isosceles parent of $I_{\omega_{51}}$.

We define the *van IJzeren rational function*

$$v(s) = \frac{(4s-5)^2\left((4s-5)^2 - 4S(4s-7)\right)\left(s(4s-5)^2 - S(4s+1)\right)}{-16\left(16s^2 - 32s - 1\right)^2} \tag{17}$$

with parameter S, double zero at $s = \frac{5}{4}$ and double poles at $s = 1 + \frac{\sqrt{17}}{4} \approx 2.031$ $\big($if $S \ne \frac{5+3\sqrt{17}}{8}\big)$ and at $s = 1 - \frac{\sqrt{17}}{4} \approx -0.031$ $\big($if $S \ne \frac{5-3\sqrt{17}}{8}\big)$. For

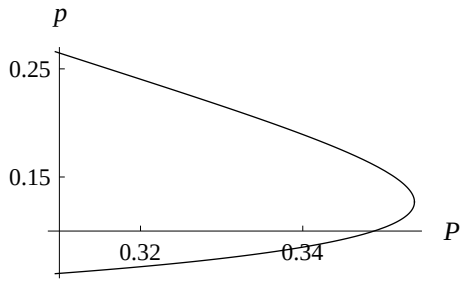

Figure 12. p–values as function of P in (16) and (19)

$S = \frac{5+3\sqrt{17}}{8}$, $v\big(1+\frac{\sqrt{17}}{4}\big) = \frac{1651-251\sqrt{17}}{2176} \approx 0.283$ by continuous extension; the situation is analogous for $S = \frac{5-3\sqrt{17}}{8}$. $v(s)$ is obtained from (6) by solving $S = \rho_1(s,p)$ for p and replacing then p in $\rho_2(s,p)\,(= P)$.

Theorem 10 (Parents)**.** *The parents* $\rho^{-1}(\Delta_1^*)$ *(in* $\mathbf{R^2}$*) of any* $\Delta_1^* = (S,P) \in \mathcal{T}^* \setminus \{(0,0)\}$ *are the points* $(s,p) \in \mathbf{R^2}$ *with*

$$s \in \left]0, \tfrac{9}{4}\right] \setminus \{\tfrac{5}{4}\},\ s \neq \tfrac{9}{4} \text{ if } (S,P) = (2,0),\ v(s) = P,$$
$$p = \frac{s(4s-5)^2 - S(4s+1)}{-16\big((4s-5)^2 - 4S(4s-7)\big)} \tag{18}$$

or

$$S = \frac{5+3\sqrt{17}}{8},\ s = 1+\frac{\sqrt{17}}{4},\ \frac{p(4s-5)^6}{(4s+1+64p(4s-7))^2} = P, \tag{19}$$

i.e.,

$$p = \frac{8(\sqrt{17}+1)P+65\sqrt{17}-297 \pm \sqrt{128\big(101-29\sqrt{17}\big)P-38610\sqrt{17}+160034}}{512\big(3\sqrt{17}-13\big)P}$$

with two values for $P < \frac{181\sqrt{17}-701}{128}$ *and one for* $P = \frac{181\sqrt{17}-701}{128}$ (Figure 12).

The denominators are never zero. All between three and seven parents of $(S,P) \in \mathcal{T}^* \setminus \Gamma$ *lie in* $\mathcal{T}^* \setminus \Gamma$ *except the rightmost parent* $\big(\frac{5}{4}+\sin\alpha, \frac{1+\sin\alpha}{64(1-\sin\alpha)}\big)$ *of* I_α^* *for* $\omega_{66} < \alpha < \frac{\pi}{2}$.

Note that the parents of $(S,0) \in \Gamma \setminus \{(0,0)\}$ have already been described – in a simpler way – in Theorem 8.

The children $(S,P) = \rho(s_0,p)$ of the points $(s_0,p) \in \mathcal{T}^*$ with constant abscissa $s_0 \in \left]0, \frac{9}{4}\right] \setminus \left\{\frac{5}{4}, \frac{7}{4}, 1+\frac{\sqrt{17}}{4}\right\}$ constitute a parabola arc $P = v(s_0)$ with end points on $\Gamma \cup \Lambda$. If $s_0 > \frac{1}{4}$, there is one point $(s_0,p_0) \in \mathcal{T}^* \setminus \Lambda$ whose child is on the roof: the parabola arc is then tangent to Λ at $\rho(s_0,p_0)$ (see curve Φ in Figure 34). If $s_0 = \frac{1}{4}$, the parabola arc is tangent to Λ at $(2,0)$.

Choose any $S \in \left]0, \frac{9}{4}\right]$ as $S = 2t(3-2t)$, $0 < t \leq \frac{3}{4}$, and draw the curve $y = v(s)$; choose then any $P \in [P_{\min}, P_{\max}] = \big[\max\big(0, 4(\frac{3}{2}-t)^3(t-\frac{1}{2})\big), 4t^3(1-t)\big]$: by Theorem 10 the parents (s,p) of (S,P) for which $s \neq 1+\frac{\sqrt{17}}{4}$ have the same

abscissae as the points with ordinate $y = P$ on the curve $y = v(s),\ s \in \left]0, \frac{9}{4}\right] \setminus \{\frac{5}{4}\}$ with $s \neq \frac{9}{4}$ if $(S, P) = (2, 0)$ – and each such abscissa corresponds to only one parent!

The (not included) start value $t = 0$, the transition values $t = \frac{1}{2}$, $\frac{9-\sqrt{17}}{8} \approx 0.61$, $\sqrt{2} - \frac{3}{4} \approx 0.664$, $\frac{29-6\sqrt{6}}{20} \approx 0.715$ and the end value $t = \frac{3}{4}$ delimit open subintervals where the curve $y = v(s)$ has constant characteristic features. These t–values correspond to $S = 0,\ 2,\ \frac{5+3\sqrt{17}}{8} \approx 2.171,\ 12\sqrt{2} - \frac{59}{4} \approx 2.221,\ \frac{168\sqrt{6}-187}{100} \approx 2.245$ and $\frac{9}{4}$. Each of the figures 14–26 has to be read as follows for the corresponding $S \in \left]0, \frac{9}{4}\right]$: the abscissae s of the curve points at the altitude $P > 0$, $P \in [P_{\min}, P_{\max}]$, tell whether the corresponding parents (s, p) of $(S, P) = \Delta_1^* \in \mathcal{T} \setminus \Gamma$ are the coordinates of obtuse, right–angled or acute parents Δ of Δ_1 (except when $(s, p) \notin \mathcal{T}$); filled circles on the boundary $y = P_{\min},\ P_{\max}$ mark the abscissa of an isosceles parent I_α, an empty square indicates a parent (s, p) outside $\mathcal{T}^*$ or the exceptional cases for $S = \frac{5+3\sqrt{17}}{8}$, and the dashed line $s = 1 + \frac{\sqrt{17}}{4}$ goes through the pole. In Figure 14–17 – where $S \in]0, 2]$ – the parents $(s, 0)$ of $(S, 0)$ are given by $v(s) = 0$, $s \in]0, 2] \setminus \{\frac{5}{4}\}$: empty circles mark the other zeros. For $S \in]0, 2]$ and $P \to 0$, the parents (s, p) of (S, P) with $s \to \frac{5}{4}$ tend to $I^*_{\pi/6}$ since $p \to \frac{3}{64}$ by (18).

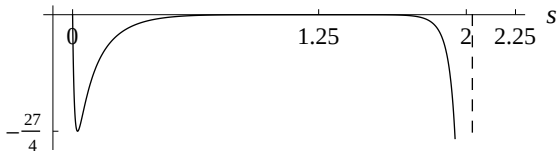

Figure 13. $y = v(s)$ for $S = 0$ with simple root at $s = 0$ and sextuple root at $s = \frac{5}{4}$, which are the abscissae of the parents of $(0, 0)$ in $\mathbf{R^2}$

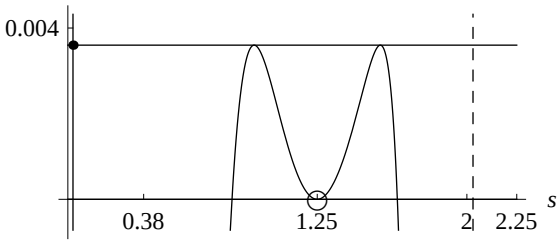

Figure 14. $S = 0.56$, top for $I^*_{\arcsin\sqrt{0.1}} \approx I^*_{18.435^\circ}$, bottom for $\Pi^*_{\arcsin\sqrt{0.28}}$

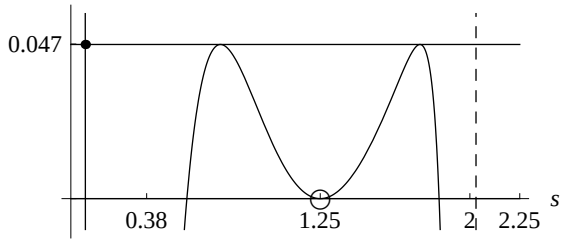

Figure 15. $S = \frac{5}{4}$, top for $I^*_{30^\circ}$, bottom for $\Pi^*_{\omega_{52}}$

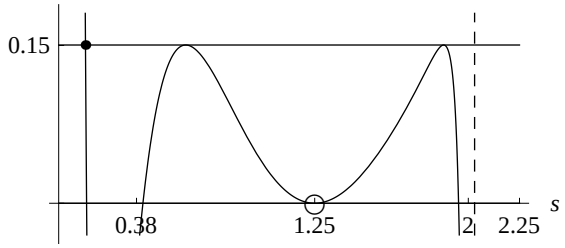

Figure 16. $S = \frac{7}{4}$, top for $I^*_{\arcsin\frac{\sqrt{3-\sqrt{2}}}{2}} \approx I^*_{23.356^\circ}$, bottom for $\Pi^*_{90^\circ-\omega_{21}}$

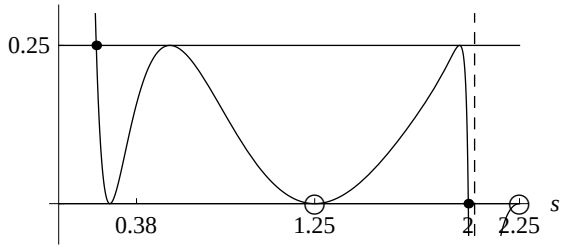

Figure 17. $S = 2$, transition case of the right–angled triangles, top for $I^*_{\pi/4}$, bottom for $\Pi^*_{\pi/2}$. A raising bump culminates at $(\frac{9}{4}, 0)$. The right–angled $\Delta_1 = \{\frac{\pi}{2}, \alpha, \frac{\pi}{2} - \alpha\}$ corresponds to $P = \frac{1}{4}\sin^2 2\alpha$.

Proof of Theorem 10 and of Figures 13–26. Theorem 10 is already proven except for the number of parents of $(S, P) \in \mathcal{T}^* \setminus \Gamma$, their location and the aspect of the curve $y = v(s)$ given by (17). The derivative of $v(s)$ can be factored as $v'(s) =$

$$\frac{(4s-5)\big(192s^3-528s^2+s(128S+100)+136S+125\big)\big(256s^4-1280s^3+2016s^2-1040s+64S+25\big)}{-16(16s^2-32s-1)^3} \tag{20}$$

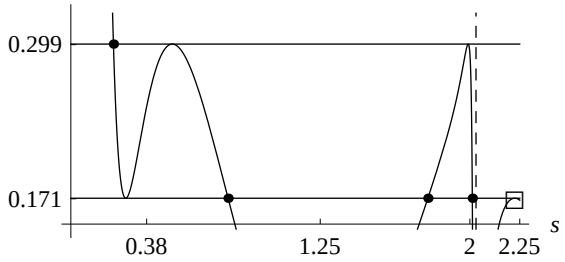

Figure 18. $S = 2.09$, top for $I^*_{\arcsin\sqrt{0.55}} \approx I^*_{47.87^\circ}$, bottom for $I^*_{\arcsin\sqrt{0.95}} \approx I^*_{77.079^\circ}$, □ parent outside $\mathcal{T}^*$

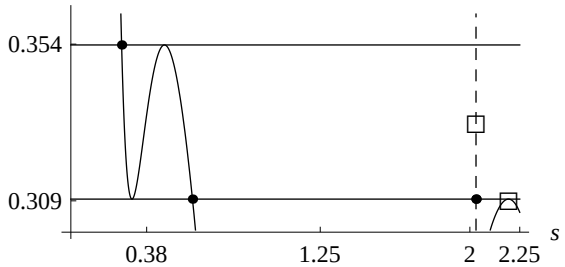

Figure 19. $S = \frac{5+3\sqrt{17}}{8} \approx 2.171$, transition case, top for $I^*_{\omega_{51}}$, bottom for $I^*_{\omega_{71}}$. □ There are *two* parents with $s = 1 + \frac{\sqrt{17}}{4}$ (pole) if $P \in [P_{\min}, P_{\max}[$ and one for $P = P_{\max}$; both such parents of $I_{\omega_{71}}$ are isosceles. □ There is a parent outside $\mathcal{T}^*$.

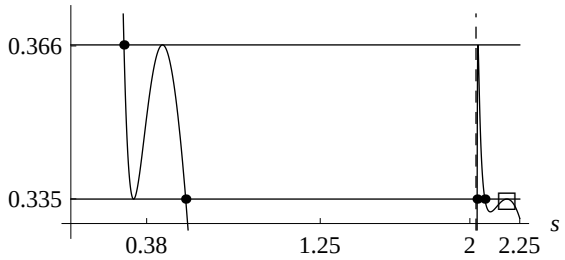

Figure 20. $S = 2.1875$, top for $I^*_{\omega_{52}}$, bottom for $I^*_{90^\circ-\omega_{21}}$, □ parent outside $\mathcal{T}^*$

with 3rd degree factor $q_3(s)$ and 4th degree factor $q_4(s)$ (Figure 27).

For $S = 2t(3-2t)$, $t \in \mathbf{R}$, which is invariant under $t \mapsto \frac{3}{2} - t$, one has

$$q_4(s) = (16s^2 - 40s - 16t + 25)(16s^2 - 40s - 16(\tfrac{3}{2} - t) + 25) \qquad (21)$$

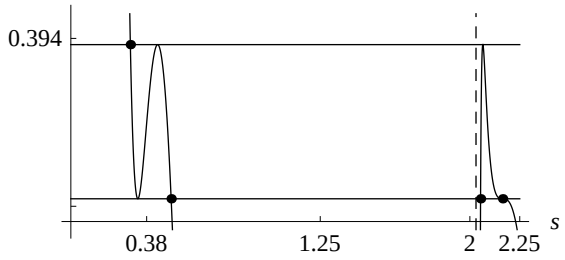

Figure 21. $S = 12\sqrt{2} - \frac{59}{4} \approx 2.221$, transition case, top for $I^*_{\arcsin\sqrt{\sqrt{2}-3/4}} \approx I^*_{54.587^\circ}$, bottom for $I_{\omega_{66}}$. The rightmost root of $v(s) = P_{\min}$ is triple.

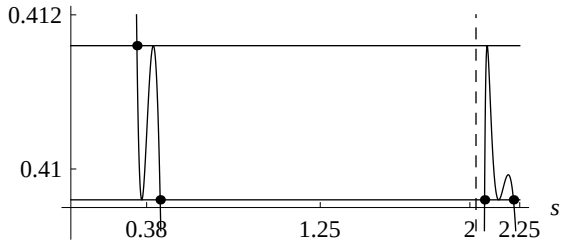

Figure 22. $S = 2.24$, top for $I^*_{\arcsin\sqrt{0.7}} \approx I^*_{56.789^\circ}$, bottom for $I^*_{\arcsin\sqrt{0.8}} \approx I^*_{63.435^\circ}$

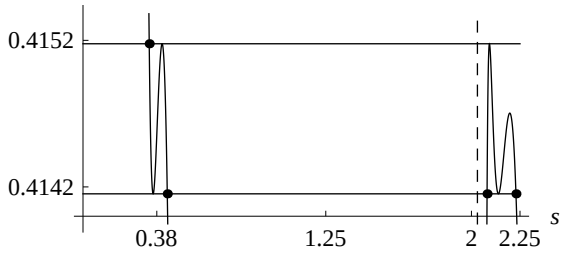

Figure 23. $S = 2.2436$, top for $I^*_{\arcsin\sqrt{0.71}} \approx I^*_{57.417^\circ}$, bottom for $I^*_{\arcsin\sqrt{0.79}} \approx I^*_{62.725^\circ}$

and $v(s) - 4t^3(1-t) =$

$$\frac{\left(16s^2-40s-16t+25\right)^2\left(16s^3+s^2\left(64t^2-96t-40\right)+s\left(-96t^2+176t+25\right)-44t^2-6t\right)}{-16\left(16s^2-32s-1\right)^2} \tag{22}$$

with numerator's squared 2nd degree factor $(Q_2(s))^2$ and 3rd degree factor

$$Q_3(s) = 16s^3+s^2\left(64t^2-96t-40\right)+s\left(-96t^2+176t+25\right)-44t^2-6t. \tag{23}$$

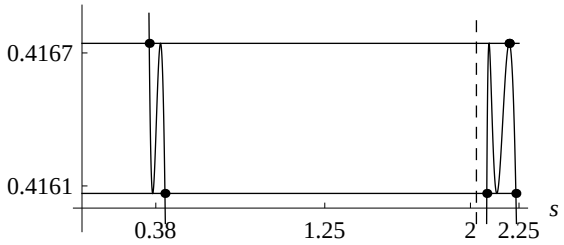

Figure 24. $S = \frac{168\sqrt{6}-187}{100} \approx 2.245$, transition case, top for $I^*_{\omega_{58}}$, bottom for $I^*_{\omega_{62}}$. (S, P) has 7 parents for all $P \in]P_{\min}, P_{\max}[$.

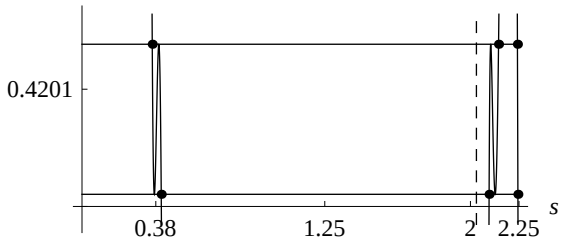

Figure 25. $S = 2.2484$, top for $I^*_{\arcsin\sqrt{0.73}} \approx I^*_{58.694^\circ}$, bottom for $I^*_{\arcsin\sqrt{0.77}} \approx I^*_{61.342^\circ}$

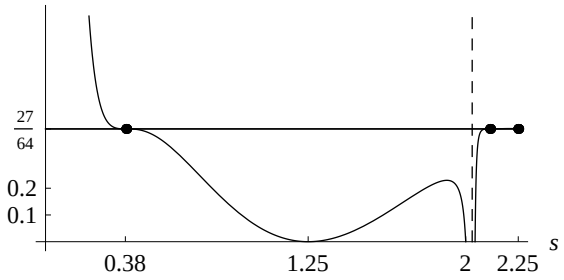

Figure 26. $t = \frac{3}{4}$, $S = \frac{9}{4}$, end case for $I^*_{60^\circ}$. $v(s) - \frac{27}{64}$ has triple roots at $s = \frac{5\pm2\sqrt{3}}{4}$ and a simple root at $s = \frac{9}{4}$.

Since for $t \geq 0$

$$Q_2(s) = 16\big(s - \tfrac{5}{4} - \sqrt{t}\,\big)\big(s - \tfrac{5}{4} + \sqrt{t}\,\big), \tag{24}$$

one can factor (21) further for $S = 2t(3-2t)$, $t \in \big[0, \frac{3}{2}\big]$:

$$q_4(s) = 256\big(s - \tfrac{5}{4} - \sqrt{t}\,\big)\big(s - \tfrac{5}{4} + \sqrt{t}\,\big)\big(s - \tfrac{5}{4} - \sqrt{\tfrac{3}{2} - t}\,\big)\big(s - \tfrac{5}{4} + \sqrt{\tfrac{3}{2} - t}\,\big). \tag{25}$$

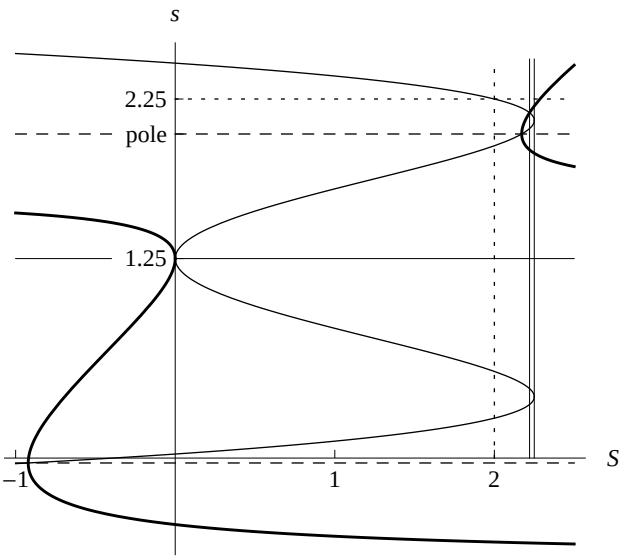

Figure 27. Poles and real zeros of $v'(s)$ as a function of S with constant zero $\frac{5}{4}$, thick curve for the zeros of $q_3(s)$, plain curve for the zeros of $q_4(s)$ and vertical lines at $S = 12\sqrt{2} - \frac{59}{4}$ and $S = \frac{9}{4}$

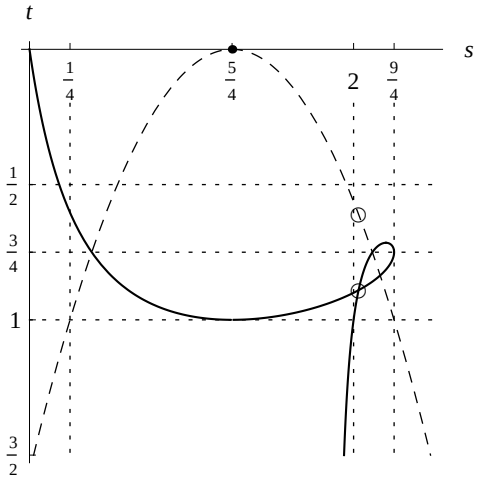

Figure 28. At height t, solutions s of $v(s) = 4t^3(1-t)$ for $S = 2t(3-2t)$, $s \neq 1 + \frac{\sqrt{17}}{4}$: roots of $(Q_2(s))^2$ on the parabola $t = (s - \frac{5}{4})^2$ and roots of $Q_3(s)$ on the bold curve (with one simple and one double root for $t = 0$, $\frac{29-6\sqrt{6}}{20}$, $\frac{3+\sqrt{17}}{8}$ and 1); abscissae of the parents of I^*_α at height $t = \sin^2\alpha$ for $0 < \alpha < \frac{\pi}{2}$, with parents outside $\mathcal{T}^*$ on the right parabola section under the bold curve

For $t \in \left[0, \frac{3}{2}\right]$ and $S = 2t(3-2t) \in \left[0, \frac{9}{4}\right]$, the roots of (22) are thus – except $s = 1 + \frac{\sqrt{17}}{4}$ for $t = \frac{3}{4} \pm \frac{\sqrt{17}-3}{8}$ – the roots $s = \frac{5}{4} \pm \sqrt{t}$ of $(Q_2(s))^2$ on the parabola $t = (s - \frac{5}{4})^2$ and the real roots of $Q_3(s)$ (Figure 28): if $t = \sin^2\alpha \in]0,1[$, these roots, in particular $s = \frac{5}{4} \pm \sin\alpha$, are the abscissae of the parents of I^*_α. The pole $s = 1 + \frac{\sqrt{17}}{4}$ is equal to $\frac{5}{4} + \sin\alpha$ for $t = \frac{3}{4} - \frac{\sqrt{17}-3}{8}$ and to a double root of $Q_3(s)$ for $t = \frac{3}{4} + \frac{\sqrt{17}-3}{8}$: $I^*_{\omega_{51}}$ and $I^*_{\omega_{71}}$ have no parent with $s = 1 + \frac{\sqrt{17}}{4}$ from these sources. The parent of I^*_α with abscissa $s = \frac{5}{4} + \sin\alpha \neq 1 + \frac{\sqrt{17}}{4}$ has the ordinate $p = \frac{1+\sin\alpha}{64(1-\sin\alpha)}$ according to (18). One gets $D(s,p) = \frac{(2\cos 2\alpha+1)^2(2\cos 2\alpha - 4\sin\alpha + 5)}{16(1-\sin\alpha)^2}$, which is < 0 for $\alpha > \omega_{66}$ (parent outside $\mathcal{T}^*$), $= 0$ for $\alpha = \frac{\pi}{3}$ or $\alpha = \omega_{66}$ (isosceles parent of I_α) and > 0 otherwise (non-isosceles parent of I_α): this parent is obtuse for $\alpha < \arcsin\frac{3}{4} = \omega_{49}$, right–angled for $\alpha = \omega_{49}$ and acute for $\omega_{49} < \alpha \leq \omega_{66}$; it is the acute class I_{75° for $\alpha = \frac{\pi}{3}$. The parent with abscissa $s = \frac{5}{4} - \sin\alpha$ has the ordinate $p = \frac{1-\sin\alpha}{64(1+\sin\alpha)}$ and $D(s,p)$ is then $= 0$ for $\alpha = \frac{\pi}{3}$ and > 0 otherwise: the corresponding parent of I_α is always obtuse since $s < 2$. Since the number of real roots of $Q_3(s)$ counted with their multiplicity (Figure 28) coincides with the number of isosceles parents of I_α for all $\alpha \neq \omega_{58}$, we have the following result: with the only exception of the rightmost solution of $v(s) = P_{\max}$ for $S = \frac{168\sqrt{6}-187}{100}$ (giving an isosceles parent of $I_{\omega_{58}}$), double roots of (the denominator of) $v(s) - P_{\max}$ or of $v(s) - P_{\min}$, $P_{\min} > 0$, correspond to non-isosceles parents of the considered isosceles triangle class (unless (s,p) lies outside $\mathcal{T}^*$), and simple or triple roots correspond to isosceles parents. Note that $\frac{168\sqrt{6}-187}{100}$ is the abscissa of the end $I^*_{\omega_{58}}$ of the appendix formed by the roof under the reflection map ρ. For $S \in \left[0, \frac{9}{4}\right]$, the growth of $v(s)$ on $\mathbf{R} \setminus \{1 \pm \frac{\sqrt{17}}{4}\}$ is given by the sign of $v'(s)$ according to (20), (21) and Figure 27. If one considers $S \in \left]0, \frac{9}{4}\right[$, writes it as $S = 2t(3-2t)$ with $t \in \left]0, \frac{3}{4}\right[$ and excludes partly the transition values $t = \frac{1}{2}$, $\frac{9-\sqrt{17}}{8}$, $\sqrt{2} - \frac{3}{4}$, $\frac{29-6\sqrt{6}}{20}$, *i.e.*, $S = 2$, $\frac{5+3\sqrt{17}}{8}$, $12\sqrt{2} - \frac{59}{4}$, $\frac{168\sqrt{6}-187}{100}$, $v(s)$ has exactly two local extrema (always maxima) at height $P_{\max} = 4t^3(1-t)$ – for $s = \frac{5}{4} \pm \sqrt{t}$ – and exactly two local extrema (a minimum on the left) at height $4(\frac{3}{2}-t)^3(1-(\frac{3}{2}-t))$ – for $s = \frac{5}{4} \pm \sqrt{\frac{3}{2} - t}$. Note that $4(\frac{3}{2}-t)^3(1-(\frac{3}{2}-t)) = P_{\min}$ for $t \in \left[\frac{1}{2}, \frac{3}{4}\right]$ and that t and $\frac{3}{2} - t$ are symmetric with respect to $\frac{3}{4}$ in Figure 28. □

Theorem 11. *The parents in $\mathcal{T}$ of I_α, $\alpha \neq \frac{\pi}{3}$, are – up to the exceptions mentioned below – the two non-isosceles classes $\{\alpha'_\pm, \beta'_\pm, \gamma'_\pm\}$ given by the non-obtuse angles*

$$\begin{aligned}
\alpha'_\pm &= \tfrac{\pi}{4} \pm \tfrac{\alpha}{2}, \\
\beta'_\pm &= \operatorname{arccot}\left(2\cos\alpha + 2\sqrt{2 - \left(\frac{1}{2} \pm \sin\alpha\right)^2}\right), \\
\gamma'_\pm &= \operatorname{arccot}\left(2\cos\alpha - 2\sqrt{2 - \left(\frac{1}{2} \pm \sin\alpha\right)^2}\right)
\end{aligned}$$

in $]0,\pi[$ *– with coordinates* $\left(\frac{5}{4}\pm\sin\alpha,\frac{(1\pm\sin\alpha)^2}{64(1-\sin^2\alpha)}\right)\in\mathcal{T}^*$ *– and the isosceles triangle classes with coordinates* (s,p) (automatically on the roof) *corresponding to each real root* s *of* $Q_3(s)$ *given by* (23) *for* $t=\sin^2\alpha$*, with* p *as in Theorem 10.*

For $\alpha=\omega_{66}$ *the triangle class* $\{\alpha'_+,\beta'_+,\gamma'_+\}$ *is isosceles with equal angles* ω_{50} *and corresponds to the triple root* $s=\sqrt{2}+\frac{3}{4}$ *of* $v(s)=P_{\min}$ *for* $S=12\sqrt{2}-\frac{59}{4}$*. For* $\alpha>\omega_{66}$ *the non-isosceles class* $\{\alpha'_+,\beta'_+,\gamma'_+\}$ *doesn't exist: it corresponds to the parent outside* $\mathcal{T}^*$ *and* $\beta'_+,\gamma'_+\notin\mathbf{R}$*.*

Proof. Parts of this theorem have been already demonstrated in the proof of Theorem 10. Theorem 2 for $s=\frac{5}{4}-\sin\alpha$, $p=\frac{1-\sin\alpha}{64(1+\sin\alpha)}$ gives an obtuse parent $\{\alpha',\beta',\gamma'\}$ of I_α with $\sin^2\alpha'=\frac{1-\sin\alpha}{2}$, *i.e.*, $\sin\alpha=\cos 2\alpha'=\sin\left(\frac{\pi}{2}-2\alpha'\right)$,

$$\sin^2\beta'=\frac{3+\sin\alpha-2\sin^2\alpha-\cos\alpha\sqrt{7+4\sin\alpha-4\sin^2\alpha}}{8(1+\sin\alpha)},$$

$$\sin^2\gamma'=\frac{3+\sin\alpha-2\sin^2\alpha+\cos\alpha\sqrt{7+4\sin\alpha-4\sin^2\alpha}}{8(1+\sin\alpha)}.$$

Because $\sin^2\gamma'\geq\sin^2\alpha',\sin^2\beta'$ for $0<\alpha<\frac{\pi}{2}$, α', β' are acute, thus $\alpha'=\frac{\pi}{4}-\frac{\alpha}{2}$, and γ' is obtuse. One gets

$$\cot^2\beta'=\frac{1}{\sin^2\beta'}-1=\left(2\cos\alpha+\sqrt{7+4\sin\alpha-4\sin^2\alpha}\right)^2$$

and, with negative parenthesis, $\cot^2\gamma'=\left(2\cos\alpha-\sqrt{7+4\sin\alpha-4\sin^2\alpha}\right)^2$.

For $s=\frac{5}{4}+\sin\alpha$, $p=\frac{1+\sin\alpha}{64(1-\sin\alpha)}$ one gets similarly $\sin^2\alpha'=\frac{1+\sin\alpha}{2}$, *i.e.*, $\sin\alpha=-\cos 2\alpha'=\sin\left(2\alpha'-\frac{\pi}{2}\right)$, $\sin^2\beta'=\frac{3-\sin\alpha-2\sin^2\alpha-\cos\alpha\sqrt{7-4\sin\alpha-4\sin^2\alpha}}{8(1-\sin\alpha)}$ and $\sin^2\gamma'=\frac{3-\sin\alpha-2\sin^2\alpha+\cos\alpha\sqrt{7+4\sin\alpha-4\sin^2\alpha}}{8(1-\sin\alpha)}$ with $\sin^2\gamma',\sin^2\alpha'\geq\sin^2\beta'$ for $0<\alpha\leq\omega_{66}$ and $\sin^2\gamma'>\sin^2\alpha'$ for $0<\alpha\leq\omega_{49}$, *i.e.*, when $\{\alpha',\beta',\gamma'\}$ is obtuse or right–angled. Since α' is always acute, $\alpha'=\frac{\pi}{4}+\frac{\alpha}{2}$. One gets $\cot^2\beta'=\left(2\cos\alpha+\sqrt{7-4\sin\alpha-4\sin^2\alpha}\right)^2$ and, with parenthesis changing sign at $\alpha=\omega_{49}$ from <0 to >0, $\cot^2\gamma'=\left(2\cos\alpha-\sqrt{7-4\sin\alpha-4\sin^2\alpha}\right)^2$. □

For $\alpha=0$, a triangle with angles $\{\alpha_\pm,\beta_\pm,\gamma_\pm\}=\{45^\circ,\omega_{12},135^\circ-\omega_{12}\}$ is the parent of an isosceles degenerate triangle with three different vertices from Theorem 5. For $\alpha=\frac{\pi}{2}$, $\{\alpha_-,\beta_-,\gamma_-\}$ is the parent $\Pi_{\omega_{21}}$ of $\Pi_{\pi/2}$. The points $(s,p)=\left(\frac{5}{4}\pm\sin\alpha,\frac{(1\pm\sin\alpha)^2}{64(1-\sin^2\alpha)}\right)$ constitute the hyperbola arc $p=\frac{1-4s}{64(4s-9)}$, $\frac{1}{4}\leq s<\frac{9}{4}$, which starts on Γ, is tangent to Λ at $I^*_{\pi/12}$ and $I^*_{5\pi/12}$ and lies outside $\mathcal{T}^*$ between $s=\sqrt{2}+\frac{3}{4}$ and the pole $s=\frac{9}{4}$.

One gets the following non-isosceles parents of isosceles triangles with integer angles (see curve Φ in Figure 34): $\{42^\circ,12^\circ,126^\circ\}$ for I_{6°, $\{36^\circ,12^\circ,132^\circ\}$ for I_{18°, $\{60^\circ,15^\circ,105^\circ\}$ for I_{30°, $\{66^\circ,18^\circ,96^\circ\}$ for I_{42°, $\{72^\circ,24^\circ,84^\circ\}$ for I_{54°, $\{54^\circ,48^\circ,78^\circ\}$ for I_{66° and $\{18^\circ,6^\circ,156^\circ\}$ for I_{78°.

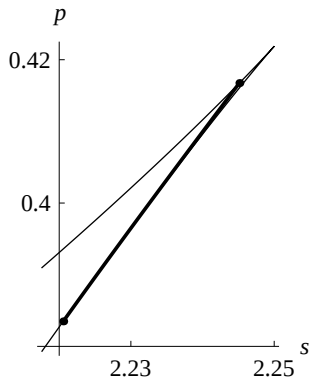

Figure 29. Curve of the coordinates of the hexagenerated triangles

The isosceles parent of the right–angled $I_{\pi/4}$ is I_α with

$$\alpha = \arcsin\sqrt{\frac{1}{12}\left(8 - \frac{13}{\sqrt[3]{73-6\sqrt{87}}} - \sqrt[3]{73-6\sqrt{87}}\right)} \approx 10.1986^\circ.$$

The two isosceles parents of $I_{\omega_{58}}$ have equal angles $\arcsin\sqrt{\frac{11-4\sqrt{6}}{20}} \approx 14.191^\circ$ and ω_{68} (corresponding to the rightmost double root of $v(s) = P_{\max}$ for $S = \frac{168\sqrt{6}-187}{100}$), respectively.

Consider $(S,P) \in \mathcal{T}^*$ neither on the roof nor on the ground. Figures 14–26 show that (S,P) has 5 parents if $S \le 12\sqrt{2} - \frac{59}{4}$ and 7 parents if $S \ge \frac{168\sqrt{6}-187}{100}$, whereas the interval $12\sqrt{2} - \frac{59}{4} < S < \frac{168\sqrt{6}-187}{100}$ assures the mutation from "pentagenerated" to "heptagenerated" non-isosceles classes of $\mathcal{T}$: in this last case, the number of parents of (S,P) depends on P and jumps (over 6 at the level P_6) from 7 near the bottom $P_{\min}$ to 5 near the top $P_{\max}$, and the ordinate $P_6 = P_6(S)$ of the hexagenerated triangle class climbs with growing S. This mutation is achieved at the abscissa $S = \frac{168\sqrt{6}-187}{100}$ of the end $I^*_{\omega_{58}}$ of the appendix formed by the roof under the reflection map ρ. Triangle classes have thus infinitely many or exactly 7, 6, 5, 4, 3 or 2 parents in $\mathcal{T}$ but never only one parent!

For $12\sqrt{2} - \frac{59}{4} < S \le \frac{168\sqrt{6}-187}{100}$, the largest of the three real roots s of

$$q_3(s) = 192s^3 - 528s^2 + s(128S + 100) + 136S + 125$$

in (20) is the abscissa of the first maximum of $v(s)$ left from $\frac{9}{4}$: this gives the ordinate P_6 of the hexagenerated triangle class exactly (Figures 27, 29 and 30).

Figures 14–17 show that finite obtuse or right–angled triangles have only obtuse parents.

All acute triangles with abscissa $> s(I_{\omega_{49}}) = \frac{135}{64} = 2.109375$ have both acute and obtuse parents. The coordinates $(S,P) = r\big(\{\alpha, \frac{\pi}{2} - \alpha, \frac{\pi}{2}\}\big)^*$ of the triangles with right–angled parents form the parabola arc $P = v(2) = \frac{81}{4}(S-2)(\frac{9}{4} - S)$,

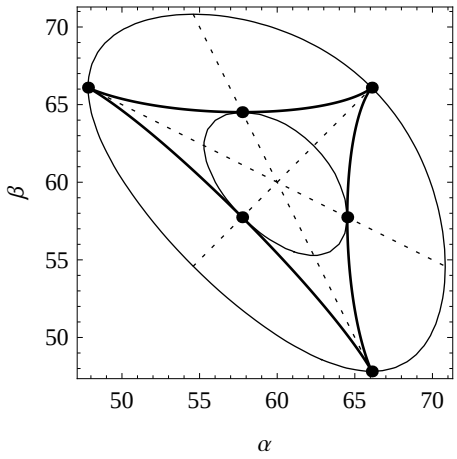

Figure 30. Level curves $s(\Delta) = 12\sqrt{2} - \frac{59}{4}$ and $s(\Delta) = \frac{168\sqrt{6}-187}{100}$ in the $\alpha\beta$–plane for two angles $\alpha,\ \beta$ (in $^\circ$) of the triangle Δ: the curve of the hexagenerated triangles separates the pentagenerated from the heptagenerated ones. The *pentagenerated* cusps correspond to $I_{\omega_{66}}$, the three other points to $I_{\omega_{58}}$.

$2 \le S \le \frac{54}{25} = 2.16$, given by (17): S grows with α from 2 for $r(\Pi_{\pi/2}) = \Pi_{\pi/2}$ to 2.16 for $r(I_{\pi/4})$, which is $I_{\arcsin 3/\sqrt{10}} = I_{\omega_{72}}$ since $Q_3(s) = 2$ if and only if $t \in \{\frac{9}{10}, 1\}$. The parabola arc starts and ends on the right roof section and is tangent to the left roof section for $S = \frac{135}{64}$ at $I^*_{\omega_{49}}$. Acute triangles with abscissa > 2.16 have thus no right–angled parents.

A non-isosceles parent of an isosceles class $I_\alpha \in \mathcal{T}$ generates two different parents of a corresponding given isosceles triangle. By considering congruent non-identical triangles as different, we have proven the following result.

Theorem 12. *Let ABC be a proper triangle with vertices A, B, C and angles $\alpha,\ \beta,\ \gamma$. Let*

$$S = \sin^2\alpha + \sin^2\beta + \sin^2\gamma,\ P = \sin^2\alpha \cdot \sin^2\beta \cdot \sin^2\gamma.$$

ABC is the reflection triangle of between 5 and 7 parents.
(1) *If ABC is obtuse and non-isosceles, it has exactly 5 parents, which are all obtuse, non-isosceles and pairwise non-similar.*
(2) *If ABC is acute and non-isosceles* (Figure 30)*, it has between 5 and 7 parents depending on S and P. These parents are all non-isosceles and pairwise non-similar:*

(a) $2 < S \le \frac{135}{64} = 2.109375$*: 5 parents, 4 of them obtuse and the last one obtuse, right–angled or acute according as* $P \gtreqless \frac{81}{4}(S-2)(\frac{9}{4}-S)$*;*
(b) $2.109375 \le S \le \frac{54}{25} = 2.16$*: 5 parents, 3 of them obtuse, one acute and the last obtuse, right–angled or acute according as* $P \lesseqgtr \frac{81}{4}(S-2)(\frac{9}{4}-S)$*;*
(c) $2.16 \le S \le 12\sqrt{2} - \frac{59}{4} \approx 2.221$*: 5 parents, 3 of them obtuse and 2 acute;*

(d) $12\sqrt{2} - \frac{59}{4} \leq S \leq \frac{168\sqrt{6}-187}{100} \approx 2.245$*: 5, 6 or 7 parents, 3 of them obtuse, 2 acute and zero, one or two additional acute parents according as* $P \gtreqless P_6 = P_6(S)$ *given by Figure 29;* P_6 *grows with* S *from* $\frac{371}{\sqrt{2}} - \frac{16765}{64} \approx 0.383$ *to* $\frac{3\left(135664\sqrt{6}-326751\right)}{40000} \approx 0.417$.

(e) $\frac{168\sqrt{6}-187}{100} \leq S < \frac{9}{4}$*: 7 parents, 3 of them obtuse and* 4 *acute.*

(3) *If* ABC *is isosceles with equal angles* α*, it has* 5 *parents except for* $\alpha = \omega_{58}$ $(6$ *parents*$)$ *and for* $\omega_{58} < \alpha < \omega_{66}$ $(7$ *parents*$)$*:*

(a) $0^\circ < \alpha < \omega_{49}$*: one isosceles obtuse parent, a pair of non-similar non-isosceles obtuse parents and their mirror images in the axis of* ABC*;*

(b) $\alpha = \omega_{49}$ $(S = \frac{135}{64})$*: one isosceles obtuse parent, one non-isosceles obtuse and one non-isosceles right–angled parent and their mirror images;*

(c) $\omega_{49} < \alpha < \omega_{58}$*: one isosceles obtuse parent, one non-isosceles obtuse and one non-isosceles acute parent and their mirror images;*

(d) $\alpha = \omega_{58}$ $\left(S = \frac{168\sqrt{6}-187}{100}\right)$*: one isosceles obtuse and one isosceles acute parent, one non-isosceles obtuse and one non-isosceles acute parent and their mirror images;*

(e) $\omega_{58} < \alpha < \omega_{66}$, $\alpha \neq 60^\circ$*: one isosceles obtuse and two non-similar isosceles acute parents, one non-isosceles obtuse and one non-isosceles acute parent and their mirror images;*

(f) $\alpha = 60^\circ$*: one equilateral parent, three congruent isosceles parents with equal angles* 15° *and three with equal angles* 75° (Figure 2)*;*

(g) $\omega_{66} \leq \alpha < \omega_{72}$ $\left(S = 12\sqrt{2} - \frac{59}{4}$ *for* $\alpha = \omega_{66}\right)$*: one isosceles obtuse and two non-similar isosceles acute parents, one non-isosceles obtuse parent and its mirror image;*

(h) $\alpha = \omega_{72}$*: three isosceles parents (one obtuse, one right–angled and one acute), one non-isosceles obtuse parent and its mirror image;*

(i) $\omega_{72} < \alpha < 90^\circ$*: a pair of non-similar isosceles obtuse parents, one acute isosceles parent, one non-isosceles obtuse parent and its mirror image.*

In order to count and describe the parents of the corresponding coordinates $(S, P) \in \mathcal{T}^* \setminus \Gamma$ in Theorem 12, one has to neglect the mirror images and the repetitions of congruent triangles and to add one exterior parent of I^*_α for $\omega_{66} < \alpha < \frac{\pi}{2}$.

9. Convergence to an equilateral or degenerate limit

After continuous extension, all level curves of ρ_1 and of ρ_2 given by (6) are tangent to Λ at $I^*_{\pi/6} = (\frac{5}{4}, \frac{3}{64})$. By (15) one has $\rho_1(s,p) = s$ for $(s,p) \neq I^*_{\pi/6}$ if and only if $p = \frac{s(s-2)(4s-3)}{4(12s-25)}$: this curve lies in $\mathcal{T}^*$ if and only if $s \in \{0\} \cup \left[\frac{3}{4}, 2\right] \cup \{\frac{9}{4}\}$ and is tangent to Λ at $I^*_{\pi/6}$. One has $\rho_2(s,p) = p$ for $(s,p) \neq I^*_{\pi/6}$ if and only if $p = 0$ or $s = \frac{7}{4}$ or $p = \frac{1}{4}(s-1)^2 + \frac{1}{32}$ or $p = \frac{(4s-5)^3+4s+1}{-64(4s-7)}$: both last curves are tangent to Λ at $I^*_{\pi/6}$ from outside $\mathcal{T}^*$ and the parabola has no other point in $\mathcal{T}^*$.

The arrows $\nearrow, \nwarrow, \swarrow, \searrow$ in Figure 31 show the constant quadrant of the vector $\rho(s,p) - (s,p)$ in each of the zones of $\mathcal{T}^*$ delimited by the curves $\rho_1(s,p) = s$

and $\rho_2(s,p) = p$, whose intersections are the fixed points of ρ. Note that zone VII is the thin region bounded below by $\rho_1 = s$ and above by the curved branch of $\rho_2 = p$ and by the roof. Since $\rho(s,p)$ lies strictly eastwards and northwards from (s,p) for all $(s,p) \in \mathcal{T}^*$ with $2 \le s < \frac{9}{4}$, $p > 0$, the sequence $\big(\rho^n(s,p)\big)_{n\in\mathbf{N}}$ for such an (s,p) converges to or reaches $I^*_{\pi/3}$ with strictly increasing coordinates. The first part of the following theorem is proven.

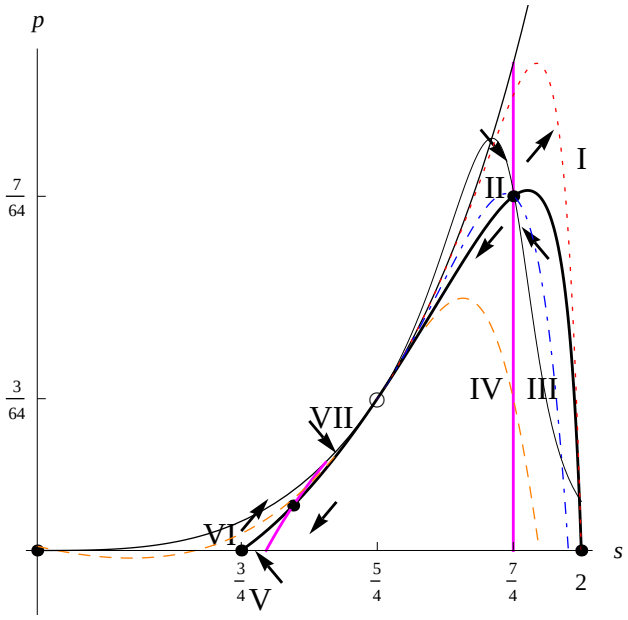

Figure 31. Quadrant of the vector $\rho(s,p) - (s,p)$ depending on the zone of $(s,p) \in \mathcal{T}^*$ with curves $\rho_1 = s$ (black, thick), $\rho_1 = p$ (magenta, thick), $\rho_1 = \frac{5}{4}$ (dashed, orange) and, for $s \ge \frac{5}{4}$, $\rho_1 = \frac{7}{4}$ (dot–dashed, blue), $\rho_1 = 2$ (dotted, red), $\rho_2 = p_{\text{top}}$ (thin)

Theorem 13. (1) *An acute or right–angled proper triangle has always an acute reflection triangle and its iterated reflection triangle converges to an equilateral limit with strictly growing coordinates.*
(2) *An acute or right–angled triangle becomes equilateral after a finite number of reflection steps if and only if its class is an isosceles acute ancestor of* I_{60° *given by the infinite sequence of successive parents* I_{60°, I_{75°, $I_{84.6588\ldots^\circ}$, $I_{88.205\ldots^\circ}$, $\ldots$ *whose equal angles grow towards* 90°.

Proof. (2) Each I_α with $\alpha \ge 75^\circ$ has exactly one acute or right–angled parent: an isosceles one with equal angles $> \alpha$ (Figure 10). □

Theorem 14. $(s,p) \in \mathcal{T}^* \setminus \big(\Gamma \cup \big\{(\frac{7}{4}, \frac{7}{64})\big\}\big)$ *converges to* $I^*_{\pi/3}$ *under iteration of* ρ *(with strictly growing coordinates except possibly for the first reflection step) when*
(1) (s,p) *is in zone I of Figure 31 with boundary,* i.e., $s \ge \frac{7}{4}$ *and* $\rho_1(s,p) \ge s$, *or*
(2) $\rho_1(s,p) \ge \frac{7}{4}$ *and* $\rho_2(s,p) \ge p_{\text{top}}$ *where* $p_{\text{top}} \approx 0.11118$ *is the ordinate of the*

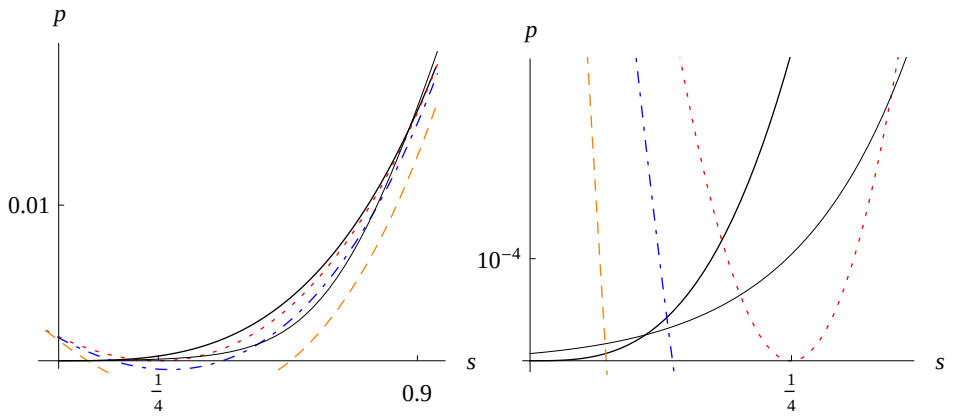

Figure 32. Detailed views of the left part of Figure 31. In the right figure, the intersection points of the roof (black, thick) with $\rho_1(s,p) = 2$ (dotted, red) and $\rho_1(s,p) = \frac{5}{4}$ (dashed, orange) give the coordinates of the isosceles parents of $I_{\pi/4}$ and $I_{\pi/6}$, respectively. $(\frac{1}{4}, 0)$ is the parent $\Pi^*_{\omega_{21}}$ of $\Pi^*_{\pi/2}$.

maximum point of the curve $\rho_1(s,p) = s$ (Figures 31 and 32), *or*
(3) $\rho_1(s,p) \geq 2$.

Note that $576p_{\text{top}}$ *is the middle root of* $p^3 - 294p^2 + 13209p + 97200$.

Proof. We only have to prove that the corner of zone I near the heptagonal fixed point $(\frac{7}{4}, \frac{7}{64})$ is mapped by ρ to zone I and not to zone III, and this is true: the points with $\rho_1(s,p) = s$, $s > \frac{7}{4}$, $p > 0$, are mapped upwards by ρ and $\frac{\partial \rho_2}{\partial p}(s,p) = \frac{(5-4s)^6(64p(4s-7)-4s-1)}{-(64p(4s-7)+4s+1)^3}$ is strictly positive in the rectangle $\frac{7}{4} < s < 2$, $\frac{7}{64} < p < \frac{1}{8}$ containing the maximum point of the curve $\rho_1(s,p) = s$. □

Theorem 14 gives Figure 33 where each (α, β) is identified with the triangle class $\{\alpha, \beta, 180^\circ - \alpha - \beta\} \in \mathcal{T}$. The large points are the fixed points of r; the small points are I_{30°, its isosceles parent and grandparent and the parent $\Pi_{\omega_{21}}$ of Π_{90°. The squares mark the right–angled I_{45° and its isosceles parent on the thin dotted curve $\rho_1(s,p) = 2$. The curve $s = \frac{5}{4}$ is dot–dashed and goes through $I_{30^\circ} = (30^\circ, 30^\circ)$; its parent curves are dashed: one of them goes through the parent $(60^\circ, 15^\circ)$ of I_{30° corresponding to $(s,p) = (\frac{7}{4}, \frac{3}{64})$. There are points with $\rho_1(s,p) \geq 2$ in zones I, II, VII and VI of Figure 31; there are points with $\rho_1(s,p) \geq \frac{7}{4}$ and $\rho_2(s,p) \geq p_{\text{top}}$ in zones I, II, III and VI. Note that every neighborhood of the heptagonal fixed point $\left(\frac{360^\circ}{7}, \frac{180^\circ}{7}\right)$ contains triangle classes with equilateral limit. Because the leftmost roots of $v(s) = P$ for $S = \frac{5}{4}$ are almost equal for all P, the inner branch of parents of $s = \frac{5}{4}$ that passes through $I_{6.33\ldots^\circ}$ in Figure 33 is nearly a level curve of s; furthermore, the nearby arc of the curve $\rho_1(s,p) = 2$ that joins the pair of points representing $\Pi_{\omega_{21}}$ is almost parallel to the square diagonal $s = 2$: the fractal structure is born.

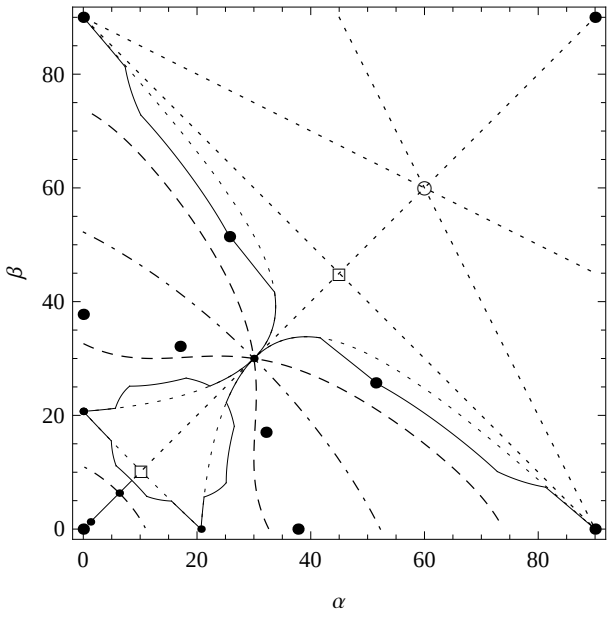

Figure 33. Convergence to an equilateral limit is ensured when two angles (α, β) of the base triangle are in the zone enclosed by or north–east from the plain curve, or on this curve, filled points excepted.

We now describe the set of triangles with equilateral or degenerate limit systematically. We denote by $\mathcal{A}_n$ and $\mathcal{D}_n$ the set of classes in $\mathcal{T}$ that become acute and degenerate after exactly n applications of the reflection map r, $n \in \mathbf{N}$. $\mathcal{A}_n^*$ and $\mathcal{D}_n^*$ are the corresponding subsets of $\mathcal{T}^*$: $\mathcal{A}_n^*$, $n \geq 1$, consists of the points $(s, p) \in \mathcal{T}^*$ for which the first coordinates of $\rho^{n-1}(s, p)$ and of $\rho^n(s, p)$ are ≤ 2 and > 2, respectively. Since $\mathcal{O}^*$ is a repelling fixed point of ρ, the basins of attraction of $I_{\pi/3}^*$ and $\mathcal{O}^*$ in $\mathcal{T}^*$ are the disjoint unions $\mathcal{A}^* = \bigcup_{n\geq 0} \mathcal{A}_n^*$ and $\mathcal{D}^* = \bigcup_{n\geq 0} \mathcal{D}_n^*$, respectively. Figure 34 shows the "wing" $\bigcup_{n=1}^3 \mathcal{A}_n$ with skeleton $\bigcup_{n=1}^3 \mathcal{D}_n$, where (α, β) represents $\{\alpha, \beta, 180° - \alpha - \beta\} \in \mathcal{T}$.

The boundary curve of $\mathcal{A}_n^*$, $n \geq 1$, consists of the following points:

(1) the points $(s, p) \in \mathcal{T}^*$ for which the first coordinate of $\rho^{n-1}(s, p)$ or of $\rho^n(s, p)$ is 2
(2) the members of $\rho^{-k}\big(I_{\pi/6}^*\big)$ (lying thus on $\mathcal{D}_{k+1}^*$) for $0 \leq k \leq n - 1$
(3) the members of $\rho^{-n}\big(\Pi_{\pi/2}^*\big) = \bigcup_{k=0}^n \rho^{-k}\big(\Pi_{\pi/2}^*\big)$ (lying thus on Γ)
(4) the roof section between the roof member of $\rho^{-(n-1)}\big(I_{\pi/4}^*\big)$ and its roof parent.

$\mathcal{A}_n^*$, $n \geq 1$, is composed of $5^{n-1} + 1$ maximal simply connected subsets. $\mathcal{T}^* \setminus \bigcup_{k=0}^n \overline{\mathcal{A}_k^*}$, $n \geq 0$, consists of $\frac{5^n+3}{4}$ maximal simply connected components – the overline denoting set closure. For $n \geq 1$, $\frac{3^n-1}{2}$ such components are juxtaposed arches whose feet are the $\frac{3^n+1}{2}$ members of $\rho^{-n}\big(\Pi_{\pi/2}^*\big)$ on Γ. Starting

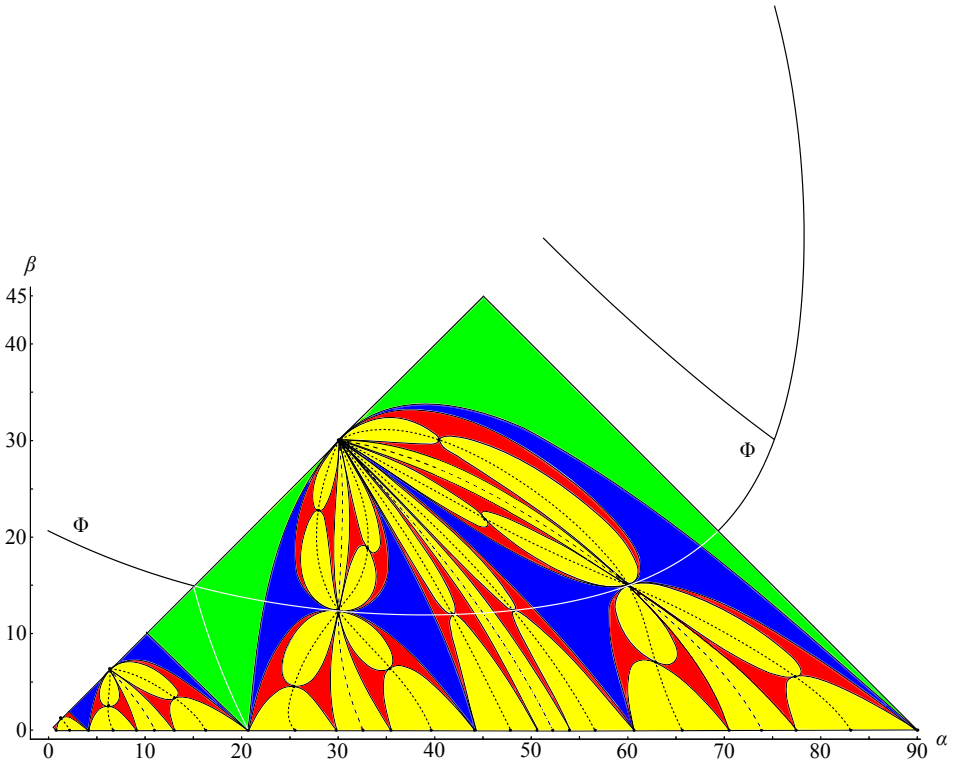

Figure 34. Wing of the obtuse triangles that become acute after one ($\mathcal{A}_1$, green), two (blue) or three reflection steps (red) with curves of the triangles that become degenerate after one ($\mathcal{D}_1$, dot–dashed), two (dashed) or three reflection steps (dotted)

from the rightmost $\Pi^*_{\pi/2}$, the members of $\rho^{-n}\big(\Pi^*_{\pi/2}\big)$ and the $\frac{3^n-1}{2}$ members of $\bigcup_{k=0}^{n-1}\rho^{-k}\big(\Pi^*_{\omega_{52}}\big)$ alternate on Γ. Each member of $\rho^{-k}\big(\Pi^*_{\omega_{52}}\big)$ – lying between the leftmost member of $\rho^{-m}\big(\Pi^*_{\pi/2}\big)$ and the leftmost member of $\rho^{-(m+1)}\big(\Pi^*_{\pi/2}\big)$, say – is the starting point of one of the 3^k curves of $\mathcal{D}^*_{k+1}$: after continuous extension at some points of $\bigcup_{\ell=0}^{k}\rho^{-\ell}\big(I^*_{\pi/6}\big)$, this curve ends at the roof member of $\rho^{-m}\big(I^*_{\pi/6}\big)$. One has further $\overline{\mathcal{D}^*_n}=\mathcal{D}^*_n\cup\bigcup_{k=0}^{n-1}\rho^{-k}\big(I^*_{\pi/6}\big)$ and $\overline{\mathcal{A}^*_n}\cap\overline{\mathcal{D}^*_n}=\bigcup_{k=0}^{n-1}\rho^{-k}\big(I^*_{\pi/6}\big)$, $n\geq 1$.

Figure 34 shows the frontier line Φ of the non-isosceles parents of the isosceles triangle classes given by Theorem 11. The same classes are represented two times on the branches issued from the left bifurcation, three times after the right bifurcation. Φ cuts the dot–dashed middle curve $\mathcal{D}_1$ at $(45^\circ,\omega_{12})$: a triangle with these angles is the parent of an isosceles degenerate triangle (*i.e.*, a segment and its midpoint). The intersection point of Φ with the line $\beta=\alpha$ corresponding to the roof is the isosceles parent I_{15° of I_{60° and its left end is the parent $\Pi_{\omega_{21}}$ of Π_{90°. Φ intersects the line $s=2$ at the right–angled parent $(90^\circ-\omega_{21},\omega_{21})$ of

$I_{\omega_{49}}$, the right bifurcation point is the isosceles parent I_{75° of I_{60° and the end of the following left branch is the isosceles parent $I_{\omega_{50}}$ of the end class $I_{\omega_{66}}$.

Consider Figure 34 filled with $\mathcal{A}$ and $\mathcal{D}$. Let $\mathcal{P}_n$, $n \geq 1$, be the closure of the component of $\mathcal{A}_n$ with a boundary segment on the "roof" $\beta = \alpha$ together with the underlying arch bounded by the α–axis. Let $\mathcal{S}_n$, $n \geq 1$, be the following subset of $\mathcal{P}_1$: the closure of both pairs of components of $\mathcal{A}_{n+1}$ connecting the α–axis with I_{30° on both sides of the middle curve $\mathcal{D}_1$ together with both underlying arches and enclosed bubbles. Let $\mathcal{S}_n^{lb}$, $\mathcal{S}_n^{lt}$, $\mathcal{S}_n^{rb}$ and $\mathcal{S}_n^{rt}$ be the left bottom, left top, right bottom and right top parts of $\mathcal{S}_n$ delimited by Φ left and right from $\mathcal{D}_1$.

Every class of proper non-acute and non-isosceles triangles has exactly 5 parents, every class of infinite triangles except Π_{90° has exactly 3 parents, and every I_α, $0^\circ < \alpha \leq 45^\circ$, has exactly one isosceles and two non-isosceles parents. Here are these mappings.

The reflection map r is a bijective fractal blow–up of $\mathcal{P}_{n+1}$, $n \geq 1$, to $\mathcal{P}_n$, *i.e.*, every component, boundary or point of $\mathcal{A}_k$, $\mathcal{D}_k$, $\ldots$ in $\mathcal{P}_{n+1}$ is blown up bijectively for all $k \geq n+1$ (with appropriate orientation–preserving distortion and translation) to the geographically corresponding component, boundary or point of $\mathcal{A}_{k-1}$, $\mathcal{D}_{k-1}$, $\ldots$ in $\mathcal{P}_n$. r is a bijective fractal blow–up or blow–down to $\mathcal{P}_n$ of $\mathcal{S}_n^{rb}$ and of $\mathcal{S}_n^{lb}$ flipped about a vertical axis. And r is a bijective fractal blow–up or blow–down to $\mathcal{P}_n$ without α–axis of $\mathcal{S}_n^{rt} \setminus \{I_{30^\circ}\}$ flipped about the line $\beta = \alpha$ and of $\mathcal{S}_n^{lt} \setminus \{I_{30^\circ}\}$ after a half–turn. Note that the top of $\mathcal{S}_n^{rt}$ and of $\mathcal{S}_n^{lt}$ has first to be stretched after I_{30° has been removed!

Every point of $\mathcal{P}_n$, $n \geq 1$, has thus one parent in $\mathcal{P}_{n+1}$ and all its other parents in $\mathcal{P}_1$, more precisely in $\mathcal{S}_n$. If one identifies the set of classes of infinite triangles with the interval $[0^\circ, 90^\circ]$ of the α–axis, the action of r on the infinite classes consists of three bijective fractal blow–ups to $[0^\circ, 90^\circ]$: one of $[0^\circ, \omega_{21}]$, one of $[\omega_{21}, \omega_{52}]$ after a flip and one of $[\omega_{52}, 90^\circ]$.

For a global description of the reflection map r we identify $\mathcal{T}$ in Figure 35 with $\left\{(\alpha, \beta) \mid 0^\circ \leq \beta \leq \alpha \leq 90^\circ - \frac{\beta}{2}\right\}$ and consider the set $\mathcal{T}_1$ of the non-acute, nondegenerate classes and the set $\mathcal{T}_2$ of the non-obtuse classes – $\mathcal{T}_1$ and $\mathcal{T}_2$ sharing the set $\mathcal{T}_\perp$ of the right–angled classes. The zones i–v and 1–7 of $\mathcal{T}$ are delimited by the following plain curves:

(1) the curve $\mathcal{D}_1$ of the nondegenerate classes that degenerate at the first stage,
(2) the curve of the parents of the right–angled classes, whose 5 segments without I_{30° – between zones 1 and v, 2 and iv, 3 and iii, 5 and ii, 4 and i, respectively – are each mapped bijectively to $\mathcal{T}_\perp$ or $\mathcal{T}_\perp \setminus \{\Pi_{90^\circ}\}$,
(3) the curve Φ of the non-isosceles parents of the isosceles classes,
(4) the curve between zone 6 and zone 7 (from $I_{\omega_{50}}$ to $I_{\omega_{68}}$) that corresponds to the rightmost parents of the hexagenerated points of $\mathcal{T}^*$ and whose dotted child curve (from $I_{\omega_{66}}$ to $I_{\omega_{58}}$) is the thick line of hexagenerated triangles of Figure 30.

The reflection map r can be described as follows if one considers zones i–iv without $\mathcal{D}_1$: the curve $\mathcal{D}_1$ and $(0, 0)$ are mapped to $(0, 0)$; zone i, zone iv flipped about a vertical axis and zone v without origin are each scaled bijectively and fractally to

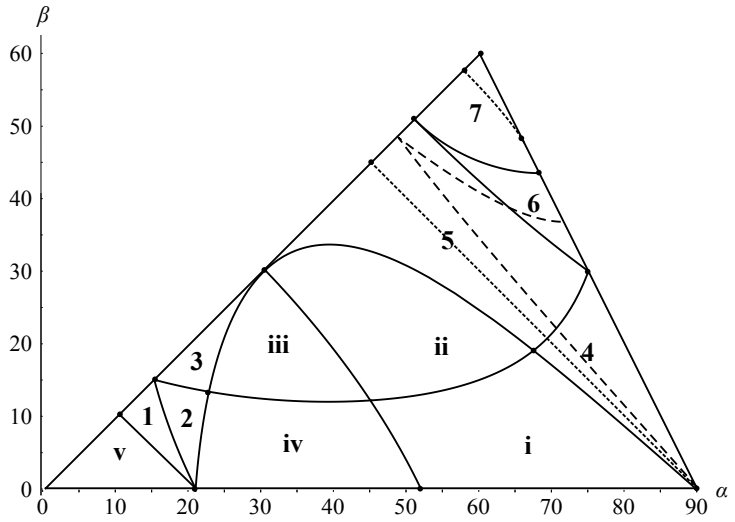

Figure 35. Decomposition of the reflection map r into bijective submappings

$\mathcal{T}_1$; zone ii flipped about the line $\beta = \alpha$ and zone iii after a half–turn are each scaled bijectively and fractally to $\mathcal{T}_1$ without α–axis. Zone 1, zone 2 flipped about a vertical axis and zone 4 are each scaled bijectively and fractally to $\mathcal{T}_2$; zone 3 without I_{30° after a half–turn and zone 5 without I_{30° flipped about the line $\beta = \alpha$ are each scaled bijectively and fractally to $\mathcal{T}_2$ without Π_{90°. Note that the upper border section of zone 5 from I_{75° to I_{30° is mapped to the whole right "roof" section from I_{60° to Π_{90°. Zone 6 after a half–turn and zone 7 flipped about a vertical axis are each scaled bijectively and fractally to the heptagenerated tip of $\mathcal{T}_2$.

The triangle classes $r\big(\{\alpha, 90^\circ - \alpha, 90^\circ\}\big)$ with right–angled parents constitute the dashed curve $r(\mathcal{T}_\perp)$ of Figure 35 joining with decreasing α the fixed point Π_{90° to $r(I_{45^\circ}) = I_{\omega_{72}}$ over $r\big(\{90^\circ - \omega_{21}, \omega_{21}, 90^\circ\}\big) = I_{\omega_{49}}$. Their coordinates (S, P) form the parabola arc $P = \frac{81}{4}(S-2)(\frac{9}{4} - S)$, $2 \leq S \leq 2.16$.

A class of non-isosceles finite triangles in Figure 35 has 5, 6 or 7 parents when it is located below, on or above the upper dotted curve, respectively; it has (exactly) one right–angled parent if and only if it is on $r(\mathcal{T}_\perp)$; exactly 3, 4 or 5 of its parents are obtuse when it is located on or above the upper section of $r(\mathcal{T}_\perp)$, below this section but not below the bottom section, or below $r(\mathcal{T}_\perp)$, respectively. The preceding sentence is also true for finite isosceles *triangles*, except that triangles in the class $I_{\omega_{66}}$ have only 5 parents (instead of 6) and that triangles in the class $I_{\omega_{49}}$ have two right–angled parents (instead of one acute and one right–angled) and three obtuse parents.

10. Periodic orbits

We use the notations of Section 9.

Theorem 15. *$\rho\big|_{\mathcal{T}^*\setminus\Gamma}$ has n–periodic points for all integers $n \geq 1$.*

Proof. Consider the bottom half $\mathcal{S}_n^{lt\downarrow}$ of $\mathcal{S}_n^{lt}$ delimited by Φ and by the upper parent curve of Φ. r^n is a bijective continuous mapping from $\mathcal{S}_n^{lt\downarrow}$ to the top $r^n\big(\mathcal{S}_n^{lt\downarrow}\big)$ of $\mathcal{T}_1$ delimited by Φ, and the inverse mapping is continuous also. Since $r^n\big(\mathcal{S}_n^{lt\downarrow}\big)$ is homeomorphic to a closed disk and since $r^n\big(\mathcal{S}_n^{lt\downarrow}\big) \supset \mathcal{S}_n^{lt\downarrow}$, $\mathcal{S}_n^{lt\downarrow}$ contains a fixed point of r^n by the Brouwer Theorem. For $n \geq 2$, $\bigcup_{k=1}^{n-1} r^k\big(\mathcal{S}_n^{lt\downarrow}\big)$ doesn't intersect $\mathcal{S}_n^{lt\downarrow}$: all fixed points of r^n in $\mathcal{S}_n^{lt\downarrow}$ have thus order n. □

The same argument is valid for $\mathcal{S}_n^{rt\downarrow}$. For $\mathcal{S}_n^{lb}$ and $\mathcal{S}_n^{rb}$ the fixed point can be a class of infinite triangles (we will show that it is always such a class). For $n = 1$ there is exactly one fixed point of r in $\mathcal{S}_1^{lt\downarrow}$, $\mathcal{S}_1^{rt\downarrow}$, $\mathcal{S}_1^{lb}$ and $\mathcal{S}_1^{rb}$: the triangle class with coordinates $\big(\frac{6-\sqrt{5}}{4}, \frac{8\sqrt{5}-17}{64}\big)$, the heptagonal class, $\Pi_{\omega_{38}}$ and Π_{90°, respectively. $(39.952203015767141115\ldots^\circ, 18.346346518943955680\ldots^\circ)$ in $\mathcal{S}_3^{lt\downarrow}$ is for example a 3–periodic triangle class. All computations in this section were done with 1000–digit precision.

The following construction generates all cycles for classes of finite triangles in $\mathcal{T}_1$, as we will show in Section 11: take any fractal ancestor copy $\mathcal{C}$ of $\mathcal{P}_1 \setminus \alpha$–axis that is included in $\mathcal{P}_1$ and not bordered by the α–axis; the outer layer of $\mathcal{C}$ belongs to $\mathcal{A}_{n+1}$ for some unique $n \geq 1$; cut away the part of $\mathcal{C}$ beyond the ancestor curve of Φ through $\mathcal{C}$ that is as far as possible from and n generations older than the ancestor curve of Φ bordering $\mathcal{C}$ (this ancestor may be Φ here); denote by $\mathcal{R}$ the rest of $\mathcal{C}$; take the smallest integer $N \geq 1$ with $r^N(\mathcal{R}) \supset \mathcal{R}$: one has $N \leq n$ since $r^n(\mathcal{R}) \supset \mathcal{R}$; r^N is then a bijective continuous mapping from $\mathcal{R}$ to $r^N(\mathcal{R}) \supset \mathcal{R}$ with continuous inverse and there is at least one N–cycle as in the proof of Theorem 15 since $\bigcup_{k=1}^{N-1} r^k(\mathcal{R})$ doesn't intersect $\mathcal{R}$ if $N \geq 2$. This N–cycle is unique and the same cycle is generated in this way by infinitely many different fractal copies of $\mathcal{P}_1 \setminus \alpha$–axis in $\mathcal{P}_1$ (see Section 11).

$$(25.478876347440316089\ldots^\circ, 3.6818528532788970876\ldots^\circ)$$
$$(62.431567122689586325\ldots^\circ, 12.276789619498866686\ldots^\circ)$$
$$(32.460249346540695688\ldots^\circ, 24.998279789538063086\ldots^\circ)$$

is a 3–cycle not leaving $\mathcal{S}_1$.

$$(37.865926747917574986\ldots^\circ, 18.061811244908607526\ldots^\circ)$$
$$(10.468235814868372615\ldots^\circ, 4.8401011494351450701\ldots^\circ)$$
$$(48.638604189899250723\ldots^\circ, 22.211186045240131467\ldots^\circ)$$

is a 3–cycle of triangle classes in order in $\mathcal{S}_2^{lt}$, $\mathcal{P}_2$ and $\mathcal{S}_1^{rt}$.

$$(42.090874141099660640\ldots^\circ, 15.557122843876427568\ldots^\circ)$$
$$(1.2635523114915185243\ldots^\circ, 0.8247788078196525102\ldots^\circ)$$
$$(6.3075862480243139879\ldots^\circ, 4.1172394455012728648\ldots^\circ)$$
$$(30.390568589226577771\ldots^\circ, 19.803092968967591208\ldots^\circ)$$

is a 4–cycle of triangle classes in order in $\mathcal{S}_3^{lt}$, $\mathcal{P}_3$, $\mathcal{P}_2$ and $\mathcal{S}_1^{lt}$.

$$(37.247939372886625265\ldots^\circ, 19.189939461450692321\ldots^\circ)$$
$$(10.723421490339811872\ldots^\circ, 4.2741308209904622975\ldots^\circ)$$
$$(49.920751710266512618\ldots^\circ, 19.633287363391045768\ldots^\circ)$$
$$(30.697646461742403045\ldots^\circ, 17.370185973399543132\ldots^\circ)$$

is a 4–cycle of triangle classes in order in $\mathcal{S}_2^{lt}$, $\mathcal{P}_2$, $\mathcal{S}_1^{rt}$ and $\mathcal{S}_1^{lt}$.

$$(37.630255649010598209\ldots^\circ, 18.570369773326372964\ldots^\circ)$$
$$(10.420573639194774736\ldots^\circ, 4.5115591822140415293\ldots^\circ)$$
$$(48.550547727001821453\ldots^\circ, 20.765781310885329500\ldots^\circ)$$
$$(32.363595430957208503\ldots^\circ, 16.384331092939721789\ldots^\circ)$$
$$(30.729181801658592737\ldots^\circ, 17.688152298022029834\ldots^\circ)$$

is a 5–cycle of triangle classes in order in $\mathcal{S}_2^{lt}$, $\mathcal{P}_2$, $\mathcal{S}_1^{rt}$, $\mathcal{S}_1^{lt}$ and $\mathcal{S}_1^{lt}$.

$$(37.930269796367360642\ldots^\circ, 18.102923174699484745\ldots^\circ)$$
$$(10.135362642153623417\ldots^\circ, 4.6659841044983596966\ldots^\circ)$$
$$(47.278732653265572140\ldots^\circ, 21.526719537744220795\ldots^\circ)$$
$$(32.908073875879027270\ldots^\circ, 15.212876460421699178\ldots^\circ)$$
$$(27.941680542770112113\ldots^\circ, 18.655538982479742580\ldots^\circ)$$
$$(48.659125226707857104\ldots^\circ, 22.220242130215287975\ldots^\circ)$$

is a 6–cycle of triangle classes in order in $\mathcal{S}_2^{lt}$, $\mathcal{P}_2$, $\mathcal{S}_1^{rt}$, $\mathcal{S}_1^{lt}$, $\mathcal{S}_1^{lt}$ and $\mathcal{S}_1^{rt}$.

$$(39.305662309899846302\ldots^\circ, 17.677017538458936691\ldots^\circ)$$
$$(5.7747047491290930782\ldots^\circ, 2.8485972409982163053\ldots^\circ)$$
$$(28.121014496985812289\ldots^\circ, 13.853288022731393651\ldots^\circ)$$
$$(36.786251566382858823\ldots^\circ, 31.096467455697263241\ldots^\circ)$$
$$(66.202454138266987877\ldots^\circ, 11.299882269350171350\ldots^\circ)$$
$$(38.901818026182387037\ldots^\circ, 25.434990337954490686\ldots^\circ)$$
$$(30.886718722856714101\ldots^\circ, 7.0225504408166614203\ldots^\circ)$$

is a 7–cycle of triangle classes in order in $\mathcal{S}_2^{lt}$, $\mathcal{P}_2$, $\mathcal{S}_1^{lt}$, $\mathcal{S}_1^{rt}$, $\mathcal{S}_1^{rb}$, $\mathcal{S}_1^{rt}$ and $\mathcal{S}_1^{lb}$.

$$(38.468777685667500548\ldots^\circ, 18.102890974997997195\ldots^\circ)$$
$$(8.0151057516993356943\ldots^\circ, 3.7150704462974721546\ldots^\circ)$$
$$(38.254172619328622821\ldots^\circ, 17.649186686577651211\ldots^\circ)$$
$$(9.7328922219345150314\ldots^\circ, 4.7538361797984130640\ldots^\circ)$$
$$(45.519097683522135284\ldots^\circ, 22.022284341558206040\ldots^\circ)$$
$$(31.297303214442445113\ldots^\circ, 13.020261718008364724\ldots^\circ)$$
$$(28.711664232298528730\ldots^\circ, 25.939377664641886290\ldots^\circ)$$
$$(66.695344715752296964\ldots^\circ, 8.3394888580526813797\ldots^\circ)$$

is a 8–cycle of triangle classes in order in $\mathcal{S}_2^{lt}$, $\mathcal{P}_2$, $\mathcal{S}_2^{lt}$, $\mathcal{P}_2$, $\mathcal{S}_1^{rt}$, $\mathcal{S}_1^{lt}$, $\mathcal{S}_1^{lt}$ and $\mathcal{S}_1^{rb}$.

As for $\mathcal{S}_n^{lb}$ and $\mathcal{S}_n^{rb}$, any fractal ancestor copy $\mathcal{C}$ of $\mathcal{P}_1$ that is bordered by the α–axis and included in $\mathcal{P}_1$ is covered for the first time by $r^n(\mathcal{C})$ for some $n \geq 1$; r^n is then a bijective continuous mapping from $\mathcal{C}$ to $r^n(\mathcal{C}) \supset \mathcal{C}$ with continuous inverse and – since $\bigcup_{k=1}^{n-1} r^k(\mathcal{C})$ doesn't intersect $\mathcal{C}$ for $n \geq 2$ – there is at least one n–cycle. We show in Section 11 that this n–cycle is unique and consists of classes of infinite triangles and that each cycle of such classes can be generated in this way by infinitely many different fractal copies of $\mathcal{P}_1$ bordered by the α–axis in $\mathcal{P}_1$.

Theorem 16. *$\mathcal{T} \setminus \big(\mathcal{A} \cup \mathcal{D}\big)$ is totally path–disconnected if $\mathcal{T} = \big\{(\alpha, \beta) \mid 0^\circ \leq \beta \leq \alpha \leq 90^\circ - \frac{\beta}{2}\big\}$.*

Proof. Otherwise some fixed continuous curve between two different points of $\mathcal{T} \setminus \big(\mathcal{A} \cup \mathcal{D}\big)$ would be included in each member of an infinite nested family of shrinking fractal ancestor copies of $\mathcal{P}_1$ or of $\mathcal{P}_1 \setminus \alpha$–axis whose diameters tend to 0, a contradiction. □

11. Reflection triangles as symbolic dynamics

We use the notations of Section 9. Referring to Figure 36, which is based on Figure 8, we code a class Π_α of infinite triangles by the infinite sequence $x = x_1x_2x_3\ldots$ of digits $x_k \in \{0, 1, 2\}$ giving the position of α in "base 3" with respect to the fractal subdivision of $[0^\circ, 90^\circ]$ induced by the monotonicity intervals of $\rho|_\Gamma$ and its iterates. If x is eventually periodic we overline the period's digits. We identify the ends $0\overline{2}$ and $1\overline{0}$ as well as $1\overline{2}$ and $2\overline{0}$. For a class x of infinite triangles or for the zero sequence x coding $\mathcal{O}$, the reflection class $r(x)$ is then given by a left shift when $x_1 = 0$ or 2 and a left shift with permutation $0 \leftrightarrow 2$ in x when $x_1 = 1$. Note that $r^n(x) = x_{n+1}\ldots$ or $r^n(x) = (x_{n+1}\ldots)_{0\leftrightarrow 2}$ according as $x_1\ldots x_n$ contains an even or odd number of 1's.

One has $\mathcal{O} = \overline{0}$, $\Pi_{\omega_{21}} = 1\overline{0}$, $\Pi_{\omega_{38}} = \overline{1}$, $\Pi_{\omega_{52}} = 2\overline{0}$, and $\Pi_{\pi/2} = \overline{2}$. The lexicographic order of two sequences is the same as the order $\alpha < \beta \leq \frac{\pi}{2}$ for the corresponding infinite triangles Π_α and Π_β. The parents of x are $0x$, $2x$ and $1x_{0\leftrightarrow 2}$ (if one neglects the parents of $x = \mathcal{O}$ that are classes of finite triangles). A sequence is an ancestor of $\overline{0}$ ($\overline{0}$ included) if and only if it contains an even number of 1's with end $\overline{0}$ or an odd number of 1's with end $\overline{2}$. A sequence is an ancestor of $\overline{2}$ ($\overline{2}$ included) if and only if it contains an even number of 1's with end $\overline{2}$ or an odd number of 1's with end $\overline{0}$. The three 2–cycles are generated by $\overline{02} = \Pi_{\omega_{12}}$, $\overline{0121}$ and $\overline{1012}$. (See the discussion after Theorem 8.)

x generates a periodic orbit if and only if the sequence is periodic: if $r^n(x) = x$ for some $n \in \mathbf{N}\setminus\{0\}$, one has indeed $x = \overline{x_1\ldots x_n}$ or $x = \overline{x_1\ldots x_n(x_1\ldots x_n)_{0\leftrightarrow 2}}$ according as $x_1\ldots x_n$ contains an even or odd number of 1's; conversely, if $x = \overline{x_1\ldots x_n}$, one has $r^n(x) = x$ or $r^n(x) = x_{0\leftrightarrow 2}$ and thus $r^n(x) = x$ or $r^{2n}(x) = x$: the orbit is periodic. x generates an infinite forward orbit if and only if the sequence never becomes periodic.

We code a class of non-acute nondegenerate triangles (*i.e.*, a class of $\mathcal{T}_1$) by a nonempty sequence $z = w_1y_1w_2y_2\ldots$ of digits $w_k \in \mathbf{N} \setminus \{0\}$ and $y_k \in$

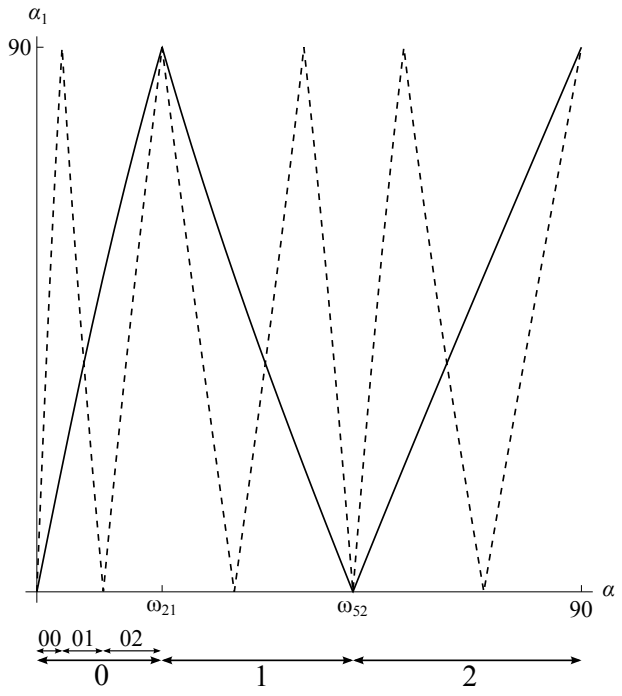

Figure 36. Fractal subdivision of $[0°, 90°]$ induced by $\Pi_{\alpha_1} = r(\Pi_\alpha)$ and its iterates

$\{D, E, i, ii, iii, iv\}$ with the following property: if z is a finite sequence, it ends with E – for "exterior" – or with D – for "becoming degenerate" – and these are the only occurrences of D and E. At each zooming stage k (see Figures 34 and 35), w_k numerates the side–by–side fractal copies of $\mathcal{P}_1$ or $\mathcal{P}_1 \setminus \alpha$–axis (starting from the border in $\mathcal{A}_k$) and y_k locates the triangle class in this copy: D if the triangle class is on the midline that becomes eventually degenerate, E if it is in one of the two components of $\mathcal{A}$ bordering this copy and i, ii, iii or iv if it is in the bottom right, top right, top left or bottom left inside quarter (without midline), respectively. The triangle classes of $\mathcal{S}_2^{lb}$ correspond for example to sequences beginning with $1iv2\ldots$

All triangle classes on the same midline section are thus coded identically, as are the triangle classes in the components of $\mathcal{A}$ bordering the same copy. The infinite sequences z containing neither ii nor iii code the classes of infinite triangles that don't become degenerate. An infinite sequence z containing only $y_k \in \{i, iv\}$ for all $k > k_0$ after a last $y_{k_0} \in \{ii, iii\}$ is identified with the finite sequence obtained by putting $y_{k_0+1} = D$: for example $1i1ii\overline{1i1iv} = 1i1ii1D$. The preceding sentence is also true if one interchanges i, iv with ii, iii. An infinite sequence z containing only $y_k \in \{ii, iii\}$ is identified with $w_1 D$. Triangle classes ending in E or D have two representations when they are on the curve separating quarter i from ii or iii from iv at the last stage: $(60°, 15°)$ is for example $1i1D$ or $1ii1D$.

Classes of infinite triangles ending in $\overline{1i}$ – except $z = \overline{1i}$ – or in $\overline{1iv}$ have a second representation ending in $\overline{1iv}$ or $\overline{1i}$, respectively.

We consider the following involutive permutations of $\{i, ii, iii, iv\}$: σ_i is the identity, σ_{ii} interchanges $i \leftrightarrow ii$ and $iii \leftrightarrow iv$, σ_{iii} interchanges $i \leftrightarrow iii$ and $ii \leftrightarrow iv$ and σ_{iv} interchanges $i \leftrightarrow iv$ and $ii \leftrightarrow iii$. These permutations form a dihedral group $C_2 \times C_2$ under composition – with $\sigma_{iii} \circ \sigma_{ii} = \sigma_{ii} \circ \sigma_{iii} = \sigma_{iv}$, and cyclically. The reflection class $r(z)$ is then given by the following transformation of $z = w_1 y_1 w_2 y_2 \cdots \in \mathcal{T}_1$:

(1) if $w_1 > 1$, $r(z) = (w_1 - 1) y_1 w_2 y_2 \ldots$,
(2) $r(1E) =$ acute triangle outside $\mathcal{T}_1$,
(3) $r(1D) =$ degenerate triangle $(0°, 0°)$ outside $\mathcal{T}_1$,
(4) $r(1 y_1 w_2 y_2 \ldots) = \sigma_{y_1}(w_2 y_2 \ldots)$ for $y_1 \in \{i, ii, iii, iv\}$ except when all $y_k \in \{ii, iii\}$ (then $1 y_1 w_2 y_2 \cdots = 1D$).

The parents of z are $(w_1 + 1) y_1 \ldots$, $1y\,\sigma_y(z)$ for $y = i, iv$, and – if z codes a class of proper triangles – $1y\,\sigma_y(z)$ for $y = ii, iii$. An infinite triangle tends to $\Pi_{\pi/2}$ under iteration of r if and only if its code ends in $\overline{1i}$ or in $\overline{1iv}$. The fixed points of r in $\mathcal{T}_1$ are the heptagonal class $\overline{1ii1i}$, the triangle class $\overline{1iii1i}$ with coordinates $\left(\frac{6-\sqrt{5}}{4}, \frac{8\sqrt{5}-17}{64}\right)$, $\Pi_{\omega_{38}} = \overline{1iv1i}$ and $\Pi_{\pi/2} = \overline{1i}$.

If $r^n(z)$ causes a left shift of $2m$ digits, $m \geq 1$, one has

$$r^n(z) = \sigma_y\big((w_{m+1} - \nu) y_{m+1} w_{m+2} y_{m+2} \ldots\big)$$

where $y \in \{i, ii, iii, iv\}$ is given by $t_1 = y_1$, $t_{k+1} = \sigma_{\sigma_{t_k}(y_{k+1})}(t_k)$ for $1 \leq k \leq m-1$, $y = t_m$ and where ν is an integer $\in [0, w_{m+1} - 1]$; one has $n = \nu + \sum_{k=1}^{m} w_k$.

Theorem 17. (1) *The following situations are equivalent:*

(a) $n \geq 1$, $r^n(z) = z$ *and* $r^n(z)$ *causes a left shift of* $2m$ *digits.*
(b) $m \geq 1$,

$$z = (w_1 - \nu) y_1 w_2 y_2 \ldots w_m y_m \,\overline{\sigma_y(w_1 y_1 w_2 y_2 \ldots w_m y_m)\, w_1 y_1 w_2 y_2 \ldots w_m y_m} \tag{26}$$

for some integer $\nu \in [0, w_1 - 1]$, $n = \sum_{k=1}^{m} w_k$ *and* y *is given by* $t_1 = y_1$, $t_{k+1} = \sigma_{\sigma_{t_k}(y_{k+1})}(t_k)$ *for* $1 \leq k \leq m-1$, $y = t_m$.

The forward (periodic) orbit of z *is then generated by*

$$r^{n-\nu}(z) = \overline{w_1 y_1 w_2 y_2 \ldots w_m y_m\, \sigma_y(w_1 y_1 w_2 y_2 \ldots w_m y_m)} \tag{27}$$

and the sequence z *is periodic if and only if* $\nu = 0$.
(2) *For each integer* $N \geq 1$ *the number of* N*–periodic orbits is finite and nonzero for both finite and infinite triangles.*
(3) *A triangle class of* $\mathcal{T}_1$ *belongs to the backward orbit of a periodic orbit of* $\mathcal{T}_1$ *if and only if its sequence* z *is eventually periodic and contains infinitely many* $y_k \in \{i, iv\}$.
(4) *A triangle class of* $\mathcal{T}_1$ *belongs to an infinite divergent forward orbit if and only if its sequence* z *is infinite, never becomes periodic and contains either no* $y_k \in \{ii, iii\}$ *or both infinitely many* $y_k \in \{ii, iii\}$ *and infinitely many* $y_k \in \{i, iv\}$.

(5) *Every periodic orbit in $\mathcal{T}_1$ is repelling. An infinite forward orbit in $\mathcal{T}_1$ is thus never asymptotically periodic.*

Proof. (1) By setting $r^n(z) = z$ in the paragraph preceding the theorem.

(2) There is at least one N–periodic orbit for classes of both finite and infinite triangles by Theorems 15 and 8 and there are finitely many sequences with the necessary form (27) for $n = N$.

(3) The ancestors of a generator (27) of a periodic orbit are eventually periodic sequences.

Conversely, if the sequence z is eventually periodic, $r^{k_0}(z)$ is periodic for infinitely many k_0. Fix such a k_0 with $r^{k_0}(z) = \overline{w_1y_1w_2y_2\dots w_My_M}$. If $n = \sum_{k=1}^{M} w_k$ the sequences $r^{k_0+\ell n}(z)$, $\ell \in \mathbf{N}$, are then $\sigma_{\tilde{y}_\ell}\big(r^{k_0}(z)\big)$ for some $\tilde{y}_\ell \in \{i, ii, iii, iv\}$: since there are two equal $\tilde{y}_\ell$ in $\{\tilde{y}_0, \dots, \tilde{y}_4\}$ some descendant $r^{k_0+\ell n}(z)$ of z with $0 \le \ell \le 3$ generates a periodic orbit.

(4) follows from the preceding results.

(5) We already know that the fixed point $\Pi_{\pi/2}$ is repelling. Consider another periodic orbit: it is generated as in (27) by a sequence

$$z_0 = \overline{w_1y_1w_2y_2\dots w_my_m\,\sigma_y(w_1y_1w_2y_2\dots w_my_m)}$$

with $r^n(z_0) = z_0$ for $n = \sum_{k=1}^{m} w_k$ that corresponds to the triangle class $\Delta_0 \neq \Pi_{\pi/2}$. Let $\varepsilon > 0$ be the distance between Δ_0 and $\mathcal{A}_n$ in $\mathcal{T}_1$. We consider $\Delta \neq \Delta_0$ in the ε–neighborhood of Δ_0 with sequence z. If z is finite, some descendant of Δ will be degenerate or acute, *i.e.*, some $r^{\ell_0 n}(\Delta)$ will be outside the ε–neighborhood of $r^{\ell_0 n}(\Delta_0) = \Delta_0$. If $\Delta \notin \mathcal{A} \cup \mathcal{D}$ the first $2m$ digits of z and z_0 coincide. Let $k_0 \in \,]\ell_0 m, (\ell_0+1)m]$ with $\ell_0 \in \mathbf{N} \setminus \{0\}$ be the index of the first different digit. Then $r^{\ell_0 n}(z)$ and $r^{\ell_0 n}(z_0) = z_0$ differ in one of the first $2m$ digits: $r^{\ell_0 n}(\Delta)$ is outside the ε–neighborhood of $r^{\ell_0 n}(\Delta_0) = \Delta_0$, the periodic orbit is repelling. □

Note that the forward orbit of z in (27) may have less than n points, even if $y \neq i$: for example

$$\overline{1i1ii1ii1i1i1ii\,\sigma_y(1i1ii1ii1i1i1ii)} = \overline{1i1ii1ii1i} = \overline{1i1ii\,\sigma_{\tilde{y}}(1i1ii)}$$

since $y = \tilde{y} = ii$.

We now analyze the construction of Section 10. Suppose without restricting the generality that a cycle is generated by (26). This cycle contains a triangle class of $\mathcal{P}_1$ beginning with $1y_1w_2y_2\dots w_my_mw_1$. Take the fractal copy $\mathcal{C}$ of $\mathcal{P}_1$ with this address (conversely, the address $1y_1w_2y_2\dots w_my_mw_1$ of any fractal copy $\mathcal{C}$ of $\mathcal{P}_1$ in $\mathcal{P}_1$ can be chosen as begin of (26)). Suppose that the cycle is a N–cycle with $2M$ shifts: note that $N = \sum_{k=1}^{M} w_k$ divides $n = \sum_{k=1}^{m} w_k$. The given cycle (26) is then generated by

$$z = 1y_1w_2y_2\dots w_My_M\,\overline{\sigma_{\tilde{y}}(w_1y_1w_2y_2\dots w_My_M)\,w_1y_1w_2y_2\dots w_My_M}$$

and is exactly the cycle generated by $\mathcal{C}$ in the construction of Section 10 since the addresses of $r^k(\mathcal{C})$, $0 \le k \le N-1$, are correct: there is thus only one such cycle. The same cycle is also generated by

$$1\underbrace{y_1w_2y_2\dots w_my_m\sigma_y(w_1y_1w_2y_2\dots w_my_m)\,w_1y_1w_2y_2\dots w_my_m}_{\text{head}}\overline{\sigma_y(w_1\text{head})w_1\text{head}}$$

and the segment $\sigma_y(w_1y_1w_2y_2\dots w_my_m)\,w_1y_1w_2y_2\dots w_my_m$ can be concatenated any finite number of times in the head: this gives addresses of infinitely many nested $\mathcal{C}$ generating the same cycle. The more concatenations of this segment the head contains, the more the starting $\mathcal{C}$ and its first $N-1$ descendants $r(\mathcal{C}),\ \dots,\ r^{N-1}(\mathcal{C})$ converge to the orbit points.

The three 2–cycles for classes of infinite triangles are generated by $\overline{2i} = \Pi_{\omega_{12}}$, $\overline{2iv2i}$ and $\overline{1i1iv1iv1i}$. In the same order as in Section 6 the seven 2–cycles for classes of finite triangles are generated by $\overline{2iii2i}$, $\overline{1iii1ii1iv1i}$, $\overline{1i1ii1ii1i}$, $\overline{2ii2i}$, $\overline{1iii1iv1ii1i}$, $\overline{1ii1iii1iv1i}$ and $\overline{1iii1iii1i1i}$.

Table 1 contains the fundamental periods of periodic generators of the 40 different 3–cycles. The explicit 3–cycles of Section 10 are generated in order by $\overline{3iii3i}$, $\overline{1i1iii1ii1ii1iv1i}$ and $\overline{2ii1iv2iii1i}$. The explicit 8–cycle is generated by

$$\overline{2iii2iv1ii1iv1iv1iv1ii\,\sigma_{iv}(2iii2iv1ii1iv1iv1ii)} = (8.015\dots^\circ, 3.715\dots^\circ).$$

Theorem 18. *Under the reflection map r, there are in $\mathcal{T}_1$ uncountably many disjoint infinite forward orbits of classes of both finite and infinite triangles.*

Proof. The infinite sequence $z = \underbrace{1i}_{1\times}1ii1i\underbrace{1i1i}_{2\times}1ii1i\underbrace{1i1i1i}_{3\times}\dots$ codes a class of finite triangles with unique representation and generates an infinite forward orbit in $\mathcal{P}_1$: z begins indeed with one copy of $1i$, $r^3(z)$ with two copies, $r^7(z)$ with three copies, $r^{12}(z)$ with four copies and so on. The backward orbit of this (and of every) infinite forward orbit is countable. One can thus replace the occurrence numbers $1, 2, 3, 4, \dots$ of $1i$ in the successive groups (separated by $1ii1i$) by the successive digits of uncountably many irrational numbers in such a way that all generated forward orbits, which are infinite, are disjoint. By replacing ii by iv in z one gets an infinite orbit of infinite triangles. Note that one can also consider the infinite triangle $x = 021102021102020211\dots$ □

$z = w_1y_1w_2y_2\dots$ with $w_k = k$ for all $k \geq 1$ and $(y_k)_{k\geq1} = \overline{i, ii, iii, iv}$ generates an infinite forward orbit of classes of finite triangles, too (with accumulation point $\mathcal{O}$).

Theorem 19. *$\mathcal{A}$ is a dense open subset of $\mathcal{T} = \big\{(\alpha,\beta) \mid 0^\circ \leq \beta \leq \alpha \leq 90^\circ - \frac{\beta}{2}\big\}$. Any neighborhood of a point of $\mathcal{T}\setminus\mathcal{A}$ intersects countably many periodic orbits and uncountably many disjoint divergent forward orbits; the rest of the neighborhood consists of uncountably many points of $\mathcal{D}$, uncountably many points of $\mathcal{A}$ and countably many other points that become eventually periodic.*

Proof. A point of $\mathcal{A}_n$, $n \in \mathbf{N}$, has some neighborhood in $\mathcal{A}_{n-1} \cup \mathcal{A}_n$ if one sets $\mathcal{A}_{-1} = \mathcal{A}_0$. The rest follows from the fact that every neighborhood of a point of $\mathcal{T}\setminus\mathcal{A}$ contains (infinitely many) fractal copies of $\mathcal{P}_1\setminus\alpha$–axis: take such a copy and let $w_1y_1\dots w_M$ be its address; this head can be prolonged to get the given number

$\overline{1i1i1ii1ii1i}$	:	$(77.992, 5.4261)$,	$(61.422, 14.969)$,	$(32.443, 31.271)$	
$\overline{1i1i1iii1iii1iii1i}$	:	$(77.137, 5.2765)$,	$(59.569, 14.357)$,	$(28.774, 27.798)$	
$\overline{1i1i1iv1iv1iv1i}$	:	$(78.072, 0.0000)$,	$(62.116, 0.0000)$,	$(24.228, 0.0000)$	$\leftarrow$
$\overline{1i1ii1i}$	:	$(77.538, 5.7639)$,	$(60.431, 15.811)$,	$(32.623, 31.329)$	
$\overline{1i1ii1iii1iii1iv1i}$	:	$(64.111, 12.369)$,	$(35.593, 26.667)$,	$(24.946, 3.6423)$	
$\overline{1i1ii1iv1iv1iii1i}$	:	$(76.703, 5.5669)$,	$(58.628, 15.057)$,	$(28.720, 27.668)$	
$\overline{1i1iii1i}$	:	$(63.351, 7.1712)$,	$(31.121, 13.087)$,	$(29.183, 26.185)$	
$\overline{1i1iii1ii1ii1iv1i}$	:	$(62.432, 12.277)$,	$(32.460, 24.998)$,	$(25.479, 3.6819)$	
$\overline{1i1iii1iv1iv1ii1i}$	:	$(61.950, 7.8678)$,	$(28.710, 13.651)$,	$(35.158, 30.232)$	
$\overline{1i1iv1i}$	:	$(69.448, 0.0000)$,	$(41.773, 0.0000)$,	$(26.919, 0.0000)$	$\leftarrow$
$\overline{1i1iv1ii1ii1iii1i}$	:	$(63.532, 6.4266)$,	$(31.070, 11.546)$,	$(29.295, 26.539)$	
$\overline{1i1iv1iii1iii1ii1i}$	:	$(62.337, 6.7728)$,	$(28.805, 11.523)$,	$(34.391, 30.234)$	
$\overline{1ii1i1iii1iv1iii1i}$	:	$(45.654, 26.671)$,	$(50.356, 18.460)$,	$(27.406, 16.857)$	
$\overline{1ii1i1iv1iii1iv1i}$	:	$(53.737, 20.669)$,	$(39.419, 24.424)$,	$(25.777, 6.4984)$	
$\overline{1ii1iii1i}$	:	$(39.242, 25.752)$,	$(34.431, 7.9491)$,	$(28.909, 15.731)$	
$\overline{1ii1iii1ii1i1iv1i}$	:	$(36.334, 27.318)$,	$(36.353, 5.6518)$,	$(29.022, 10.379)$	
$\overline{1ii1iv1i}$	:	$(53.953, 18.520)$,	$(33.152, 22.790)$,	$(26.294, 5.8906)$	
$\overline{1ii1iv1ii1i1iii1i}$	:	$(47.415, 21.434)$,	$(32.805, 15.325)$,	$(28.339, 18.663)$	
$\overline{1iii1i1iv1ii1iv1i}$	:	$(31.077, 14.761)$,	$(32.071, 23.138)$,	$(34.174, 7.1741)$	
$\overline{1iii1ii1iii1i1iv1i}$	:	$(31.634, 24.738)$,	$(35.739, 5.4231)$,	$(30.966, 10.501)$	
$\overline{2i1i}$	:	$(17.076, 0.0000)$,	$(76.815, 0.0000)$,	$(59.165, 0.0000)$	$\leftarrow$
$\overline{2i1ii2ii1i}$	:	$(14.181, 2.6145)$,	$(64.753, 11.579)$,	$(36.335, 25.097)$	
$\overline{2i1iii2iii1i}$	:	$(13.882, 2.5866)$,	$(63.564, 11.512)$,	$(34.082, 23.968)$	
$\overline{2i1iv2iv1i}$	:	$(15.623, 0.0000)$,	$(71.266, 0.0000)$,	$(46.083, 0.0000)$	$\leftarrow$
$\overline{2ii1i}$	:	$(10.110, 5.3306)$,	$(46.937, 24.481)$,	$(43.827, 17.928)$	
$\overline{2ii1ii2i1i}$	:	$(8.2127, 6.0759)$,	$(38.467, 28.345)$,	$(50.539, 10.136)$	
$\overline{2ii1iii2iv1i}$	:	$(8.3357, 5.7834)$,	$(39.101, 27.004)$,	$(42.786, 9.3457)$	
$\overline{2ii1iv2iii1i}$	:	$(10.468, 4.8401)$,	$(48.639, 22.211)$,	$(37.866, 18.062)$	
$\overline{2iii1i}$	:	$(6.3707, 4.0384)$,	$(30.697, 19.423)$,	$(40.263, 15.637)$	
$\overline{2iii1ii2iv1i}$	:	$(6.4310, 4.7667)$,	$(30.826, 22.812)$,	$(43.381, 9.8110)$	
$\overline{2iii1iii2i1i}$	:	$(6.2608, 4.8616)$,	$(30.025, 23.283)$,	$(49.365, 10.426)$	
$\overline{2iii1iv2ii1i}$	:	$(6.2109, 4.2180)$,	$(29.925, 20.291)$,	$(44.884, 15.582)$	
$\overline{2iv1i}$	:	$(6.8623, 0.0000)$,	$(33.576, 0.0000)$,	$(49.511, 0.0000)$	$\leftarrow$
$\overline{2iv1ii2iii1i}$	:	$(6.2470, 1.7815)$,	$(30.485, 8.6796)$,	$(36.590, 21.684)$	
$\overline{2iv1iii2ii1i}$	:	$(6.1133, 1.7573)$,	$(29.860, 8.5706)$,	$(38.323, 22.175)$	
$\overline{2iv1iv2i1i}$	:	$(6.4721, 0.0000)$,	$(31.739, 0.0000)$,	$(54.842, 0.0000)$	$\leftarrow$
$\overline{3i}$	:	$(2.2468, 0.0000)$,	$(11.207, 0.0000)$,	$(53.139, 0.0000)$	$\leftarrow$
$\overline{3ii3i}$	:	$(1.7190, 0.7883)$,	$(8.5745, 3.9322)$,	$(40.696, 18.552)$	
$\overline{3iii3i}$	:	$(1.6847, 0.7779)$,	$(8.4041, 3.8806)$,	$(39.952, 18.346)$	
$\overline{3iv3i}$	:	$(2.1646, 0.0000)$,	$(10.798, 0.0000)$,	$(51.375, 0.0000)$	$\leftarrow$

Table 1. Periodic generators of the forty 3–cycles with their approximate angles (in $^\circ$) and the approximate angles of their child and grandchild in order ($\leftarrow$ denotes classes of infinite triangles)

of points of the desired type in the same copy; the given neighborhood cannot contain uncountably many eventually periodic triangles outside $\mathcal{A} \cup \mathcal{D}$ since their total number in $\mathcal{T}$ is countable. □

One can construct codes z with almost any behavior under iteration of the reflection map, as for the sequences of pedal triangles [1]. We design for example a code z whose forward orbit is dense in $\mathcal{T} \setminus \mathcal{A}$: write all words $w_1 y_1 \dots w_. y_.$ of finite length with digits $w \in \mathbf{N} \setminus \{0\}$ and $y \in \{i, ii, iii, iv\}$; order these words by lexicographic order of the w's and then of the y's for each sum 1, 2, 3, ... of the w's; concatenate the words and submit each of them in order to an appropriate permutation $\sigma_{i,ii,iii,iv}$ such that the original word will appear as head of the corresponding descendant of z.

Theorem 20. *The backward orbit of a class of proper triangles of $\mathcal{T} \setminus \mathcal{A}$ is dense in $\mathcal{T} \setminus \mathcal{A}$.*

Proof. Consider a class of proper triangles $\Delta_0 \in \mathcal{T} \setminus \mathcal{A}$ and suppose that $\Delta_0 \in \mathcal{P}_N \setminus \alpha$–axis. Fix a neighborhood of $\Delta \in \mathcal{T} \setminus \mathcal{A}$ and choose a fractal copy $\mathcal{C}$ of $\mathcal{P}_1 \setminus \alpha$–axis in this neighborhood. Take $n \geq 1$ such that r^n maps $\mathcal{C}$ bijectively to $\mathcal{P}_1 \setminus \alpha$–axis (such a n exists) and take the copy $\mathcal{C}' \subset \mathcal{C}$ that is the inverse image of $\mathcal{S}_N^{lb} \setminus \alpha$–axis under this mapping. r^{n+1} maps then $\mathcal{C}'$ bijectively to $\mathcal{P}_N \setminus \alpha$–axis: there is thus some $\Delta' \in \mathcal{C}'$ with $r^{n+1}(\Delta') = \Delta_0$. □

Note that the backward orbit of the degenerate class contains the backward orbit of $I_{\pi/6}$ – and of every class Δ of proper triangles with $s(\Delta) = \frac{5}{4}$ – and is thus also dense in $\mathcal{T} \setminus \mathcal{A}$. If Δ_0 is a class of proper triangles outside $\mathcal{A} \cup \mathcal{D}$ with code z_0, the code of some ancestor of Δ_0 in a fixed neighborhood of $\Delta \in \mathcal{T} \setminus \mathcal{A}$ can be constructed as follows: take a fractal copy $\mathcal{C}$ of $\mathcal{P}_1 \setminus \alpha$–axis with address $w_1 y_1 \dots w_M$ in this neighborhood; take this address as head of a code z whose tail is z_0 and fill the space between head and tail with one i, ii, iii or iv in such a way that z_0 will appear as a descendant of z: the triangle class with code z is an ancestor of Δ_0 in the given neighborhood of Δ.

References

[1] J. C. Alexander, The symbolic dynamics of the sequence of pedal triangles, *Math. Mag.*, 66 (1993) 147–158.

[2] O. Bottema, De constructie van een driehoek als de spiegelpunten van de hoekpunten in de overstaande zijden gegeven zijn, *Nieuw Tijdschrift voor Wiskunde*, 24 (1936/37) 248–251.

[3] O. Bottema, *Topics in Elementary Geometry*, Springer Science+Business Media, New York, 2008.

[4] J. C. Fisher, H. Weston, and A. K. Demis, Problem 3224 *Crux Math.*, 33 (2007) 112, 115; solution, 34 (2008) 120–124.

[5] D. Grinberg, On the Kosnita point and the reflection triangle, *Forum Geom.*, 3 (2003) 105–111.

[6] A. P. Hatzipolakis and P. Yiu, Reflections in triangle geometry, *Forum Geom.*, 9 (2009) 301–348.

[7] R. Honsberger, *Episodes in Nineteenth and Twentieth Century Euclidean Geometry*, Math. Assoc. Amer., Washington DC, 1995.

[8] J. van IJzeren, Spiegelpuntsdriehoeken, *Nieuw Tijdschrift voor Wiskunde*, 71 (1983/84) 95–106.

[9] J. van IJzeren, *Driehoeken met gegeven spiegelpuntsdriehoek*, Eindhoven University of Technology, EUT Report 84–WSK–03 (1984) 356–373 .
[10] R. A. Johnson, *Advanced Euclidean Geometry*, Dover reprint, 2007.
[11] L. Kuipers, Het beeld van spiegelingen van de hoekpunten van een driehoek in de overstaande zijlijnen, *Nieuw Tijdschrift voor Wiskunde*, 70 (1982/83) 58–59.
[12] G. R. Veldkamp, Spiegel(punts)driehoeken, *Nieuw Tijdschrift voor Wiskunde*, 73 (1985/86) 143–156.

University of Applied Sciences of Western Switzerland
Route du Rawyl 47, CH–1950 Sion, Switzerland
E-mail address: gregoire.nicollier@hevs.ch

Forum Geometricorum
Volume 12 (2012) 129.

FORUM GEOM
ISSN 1534-1178

Correction to Grégoire Nicollier, Reflection Triangles and Their Iterates, *Forum Geom.*, 12 (2012) 83–128.

An error was regretfully introduced in the statement of Theorem 11 in the bottom of p.108 during the typesetting process. Here is the corrected statement.

Theorem 11. *The parents in $\mathcal{T}$ of I_α, $\alpha \neq \frac{\pi}{3}$, are – up to the exceptions mentioned below – the two non-isosceles classes $\{\alpha'_\pm, \beta'_\pm, \gamma'_\pm\}$ given by the non-obtuse angles*

$$\alpha'_\pm = \tfrac{\pi}{4} \pm \tfrac{\alpha}{2}, \qquad \beta'_\pm = \operatorname{arccot}\left(2\cos\alpha + 2\sqrt{2 - \left(\frac{1}{2} \pm \sin\alpha\right)^2}\right),$$

and by

$$\gamma'_\pm = \operatorname{arccot}\left(2\cos\alpha - 2\sqrt{2 - \left(\frac{1}{2} \pm \sin\alpha\right)^2}\right)$$

in $]0, \pi[$ – with coordinates $\left(\frac{5}{4} \pm \sin\alpha, \frac{(1\pm\sin\alpha)^2}{64(1-\sin^2\alpha)}\right) \in \mathcal{T}^*$ – and the isosceles triangle classes with coordinates (s, p) (automatically on the roof) *corresponding to each real root s of $Q_3(s)$ given by* (23) *for $t = \sin^2\alpha$, with p as in Theorem 10.*

For $\alpha = \omega_{66}$ the triangle class $\{\alpha'_+, \beta'_+, \gamma'_+\}$ is isosceles with equal angles ω_{50} and corresponds to the triple root $s = \sqrt{2} + \frac{3}{4}$ of $v(s) = P_{\min}$ for $S = 12\sqrt{2} - \frac{59}{4}$. For $\alpha > \omega_{66}$ the non-isosceles class $\{\alpha'_+, \beta'_+, \gamma'_+\}$ doesn't exist: it corresponds to the parent outside $\mathcal{T}^*$ and $\beta'_+, \gamma'_+ \notin \mathbf{R}$.

Publication Date: April 20, 2012. Communicating Editor: Paul Yiu.

Forum Geometricorum
Volume 12 (2012) 131–139.

FORUM GEOM
ISSN 1534-1178

Three Conics Derived from Perpendicular Lines

Alberto Mendoza

Abstract. Given a triangle ABC and a generic point P on its plain, we consider the rectangular hyperbola $\mathcal{H}$ which is the isogonal conjugate of the line OP where O is the circumcenter of the triangle. We also consider the line $\mathcal{L}$ perpendicular to OP at the point P, the conic $\mathcal{E}$ which is the isogonal conjugate of this line and the inscribed parabola $\mathcal{P}$, tangent to the line $\mathcal{L}$. We discuss some relations between this three conics.

Let ABC be a triangle with sides a, b and c. Let P be a generic point with homogenous barycentric coordinates $(u : v : w)$ and

$$O = (a^2 S_A : b^2 S_B : c^2 S_C),$$

the circumcenter of the triangle ABC. The line OP is given by

$$\sum_{\text{cyclic}} (c^2 S_C v - b^2 S_B w)x = 0. \tag{1}$$

Let us define

$$p_a = -u + v + w, \quad p_b = u - v + w, \quad p_c = u + v - w,$$

and

$$\lambda_a = p_b\, S_B - p_c\, S_C, \quad \lambda_b = p_c\, S_C - p_a\, S_A, \quad \lambda_c = p_a\, S_A - p_b\, S_B.$$

Lemma 1. *In terms of these expressions,*
(a) *the line OP can be expressed as*

$$\sum_{\text{cyclic}} (b^2 \lambda_c + c^2 \lambda_b)x = 0, \tag{2}$$

(b) *the point at infinity of the line OP is given by*

$$I_{OP} = (\lambda_b\, S_B - \lambda_c\, S_C : \lambda_c\, S_C - \lambda_a\, S_A : \lambda_a\, S_A - \lambda_b\, S_B)\,, \tag{3}$$

(c) *and the infinite point of perpendicular lines to OP is given by*

$$I_{\mathcal{L}} = (\lambda_a : \lambda_b : \lambda_c). \tag{4}$$

Publication Date: April 20, 2012. Communicating Editor: Paul Yiu.

The author would like to thank the referee as his suggestions led to improvements of the original version of this paper.

Equations (2), (3) and (4) follow easily from (1) and the definitions.

Let $\mathcal{L}$ be the line perpendicular to the line OP at the point P, with equation

$$\mathcal{L}: \quad (\lambda_c\, v - \lambda_b\, w)\, x + (\lambda_a\, w - \lambda_c\, u)\, y + (\lambda_b\, u - \lambda_a\, v)\, z = 0.$$

Next we shall consider the isogonal conjugates of the lines OP and $\mathcal{L}$. The isogonal conjugate of the line OP is the rectangular hyperbola

$$\mathcal{H}: \quad \sum_{\text{cyclic}} a^2 \left(b^2\lambda_c + c^2\lambda_b\right) y\, z = 0.$$

The fourth point of intersection of the hyperbola $\mathcal{H}$ with the circumcircle is the isogonal conjugate of the point I_{OP}:

$$H' = \left(\frac{a^2}{\lambda_b\, S_B - \lambda_c\, S_C} : \frac{b^2}{\lambda_c\, S_C - \lambda_a\, S_A} : \frac{c^2}{\lambda_a\, S_A - \lambda_b\, S_B}\right).$$

The center M of $\mathcal{H}$ (on the nine point circle) is the midpoint of the points H and H', where H is the orthocenter of the triangle ABC,

$$M = \left(\left(b^2\lambda_c + c^2\lambda_b\right)\lambda_a : \left(c^2\lambda_a + a^2\lambda_c\right)\lambda_b : \left(a^2\lambda_b + b^2\lambda_a\right)\lambda_c\right).$$

The circumconic $\mathcal{E}$ is the isogonal conjugate of $\mathcal{L}$:

$$\mathcal{E}: \quad \sum_{\text{cyclic}} a^2\, (\lambda_c\, v - \lambda_b\, w)\, yz = 0.$$

The center of the circumconic $\mathcal{E}$ is the point

$$N = \left(a^2\, (\lambda_c\, v - \lambda_b\, w)\left(b^2\lambda_c w - c^2\lambda_b v + \lambda_b\lambda_c\right) : \cdots : \cdots\right).$$

The fourth intersection of $\mathcal{E}$ with the circumcircle is the isogonal conjugate of the point $I_{\mathcal{L}}$

$$E = \left(a^2\lambda_b\lambda_c : b^2\lambda_c\lambda_a : c^2\lambda_a\lambda_b\right).$$

The points H' and E are antipodes in circumcenter being the isogonal conjugates of points at infinity on perpendicular lines.

Finally we will consider the inscribed parabola tangent to the line $\mathcal{L}$. This is the parabola

$$\mathcal{P}: \quad \sum_{\text{cyclic}} \left(\lambda_a^2\, (\lambda_c\, v - \lambda_b\, w)^2\, x^2 - 2\lambda_b\, \lambda_c\, (\lambda_a\, w - \lambda_c\, u)\, (\lambda_b\, u - \lambda_a\, v)\, y\, z\right) = 0.$$

The center of the parabola $\mathcal{P}$ is the infinite point

$$J = ((\lambda_c\, v - \lambda_b\, w)\, \lambda_a : (\lambda_a\, w - \lambda_c\, u)\, \lambda_b : (\lambda_b\, u - \lambda_a\, v)\, \lambda_c).$$

The focus of $\mathcal{P}$ is the isogonal conjugate of J

$$F = \left(\frac{a^2\lambda_b\, \lambda_c}{\lambda_c\, v - \lambda_b\, w} : \frac{b^2\lambda_c\, \lambda_a}{\lambda_a\, w - \lambda_c\, u} : \frac{c^2\lambda_a\, \lambda_b}{\lambda_b\, u - \lambda_a\, v}\right),$$

and the perspector of $\mathcal{P}$, on the Steiner circumellipse $\mathcal{E}_0$, is the isotomic conjugate of J:

$$Q = \left(\frac{\lambda_b\, \lambda_c}{\lambda_c\, v - \lambda_b\, w} : \frac{\lambda_c\, \lambda_a}{\lambda_a\, w - \lambda_c\, u} : \frac{\lambda_a\, \lambda_b}{\lambda_b\, u - \lambda_a\, v}\right).$$

The point of contact between $\mathcal{P}$ and $\mathcal{L}$ is the point

$$T = \left(\frac{\lambda_a}{\lambda_c\, v - \lambda_b\, w} : \frac{\lambda_b}{\lambda_a\, w - \lambda_c\, u} : \frac{\lambda_c}{\lambda_b\, u - \lambda_a\, v} \right).$$

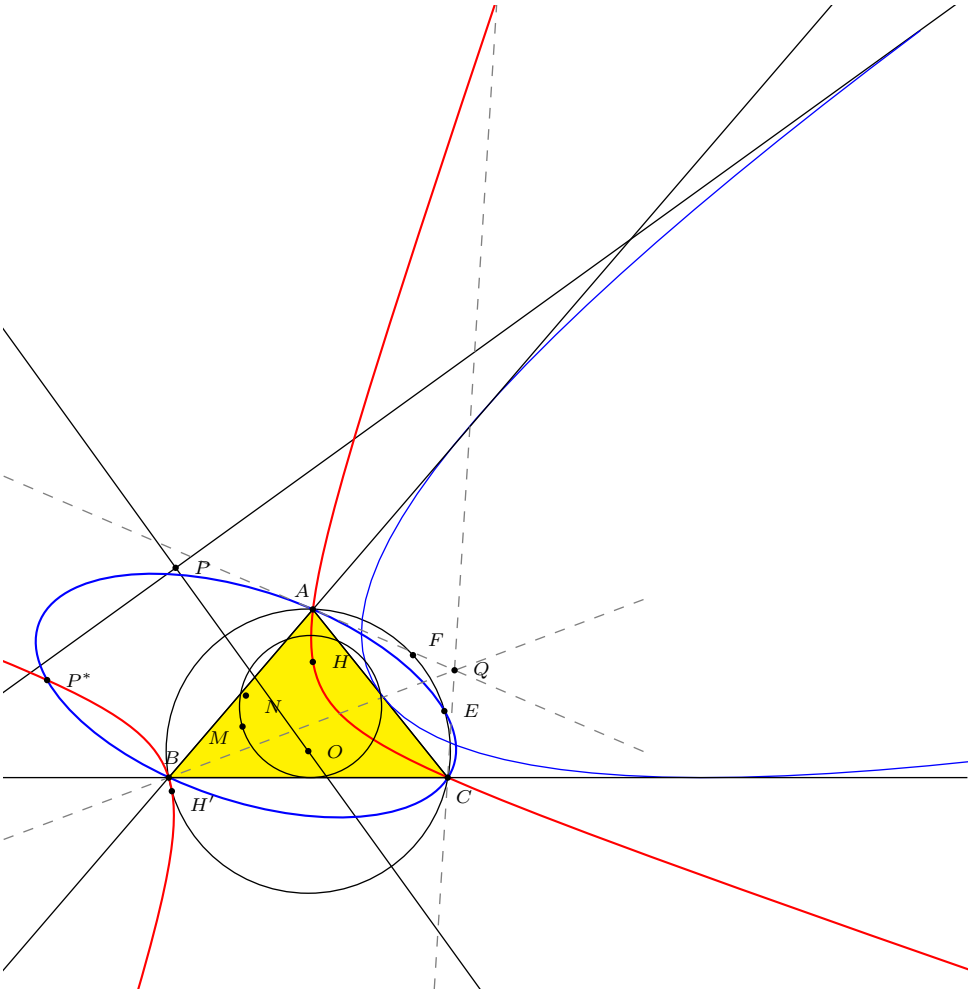

Figure 1. Three conics

Theorem 2. *The tangent to $\mathcal{E}$ at E*
(a) *passes through the focus F of $\mathcal{P}$;*
(b) *is parallel to the tangent to $\mathcal{E}$ at P^*, the isogonal conjugate of the point P;*
(c) *has as its pole K with respect to $\mathcal{P}$ on $\mathcal{H}$.*

Proof. (a) The tangent $\mathcal{T}$ to $\mathcal{E}$ at the point E has the equation

$$\frac{(\lambda_c\, v - \lambda_b\, w)\, \lambda_a^2}{a^2} x + \frac{(\lambda_a\, w - \lambda_c\, u)\, \lambda_b^2}{b^2} y + \frac{(\lambda_b\, u - \lambda_a\, v)\, \lambda_c^2}{c^2} z = 0. \qquad (5)$$

If $(x : y : z)$ are the coordinates of the point F, the left hand side of the above expression simplifies to a constant multiplied by $\lambda_a + \lambda_b + \lambda_c$. But this sum is equal to zero, verifying that the point F is on the tangent $\mathcal{T}$.

(b) The tangent to $\mathcal{E}$ at the point P^* is given by

$$\frac{(\lambda_c\, v - \lambda_b\, w)\, u^2}{a^2} x + \frac{(\lambda_a\, w - \lambda_c\, u)\, v^2}{b^2} y + \frac{(\lambda_b\, u - \lambda_a\, v)\, w^2}{c^2} z = 0.$$

The point of intersection of this line with the line $\mathcal{T}$ may be written as

$$\left((\lambda_c\, v + \lambda_b\, w)\, a^2 : (\lambda_a\, w + \lambda_c\, u)\, b^2 : (\lambda_b\, u + \lambda_a\, v)\, c^2\right)$$

The sum of this coordinates gives

$$\left(b^2\lambda_c + c^2\lambda_b\right) u + \left(c^2\lambda_a + a^2\lambda_c\right) v + \left(a^2\lambda_b + b^2\lambda_a\right) w.$$

The sum is equal to zero because this is the condition that the point P is on the line OP (2). This shows that the tangents to $\mathcal{E}$ at E and P^* are parallel.

(c) The polar K of the line $\mathcal{T}$ with respect to the parabola is given by

$$K = \left(\frac{\left(b^2\lambda_c + c^2\lambda_b\right) a^2}{(\lambda_c\, v - \lambda_b\, w)\, \lambda_a} : \frac{\left(c^2\lambda_a + a^2\lambda_c\right) b^2}{(\lambda_a\, w - \lambda_c\, u)\, \lambda_b} : \frac{\left(a^2\lambda_b + b^2\lambda_a\right) c^2}{(\lambda_b\, u - \lambda_a\, v)\, \lambda_c} \right).$$

Inserting the coordinates of the point K in the left hand side of the equation of $\mathcal{H}$, simplifies to

$$\left(\prod_{\text{cyclic}} \frac{\left(b^2\lambda_c + c^2\lambda_b\right) a^2}{(\lambda_c\, v - \lambda_b\, w)\, \lambda_a} \right) \sum_{\text{cyclic}} \left((\lambda_c\, v - \lambda_b\, w)\, \lambda_a\right).$$

But the sum is zero the as it represent the fact that the point $(\lambda_a : \lambda_b : \lambda_c)$ is on the line $\mathcal{L}$. This shows that the point K is on the hyperbola $\mathcal{H}$. □

Corollary 3. *The center N of the conic $\mathcal{E}$ is the midpoint of the points P^* and E.*

Corollary 4. *The directrix of the parabola is the line HK.*

Let R be the fourth intersection of the hyperbola $\mathcal{H}$ with the Steiner circumellipse.

Theorem 5. *The lines FH', EP^* and QR concur at the point K on $\mathcal{H}$.*

Proof. The equations of the lines FH' and EP^* are given by

$$FH' : \qquad \sum_{\text{cyclic}} \frac{\lambda_a}{a^2} \left(\lambda_b\, S_B - \lambda_c\, S_C\right) (\lambda_c\, v - \lambda_b\, w)\, x = 0$$

and

$$EP^* : \qquad \sum_{\text{cyclic}} \frac{\lambda_a}{a^2} (\lambda_c\, v - \lambda_b\, w)\, u\, x = 0.$$

It is easy to verify that the cross product of the line coordinates of this lines are proportional to the coordinates of the point K. The constant of proportionality is

$$\frac{\lambda_a\lambda_b\lambda_c}{2a^2b^2c^2}(u + v + w)\, (\lambda_c\, v - \lambda_b\, w)\, (\lambda_a\, w - \lambda_c\, u)\, (\lambda_b\, u - \lambda_a\, v).$$

On the other hand, the equation of the line QR is given by

$$\sum_{\text{cyclic}} a^2\lambda_a \left(b^2\lambda_c - c^2\lambda_b\right)(\lambda_c\, v - \lambda_b\, w)\, x = 0.$$

Inserting the coordinates of the point K gives

$$a^4\left(b^4\lambda_c^2 - c^4\lambda_b^2\right) + b^4\left(a^4\lambda_c^2 - c^4\lambda_a^2\right) + c^4\left(a^4\lambda_b^2 + b^4\lambda_a^2\right),$$

which is clearly equal to zero. □

Let D be the fourth intersection of the conic $\mathcal{E}$ with the Steiner circum-ellipse $\mathcal{E}_0$,

$$D = \left(\frac{1}{(\lambda_a\, w - \lambda_c\, u)\, b^2 + (\lambda_a\, v - \lambda_b\, u)\, c^2} : \cdots : \cdots\right).$$

Theorem 6. *The point D is on the line EQ.*

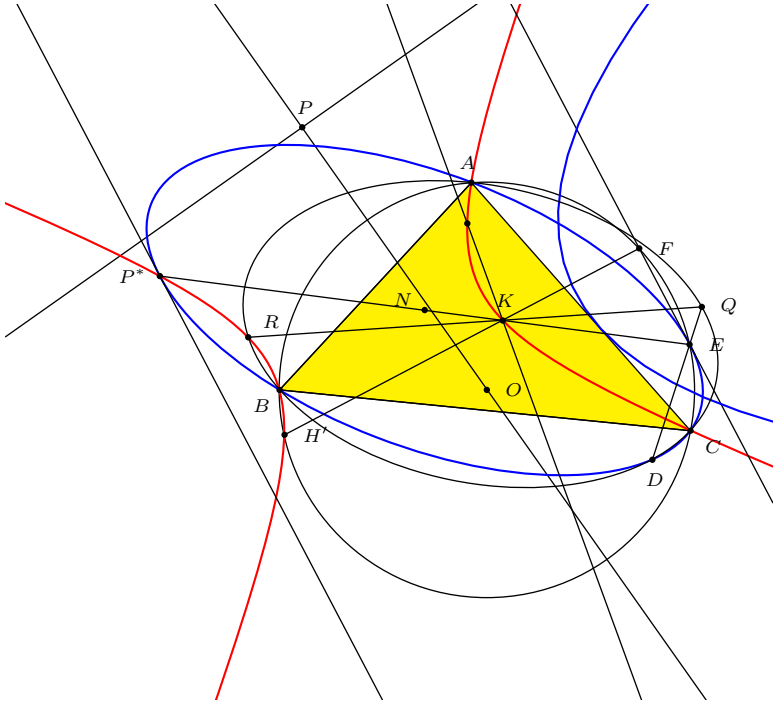

Figure 2. Collinearities

Proof. The line EQ can be written as

$$\sum_{\text{cyclic}} \lambda_a \left((\lambda_a\, w - \lambda_c\, u)\, b^2 + (\lambda_a\, v - \lambda_b\, u)\, c^2\right)(\lambda_c\, v - \lambda_b\, w)\, x = 0$$

A direct calculation shows that, inserting the coordinates of the point D in this equation, simplifies to zero. □

Theorem 7. *The following pairs of* (*perpendicular*) *lines are parallel to the asymptotes of* $\mathcal{H}$*:*
(a) *the axes of* $\mathcal{E}$*,*
(b) *the tangents from* K *to the parabola* $\mathcal{P}$*.*

Proof. Let us denote with L_1 and L_2 the points of intersection of the line OP with the circumcircle of the triangle

$$L_1 = \left(a\,b\,c\,(\lambda_b\,S_B - \lambda_c\,S_C) + a^2 S_A\mu : \cdots : \cdots\right),$$
$$L_2 = \left(a\,b\,c\,(\lambda_b\,S_B - \lambda_c\,S_C) - a^2 S_A\mu : \cdots : \cdots\right),$$

where $\mu = \sqrt{\lambda_a^2\,S_A + \lambda_b^2\,S_B + \lambda_c^2\,S_C}$.

(a) The isogonal conjugates L_1^* and L_2^*, are the points where the asymptotes of the hyperbola $\mathcal{H}$ meet the line at infinity. The polars of L_1^* and L_2^* with respect to the conic $\mathcal{E}$ are diameters of the conic. If this diameters are conjugate with respect to $\mathcal{E}$, then they are orthogonal and are the axis of the said conic [1, page 220, §297]. But the polar of a point is conjugate to the one of another point if this last point is on the polar of the first point. The polar of the point L_1^* is the line

$$\sum_{\text{cyclic}} \left(\frac{b^2c^2\,(\lambda_b\,u - \lambda_a\,v)}{abc\,(\lambda_c\,S_C - \lambda_a\,S_A) + b^2 S_B\mu} + \frac{b^2c^2\,(\lambda_a\,w - \lambda_c\,u)}{abc\,(\lambda_a\,S_A - \lambda_b\,S_B) + c^2 S_C\mu} \right) x = 0$$

and a (not so short) calculation shows that, indeed L_2^* is on this polar. Thus the diameters are orthogonal and conjugate, and are the axis of the conic $\mathcal{E}$.

(b) As the point K lies on the directrix of $\mathcal{P}$ the tangents from K to $\mathcal{P}$ are perpendicular. Thus it suffice to show that the line KL_1^* is tangent to $\mathcal{P}$. The line KL_1^* can be expressed as

$$\sum_{\text{cyclic}} \left(\frac{b^2c\,\left(c^2\lambda_a + a^2\lambda_c\right)}{\lambda_b\,(\lambda_a\,w - \lambda_c\,u)\,f(c,a,b)} - \frac{bc^2\,\left(a^2\lambda_b + b^2\lambda_a\right)}{\lambda_c\,(\lambda_b\,u - \lambda_a\,v)\,f(b,c,a)} \right) x = 0$$

where $f(a,b,c) = b\,c\,(\lambda_b\,S_B - \lambda_c S_C) + a\,S_A\mu$. A long calculation shows that the line KL_1^* is tangent to $\mathcal{P}$. □

Let S be the second intersection of the line EP^* with the circumcircle,

$$S = \left(\frac{a^2}{(\lambda_c\,v - \lambda_b\,w)\,u} : \frac{b^2}{(\lambda_a\,w - \lambda_c\,u)\,v} : \frac{c^2}{(\lambda_b\,u - \lambda_a\,v)\,w} \right).$$

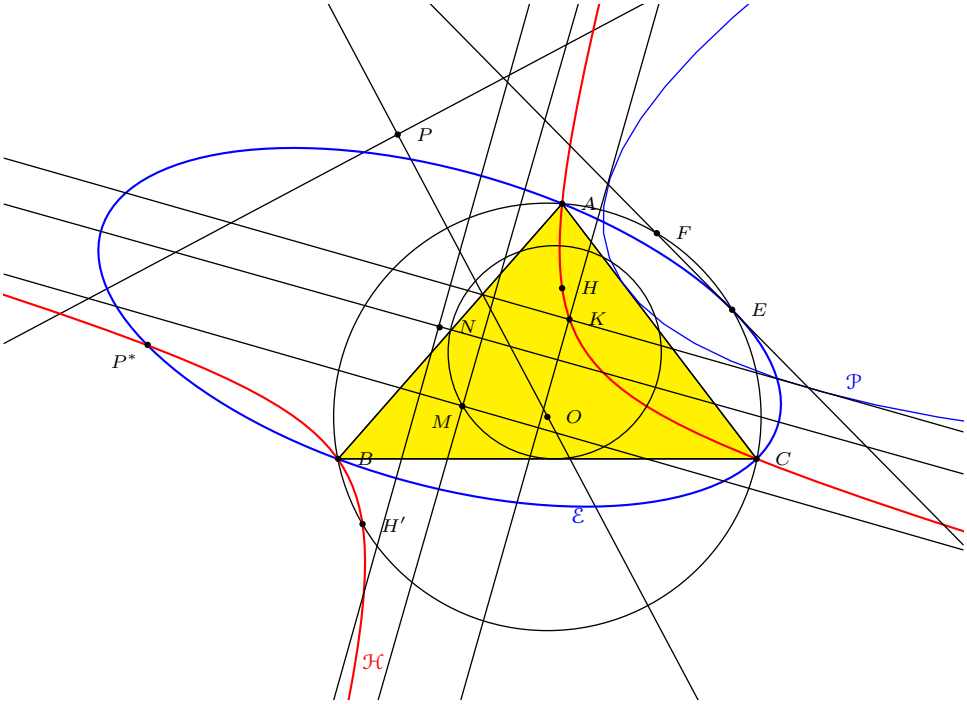

Figure 3. Asymptotes, axis and tangents

Theorem 8. *The pole P' of the line $\mathcal{L}$ is on the line FS.*

Proof. The line FS is given by

$$\frac{\lambda_a\,(\lambda_c\,v-\lambda_b\,w)^2\,u}{a^2}x+\frac{\lambda_b\,(\lambda_a\,w-\lambda_c\,u)^2\,v}{b^2}y+\frac{\lambda_c\,(\lambda_b\,u-\lambda_a\,v)^2\,w}{c^2}z=0,$$

and the point P' by

$$P'=\left((\lambda_c\,v-\lambda_b\,w)\,a^2-(\lambda_a\,w-\lambda_c\,u)\,b^2-(\lambda_b\,u-\lambda_a\,v)\,c^2:\cdots:\cdots\right).$$

Inserting the coordinates of P' in the equation of the line FS simplifies to

$$\left(\prod_{\text{cyclic}}(\lambda_c\,v-\lambda_b\,w)\right)\sum_{\text{cyclic}}\left(b^2\lambda_c+c^2\lambda_b\right)u$$

and, as already seen, the sum is equal to zero. □

P' is also the inverse in circumcircle of the point P. If T, on the line $\mathcal{L}$, is the pole of the line FS it follows that points O, P, F, S, and T are concyclic.

The point T can be expressed as

$$T=\left(\frac{(\lambda_c\,v+\lambda_b\,w)\,a^2}{(\lambda_c\,v-\lambda_b\,w)}:\frac{(\lambda_a\,w+\lambda_c\,u)\,b^2}{(\lambda_a\,w-\lambda_c\,u)}:\frac{(\lambda_b\,u+\lambda_a\,v)\,c^2}{(\lambda_b\,u-\lambda_a\,v)}\right).$$

The point T is also the center of a circle $\mathcal{C}$ through the points F and S. The circle $\mathcal{C}$ is orthogonal to the circumcircle.

Theorem 9. *Points on $\mathcal{C}$ are*
(a) *the point K,*
(b) *the intersections of the line $\mathcal{L}$ with the tangents from the point K to the parabola $\mathcal{P}$.*

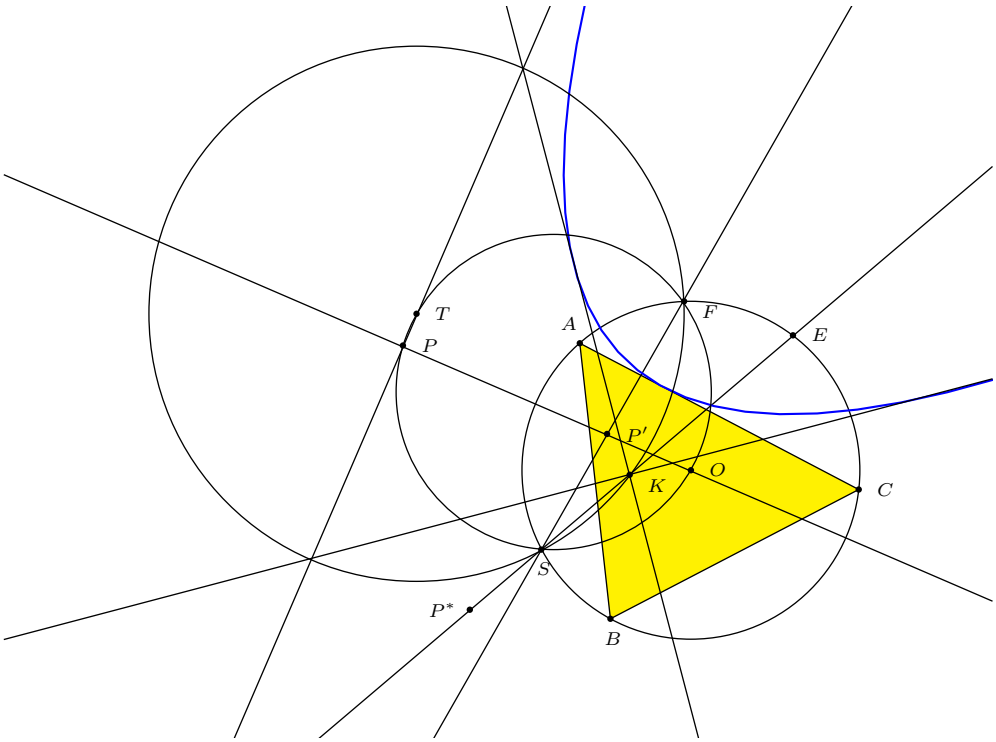

Figure 4. Circles

Proof. (a) A long calculation allows one to show that indeed, the point T is equidistant to the points F and K. [1] The common distance of the point T to the points F and S can be expressed as $d_1/(d_2 d_3)$ where

$$\begin{aligned} d_1 &= \sum_{\text{cyclic}} a^4 S_A \left(b^2 w^2 \nu_c^2 - c^2 v^2 \nu_b^2\right)^2, \\ d_2 &= (a^2 \nu_b \nu_c v w + b^2 \nu_c \nu_a w u + c^2 \nu_a \nu_b u v)^2, \\ d_3 &= \left(\sum_{\text{cyclic}} \frac{a^2 (w\lambda_b + v\lambda_c)}{\nu_a}\right)^2, \end{aligned}$$

and

$$\nu_a = \lambda_c v - \lambda_b w, \quad \nu_b = \lambda_a w - \lambda_c u, \quad \nu_c = \lambda_b u - \lambda_a v.$$

[1] For an equation of the distance of two points in barycentric coordinates see [2, Chapter 7].

(b) Consider the triangle whose sides are the line $\mathfrak{L}$ and the tangents to the parabola from the point K. The three sides of this triangle are tangent to the parabola. Thus the focus F is on the circumcircle of this triangle and the center of this circle is on the line $\mathfrak{L}$. But by part (a) of the proof, the only circle through the points F and K with center on $\mathfrak{L}$ is the circle $\mathcal{C}$. □

Interesting examples of the relations shown in this work arise if one takes the point P as the inverse in circumcircle of the symmedian point of the triangle[2], the inverse in circumcircle of the orthocenter, or when P is the intersection of the line OI, where I is the incenter, with the radical axis of the circumcircle and the incircle.

References

[1] L. Cremona, *Elements of Projective Geometry*, Dover, 1960.

[2] P. Yiu, *Introduction to the Geometry of the Triangle*, Florida Atlantic University Lecture Notes, 2001.

Alberto Mendoza: Universidad Simón Bolívar, Departamento de Matemáticas, Caracas, Venezuela.
E-mail address: jacob@usb.ve

[2] In this case the points E and Q are the same and there is no point D, the conics $\mathcal{E}$ and $\mathcal{E}_0$ coincide.

Forum Geometricorum
Volume 12 (2012) 141–148.

FORUM GEOM
ISSN 1534-1178

On the Intersections of the Incircle and the Cevian Circumcircle of the Incenter

Luiz González and Cosmin Pohoata

Abstract. We give a characterization of the other point of intersection of the incircle with the circle passing through the feet of the internal angle bisectors, different from the Feuerbach point.

1. Introduction

The famous Feuerbach theorem states that the nine-point circle of a triangle is tangent to the incircle and to each of the excircles. Of particular interest is the tangency between the nine-point circle and the incircle, for it is this tangency point among the four that is a triangle center in the sense of Kimberling [5]. Thus, it is this point which was coined as the *Feuerbach point* of the triangle. Besides, its existence, being perhaps one of the first more difficult results that arise in triangle geometry, has been the subject of many discussions over the years, and consequently, many proofs, variations, and related results have appeared in the literature. A celebrated collection of such results is provided by Emelyanov and Emelyanova in [3]. In this note, we shall dwell on a particular theorem, for which they gave a magnificient synthetic proof in [2].

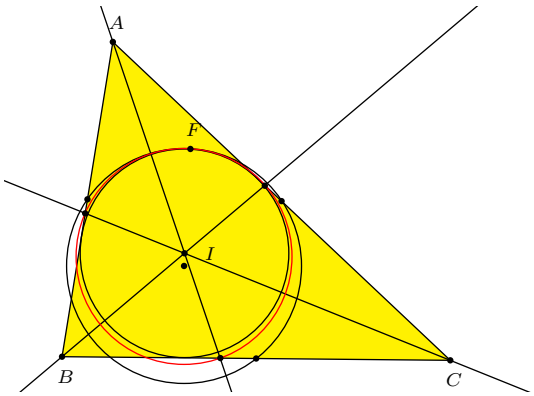

Figure 1

Theorem 1 (Emelyanov and Emelyanova)**.** *The circle through the feet of the internal angle bisectors of a given triangle passes through the Feuerbach point of the triangle.*

Publication Date: April 25, 2012. Communicating Editor: Paul Yiu.

We focus on the second intersection of the incircle with this cevian circumcircle of the incenter. Following an idea of Suceavă and Yiu [7], we give a natural characterization of this point in terms of the reflections of a given line in the sidelines of the cevian triangle of the incircle. We begin with some preliminaries on the *Poncelet point* of a quadrilateral and the *anti-Steiner point* of a line passing through the orthocenter of the triangle.

2. Preliminaries

In essence, the result that lies at the heart of the theory of anti-Steiner point is the following concurrency due to Collings [1].

Theorem 2 (Collings)**.** *If $\mathcal{L}$ is a line passing through the orthocenter H of a triangle ABC, then the reflections of $\mathcal{L}$ in the sides BC, CA, AB are concurrent on the circumcircle of ABC at a point called the* anti-Steiner point *of $\mathcal{L}$.*

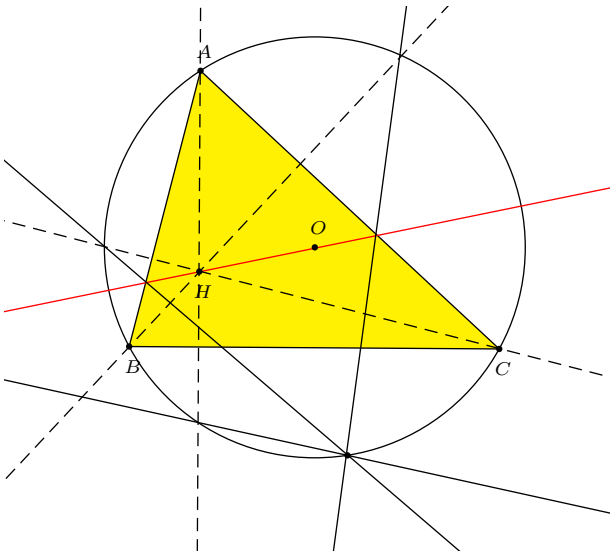

Figure 2

The proof for this is quite straightforward and it consists of a simple angle chasing (see [1] or [4]). It is also well-known that the orthocenter of the intouch triangle lies on the line determined by the circumcenter O and the incenter I of the triangle. This can be proved in many ways synthetically. The most beautiful approach however is by using inversion with respect to the incircle; we refer to [6] for this proof. Given this fact, it is natural now to ask about the anti-Steiner point of OI with reference to the intouch triangle. Suceavă and Yiu did this and obtained the following result.

Theorem 3 (Suceavă and Yiu)**.** *The reflections of the OI-line in the sides of the intouch triangle of ABC concur at the Feuerbach point of ABC.*

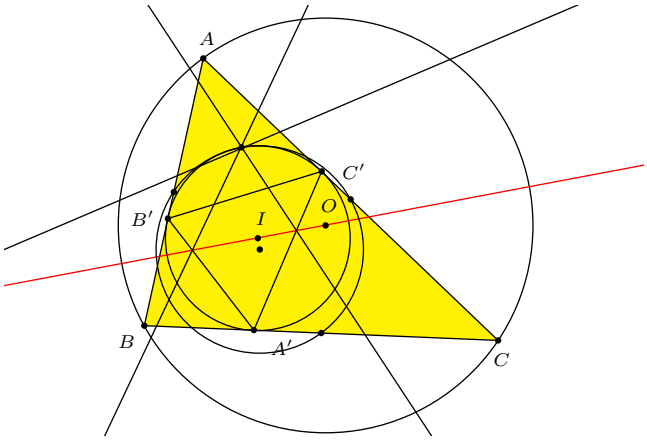

Figure 3

We proceed to give a geometric characterization of the "second" intersection of the cevian circumcenter of the incenter with the incircle, apart from the Feuerbach point.

3. The main result

Theorem 4. *Let I be the incenter of triangle ABC, and H_1 the orthocenter of cevian triangle $A_1B_1C_1$ of I. The anti-Steiner point of the line IH_1* (with respect to $A_1B_1C_1$) *is the "second" intersection of the incircle with the cevian circumcircle of I.*

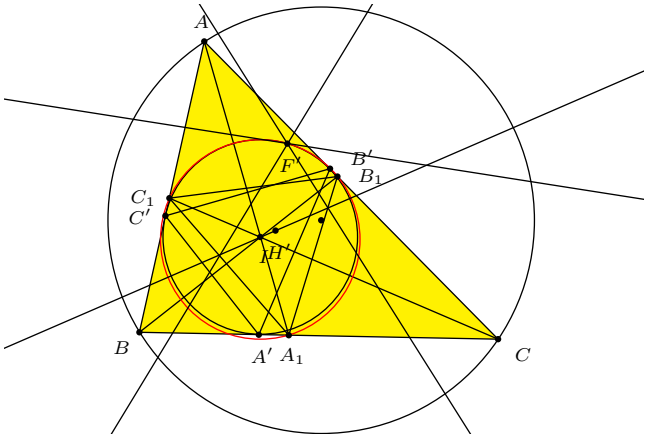

Figure 4

In other words, the anti-Steiner point of the line IH_1 with respect to triangle $A_1B_1C_1$ lies on the incircle of ABC. This is in general different from the Feuerbach point of ABC, unless the incircle and the cevian circumcircle of the incenter are tangent to one another.

We prove Theorem 4 synthetically, with the aid of a few lemmas. Lemma 5 provides more insight on the standard anti-Steiner point configuration.

Lemma 5. *Let P be a point in the plane of a given triangle ABC with orthocenter H. Let A_1, B_1, C_1 be the points where the lines AP, BP, and CP, intersect again the circumcircle. Furthermore, let A_2, B_2, C_2 be the reflections of P across the sidelines BC, CA, and AB, respectively. Then, the circumcircles of triangles ABC, PA_1A_2, PB_1B_2, and PC_1C_2 are concurrent at the anti-Steiner point of the line PH with respect to triangle ABC.*

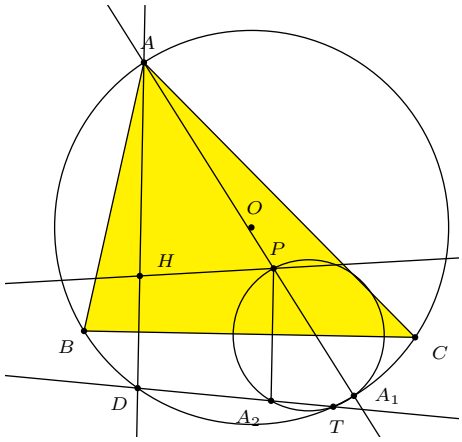

Figure 5

Proof. The line AH cuts the circumcircle of triangle ABC again at the reflection D of H across BC. Thus, the line DA_2 is the reflection of PH with respect to BC and intersects the circumcircle of triangle ABC again at the anti-Steiner point T of PH with respect to ABC. Since the directed angles

$$(TA_1, TA_2) = (TA_1, TD) = (AA_1, AD) = (PA_1, PA_2) \mod 180^\circ,$$

it follows that T lies on the circumcircle of PA_1A_2. Similarly, T lies on the circumcircles of triangles PB_1B_2 and PC_1C_2. □

Lemma 6 is a property of Poncelet points of general quadrilaterals. By definition (see [4]), the Poncelet point T associated with the four points A, B, C, D is the concurrency point of 8 circles: the nine-point circles of triangles ABC, BCD, CDA, DAB, and the pedal circles of the points A, B, C, and D, with respect to the triangles BCD, CDA, DAB, and ABC, respectively.

Lemma 6. *Let P be a point in the plane of triangle ABC and $P_AP_BP_C$ its pedal triangle with respect to ABC. Let A', B', C' be the midpoints of the segments PA, PB, and PC, respectively, and let P_1, P_2, P_3 be the points where the lines PP_A, PP_B, PP_C meet again the pedal circle $P_AP_BP_C$. Then, the lines P_1A', P_2B', and P_3C' concur at a point on the pedal circle $P_AP_BP_C$.*

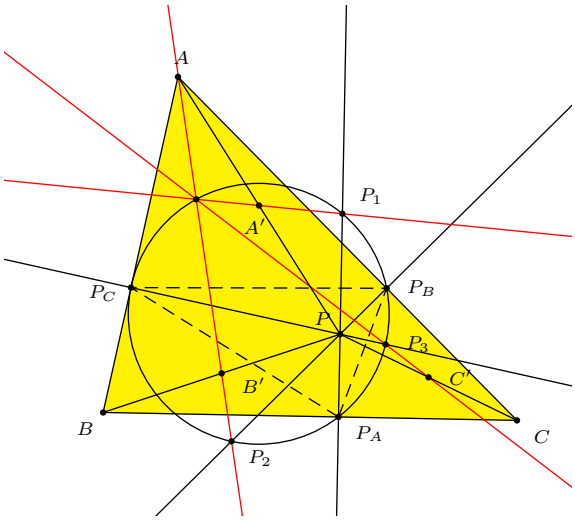

Figure 6

Proof. Let U be the Poncelet point of the quadrilateral $ABCP$. By definition, this point lies on the pedal circle of P with respect to triangle ABC. Now, let D be the second intersection of BC with the pedal circle $P_AP_BP_C$ and let R be the orthogonal projection of A on PC. We have that $URA'C'$ is the nine-point circle of triangle APC. Furthermore, we also get that

$$\begin{aligned}\angle DUC' &= \angle DUP_B - \angle C'UP_B \\ &= 180^\circ - \angle CPP_B - \angle PRP_B \\ &= \angle PAC - \angle CPP_B \\ &= \angle PAC - \angle RAC \\ &= 90^\circ - \angle APC.\end{aligned}$$

Thus,

$$\begin{aligned}\angle DUA' &= \angle DUC' + \angle C'UA' \\ &= 90^\circ - \angle APC + \angle APC \\ &= 90^\circ.\end{aligned}$$

Therefore, since $\angle DUP_1 = 90^\circ$, it follows that U lies on the line P_1A'. Similarly, P_2B' and P_3C' pass through the Poncelet point P. □

Finally, we prove the lemma which lies at the core of the proof of the main Theorem 4.

Lemma 7. *Given a triangle ABC with circumcenter O and medial triangle DEF, let P be a point with orthogonal projections P_1, P_2, P_3 on these sides. Let A' be the intersection of the lines EF and P_2P_3, and define B', C' cyclically. Then, the lines P_1A' P_2B' P_3C' concur at the intersection point U of the circumcircles $P_1P_2P_3$ and DEF that is different from the Poncelet point of A, B, C and P. Furthermore, U is the anti-Steiner point of the line OP with respect to the medial triangle DEF.*

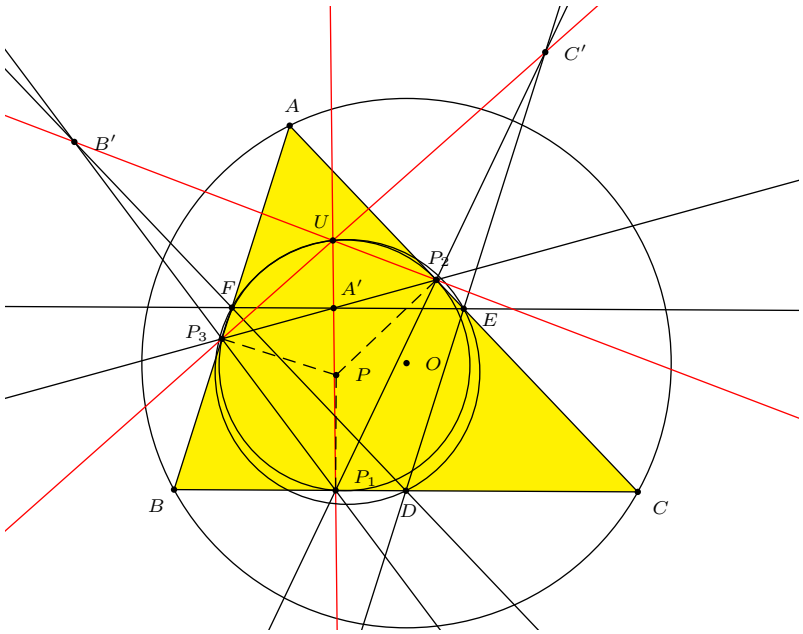

Figure 7

Proof. The orthogonal projection V of A on OP is clearly the second intersection of the circumcircles of the cyclic quadrilaterals PP_2AP_3 and $OEAF$ with diameters AP and AO, respectively. Also, note that V is the Miquel point of the complete quadrilateral bounded by the lines AB, AC, EF, and P_2P_3. Thus, it follows by the standard characterization of Miquel points that V lies on the circumcircle of $FA'P_3$.

On the other hand, let PP_1 intersect the circle AP_2P_3 again at T. Since AP is a diameter of AP_2P_3, $\angle ATP = 90^\circ$, and AT is parallel to EF. In other words, EF is the perpendicular bisector of TP_1, and $\angle TAF = \angle AFE$. We have shown above V lies on the circumcircle of $FA'P_3$. Therefore, $\angle A'VP_3 = \angle AFE$, and A' lies on VT. Furthermore, since A' lies on the radical axis P_2P_3 of the circumcircles AP_2P_3 and $P_1P_2P_3$, it also follows that A' has equal powers with respect to AP_2P_3 and $P_1P_2P_3$. Consequently, if P_1A' cuts the circle $P_1P_2P_3$ again at U,

then $TUVP_1$ is an isosceles trapezoid with bases UV and TP_1. Therefore, U is the reflection of V across EF. Finally, since the circumcircles AEF and DEF are symmetric with respect to EF, the point U, which lies on the circumcircle DEF, is the anti-Steiner point of OP with respect to triangle DEF. □

Now we conclude with a proof of Theorem 4.

Let DEF be the intouch triangle of ABC, and $A_0B_0C_0$ the antimedial triangle of DEF. Since the lines B_0C_0, C_0A_0, A_0B_0 are perpendicular to the lines IA, IB, IC respectively, the feet of the internal angle bisectors, A_1, B_1, C_1, are the poles of B_0C_0, C_0A_0, A_0B_0 with respect to the incircle (I). Therefore, by duality, the points A_0, B_0, C_0 are the poles of the lines B_1C_1, C_1A_1, A_1B_1 with respect to (I).

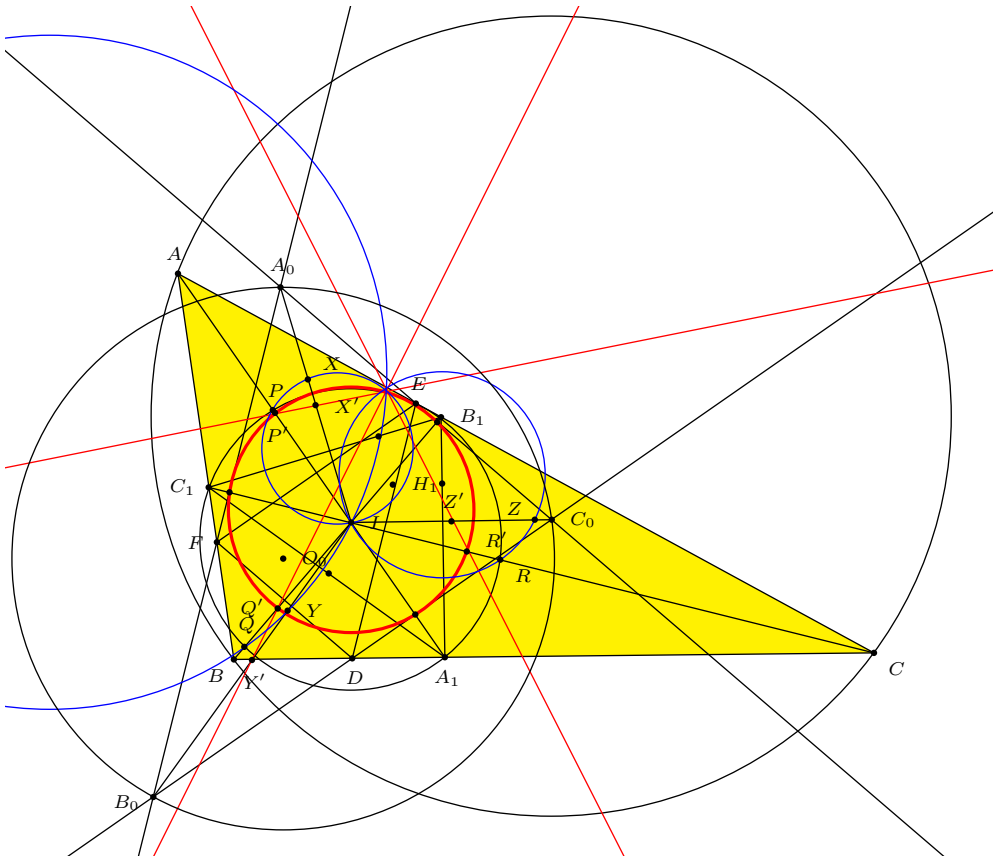

Figure 8

Now, let the segments IA, IB, IC intersect the cevian circumcircle $(A_1B_1C_1)$ of I at P, Q, R respectively, and let X, Y, Z be the reflections of I across the lines B_1C_1, C_1A_1, and A_1B_1, respectively. Inversion with respect to (I) takes ω into the pedal circle ω' of I with respect to triangle $A_0B_0C_0$. Thus, the segments IA, IB, IC cut ω' at the inverse images P', Q', R' of P, Q, R respectively, and

the midpoints X', Y', Z' of IA_0, IB_0, IC_0 are the inverse images of X, Y, Z. It follows from Lemma 6 that $P'X'$, $Q'Y'$, $R'Z'$ all meet at the Poncelet point F' of $A_0B_0C_0I$, which, as a matter of fact, lies on ω'. On the other hand, by Lemma 5, the inverses of these lines are the circles (IXP), (IYQ), and (IZR) concurring at the anti-Steiner point of I with respect to triangle $A_1B_1C_1$. Therefore, the intersection points of $(A_1B_1C_1)$ and the incircle (I) are precisely the anti-Steiner point F' of IH_1 with respect to triangle $A_1B_1C_1$ and the Feuerbach point of ABC. Moreover, if O_0 is the circumcenter of triangle $A_0B_0C_0$, then according to Lemma 7, F' is in general different from the anti-Steiner point of IO_0 with respect to triangle DEF. Thus, we conclude that the anti-Steiner point F' of IH_1 with respect to triangle $A_1B_1C_1$ is indeed the intersection of $(I) \cap \omega$, which is different from the Feuerbach point, since by Theorem 3 the anti-Steiner point of IO_0 with respect to DEF is the Feuerbach point of ABC.

This completes the proof of Theorem 4.

References

[1] S. N. Collings: Reflections on a triangle 1, *Math. Gazette*, 57 (1973) 291–293.
[2] L. A. Emelyanov and T. L. Emelyanova, A note on the Feuerbach point, *Forum Geom.*, 1 (2001) 121–124.
[3] L. A. Emelyanov and T. L. Emelyanova, Semejstvo Feuerbacha, *Matematicheskoe Prosveshjenie*, 2002, 1–3.
[4] D. Grinberg, Anti-Steiner points with respect to a triangle, available at `http://www.cip.ifi.lmu.de/ grinberg`
[5] C. Kimberling, Triangle centers and central triangles, *Congressus Numerantium*, 129 (1998) 1–285.
[6] C. Pohoata, Homothety and Inversion, AwesomeMath Year-Round Program material, 2012.
[7] B. Suceavă and P. Yiu, The Feuerbach point and Euler lines, *Forum Geom.*, 6 (2006) 191–197.

Luis González: 5 de Julio Avenue, Maracaibo, Venezuela
E-mail address: `Luisgeometria@hotmail.com`

Cosmin Pohoata: 215 1938 Hall, Princeton University, USA
E-mail address: `apohoata@princeton.edu`

Forum Geometricorum
Volume 12 (2012) 149–152.

FORUM GEOM
ISSN 1534-1178

Some Properties of the Newton-Gauss Line

Cătălin Barbu and Ion Pătraşcu

Abstract. We present some properties of the Newton-Gauss lines of the complete quadrilaterals associated with a cyclic quadrilateral.

1. Introduction

A complete quadrilateral is the figure determined by four lines, no three of which are concurrent, and their six points of intersection. Figure 1 shows a complete quadrilateral $ABCDEF$, with its three diagonals AC, BD, and EF (compared to two for an ordinary quadrilateral). The midpoints M, N, L of these diagonals are collinear on a line, called the *Newton-Gauss line* of the complete quadrilateral ([1, pp.152–153]). In this note, we present some properties of the Newton - Gauss lines of complete quadrilaterals associated with a cyclic quadrilateral.

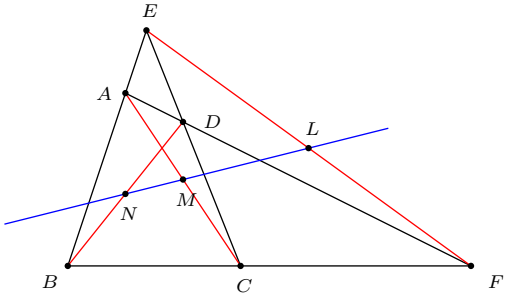

Figure 1.

2. An equality of angles determined by Newton - Gauss line

Given a cyclic quadrilateral $ABCD$, denote by F the point of intersection at the diagonals AC and BD, E the point of intersection at the lines AB and CD, N the midpoint of the segment EF, and M the midpoint of the segment BC (see Figure 2).

Theorem 1. *If P is the midpoint of the segment BF, the Newton - Gauss line of the complete quadrilateral $EAFDBC$ determines with the line PM an angle equal to $\angle EFD$.*

Proof. We show that triangles NPM and EDF are similar.

Since $BE \| PN$ and $FC \| PM$, $\angle EAC = \angle NPM$ and $\frac{BE}{PN} = \frac{FC}{PM} = 2$.

In the cyclic quadrilateral $ABCD$, we have

$$\angle EDF = \angle EDA + \angle ADF = \angle ABC + \angle ACB = \angle EAC.$$

Publication Date: May 2, 2012. Communicating Editor: Paul Yiu.

Therefore, $\angle NPM = \angle EDF$.

Let R_1 and R_2 be the radii of the circumcircles of triangles BED and DFC respectively. Applying the law of sines to these triangles, we have

$$\frac{BE}{FC} = \frac{2R_1 \sin EDB}{2R_2 \sin FDC} = \frac{R_1}{R_2} = \frac{2R_1 \sin EBD}{2R_2 \sin FCD} = \frac{DE}{DF}.$$

Since $BE = 2PN$ and $FC = 2PM$, we have shown that $\frac{PN}{PM} = \frac{DE}{DF}$. The similarity of triangles NPM and EDF follows, and $\angle NMP = \angle EFD$. □

Remark. If Q is the midpoint of the segment FC, the same reasoning shows that that $\angle NMQ = \angle EFA$.

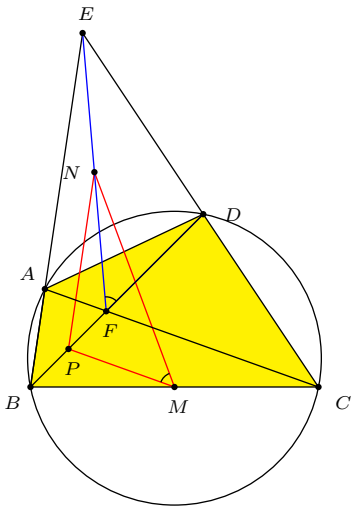

Figure 2

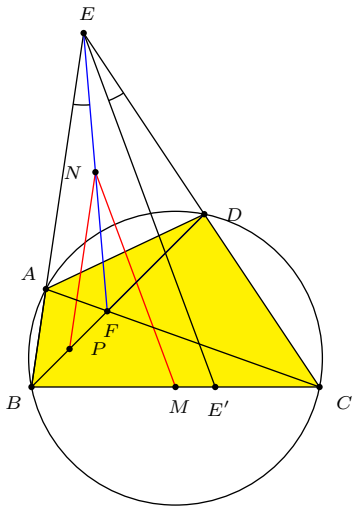

Figure 3

3. A parallel to the Newton-Gauss line

Theorem 2. *The parallel from E to the Newton - Gauss line of the complete quadrilateral $EAFDBC$ and the line EF are isogonal lines of angle BEC.*

Proof. Since triangles EDF and NPM are similar, we have $\angle DEF = \angle PNM$.

Let E' be the intersection of the side BC with the parallel of NM through E. Because $PN \| BE$ and $NM \| EE'$, $\angle BEF = \angle PNF$ and $\angle FNM = \angle E'EF$. Thus,

$$\angle CEE' = \angle DEF - \angle E'EF = \angle PNM - \angle FNM = \angle PNF = \angle BEF.$$

□

4. Two cyclic quadrilaterals determined the Newton-Gauss line

Let G and H be the orthogonal projections of the point F on the lines AB and CD respectively (see Figure 4).

Theorem 3. *The quadrilaterals $MPGN$ and $MQHN$ are cyclic.*

Proof. By Theorem 1, $\angle EFD = \angle PMN$. The points P and N are the circumcenters of the right triangles BFG and EFG, respectively. It follows that $\angle PGF = \angle PFG$ and $\angle FGN = \angle GFN$. Thus,

$$\begin{aligned}\angle PGN + \angle PMN &= (\angle PGF + \angle FGN) + \angle PMN \\ &= \angle PFG + \angle GFN + \angle EFD \\ &= 180^\circ.\end{aligned}$$

Therefore, $MPGN$ is a cyclic quadrilateral. In the same way, the quadrilateral $MQHN$ is also cyclic. □

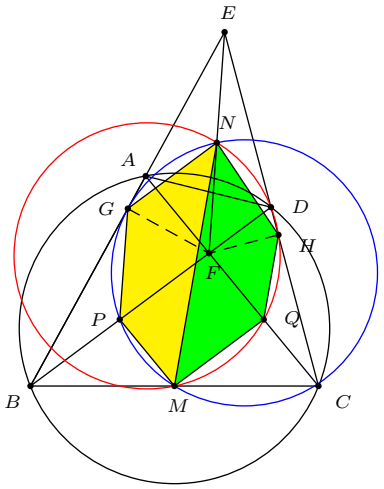

Figure 4

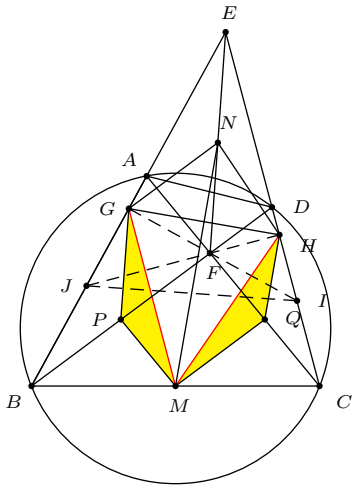

Figure 5

5. Two complete quadrilaterals with the same Newton-Gauss line

Extend the lines GF and HF to intersect EC and EB at I and J respectively (see Figure 5).

Theorem 4. *The complete quadrilaterals $EGFHJI$ and $EAFDBC$ have the same Newton-Gauss line.*

Proof. The two complete quadrilaterals have a common diagonal EF. Its midpoint N lies on the Newton-Gauss lines of both quadrilaterals. Note that N is equidistant from G and H since it is the circumcenter of the cyclic quadrilateral $EGFH$. We show that triangles MPG and HQM are congruent. From this, it follows that M

lies on the perpendicular bisector of GH. Therefore, the line MN contains the midpoint of GH, and is the Newton-Gauss line of $EGFHJI$.

Now, to show the congruence of the triangles MPG and HQM, first note that since M and P are the midpoints of BF and BC, $PMQF$ is a parallelogram. From these, we conclude
(i) $MP = QF = HQ$,
(ii) $GP = PF = MQ$,
(iii) $\angle MPF = \angle FQM$.

Note also that

$$\angle FPG = 2\angle PBG = 2\angle DBA = 2\angle DCA = 2\angle HCF = \angle HQF.$$

Together with (iii) above, this yields

$$\angle MPG = \angle MPF + \angle FPG = \angle FQM + \angle HQF = \angle HQF + \angle FQM = \angle HQM.$$

Together with (i) and (ii), this proves the congruence of triangles MPG and HQM. □

Remark. Because MPG and HQM are congruent triangles, their circumcircles, namely, $(MPGN)$ and $(MQHN)$ are congruent (see Figure 4).

Reference

[1] R. A. Johnson, *A Modern Geometry: An Elementary Treatise on the Geometry of the Triangle and the Circle*, Houghton Mifflin, Boston, 1929.

Cătălin Barbu: Vasile Alecsandri College, Bacău, str. Iosif Cocea, nr. 12, sc. A, ap. 13, Romania
E-mail address: kafka_mate@yahoo.com

Ion Pătraşcu: Fraţii Buzeşti College, Craiova, str. Ion Cantacuzino, nr. 15, bl S33, sc. 1, ap. 8, , Romania
E-mail address: patrascu_ion@yahoo.com

Forum Geometricorum
Volume 12 (2012) 153–159.

FORUM GEOM
ISSN 1534-1178

Harmonic Conjugate Circles Relative to a Triangle

Nikolaos Dergiades

Abstract. We use the term harmonic conjugate conics, for the conics $\mathcal{C}, \mathcal{C}^*$ with equations $\mathcal{C}: fx^2+gy^2+hz^2+2pyz+2qz+2rxy=0$ and $\mathcal{C}^*: fx^2+gy^2+hz^2-2pyz-2qz-2rxy=0$, in barycentric coordinates because if A_1, A_2 are the points where $\mathcal{C}$ meets the sideline BC of the reference triangle ABC, then $\mathcal{C}^*$ meets the same side at the points A_1', A_2' that are harmonic conjugates of A_1, A_2 respectively relative to BC and similarly for the other sides of ABC [1]. So we investigate the interesting case where both $\mathcal{C}$ and $\mathcal{C}^*$ are circles.

1. Introduction

We work with barycentric coordinates with reference to a given triangle ABC. A conic $\mathcal{C}$ with matrix

$$M=\begin{pmatrix} f & r & q \\ r & g & p \\ q & p & h \end{pmatrix}$$

and equation

$$fx^2+gy^2+hz^2+2pyz+2qzx+2rxy=0 \tag{1}$$

intersects the sideline BC of triangle ABC at the points $A_1=(0:y_1:z_1)$ and $A_2=(0:y_2:z_2)$ with y_i, z_i $(i=1,2)$ satisfying $gy^2+2pyz+hz^2=0$. Similarly, the conic $\mathcal{C}^*$ with matrix

$$M^*=\begin{pmatrix} f & -r & -q \\ -r & g & -p \\ -q & -p & h \end{pmatrix}$$

and equation

$$fx^2+gy^2+hz^2-2pyz-2qzx-2rxy=0 \tag{2}$$

intersects the sideline BC of triangle ABC at the points $A_1'=(0:-y_1:z_1)$ and $A_2'=(0:-y_2:z_2)$. For $i=1,2$, the points A_i and A_i' are harmonic conjugates with respect to B and C. Similarly the intersections of $\mathcal{C}$ and $\mathcal{C}^*$ with the other two sides CA, AB are also harmonic conjugates. We call these conics harmonic conjugates relative to triangle ABC (see Figure 1), and it is very interesting to consider their properties and construction if these conics are both circles. If the conic $\mathcal{C}$ is a bicevian conic (passing through the vertices of the cevian triangles of

Publication Date: May 9, 2012. Communicating Editor: Paul Yiu.

two points P, Q), then its harmonic conjugate conic is a pair of lines (the trilinear polars of P and Q).

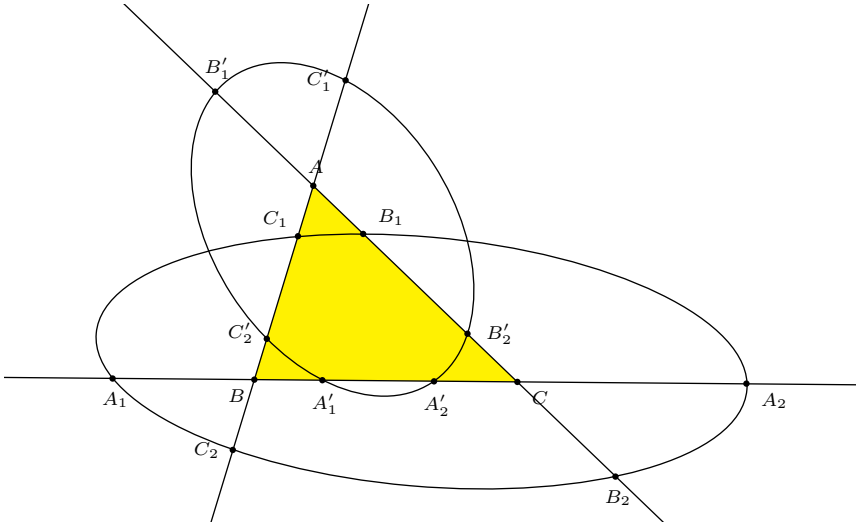

Figure 1. Harmonic conjugate conics

2. Harmonic conjugate circles relative to ABC

Theorem 1. *The harmonic conjugate conic of the circle*

$$a^2yz + b^2zx + c^2xy - (x + y + z)(Px + Qy + Rz) = 0 \tag{3}$$

is a circle if and only if $(P, Q, R) = m(S_A, S_B, S_C)$ *for some* m.

Proof. The matrix of the circle (3) being

$$\begin{pmatrix} -2P & c^2 - P - Q & b^2 - R - P \\ c^2 - P - Q & -2Q & a^2 - Q - R \\ b^2 - R - P & a^2 - Q - R & -2R \end{pmatrix},$$

its harmonic conjugate conic has matrix

$$\begin{pmatrix} -2P & -c^2 + P + Q & -b^2 + R + P \\ -c^2 + P + Q & -2Q & -a^2 + Q + R \\ -b^2 + R + P & -a^2 + Q + R & -2R \end{pmatrix}.$$

This is the conic

$$(2Q+2R-a^2)yz+(2R+2P-b^2)zx+(2P+2Q-c^2)xy-(x+y+z)(Px+Qy+Rz) = 0.$$

It is a circle if and only if

$$2Q + 2R - a^2 : 2R + 2P - b^2 : 2P + 2Q - c^2 = a^2 : b^2 : c^2,$$

i.e.,

$$P : Q : R = b^2 + c^2 - a^2 : c^2 + a^2 - b^2 : a^2 + b^2 - c^2 = S_A : S_B : S_C.$$

This is the case if and only if $(P, Q, R) = m(S_A, S_B, S_C)$ for some m. □

Denote by $\mathcal{C}_m$ the circle with equation

$$a^2yz + b^2zx + c^2xy - m(x+y+z)(S_Ax + S_By + S_Cz) = 0.$$

A simple application of the formula in [3, §10.7.2] shows that the center of $\mathcal{C}_m$ is the point

$$O_m = ((1-m)a^2S_A + m\cdot 2S_{BC} : (1-m)b^2S_B + m\cdot 2S_{CA} : (1-m)c^2S_C + m\cdot 2S_{AB}),$$

which divides OH in the ratio

$$OO_m : O_mH = m : 1-m.$$

Proposition 2. *If $m \neq \frac{1}{2}$, the harmonic conjugate circle of $\mathcal{C}_m$ is the circle $\mathcal{C}_{m'}$, where $m' = \frac{m}{2m-1}$.*

Proof. By the proof of Theorem 1, the harmonic conjugate circle of $\mathcal{C}_m$ is the circle

$$(2m(S_B+S_C) - a^2)yz + (2m(S_C+S_A) - b^2)zx + (2m(S_A+S_B) - c^2)xy$$
$$- m(x+y+z)(S_Ax + S_By + S_Cz) = 0,$$

namely,

$$a^2yz + b^2zx + c^2xy - \frac{m}{2m-1}(x+y+z)(S_Ax + S_By + S_Cz) = 0.$$

This is the circle $\mathcal{C}_{m'}$ with $m' = \frac{m}{2m-1}$. □

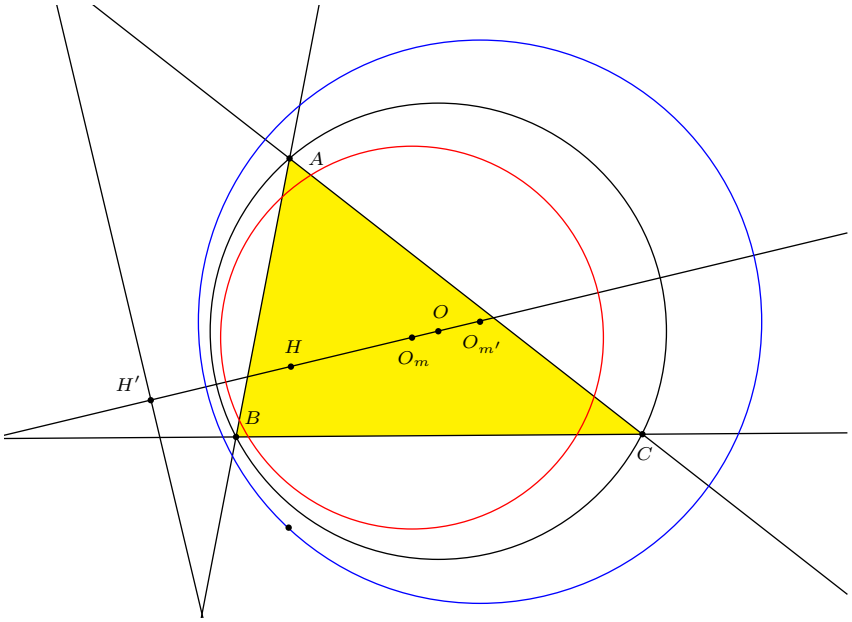

Figure 2. Harmonic conjugate circles

Remark. For $m = \frac{1}{2}$, $\mathcal{C}_m$ is the nine-point circle, the bicevian circle of the centroid and the orthocenter. Its harmonic conjugate conic is the pair of lines consisting of the line at infinity and the orthic axis.

Proposition 3. *The centers of a pair of harmonic conjugate circles divide the segment OH harmonically.*

Proof. Let the harmonic conjugate circles be $\mathcal{C}_m$ and $\mathcal{C}_{m'}$, with $m' = \frac{m}{2m-1}$. Their centers are points O_m and $O_{m'}$ satisfying

$$\begin{aligned} OO_{m'} : O_{m'}H &= m' : 1 - m' = \frac{m}{2m-1} : \frac{m-1}{2m-1} \\ &= m : -(1-m) \\ &= OO_m : -O_mH. \end{aligned}$$

Therefore O_m and $O_{m'}$ divide OH harmonically. □

Since $m = m'$ if and only if $m = 0$ or 1, we have the following corollary.

Corollary 4. *The circumcircle and the polar circle (with center H) are the only circles which are their own harmonic conjugate circles.*

Remark. The polar circle is real only when the triangle contains an angle $\geq 90°$. For the construction of the polar circle, see §4.2 below.

3. Construction of coaxial circles

3.1. *Prescribed center.* Given a circle $O(R)$ and a line $\mathcal{L}$ generating a coaxial family of circles, we address the construction problem of the circle in the family with a prescribed center P on the line through O perpendicular to $\mathcal{L}$.

Any intersection of $\mathcal{L}$ and $O(R)$ is common to the circles in the coaxial family. The construction problem is trivial when $\mathcal{L}$ and $O(R)$ intersect.

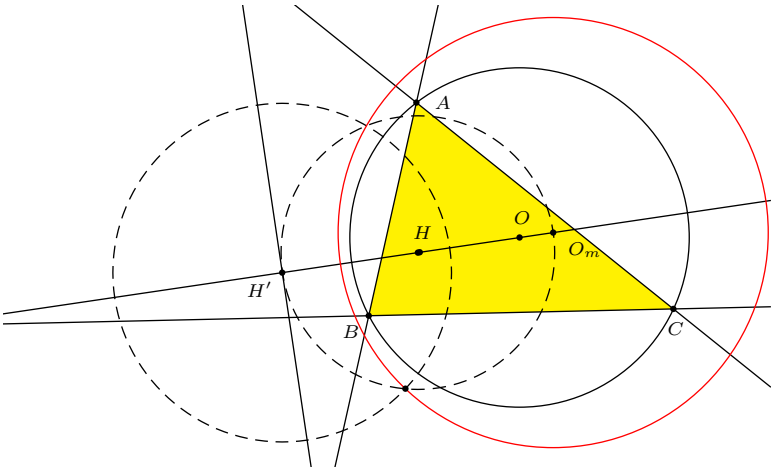

Figure 3. Construction of circles in coaxial family

Suppose $\mathcal{L}$ does not intersect the circle $O(R)$. Let H' be the orthogonal projection of O on the line $\mathcal{L}$. Set up a Cartesian coordinates with origin at H', y-axis along $\mathcal{L}$, and positive x-axis along the half-line $H'O$. If the point O has coordinates $(k_0, 0)$ for $k_0 > R$, the circle $O(R)$ has equation $(x - k_0)^2 + y^2 = R^2$, or

$$x^2 + y^2 - 2k_0x + k_0^2 - R^2 = 0.$$

Construct the circle (H') orthogonal to (O). This circle has radius $\sqrt{k_0^2 - R^2}$.

The real circles in the coaxial family have equations

$$x^2 + y^2 - 2kx + k_0^2 - R^2 = 0, \qquad k^2 \geq k_0^2 - R^2.$$

Given the center $K(k, 0)$, here is a simple construction of the circle.

(i) Suppose $k > 0$. Construct the circle with diameter $H'K$ to intersect the circle (H') at a point P. Then the circle $K(P)$ is the one in the coaxial family with center K (see Figure 3).

(ii) Suppose $k < 0$. Apply (i) to construct the circle in the family with center $(-k, 0)$. Reflect this in the line $\mathcal{L}$ to yield the circle with center $K(k, 0)$.

3.2. *Through a given point.* Given a point P not on the line $\mathcal{L}$, to construct the circle in the coaxial family which contains P, we need only note that this circle, being orthogonal to (H'), should also contain the inversive image P' of P in (H'). The intersection of the perpendicular bisector of PP' and the perpendicular to $\mathcal{L}$ from O is the center K of the circle.

4. Harmonic conjugate circles for special triangles

4.1. *Equilateral triangles.* If ABC is equilateral with circumcenter O and circumradius R, the only harmonic conjugate circle pairs are concentric circles at O, with radii ρ and ρ' related by

$$\left(\rho^2 - \frac{R^2}{4}\right)\left(\rho'^2 - \frac{R^2}{4}\right) = \left(\frac{3R^2}{4}\right)^2.$$

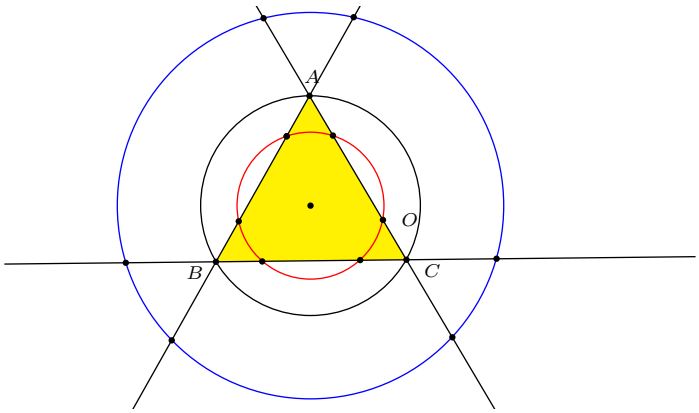

Figure 4. Harmonic conjugate circles of an equilateral triangle

4.2. *Nonacute triangles.* If ABC contains an angle $\geq 90^\circ$, then its orthic axis intersects the circumcircle at real points. [1] Therefore the harmonic conjugate circles pairs can be easily constructed knowing that their centers are harmonic conjugates with respect to OH.

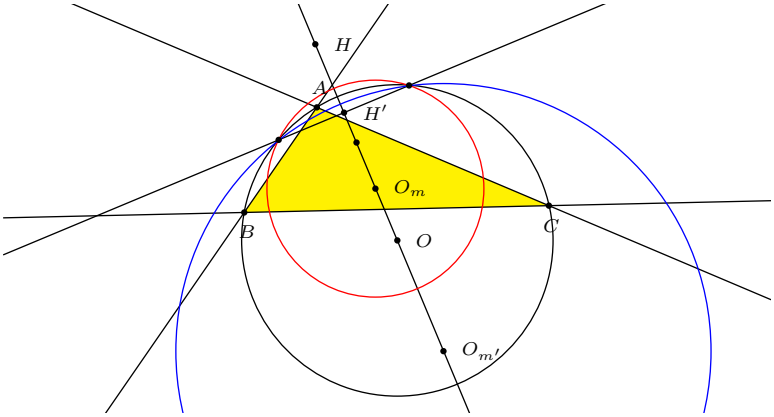

Figure 5. Harmonic conjugate circles of an obtuse triangle

5. Congruent harmonic conjugate circles

There is a unique pair of congruent harmonic conjugate circles. Their centers on the Euler line are symmetric with respect to H'. These two points are therefore the intersection of the Euler line with the circle, center H', orthogonal to the circle with diameter OH.

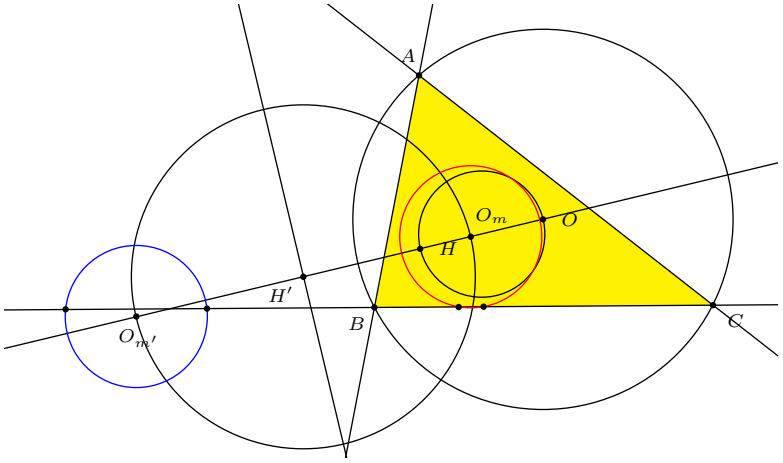

Figure 6. Congruent harmonic conjugate circles

[1] If ABC contains a right angle, then the right angle vectex is on the orthic axis (and the circumcircle).

References

[1] A. P. Hatzipolakis, F. M. van Lamoen, B. Wolk, and P. Yiu, Concurrency of four Euler lines, *Forum Geom.*, 1 (2001) 59–68.
[2] S. H. Lim, Hyacinthos message 20518, December 11, 2011
[3] P. Yiu, *Introduction to the Geometry of the Triangle*, Florida Atlantic University Lecture Notes, 2001.

Nikolaos Dergiades: I. Zanna 27, Thessaloniki 54643, Greece
E-mail address: ndergiades@yahoo.gr

Forum Geometricorum
Volume 12 (2012) 161–189.

FORUM GEOM
ISSN 1534-1178

The Perpendicular Bisector Construction, the Isoptic point, and the Simson Line of a Quadrilateral

Olga Radko and Emmanuel Tsukerman

Abstract. Given a noncyclic quadrilateral, we consider an iterative procedure producing a new quadrilateral at each step. At each iteration, the vertices of the new quadrilateral are the circumcenters of the triad circles of the previous generation quadrilateral. The main goal of the paper is to prove a number of interesting properties of the limit point of this iterative process. We show that the limit point is the common center of spiral similarities taking any of the triad circles into another triad circle. As a consequence, the point has the isoptic property *i.e.*, all triad circles are visible from the limit point at the same angle. Furthermore, the limit point can be viewed as a generalization of a circumcenter. It also has properties similar to those of the isodynamic point of a triangle. We also characterize the limit point as the unique point for which the pedal quadrilateral is a parallelogram. Continuing to study the pedal properties with respect to a quadrilateral, we show that for every quadrilateral there is a unique point (which we call the Simson point) such that its pedal consists of four points on a line, which we call the Simson line, in analogy to the case of a triangle. Finally, we define a version of isogonal conjugation for a quadrilateral and prove that the isogonal conjugate of the limit point is a parallelogram, while that of the Simson point is a degenerate quadrilateral whose vertices coincide at infinity.

1. Introduction

The perpendicular bisector construction that we investigate in this paper arises very naturally in an attempt to find a replacement for a circumcenter in the case of a noncyclic quadrilateral $Q^{(1)} = A_1B_1C_1D_1$. Indeed, while there is no circle going through all four vertices, for every triple of vertices there is a unique circle (called the *triad circle*) passing through them. The centers of these four triad circles can be taken as the vertices of a new quadrilateral, and the process can be iterated to obtain a sequence of noncyclic quadrilaterals: $Q^{(1)}, Q^{(2)}, Q^{(3)}, \ldots$.

To reverse the iterative process, one finds the isogonal conjugates of each of the vertices with respect to the triangle formed by the remaining vertices of the quadrilateral.

It turns out that all odd generation quadrilaterals are similar, and all even generation quadrilaterals are similar. Moreover, there is a point that serves as the center of spiral similarity for any pair of odd generation quadrilaterals as well as for any

Publication Date: June 1, 2012. Communicating Editor: Paul Yiu.

pair of even generation quadrilaterals. The angle of rotation is 0 or π depending on whether the quadrilateral is concave or convex, and the ratio r of similarity is a constant that is negative for convex noncyclic quadrilaterals, zero for cyclic quadrilaterals, and ≥ 1 for concave quadrilaterals. If $|r| \neq 1$, the same special point turns out to be the limit point for the iterative process or for the reverse process.

The main goal of this paper is to prove the following theorem.

Theorem 1. *For each quadrilateral $Q^{(1)} = A_1B_1C_1D_1$ there is a unique point W that has any (and, therefore, all) of the following properties:*

(1) *W is the center of the spiral similarity for any two odd (even) generation quadrilaterals in the iterative process;*
(2) *Depending on the value of the ratio of similarity in the iterative process, there are the following possibilities:*
   (a) *If $|r| < 1$, the quadrilaterals in the iterated perpendicular bisectors construction converge to W;*
   (b) *If $|r| = 1$, the iterative process is periodic (with period 2 or 4); W is the common center of rotations for any two odd (even) generation quadrilaterals;*
   (c) *If $|r| > 1$, the quadrilaterals in the reverse iterative process (obtained by isogonal conjugation) converge to W;*
(3) *W is the common point of the six circles of similitude $CS(o_i, o_j)$ for any pair of triad circles o_i, o_j, $i, j \in \{1, 2, 3, 4\}$, where $o_1 = (D_1A_1B_1)$, $o_2 = (A_1B_1C_1)$, $o_3 = (B_1C_1D_1)$, $o_4 = (C_1D_1A_1)$.*
(4) *(isoptic property) Each of the triad circles is visible from W at the same angle.*
(5) *(generalization of circumcenter) The (directed) angle subtended by any of the quadrilateral's sides at W equals to the sum of the angles subtended by the same side at the two remaining vertices.*
(6) *(isodynamic property) The distance from W to any vertex is inversely proportional to the radius of the triad circle determined by the remaining three vertices.*
(7) *W is obtained by inversion of any of the vertices of the original quadrilateral in the corresponding triad-circle of the second generation:*

$$W = Inv_{o_1^{(2)}}(A) = Inv_{o_2^{(2)}}(B) = Inv_{o_3^{(2)}}(C) = Inv_{o_4^{(2)}}(D),$$

   where $o_1^{(2)} = (D_2A_2B_2)$, $o_2^{(2)} = (A_2B_2C_2)$, $o_3^{(2)} = (B_2C_2D_2)$, $o_4^{(2)} = (C_2D_2A_2)$.
(8) *W is obtained by composition of isogonal conjugation of a vertex in the triangle formed by the remaining vertices and inversion in the circumcircle of that triangle.*
(9) *W is the center of spiral similarity for any pair of triad circles (of possibly different generations). That is, $W \in CS(o_i^{(k)}, o_j^{(l)})$ for all i, j, k, l.*
(10) *The pedal quadrilateral of W is a (nondegenerate) parallelogram. Moreover, its angles equal to the angles of the Varignon parallelogram.*

Many of these properties of W were known earlier. In particular, several authors (G. T. Bennett in an unpublished work, De Majo [11], H. V. Mallison [12]) have considered a point that is defined as the common center of spiral similarities. Once the existence of such a point is established, it is easy to conclude that all the triad circles are viewed from this point under the same angle (this is the so-called *isoptic property*). Since it seems that the oldest reference to the point with such an isoptic property is to an unpublished work of G. T. Bennett given by H. F. Baker in his *Principles of Geometry*, volume 4 [1, p.17], in 1925, we propose to call the center of spiral similarities in the iterative process *Bennett's isoptic point*.

C. F. Parry and M. S. Longuet-Higgins [14] showed the existence of a point with property 7 using elementary geometry.

Mallison [12] defined W using property 3 and credited T. McHugh for observing that this implies property 5.

Several authors, including Wood [19] and De Majo [11], have looked at the properties of the isoptic point from the point of view of the unique rectangular hyperbola going through the vertices of the quadrilateral, and studied its properties related to cubics. For example, P.W. Wood [19] considered the diameters of the rectangular hyperbola that go through A, B, C, D. Denoting by $\bar{A}, \bar{B}, \bar{C}, \bar{D}$ the other endpoints of the diameters, he showed that the isogonal conjugates of these points in triangles BCD, CAD,ABD, ABC coincide. Starting from this, he proved properties 4 and 7 of the theorem. He also mentions the reversal of the iterative process using isogonal conjugation (also found in [19], [17], [5]). Another interesting property mentioned by Wood is that W is the Fregier point of the center of the rectangular hyperbola for the conic $ABCDO$, where O is the center of the rectangular hyperbola.

De Majo [11] uses the property that inversion in a point on the circle of similitude of two circles transforms the original circles into a pair of circles whose radii are inversely proportional to those of the original circles to show that that there is a common point of intersection of all 6 circles of similitude. He describes the iterative process and states property 1, as well as several other properties of W (including 8). Most statements are given without proofs.

Scimemi [17] describes a Möbius transformation that characterizes W: there exists a line going through W and a circle centered at W such that the product of the reflection in the line with the inversion in the circle maps each vertex of the first generation into a vertex of the second generation.

The question of proving that the third generation quadrilateral is similar to the original quadrilateral and finding the ratio of similarity was first formulated by J. Langr [8]. Independently, the result appeared in the form of a problem by V.V. Prasolov in [15, 16]. The expression for the ratio (under certain conditions) was obtained by J. Langr [8] , and the expression for the ratio (under certain conditions) was obtained by D. Bennett [2] (apparently, no relation to G. T. Bennett mentioned above), and J. King [7]. A paper by G. C. Shepard [18] found an expression for the ratio as well. (See [3] for a discussion of these works).

Properties 9 and 10 appear to be new.

For the convenience of the reader, we give a complete and self contained exposition of all the properties in the Theorem above, as well as proofs of several related statements.

In addition to investigating properties of W, we show that there is a unique point for which the feet of the perpendiculars to the sides lie on a straight line. In analogy with the case of a triangle, we call this line the *Simson line* of a quadrilateral and the point – the *Simson point.* The existence of such a point is stated in [6] where it is obtained as the intersection of the Miquel circles of the complete quadrilateral.

Finally, we introduce a version of isogonal conjugation for a quadrilateral and show that the isogonal conjugate of W is a parallelogram, and that of the Simson point is a degenerate quadrilateral whose vertices are at infinity, in analogy with the case of the points on the circumcircle of a triangle.

2. The iterative process

Let $A_1B_1C_1D_1$ be a quadrilateral. If $A_1B_1C_1D_1$ is cyclic, the center of the circumcircle can be found as the intersection of the four perpendicular bisectors to the sides of the quadrilateral.

Assume that $Q^{(1)} = A_1B_1C_1D_1$ is a noncyclic quadrilateral.[1] Is there a point that, in some sense, plays the role of the circumcenter? Let $Q^{(2)} = A_2B_2C_2D_2$ be the quadrilateral formed by the intersections of the perpendicular bisectors of the sides of $A_1B_1C_1D_1$. The vertices A_2, B_2, C_2, D_2 of the new quadrilateral are the circumcenters of the triangles $D_1A_1B_1$, $A_1B_1C_1$, $B_1C_1D_1$ and $C_1D_1A_1$ formed by vertices of the original quadrilateral taken three at a time.

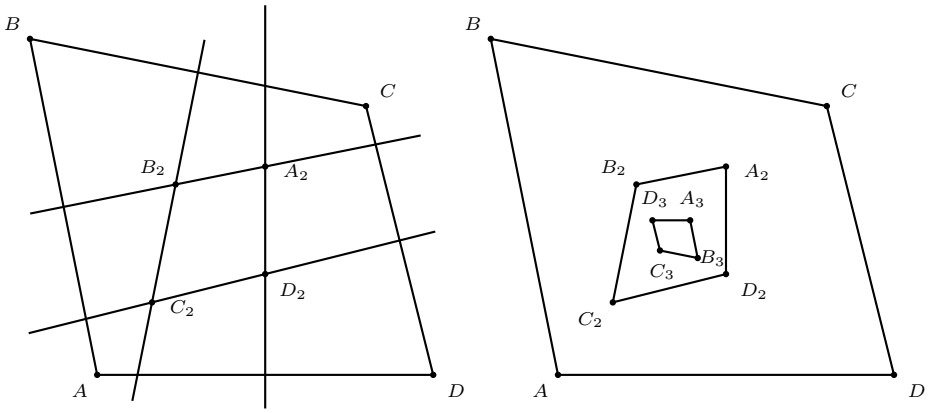

Figure 1. The perpendicular bisector construction and $Q^{(1)}, Q^{(2)}, Q^{(3)}$.

Iterating this process, *i.e.*, constructing the vertices of the next generation quadrilateral by intersecting the perpendicular bisectors to the sides of the current one, we obtain the successive generations, $Q^{(3)} = A_3B_3C_3D_3$, $Q^{(4)} = A_4B_4C_4D_4$ and so on, see Figure 1.

[1]Sometimes we drop the lower index 1 when denoting vertices of $Q^{(1)}$, so $ABCD$ and $A_1B_1C_1D_1$ are used interchangeably throughout the paper.

The first thing we note about the iterative process is that it can be reversed using isogonal conjugation. Recall that given a triangle ABC and a point P, the *isogonal conjugate* of P with respect to the triangle (denoted by $\mathrm{Iso}_{ABC}(P)$) is the point of intersection of the reflections of the lines AP, BP and CP in the bisectors of angles A, B and C respectively. One of the basic properties of isogonal conjugation is that the isogonal conjugate of P is the circumcenter of the triangle obtained by reflecting P in the sides of ABC (see, for example, [5] for more details). This property immediately implies

Theorem 2. *The original quadrilateral $A_1B_1C_1D_1$ can be reconstructed from the second generation quadrilateral $A_2B_2C_2D_2$ using isogonal conjugation:*

$$\begin{aligned} A_1 &= \mathit{Iso}_{D_2A_2B_2}(C_2), \\ B_1 &= \mathit{Iso}_{A_2B_2C_2}(D_2), \\ C_1 &= \mathit{Iso}_{B_2C_2D_2}(A_2), \\ D_1 &= \mathit{Iso}_{C_2D_2A_2}(B_2). \end{aligned}$$

The following theorem describes the basic properties of the iterative process.

Theorem 3. *Let $Q^{(1)}$ be a quadrilateral. Then*

(1) *$Q^{(2)}$ degenerates to a point if and only if $Q^{(1)}$ is cyclic.*
(2) *If $Q^{(1)}$ is not cyclic, the corresponding angles of the first and second generation quadrilaterals are supplementary:*

$$\angle A_1 + \angle A_2 = \angle B_1 + \angle B_2 = \angle C_1 + \angle C_2 = \angle D_1 + \angle D_2 = \pi.$$

(3) *If $Q^{(1)}$ is not cyclic, all odd generation quadrilaterals are similar to each other and all the even generation quadrilaterals are similar to each other:*

$$\begin{aligned} Q^{(1)} \sim Q^{(3)} \sim Q^{(5)} \sim \dots, \\ Q^{(2)} \sim Q^{(4)} \sim Q^{(6)} \sim \dots. \end{aligned}$$

(4) *All odd generation quadrilaterals are related to each other via spiral similarities with respect to a common center.*
(5) *All even generation quadrilaterals are also related to each other via spiral similarities with respect to a common center.*
(6) *The angle of rotation for each spiral similarity is π (for a convex quadrilateral) or a 0 (for a concave quadrilateral). The ratio of similarity is*

$$r = \frac{1}{4}(\cot\alpha + \cot\gamma) \cdot (\cot\beta + \cot\delta), \tag{1}$$

where $\alpha = \angle A_1$, $\beta = \angle B_1$, $\gamma = \angle C_1$ and $\delta = \angle D_1$ are the angles of $Q^{(1)}$.
(7) *The center of spiral similarities is the same for both the odd and the even generations.*

Proof. The first and second statements follow immediately from the definition of the iterative process. To show that all odd generation quadrilaterals are similar to each other and all even generation quadrilaterals are similar to each other, it is enough to notice that both the corresponding sides and the corresponding diagonals of all odd (even) generation quadrilaterals are pairwise parallel.

Let $W_1 := A_1A_3 \cap B_1B_3$ be the center of spiral similarity taking $Q^{(1)}$ into $Q^{(3)}$. Similarly, let W_2 be the center of spiral similarity taking $Q^{(2)}$ into $Q^{(4)}$. Denote the midpoints of segments A_1B_1 and A_3B_3 by M_1 and M_3. (See fig. 2). To show that W_1 and W_2 coincide, notice that $B_1M_1A_2 \sim B_3M_3A_4$. Since the corresponding sides of these triangles are parallel, they are related by a spiral similarity. Since $B_1B_3 \cap M_1M_3 = W_1$ and $M_1M_3 \cap B_2B_4 = W_2$, it follows that $W_1 = W_2$. Let now W_3 be the center of spiral similarity that takes $Q^{(3)}$ into $Q^{(5)}$. By the same reasoning, $W_2 = W_3$, which implies that $W_1 = W_3$. Continuing by induction, we conclude that the center of spiral similarity for any pair of odd generation quadrilaterals coincides with that for any pair of even generation quadrilaterals. We denote this point by W. □

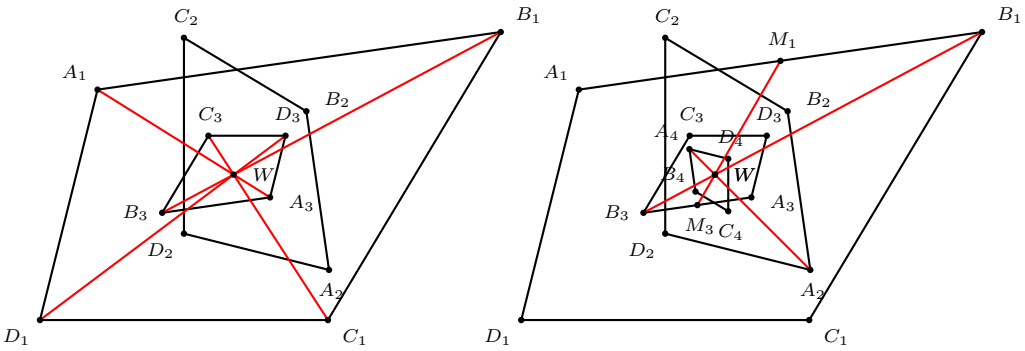

Figure 2. W as the center of spiral similarities.

From parts (2) and (3) of Theorem 3 we obtain the following corollary.

Corollary 4. *The even and odd generation quadrilaterals are similar to each other if and only if $Q^{(1)}$ is a trapezoid.*

The ratio of similarity $r = r(\alpha, \beta, \gamma, \delta)$ takes values in $(-\infty, 0] \cup [1, \infty)$ and characterizes the shape of $Q^{(1)}$ in the following way:

(1) $r \leq 0$ if and only if $Q^{(1)}$ is convex. Moreover, $r = 0$ if and only if $Q^{(1)}$ is cyclic.

(2) $r \geq 1$ if and only if $Q^{(1)}$ is concave. Moreover, $r = 1$ if and only if $Q^{(1)}$ is *orthocentric* (that is, each of the vertices is the orthocenter of the triangle formed by the remaining three vertices. Alternatively, an orthocentric quadrilateral is characterized by being a concave quadrilateral for which the two opposite acute angles are equal).

For convex quadrilaterals, r can be viewed as a measure of how noncyclic the original quadrilateral is. Recall that since the opposite angles of a cyclic quadrilateral add up to π, the difference

$$|(\alpha + \gamma) - \pi| = |(\beta + \delta) - \pi| \tag{2}$$

can be taken as the simplest measure of noncyclicity. This measure, however, treats two quadrilaterals with equal sums of opposite angles as equally noncyclic. The

ratio r provides a refined measure of noncyclicity. For example, for a fixed sum of opposite angles, $\alpha + \gamma = C$, $\beta + \delta = 2\pi - C$, where $C \in (0, 2\pi)$, the convex quadrilateral with the smallest $|r|$ is the parallelogram with $\alpha = \gamma = \frac{C}{2}$, $\beta = \delta$.

Similarly, for concave quadrilaterals, r measures how different the quadrilateral is from being orthocentric.

Since the angles between diagonals are the same for all generations, it follows that the ratio is the same for all pairs of consecutive generations:

$$\frac{\text{Area}(Q^{(n)})}{\text{Area}(Q^{(n-1)})} = |r|.$$

Assuming the quadrilateral is noncyclic, there are the following three possibilities:

(1) When $|r| < 1$ (which can only happen for convex quadrilaterals), the quadrilaterals in the iterative process converge to W.
(2) When $|r| > 1$, the quadrilaterals in the inverse iterative process converge to W.
(3) When $|r| = 1$, all the quadrilaterals have the same area. The iterative process is periodic with period 4 for all quadrilaterals with $|r| = 1$, except for the following two special cases. If $Q^{(1)}$ is either a parallelogram with angle $\frac{\pi}{4}$ (so that $r = -1$) or forms an orthocentric system (so that $r = 1$), we have $Q^{(3)} = Q^{(1)}$, $Q^{(4)} = Q^{(2)}$, and the iterative process is periodic with period 2.

By setting $r = 0$ in formula (1), we obtain the familiar relations between the sides and diagonals of a cyclic quadrilateral $ABCD$:

$$AC \cdot BD = AB \cdot CD + BC \cdot AD, \qquad \text{(Ptolemy's theorem)} \tag{3}$$

$$\frac{AC}{BD} = \frac{AB \cdot AD + CB \cdot CD}{BA \cdot BC + DA \cdot DC.} \tag{4}$$

Since the vertices of the next generation depend only on the vertices of the previous one (but not on the way the vertices are connected), one can see that W and r for the (self-intersecting) quadrilaterals $ACBD$ and $ACDB$ coincide with those for $ABCD$. This observation allows us to prove the following

Corollary 5. *The angles between the sides and the diagonals of a quadrilateral satisfy the following identities:*

$$(\cot\alpha + \cot\gamma) \cdot (\cot\beta + \cot\delta) = (\cot\alpha_1 - \cot\beta_2) \cdot (\cot\delta_2 - \cot\gamma_1),$$
$$(\cot\alpha + \cot\gamma) \cdot (\cot\beta + \cot\delta) = (\cot\delta_1 - \cot\alpha_2) \cdot (\cot\beta_1 - \cot\gamma_2)$$

where $\alpha_i, \beta_i, \gamma_i, \delta_i$, $i = 1, 2$ are the directed angles formed between sides and diagonals of a quadrilateral (see Figure 3).

Proof. Since the (directed) angles of $ACBD$ are $-\alpha_1, \beta_2, \gamma_1, -\delta_2$ and the directed angles of $ACDB$ are $\alpha_2, \beta_1, -\gamma_2, -\delta_1$, the identities follow from formula (1) for the ratio of similarity. □

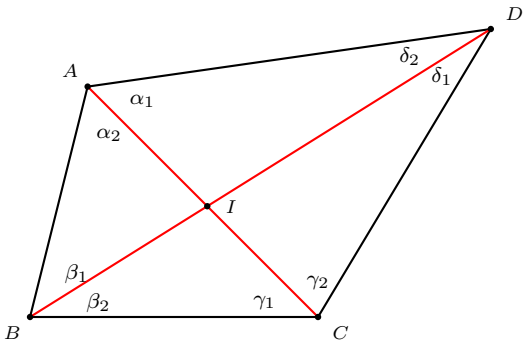

Figure 3. The angles between the sides and diagonals of a quadrilateral.

3. Properties of the center of spiral similarity

We will show that W, defined as the limit point of the iterated perpendicular bisectors construction in the case that $|r| < 1$ (or of its reverse in the case that $|r| > 1$), is the common center of all spiral similarities taking any of the triad circles into another triad circle in the iterative process.

First, we will prove that any of the triad circles of the first generation quadrilateral can be taken into another triad circle of the first generation by a spiral similarity centered at W (Theorem 9). This result allows us to view W as a generalization of the circumcenter for a noncyclic quadrilateral (Corollary 10 and Corollary 13), to prove its isoptic (Theorem 11), isodynamic (Corollary 14) and inversive (Theorem 15) properties, as well as to establish some other results. We then prove several statements that allow us to conclude (see Theorem 24) that W serves as the center of spiral similarities for any pair of triad circles of any two generations.

Several objects associated to a configuration of two circles on the plane will play a major role in establishing properties of W. We will start by recalling the definitions and basic constructions related to these objects.

3.1. *Preliminaries: circle of similitude, mid-circles and the radical axis of two circles.* Let o_1 and o_2 be two (intersecting[2]) circles on the plane with centers O_1 and O_2 and radii R_1 and R_2 respectively. Let A and B be the points of intersection of the two circles. There are several geometric objects associated to this configuration (see Figure 4):

(1) The *circle of similitude* $CS(o_1, o_2)$ is the set of points P on the plane such that the ratio of their distances to the centers of the circles is equal to the ratio of the radii of the circles:
$$\frac{PO_1}{PO_2} = \frac{R_1}{R_2}.$$
In other words, $CS(o_1, o_2)$ is the Apollonian circle determined by points O_1, O_2 and ratio R_1/R_2.

[2]Most of the constructions remain valid for non-intersecting circles. However, they sometimes have to be formulated in different terms. Since we will only deal with intersecting circles, we will restrict our attention to this case.

(2) The *radical axis* $RA(o_1, o_2)$ can be defined as the line through the points of intersection.
(3) The two *mid-circles* (sometimes also called the *circles of antisimilitude*) $MC_1(o_1, o_2)$ and $MC_2(o_1, o_2)$ are the circles that invert o_1 into o_2, and vice versa:

$$\mathrm{Inv}_{MC_i(o_1,o_2)}(o_1) = o_2, \qquad i = 1, 2.$$

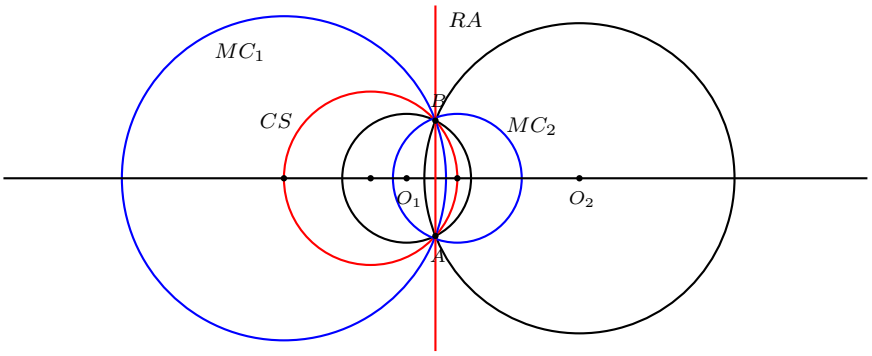

Figure 4. Circle of similitude, mid-circles and radical axis.

Here are several important properties of these objects (see [6] and [4] for more details):

(1) $CS(o_1, o_2)$ is the locus of centers of spiral similarities taking o_1 into o_2. For any $E \in CS(o_1, o_2)$, there is a spiral similarity centered at E that takes o_1 into o_2. The ratio of similarity is R_2/R_1 and the angle of rotation is $\angle O_1 E O_2$.
(2) Inversion with respect to $CS(o_1, o_2)$ takes centers of o_1 and o_2 into each other:

$$\mathrm{Inv}_{CS(o_1,o_2)}(O_1) = O_2.$$

(3) Inversion with respect to any of the mid-circles exchanges the circle of similitude and the radical axis:

$$\mathrm{Inv}_{MC_i(o_1,o_2)}(CS(o_1, o_2)) = RA(o_1, o_2), \qquad i = 1, 2.$$

(4) The radical axis is the locus of centers of all circles k that are orthogonal to both o_1 and o_2.
(5) For any $P \in CS(o_1, o_2)$, inversion in a circle centered at P takes the circle of similitude of the original circles into the radical axis of the images, and the radical axis of the original circles into the circle of similitude of the images:

$$CS(o_1, o_2)' = RA(o_1', o_2'),$$
$$RA(o_1, o_2)' = CS(o_1', o_2').$$

Here $'$ denotes the image of an object under the inversion in a circle centered at $P \in CS(o_1, o_2)$.

(6) Let K, L, M be points on the circles $o_1, o_2, CS(o_1, o_2)$ respectively. Then

$$\angle AMB = \angle AKB + \angle ALB, \tag{5}$$

where the angles are taken in the sense of directed angles.

(7) Let A_1B_1 be a chord of a circle k_1 and A_2B_2 be a chord of a circle k_2. Then A_1, B_1, A_2, B_2 are on a circle o if and only if $A_1B_1 \cap A_2B_2 \in RA(k_1, k_2)$.

It is also useful to recall the construction of the center of a spiral similarity given the images of two points. Suppose that A and B are transformed into A' and B' respectively. Let $P = AA' \cap BB'$. The center O of the spiral similarity can be found as the intersection $O = (ABP) \cap (A'B'P)$. (Here and henceforth (ABP) stands for the circle going through A, B, P). We will call point P in this construction the *joint point* associated to two given points A, B and their images A', B' under spiral similarity.

There is another spiral similarity associated to the same configuration of points. Let $P' = AB \cap A'B'$ be the joint point for the spiral similarity taking A and A' into B and B' respectively. A simple geometric argument shows that the center of this spiral similarity, determined as the intersection of the circles $(AA'P') \cap (BB'P')$, coincides with O. We will call such a pair of spiral similarities centered at the same point *associated spiral similarities*.

Let $H^W_{i,j}$ be the spiral similarity centered at W that takes o_i into o_j. The following Lemma will be useful when studying properties of the limit point of the iterative process (or of its inverse):

Lemma 6. *Let o_1 and o_2 be two circles centered at O_1 and O_2 respectively and intersecting at points A and B. Let $W, R, S \in CS(o_1, o_2)$ be points on the circle of similitude such that R and S are symmetric to each other with respect to the line of centers, O_1O_2. Then the joint points corresponding to taking $O_1 \to O_2$, $R \to R_{1,2} := H^W_{1,2}(R)$ by $H^W_{1,2}$ and taking $O_2 \to O_1$, $S \to S_{2,1} := H^W_{2,1}(S)$ by $H^W_{2,1}$ coincide. The common joint point lies on O_1O_2.*

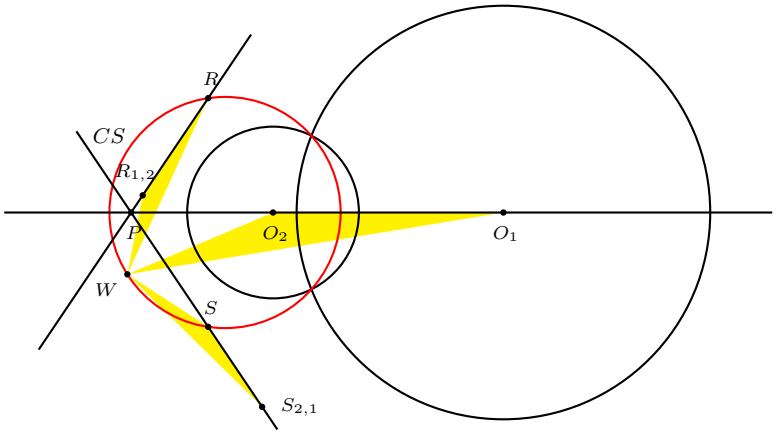

Figure 5. Lemma 6.

Proof. Perform inversion in the mid-circle. The image of $CS(o_1, o_2)$ is the radical axis $RA(o_1, o_2)$, *i.e.*, the line through A and B. The images of R and S lie on the line AB and are symmetric with respect to $I := AB \cap O_1O_2$. Similarly, the images of O_1 and O_2 are symmetric with respect to I and lie on the line of centers. By abuse of notation, we will denote the image of a point under inversion in the mid-circle by the same letter.

The lemma is equivalent to the statement that $P := (WO_1R) \cap O_1O_2$ lies on the circle (WO_2S). To show this, note that since P, R, O_1 and W lie on a circle, we have $|IP| \cdot |IO_1| = |IW| \cdot |IR|$. Since $|IO_2| = |IO_1|$ and $|IR| = |IS|$, it follows that $|IP| \cdot |IO_2| = |IW| \cdot |IS|$, which implies that W, P, O_2, S lie on a circle. After inverting back in the mid-circle, we obtain the result of the lemma. □

Notice that the lemma is equivalent to the statement that

$$RR_{1,2} \cap SS_{2,1} = (WRO_1) \cap (WSO_2) \in O_1O_2.$$

3.2. *W as the center of spiral similarities for triad circles of $Q^{(1)}$.* Denote by o_1, o_2, o_3 and o_4 the triad circles $(D_1A_1B_1)$, $(A_1B_1C_1)$, $(B_1C_1D_1)$ and $(C_1D_1A_1)$ respectively.[3] For triad circles in other generations, we add an upper index indicating the generation. For example, $o_1^{(3)}$ denotes the first triad-circle in the 3rd generation quadrilateral, *i.e.*, circle $(D_3A_3B_3)$. Let T_1, T_2, T_3 and T_4 be the triad triangles $D_1A_1B_1$, $A_1B_1C_1$, $B_1C_1D_1$ and $C_1D_1A_1$ respectively.

Consider two of the triad circles of the first generation, o_i and o_j, $i \neq j \in \{1, 2, 3, 4\}$. The set of all possible centers of spiral similarity taking o_i into o_j is their circle of similitude $CS(o_i, o_j)$. If $Q^{(1)}$ is a nondegenerate quadrilateral, it can be shown that $CS(o_1, o_2)$ and $CS(o_1, o_4)$ intersect at two points and are not tangent to each other. Let W be the other point of intersection of $CS(o_1, o_2)$ and $CS(o_1, o_4)$.[4]

Let $H_{k,l}^W$ be the spiral similarity centered at W that takes o_k into o_l for any $k, l \in \{1, 2, 3, 4\}$.

Lemma 7. *Spiral similarities $H_{k,l}^W$ have the following properties:*

(1) $H_{1,2}^W(B_1) = A_1 \Longleftrightarrow H_{2,4}^W(A_1) = C_1$.
(2) $H_{1,2}^W(B_1) = A_1 \Longleftrightarrow H_{1,4}^W(B_1) = C_1$.

Proof. Assume that $H_{1,2}^W(B_1) = A_1$. Let $P_{1,2} := A_1B_1 \cap A_2B_2$ be the joint point of the spiral similarity (centered at W) taking B_1 into A_1 and A_2 into B_2. Since points $B_1, P_{1,2}, W, A_2$ lie on a circle (see Lemma 6), it follows that $\angle BWA_1 = \angle BP_{1,2}A_2 = \pi/2$. Thus, A_2B_1 is a diameter of $k_1 := (B_1P_{1,2}WA_2)$. Since o_1 is centered at A_2, the circles o_1 and k_1 are tangent at B_1. It is easy to see that the converse is also true: if o_1 and (B_1WA_2) are tangent at B_1, then $H_{1,2}^W(B_1) = A_1$.

[3] In short, the middle vertex defining the circle o_i is vertex number i (the first vertex being A_1, the second being B_1, the third being C_1 and the last being D_1).

[4] This will turn out to be the same point as the limit point of the iterative process defined in section 2, so the clash of notation is intentional.

Since $A_1, P_{1,2}, W, B_2$ lie on a circle, it follows that $\angle A_1 W B_2 = \angle A_1 P_{1,2} B_2 = \pi/2$. Since $B_1 \mapsto A_1$ and $A_2 \mapsto B_2$ under $H^W_{1,2}$, $\angle B_1 W A_2 = \angle A_1 W B_2 = \pi/2$. This implies that the circles $k_2 := (A_1 P_{1,2} W B_2)$ and o_2 are tangent at A_1. It is easy to see that k_2 is tangent to o_2 if and only if k_1 is tangent to o_1.

Similarly to the above, let $P_{2,4} := A_1 H^W_{2,4}(A_1) \cap B_2 D_2$ be the joint point of the spiral similarity centered at W and taking o_2 into o_4. Then $P_{2,4} \in k_2$. Similarly to the argument above, k_2 is tangent to o_2 if and only if $k_4 := (C_1 P_{2,4} W D_2)$ is tangent to o_4. This is equivalent to $H^W_{2,4}(A_1) = C_1$.

The second statement follows since $H^W_{1,4}(B_1) = H^W_{2,4} \circ H^W_{1,2}(B_1) = H^W_{2,4}(A_1) = C_1$. (Here and below the compositions of transformations are read right to left). □

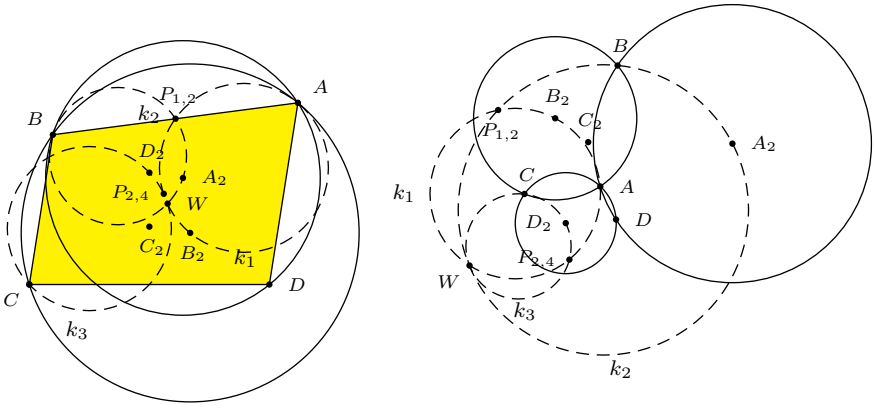

Figure 6. Proofs of Lemma 7 and Lemma 8.

Notice that circles o_1 and o_4 have two common vertices, A_1 and D_1. The next Lemma shows that $H^W_{1,4}$ takes B_1 (the third vertex on o_1) to C_1 (the third vertex on o_4). This property is very important for showing that any triad circle from the first generation can be transformed into another triad circle from the first generation by a spiral similarity centered at W. Similar properties hold for $H^W_{1,2}$ and $H^W_{2,4}$. Namely, we have

Lemma 8. $H^W_{1,4}(B_1) = C_1$, $H^W_{1,2}(D_1) = C_1$, $H^W_{4,2}(D_1) = B_1$.

Proof. Lemma 7 shows that $H^W_{1,2}(B_1) = A_1$ implies $H^W_{1,4}(B_1) = C_1$. Assume that $H^W_{1,2}(B_1) \neq A_1$. To find the image of B_1 under $H^W_{1,4}$, represent the latter as the composition $H^W_{2,4} \circ H^W_{1,2}$. First, $H^W_{1,2}(B_1) = P_{1,2}B_1 \cap (P_{1,2}B_2W)$, where $P_{1,2}$ is as in Lemma 7, see Figure 6. For brevity, let $B_{1,2} := H^W_{1,2}(B_1)$. (The indices refer to the fact that $B_{1,2}$ is the image of B under spiral similarity taking o_1 into o_2).

Now we construct $H^W_{1,4}(B_1) = H^W_{2,4}(B_{1,2})$. By Lemma 6, $H^W_{1,4}(B_1) = P_{2,4}B_{1,2} \cap (WP_{2,4}D_2)$, where $P_{2,4}$ is as in Lemma 7. Applying Lemma 6 to the circle $(WP_{2,4}D_2)$, we conclude that it passes through C_1. Since by assumption $H^W_{1,2}(B_1) \neq$

A_1, it follows that $H^W_{2,4} \circ H^W_{1,2}(B_1) = C_1$. Thus, $H^W_{1,4}(B_1) = C_1$. The other statements in the Lemma can be shown in a similar way. □

The last Lemma allows us to show that W lies on all of the circles of similitude $CS(o_i, o_j)$.

Theorem 9. *$W \in CS(o_i, o_j)$ for all $i, j \in \{1, 2, 3, 4\}$.*

Proof. By definition, $W \in CS(o_1, o_2) \cap CS(o_1, o_4) \cap CS(o_2, o_4)$. We will show that $W \in CS(o_3, o_i)$ for any $i \in \{1, 2, 4\}$.

Recall that $B_1 \in CS(o_1, o_2) \cap CS(o_2, o_3)$. Let $\widetilde{W}$ be the second point in the intersection $CS(o_1, o_2) \cap CS(o_2, o_3)$, so that $CS(o_1, o_2) \cap CS(o_2, o_3) = \{B_1, \widetilde{W}\}$. By Lemma 8, $H^{\widetilde{W}}_{1,2}(D_1) = C_1$. Since $H^{\widetilde{W}}_{1,2}(A_2) = B_2$, it follows that $H^{\widetilde{W}}_{1,2} = H^W_{1,2}$, which implies that $\widetilde{W} = W$. Therefore, W is the common point for all the circles of similitude $CS(o_i, o_j)$, $i, j \in \{1, 2, 3, 4\}$. □

3.3. *Properties of W.* The angle property (5) of the circle of similitude implies

Corollary 10. *The angles subtended by the quadrilateral's sides at W are as follows (see Figure 7):*

$$\begin{aligned} \angle AWB &= \angle ACB + \angle ADB, \\ \angle BWC &= \angle BAC + \angle BDC, \\ \angle CWD &= \angle CAD + \angle CBD, \\ \angle DWA &= \angle DBA + \angle DCA. \end{aligned}$$

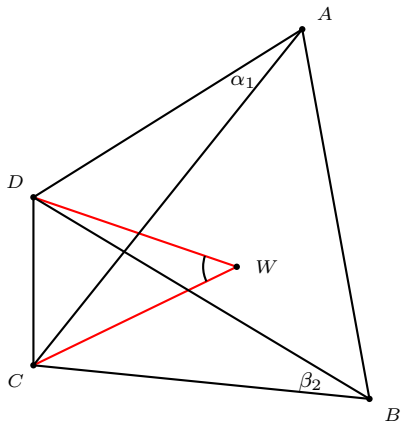

Figure 7. $\angle CWD = \angle CAD + \angle CBD$.

This allows us to view W as a replacement of the circumcenter in a certain sense: the angle relations above are generalizations of the relation $\angle AOB = \angle ACB + \angle ADB$ between the angles in a cyclic quadrilateral $ABCD$ with circumcenter O. (Of course, in this special case, $\angle ACB = \angle ADB$).

Since $W \in CS(o_i, o_j)$ for all i, j, W can be used as the center of spiral similarity taking any of the triad circles into another triad circle. This implies the following

Theorem 11. *(Isoptic property) All the triad circles o_i subtend equal angles at W.*

In particular, W is inside of all of the triad circles in the case of a convex quadrilateral and outside of all of the triad circles in the case of a concave quadrilateral. (This was pointed out by Scimemi in [17]). If W is inside of a triad circle, the isoptic angle equals to $\angle TOT'$, where T and T' are the points on the circle so that TT' goes through W and $TT' \perp OW$. (See Figure 8, where $\angle T_1A_2W$ and $\angle T_4B_2W$ are halves of the isoptic angle in o_1 and o_4 respectively). If W is outside of a triad circle centered at O and WT is the tangent line to the circle, so that T is point of tangency, $\angle OTW$ is half of the isoptic angle. Inverting in a triad circle of the second generation, we get that the triad circles are viewed at equal angles from the vertices opposite to their centers (see Figure 8).

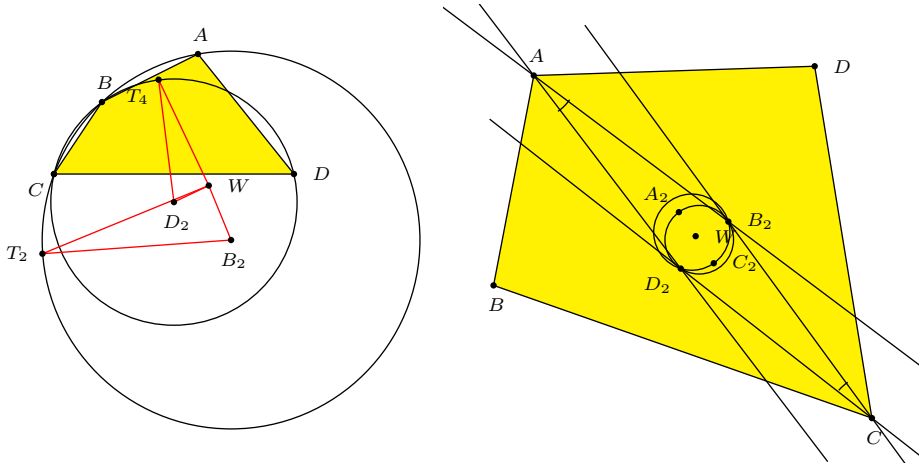

Figure 8. The isoptic angles before and after inversion.

Recall that the *power of a point* P with respect to a circle o centered at O with radius R is the square of the length of the tangent from P to the circle, that is,

$$h = |PO|^2 - R^2.$$

The isoptic property implies the following

Corollary 12. *The powers of W with respect to triad circles are proportional to the squares of the radii of the triad circles.*

This property of the isoptic point was shown by Neville in [13] using tetracyclic coordinates and the Darboux-Frobenius identity.

Let a, b, c, d be sides of the quadrilateral. For any $x \in \{a, b, c, d\}$, let F_x be the foot of the perpendicular bisector of side x on the opposite side. (E.g., F_a is the intersection of the perpendicular bisector to the side AB and the side CD). The following corollary follows from Lemma 8 and expresses W as the point of intersection of several circles going through the vertices of the first and second

generation quadrilaterals, as well as the intersections of the perpendicular bisectors of the original quadrilateral with the opposite sides (see Figure 9).

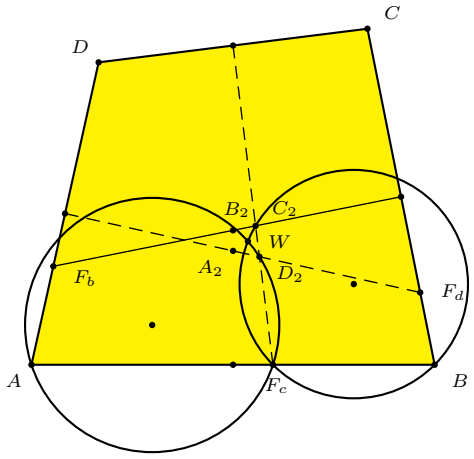

Figure 9. W as the intersection of circles $(A_1F_cD_2)$ and $(B_1F_cC_2)$ in (6).

Corollary 13. *W is a common point of the following eight circles:*

$$\begin{array}{llll}(A_1F_bB_2), & (A_1F_cD_2), & (B_1F_cC_2), & (B_1F_dA_2),\\ (C_1F_dD_2), & (C_1F_aB_2), & (D_1F_aA_2), & (D_1F_bC_2).\end{array} \tag{6}$$

Remark. This property can be viewed as the generalization of the following property of the circumcenter of a triangle:

Given a triangle ABC with sides a, b, c opposite to vertices A, B, C, let F_{kl} denote the feet of the perpendicular bisector to side k on the side l (or its extension), where $k, l \in \{a, b, c\}$. Then the circumcenter is the common point of three circles going through vertices and feet of the perpendicular bisectors in the following way [5]:

$$O = (ABF_{ab}F_{ba}) \cap (BCF_{bc}F_{cb}) \cap (CAF_{ca}F_{ac}), \tag{7}$$

see Figure 10.

The similarity between (7) and (6) supports the analogy of the isoptic point with the circumcenter.

The last corollary provides a quick way of constructing W. First, construct two vertices (e.g., A_2 and D_2) of the second generation by intersecting the perpendicular bisectors. Let F_d be the intersection of the lines A_2D_2 and B_1C_1. Then W is obtained as the second point of intersection of the two circles $(B_1F_bA_2)$ and $(C_1F_bD_2)$.

[5]Note also that this statement is related to Miquel's theorem as follows. Take any three points P, Q, R on the three circles in (7), so that A, B, C are points on the sides PQ, QR, PQ of PQR. Then the statement becomes Miquel's theorem for PQR and points A, B, C on its sides, with the extra condition that the point of intersection of the circles (PAC), (QAB), (RBC) is the circumcenter of ABC.

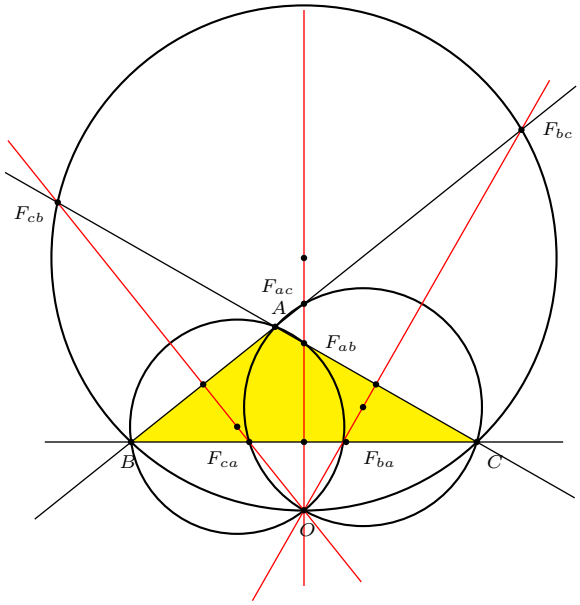

Figure 10. Circumcenter as intersection of circles in (7).

Recall the definition of isodynamic points of a triangle. Let $A_1A_2A_3$ be a triangle with sides a_1, a_2, a_3 opposite to the vertices A_1, A_2, A_3. For each $i, j \in \{1, 2, 3\}$, where $i \neq j$, consider the circle o_{ij} centered at A_i and going through A_j. The circle of similitude $CS(o_{ij}, o_{kj})$ of two distinct circles o_{ij} and o_{kj} is the Apollonian circle with respect to points A_i, A_k with ratio $r_{ik} = \frac{a_k}{a_i}$. It is easy to see that the three Apollonian circles intersect in two points, S and S', which are called the *isodynamic points* of the triangle.

Here are some properties of isodynamic points (see, e.g., [6], [4] for more details):

(1) The distances from S (and S') to the vertices are inversely proportional to the opposite side lengths:

$$|SA_1| : |SA_2| : |SA_3| = \frac{1}{a_1} : \frac{1}{a_2} : \frac{1}{a_3}. \tag{8}$$

Equivalently,

$$|SA_i| : |SA_j| = \sin\alpha_j : \sin\alpha_i, \qquad i \neq j \in \{1, 2, 3\},$$

where α_i is the angle $\angle A_i$ in the triangle. The isodynamic points can be characterized as the points having this distance property. Note that since the radii of the circles used to define the circles of similitude are the sides, the last property means that distances from isodynamic points to the vertices are inversely proportional to the radii of the circles.

(2) The pedal triangle of a point on the plane of $A_1A_2A_3$ is equilateral if and only if the point is one of the isodynamic points.

(3) The triangle whose vertices are obtained by inversion of A_1, A_2, A_3 with respect to a circle centered at a point P is equilateral if and only if P is one of the isodynamic points of $A_1A_2A_3$.

It turns out that W has properties (Corollary 14, Theorem 30, Theorem 27) similar to properties 1–3 of S.

Corollary 14. *(Isodynamic property of W) The distances from W to the vertices of the quadrilateral are inversely proportional to the radii of the triad-circles going through the remaining three vertices:*

$$|WA_1| : |WB_1| : |WC_1| : |WD_1| = \frac{1}{R_3} : \frac{1}{R_4} : \frac{1}{R_1} : \frac{1}{R_2},$$

where R_i is the radius of the triad-circle o_i. Equivalently, the ratios of the distances from W to the vertices are as follows:

$$\begin{aligned} |WA_1| : |WB_1| &= |A_1C_1| \sin\gamma : |B_1D_1| \sin\delta, \\ |WA_1| : |WC_1| &= \sin\gamma : \sin\alpha, \\ |WB_1| : |WD_1| &= \sin\delta : \sin\beta. \end{aligned}$$

From analysis of similar triangles in the iterative process, it is easy to see that the limit point of the process satisfies the above distance relations. Therefore, W (defined at the beginning of this section as the second point of intersection of $CS(o_1, o_2)$ and $CS(o_1, o_4)$) is the limit point of the iterative process.

One more property expresses W as the image of a vertex of the first generation under the inversion in a triad circle of the second generation. Namely, we have the following

Theorem 15 (Inversive property of W)**.**

$$W = Inv_{o_1^{(2)}}(A_1) = Inv_{o_2^{(2)}}(B_1) = Inv_{o_3^{(2)}}(C_1) = Inv_{o_4^{(2)}}(D_1). \tag{9}$$

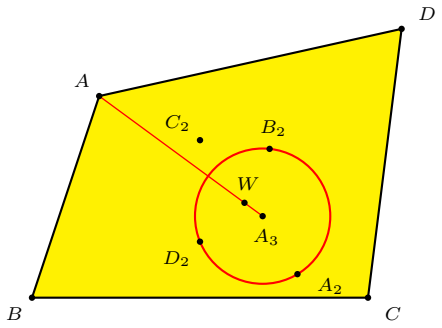

Figure 11. Inversive property of W

Proof. To prove the first equality, perform inversion in a circle centered at A_1. The image of a point under the inversion will be denoted by the same letter with a prime. The images of the circles of similitude $CS(o_1, o_2)$, $CS(o_4, o_1)$ and $CS(o_2, o_4)$ are

the perpendicular bisectors of the segments $A_2'B_2'$, $D_2'A_2'$ and $B_2'D_2'$ respectively. By Theorem 9, these perpendicular bisectors intersect in W'. Since W' is the circumcenter of $D_2'A_2'B_2'$, it follows that $\text{Inv}_{o_1^{(2)\prime}}(W') = A_1'$. Inverting back in the same circle centered at A_1, we obtain $\text{Inv}_{o_1^{(2)}}(W) = A_1$. The rest of the statements follow analogously. □

The fact that the inversions of each of the vertices in triad circles defined by the remaining three vertices coincide in one point was proved by Parry and Longuet-Higgins in [14].

Notice that the statement of Theorem 15 can be rephrased in a way that does not refer to the original quadrilateral, so that we can obtain a property of circumcenters of four triangles taking a special configuration on the plane. Recall that an inversion takes a pair of points which are inverses of each other with respect to a (different) circle into a pair of points which are inverses of each other with respect to the image of the circle, that is if $S = \text{Inv}_k(T)$, then $S' = \text{Inv}_{k'}(T')$, where $'$ denotes the image of a point (or a circle) under inversion in a given circle. Using this and property 2 of circles of similitude, we obtain the corollary below. In the statement, A, B, C, P, X, Y, Z, O play the role of $A_2', B_2', D_2', A_1, B_1', C_1', D_1', W_1'$ in Theorem 15.

Corollary 16. *Let P be a point on the plane of ABC. Let points O, X, Y and Z be the circumcenters of ABC, APB, BPC and CPA respectively.* Then

$$\textit{Inv}_{(ZOX)}(A) = \textit{Inv}_{(XOY)}(B) = \textit{Inv}_{(YOZ)}(C) = \textit{Inv}_{(XYZ)}(P). \qquad (10)$$

Furthermore,

$$Iso_{ZOX}(A) = Y, \quad Iso_{XOY}(B) = Z, \quad Iso_{YOZ}(C) = X.$$

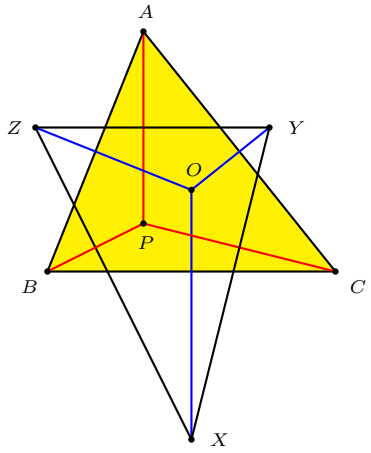

Figure 12. Corollary 16.

Combining the description of the reverse iterative process (Theorem 2) and the inversive property of W (Theorem 15), we obtain one more direct way of constructing W without having to refer to the iterative process:

Theorem 17. *Let A, B, C, D be four points in general position. Then*

$$W = \mathit{Inv}_{o_3} \circ Iso_{T_3}(A_1) = \mathit{Inv}_{o_4} \circ Iso_{T_4}(B_1) = \mathit{Inv}_{o_1} \circ Iso_{T_1}(C_1) = \mathit{Inv}_{o_2} \circ Iso_{T_2}(D_1),$$

*where o_i is the i*th *triad circle, and T_i is the i*th *triad triangle.*

This property suggests a surprising relation between inversion and isogonal conjugation.

Taking into account that the circumcenter and the orthocenter of a triangle are isogonal conjugates of each other, we obtain the following

Corollary 18. *W is the point at infinity if and only if the vertices of the quadrilateral form an orthocentric system.*

3.4. *W as the center of similarity for any pair of triad circles.* To show that W is the center of spiral similarity for any pair of triad circles (of possibly different generations), we first need to prove Lemmas 19—21 below.

The following lemma shows that given three points on a circle — two fixed and one variable — the locus of the joint points of the spiral similarities taking one fixed point into the other applied to the variable point is a line.

Lemma 19. *Let $M, N \in o$ and $W \notin o$. For every point $L \in o$, define*

$$J := (MWL) \cap NL.$$

The locus of points J is a straight line going through W.

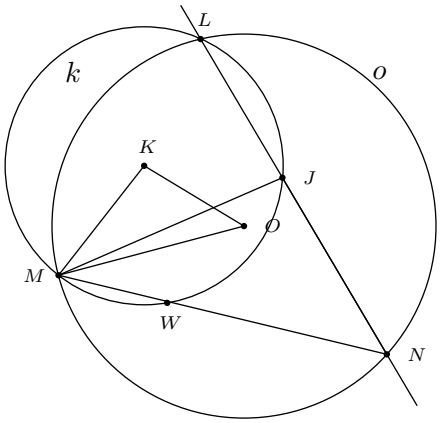

Figure 13. Lemma 19.

Proof. For each point $L \in o$, let K be the center of the circle $k := (MWL)$. The locus of centers of the circles k is the perpendicular bisector of the segment MW. Since $M \in o \cap k$, there is a spiral similarity centered at M with joint point L that takes k into o. This spiral similarity takes $K \mapsto O$ and $J \mapsto N$, where O is the center of o. Thus, $MOK \simeq MNJ$. Since M, O, K are fixed and the locus of K is a line (the perpendicular bisector), the locus of points J is also a line.

To show that the line goes through W, let $L = NW \cap o$. Then $J = W$. □

In the setup of the lemma above, let $H^W_{L,N}$ be the spiral similarity centered at W that takes L into N. Let M' be the image of M under this spiral similarity. Then J is the joint point for the spiral similarity taking $L \mapsto N$ and $M \mapsto M'$.

The following two results are used for proving that W lies on the circle of similitude of o_3 and $o_1^{(2)}$.

Lemma 20. *Let AC, ZX be two distinct chords of a circle o, and W be the center of spiral similarity taking ZX into AC. Let $H^W_{B,C}$ be the spiral similarity centered at W that takes a point $B \in o$ into C. Then $H^W_{B,C}(Z) \in o$.*

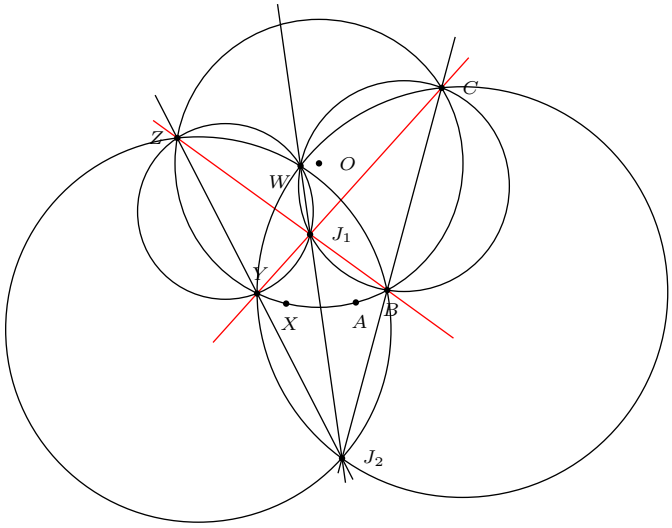

Figure 14. Lemma 20.

Proof. Let l be the locus of the joint points corresponding to $M = Z$, $N = C$ in Lemma 19. Let J_1 be the joint point corresponding to $L = B$. Then $J_1, W \in l$.

Let J_2 be the joint point corresponding to $M = C$, $N = Z$ and $L = B$ in Lemma 19.

Let $Y = J_2C \cap J_1Z$. By properties of spiral similarity, $Y = H^W_{B,C}(Z)$.

Notice that by definition of J_1, points J_1, B, C are on a line. Similarly, by definition of J_2, points J_2, B, Z are on a line as well. By definition of Y, points Y, J_2, C are on a line, as are points Z, Y, J_1. The intersections of these four lines form a complete quadrilateral. By Miquel's theorem, the circumcircles of the triangles $BJ_1Z,\ BJ_2C,\ J_2YZ,\ CJ_1Y$ have a common point, the Miquel point for the complete quadrilateral. By definitions of J_1 and J_2 , $(BJ_2C) \cap (BZJ_1) = \{B, W\}$. Thus, the Miquel point is either B or W. It is easy to see that B can not be the Miquel point (if $B \neq C, Z$). Thus, W is the Miquel point of the complete quadrilateral. This implies that (YCJ_1), (YZJ_2) both go through W.

Consider the circles $k_1 = (ZWJ_2Y)$ and $k_2 = (CWJ_2B)$. Then $RA(k_1, k_2) = l$. Since $ZY \cap BC = J_1 \in l = RA(k_1, k_2)$, by property 7 in section 3.1, points Z, Y, B, C are on a circle. Thus, $Y \in o$. □

Remark. Notice that in the proof of the Lemma above there are three spiral similarities centered at W that take each of the sides of XYZ into the corresponding side of CBA. We will call such a construction a *cross-spiral* and say that the two triangles are obtained from each other via a cross-spiral. [6]

Lemma 21. *Let PQ be a chord on a circle o centered at O. If $W \notin (POQ)$, there is a spiral similarity centered at W that takes PQ into another chord of the circle o.*

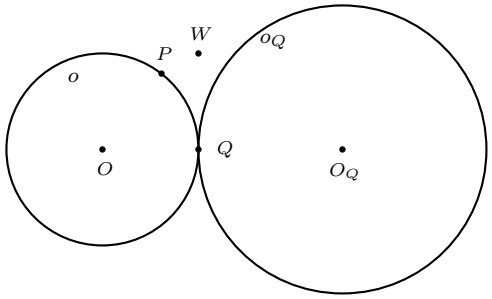

Figure 15. Proof of Lemma 21.

Proof. Let $H^W_{P,P'}$ be the spiral similarity centered at W that takes P into another point P' on circle o. As P' traces out o, the images $H^W_{P,P'}(Q)$ of Q trace out another circle, o_Q. To see this, consider the associated spiral similarity and notice that $H^W_{P,Q}(P') = Q'$. Since P' traces out o, $H^W_{P,Q}(o) = o_Q$. Since $Q = H^W_{P,P}(Q) \in o_Q$, it follows that $Q \in o \cap o_Q$.

Suppose that o and o_Q are tangent at Q. From $H_{P,Q}(o) = o_Q$ it follows that the joint point is Q, and therefore the quadrilateral $PQWO$ must be cyclic. Since $W \notin (POQ)$, this can not be the case. Thus, the intersection $o \cap o_Q$ contains two points, Q and Q'. This implies that there is a unique chord, $P'Q'$, of o to which PQ can be taken by a spiral similarity centered at W. □

Theorem 22. $W \in CS(o_3, o_1^{(2)})$.

Proof. We've shown previously that W is on all six circles of similitude of $A_1B_1C_1D_1$. Since W has the property that

$$H^W_{C_1,B_2}:\ C_1 \mapsto B_2, D_1 \mapsto A_2,$$
$$H^W_{B_1,A_2}:\ B_1 \mapsto A_2, C_1 \mapsto D_2,$$

it follows that

$$H^W_{B_2,C_1} H^W_{B_1,A_2}(B_1) = H^W_{B_2,C_1}(A_2) = D_1.$$

[6] Clearly, the sides of any triangle can be taken into the sides of any other triangle by three spiral similarities. The special property of the cross-spiral is that the centers of all three spiral similarities are at the same point.

Since the spiral similarities centered at W commute, it follows that

$$H^W_{B_2,C_1}H^W_{B_1,A_2}(B_2) = H^W_{B_1,A_2}H^W_{B_2,C_1}(B_2) = H^W_{B_1A_2}(C_1) = D_2.$$

This means that there is a spiral similarity centered at W that takes B_1D_1 into B_2D_2. Therefore, $B_1C_1D_1$ and $D_2A_2B_2$ are related by a cross-spiral centered at W.

We now show that there is a cross-spiral that takes $D_2A_2B_2$ into another triangle, XYZ, with vertices on the same circle, $o_1^{(2)} = (D_2A_2B_2)$. This will imply that there is a spiral similarity centered at W that takes $B_1C_1D_1$ into XYZ. This, in turn, implies that W is a center of spiral similarity taking o_3 into $o_1^{(2)}$.

Assume that $W \in (B_2A_3D_2)$. Since inversion in $(D_2A_2B_2)$ takes W into A_1 and $(B_2A_3D_2)$ into B_2D_2, it follows that $A_1 \in B_2D_2$. This can not be the case for a nondegenerate quadrilateral. Thus, $W \in (B_2A_3D_2)$.

By Lemma 21, there is a spiral similarity centered at W that takes the chord B_2D_2 into another chord, XZ, of the circle $(D_2A_2B_2)$. Thus, there is a spiral similarity taking B_2D_2 into XZ and centered at W.

By Lemma 20, there is a point $Y \in o_1^{(2)}$ such that XYZ and $B_2A_2D_2$ are related by a cross-spiral centered at W. (See also the remark after Lemma 20).

By composing the two cross-spirals, we conclude that $XYZ \sim D_1C_1B_1$. Since $(XYZ) = o_1^{(2)}$ and $(D_1C_1B_1) = o_3$, it follows that $W \in CS(o_1^{(2)}, o_3)$. □

Corollary 23. *$W \in CS(o_i^{(1)}, o_j^{(k)})$ for any i, j, k.*

Proof. Since there is a spiral similarity centered at W that takes A_1B_1 into C_2D_2, Theorem 22 implies that $W \in CS(o_1, o_4^{(2)})$. Since $W \in CS(o_1, o_2)$, it follows that $W \in CS(o_4^{(2)}, o_2)$. Since W is on two circles of similitude for the second generation, it follows that it is on all four. Furthermore, we can apply Theorem 22 to the triad circles of the second and third generation to show that W is also on all four circles of similitude of the third generation.

Finally, a simple induction argument shows that $W \in CS(o_j^{(1)}, o_i^{(k)})$. Assuming $W \in CS(o_j^{(1)}, o_i^{(k-1)})$, Theorem 22 implies that $W \in CS(o_i^{(k-1)}, o_i^{(k)})$. Thus, $W \in CS(o_j^{(1)}, o_i^{(k)})$. □

Using this, we can show that W lies on all the circles of similitude:

Theorem 24. *$W \in CS(o_i^{(k)}, o_j^{(l)})$ for all $i, j \in \{1, 2, 3, 4\}$ and any k, l.*

Recall that the *complete quadrangle* is the configuration of 6 lines going through all possible pairs of 4 given vertices.

Theorem 25. *(Inversion in a circle centered at W) Consider the complete quadrangle determined by a nondegenerate quadrilateral. Inversion in W transforms*

- *6 lines of the complete quadrilateral into the 6 circles of similitude of the triad circles of the image quadrilateral;*
- *6 circles of similitude of the triad circles into the 6 lines of the image quadrangle.*

Proof. Observe that the 6 lines of the quadrangle are the radical axes of the triad circles taken in pairs. Since W belongs to all the circles of similitude of triad circles, by property 5 in section 3.1, inversion in a circle centered in W takes radical axes into the circles of similitude. This implies the statement. □

4. Pedal properties

4.1. *Pedal of W with respect to the original quadrilateral.* Since W has a distance property similar to that of the isodynamic points of a triangle (see Corollary 14), it is interesting to investigate whether the analogy between these two points extends to pedal properties. In this section we show that the pedal quadrilateral of W with respect to $A_1B_1C_1D_1$ (and, more generally, with respect to any $Q^{(n)}$) is a nondegenerate parallelogram. Moreover, W is the unique point whose pedal has such a property. These statements rely on the fact that W lies on the intersection of two circles of similitude, $CS(o_1, o_3)$ and $CS(o_2, o_4)$.

First, consider the pedal of a point that lies on one of these circles of similitude.

Lemma 26. *Let $P_aP_bP_cP_d$ be the pedal quadrilateral of P with respect to $ABCD_1$. Then*

- *$P_aP_bP_cP_d$ is a trapezoid with $P_aP_d||P_bP_c$ if and only if $P \in CS(o_2, o_4)$;*
- *$P_aP_bP_cP_d$ is a trapezoid with $P_aP_b||P_cP_d$ if and only if $P \in CS(o_1, o_3)$.*

Proof. Assume that $P \in CS(o_2, o_4)$. Let $K = AC \cap P_aP_d$ and $L = AC \cap P_bP_c$. We will show that $\angle AKP_d + \angle CLP_c = \pi$, which implies $P_aP_d||P_bP_c$.

Let $\theta = \angle APP_a$. Since AP_aPP_d is cyclic, $\angle AP_dP_a = \theta$. Then

$$\angle AKP_d = \pi - \alpha_1 - \theta. \tag{11}$$

On the other hand, $\angle CLP_c = \pi - \gamma_2 - \angle LP_cC$. Since PP_bCP_c is cyclic, it follows that $\angle LP_cC = \angle P_bPC$.

We now find the latter angle. Since $P \in CS(o_2, o_4)$, by property (5) of the circle of similitude (see §3.1), it follows that $\angle APC = \pi + \delta + \beta$. Since P_aPP_bB is cyclic, $\angle P_aPP_b = \pi - \beta$. Therefore, $\angle P_bPC = \delta - \theta$. This implies that

$$\angle CLP_c = \pi - \gamma_2 - \delta + \theta. \tag{12}$$

Adding (11) and (12), we obtain $\angle AKP_d + \angle CLP_c = \pi$.

Reasoning backwards, it is easy to see that $P_aP_d||P_bP_c$ implies that $P \in CS(o_2, o_4)$. □

Let S be the second point of intersection of $CS(o_1, o_3)$ and $CS(o_2, o_4)$, so that $CS(o_1, o_3) \cap CS(o_2, o_4) = \{W, S\}$. The Lemma above implies that the pedal quadrilateral of a point is a parallelogram if and only if this point is either W or S.

Theorem 27. *The pedal quadrilateral of W is a parallelogram whose angles equal to those of the Varignon parallelogram.*

Proof. Since $W \in CS(o_1, o_2) \cap CS(o_3, o_4)$, property (5) of the circle of similitude implies that

$$\begin{aligned} \angle AWB &= \angle ACB + \angle ADB = \gamma_1 + \delta_2, \\ \angle CWD &= \angle CAD + \angle CBD = \alpha_1 + \beta_2, \end{aligned}$$

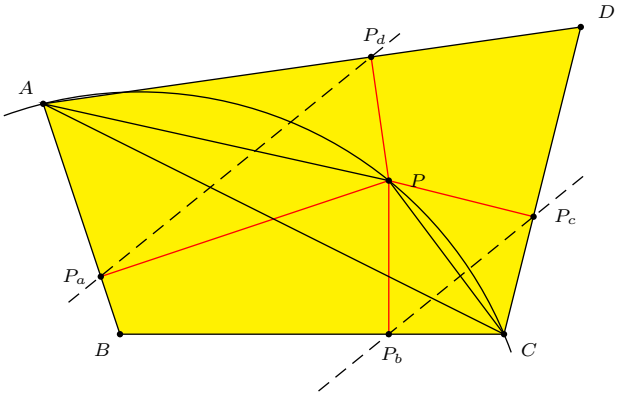

Figure 16. The pedal quadrilateral of a point on $CS(o_2, o_4)$ has two parallel sides.

where $\alpha_i, \beta_i, \gamma_i, \delta_i$ are the angles between the quadrilateral's sides and diagonals, as before (see Figure 3). Let $\angle AWW_a = x$ and $\angle W_cWC = y$. Since the quadrilaterals W_aWW_dA and W_cWW_bC are cyclic, $\angle W_aW_dA = x$ and $\angle W_cW_bC = y$. Therefore,

$$\angle W_aW_bB = \angle AWB - \angle AWW_a = \gamma_1 + \delta_2 - x,$$
$$\angle W_cW_dD = \angle CWD - \angle W_cWC = \alpha_1 + \beta_2 - y.$$

Finding supplements and adding, we obtain

$$\begin{aligned}\angle W_aW_dW_c + \angle W_aW_bW_c &= (\pi - x - \alpha_1 - \beta_2 + y) + (\pi - y - \gamma_1 - \delta_2 + x)\\ &= 2\pi - \alpha_1 - \beta_2 - \gamma_1 - \delta_2\\ &= 2\pi - (2\pi - 2\angle AIC) = 2\angle AIC,\end{aligned}$$

where $\angle AIC$ is the angle formed by the intersection of the diagonals. Thus, $W_aW_bW_cW_d$ is a parallelogram with the same angles as those of the Varignon parallelogram $M_aM_BM_bM_c$, where M_x is the midpoint of side x, for any $x \in \{a, b, c, d\}$. □

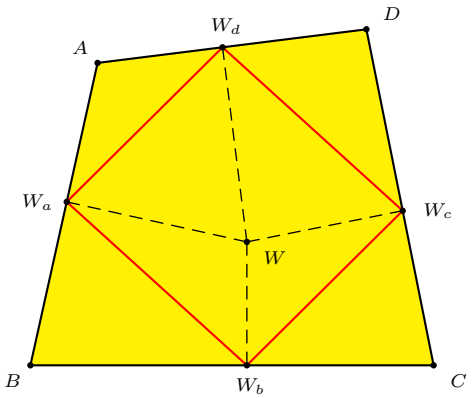

Figure 17. The pedal parallelogram of W.

It is interesting to note the following

Corollary 28. *The pedal of W with respect to the self-intersecting quadrilateral $ACBD$ (whose sides are the two diagonals and two opposite sides of the original quadrilateral) is also a parallelogram.*

The Theorem above also implies that the pedal of W is nondegenerate. (We will see later that the pedal of S degenerates to four points lying on a straight line). While examples show that the pedal of W and the Varignon parallelogram have different ratios of sides (and, therefore, are not similar in general), it is easy to see that they coincide in the case of a cyclic quadrilateral:

Corollary 29. *The Varignon parallelogram $M_aM_bM_cM_d$ is a pedal parallelogram of a point if and only if the quadrilateral is cyclic and the point is the circumcenter. In this case, $M_aM_bM_cM_d = W_aW_bW_cW_d$.*

Theorem 30. *The pedal quadrilateral of a point with respect to quadrilateral $ABCD$ is a nondegenerate parallelogram if and only if this point is W.*

Proof. By Lemma 26, if $P \in CS(o_1, o_3) \cap CS(o_2, o_4)$, then both pairs of opposite sides of the pedal quadrilateral $P_aP_bP_cP_d$ are parallel.

Assume that the pedal quadrilateral $P_aP_bP_cP_d$ of P is a nondegenerate parallelogram. Since P_dAP_aP is a cyclic quadrilateral,

$$\begin{aligned} |P_aP_d| &= \frac{|PA|}{2\sin\alpha}, \\ |P_bP_c| &= \frac{|PC|}{2\sin\gamma}. \end{aligned}$$

The assumption $|P_aP_d| = |P_bP_c$— implies that $|PA| : |PC| = \sin\gamma : \sin\alpha$. Similarly, $|P_aP_b| = |P_cP_d|$ implies $|PB| : |PD| = \sin\delta : \sin\beta$, so that P must be on the Apollonian circle with respect to A, C with ratio $\sin\gamma : \sin\alpha$ and on the Apollonian circle with respect to B, D with ratio $\sin\delta : \sin\beta$. These Apollonian circles are easily shown to be $CS(o_1^{(0)}, o_3^{(0)})$ and $CS(o_2^{(0)}, o_4^{(0)})$, the circles of similitude of the previous generation quadrilateral. One of the intersections of these two circles of similitude is W. Let Y be the other point of intersection. Computing the ratios of distances from Y to the vertices, one can show that the pedal of Y is an isosceles trapezoid. That is, instead of two pairs of equal opposite sides, it has one pair of equal opposite sides and two equal diagonals. This, in particular, means that Y does not lie on $CS(o_1, o_3) \cap CS(o_2, o_4)$. It follows that W is the only point for which the pedal is a nondegenerate parallelogram. □

Remark. Note that another interesting pedal property of a quadrilateral was proved by Lawlor in [9, 10]. For each vertex, consider its pedal triangle with respect to the triangle formed by the remaining vertices. The four resulting pedal triangles are directly similar to each other. Moreover, the center of similarity is the so-called *nine-circle point*, denoted by H in Scimemi's paper [17].

4.2. *Simson line of a quadrilateral.* Recall that for any point on the circumcircle of a triangle, the feet of the perpendiculars dropped from the point to the triangle's sides lie on a line, called the *Simson line* corresponding to the point (see Figure

18). Remarkably, in the case of a quadrilateral, Lemma 26 and Theorem 30 imply that there exists a unique point for which the feet of the perpendiculars dropped to the sides are on a line (see Theorem 31 below).

In the case of a noncyclic quadrilateral, this point turns out to be the second point of intersection of $CS(o_1, o_3)$ and $CS(o_2, o_4)$, which we denote by S. For a cyclic quadrilateral $ABCD$ with circumcenter O, even though all triad circles coincide, one can view the circles (BOD) and (AOC) as the replacements of $CS(o_1, o_3)$ and $CS(o_2, o_4)$ respectively. The second point of intersection of these two circles, $S \in (BOD) \cap (AOC)$, $S \neq W$ also has the property that the feet of the perpendiculars to the sides lie on a line. Similarly to the noncyclic case (see Lemma 26), one can start by showing that the pedal quadrilateral of a point is a trapezoid if and only if the point lies on one of the two circles, (BOD) or (AOC).

In analogy with the case of a triangle, we will call the line $S_aS_bS_cS_d$ the *Simson line* and S the *Simson point of a quadrilateral*, see Fig. 18.

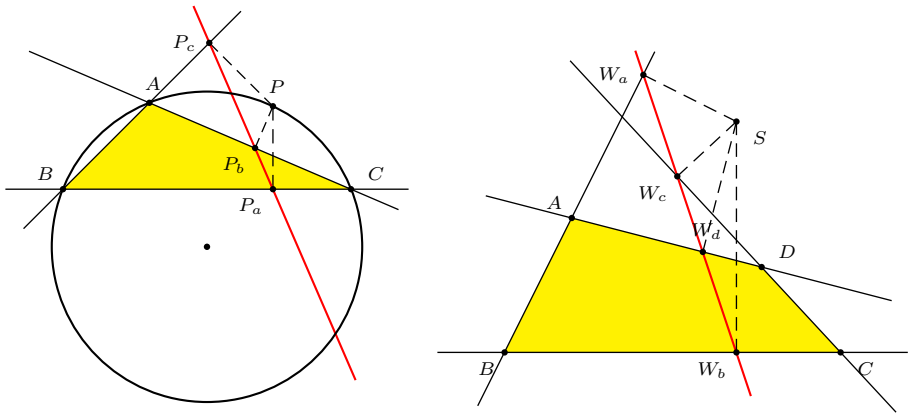

Figure 18. A Simson line for a triangle and the Simson line of a quadrilateral.

Theorem 31. *(The Simson line of a quadrilateral) The feet of the perpendiculars dropped to the sides from a point on the plane of a quadrilateral lie on a straight line if and only if this point is the Simson point.*

Unlike in the case of a triangle, where every point on the circumcircle produces a Simson line, the Simson line of a quadrilateral is unique. When the original quadrilateral is a trapezoid, the Simson point is the point of intersection of the two nonparallel sides. In particular, when the original quadrilateral is a parallelogram, the Simson point is point at infinity. The existence of this point is also mentioned in [6].

Recall that all circles of similitude intersect at W. The remaining $\binom{6}{2} = 15$ intersections of pairs of circles of similitude are the Simson points with respect to the $\binom{6}{4} = 15$ quadrilaterals obtained by choosing 4 out of the lines forming the complete quadrangle. Thus for each of the 15 quadrilaterals associated to a complete quadrangle there is a Simson point lying on a pair of circles of similitude.

4.3. *Isogonal conjugation with respect to a quadrilateral.* Recall that the isogonal conjugate of the first isodynamic point of a triangle is the Fermat point, *i.e.*, the point minimizing the sum of the distances to vertices of the triangle. Continuing to explore the analogy of W with the isodynamic point, we will now define isogonal conjugation with respect to a quadrilateral and study the properties of W and S with respect to this operation.

Let P be a point on the plane of $ABCD$. Let l_A, l_B, l_C, l_D be the reflections of the lines AP, BP, CP, DP in the bisectors of $\angle A$, $\angle B$, $\angle C$ and $\angle D$ respectively.

Definition. Let $P_A = l_A \cap l_B$, $P_B = l_B \cap l_C$, $P_C = l_C \cap l_D$, $P_D = l_D \cap l_A$. The quadrilateral $P_A P_B P_C P_D$ will be called the *isogonal conjugate of* P with respect to $ABCD$ and denoted by $Iso_{ABCD}(P)$.

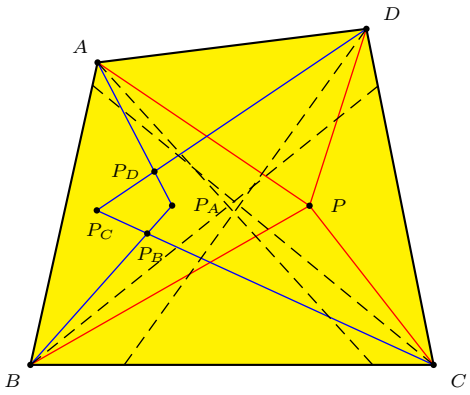

Figure 19. Isogonal conjugation with respect to a quadrilateral

The following Lemma relates the isogonal conjugate and pedal quadrilaterals of a given point:

Lemma 32. *The sides of the isogonal conjugate quadrilateral and the pedal quadrilateral of a given point are perpendicular to each other.*

Proof. Let b_A be the bisector of the $\angle DAB$. Let $I = l_A \cap P_a P_d$ and $J = b_A \cap P_a P_d$. Since AP_aPP_d is cyclic, it follows that $\angle P_d AP = \angle P_d P_a P$. Since $PP_a \perp P_a A$, it follows that $AI \perp P_a P_d$. Therefore, $P_A P_D \perp P_a P_d$. The same proof works for the other sides, of course. □

The Lemma immediately implies the following properties of the isogonal conjugates of W and S:

Theorem 33. *The isogonal conjugate of W is a parallelogram. The isogonal conjugate of S is the degenerate quadrilateral whose four vertices coincide at infinity.*

The latter statement can be viewed as an analog of the following property of isogonal conjugation with respect to a triangle: the isogonal conjugate of any point on the circumcircle is the point at infinity.

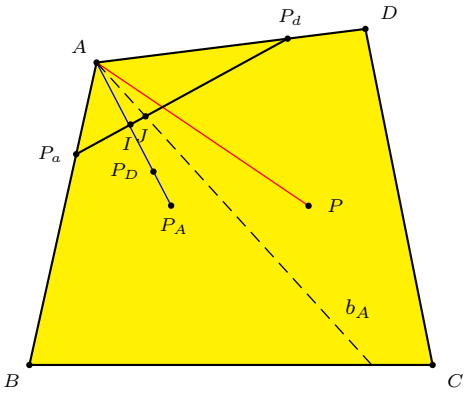

Figure 20. Lemma 32.

4.4. *Reconstruction of the quadrilateral.* The paper by Scimemi [17] has an extensive discussion of how one can reconstruct the quadrilateral from its central points. Here we just want to point out the following 3 simple constructions:

(1) Given W and its pedal parallelogram $W_aW_bW_cW_d$ with respect to $A_1B_1C_1D_1$, one can reconstruct $A_1B_1C_1D_1$ by drawing lines through W_a, W_b, W_c, W_d perpendicular to WW_a, WW_b, WW_c, WW_d respectively. The construction is actually simpler than reconstructing $A_1B_1C_1D_1$ from midpoints of sides *i.e.*, vertices of the Varignon parallelogram and the point of intersection of diagonals.

(2) Similarly, one can reconstruct the quadrilateral from the Simson point S and the four pedal points of S on the Simson line.

(3) Given three vertices A_1, B_1, C_1 and W, one can reconstruct D_1. Here is one way to do this. The given points determine the circles $o_2 = (A_1B_1C_1)$, $CS(o_2, o_1) = (A_1WB_1)$ and $CS(o_2, o_3) = (B_1WC_1)$. Given o_2 and $CS(o_2, o_1)$, we construct the center of o_1 as $A_2 = \text{Inv}_{CS(o_2,o_1)}(B_2)$ (see property 2 in the Preliminaries of Section 3). Similarly, $C_2 = \text{Inv}_{CS(o_2,o_3)}(B_2)$. Then D_1 is the second point of intersection of o_1 (the circle centered at A_2 and going through A_1, B_1) and o_3 (the circle centered at C_2 and going through B_1, C_1). Alternatively, one can use the property that $D_1 = \text{Iso}_{T_2} \circ \text{Inv}_{o_2}(W)$.

References

[1] H. F. Baker, *Principles of Geometry*, volume 4, Cambridge, 1925.

[2] D. Bennett, Dynamic geometry renews interest in an old problem, in *Geometry Turned On*, (ed. J. King), MAA Notes 41, 1997, pp.25–28.

[3] A. Bogomolny, Quadrilaterals formed by perpendicular bisectors, *Interactive Mathematics Miscellany and Puzzles*, `http://www.cut-the-knot.org/Curriculum/Geometry/PerpBisectQuadri.shtml`.

[4] H. S. M. Coxeter and S. L. Greitzer, *Geometry Revisited*, Washington, DC: Math. Assoc. Amer., 1967.

[5] D. Grinberg, Isogonal conjugation with respect to triangle, unpublished notes, `http://www.cip.ifi.lmu.de/~grinberg/Isogonal.zip`.

[6] R. A. Johnson, *Advanced Euclidean Geometry*, Dover Publications, Mineola, NY, 2007.
[7] J. King, Quadrilaterals formed by perpendicular bisectors, in *Geometry Turned On*, (ed. J. King), MAA Notes 41, 1997, pp.29–32.
[8] J. Langr, Problem E1050, *Amer. Math. Monthly*, 60 (1953) 551.
[9] J. K. Lawlor, Pedal triangles and pedal circles, *Math. Gazette*, 9 (1917) 127–130.
[10] J. K. Lawlor, Some properties relative to a tetrastigm, *Math Gazette*, 10 (1920) 135–139.
[11] A. De Majo, Sur un point remarquable du quadrangle, *Mathesis*, 63 (1953) 236–240.
[12] H. V. Mallison, Pedal circles and the quadrangle, *Math. Gazette*, 42 (1958) 17–20.
[13] E. H. Neville, Isoptic point of a quadrangle, *J. London Math. Soc.*, (1941) 173–174.
[14] C. F. Parry and M. S. Longuet-Higgins, (Reflections)^3, *Math. Gazette*, 59 (1975) 181–183.
[15] V. V. Prasolov, *Plane Geometry Problems*, vol. 1 (in Russian), 1991; Problem 6.31.
[16] V. V. Prasolov, *Problems in Plane and Solid Geometry*, vol. 1 (translated by D. Leites), available at `http://students.imsa.edu/~tliu/Math/planegeo.eps`.
[17] B. Scimemi, Central points of the complete quadrangle, *Milan. J. Math.*, 75 (2007) 333–356.
[18] G. C. Shephard, The perpendicular bisector construction, *Geom. Dedicata*, 56 (1995) 75–84.
[19] P. W. Wood, Points isogonally conjugate with respect to a triangle, *Math. Gazette*, 25 (1941) 266–272.
[20] Hyacinthos forum, message 6411, http://tech.dir.groups.yahoo.com/group/Hyacinthos/message/6411.

Olga Radko: Department of Mathematics, UCLA, Los Angeles, California 90095-1555, USA
E-mail address: `radko@math.ucla.edu`

Emmanuel Tsukerman: P. O. Box 16061, Stanford, Stanford University, Santa Clara, California 94309, USA
E-mail address: `emantsuk@stanford.edu`

Forum Geometricorum
Volume 12 (2012) 191–192.

FORUM GEOM
ISSN 1534-1178

A Highway from Heron to Brahmagupta

Albrecht Hess

Abstract. We give a simple derivation of Brahmagupta's area formula for a cyclic quadrilateral from Heron's formula for the area of a triangle.

Brahmagupta's formula

$$A = \frac{1}{4}\sqrt{(-a+b+c+d)(a-b+c+d)(a+b-c+d)(a+b+c-d)}$$

for the area of a cyclic quadrilateral is very similar to Heron's formula

$$\Delta = \frac{1}{4}\sqrt{(a+b+c)(-a+b+c)(a-b+c)(a+b-c)}$$

for the area of a triangle, which is itself a consequence of Brahmagupta's formula for $d = 0$. Although I have searched extensively ([1, §3], [2, §9], [3], [4, Theorem 3.22], [5, Theorem 109]), the following derivation of the area of a cyclic quadrilateral from Heron's formula seems to be unknown.

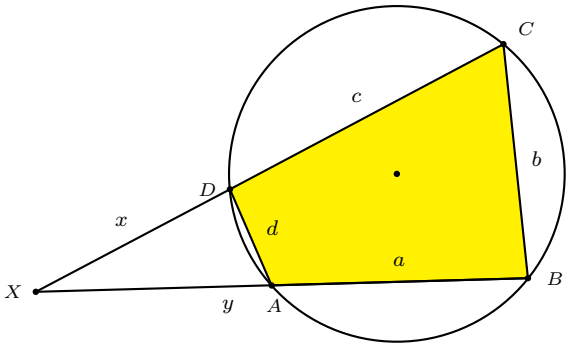

Figure 1

Let $ABCD$ be a cyclic quadrilateral with sides $AB = a$, $BC = b$, $CD = c$, $DA = d$. Brahmagupta's formula is obvious if both pairs of opposite sides are parallel. We may assume that AB and CD intersect at point X and that $XD = x$, $XB = y$. Let S_1, S_2, S_3, S_4 be the four factors under the radical in Heron's

Publication Date: June 6, 2012. Communicating Editor: Paul Yiu.

formula for the area of triangle XBC. Note that from the similarity of triangles XBC and XDA (with ratio λ),

$$\begin{aligned} 4A &= 4\Delta(XBC) - 4\Delta(XDA) \\ &= \sqrt{S_1S_2S_3S_4} - \sqrt{(\lambda S_1)(\lambda S_2)(\lambda S_3)(\lambda S_4)} \\ &= \sqrt{(S_1-\lambda S_1)(S_2-\lambda S_2)(S_3+\lambda S_3)(S_4+\lambda S_4)}. \end{aligned}$$

Upon simplification, x and y vanish in these factors:

$$\begin{aligned} S_1-\lambda S_1 &= (b+(c+x)+y)-(d+(y-a)+x) = a+b+c-d, \\ S_2-\lambda S_2 &= (-b+(c+x)+y)-(-d+(y-a)+x) = a-b+c+d, \\ S_3+\lambda S_3 &= (b-(c+x)+y)+(d-(y-a)+x) = a+b-c+d, \\ S_4+\lambda S_4 &= (b+(c+x)-y)+(d+(y-a)-x) = -a+b+c+d, \end{aligned}$$

and Brahmagupta's formula appears.

References

[1] C. A. Bretschneider, Trigonometrische Relationen zwischen den Seiten und Winkeln zweier beliebiger ebener oder sphärischer Dreiecke, *Archiv der Math.*, 2 (1842) 132–145.

[2] C. A. Bretschneider, Untersuchung der trigonometrischen Relationen des geradlinigen Viereckes, *Archiv der Math.*, 2 (1842) 225–261.

[3] J. L. Coolidge, A historically interesting formula for the area of a quadrilateral, *Amer. Math. Monthly*, 46 (1939) 345–347.

[4] H. S. M. Coxeter and S. L. Greitzer, *Geometry Revisited*, Math. Assoc. Amer. 1967.

[5] R. A. Johnson, *Advanced Euclidean Geometry*, Dover reprint, 2007.

Albrecht Hess: Deutsche Schule Madrid, Avenida Concha Espina 32, 28016 Madrid, Spain
E-mail address: albrecht.hess@gmail.com

Forum Geometricorum
Volume 12 (2012) 193–196.

FORUM GEOM
ISSN 1534-1178

Alhazen' s Circular Billiard Problem

Debdyuti Banerjee and Nikolaos Dergiades

Abstract. In this paper we give two simple geometric constructions of two versions of the famous Alhazen's circular billiard problem.

1. Introduction

The famous Alhazen problem [2, Problem 156] has to do with a circular billiard and there are two versions of the problem. The first case is to find at the edge of the circular billiard two points B, C such that a billiard ball moving from a given point A inside the circle of the billiard after reflection at B, C passes through the point A again (see Figure 1A). It is obvious that if O is the center of the circle and the points O, A, B, C are collinear then the problem is trivial.

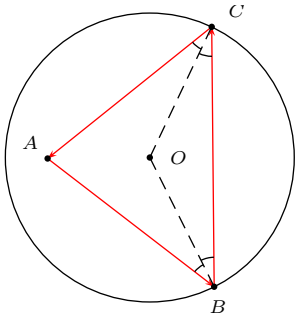

Figure 1A: The first case

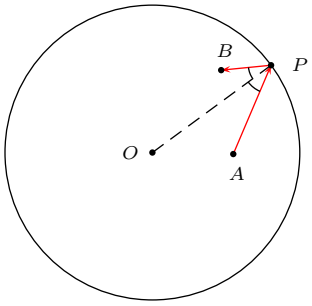

Figure 1B: The second case

The second case is, given two fixed points A and B inside the circle, to find a point P on the edge of the circular billiard such that the ball moving from A after one reflection at P will pass from B (see Figure 1B). It is obvious again that if the points A, B and O are on a diameter of the circle then the problem is trivial.

2. Alhazen' s problem 1

Given a point A inside a circle (O), to construct points B and C on the circle such that the reflection of AB at B passes through C and the reflection of BC at C passes through A.

Since the radii OB and OC are bisectors of angles B and C of triangle ABC, O is the incenter of ABC, which is isosceles with $AB = AC$ (see Figure 2). The

Publication Date: June 21, 2012. Communicating Editor: Paul Yiu.

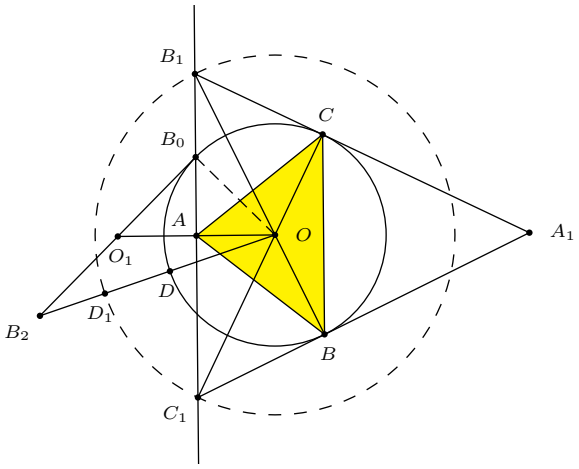

Figure 2.

points B and C are symmetric in OA. The tangents to the circle at B and C, together with the perpendicular to OA at A, bound the antipedal triangle $A_1B_1C_1$ of O (relative to ABC). Hence, O is the orthocenter of triangle $A_1B_1C_1$, and BB_1, CC_1 are altitudes of $A_1B_1C_1$ passing through O. Therefore, to construct the reflection points B and C, it is sufficient to construct B_1 and C_1.

Suppose the circle (O) has radius R and $OA = d$. If $OB_1 = x$, then from the similar right triangles B_1AO and B_1BC_1, we have

$$\frac{B_1A}{B_1O} = \frac{B_1B}{B_1C_1} \implies \frac{B_1A}{x} = \frac{x+R}{2B_1A}.$$

Since $B_1A^2 = x^2 - d^2$, this reduces to $x(x+R) = 2(x^2-d^2)$, or

$$x^2 - Rx - 2d^2 = 0. \tag{1}$$

This has a unique positive solution x. This leads to the following construction.
(i) Let B_0 be an intersection of the given circle with the perpendicular to OA at A, O_1 the symmetric of O in A, and B_2 the symmetric of B_0 in O_1. Note that $O_1B_0 = OB_0 = R$.
(ii) Construct the segment OB_2 to intersect the given circle at D, and let D_1 be the midpoint of DB_2.
(iii) Construct the circle with center O to pass through D_1. The intersections of this circle with the line AB_0 are the points B_1 and C_1.

To validate this, let $OD_1 = y$. Then $OB_2 = 2y - R$. Applying Apollonius' theorem to the median OO_1 of triangle OB_0B_2, we have

$$(2y-R)^2 + R^2 = 2(2d)^2 + 2R^2.$$

This leads to

$$y^2 - Ry - 2d^2 = 0. \tag{2}$$

Comparison of (1) and (2) gives $y = x$.

3. Alhazen's problem 2

Given two points A and B inside a circle (O), to construct a point P on the circle such that the reflection of AP at P passes through B.

It is well known that P cannot be constructed with ruler and compass only; see, for example, [3]. The analysis below leads to a simple construction with conics.

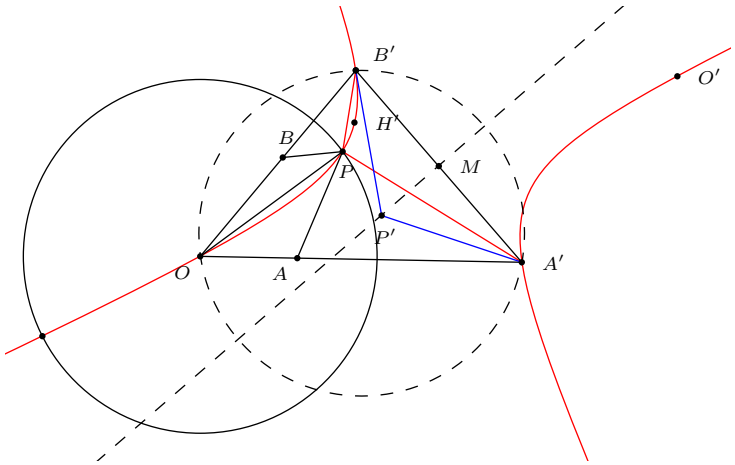

Figure 3

Let A' and B' be the inverses of A and B in the circle (O). Since $OA \cdot OA' = OP^2$, the triangles $PA'O$ and APO are similar, and $\angle PA'O = \angle APO$. Similarly, $\angle PB'O = \angle BPO$. Since $\angle APO = \angle BPO$, we have $\angle PA'O = \angle PB'O$. Consider the reflections of PA' and PB' respectively in the bisectors of angles A' and B' of triangle $OA'B'$. These reflection lines intersect at the isogonal conjugate P' of P (in triangle $OA'B'$). Note that $\angle P'A'B' = \angle PA'O = \angle PB'O = \angle P'B'A'$. Therefore, P' is a point on the perpendicular bisector of $A'B'$ (which contains the circumcenter center of $O'A'B'$). It follows that P lies on the isogonal conjugate of the perpendicular bisector of $A'B'$. This is a rectangular circum-hyperbola of triangle $OA'B'$, whose center is the midpoint of $A'B'$. It also contains the orthocenter of the triangle. This leads to the following construction of the point P.

(i) Construct the orthocenter H' of triangle $OA'B'$ and complete the parallelogram $OA'O'B'$.

(ii) The point P can be constructed as an intersection of the given circle (O) with the conic (rectangular hyperbola) containing O, A', B', H' and O'.

We conclude with two special cases when P can be constructed easily with ruler and compass.

3.1. *Special case: A and B on a diameter.* If the points A, B, O are collinear, then the triangle $OA'B'$ degenerates into a line. Let O_1 be the harmonic conjugate of O relative to AB; see Figure 4. The point P lies on the circle with diameter OO_1 ([1]).

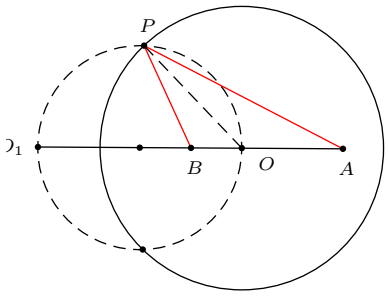

Figure 4

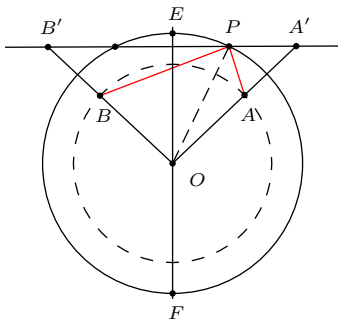

Figure 5

3.2. *Special case:* $OA = OB$. If $OA = OB = d$, then $OA'B'$ is isosceles and the rectangular circum-hyperbola degenerates into a pair of perpendicular lines, the perpendicular bisector of AB and the line $A'B'$. The first line gives the endpoints E and F of the diameter perpendicular to AB. The second line $A'B'$ intersects the circle (O) at two real points (solution to Alhazen's problem) if and only if $\angle AOB < 2\arccos\frac{d}{R}$ (see Figure 5).

References

[1] F. Bellot, Hyacinthos message 20974, April 11, 2012.
[2] F. G.-M., *Exercices de Géométrie*, 6th ed., 1920; Gabay reprint, Paris, 1991.
[3] P. M. Neumann, Reflections on reflection in spherical mirror, *Amer. Math. Monthly*, 105 (1998) 523–528.

Debdyuti Banerjee: 16/1/C Goala Para Lane, Chatra, Serampore, Hooghly, West Bengal 712204, India
E-mail address: chandana.snbv@gmail.com

Nikolaos Dergiades: I. Zanna 27, Thessaloniki 54643, Greece
E-mail address: ndergiades@yahoo.gr

Forum Geometricorum
Volume 12 (2012) 197–209.

FORUM GEOM
ISSN 1534-1178

Non-Euclidean Versions of Some Classical Triangle Inequalities

Dragutin Svrtan and Darko Veljan

Abstract. In this paper we recall with short proofs of some classical triangle inequalities, and prove corresponding non-Euclidean, *i.e.*, spherical and hyperbolic versions of these inequalities. Among them are the well known Euler's inequality, Rouché's inequality (also called "the fundamental triangle inequality"), Finsler–Hadwiger's inequality, isoperimetric inequality and others.

1. Introduction

As it is well known, the Euclid's Fifth Postulate (through any point in a plane outside of a given line there is only one line parallel to that line) has many equivalent formulations. Recall some of them: sum of the angles of a triangle is π (or 180°), there are similar (non-congruent) triangles, there is the area function (with usual properties), every triangle has unique circumcircle, Pythagoras' theorem and its equivalent theorems such as the law of cosines, the law of sines, Heron's formula and many more.

The negations of the Fifth Postulate lead to spherical and hyperbolical geometries. So, negations of some equalities characteristic for the Euclidean geometry lead to inequalities specific for either spherical or hyperbolic geometry. For example, for a triangle in the Euclidean plane we have the law of cosines

$$c^2 = a^2 + b^2 - 2ab\cos C,$$

where we stick with standard notations (that is a, b and c are the side lengths and $A,\ B$ and C are the angles opposite, respectively to the sides a, b and c).

It can be proved that the following Pythagoras' inequalities hold. In spherical geometry one has the inequality

$$c^2 < a^2 + b^2 - 2ab\cos C,$$

and in the hyperbolic geometry the opposite inequality

$$c^2 > a^2 + b^2 - 2ab\cos C.$$

In fact, in the hyperbolic case we have

$$a^2 + b^2 - 2ab\cos C < c^2 < a^2 + b^2 + 2ab\cos(A + B).$$

See [13] for details.

Publication Date: June 27, 2012. Communicating Editor: Paul Yiu.

On the other hand, there are plenty of interesting inequalities in (ordinary or Euclidean) triangle geometry relating various triangle elements. In this paper we prove some of their counterparts in non-Euclidean cases.

Let us fix (mostly standard) notations. For a given triangle $\triangle ABC$, let a, b, c denote the side lengths (a opposite to the vertex A, etc.), A, B, C the corresponding angles, $2s = a+b+c$ the perimeter, S its area, R the circumradius, r the inradius, and r_a, r_b, r_c the radii of excircles.

We use the symbols of cyclic sums and products such as:

$$\begin{aligned}\sum f(a) &= f(a)+f(b)+f(c),\\ \sum f(A) &= f(A)+f(B)+f(C),\\ \sum f(a,b) &= f(a,b)+f(b,c)+f(c,a),\\ \prod f(a) &= f(a)f(b)f(c),\\ \prod f(x) &= f(x)f(y)f(z).\end{aligned}$$

2. Euler's inequality

In 1765, Euler proved that the triangle's circumradius R is at least twice as big as its inradius r, *i.e.*,

$$R \geq 2r,$$

with equality if and only if the triangle is equilateral.Here is a short proof. $R \geq 2r \Leftrightarrow \frac{abc}{4S} \geq \frac{2S}{s} \Leftrightarrow sabc \geq 8S^2 = 8s\underbrace{(s-a)}_{=x}\underbrace{(s-b)}_{=y}\underbrace{(s-c)}_{=z} \Leftrightarrow \prod(s-x) \geq 8\prod x \Leftrightarrow s\sum xy - \prod x \geq 8\prod x \Leftrightarrow \sum x \cdot \sum xy \geq 9\prod x \Leftrightarrow \sum x^2y \geq 6\prod x \overset{A-G}{\Longleftrightarrow} \sum x^2y \geq 6(\prod x^2y)^{\frac{1}{6}} = 6\prod x.$ [1] The equality case is clear.

The inequality $8S^2 \leq sabc$ (equivalent to Euler's) can also be easily obtained as a consequence (via $A-G$) of the "isoperimetric triangle inequality":

$$S \leq \frac{\sqrt{3}}{4}(abc)^{\frac{2}{3}},$$

which we shall prove in §4.

The Euler inequality has been improved and generalized (*e.g.*, for simplices) many times. A recent and so far the best improvement of Euler's inequality is given by (see [11], [14]) (and it improves [17]):

$$\frac{R}{r} \geq \frac{abc+a^3+b^3+c^3}{2abc} \geq \frac{a}{b}+\frac{b}{c}+\frac{c}{a}-1 \geq \frac{2}{3}\left(\frac{a}{b}+\frac{b}{c}+\frac{c}{a}\right) \geq 2.$$

Now we turn to the non-Euclidean versions of Euler's inequality. Let k be the (constant) curvature of the hyperbolic plane in which a hyperbolic triangle $\triangle ABC$ sits. Let $\delta = \pi - (A+B+C)$ be the triangle's defect. The area of the hyperbolic triangle is given by $S = k^2\delta$.

[1] Yet another way to prove the last inequality: $x^2y + yz^2 = y(x^2+z^2) \geq 2xyz$, and add such three similar inequalities.

Theorem 1 (Hyperbolic Euler's inequality)**.** *Suppose a hyperbolic triangle has a circumcircle and let R be its radius. Let r be the radius of the triangle's incircle. Then*

$$\tanh\frac{R}{k} \geq 2\tanh\frac{r}{k}. \tag{1}$$

The equality is achieved for an equilateral triangle for any fixed defect.

Proof. Recall that the radius R of the circumcircle of a hyperbolic triangle (if it exists) is given by

$$\tanh\frac{R}{k} = \sqrt{\frac{\sin\frac{\delta}{2}}{\prod\sin(A+\frac{\delta}{2})}} = \frac{2\prod\sinh\frac{a}{2k}}{\sqrt{\sinh\frac{s}{k}\prod\sinh\frac{s-a}{k}}} \tag{2}$$

Also, the radius of the incircle (radius of the inscribed circle) r of the hyperbolic triangle is given by

$$\tanh\frac{r}{k} = \sqrt{\frac{\prod\sinh\frac{s-a}{k}}{\sinh\frac{s}{k}}} \tag{3}$$

See, *e.g.*, [5], [6], [7], [8], [9]. We can take $k=1$ in the above formulas. Then it is easy to see that (1) is equivalent to

$$\prod\sinh(s-a) \leq \prod\sinh\frac{a}{2},$$

or, by putting (as in the Euclidean case) $x=s-a$, $y=s-b$, $z=s-c$, to

$$\prod\sinh x \leq \prod\sinh\frac{s-x}{2}. \tag{4}$$

By writing $2x$ instead of x etc., (4) becomes

$$\prod\sinh 2x \leq \prod\sinh(s-x) = \prod\sinh(y+z).$$

Now by the double formula and addition formula for $\sinh$, after multiplications we get

$$8\prod\sinh x\cdot\prod\cosh x \leq \sum\sinh^2 x\ \sinh y\ \cosh y\ \cosh^2 z + 2\prod\sinh x\prod\cosh x.$$

Hence,

$$6\prod\sinh x\cdot\prod\cosh x \leq \sum\sinh^2 x\ \sinh y\ \cosh y\ \cosh^2 z. \tag{5}$$

However, (5) is simply the $A-G$ inequality for the six (nonnegative) numbers $\sinh x$, $\cosh x$, …, $\cosh z$. The equality case follows easily. This proves the hyperbolic Euler's inequality. □

Note also that (5) can be proved alternatively in the following way, using three times the simplest $A-G$ inequality:

$$\begin{aligned}
&\sinh^2 x\ \sinh y\ \cosh y\ \cosh^2 z + \cosh^2 x\ \sinh y\ \cosh y\ \sinh^2 z\\
&= \sinh y\ \cosh y[(\sinh x\ \cosh z)^2 + (\cosh x\ \sinh z)^2]\\
&\geq 2\sinh y\ \cosh y\ \sinh x\ \cosh z\ \cosh x\ \sinh z.
\end{aligned}$$

In the spherical case the analogous formula to (2) and (3) and similar reasoning to the previous proof boils down to proving analogous inequality to (4):

$$\prod \sin x \le \prod \sin \frac{s-x}{2} \tag{6}$$

But (6) follows in the same manner as above. So, we have the following.

Theorem 2 (Spherical Euler's inequality)**.** *The circumradius R and the inradius r of a spherical triangle on a sphere of radius ρ are related by*

$$\tan \frac{R}{\rho} \ge 2 \tan \frac{r}{\rho}. \tag{7}$$

The equality is achieved for an equilateral triangle for any fixed spherical excess $\varepsilon = (A+B+C) - \pi$.

Remark. At present, we do not know how to improve these non-Euclidean Euler inequalities in the sense of the previous discussions in the Euclidean case. It would also be of interest to have the non-Euclidean analogues of the Euler inequality $R \ge 3r$ for a tetrahedron (and simplices in higher dimensions).

3. Finsler–Hadwiger's inequality

In 1938, Finsler and Hadwiger [3] proved the following sharp upper bound for the area S in terms of side lengths a, b, c of a Euclidean triangle (improving upon Weitzenboeck's inequality):

$$\sum a^2 \ge \sum (b-c)^2 + 4\sqrt{3}S. \tag{8}$$

Here are two short proofs of (8). First proof ([10]): Start with the law of cosines $a^2 = b^2 + c^2 - 2bc\cos A$, or equivalently $a^2 = (b-c)^2 + 2bc(1-\cos A)$. From the area formula $2S = bc\sin A$, it then follows $a^2 = (b-c)^2 + 4S\tan\frac{A}{2}$. By adding all three such equalities we obtain

$$\sum a^2 = \sum (b-c)^2 + 4S \sum \tan \frac{A}{2}.$$

By applying Jensen's inequality to the sum $\sum \tan\frac{A}{2}$ (*i.e.*, using convexity of $\tan\frac{x}{2}$, $0 < x < \pi$) and the equality $A+B+C = \pi$, (8) follows at once.

Second proof ([8]): Put $x = s-a$, $y = s-b$, $z = s-c$. Then

$$\sum [a^2 - (b-c)^2] = 4\sum xy.$$

On the other hand, Heron's formula can be written as $4\sqrt{3}S = 4\sqrt{3\sum x \prod x}$. Then (8) is equivalent to $\sqrt{3\sum x \cdot \prod x} \le \sum xy$, and this is equivalent to $\sum x^2 yz \le \sum (xy)^2$, which in turn is equivalent to $\sum [x(y-z)]^2 \ge 0$, and this is obvious.

Remark. The seemingly weaker Weitzenboeck's inequality

$$\sum a^2 \ge 4\sqrt{3}S$$

is, in fact, equivalent to (8) (see [17]).

There are many ways to rewrite Finsler–Hadwiger's inequality. For example, since

$$\sum[a^2-(b-c)^2]=4r(r+4R),$$

it follows that (8) is equivalent to

$$r(r+4R)\geq\sqrt{3}S,$$

or, since $S=rs$, it is equivalent to

$$s\sqrt{3}\leq r+4R.$$

There are also many generalizations, improvements and strengthening of (8) (see [4]). Let us mention here only two recent ones. One is (see [1]):

$$\sum(b+c)\cdot\sum\frac{1}{b+c}\leq 10-\frac{r}{s^2}[s\sqrt{3}+2(r+4R)],$$

and the other one is (see [15])

$$\sum a^2\geq 4\sqrt{3}S+\sum(a-b)^2+\sum[\sqrt{a(b+c-a)}-\sqrt{b(c+a-b)}]^2.$$

The opposite inequality of (8) is (see [17]):

$$\sum a^2\leq 4\sqrt{3}S+3\sum(b-c)^2.$$

Note that all these inequalities are sharp in the sense that equalities hold if and only if the triangles are equilateral (regular).

For the hyperbolic case, we need first an analogue of the area formula $2S=bc\sin A$. It is not common in the literature, so for the reader's convenience we provide its short proof (see *e.g.*, [5]).

Lemma 3 (Cagnolli's first formula)**.** *The area $S=k^2\delta$ of a hyperbolic triangle ABC is given by*

$$\sin\frac{S}{2k^2}=\frac{\sinh\frac{a}{2k}\sinh\frac{b}{2k}\sin C}{\cosh\frac{c}{2k}} \tag{9}$$

Proof. From the well known second (or "polar") law of cosines in elementary hyperbolic geometry

$$\cosh\frac{a}{k}=\frac{\cos A+\cos B\cos C}{\sin B\sin C},$$

we get

$$\cosh\frac{a}{2k}=\sqrt{\frac{\sin\left(B+\frac{\delta}{2}\right)\sin\left(C+\frac{\delta}{2}\right)}{\sin B\sin C}},\ \ \sinh\frac{a}{2k}=\sqrt{\frac{\sin\left(\frac{\delta}{2}\right)\sin\left(A+\frac{\delta}{2}\right)}{\sin B\sin C}}. \tag{10}$$

By multiplying two expressions $\sinh\frac{a}{2k}\cdot\sinh\frac{b}{2k}$, and using (10) we get

$$\sinh\frac{a}{2k}\cdot\sinh\frac{b}{2k}=\frac{\sin\frac{\delta}{2}}{\sin C}\cosh\frac{c}{2k}.$$

This implies (9). □

Theorem 4 (Hyperbolic Finsler–Hadwiger's inequality)**.** *For a hyperbolic triangle ABC we have:*

$$\sum \cosh\frac{a}{k} \geq \sum \cosh\frac{b-c}{k} + 12\sin\frac{S}{2k^2}\prod \cosh\frac{a}{2k}\tan\frac{\pi-\delta}{6} \tag{11}$$

The equality in (11) *holds if and only if for any fixed defect δ, the triangle is equilateral.*

Proof. The idea is to try to mimic (as much as possible) the first proof of (8). Start with the hyperbolic law of cosines

$$\cosh\frac{a}{k} = \cosh\frac{b}{k}\cosh\frac{c}{k} - \sinh\frac{b}{k}\sinh\frac{c}{k}\cos A.$$

By adding and subtracting $\sinh\frac{b}{k}\sinh\frac{c}{k}$, we obtain

$$\begin{aligned}\cosh\frac{a}{k} &= \cosh\frac{b-c}{k} + \sinh\frac{b}{k}\sinh\frac{c}{k} - \sinh\frac{b}{k}\sinh\frac{c}{k}\cos A\\ &= \cosh\frac{b-c}{k} + \sinh\frac{b}{k}\sinh\frac{c}{k}\cdot 2\sin^2\frac{A}{2}\\ &= \cosh\frac{b-c}{k} + 4\sinh\frac{b}{2k}\sinh\frac{c}{2k}\cosh\frac{b}{2k}\cosh\frac{c}{2k}\cdot 2\sin^2\frac{A}{2}.\end{aligned}$$

By Cagnolli's formula (9), substitute here the part $\sinh\frac{b}{2k}\sinh\frac{c}{2k}$ to obtain

$$\cosh\frac{a}{k} = \cosh\frac{b-c}{k} + 4\cosh\frac{a}{2k}\cosh\frac{b}{2k}\cosh\frac{c}{2k}\sin\frac{S}{2k^2}\tan\frac{A}{2}. \tag{12}$$

Apply to both sides of (12) the cyclic sum operator $\sum$, and (again) apply Jensen's inequality (*i.e.*, convexity of $\tan\frac{x}{2}$):

$$\frac{1}{3}\sum\tan\frac{A}{2} \geq \tan\left(\frac{1}{3}\sum\frac{A}{2}\right) = \tan\frac{\pi-\delta}{6}.$$

This implies (11). The equality claim is also clear from the above argument. □

The corresponding spherical Finsler–Hadwiger inequality can be obtained mutatis mutandis from the hyperbolic case. The area S of a spherical triangle ABC on a sphere of radius ρ is given by $S = \rho^2\varepsilon$, where $\varepsilon = A + B + C - \pi$ is the triangle's excess. The spherical Cagnolli formula (like 9) reads as follows:

$$\sin\frac{S}{2\rho^2} = \frac{\sin\frac{a}{2\rho}\sin\frac{b}{2\rho}\sin C}{\cos\frac{c}{2\rho}}. \tag{13}$$

So, starting with the spherical law of cosines, using (13) and Jensen's inequality, one can show the following.

Theorem 5 (Spherical Finsler–Hadwiger's inequality)**.** *For a spherical triangle ABC on a sphere of radius ρ we have*

$$\sum\cos\frac{a}{\rho} \geq \sum\cos\frac{b-c}{\rho} + 12\sin\frac{S}{2\rho^2}\cos\frac{a}{2\rho}\cos\frac{b}{2\rho}\cos\frac{c}{2\rho}\tan\frac{\varepsilon-\pi}{6}. \tag{14}$$

The equality in (14) *holds if and only if for any fixed ε, the triangle is equilateral.*

Remark. Note that both hyperbolic and spherical inequalities (11) and (14) reduce to Finsler–Hadwiger's inequality (8) when $k \to \infty$ in (11), or $\rho \to \infty$ in (14). This is immediate from the power sum expansions of trigonometric or hyperbolic functions.

4. Isoperimetric triangle inequalities

In the Euclidean case, if we multiply all three area formulas, one of which is $S = \frac{1}{2}bc\sin A$, we obtain a symmetric formula for the triangle area

$$S^3 = \frac{1}{8}(abc)^2 \sin A \ \sin B \ \sin B. \tag{15}$$

By using the $A-G$ inequality and the concavity of the function $\sin x$ on $[0,\pi]$ (or, Jensen's inequality again), we have:

$$\begin{aligned}\sin A \ \sin B \ \sin C &\le \left(\frac{\sin A + \sin B + \sin C}{3}\right)^3 \\ &\le \left(\sin\frac{A+B+C}{3}\right)^3 = \sin^3\frac{\pi}{3} = \frac{3\sqrt{3}}{8}.\end{aligned}$$

This and (15) imply the so called "isoperimetric inequality" for a triangle:

$$S^3 \le \frac{3\sqrt{3}}{64}(abc)^2, \text{or in a more appropriate form}$$

$$S \le \frac{\sqrt{3}}{4}(abc)^{\frac{2}{3}}. \tag{16}$$

Inequality (16) and $A-G$ imply that $S \le \frac{\sqrt{3}}{36}(a+b+c)^2$, and this is why we call it the "isoperimetric inequality".

By Heron's formula we have $(4S)^2 = 2sd_3(a,b,c)$, where $2s = a+b+c$ and $d_3(a,b,c) := (a+b-c)(b+c-a)(c+a-b)$. By [11, Cor. 6.2], we have a sharp inequality

$$d_3(a,b,c) \le \frac{(2abc)^2}{a^3+b^3+c^3+abc}. \tag{17}$$

From Heron's formula and (17) it easily follows

$$S \le \frac{1}{2}abc\sqrt{\frac{a+b+c}{a^3+b^3+c^3+abc}}. \tag{18}$$

We claim that (18) improves the "isoperimetric inequality" (16). Namely, we claim

$$\frac{1}{2}abc\sqrt{\frac{a+b+c}{a^3+b^3+c^3+abc}} \le \frac{\sqrt{3}}{4}\sqrt[3]{(abc)^2}. \tag{19}$$

But (19) is equivalent to

$$\left(\frac{a^3+b^3+c^3+abc}{4}\right)^3 \ge (abc)^2\left(\frac{a+b+c}{3}\right)^3. \tag{20}$$

To prove (20) we can take $abc = 1$ and prove

$$\frac{a^3+b^3+c^3+1}{4} \geq \frac{a+b+c}{3}. \tag{21}$$

Instead, we prove an even stronger inequality

$$\frac{a^3+b^3+c^3+1}{4} \geq \sqrt[3]{\frac{a^3+b^3+c^3}{3}}. \tag{22}$$

Inequality (22) is stronger than (21) because the means are increasing, *i.e.*,

$$M_p(a,b,c) \leq M_q(a,b,c) \quad \text{for } a,b,c>0 \text{ and } 0 \leq p \leq q,$$

where $M_p(a,b,c) = \left[\frac{(a^p+b^p+c^p)}{3}\right]^{\frac{1}{p}}$. To prove (22), denote $x = a^3+b^3+c^3$ and consider the function

$$f(x) = \left(\frac{x+1}{4}\right)^3 - \frac{x}{3}.$$

Since (by $A-G$) $\frac{x}{3} \geq abc = 1$, *i.e.*, $x \geq 3$, we consider $f(x)$ only for $x \geq 3$. Since $f(3) = 0$ and the derivative $f'(x) \geq 0$ for $x \geq 3$, we conclude $f(x) \geq 0$ for $x \geq 3$ and hence prove (19).

Putting all together, we finally have a chain of inequalities for the triangle area S symmetrically expressed in terms of the side lengths a, b, c.

Theorem 6 (Improved Euclidean isoperimetric triangle inequalities)**.**

$$S \leq \frac{1}{2}abc\sqrt{\frac{a+b+c}{a^3+b^3+c^3+abc}} \leq \frac{1}{4}\sqrt[6]{\frac{3(a+b+c)^3(abc)^4}{a^3+b^3+c^3}} \leq \frac{\sqrt{3}}{4}(abc)^{\frac{2}{3}} \tag{23}$$

We shall now make an analogue of the "isoperimetric inequality" (16) in the hyperbolic case.

Start with Cagnolli's formula (9) and multiply all such three formulas to get (since $S = \delta k^2$):

$$\sin^3\frac{\delta}{2} = \prod \sinh\frac{a}{2k} \prod \tanh\frac{a}{2k} \prod \sin A. \tag{24}$$

As in the Euclidean case we have

$$\prod \sin A \leq \left(\frac{\sin A + \sin B + \sin C}{3}\right)^3 \leq \left(\sin\frac{A+B+C}{3}\right)^3 = \left(\sin\frac{\pi-\delta}{3}\right)^3$$

So, this inequality together with (24) implies the following.

Theorem 7. *The area $S = \delta k^2$ of a hyperbolic triangle with side lengths a, b, c satisfies the following inequality*

$$\left(\frac{\sin\frac{\delta}{2}}{\sin\frac{\pi-\delta}{3}}\right)^3 \leq \prod \sinh\frac{a}{2k} \cdot \prod \tanh\frac{a}{2k}. \tag{25}$$

For an equilateral triangle ($a = b = c, A = B = C$) *and any fixed defect δ, the inequality* (25) *becomes an equality* (by Cagnolli's formula (9)).

The corresponding isoperimetric inequality can be obtained for a spherical triangle:

$$\left(\frac{\sin\frac{\varepsilon}{2}}{\sin\frac{\varepsilon-\pi}{3}}\right)^3 \leq \prod \sin\frac{a}{2\rho}\cdot\prod\tan\frac{a}{2\rho}. \tag{26}$$

Remark. In the 3–dimensional case we have a well known upper bound of the volume V of a (Euclidean) tetrahedron in terms of product of lengths of its edges (like (16)) :

$$V \leq \frac{\sqrt{2}}{12}\sqrt{abcdef}$$

with equality if and only if the tetrahedron is regular (and similarly in any dimension); see [12].

Non–Euclidean tetrahedra (and simplices) lack good volume formulas of Heron's type, except the Cayley–Menger determinant formulas in all three geometries. Kahan's formula [2] for volume of a Euclidean tetrahedron is known only for the Euclidean case. There are some volume formulas for tetrahedra in all three geometries now available on Internet, but they are rather involved. We don't know at present how to use them to obtain a good and simple enough upper bound.

In dimension 2, Heron's formula in all three geometries can very easily be deduced. A very short proof of Heron's formula is as follows. Start with the triangle area $4S = 2ab\sin C$ and the law of cosines $a^2+b^2-c^2 = 2ab\cos C$. Now square and add them. The result is a form of the Heron's formula $(4S)^2+(a^2+b^2-c^2)^2 = (2ab)^2$. In a similar way one can get triangle area formulas in the non-Euclidean case by starting with Cagnolli's formula ((9) or (13)) and the appropriate law of cosines.

The result in the hyperbolic geometry is the formula

$$\left(4\sin\frac{\delta}{2}\prod\cosh\frac{a}{2k}\right)^2+\left(\cosh\frac{a}{k}\cosh\frac{b}{k}-\cosh\frac{c}{k}\right)^2=\left(\sinh\frac{a}{k}\sinh\frac{b}{k}\right)^2$$

or

$$\left(4\sin\frac{\delta}{2}\prod\cosh\frac{a}{2k}\right)^2+\sum\cosh^2\frac{a}{k}=1+2\prod\cosh\frac{a}{k}.$$

Remark. In order to improve the non-Euclidean 2–dimensional isoperimetric inequality analogous to (23) we would need an analogue of the function $d_3(a,b,c)$ and a corresponding inequality like (17). This inequality was proved in [11] as a consequence of the inequality $d_3(a^2,b^2,c^2) \leq d_3^2(a,b,c)$, and this follows from an identity expressing the difference $d_3^2(a,b,c) - d_3(a^2,b^2,c^2)$ as a sum of four squares. But at present we do not know the right hyperbolic analogue $d_3^H(a,b,c)$ or spherical analogue $d_3^S(a,b,c)$ of the function $d_3(a,b,c)$.

[2] see www.cs.berkeley.edu/~wkahan/VtetLang.pdf, 2001.

5. Rouché's inequality and Blundon's inequality

The following inequality is a necessary and sufficient condition for the existence of an (Euclidean) triangle with elements R, r and s (see [4]):

$$2R^2+10Rr-r^2-2(R-2r)\sqrt{R^2-2Rr}\le s^2$$
$$\le 2R^2+10Rr-r^2+2(R-2r)\sqrt{R^2-2Rr}. \tag{27}$$

This inequality (sometimes called "the fundamental triangle inequality") was first proved by É. Rouché in 1851, answering a question of Ramus. It was recently improved in [16].

A short proof of (27) is as follows. Let r_a, r_b, r_c be the excircle radii of the triangle ABC. It is well known (and easy to check) that $\sum r_a = 4R+r$, $\sum r_a r_b = s^2$ and $r_a r_b r_c = rs^2$. Hence r_a, r_b, r_c are the roots of the cubic

$$x^3-(4R+r)x^2+s^2x-rs^2=0. \tag{28}$$

Now consider the discriminant of this cubic, *i.e.*, $D=\prod(r_a-r_b)^2$.
In terms of the elementary symmetric functions e_1, e_2, e_3 in the variables r_a, r_b, r_c,

$$D=e_1^2e_2^2-4e_2^3-4e_1^3e_3+18e_1e_2e_3-27e_3^2. \tag{29}$$

Since $e_1=\sum r_a=4R+r$, $e_2=\sum r_ar_b=s^2$, $e_3=\prod r_a=rs^2$, we have

$$D=s^2[(4R+r)^2s^2-4s^4-4(4R+r)^3r+18(4R+r)rs^2-27r^2s^2].$$

From $D\ge 0$, (27) follows easily. In fact, the inequality $D\ge 0$ reduces to the quadratic inequality in s^2:

$$s^4-2(2R^2+10Rr-r^2)s^2+(4R+r)^3r\le 0. \tag{30}$$

The "fundamental" inequality (27) implies a sharp linear upper bound of s in terms of r and R, known as Blundon's inequality [2]:

$$s\le(3\sqrt{3}-4)r+2R. \tag{31}$$

To prove (31), it is enough to prove that

$$2R^2+10Rr-r^2+2(R-2r)\sqrt{R^2-2Rr}\le[(3\sqrt{3}-4)r+2R]^2.$$

A little computation shows that this is equivalent to the following cubic inequality (with $x=R/r$):

$$f(x):=4(3\sqrt{3}-5)x^3-3(60\sqrt{3}-103)x^2+12(48\sqrt{3}-83)x+4(229-132\sqrt{3})\ge 0.$$

By Euler's inequality $x\ge 2$, $f(2)=0$ and hence clearly $f(x)\ge 0$ for $x\ge 2$.

Yet another (standard) way to prove Blundon's inequality (31) is to use the convexity of the biquadratic function on the left hand side of the inequality (30).

Blundon's inequality is also sharp in the sense that equality holds in (31) if and only if the triangle is equilateral. (Recall by the way that a triangle is a right triangle if and only if $s=r+2R$).

Let us turn to non-Euclidean versions of the "fundamental triangle inequality".

Suppose a hyperbolic triangle has a circumscribed circle. As before, denote by R, r, and r_a, r_b, r_c, respectively, the radii of the circumscribed, inscribed and

escribed circles of the triangle. Then by (2) and (3) we know R and r, while r_a (and similarly r_b and r_c) is given by

$$\tanh\frac{r_a}{k}=\sinh\frac{s}{k}\tan\frac{A}{2}, \tag{32}$$

and by using

$$\tan\frac{A}{2}=\sqrt{\frac{\sinh\frac{s-b}{k}\sinh\frac{s-c}{k}}{\sinh\frac{s}{k}\sinh\frac{s-a}{k}}}. \tag{33}$$

The combination of these two expresses r_a in terms of $a, b,$ and c. In order to obtain for the hyperbolic triangle the analogue of the cubic equation (28) whose roots are $x_1=\tanh\frac{r_a}{k}$, $x_2=\tanh\frac{r_b}{k}$, $x_3=\tanh\frac{r_c}{k}$, we have to compute the elementary symmetric functions e_1, e_2, e_3 in the variables x_1, x_2, x_3. We compute first (the easiest) e_3. Equations (32), (33) and (3) yield

$$e_3=\prod\tanh\frac{r_a}{k}=\sinh^2\frac{s}{k}\tanh\frac{r}{k}. \tag{34}$$

Next, by (32) and (33):

$$e_2=\sum\tanh\frac{r_a}{k}\cdot\tanh\frac{r_b}{k}=\sinh^2\frac{s}{k}\sum\tan\frac{A}{2}\tan\frac{B}{2}=\sinh\frac{s}{k}\sum\sinh\frac{s-a}{k}.$$

Applying the identity

$$\sinh(x+y+z)-(\sinh x+\sinh y+\sinh z)=4\sinh\frac{y+z}{2}\sinh\frac{z+x}{2}\sinh\frac{x+y}{2},$$

with $x=\frac{s-a}{2}, y=\frac{s-b}{2}, z=\frac{s-c}{2}$, we obtain

$$\sinh\frac{s}{k}-\sum\sinh\frac{s-a}{k}=4\prod\sinh\frac{a}{2k}. \tag{35}$$

And now from (2) and (3) we get

$$e_2=\sinh^2\frac{s}{k}\left(1-2\tanh\frac{r}{k}\tanh\frac{R}{k}\right). \tag{36}$$

Finally, to compute e_1, we use the identity

$$\tan(x+y+z)=\frac{\tan x+\tan y+\tan z-\tan x\tan y\tan z}{1-\tan x\tan y-\tan y\tan z-\tan z\tan x}. \tag{37}$$

By (32), $e_1=\sinh\frac{s}{k}\sum\tan\frac{A}{2}$. Now from (37):

$$\sum\tan\frac{A}{2}=\tan\frac{A+B+C}{2}\left(1-\sum\tan\frac{A}{2}\tan\frac{B}{2}\right)+\prod\tan\frac{A}{2},$$

$$\tan\frac{A+B+C}{2}=\tan\frac{\pi-\delta}{2}=\cot\frac{\delta}{2}.$$

From (3), we have $\prod\tan\frac{A}{2}=\frac{\tanh\frac{r}{k}}{\sinh\frac{s}{k}}$.

By (33), (35), and (2), (3) it follows easily

$$1-\sum\tan\frac{A}{2}\tan\frac{B}{2}=2\tanh\frac{r}{k}\tanh\frac{R}{k}\sinh\frac{s}{k}.$$

Finally, putting all together yields

$$e_1 = \tanh\frac{r}{k}\left(1 + 2\tanh\frac{R}{k}\sinh\frac{s}{k}\cot\frac{\delta}{2}\right). \tag{38}$$

Equations (34), (36) and (38) yield via $x^3 - e_1x^2 + e_2x - e_3 = 0$ the cubic equation

$$\begin{aligned} x^3 &- \tanh\frac{r}{k}\left(1 + 2\tanh\frac{R}{k}\sinh\frac{s}{k}\cot\frac{\delta}{2}\right)x^2 \\ &+ \sinh^2\frac{s}{k}\left(1 - 2\tanh\frac{r}{k}\tanh\frac{R}{k}\right)x - \sinh^2\frac{s}{k}\tanh\frac{r}{k} = 0. \end{aligned} \tag{39}$$

This cubic (with roots $\tanh\frac{r_a}{k}$ etc.) reduces to the cubic (28) by letting $k \to \infty$. This follows from the identity

$$\frac{\sinh\frac{s}{k}\cdot\tanh\frac{r}{k}}{\sin\frac{\delta}{2}} = 2\prod\cosh\frac{a}{2k}.$$

If $k \to \infty$, then the right hand side tends to 2 and therefore the coefficient by x^2 in (39) goes to $r + 4R$ which appears in (28); similarly for the other coefficients.

Consider the discriminant of (39)

$$D = \prod\left(\tanh\frac{r_a}{k} - \tanh\frac{r_b}{k}\right)^2.$$

Now, by applying (29) and (34), (36) and (38) we obtain the quartic polynomial (in fact degree 6) in $\sinh\frac{s}{k}$ for an expression D. By the following legend

$$\begin{aligned} r &\longleftrightarrow \tanh\tfrac{r}{k} \qquad \delta \longleftrightarrow \cot\tfrac{\delta}{2} \\ R &\longleftrightarrow \tanh\tfrac{R}{k} \qquad s \longleftrightarrow \sinh\tfrac{s}{k} \end{aligned} \tag{40}$$

we can write D as follows (after some computation); note that it has almost double number of terms than the corresponding Euclidean discriminant

$$\begin{aligned} D = \quad & s^2[(r^2R^2\delta^2 + 4r^4R^4\delta^2 - 4r^3R^3\delta^2 - 1 + 6rR - 12r^2R^2 + 8r^3R^3)s^4 \\ & + r^2R\delta(1 - 4rR + 4r^2R^2\delta - 8r^2R^2\delta^2 + 9\delta + 18rR\delta)s^3 \\ & + r^2(r^2R^2 - 10rR - 12r^2R^2\delta^2 - 2)s^2 \\ & - 6r^4R\delta s - r^4]. \end{aligned} \tag{41}$$

By definition $D \geq 0$, so the quartic polynomial in s (in fact in $\sinh\frac{s}{k}$), *i.e.*, the polynomial in brackets in (41) is ≥ 0.

So the hyperbolic analogue of the "fundamental triangle inequality" (27), or rather degree–four polynomial inequality (30) is the quartic (in s) polynomial inequality $\frac{D}{s^2} \geq 0$.

Theorem 8 (Hyperbolic "fundamental triangle inequality")**.** *For a hyperbolic triangle that has a circumcircle of radius R, incircle of radius r, semiperimeter s, and excess δ, we have*

$$\frac{D}{s^2} \geq 0, \tag{42}$$

where D is given by (41) *together with the legend* (40). *When $k \to \infty$,* (42) *reduces to* (30).

Blundon's hyperbolic inequality can also be derived as a corollary of Theorem 8.

The spherical version of the "fundamental inequality" as well as the corresponding spherical Blundon's inequality can also be obtained, but we omit them here.

In conclusion, we may say that all these triangle inequalities give more information and better insight to the geometry of 2– and 3– manifolds.

References

[1] S. J. Bilichev and P. M. Vlamos, About some improvements of the Finsler–Hadwiger's inequality, *Geometry and Math. Competitions, 4th. Congress of the World Fed. of Mat., Math. Comp.*, Melbourne, 2002; 19–36.

[2] W. J. Blundon, Inequalities associated with the triangle, *Canad. Math. Bull.*, 8 (1965) 615–626.

[3] P. Finsler and H. Hadwiger, Einige Relationen im Dreieck, *Comment. Math. Helv.*, 10 (1938) 316–326.

[4] D. S. Mitrinović, J. E. Pečarić, V. Volenec, *Recent Advances in Geometric Inequalities*, Kluver Acad. Publ., Amsterdam, 1989.

[5] N. M. Nestorovich, *Geometricheskie postroenija v ploskosti Lobachevskogo*, (in Russian) M.–L.:GITTL, Leningrad, 1951.

[6] V. V. Prasolov, V. M. Tikhomirov, *Geometry*, Translations of Mathematical Monographs, AMS, Providence, R.I., 2001.

[7] V. V. Prasolov, *Geometrija Lobachevskogo*, (in Russian) MCNMO, Moscow, 2004.

[8] V. V. Prasolov, *Problems in Planimetry*, (in Russian) MCNMO, OAO, "Moscow textbooks", Moscow, 2006.

[9] J. G. Ratcliffe, *Foundations of Hyperbolic Manifolds*, GTM, Springer Verlag, New York, 1994.

[10] J. M. Steele, *The Cauchy–Schwarz Master Class*, MAA, Cambridge University Press, Cambridge, 2004.

[11] D. Svrtan, I. Urbiha, Verification and strengthening of the Atiyah–Sutcliffe conjectures for the sine theorem and several types of configurations, arXiv:math/0609174

[12] D. Veljan, Inequalities for volumes of simplices and determinants, *Lin. Alg. and its Appl.*, 219 (1995) 79–91.

[13] D. Veljan, Geometry and convexity of $\cos\sqrt{x}$, *Amer. Math. Monthly*, 111 (2004) 592–595.

[14] D. Veljan, S. Wu, Parametrized Klamkin's inequality and improved Euler's inequality, *Math. Inequalities Appl.*, 11 (2008) 729–737.

[15] Sh.–H. Wu, Generalizations and sharpness of Finsler–Hadwiger's inequality and its applications, *Math. Inequalities Appl.*, 9 (2006) 421–426.

[16] S. Wu, A sharpened version of the fundamental triangle inequality, *Math. Inequalities Appl.*, 11 (2008) 477–482.

[17] Sh.–H. Wu, Zh.–H. Zhang, and Zh.–G. Xiao, On Weitzenboeck's inequality and its generalizations, *RGMIA Research Report Collection*, 6(4), Article 14, 2003.

Dragutin Svrtan: Department of Mathematics, University of Zagreb,, Bijenička cesta 30, 10000 Zagreb, Croatia

E-mail address: dsvrtan@math.hr

Darko Veljan: Department of Mathematics, University of Zagreb,, Bijenička cesta 30, 10000 Zagreb, Croatia

E-mail address: darko.veljan@gmail.com

Forum Geometricorum
Volume 12 (2012) 211–213.

FORUM GEOM
ISSN 1534-1178

Finding Integer-Sided Triangles With $P^2 = nA$

John F. Goehl, Jr.

Abstract. A surprising property of certain parameters leads to algorithms for finding integer-sided triangles with $P^2 = nA$, where P is the perimeter, A is the area, and n is an integer. Examples of triangles found for each of two values of n are given.

1. Introduction

MacLeod [1] considered the problem of finding integer-sided triangles with sides a, b, and c and $P^2 = nA$, where P is the perimeter, A is the area, and n is an integer. He showed that they could be found from solutions of the equation:

$$16(a+b+c)^3 = n^2(a+b-c)(a+c-b)(b+c-a). \tag{1}$$

It was shown that n must be an integer greater than or equal to 21. Define

$$2\alpha = a+b-c, \quad 2\beta = a+c-b, \qquad 2\gamma = b+c-a,$$

then

$$16(\alpha+\beta+\gamma)^3 = n^2\alpha\beta\gamma. \tag{2}$$

Note that the parameters α, β, and γ are the lengths of the segments into which the inscribed circle divides the sides.

2. Special case: n a prime number

Consider the special case when n is a prime number. Then $\alpha+\beta+\gamma = nw$ for some integer w. So equation (2) becomes $16nw^3 = \alpha\beta\gamma$. Then one of the parameters α, β, or γ must be divisible by n. Choose $\gamma = n\gamma'$ and so $16w^3 = \alpha\beta\gamma'$. Let $\alpha = 2^i\alpha_1$, $\beta = 2^j\beta_1$, and $\gamma' = 2^k\gamma_1$, where $i+j+k = 4$. Then $w^3 = \alpha_1\beta_1\gamma_1$. Note that it can be assumed that α_1, β_1, and γ_1 have no common factor since the sides of the corresponding triangle can be reduced by that factor to an equivalent triangle with the same P^2/A ratio. Hence $w = w'\alpha_0$ for some w' and a factor unique to α_1 so $\alpha_1 = \alpha_0^3$. Similarly, $\beta_1 = \beta_0^3$, $\gamma_1 = \gamma_0^3$, and $w = \alpha_0\beta_0\gamma_0$. Finally, the sides can be found from $\alpha = 2^i\alpha_0^3$, $\beta = 2^j\beta_0^3$, and $\gamma = 2^k n\gamma_0^3$.

Publication Date: July 6, 2012. Communicating Editor: Paul Yiu.

3. Algorithms

From equation (2), $16(\alpha+\beta+\gamma)^3 = n^2\alpha\beta\gamma = n^2 2^i\alpha_0^3 2^j\beta_0^3 2^k n\gamma_0^3$, or

$$2^i\alpha_0^3 + 2^j\beta_0^3 + 2^k n\gamma_0^3 = n\alpha_0\beta_0\gamma_0. \tag{3}$$

First note that

$$2^i\alpha_0^3 + 2^j\beta_0^3 = nv \tag{4}$$

for some v. Equation (4) is used to find allowed integer values of α_0, β_0, and v. Then allowed integer values of γ_0 are found from solutions of the cubic equation:

$$2^k\gamma_0^3 - \alpha_0\beta_0\gamma_0 + v = 0. \tag{5}$$

4. An example

Consider $n = 31$. Values for α_0 and β_0 up to 600 resulted in the integer solutions of equations (4) and (5) shown in Table 1. Solutions for which α_0 and β_0 have a common factor result in duplicate triangles and have been omitted. Entries for α_0, β_0, and v that result in duplicate triangles have also been omitted. In both tables that follow, the values for α, β, and γ and the values of the corresponding sides, $a = \alpha+\beta$, $b = \alpha+\gamma$, and $c = \beta+\gamma$ have been reduced by the common factor. The second solution in Table 1 is the triangle found by MacLeod.

i	4	3	3	3	3
j	0	1	1	0	0
k	0	0	0	1	1
α_0	2	1	5	17	29
β_0	3	3	13	18	35
v	5	2	174	1456	7677
γ_0	1	1	6	7	9
α	128	8	500	19652	195112
β	27	54	2197	2916	42875
γ	31	31	3348	10633	45198
a	155	62	2697	22568	237987
b	159	39	3848	30285	240310
c	58	85	5545	13549	88073

Table 1

5. General case: n a composite number

Consider a possible factorization of n: $n = n_1n_2n_3$. Similar arguments lead to $\alpha = 2^i n_1\alpha_0^3$, $\beta = 2^j n_2\beta_0^3$, and $\gamma = 2^k n_3\gamma_0^3$, where $i+j+k = 4$. All the MacLeod triangles are of this form.

6. General algorithm

With the above choices for α, β, and γ, equation (2) becomes

$$2^i n_1 \alpha_0^3 + 2^j n_2 \beta_0^3 + 2^k n_3 \gamma_0^3 = n_1 n_2 n_3 \alpha_0 \beta_0 \gamma_0. \tag{6}$$

First note that

$$2^i n_1 \alpha_0^3 + 2^j n_2 \beta_0^3 = n_3 v \tag{7}$$

for some v. Equation (7) is used to find allowed integer values of α_0, β_0, and v. Then allowed integer values of γ_0 are found from solutions of the cubic equation:

$$2^k \gamma_0^3 - n_1 n_2 \alpha_0 \beta_0 \gamma_0 + v = 0. \tag{8}$$

7. An example

Consider $n = 42$. Integer solutions of equations (7) and (8) are shown in Table 2. Note that the fourth entry in Table 2 is the triangle found by MacLeod.

i	0	2	2	0	0	0	0
j	0	2	2	2	2	2	2
k	4	0	0	2	2	2	2
n_1	1	1	1	2	2	2	2
n_2	1	1	1	3	3	3	3
n_3	42	42	42	7	7	7	7
α_0	11	43	227	1	4	92	109
β_0	19	47	487	1	1	53	121
v	195	17460	12114132	2	20	477700	3406970
γ_0	3	9	129	1	1	17	49
α	1331	159014	23394166	1	32	389344	1295029
β	6859	207646	231002606	6	3	446631	10629366
γ	18144	15309	45080469	14	7	34391	1647086
a	8190	366660	254396772	7	35	835975	11924395
b	19475	174323	68474635	15	39	423735	2942115
c	25003	222955	276083075	20	10	481022	12276452

Table 2

Reference

[1] A. J. MacLeod, On integer relations between the area and perimeter of Heron triangles, *Forum Geom.*, 9 (2009) 41–46.

John F. Goehl, Jr.: Department of Physical Sciences, Barry University, 11300 NE Second Avenue, Miami Shores, Florida 33161, USA

E-mail address: jgoehl@mail.barry.edu

Forum Geometricorum
Volume 12 (2012) 215–218.

FORUM GEOM
ISSN 1534-1178

The Spheres Tangent Externally to the Tritangent Spheres of a Triangle

Floor van Lamoen

Abstract. We consider the tritangent circles of a triangle as the great circles of spheres in three dimensional space, and identify the spheres tangent externally to these four spheres.

In the plane of a triangle ABC we consider the tritangent circles, the incircle and the three excircles. It is well known that the nine-point circle is tangent to the excircles externally and to the incircle internally. Together with the sidelines of ABC, considered as degenerate circles, this is the only circle tangent to all four tritangent circles. Considering the tritangent circles as the sections of spheres by the plane containing their centers, we wonder if there are spheres quadritangent to these "tritangent spheres", apart from the one containing the nine-point circle. In this paper we identify the spheres tangent externally to the four tritangent spheres. We use methods similar to [4]. By symmetry it is enough to consider spheres on one side of the plane.

Let us start with the excircles $\mathcal{C}_a = I_a(r_a)$, $\mathcal{C}_b = I_b(r_b)$ and $\mathcal{C}_c = I_c(r_c)$, and the excircle-spheres $\mathcal{S}_a$, $\mathcal{S}_b$, $\mathcal{S}_c$ in 3-dimensional space with the same centers and radii. Consider a sphere with radius ρ, and center D at a distance d above the plane of triangle ABC, and tangent to the three excircle-spheres. Clearly, $\rho \geq \frac{R}{2}$, where R is the circumradius of triangle ABC. The orthogonal projection of the center onto the plane is the radical center of the circles $I_a(r_a+\rho)$, $I_b(r_b+\rho)$ and $I_c(r_c+\rho)$. For $\rho = \frac{R}{2}$, this is the nine-point center N. In general, this projection lies on the line joining N to the radical center of the excircles, namely, the Spieker center $S_{\rm p}$. The power of $S_{\rm p}$ with respect to each excircle is $\frac{r^2+s^2}{4}$, where r and s are the inradius and semiperimeter of the triangle (see, for example, [2, Theorem 4]).

Let P be the reflection of $S_{\rm p}$ in N. A simple application of Menelaus' theorem (to triangle $PIS_{\rm p}$ with transversal GNH) shows that it is also the midpoint between the incenter I and the orthocenter H (see Figure 1).

Theorem 1. *The sphere $\mathcal{Q}$ with radius R, and center at $\frac{\sqrt{bc+ac+ab}}{2}$ above the point P, is tangent externally to the four tritangent spheres.*

Proof. Consider triangle $I_aPS_{\rm p}$ with median I_aN. Note that $I_aN = \frac{R}{2} + r_a$ and $NS_{\rm p} = \frac{1}{2}OI$, where O is the circumcenter. It follows that $NS_{\rm p}^2 = \frac{1}{4}R(R-2r)$ by Euler's formula. Since the power of $S_{\rm p}$ with respect to each excircle is $\frac{1}{4}(r^2+s^2)$,

Publication Date: July 13, 2012. Communicating Editor: Paul Yiu.

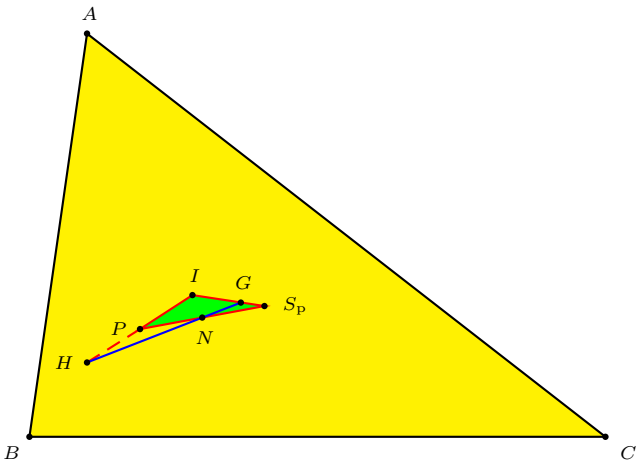

Figure 1.

$I_aS_{\rm p}^2 = \frac{r^2+s^2}{4} + r_a^2$. Applying Apollonius' theorem to triangle $I_aPS_{\rm p}$, we have

$$\begin{aligned} I_aP^2 &= 2I_aN^2 + 2NS_{\rm p}^2 - I_aS_{\rm p}^2 \\ &= 2\left(\frac{R}{2} + r_a\right)^2 + \frac{1}{2}R(R-2r) - \frac{r^2+s^2}{4} - r_a^2 \\ &= (R+r_a)^2 - \frac{r^2+s^2+4Rr}{4} \\ &= (R+r_a)^2 - \frac{ab+bc+ca}{4}. \end{aligned}$$

The last equality follows from $R = \frac{abc}{4\Delta}$, $r = \frac{\Delta}{s}$ and Heron's formula for the area Δ. Similarly,

$$I_bP^2 = (R+r_b)^2 - \frac{ab+bc+ca}{4} \quad \text{and} \quad I_cP^2 = (R+r_c)^2 - \frac{ab+bc+ca}{4}.$$

By letting D be the point at a distance $d := \frac{\sqrt{ab+bc+ca}}{2} = \frac{\sqrt{r^2+s^2+4Rr}}{2}$ above P, we have

$$I_aD = R + r_a, \quad I_bD = R + r_b, \quad I_cD = R + r_c.$$

Therefore the sphere $\mathcal{Q}$ with center D, radius R, is tangent to each of $\mathcal{S}_a$, $\mathcal{S}_b$, $\mathcal{S}_c$. Since the point P is also the midpoint of IH, and $IH^2 = 4R^2 + 4Rr + 3r^2 - s^2$ (see [1, p.50]), we have

$$DI^2 = \frac{r^2+s^2+4Rr}{4} + \frac{4R^2+4Rr+3r^2-s^2}{4} = (R+r)^2.$$

This shows that $\mathcal{Q}$ is also tangent to the incircle-sphere $\mathcal{S}$. □

The point P, which is the reflection of $S_{\rm p}$ in N (also the midpoint of IH), is the triangle center

$$X_{946} = (a^3(b+c) + (b-c)^2(a^2 - a(b+c) - (b+c)^2) : \cdots : \cdots)$$

in [3].

The orthogonal projections to the plane of ABC of the points of contact of $\mathcal{Q}$ with the excircle-spheres form a triangle $A'B'C'$. The point A', for instance, is the point that divides the segment PI_a in ratio $R : r_a$. Let AA' intersect the line IP at Q (see Figure 2). Applying Menelaus' theorem to triangle PII_a with transversal AXA', we have

$$\frac{PQ}{QI} \cdot \frac{IA}{AI_a} \cdot \frac{I_aA'}{A'P} = -1 \implies \frac{PQ}{QI} \cdot \frac{-r}{r_a} \cdot \frac{r_a}{R} = -1 \implies \frac{PQ}{QI} = \frac{R}{r}.$$

Similarly, the lines BB' and CC' intersect IP at the same point Q, which divides PI in the ratio $R : r$. This is the orthogonal projection of the point of tangency of $\mathcal{Q}$ with the incircle-sphere $\mathcal{S}$. It has barycentric coordinates

$$\left(\frac{b+c}{b+c-a} : \frac{c+a}{c+a-b} : \frac{a+b}{a+b-c}\right),$$

and is the triangle center X_{226} in [3].

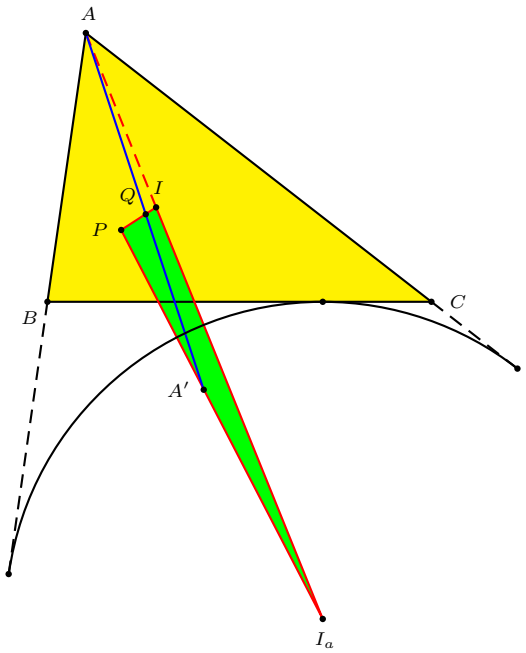

Figure 2.

References

[1] O. Bottema, R. Z. Djordjevic, R. R. Janic, D. S. Mitrinovic, and P. M. Vasic, *Geometric Inequalities*, Wolters-Noordhoff, 1968.

[2] D. Grinberg and P. Yiu, The Apollonius circle as a Tucker circle, *Forum Geom.*, 2 (2002) 175–182.

[3] C. K. Kimberling, *Encyclopedia of Triangle Centers*, available at `http://faculty.evansville.edu/ck6/encyclopedia/ETC.html`.

[4] F. M. van Lamoen, A spatial view of the second Lemoine circle, *Forum Geom.*, 11 (2011) 201–203.

Floor van Lamoen: Ostrea Lyceum, Bergweg 4, 4461 NB Goes, The Netherlands
E-mail address: `fvanlamoen@planet.nl`

Forum Geometricorum
Volume 12 (2012) 219–225.

FORUM GEOM
ISSN 1534-1178

Sherman's Fourth Side of a Triangle

Paul Yiu

Abstract. We give two simple ruler-and-compass constructions of the line which, like the sidelines of the triangle, is tangent to the incircle and cuts the circumcircle in a chord with midpoint on the nine-point circle.

1. Introduction

Consider the sides of a triangle as chords of its circumcircle. Each of these is tangent to the incircle and has its midpoint on the nine-point circle. Apart from these three chords, B. F. Sherman [3] has established the existence of a fourth one, which is also tangent to the incircle and bisected by the nine-point circle (see Figure 1). While Sherman called this the *fourth side* of the triangle, we refer to the line containing this fourth side as the Sherman line of the triangle. In this note we provide a simple euclidean construction of this Sherman line as a result of an analysis with barycentric coordinates.

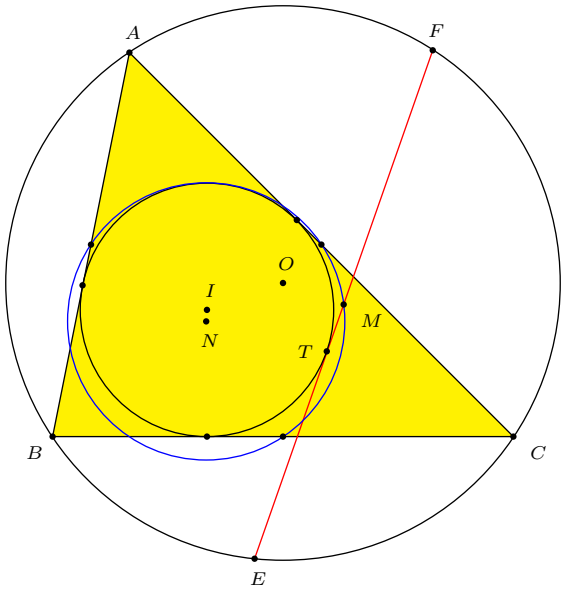

Figure 1. The fourth side of a triangle

2. Lines tangent to the incircle

Given a triangle ABC with sidelengths a, b, c, we say that the line with barycentric equation $px+qy+rz=0$ has line coordinates $[p,q,r]$. A line $px+qy+rz=0$

Publication Date: July 18, 2012. Communicating Editor: Nikolaos Dergiades.

is tangent to a conic $\mathscr{C}$ if and only if $[p : q : r]$ lies on the dual conic $\mathscr{C}^*$ (see, for example, [4, §10.6]).

Proposition 1. *If $\mathscr{C}$ is the inscribed conic tangent to the sidelines at the traces of the point $\left(\frac{1}{u} : \frac{1}{v} : \frac{1}{w}\right)$, its dual conic $\mathscr{C}^*$ is the circumconic*

$$\frac{u}{x} + \frac{v}{y} + \frac{w}{z} = 0.$$

Proof. Since the barycentric equation of $\mathscr{C}$ is

$$u^2x^2 + v^2y^2 + w^2z^2 - 2vwyz - 2wuzx - 2uvxy = 0,$$

the conic is represented by the matrix

$$M = \begin{pmatrix} u^2 & -uv & -uw \\ -uv & v^2 & -vw \\ -uw & -vw & w^2 \end{pmatrix}.$$

This has adjoint matrix

$$M^* = 8uvw \cdot \begin{pmatrix} 0 & w & v \\ w & 0 & u \\ v & u & 0 \end{pmatrix}.$$

It follows that the dual conic $\mathscr{C}^*$ is the circumconic $uyz + vzx + wxy = 0$. □

Applying this to the incircle, we have the following characterization of its tangent lines.

Proposition 2. *A line $px + qy + rz = 0$ is tangent to the incircle if and only if*

$$\frac{b+c-a}{p} + \frac{c+a-b}{q} + \frac{a+b-c}{r} = 0. \tag{1}$$

3. Lines bisected by the nine-point circle

Suppose a line $\mathscr{L} : px + qy + rz = 0$ cuts out a chord EF of the circumcircle. The chord is bisected by the nine-point circle if and only if the pedal (orthogonal projection) P of the circumcenter O on $\mathscr{L}$ lies on the nine-point circle. We shall simply say that the line is bisected by the nine-point circle.

Proposition 3. *A line $px + qy + rz = 0$ is bisected by the nine-point circle if and only if*

$$\frac{a^2(b^2+c^2-a^2)}{p} + \frac{b^2(c^2+a^2-b^2)}{q} + \frac{c^2(a^2+b^2-c^2)}{r} = 0. \tag{2}$$

Proof. The pedal of O on the line $px + qy + rz = 0$ is the point

$$\begin{aligned} P = & -b^2q^2 - c^2r^2 + (b^2+c^2-2a^2)qr + a^2rp + a^2pq \\ : & -c^2r^2 - a^2p^2 + (c^2+a^2-2b^2)rp + b^2pq + b^2qr \\ : & -a^2p^2 - b^2q^2 + (a^2+b^2-2c^2)pq + c^2qr + c^2rp. \end{aligned}$$

The superior of the pedal P is the point

$$\begin{aligned} Q &= a^2p^2 - a^2qr + (b^2 - c^2)rp - (b^2 - c^2)pq \\ &: b^2q^2 - b^2rp + (c^2 - a^2)pq - (c^2 - a^2)qr \\ &: c^2r^2 - c^2pq + (a^2 - b^2)qr - (a^2 - b^2)rp. \end{aligned}$$

The line $px + qy + rz = 0$ is bisected by the nine-point circle if and only if Q lies on the circumcircle $a^2yz + b^2zx + c^2xy = 0$. This condition is equivalent to

$$\begin{aligned} &a^2(b^2q^2 - b^2rp + (c^2 - a^2)pq - (c^2 - a^2)qr)(b^2q^2 - b^2rp + (c^2 - a^2)pq - (c^2 - a^2)qr) \\ &+ b^2(b^2q^2 - b^2rp + (c^2 - a^2)pq - (c^2 - a^2)qr)(a^2p^2 - a^2qr + (b^2 - c^2)rp - (b^2 - c^2)pq) \\ &+ c^2(a^2p^2 - a^2qr + (b^2 - c^2)rp - (b^2 - c^2)pq)(b^2q^2 - b^2rp + (c^2 - a^2)pq - (c^2 - a^2)qr) \\ &= 0. \end{aligned}$$

The quartic polynomial in p, q, r above factors as $-F \cdot G$, where

$$\begin{aligned} F = {} & a^2(b^2 + c^2 - a^2)qr + b^2(c^2 + a^2 - b^2)rp + c^2(a^2 + b^2 - c^2)pq, \\ G = {} & a^2p^2 + b^2q^2 + c^2r^2 - (b^2 + c^2 - a^2)qr - (c^2 + a^2 - b^2)rp - (a^2 + b^2 - c^2)pq. \end{aligned}$$

Now G can be rewritten as

$$G = S_A(q - r)^2 + S_B(r - p)^2 + S_C(p - q)^2.$$

As such, it is the square length of a vector of component p, q, r along the respective sidelines. Therefore, $G > 0$, and we obtained $F = 0$ as the condition for the line to be bisected by the nine-point circle. □

Corollary 4. *A line is bisected by the nine-point circle* (N) *if and only if it is tangent to the inscribed conic with center the nine-point center* N.

Proof. Let $px + qy + rz = 0$ be a line bisected by the nine-point circle. By Proposition 3, it is tangent to the inscribed conic with perspector $\left(\frac{1}{u} : \frac{1}{v} : \frac{1}{w}\right)$, where

$$u : v : w = a^2(b^2 + c^2 - a^2) : b^2(c^2 + a^2 - b^2) : c^2(a^2 + b^2 - c^2).$$

The center of the inscribed conic is

$$\begin{aligned} &v + w : w + u : u + v \\ &= b^2(c^2 + a^2) - (b^2 - c^2)^2 : \ b^2(c^2 + a^2)^2 - (c^2 - a^2)^2 : \ c^2(a^2 + b^2) - (a^2 - b^2)^2. \end{aligned}$$

This is the center N of the nine-point circle. □

The inscribed conic with center N is called the MacBeath inconic. It is well known that this has foci O and H, the circumcenter and the orthocenter (see [4, §11.1.5]). The Sherman line is the *fourth* common tangent of the incircle and the inscribed conic with center N.

N. Dergiades has kindly suggested the following alternative proof of Corollary 4. The orthogonal projection of a focus on a tangent of a conic lies on the auxiliary

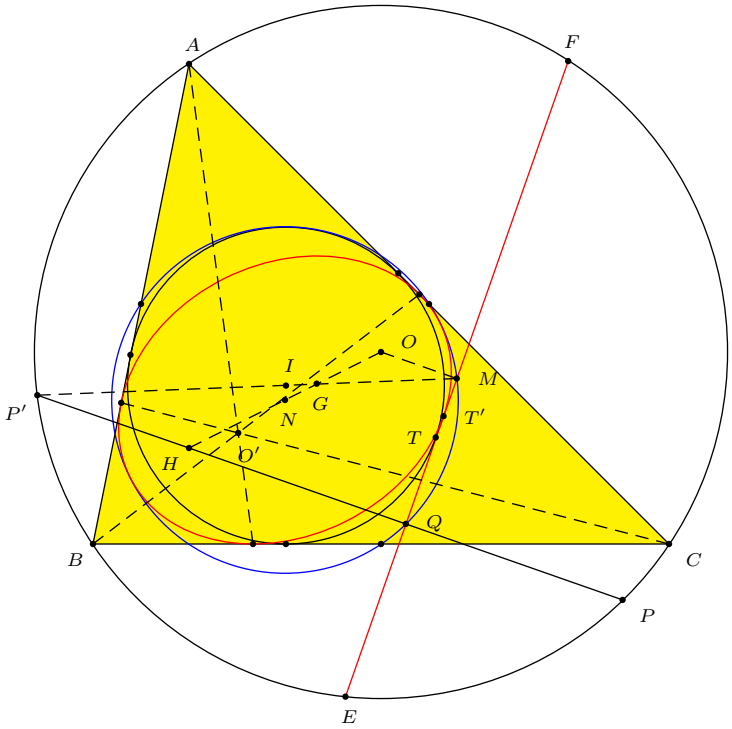

Figure 2. The fourth side of a triangle as a common tangent

circle. Since the MacBeath inconic has the nine-point circle as auxiliary circle ([1, Problem 130]), and the orthogonal projection of the focus O on the Sherman line lies on the nine-point circle, the Sherman line must be tangent to the MacBeath inconic.

4. Construction of the Sherman line

The Sherman line, being tangent to the incircle and bisected by the nine-point circle, has its line coordinates $[p : q : r]$ satisfying both (1) and (2). Regarding $px + qy + rz = 0$ as the trilinear polar of the point $S = \left(\frac{1}{p} : \frac{1}{q} : \frac{1}{r}\right)$, we have a simple characterization of S leading to an easy ruler-and-compass construction of the Sherman line.

Proposition 5. *The Sherman line is the trilinear polar of the intersection of*
(i) *the trilinear polar of the Gergonne point,*
(ii) *the isotomic line of the trilinear polar of the circumcenter* (see Figure 2).

Proof. The point S is the intersection of the two lines with equations

$$(b+c-a)x + (c+a-b)y + (a+b-c)z = 0, \quad (3)$$
$$a^2(b^2+c^2-a^2)x + b^2(c^2+a^2-b^2)y + c^2(a^2+b^2-c^2)z = 0. \quad (4)$$

These two lines can be easily constructed as follows.
(3) is the trilinear polar of the Gergonne point $\left(\frac{1}{b+c-a} : \frac{1}{c+a-b} : \frac{1}{a+b-c}\right)$.

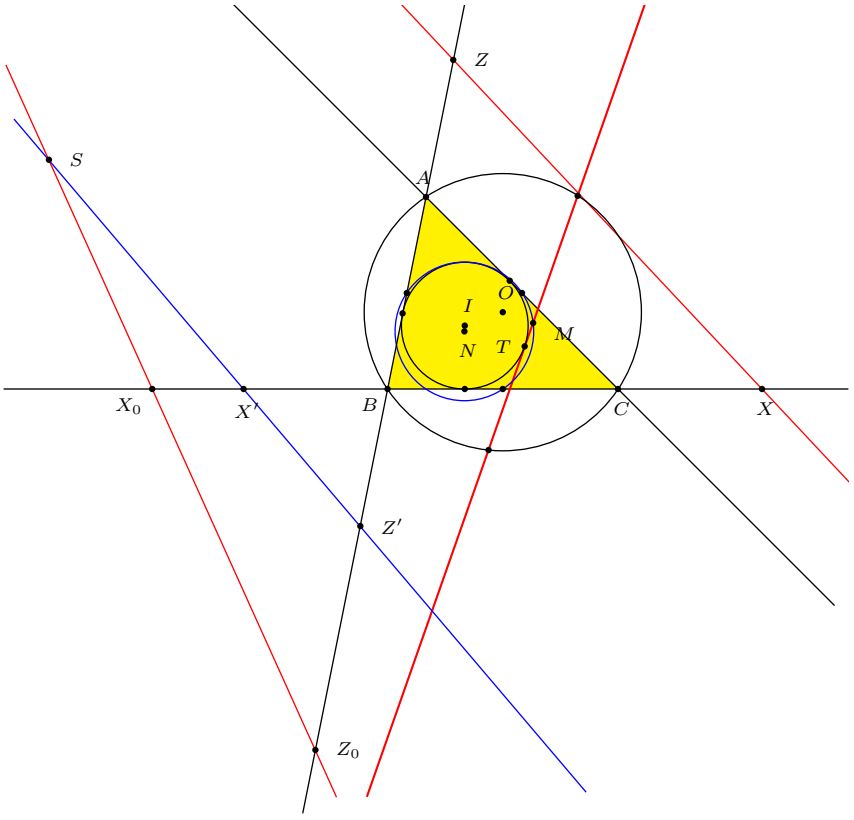

Figure 3. Construction of the tripole of the Sherman line

(4) is the trilinear polar of the isotomic conjugate of the circumcenter. It can also be constructed as follows. If the trilinear polar of the circumcenter O intersects the sidelines at X, Y, Z respectively, and if X', Y', Z' are points on the respective sidelines such that

$$BX' = XC, \qquad CY' = YA, \qquad AZ' = ZB,$$

then (4) is the line containing X', Y', Z'. This is called the isotomic line of the line containing X, Y, Z. □

5. Coordinates

For completeness, we record the barycentric coordinates of various points associated with the Sherman line configuration.

5.1. *Points on the Sherman line.* The Sherman line is the trilinear polar of

$$S = (f(a,b,c) : f(b,c,a) : f(c,a,b)),$$

where

$$f(a,b,c) := (b-c)(a^2(b+c) - 2abc - (b+c)(b-c)^2).$$

The point of tangency with the incircle is

$$T = ((b+c-a)f(a,b,c)^2 : (c+a-b)f(b,c,a)^2 : (a+b-c)f(c,a,b)^2).$$

This is the triangle center X_{3326} in [2]. The point of tangency with the MacBeath inconic is the point

$$T' = (a^2S_A \cdot f(a,b,c)^2 : b^2S_B \cdot f(b,c,a)^2 : c^2S_C \cdot (c,a,b)^2).$$

See [5].

The pedal of O on the Sherman line is the point

$$M = ((b+c-a)(b-c)S_A f(a,b,c) \cdot g(a,b,c) : \cdots : \cdots),$$

where

$$g(a,b,c) = -2a^4 + a^3(b+c) + a^2(b-c)^2 - a(b+c)(b-c)^2 + (b^2-c^2)^2.$$

The triangle centers S, T', and M do not appear in Kimberling's *Encyclopedia of Triangle Centers* [2]. However, the superior of M is the point

$$P' = \left(\frac{1}{S_A \cdot f(a,b,c)} : \cdots : \cdots\right)$$

on the circumcircle, and the line HP' is perpendicular to the Sherman line (see Figure 2). P' is the triangle center X_{1309}.

5.2. *A second construction of the Sherman line.* It is known that the MacBeath inconic is the envelope of the perpendicular bisector of HP as P traverses the circumcircle ([4, §11.1.5]). Therefore, the reflection of H in the Sherman line, like those in the three sidelines of ABC, is a point on the circumcircle. This reflection is the point

$$P = \left(\frac{a^2}{2a^4 - 2a^3(b+c) - a^2(b^2-4bc+c^2) + 2a(b+c)(b-c)^2 - (b^2-c^2)^2} : \cdots : \cdots\right),$$

According to [2], P is the triangle center X_{953}, the isogonal conjugate of the infinite point

$$X_{952} = (2a^4-2a^3(b+c)-a^2(b^2-4bc+c^2)+2a(b+c)(b-c)^2-(b^2-c^2)^2 : \cdots : \cdots).$$

This is the infinite point of the line joining the incenter to the nine-point center, namely,

$$\sum_{\text{cyclic}} (b-c)(b+c-a)(a^2-b^2+bc-c^2)x = 0.$$

This observation leads to a very easy (second) construction of the Sherman line:
(i) Construct lines through A, B, C parallel to the line IN.
(ii) Construct the reflections of the lines in (i) in the respective angle bisectors of the triangle.
(iii) The three lines in (ii) intersect at a point P on the circumcircle.
(iv) The perpendicular bisector of HP is the Sherman line.
See Figure 4. For a simpler construction, it is sufficient to construct one line in (i) and the corresponding reflection in (ii).

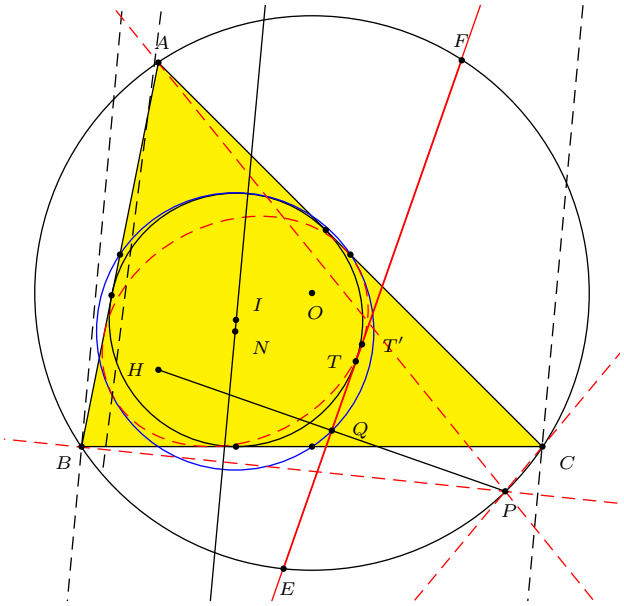

Figure 4. Construction of the Sherman line

5.3. *Pedal of orthocenter on the Sherman line.* The midpoint of the segment HP is the point

$$Q = ((b+c-2a)(b-c)f(a,b,c) : (c+a-2b)(b-c)f(b,c,a) : (a+b-2c)(b-c)f(c,a,b))$$

on the nine-point circle. This is the triangle center X_{3259} in [2] (see Figure 2).

5.4. *Distances.* Finally, we record the length of the fourth side EF of the triangle:

$$EF^2 = \frac{16r(4R^2+5Rr+r^2-s^2)(4R^3-(2r^2+s^2)R+r(s^2-r^2))}{(4R^2+4Rr+3r^2-s^2)^2},$$

where R, r, and s are the circumradius, inradius, and semiperimeter of the given triangle. The distance from O to the Sherman line is

$$OM = \frac{(R-2r)(2R+r-s)(2R+r+s)}{4R^2+4Rr+3r^2-s^2}.$$

References

[1] F. G.-M., *Exercices de Géométrie*, 6th ed., 1920; Gabay reprint, Paris, 1991.
[2] C. Kimberling, *Encyclopedia of Triangle Centers*, available at http://faculty.evansville.edu/ck6/encyclopedia/ETC.html.
[3] B. F. Sherman, The fourth side of a triangle, *Math. Mag.*, 66 (1993) 333–337.
[4] P. Yiu, *Introduction to the Geometry of the Triangle*, Florida Atlantic University Lecture Notes, 2001.
[5] P. Yiu, Hyacinthos message 14416, November 7, 2006.

Paul Yiu: Department of Mathematical Sciences, Florida Atlantic University, 777 Glades Road, Boca Raton, Florida 33431-0991, USA
E-mail address: yiu@fau.edu

Forum Geometricorum
Volume 12 (2012) 227–235.

FORUM GEOM
ISSN 1534-1178

Improving Upon a Geometric Inequality of Third Order

Toufik Mansour and Mark Shattuck

Abstract. We show that the best possible positive constant k in a certain geometric inequality of third order lies in the interval $[0.14119, 0.14364]$, which improves upon a previous known result where $k = 0$. We also consider a comparable question concerning a fourth order version of the inequality.

1. Introduction

Given a point P in the plane of triangle ABC, let R_1, R_2, and R_3 denote the respective distances AP, BP, and CP. Let a, b, and c be the lengths of the sides of triangle ABC, s the semi-perimeter, L the area, R the circumradius, and r the inradius.

Liu [4] conjectured the following geometric inequality which holds for all points P in the plane of an arbitrary triangle ABC:

$$(R_1R_2)^{\frac{3}{2}} + (R_2R_3)^{\frac{3}{2}} + (R_3R_1)^{\frac{3}{2}} \geq 24r^3. \tag{1}$$

This inequality was proven by Wu, Zhang and Chu in [5], where it was strengthened to

$$(R_1R_2)^{\frac{3}{2}} + (R_2R_3)^{\frac{3}{2}} + (R_3R_1)^{\frac{3}{2}} \geq 12Rr^2. \tag{2}$$

Observe that (1) and (2) both reduce to Euler's inequality $R \geq 2r$, see [1, p. 48, Th. 5.1], whenever P is taken to be the circumcenter of triangle ABC.

Note that (2) cannot be improved upon by a multiplicative factor since there is equality in the case when triangle ABC is equilateral with P its center. The following question involving an additional non-negative term on the right-hand side is raised by the authors at the end of [5]:

Problem. For a triangle ABC and an arbitrary point P, determine the best possible k such that the following inequality holds:

$$(R_1R_2)^{\frac{3}{2}} + (R_2R_3)^{\frac{3}{2}} + (R_3R_1)^{\frac{3}{2}} \geq 12[R + k(R - 2r)]r^2. \tag{3}$$

In this paper, we will prove the following result by a different method than that used in [5] to show (1) and (2).

Publication Date: July 25, 2012. Communicating Editor: Paul Yiu.

Theorem 1. *The best possible k such that inequality* (3) *holds lies in the interval $[y, z]$, where $y \approx 0.14119$ and $z \approx 0.14364$. In particular, we have*

$$(R_1R_2)^{\frac{3}{2}} + (R_2R_3)^{\frac{3}{2}} + (R_3R_1)^{\frac{3}{2}} \geq 12[R + \frac{7}{50}(R - 2r)]r^2.$$

2. Preliminary results

Lemma 2. [5, Eq. 3.1] *If $j > 1$, then*

$$(R_1R_2)^j + (R_2R_3)^j + (R_3R_1)^j \geq \frac{(abc)^j}{[a^{\frac{j}{j-1}} + b^{\frac{j}{j-1}} + c^{\frac{j}{j-1}}]^{j-1}}.$$

Lemma 3. *Suppose p is a fixed number with $0 < p \leq \frac{8}{27}$. Let $t := w(a, b, c) = ab + bc + ca$, where a, b and c are real numbers, and let M denote the maximum value of t subject to the constraints $a + b + c = 2$ and $abc = p$.*
(i) *M is achieved by some point (a, b, c), where two of a, b, c are the same and $a, b, c > 0$.*
(ii) *One may assume further that M is achieved by some point (a, b, c), where $a = b$ and $\frac{2}{3} \leq a < 1$.*
(iii) *If $v := \frac{M-1}{p}$, then v satisfies $p = g(v)$, where g is the function given by*

$$g(x) = \frac{-8x^2 + 36x - 27 - (9 - 8x)^{\frac{3}{2}}}{8x^3}. \tag{4}$$

Proof. (i) A standard argument using the method of Lagrange multipliers with two constraints shows that two of $\{a, b, c\}$ must be the same when t is maximized. Note that $a, b, c > 0$ when t is maximized, for if say $b, c < 0$, then $r = ab + bc + ca = 2(b + c) - (b + c)^2 + bc < 0$, and clearly t can achieve positive values for all choices of p (for example, choosing $a, b > 0$ and $c = \frac{2}{3}$). Note further that there is no minimum for t, for if c is negative, then

$$t = ab + bc + ca = ab + c(2 - c) < ab = \frac{p}{c},$$

so choosing c near zero implies t can assume arbitrarily large negative values.

(ii) By part (i) and symmetry, the equality $w(a, b, c) = M$ subject to the constraints is achieved by some point (a, b, c), where $a = b$ and $0 < a < 1$ (note that $c > 0$ implies $a < 1$). Then a is a positive root of $\alpha(x) = p$, where $\alpha(x) := 2x^2(1 - x)$. Note that the function α is increasing on $(0, \frac{2}{3})$, decreasing on $(\frac{2}{3}, 1)$, and has a maximum of $\frac{8}{27}$ at $x = \frac{2}{3}$, with $\alpha(0) = \alpha(1) = 0$. If $p = \frac{8}{27}$, then $a = b = c = \frac{2}{3}$, by the equality condition in the geometric-arithmetic mean inequality, so we will assume $p < \frac{8}{27}$. Then the equation $\alpha(x) = p$ has two roots in the interval $(0, 1)$, which we will denote by $r_1 < r_2$; note that $0 < r_1 < \frac{2}{3} < r_2 < 1$.

We will now show that the maximum value M is achieved when $a = b = r_2 > \frac{2}{3}$ by comparing it to the value of $w(a, b, c)$ when $a = b = r_1$. Let $\beta(x) := w(x, x, 2-2x) = 4x-3x^2$. Note that $\beta(r_2) > \beta(r_1)$ iff $r_1 + r_2 < \frac{4}{3}$. To show the latter, first observe that $\alpha(x) > \alpha(\frac{4}{3} - x)$ for all $x \in (0, \frac{2}{3})$ since, for the function

$\gamma(x) := \alpha(x) - \alpha(\frac{4}{3} - x)$, we have $\gamma(\frac{2}{3}) = 0$ with $\gamma'(x) = -\frac{4}{3}(2-3x)^2 < 0$. Then $\alpha(\frac{4}{3} - r_1) < \alpha(r_1) = \alpha(r_2)$ implies $r_2 < \frac{4}{3} - r_1$, as desired, since $\alpha(x)$ is decreasing when $x > \frac{2}{3}$.

(iii) By part (ii), we have $v = \frac{\beta(a)-1}{p}$, where $\frac{2}{3} \le a < 1$ satisfies $2a^2(1-a) = p$. Thus,

$$v = \frac{4a - 3a^2 - 1}{2a^2(1-a)} = \frac{3a-1}{2a^2}. \tag{5}$$

Note that $1 < v \le \frac{9}{8}$ since $1 < \frac{3x-1}{2x^2} \le \frac{9}{8}$ if $x \in [\frac{2}{3}, 1)$. Solving for a in terms of v in (5) gives

$$a = \frac{3 + (9-8v)^{\frac{1}{2}}}{4v}, \tag{6}$$

where we reject the other root since $a \ge \frac{2}{3}$. From (5) and (6), we may write

$$\begin{aligned} p = \ 2a^2(1-a) &= \frac{(1-a)(3a-1)}{v} = \frac{-3\left(\frac{3a-1}{2v}\right) + 4a - 1}{v} \\ &= \frac{-2v + 3 - (9-8v)a}{2v^2} = \frac{-8v^2 + 12v - (3 + (9-8v)^{\frac{1}{2}})(9-8v)}{8v^3}, \end{aligned}$$

which gives the requested relation. □

Lemma 4. *Let a, b, c be real numbers such that $a+b+c = 2$ with $0 < a, b, c < 1$. Then we have*

$$1 + abc < ab + bc + ca \le 1 + \frac{9}{8}abc.$$

Proof. The proof of Lemma 3 shows the right inequality. The left one follows from expanding the obvious inequality $(1-a)(1-b)(1-c) > 0$, and noting $a+b+c = 2$. □

Lemma 5. *Let D consist of the set of ordered pairs (p, u) such that there exists a triangle of perimeter 2 having side lengths a, b, c with $p = abc$ and $u = \frac{ab+bc+ca-1}{abc}$. If $1 < u' \le \frac{9}{8}$ is fixed, then $p = g(u')$ is the smallest p such that $(p, u') \in D$.*

Proof. Note first that $(p, u) \in D$ implies $0 < p \le \frac{8}{27}$ and $1 < u \le \frac{9}{8}$, the latter by Lemma 4. Given $p_o \in (0, \frac{8}{27}]$, let u_o denote the solution of the equation $g(u) = p_o$, where $u \in (1, \frac{9}{8}]$ and g is given by (4) above. Note that u_o is uniquely determined since $g(1) = 0$ and $g(\frac{9}{8}) = \frac{8}{27}$, with $g(x)$ increasing on $(1, \frac{9}{8}]$ as

$$g'(x) = \frac{81 - 8x(9-x) + (27-12x)(9-8x)^{\frac{1}{2}}}{8x^4} > 0.$$

Observe further that the proof of the third part of Lemma 3 can be modified slightly to show that points of the form $(g(u), u)$ always belong to D whenever $u \in (1, \frac{9}{8}]$. Thus, from the third part of Lemma 3, we see that u_o is the *largest* u such that $(p_o, u) \in D$.

So $u \le u_o = g^{-1}(p_o)$ for all u such that $(p_o, u) \in D$, which implies $g(u) \le p_o$ for all such u. Conversely, if $u' \in (1, \frac{9}{8}]$ is fixed and $(p, u') \in D$, then $g(u') \le p$ for all such p. In particular, $p = g(u')$ is the smallest p such that $(p, u') \in D$. □

Lemma 6. *Let $f(u)$ be given by*

$$f(u)=\frac{[(3-6u)g(u)+2]^{-\frac{1}{2}}-3(u-1)^{\frac{1}{2}}}{3(u-1)^{\frac{1}{2}}-24(u-1)^{\frac{3}{2}}},$$

where $g(u)$ is given by

$$g(u)=\frac{-8u^2+36u-27-(9-8u)^{\frac{3}{2}}}{8u^3}.$$

If m is the minimum value of $f(u)$ on the interval $(1,\frac{9}{8}]$, then $m\approx 0.141194514$.

Proof. From the definitions, we have

$$\frac{d}{du}f(u)=\frac{\frac{6g(u)-(3-6u)\frac{d}{du}g(u)}{2((3-6u)g(u)+2)^{\frac{3}{2}}}-\frac{3}{2(u-1)^{\frac{1}{2}}}}{3(u-1)^{\frac{1}{2}}(9-8u)}-\frac{(25-24u)\left(\frac{1}{((3-6u)g(u)+2)^{\frac{1}{2}}}-3(u-1)^{\frac{1}{2}}\right)}{6(u-1)^{\frac{3}{2}}(9-8u)^2},$$

where

$$\frac{d}{du}g(u)=\frac{36-16u+12(9-8u)^{\frac{1}{2}}}{8u^3}+\frac{3(8u^2-36u+27+(9-8u)^{\frac{3}{2}})}{8u^4}.$$

The equation $\frac{d}{du}f(u)=0$ can be written as

$$\frac{(3-z)^{\frac{1}{2}}(3z^6-21z^5+40z^4-21z^3-3z^2+24z-18)+6(3-3z+3z^2-z^3)^{\frac{3}{2}}(1-z^2)^{\frac{3}{2}}}{(3-3z+3z^2-z^3)^{\frac{3}{2}}(1-z^2)^{\frac{3}{2}}z^4}=0,$$

where $u=(9-z^2)/8$. The last equation implies

$$36z^{12}-324z^{11}+1197z^{10}-2421z^9+3111z^8-2877z^7+2014z^6$$
$$-702z^5-897z^4+1983z^3-2097z^2+1125z-180=0.$$

With the aid of mathematical programming (such as Maple), one can show that the above polynomial equation has four real roots

$$z_1\approx -0.876333426, z_2\approx 0.257008823, z_3\approx 0.891710246, z_4\approx 2.374529908,$$

which implies

$$u_1\approx 1.029004966, u_2\approx 1.116743308, u_3\approx 1.025606605, u_4\approx 0.420200965.$$

Now $\frac{d}{du}f(u)|_{u=u_2}=0$, with $\frac{d}{du}f(u)|_{u=u_1}<0$ and $\frac{d}{du}f(u)|_{u=u_3}<0$. Thus, the equation $\frac{d}{du}f(u)=0$ has a unique real solution $u^*=u_2\approx 1.116743308$ on the interval $(1,\frac{9}{8})$.

Since $\lim_{u\to 1^+}f(u)=\infty$, $f(u^*)=0.141194514$, and $f(\frac{9}{8})=\lim_{u\to\frac{9}{8}^-}f(u)=\frac{1}{6}$, we see that the minimum value of $f(u)$ on the interval $(1,\frac{9}{8}]$ is approximately 0.141194514. □

Lemma 7. *Let $h(a)$ be given by*

$$h(a)=\frac{a^3(1-a)^3+2[a(1-a)(-a^2+4a-2)]^{\frac{3}{2}}-6a^2(1-a)^2(2a-1)^2}{6(1-a)^2(2a-1)^2(3a-2)^2}.$$

If n is the minimum value of $h(a)$ on the interval $(2-\sqrt{2},1)$, then $n\approx 0.143630168$.

Proof. Using mathematical programming such as Maple, one can show that the equation $\frac{d}{da}h(a) = 0$ has a unique real solution $a^* \approx 0.741049808$ on the interval $2 - \sqrt{2} < a < 1$. Since $h(2 - \sqrt{2}) = 2.178511254$, $h(\frac{2}{3}) = \lim_{a \to \frac{2}{3}} h(a) = \frac{1}{4}$, $h(a^*) = 0.143630168$, and $\lim_{a \to 1^-} h(a) = \infty$, we see that the minimum of $h(a)$ on the interval $2 - \sqrt{2} < a < 1$ is approximately 0.143630168. □

3. Proof of the main result

3.1. *The lower bound.* We first treat the lower bound in Theorem 1. By Lemma 2 with $j = \frac{3}{2}$, we may consider the inequality

$$\frac{(abc)^{\frac{3}{2}}}{(a^3 + b^3 + c^3)^{\frac{1}{2}}} \geq 12[R + k(R - 2r)]r^2,$$

which can be rewritten as

$$\frac{(abc)^{\frac{3}{2}}}{(a^3 + b^3 + c^3)^{\frac{1}{2}}} \geq \frac{3(1 + k)abcL}{s^2} - \frac{24kL^3}{s^3}, \tag{7}$$

using the facts $abc = 4Rrs$ and $L = rs$, see [3, Section 1.4]. By homogeneity, we may take $s = 1$ in (7). Recalling $L = \sqrt{s(s - a)(s - b)(s - c)}$ (see [2, p. 12, 1.53]), we wish to find the best possible k such that the inequality

$$\frac{(abc)^{\frac{3}{2}}}{(a^3 + b^3 + c^3)^{\frac{1}{2}}} \geq 3(1+k)abc[(1-a)(1-b)(1-c)]^{\frac{1}{2}} - 24k[(1-a)(1-b)(1-c)]^{\frac{3}{2}} \tag{8}$$

holds for all a, b, c satisfying $a + b + c = 2$ with $0 < a, b, c < 1$.

Let $p = abc$ and $t = ab + bc + ca$. From the algebraic identity,

$$\begin{aligned} a^3 + b^3 + c^3 - 3abc &= (a + b + c)(a^2 + b^2 + c^2 - ab - bc - ca) \\ &= (a + b + c)((a + b + c)^2 - 3(ab + bc + ca)), \end{aligned}$$

and $a + b + c = 2$, we get

$$a^3 + b^3 + c^3 = 3p + 2(2^2 - 3t) = 3p - 6t + 8.$$

Furthermore, we have

$$(1 - a)(1 - b)(1 - c) = 1 - (a + b + c) + (ab + bc + ca) - abc = t - p - 1.$$

Thus, (8) may be rewritten in terms of p and t as

$$\frac{p^{\frac{3}{2}}}{(3p - 6t + 8)^{\frac{1}{2}}} \geq 3(1 + k)p(t - p - 1)^{\frac{1}{2}} - 24k(t - p - 1)^{\frac{3}{2}}. \tag{9}$$

Dividing both sides of (9) by $p^{\frac{3}{2}}$, and letting $u = \frac{t-1}{p}$, we obtain the following inequality in p and u over the domain D defined above in Lemma 5:

$$\frac{1}{(3p - 6pu + 2)^{\frac{1}{2}}} \geq 3(1 + k)(u - 1)^{\frac{1}{2}} - 24k(u - 1)^{\frac{3}{2}}. \tag{10}$$

Next consider the function $h(p,u,k)$ defined by

$$h(p,u,k) = \frac{1}{(3p-6pu+2)^{\frac{1}{2}}} - 3(1+k)(u-1)^{\frac{1}{2}} + 24k(u-1)^{\frac{3}{2}}.$$

Since for each given $u \in (1, \frac{9}{8}]$, we have

$$\frac{d}{dp}h(p,u,k) = \frac{6u-3}{2(3p-6pu+2)^{\frac{3}{2}}} > 0$$

for all $p \in (0, \frac{8}{27})$, we may consider for each u, the *smallest* p such that $(p,u) \in D$ when determining the best possible constant k. That is, we may replace p with $g(u)$ when determining the best possible k in (10), by Lemma 5, where $u \in (1, \frac{9}{8}]$ and g is given by (4).

We rewrite (10) when $p = g(u)$ as $f(u) \geq k$, where

$$f(u) = \frac{[(3-6u)g(u)+2]^{-\frac{1}{2}} - 3(u-1)^{\frac{1}{2}}}{3(u-1)^{\frac{1}{2}} - 24(u-1)^{\frac{3}{2}}}.$$

Therefore, we seek the minimum value m of $f(u)$ over the interval $(1, \frac{9}{8}]$, and choosing $k = m$ will yield the largest k for which inequality (10), and hence (7), holds. By Lemma 6, we have $m \approx 0.14119$. By Lemma 2, we see that inequality (3) holds with $k = m$ and thus the best possible k in that inequality is at least m, which establishes our lower bound.

3.2. *The upper bound.* We now treat the upper bound given in Theorem 1. For this, we consider the original inequality (3), rewritten as

$$\frac{(R_1R_2)^{\frac{3}{2}} + (R_2R_3)^{\frac{3}{2}} + (R_3R_1)^{\frac{3}{2}}}{p^{\frac{3}{2}}} \geq 3(1+k)(u-1)^{\frac{1}{2}} - 24k(u-1)^{\frac{3}{2}}, \quad (11)$$

where we have divided through both sides by $p^{\frac{3}{2}}$, and u and p are as before with $a+b+c=2$. Equivalently, we consider the inequality

$$\frac{\frac{(R_1R_2)^{\frac{3}{2}} + (R_2R_3)^{\frac{3}{2}} + (R_3R_1)^{\frac{3}{2}}}{p^{\frac{3}{2}}} - 3(u-1)^{\frac{1}{2}}}{3(u-1)^{\frac{1}{2}} - 24(u-1)^{\frac{3}{2}}} \geq k, \quad (12)$$

and seek to find a triangle ABC of perimeter 2 and a point P in its plane such that the left-hand side is small. We take ABC to be an acute isosceles triangle and the point P to be the orthocenter of triangle ABC. Note that the sides of triangle ABC are a, a, and $2-2a$ for some a, where $2-\sqrt{2} < a < 1$. After several straightforward calculations, we see that (12) in this case may be rewritten in terms of a as $h(a) \geq k$, where

$$h(a) = \frac{a^3(1-a)^3 + 2[a(1-a)(-a^2+4a-2)]^{\frac{3}{2}} - 6a^2(1-a)^2(2a-1)^2}{6(1-a)^2(2a-1)^2(3a-2)^2}.$$

By Lemma 7, we see that the minimum value of $h(a)$ on the interval $(2-\sqrt{2}, 1)$ is approximately 0.14364, which gives our upper bound for k.

4. Fourth order inequalities

Liu [4] conjectured the following geometric inequality of fourth order,

$$(R_1R_2)^2 + (R_2R_3)^2 + (R_3R_1)^2 \geq 8(R^2 + 2r^2)r^2, \tag{13}$$

which was proven in [5], where it was strengthened to

$$(R_1R_2)^2 + (R_2R_3)^2 + (R_3R_1)^2 \geq 8(R + r)Rr^2. \tag{14}$$

Note that, since $R \geq 2r$, both (13) and (14) imply the inequality

$$(R_1R_2)^2 + (R_2R_3)^2 + (R_3R_1)^2 \geq 48r^4, \tag{15}$$

which is the $k = 2$ case of Theorem 4.4 in [5]. Here, we apply the prior reasoning and sharpen inequality (15), obtaining a new lower bound for the sum which is incomparable to the bounds given in (13) and (14). We also provide an alternate proof of inequality (14), though it does not appear that we are able to sharpen it using the present method.

4.1. *Sharpened form of* (15). We prove the following strengthened version of inequality (15).

Theorem 8. *For any triangle ABC and point P in its plane, we have*

$$(R_1R_2)^2 + (R_2R_3)^2 + (R_3R_1)^2 \geq 6(7R - 6r)r^3. \tag{16}$$

Proof. By Lemma 2 when $j = 2$, it suffices to show

$$\frac{(abc)^2}{a^2 + b^2 + c^2} \geq 6(7R - 6r)r^3 \tag{17}$$

for all triangles ABC with sides a, b, and c such that $a + b + c = 2$. Note that $4Rr = abc$, $r^2 = L^2 = (1 - a)(1 - b)(1 - c) = ab + bc + ca - abc - 1$, and $a^2 + b^2 + c^2 = 4 - 2(ab + bc + ca)$, since $a + b + c = 2$. Letting $p = abc$ and $t = ab + bc + ca$, we see that inequality (17) may thus be reexpressed as

$$\frac{p^2}{4 - 2t} \geq \frac{21}{2}p(t - p - 1) - 36(t - p - 1)^2.$$

Dividing through both sides of the last inequality by p^2, letting $u = \frac{t-1}{p}$, and rearranging, we see that it is equivalent to

$$w(p, u) := \frac{1}{1 - pu} - 21(u - 1) + 72(u - 1)^2 \geq 0. \tag{18}$$

Since for each $u \in (1, \frac{9}{8}]$, we have

$$\frac{d}{dp}w(p, u) = \frac{u}{(1 - pu)^2} > 0$$

for all $p \in (0, \frac{8}{27})$, it suffices to prove (18) in the case when $p = g(u)$, by Lemma 5, where g is given by (4). Rearranging inequality (18) when $p = g(u)$, and cancelling a factor of $9 - 8u$, we show equivalently that $\ell(u) \geq 0$, where

$$\ell(u) = (72u^2 - 165u + 93)(9 - 8u)^{\frac{1}{2}} - 144u^3 + 492u^2 - 619u + 279.$$

To do so, first observe that

$$\ell'(u) = \frac{-1440u^2 + 3276u - 1857}{(9-8u)^{\frac{1}{2}}} - 432u^2 + 984u - 619,$$

whence $\ell'(1) = -88 < 0$ and $\lim_{u \to \frac{9}{8}^-} \ell'(u) = \infty$. Since

$$\ell''(u) = \frac{17280u^2 - 39024u + 22056}{(9-8u)^{\frac{3}{2}}} + (984 - 864u) > 0, \qquad 1 < u < \frac{9}{8},$$

being the sum of two positive terms, it follows that the equation $\ell'(u) = 0$ has a unique real solution u^* on the interval $(1, \frac{9}{8})$. By any numerical method, we have $u^* \approx 1.123717946$. It follows that $\ell(u^*) \approx 0.205071273$ is the minimum value of the function ℓ on the interval $(1, \frac{9}{8}]$. In particular, we have $\ell(u) \geq 0$ if $1 < u \leq \frac{9}{8}$, which establishes (18) and completes the proof of (16). □

Remark: Note that right-hand side of (16) is at least as large as the right-hand side of (14) when $R \leq \frac{9}{4}r$ and is smaller when $R > \frac{9}{4}r$.

4.2. *An alternate proof of* (14). Here, we provide an alternative proof for (14) to the one given in [5]. By the $j = 2$ case of Lemma 2, it is enough to show

$$\frac{(abc)^2}{a^2 + b^2 + c^2} \geq 8(R + r)Rr^2 \tag{19}$$

for a triangle ABC with side lengths a, b and c, where we may assume $a+b+c = 2$. Upon dividing through both sides of inequality (19) by $(abc)^2$, we see that it may be rewritten in terms of $p = abc$ and $u = \frac{ab+bc+ca-1}{abc}$ as

$$\frac{1}{2(1-pu)} \geq \frac{1}{2} + 2(u-1). \tag{20}$$

It suffices to show (20) in the case when $p = g(u)$, where g is given by (4), by Lemma 5, since the difference of the two sides is an increasing function of p for each u. To show the inequality

$$(4u-3)(1 - ug(u)) \leq 1, \qquad 1 < u \leq \frac{9}{8},$$

i.e.,

$$\frac{(4u-3)(16u^2 - 36u + 27 + (9-8u)^{\frac{3}{2}})}{8u^2} \leq 1,$$

we first rewrite it as

$$-64u^3 + 200u^2 - 216u + 81 \geq (4u-3)(9-8u)^{\frac{3}{2}}.$$

Cancelling factors of $9 - 8u$ from both sides of the last inequality then gives

$$8u^2 - 16u + 9 \geq (4u-3)(9-8u)^{\frac{1}{2}}. \tag{21}$$

Finally, to show that (21) holds for $1 < u \leq \frac{9}{8}$, note that for the function

$$v(u) := \frac{8u^2 - 16u + 9}{4u - 3} - (9-8u)^{\frac{1}{2}},$$

we have $v(1) = 0$ with

$$v'(u) = 2 - \frac{6}{(4u-3)^2} + \frac{4}{(9-8u)^{\frac{1}{2}}} > 0, \qquad 1 < u < \frac{9}{8}.$$

References

[1] O. Bottema, R. Ž. Djordević, R. R. Janić, D. S. Mitrinović, and P. M. Vasić, *Geometric Inequalities*, Wolters-Noordhoff Publishing, Groningen, The Netherlands, 1969.

[2] H. S. M. Coxeter, *Introduction to Geometry*, John Wiley & Sons, Inc., New York, 1961.

[3] H. S. M. Coxeter and S. L. Greitzer, *Geometry Revisited*, Random House Publishing, New York, 1967.

[4] J. Liu, Nine sign inequality, manuscript, (in Chinese) 33 pages, 2008.

[5] Y. D. Wu, Z. H. Zhang, and X. G. Chu, On a geometric inequality by J. Sándor, *J. Inequal. Pure and Appl. Math.* **10 (4)** (2009) Art. 118 (8 pages).

Toufik Mansour: Department of Mathematics, University of Haifa, 31905 Haifa, Israel
E-mail address: toufik@math.haifa.ac.il

Mark Shattuck: Department of Mathematics, University of Tennessee, Knoxville, Tennessee 37996, US
E-mail address: shattuck@math.utk.edu

Forum Geometricorum
Volume 12 (2012) 237–241.

FORUM GEOM
ISSN 1534-1178

Maximal Area of a Bicentric Quadrilateral

Martin Josefsson

Abstract. We prove an inequality for the area of a bicentric quadrilateral in terms of the radii of the two associated circles and show how to construct the quadrilateral of maximal area.

1. Introduction

A bicentric quadrilateral is a convex quadrilateral that has both an incircle and a circumcircle, so it is both tangential and cyclic. Given two circles, one within the other with radii r and R (where $r < R$), then a necessary condition that there can be a bicentric quadrilateral associated with these circles is that the distance δ between their centers satisfies Fuss' relation

$$\frac{1}{(R+\delta)^2} + \frac{1}{(R-\delta)^2} = \frac{1}{r^2}.$$

A beautiful elementary proof of this was given by Salazar (see [8], and quoted at [1]). According to [9, p.292], this is also a sufficient condition for the existence of a bicentric quadrilateral. Now if there for two such circles exists one bicentric quadrilateral, then according to Poncelet's closure theorem there exists infinitely many; any point on the circumcircle can be a vertex for one of these bicentric quadrilaterals [11]. That is the configuration we shall study in this note. We derive a formula for the area of a bicentric quadrilateral in terms of the inradius, the circumradius and the angle between the diagonals, conclude for which quadrilateral the area has its maximum value in terms of the two radii, and show how to construct that maximal quadrilateral.

2. More on the area of a bicentric quadrilateral

In [4] and [3, §6] we derived a few new formulas for the area of a bicentric quadrilateral. Here we will prove another area formula using properties of bicentric quadrilaterals derived by other authors.

Theorem 1. *If a bicentric quadrilateral has an incircle and a circumcircle with radii r and R respectively, then it has the area*

$$K = r\left(r + \sqrt{4R^2 + r^2}\right)\sin\theta$$

Publication Date: October 18, 2012. Communicating Editor: Paul Yiu.

where θ is the angle between the diagonals.

Proof. We give two different proofs. Both of them uses the formula

$$K = \tfrac{1}{2}pq\sin\theta \tag{1}$$

which gives the area of a convex quadrilateral with diagonals p, q and angle θ between them.

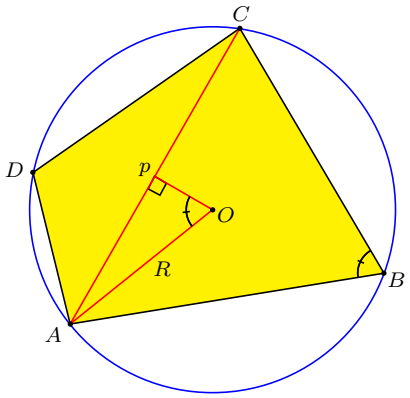

Figure 1. Using the inscribed angle theorem

First proof. In a cyclic quadrilateral it is easy to see that the diagonals satisfy $p = 2R\sin B$ and $q = 2R\sin A$ (see Figure 1). Inserting these into (1) we have that a cyclic quadrilateral has the area [1]

$$K = 2R^2\sin A\sin B\sin\theta. \tag{2}$$

In [13] Yun proved that in a bicentric quadrilateral $ABCD$ (which he called a double circle quadrilateral),

$$\sin A\sin B = \frac{r^2 + r\sqrt{4R^2 + r^2}}{2R^2}.$$

Inserting this into (2) proves the theorem.

Second proof. In [2, pp.249, 271–275] it is proved that the inradius in a bicentric quadrilateral is given by

$$r = \frac{pq}{2\sqrt{pq + 4R^2}}.$$

Solving for the product of the diagonals gives

$$pq = 2r\left(r + \sqrt{4R^2 + r^2}\right)$$

where we chose the solution of the quadratic equation with the plus sign since the product of the diagonals is positive. Inserting this into (1) directly yields the theorem. □

[1] A direct consequence of this formula is the inequality $K \leq 2R^2$ in a cyclic quadrilateral, with equality if and only if the quadrilateral is a square.

Remark. According to [12, p.164], it was Problem 1376 in the journal Crux Mathematicorum to derive the equation

$$\frac{pq}{4r^2} - \frac{4R^2}{pq} = 1$$

in a bicentric quadrilateral. Solving this also gives the product pq in terms of the radii r and R.

Corollary 2. *If a bicentric quadrilateral has an incircle and a circumcircle with radii r and R respectively, then its area satisfies*

$$K \leq r\left(r + \sqrt{4R^2 + r^2}\right)$$

where there is equality if and only if the quadrilateral is a right kite.

Proof. There is equality if and only if the angle between the diagonals is a right angle, since $\sin\theta \leq 1$ with equality if and only if $\theta = \frac{\pi}{2}$. A tangential quadrilateral has perpendicular diagonals if and only if it is a kite according to Theorem 2 (i) and (iii) in [5]. Finally, a kite is cyclic if and only if two opposite angles are right angles since it has a diagonal that is a line of symmetry and opposite angles in a cyclic quadrilateral are supplementary angles. □

We also have that the semiperimeter of a bicentric quadrilateral satisfies

$$s \leq r + \sqrt{4R^2 + r^2}$$

where there is equality if and only if the quadrilateral is a right kite. This is a direct consequence of Corollary 2 and the formula $K = rs$ for the area of a tangential quadrilateral. To derive this inequality was a part of Problem 1203 in Crux Mathematicorum according to [10, p.39]. Another part of that problem was to prove that in a bicentric quadrilateral, the product of the sides satisfies

$$abcd \leq \tfrac{16}{9}r^2(4R^2 + r^2).$$

It is well known that the left hand side gives the square of the area of a bicentric quadrilateral (a short proof is given in [4, pp.155–156]). Thus the inequality can be restated as

$$K \leq \tfrac{4}{3}r\sqrt{4R^2 + r^2}.$$

This is a weaker area inequality than the one in Corollary 2, which can be seen in the following way. An inequality between the two radii of a bicentric quadrilateral is $R \geq \sqrt{2}r$.[2] From this it follows that $4R^2 \geq 8r^2$, and so

$$3r \leq \sqrt{4R^2 + r^2}.$$

Hence, from Theorem 1, we have

$$\frac{K}{r} \leq r + \sqrt{4R^2 + r^2} \leq \tfrac{4}{3}\sqrt{4R^2 + r^2}$$

so the expression in Corollary 2 gives a sharper upper bound for the area.

[2]References to several different proofs of this inequality are given at the end of [6], where we provided a new proof of an extension to this inequality.

3. Construction of the maximal bicentric quadrilateral

Given two circles, one within the other, and assuming that a bicentric quadrilateral exist inscribed in the larger circle and circumscribed around the smaller, then among the infinitely many such quadrilaterals that are associated with these circles, Corollary 2 states that the one with maximal area is a right kite. Since a kite has a diagonal that is a line of symmetry, the construction of this is easy. Draw a line through the two centers of the circles. It intersect the circumcircle at A and C. Now all that is left is to construct tangents to the incircle through A. This is done by constructing the midpoint M between the incenter I and A, and drawing the circle with center M and radius MI according to [7]. This circle intersect the incircle at E and F. Draw the tangents AE and AF extended to intersect the circumcircle at B and D. Finally connect the points $ABCD$, which is the right kite with maximal area of all bicentric quadrilaterals associated with the two circles having centers I and O.

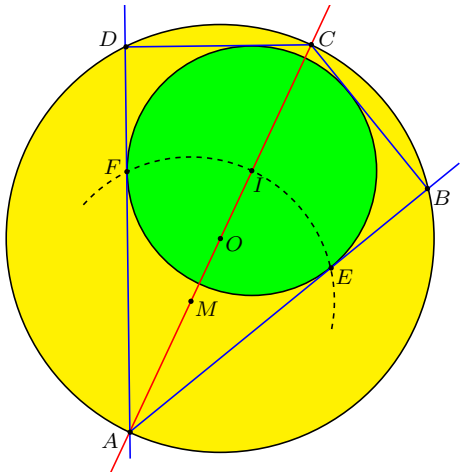

Figure 2. Construction of the right kite $ABCD$

References

[1] A. Bogomolny, Fuss' Theorem, *Interactive Mathematics Miscellany and Puzzles*, `http://www.cut-the-knot.org/Curriculum/Geometry/Fuss.shtml`

[2] H. Fukagawa and T. Rothman, *Sacred Mathematics, Japanese Temple Geometry*, Princeton university press, 2008.

[3] M. Josefsson, Calculations concerning the tangent lengths and tangency chords of a tangential quadrilateral, *Forum Geom.*, 10 (2010) 119–130.

[4] M. Josefsson, The area of a bicentric quadrilateral, *Forum Geom.*, 11 (2011) 155–164.

[5] M. Josefsson, When is a tangential quadrilateral a kite?, *Forum Geom.*, 11 (2011) 165–174.

[6] M. Josefsson, A new proof of Yun's inequality for bicentric quadrilaterals, *Forum Geom.*, 12 (2012) 79–82.

[7] *Math Open Reference*, Tangents through an external point, 2009, `http://www.mathopenref.com/consttangents.html`

[8] J. C. Salazar, Fuss' theorem, *Math. Gazette*, 90 (2006) 306–307.

[9] M. Saul, *Hadamard's Plane Geometry, A Reader's Companion,* Amer. Math. Society, 2010.
[10] E. Specht, *Inequalities proposed in "Crux Mathematicorum"*, 2007, available at http://hydra.nat.uni-magdeburg.de/math4u/ineq.pdf
[11] E. W. Weisstein, Bicentric Polygon, *MathWorld* – A Wolfram Web Resource, Accessed 22 April 2012, http://mathworld.wolfram.com/BicentricPolygon.html
[12] P. Yiu, *Notes on Euclidean Geometry*, Florida Atlantic University Lecture Notes, 1998.
[13] Z. Yun, Euler's inequality revisited, *Mathematical Spectrum*, 40 (2008) 119–121.

Martin Josefsson: Västergatan 25d, 285 37 Markaryd, Sweden
E-mail address: martin.markaryd@hotmail.com

Forum Geometricorum
Volume 12 (2012) 243–245.

FORUM GEOM
ISSN 1534-1178

The Maltitude Construction in a Convex Noncyclic Quadrilateral

Maria Flavia Mammana

Abstract. This note is linked to a recent paper of O. Radko and E. Tsukerman. We consider the maltitude construction in a convex noncyclic quadrilateral and we determine a point that can be viewed as a generalization of the anticenter.

1. Introduction

In [5] it is investigated the perpendicular bisector construction in a noncyclic quadrilateral $\mathcal{Q} = \mathcal{Q}^{(0)} = ABCD$. The perpendicular bisectors of the sides of $\mathcal{Q}$ determine a noncyclic quadrilateral $\mathcal{Q}^{(1)} = A_1B_1C_1D_1$, whose vertices are the centers of the triad circles, *i.e.*, the circles passing through three vertices of $\mathcal{Q}$. This process can be iterated to obtain a sequence of noncyclic quadrilaterals: $\mathcal{Q}^{(0)}$, $\mathcal{Q}^{(1)}$, $\mathcal{Q}^{(2)}$, ...

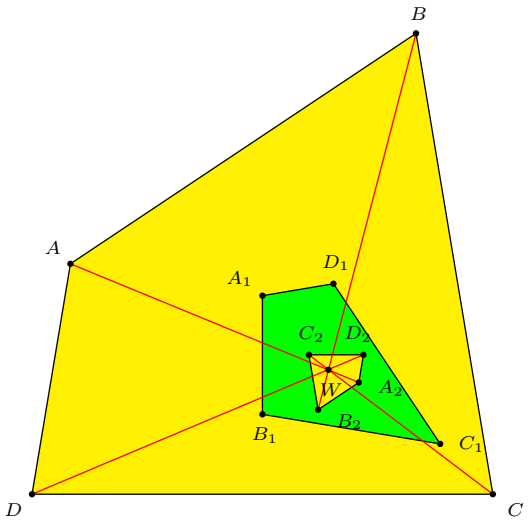

Figure 1.

All even generation quadrilaterals are similar, and all odd generation quadrilaterals are similar. Further, there is a point W that serves as the center of the spiral similarity for any pair of quadrilaterals $\mathcal{Q}^{(n)}$, $\mathcal{Q}^{(n+2)}$. If $\mathcal{Q}$ is a convex noncyclic quadrilateral, the quadrilaterals $\mathcal{Q}^{(n)}$, $\mathcal{Q}^{(n+2)}$ are homotetic, the ratio of similarity is a negative constant and the quadrilaterals in the iterated perpendicular bisectors construction converge to W. In a convex noncyclic quadrilateral the limit point W can be viewed as a generalization of the circumcenter.

Publication Date: November 5, 2012. Communicating Editor: Paul Yiu.

2. Characteristic and affinity

In [3] it is proved that if $\mathcal{Q}$ is a convex quadrilateral, then $\mathcal{Q}^{(1)}$ is affine to $\mathcal{Q}$. It follows that, for any n, $\mathcal{Q}^{(n+1)}$ is affine to $\mathcal{Q}^{(n)}$.

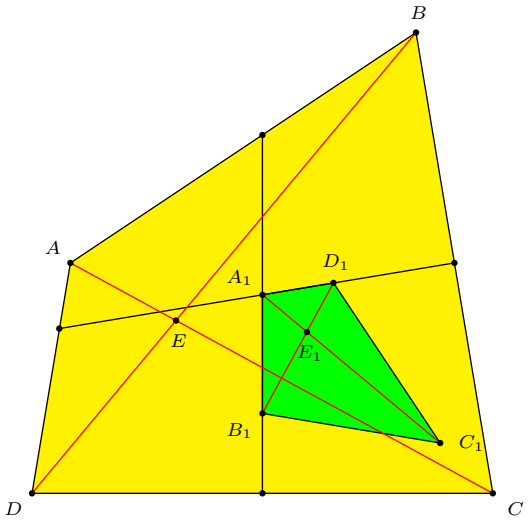

Figure 2.

For the convenience of the reader, we give a proof of this property. In [2] it is defined the characteristic of a quadrilateral $\mathcal{Q}$ as follows. Let E be the common point of the diagonals AC and BD of $\mathcal{Q}$. For the ratios $\frac{AE}{EC}$ and $\frac{CE}{EA}$, let h be the one not greater than 1. Also for the ratios $\frac{BE}{ED}$ and $\frac{DE}{EB}$, let k be the one not greater than 1. The pair $\{h, k\}$ is the characteristic of $\mathcal{Q}$. In [2] it is proved that two convex quadrilaterals are affine if and only if they have the same characteristic. We consider now the quadrilateral $\mathcal{Q}^{(1)} = A_1B_1C_1D_1$. The line A_1C_1 is perpendicular to the radical axis BD of the circle passing through B, C, D and the circle passing through A, B, D. Similarly, the line B_1D_1 is perpendicular to the line AC. Further, the lines A_1B_1, B_1C_1, C_1D_1, D_1A_1 are perpendicular to the lines DC, AD, BA, CB, respectively. It follows that, if E_1 is the common point of diagonals A_1C_1 and B_1D_1 of $\mathcal{Q}^{(1)}$, the triangle pairs ABE and $C_1D_1E_1$, BCE and $A_1D_1E_1$, CDE and $A_1B_1E_1$ are similar. Therefore we have

$$\frac{AE}{BE} = \frac{E_1D_1}{E_1C_1}, \qquad \frac{BE}{EC} = \frac{A_1E_1}{E_1D_1}, \qquad \frac{EC}{ED} = \frac{B_1E_1}{A_1E_1},$$

from which

$$\frac{AE}{EC} = \frac{A_1E_1}{E_1C_1}, \qquad \frac{BE}{ED} = \frac{B_1E_1}{E_1D_1}.$$

Thus, $\mathcal{Q}$ and $\mathcal{Q}^{(1)}$ have the same charactristic and are affine.

3. Maltitudes

In [3] it is considered also the quadrilateral $\mathcal{Q}_m$ determined by the maltitudes of a convex noncyclic quadrilateral $\mathcal{Q}$. A maltitude of $\mathcal{Q}$ is the perpendicular line

through the midpoint of a side to the opposite side [1]. In [4] it is proved that the maltitudes are concurrent in a point, called anticenter, if and only if $\mathcal{Q}$ is cyclic.

In [3] it is proved that the quadrilateral $\mathcal{Q}_m = A_1'B_1'C_1'D_1'$ is the symmetric of $\mathcal{Q}^{(1)}$ with respect to the centroid G of $\mathcal{Q}$.This property follows from the fact that the maltitudes of $\mathcal{Q}$ are transformed into the perpendicular bisectors of $\mathcal{Q}$ in the half-turn about G.

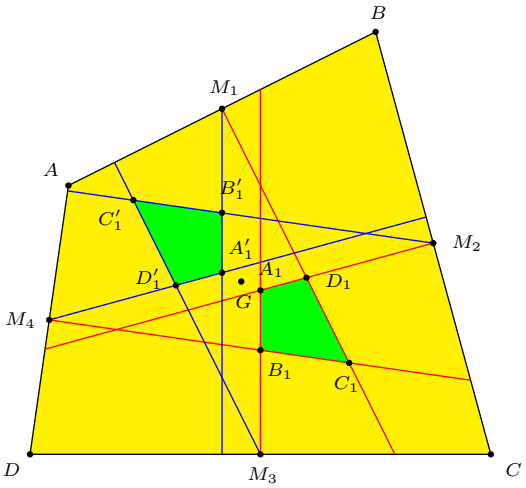

Figure 3.

The existence of the point W, as the limit point in the iterated perpendicular bisectors construction, implies that the symmetric W' of W with respect to G is the limit point in the iterated maltitudes construction. Furthermore, in a convex noncyclic quadrilateral the limit point W' can be viewed as a generalization of the anticenter.

We observe that in a cyclic quadrilateral the circumcenter and the anticenter are symmetric with respect to the centroid. If $\mathcal{Q}$ is a convex noncyclic quadrilateral, in analogy with the case of a cyclic quadrilateral, we call the line containing G, W and W' the *Euler line* of $\mathcal{Q}$.

References

[1] R. Honsberger, *Episodes in Nineteenth and Twentieth Century Euclidean Geometry*, MAA, 1995.

[2] C. Mammana and B. Micale, Una classificazione affine dei quadrilateri, *La Matematica e la sua Didattica*, 3 (1999) 323–328.

[3] M. F. Mammana and B. Micale, Quadrilaterals of triangle centres, *Math. Gazette*, 92 (2008) 466–475.

[4] B. Micale and M. Pennisi, On the altitudes of quadrilaterals, *Int. J. Math. Educ. Sci. Technol.*, 36 (2005) 15–24.

[5] O. Radko and E. Tsukerman, The perpendicular bisector construction, isoptic point and Simson line, *Forum Geom.*, 12 (2012) 161–189.

Maria Flavia Mammana: Department of Mathematics and Computer Science, University of Catania, Viale A. Doria 5, 95125, Catania, Italy

E-mail address: fmammana@dmi.unict.it

Forum Geometricorum
Volume 12 (2012) 247–254.

FORUM GEOM
ISSN 1534-1178

Using Complex Weighted Centroids to Create Homothetic Polygons

Harold Reiter and Arthur Holshouser

Abstract. After first defining weighted centroids that use complex arithmetic, we then make a simple observation which proves Theorem 1. We next define complex homothety. We then show how to apply this theory to triangles (or polygons) to create endless numbers of homothetic triangles (or polygon). The first part of the paper is fairly standard. However, in the final part of the paper, we give two examples which illustrate that examples can easily be given in which the simple basic underpinning is so disguised that it is not at all obvious. Also, the entire paper is greatly enhanced by the use of complex arithmetic.

1. Introduction to the basic theory

Suppose A, B, C, x, y are complex numbers that satisfy $xA+yB = C$, $x+y = 1$. It easily follows that $A+y\,(B-A) = C$ and $x\,(A-B)+B = C$. This simple observation with its geometric interpretation is the basis of this paper.

Definition. Suppose $M_1, M_2, \ldots, M_m$ are points in the complex plane and k_1, k_2, …, k_m are complex numbers that satisfy $\sum_{i=1}^{m} k_i = 1$. Of course, each complex point M_i is also a complex number. The weighted centroid of these complex points $\{M_1, M_2, \ldots, M_m\}$ with respect to $\{k_1, k_2, \ldots, k_m\}$ is a complex point G_M defined by $G_M = \sum_{i=1}^{m} k_i M_i$.

The complex numbers k_1, k_2, …, k_m are called weights and in the notation G_M it is always assumed that the reader knows what these weights are.

If k_1, k_2, …, k_m, $\overline{k_1}$, $\overline{k_2}$, …, $\overline{k_n}$ are complex numbers, we denote the sums $S_k = \sum_{i=1}^{m} k_i$, $S_{\overline{k}} = \sum_{i=1}^{n} \overline{k_i}$.

Suppose M_1, M_2, …, M_m, $\overline{M_1}$, $\overline{M_2}$, …, $\overline{M_n}$ are points in the complex plane. Also, k_1, k_2, …, k_m, $\overline{k_1}$, $\overline{k_2}$, …, $\overline{k_n}$ are complex numbers that satisfy $\sum_{i=1}^{m} k_i + \sum_{i=1}^{n} \overline{k_i} = 1$. Thus, $S_k + S_{\overline{k}} = 1$.

Publication Date: November 30, 2012. Communicating Editor: Paul Yiu.

Denote $G_{M\cup\overline{M}} = \sum_{i=1}^{m} k_i M_i + \sum_{i=1}^{n} \overline{k_i}\,\overline{M_i}$.

Thus, $G_{M\cup\overline{M}}$ is the weighted centroid of $\left\{M_1, \ldots, M_m, \overline{M}_1, \ldots, \overline{M}_n\right\}$ with respect to the weights $\left\{k_1, \ldots, k_m, \overline{k_1}, \ldots, \overline{k_n}\right\}$.

It is obvious that $\sum_{i=1}^{m} \frac{k_i}{S_k} = 1$ and $\sum_{i=1}^{n} \frac{\overline{k_i}}{S_{\overline{k}}} = 1$.

Denote $G_M = \sum_{i=1}^{m} \frac{k_i}{S_k} M_i$ and $G_{\overline{M}} = \sum_{i=1}^{n} \frac{\overline{k_i}}{S_{\overline{k}}} \overline{M_i}$.

Thus, G_M is the weighted centroid of $\{M_1, M_2, \ldots, M_m\}$ with respect to the weights $\left\{\frac{k_1}{S_k}, \frac{k_2}{S_k}, \ldots, \frac{k_m}{S_k}\right\}$ and $G_{\overline{M}}$ is the weighted centroid of $\left\{\overline{M_1}, \overline{M_2}, \ldots, \overline{M_n}\right\}$ with respect to the weights $\left\{\frac{\overline{k_1}}{S_{\overline{k}}}, \frac{\overline{k_2}}{S_{\overline{k}}}, \ldots, \frac{\overline{k_n}}{S_{\overline{k}}}\right\}$.

As always, these weights are understood in the notation $G_M, G_{\overline{M}}$.

Since $G_{M\cup\overline{M}} = \sum_{i=1}^{m} k_i M_i + \sum_{i=1}^{n} \overline{k_i}\,\overline{M}_i = S_k \cdot \sum_{i=1}^{m} \frac{k_i}{S_k} M_i + S_{\overline{k}} \cdot \sum_{i=1}^{n} \frac{\overline{k}_i}{S_{\overline{k}}} \overline{M}_i$ it is obvious that $(*)$ is true.

$(*)$ $S_k \cdot G_M + S_{\overline{k}} \cdot G_{\overline{M}} = G_{M\cup\overline{M}}$ where $S_k + S_{\overline{k}} = 1$.

From equation $(*)$ and $S_k + S_{\overline{k}} = 1$ it is easy to see that (1) and (2) are true.

(1) $G_M + S_{\overline{k}}\left(G_{\overline{M}} - G_M\right) \equiv G_{M\cup\overline{M}}$.

(2) $G_{\overline{M}} + S_k\left(G_M - G_{\overline{M}}\right) \equiv G_{M\cup\overline{M}}$.

2. Basic theorem

The identity $(*)$ and the formula (1) of § 1 proves the following Theorem 1.

Theorem 1. *Suppose M_1, M_2, …, M_m, $\overline{M_1}$, $\overline{M_2}$, …, $\overline{M_n}$ are points in the complex plane. Also, suppose $P = \sum_{i=1}^{m} k_i M_i + \sum_{i=1}^{n} \overline{k_i}\,\overline{M_i}$ where k_1, …, k_m, $\overline{k_1}$, …, $\overline{k_n}$ are complex numbers that satisfy $\sum_{i=1}^{m} k_i + \sum_{i=1}^{n} \overline{k_i} = 1$. Then there exists complex numbers $x_1, x_2, \ldots, x_m$ where $\sum_{i=1}^{m} x_i = 1$ and there exists complex numbers $y_1, y_2, \ldots, y_n$ where $\sum_{i=1}^{n} y_i = 1$ and there exists a complex number z such that the following are true.*

(1). *$x_1, \ldots, x_m, y_1, \ldots, y_n, z$ are rational function of k_1, …, k_m, $\overline{k_1}$, …,$\overline{k_n}$.*

(2). *$P = Q + z\,(R - Q)$ where Q, R are defined by $Q = \sum_{i=1}^{m} x_i M_i, R = \sum_{i=1}^{n} y_i \overline{M_i}$.*

As we illustrate in Section 6, the values of x_1, …, x_m, y_1, …, y_n, z as rational functions of k_1, k_2, …, k_m, $\overline{k_1}$, $\overline{k_2}$, …, $\overline{k_n}$ can be computed adhoc from any specific situation that we face in practice. We observe that Q is the weighted centroid of the complex points M_1, M_2, …, M_m using the weights x_1, x_2, …, x_m and R is

the weighted centroid of the complex points $\overline{M_1}$, $\overline{M_2}$, ..., , $\overline{M_n}$ using the weights $y_1, y_2, \ldots, y_n$. Of course, Theorem 1 is completely standard.

3. Complex homothety

If A, B are points in the complex plane, we denote $AB = B - A$. This also means that AB is the complex vector from A to B. Also, we define $|AB|$ to be the length of this vector AB. If k is any complex number, then $k = r(\cos\theta + i\sin\theta)$, $r \geq 0$, is the polar form of k. It is assumed that the reader knows that

$$[r(\cos\theta + i\sin\theta)] \cdot [\overline{r}(\cos\phi + i\sin\phi)] = r \cdot \overline{r}(\cos(\theta+\phi) + i\sin(\theta+\phi)).$$

Suppose $S, P, \overline{P}$ where $S \neq P, S \neq \overline{P}$ are points in the complex plane and $k = r(\cos\theta + i\sin\theta)$, $r > 0$, is a non-zero complex number. Also, suppose $S\overline{P} = k(SP)$ whereas always $S\overline{P} = \overline{P} - S$ and $SP = P - S$. Since

$$S\overline{P} = k(SP) = [r(\cos\theta + i\sin\theta)] \cdot (SP) = (\cos\theta + i\sin\theta) \cdot [r \cdot (SP)],$$

we see that the complex vector $S\overline{P}$ can be constructed from the complex vector SP in the following two steps.

First, we multiply the vector SP by the positive real number (or scale factor) r to define a new vector, $SP' = r \cdot (SP)$. Since $SP' = P' - S$, the new point P' is collinear with S and P with P, P' lying on the same side of S and $|SP'| = r \cdot |SP|$.

Next, we rotate the vector SP' by θ radians counterclockwise about the origin O as the axis to define the final vector $S\overline{P}$. Of course, the final point $\overline{P}$ itself is computed by rotating the point P' by θ radians counterclockwise about the axis S. If A, B, C, x, y are complex and $xA + yB = C$, $x + y = 1$, then $A + y(B - A) = C$. Therefore, $AC = y \cdot AB$ and if $y = r(\cos\theta + i\sin\theta)$,, $r \geq 0$, we see how to construct the point C.

From this construction, the following is obvious. Suppose $S \neq P$ are arbitrary variable points in the complex plane and $S\overline{P} = k \cdot (SP)$ where $k \neq 0$ is a fixed complex number.

Then the triangles $\triangle SP\overline{P}$ will always have the same geometric shape (up to similarity) since $\angle PS\overline{P} = \theta$ and $\left|S\overline{P}\right| : |SP| = r : 1$ when $k = r(\cos\theta + i\sin\theta)$, $r > 0$. Next, let us suppose that the complex triangles $\triangle ABC$ and $\triangle\overline{ABC}$ and the complex point S are related as follows:

$$S\overline{A} = k \cdot (SA),\ S\overline{B} = k \cdot (SB),\ S\overline{C} = k \cdot (SC),$$

where $k \neq 0$ is some fixed complex number.

We call this relation complex homothety (or complex similitude). Also, S is the center of homothety (or similitude) and k is the homothetic ratio (or ratio of similitude). When k is real we have the usual homothety of two triangle. Of course, for both real or complex k, it is fairly obvious that $\triangle ABC$, and $\triangle\overline{ABC}$ are always geometrically similar and $\frac{\left|\overline{AB}\right|}{|AB|} = \frac{\left|\overline{AC}\right|}{|AC|} = \frac{\left|\overline{BC}\right|}{|BC|} = |k|$.

Of course, this same definition of complex homothety also holds for two polygons $ABCDE, \ldots$ and $\overline{A}\ \overline{B}\ \overline{C}\ \overline{D}\ \overline{E}, \ldots$.

4. Using Theorem 1 to create endless homothetic triangles

Let M_1, M_2, …, M_m, $\overline{M_{a1}}$, $\overline{M_{a2}}$, …, $\overline{M_{an}}$, $\overline{M_{b1}}$, $\overline{M_{b2}}$, …, $\overline{M_{bn}}$, $\overline{M_{c1}}$, $\overline{M_{c2}}$, …, $\overline{M_{cn}}$ be any points in the plane.

As a specific example of this, we could start with a triangle $\triangle ABC$ and let M_1, M_2, …, M_m be any fixed points in the plane of $\triangle ABC$ such as the centroid, orthocenter, Lemoine point, incenter, Nagel point, etc.

Also, $\overline{M_{a1}}$, …, $\overline{M_{an}}$ are fixed points that have some relation to side BC. $\overline{M_{b1}}$, …, $\overline{M_{bn}}$ are fixed points that have some relation to side AC and $\overline{M_{c1}}$,…, $\overline{M_{cn}}$ are fixed points that have some relation to side AB.

Let k_1, k_2, …, k_m, $\overline{k_1}$, $\overline{k_2}$, …, $\overline{k_n}$ be arbitrary but fixed complex numbers that satisfy $\sum_{i=1}^{m} k_i + \sum_{i=1}^{n} \overline{k_i} = 1$.

Define points P_a, P_b, P_c as follows.

(1) $P_a = \sum_{i=1}^{m} k_i M_i + \sum_{i=1}^{n} \overline{k}_i \overline{M}_{ai}$.

(2) $P_b = \sum_{i=1}^{m} k_i M_i + \sum_{i=1}^{n} \overline{k}_i \overline{M}_{bi}$.

(3) $P_c = \sum_{i=1}^{m} k_i M_i + \sum_{i=1}^{n} \overline{k}_i \overline{M}_{ci}$.

Note that these points P_a, P_b, P_c are being defined in an analogous way. From Theorem 1, there exists complex numbers x_1, x_2, …, x_m where $\sum_{i=1}^{m} x_i = 1$, y_1, y_2, …, y_n where $\sum_{i=1}^{n} y_i = 1$, and z such that the following statements are true.

(1) x_1, …, x_m, y_1, y_2, …, y_n, z are rational functions of k_1, …, k_m, $\overline{k_1}$, …, $\overline{k_n}$.

(2) $P_a = Q + z\,(R_a - Q)$, $P_b = Q + z\,(R_b - Q)$, $R_c = P + z\,(R_c - Q)$, where $Q = \sum_{i=1}^{m} x_i M_i$, and $R_a = \sum_{i=1}^{n} y_i \overline{M}_{ai}$, $R_b = \sum_{i=1}^{n} y_i \overline{M}_{bi}$, $R_c = \sum_{i=1}^{n} y_i \overline{M}_{ci}$.

(3) $QP_a = z \cdot (QR_a)$, $QP_b = z \cdot (QR_b)$, $QP_c = z \cdot (QR_c)$.

(3) follows from (2) since, for example, $P_a - Q = QP_a$.

From (3) it also follows that $\triangle P_a P_b P_c$ is homothetic to $\triangle R_a R_b R_c$ with a center of homothety Q and a ratio of homothety $\frac{QP_a}{QR_a} = \frac{QP_b}{QR_b} = \frac{QP_c}{QR_c} = z$. Also, of course, $\triangle P_a P_b P_c \sim \triangle R_a R_b R_c$ with a ratio of similarity $\frac{|P_a P_b|}{|R_a R_b|} = \frac{|P_a P_c|}{|R_a R_c|} = \frac{|P_b P_c|}{|R_b R_c|} = |z|$.

In the above construction, we could lump some (but not all) of the points in $\{M_1, M_2, \ldots, M_m\}$ with each of the three sets of points $\{\overline{M_{a1}}, \ldots, \overline{M_{an}}\}$, $\{\overline{M_{b1}}, \ldots, \overline{M_{bn}}\}$, $\{\overline{M_{c1}}, \ldots, \overline{M_{cn}}\}$. For example, we could deal with the four sets $\{M_2, \ldots, M_m\}$, $\{M_1, \overline{M_{a1}}, \ldots, \overline{M_{an}}\}$, $\{M_1, \overline{M_{b1}}, \ldots, \overline{M_{bn}}\}$, $\{M_1, \overline{M_{c1}}, \ldots, \overline{M_{cn}}\}$. We then use the same formulas as above and we have

$$QP_a = z \cdot (QR_a), \quad QP_b = z \cdot (QR_b), \quad QP_c = z \cdot (QR_c),$$

where $Q = \sum_{i=2}^{m} x_i M_i$, $R_a = \left(\sum_{i=1}^{n} y_i \overline{M_{ai}}\right) + y_{n+1} M_1$, $R_b = \left(\sum_{i=1}^{n} y_i \overline{M_{bi}}\right) + y_{n+1} M_1$, $R_c = \left(\sum_{i=1}^{n} y_i \overline{M_{ci}}\right) + y_{n+1} M_1$ with $\sum_{i=2}^{m} x_i = 1$ and $\sum_{i=1}^{n+1} y_i = 1$.

As we illustrate in Section 7, by redefining our four sets $\{M_i\}$, $\{\overline{M_{ai}}\}$, $\{\overline{M_{bi}}\}$, $\{\overline{M_{ci}}\}$ in different ways, we can vastly expand our collections of homothetic triangles.

5. Two specific examples

5.1. *Problem 1.* Suppose $\triangle ABC$ lies in the complex plane. In $\triangle ABC$ let AD, BE, CF be the altitudes to sides BC, AC, AB respectively, where the points D, E, F lie on sides BC, AC, AB. The $\triangle DEF$ is called the orthic triangle of $\triangle ABC$. The three altitudes AD, BE, CF always intersect at a common point H which is called the orthocenter of $\triangle ABC$. Also, let O be the circumcenter of $\triangle ABC$ and let A', B', C' denote the midpoints of sides BC, AC, AB respectively. The line HO is called the Euler line of $\triangle ABC$. Define the points P_a, P_b, P_c as follows where k, e, m, n, r are fixed real numbers.

(1) $AP_a = k \cdot AH + e \cdot HD + m \cdot AO + n \cdot AA' + r \cdot OA'$.
(2) $BP_b = k \cdot BH + e \cdot HE + m \cdot BO + n \cdot BB' + r \cdot OB'$.
(3) $CP_c = k \cdot CH + e \cdot HF + m \cdot CO + n \cdot CC' + r \cdot OC'$.

Show that there exists a point Q on the Euler line HO of $\triangle ABC$, a point R_a on side BC, a point R_b on side AC, a point R_c on side AB, and a real number z such that $\triangle P_a P_b P_c$ and $\triangle R_a R_b R_c$ are homothetic with center of homothety Q and real ratio of homothety $\frac{QP_a}{QR_a} = \frac{QP_b}{QR_b} = \frac{QP_c}{QR_c} = z$.

We can also show that there exists a point S on the Euler line OH such that this $\triangle R_a R_b R_c$ is the pedal triangle of S formed by the feet of the three perpendiculars from S to sides BC, AC, BC.

Solution. We first deal with equation (1) given in Problem 1. Equations (2), (3) give analogous results.

Since $AP_a = P_a - A, AH = H - A, HD = D - A$, etc, we see that equation (1) is equivalent to

$$P_a - A = k\,(H - A) + e\,(D - H) + m\,(O - A) + n\left(A' - A\right) + r\left(A' - O\right).$$

This is equivalent to $(**)$.

$(**)$ $\quad P_a = (1 - k - m - n)A + (k - e)\,H + eD + (m - r)\,O + (n + r)\,A'$.

From geometry, we know that $AH = 2 \cdot OA', BH = 2 \cdot OB', CH = 2 \cdot OC'$. Thus, $H - A = 2\,(A' - O)$ and $A = H + 2\,(O - A')$.

Substituting this value for A in $(**)$ we have

$$\begin{aligned} P_a = {} & (1 - k - m - n)\left(H + 2O - 2A'\right) + (k - e)\,H + eD \\ & + (m - r)\,O + (n + r)\,A'. \end{aligned}$$

This is equivalent to the following.

$$\begin{aligned} P_a = {} & (1-m-n-e)\,H + (2-2k-m-2n-r)\,O + eD \\ & + (-2+2k+2m+3n+r)\,A'. \end{aligned}$$

Calling $1-m-n-e=\theta$, $2-2k-m-2n-r=\phi$, $e=\lambda$, and $-2+2k+2m+3n+r=\psi$, we have

$$P_a = \theta H + \phi O + \lambda D + \psi A',$$

where $\theta+\phi+\lambda+\psi=1$.

As in Theorem 1, we now lump H, O together and lump D, A' together. Therefore,

$$\begin{aligned} P_a = {} & [\theta H + \phi O] + \left[\lambda D + \psi A'\right] \\ = {} & (\theta+\phi)\left[\frac{\theta H}{\theta+\phi} + \frac{\phi O}{\theta+\phi}\right] + (\lambda+\psi)\left[\frac{\lambda D}{\lambda+\psi} + \frac{\psi A'}{\lambda+\psi}\right]. \end{aligned}$$

Calling $\frac{\theta H}{\theta+\phi} + \frac{\phi O}{\theta+\phi} = Q$, and $\frac{\lambda D}{\lambda+\psi} + \frac{\psi A'}{\lambda+\psi} = R_a$, we have

$$\begin{aligned} P_a = {} & (\theta+\phi)\,Q + (\lambda+\psi)\,R_a \\ = {} & Q + (\lambda+\psi)\,(R_a - Q) \\ = {} & Q + z\,(R_a - Q) \end{aligned}$$

where $z=\lambda+\psi=-2+2k+2m+3n+r+e$.

Of course, Q lies on the Euler line HO and R_a lies on the side BC since $\theta, \phi, \lambda, \psi$ are real.

By symmetry, equations (2), (3) yield the following analogous results.

$$P_b = Q + z\,(R_b - Q) \quad \text{and} \quad P_c = Q + z\,(P_c - Q),$$

where $R_b = \frac{\lambda E}{\lambda+\psi} + \frac{\psi B'}{\lambda+\psi}$, nd $R_c = \frac{\lambda F}{\lambda+\psi} + \frac{\psi C'}{\lambda+\psi}$.

Of course, Q lies on the Euler line HO, R_a lies on side BC, R_b lies on side AC and R_c lies on side AB.

Since $QP_a = (\lambda+\psi)\,(QR_a) = z \cdot QR_a$, $QP_b = (\lambda+\psi)\,(QR_b) = z \cdot QR_b$, and $QP_c = (\lambda+\psi)\,(QR_c) = z \cdot QR_c$, we see that $\triangle R_aR_bR_c \sim \triangle P_aP_bP_c$ are homothetic with ratio of homothety $\frac{QP_a}{QR_a} = \frac{QP_b}{QR_b} = \frac{QP_c}{QR_c} = z$.

Also, $\triangle R_aR_bR_c \sim \triangle P_aP_bP_c$ with ratio of similarity $\frac{|P_aP_b|}{|R_aR_b|} = \frac{|P_aP_c|}{|R_aR_c|} = \frac{|P_bP_c|}{|R_bR_c|} = |z|$.

Since D, E, F lie at the feet of the perpendiculars HD, HE, HF and since A', B', C' lie at the feet of the perpendiculars OA', OB', OC', it is easy to see that there exists a point S on the Euler line HO such that $\triangle R_aR_bR_c$ is the pedal triangle of S with respect to $\triangle ABC$.

We now deal with a special case of Problem 1. Let $k=e, m=n=r=0$. Then $\theta = 1-e = 1-k, \phi = 2-2k, \lambda = k, \psi = -2+2k$. Also, $\theta+\phi = 3-3k, \lambda+\psi = -2+3k$. Therefore, $Q = \frac{\theta H}{\theta+\phi} + \frac{\phi O}{\theta+\phi} = \frac{1}{3}H + \frac{2}{3}O$.

From geometry, we see that the center of homothety is $Q = G$ where G is the centroid of $\triangle ABC$. Also, G is still the center of homothety of $\triangle P_aP_bP_c$ and $\triangle R_aR_bR_c$ even for the case where k is complex.

Also, we see that $R_a = \frac{kD}{-2+3k} + \frac{(-2+2k)A'}{-2+3k}$, and the ratio of homothety is $z = -2 + 3k$.

If we let $k = e = 2, m = n = r = 0$, we see that $R_a = \frac{1}{2}D + \frac{1}{2}A', R_b = \frac{1}{2}E + \frac{1}{2}B', R_c = \frac{1}{2}F + \frac{1}{2}C'$.

From geometry we know that the nine point center N of $\triangle ABC$ lies at the mid point of the line segment HO.

Therefore, if $k = e = 2, m = n = r = 0$, we see that $\triangle R_aR_bR_c$ is the pedal triangle of the nine point center N. Also, when $k = e = 2, m = n = r = 0$, we see that $\triangle P_aP_bP_c$ is geometrically just the (mirror) reflections of vertices A, B, C about the three sides BC, AC, AB respectively. Also, the ratio of homothety z is $z = -2 + 3k = 4$. Thus, $\triangle P_aP_bP_c$ is four times bigger than $\triangle R_aR_bR_c$.

5.2. *Problem 2.* Suppose $\triangle ABC$ lies in the complex plane. As in Problem 1, let AD, BE, CF be the altitudes for sides BC, AC, AB respectively where D, E, F lie on sides AB, AC, BC. Let I be the incenter of $\triangle ABC$ and let the incircle (I, r) be tangent to the sides AB, AC, BC at the points X, Y, Z respectively.

Define the points P_a, P_b, P_c as follows.

(1) $P_a = D + i\,(IX)$,
(2) $P_b = E + i\,(IY)$,
(3) $P_c = F + i\,(IZ)$, where i is the unit imaginary.

We wish to find $\triangle R_aR_bR_c$ and a complex number z such that $\triangle P_aP_bP_c$ and $\triangle R_aR_bR_c$ are homothetic with a center of homothety I and a complex ratio of homothety $z = \frac{IP_a}{IR_a} = \frac{IP_b}{IR_b} = \frac{IP_b}{IR_b}$.

Solution.

We first study what $\triangle P_aP_bP_c$ is geometrically. First, we note that $i \cdot IX$, $i \cdot IY$, $i \cdot IZ$ simply rotates the vectors IX, IY, IZ by 90° in the counterclockwise direction about the origin O as the axis. Also, we note that $|IX| = |X - I| = |IY| = |Y - I| = |IZ| = |Z - I| = r$ where r is the radius of the inscribed circle $I(r)$.

Therefore, the points P_a, P_b, P_c lie on sides AB, AC, BC respectively and the distance from D to P_a is r (going in the counterclockwise direction), the distance from E to P_b is r (going counterclockwise) and the distance from F to P_c is r (going counterclockwise).

We next analyze equation (1) in the problem. The analysis of equations (2), (3) is analogous.

Now equation (1) is equivalent to

$$P_a = D + i\,(X - I) = -i \cdot I + [iX + D] = -i \cdot I + (1 + i)\left[\frac{iX}{1+i} + \frac{D}{1+i}\right].$$

Observe that $-i + (1 + i) = 1$ and $\frac{i}{1+i} + \frac{1}{1+i} = 1$.

Define $R_a = \frac{iX}{1+i} + \frac{D}{1+i} = D + \frac{i}{1+i}(X - D) = D + \frac{i}{1+i}(DX)$ since $X - D = DX$.

Therefore, $DR_a = \frac{i}{1+i}(DX) = \left(\frac{1+i}{2}\right)(DX)$ since $R_a - D = DR_a$.

Also, $P_a = -iI + (1+i)R_a = I + (1+i)(R_a - I)$. Therefore, $IP_a = (1+i)(IR_a)$ since $P_a - I = IP_a$ and $R_a - I = IR_a$.

Therefore, by symmetry, we have the following equations.

(1) $DR_a = \left(\frac{1+i}{2}\right)(DX), ER_b = \left(\frac{1+i}{2}\right)(EY), FR_c = \left(\frac{1+i}{2}\right)(FZ)$.

(2) $IP_a = (1+i)(IR_a), IP_b = (1+i)(IR_b), IP_c = (1+i)(IR_c)$.

Equation (1) tells us how to construct $\triangle R_aR_bR_c$ from the points $\{D, X\}$,$\{E, Y\}$, $\{F, Z\}$.

Also, $\triangle P_aP_bP_c$ and $\triangle R_aR_bR_c$ are homothetic with center of homothety I and complex ratio of homothety $z = 1 + i = \frac{IP_a}{IR_a} = \frac{IP_b}{IR_b} = \frac{IP_c}{IR_c}$.

Also, $\triangle P_aP_bP_c \sim \triangle R_aR_bR_c$ and $\frac{|IP_a|}{|IR_a|} = \frac{|IP_b|}{|IR_b|} = \frac{|IP_c|}{|IR_c|} = |1+i| = \sqrt{2}$. Also, $\frac{|P_aP_b|}{|R_aR_b|} = \frac{|P_aP_c|}{|R_aR_c|} = \frac{|P_bP_c|}{|R_bR_c|}$.

6. Discussion

For a deeper understanding of the many applications of Theorem 1, we invite the reader to consider the following alternative form of Problem 1 in §5.1.

Problem 1 (alternate form) The statement of the definitions P_a, P_b, P_c is the same as in Problem 1.

However, we now define A'', B'', C'' to be the (mirror) reflections of O about the sides AB, AC, BC respectively. Therefore, $OA'' = 2 \cdot OA'$, $OB'' = 2 \cdot OB'$, $OC'' = 2 \cdot OC'$. We now substitute A'', B'', C'' for A', B', C' in the problem by using $A'' - O = 2(A' - O)$, etc. and ask the reader to solve the same problem when we deal with A, B,C, H, D, E, F, O, A'', B'' ,C'' instead of A, B, C, H, D, E, F, O, A', B', C'. Also, we show that R_a, R_b, R_c will lie on lines DA'', EB'', FC'' instead of lying on sides AB, AC, BC. The pedal triangle part of the problem is ignored. The center of homothety Q will still lie on the Euler line HO. This illustrates the endless way that Theorem 1 can be used to create homothetic triangles (and polygons).

Reference

[1] N. A. Court, *College Geometry*, Barnes and Noble, Inc., New York, 1963.

Harold Reiter: Department of Mathematics, University of North Carolina Charlotte, Charlotte, North Carolina 28223, USA

E-mail address: hbreiter@email.uncc.edu

Arthur Holshouser: 3600 Bullard St., Charlotte, North Carolina 28208, USA

E-mail address: hbreiter@email.uncc.edu

Forum Geometricorum
Volume 12 (2012) 255–281.

FORUM GEOM
ISSN 1534-1178

Generalizing Orthocorrespondence

Manfred Evers

Abstract. In [3] B. Gibert investigates a transformation $P \mapsto P^{\perp}$ of the plane of a triangle ABC, which he calls *orthocorrespondence*. Important for the definition of this transformation is the tripolar line of $P^{\perp}$ with respect to ABC. This line can be interpreted as a polar-euclidean equivalent of the orthocenter H of the triangle ABC, the point P getting the role of the absolute pole of the polar-euclidean plane. We propose to substitute the center H by other triangle centers and will investigate the properties of such correspondences.

1. Foundations

1.1. *Introduction.* In [3] B. Gibert investigates the properties of orthocorrespondence, a mapping that every point P in the plane $\mathcal{E}$ of a triangle ABC assigns a point $P^{\perp}$, the tripole of the orthotransversal (line) $\mathcal{L}$ of P with respect to the triangle ABC. This orthotransversal $\mathcal{L}$ is described as follows: The perpendicular lines at P to AP, BP, CP intersect the lines BC, CA, AB respectively at points P_a, P_b, P_c which are collinear with the line $\mathcal{L}$.

We give an alternative description of the orthotransversal line $\mathcal{L}$, limiting ourselves to a point P which is neither an edge-point nor a point on the line at infinity. Let $A^*B^*C^*$ be the polar triangle of ABC with respect to a circle $\mathcal{S}$ with center P. Then $\mathcal{L}$ is the polar line with respect to $\mathcal{S}$ of the orthocenter H^* of $A^*B^*C^*$.

Because of this construction of the orthocorrespondent point $P^{\perp}$, we would like to call orthocorrespondence H^*-correspondence and generalize this by replacing H^* by some other point Q^* (especially by a center of the triangle $A^*B^*C^*$).

1.2. *Notations.* We always look on lines, conics, cubics, *etc*. as sets of points. Given a point R, a triangle Δ and a conic Γ, we write

- $R = (r_a : r_b : r_c)_{\Delta}$ if $(r_a : r_b : r_c)$ are homogeneous barycentric coordinates with respect to Δ,
- $\mathcal{L}_{\Delta}(R)$ for the tripolar line of R with respect to Δ,
- $\mathcal{C}_{\Delta}(R)$ for the circumconic and $\mathcal{J}_{\Delta}(R)$ for the inconic of Δ with perspector R,
- $\partial\Delta$ for the union of the three sidelines of Δ.

We suppose that the point $R, R = (r_a : r_b : r_c)_{\Delta}$, is not a point on $\partial\Delta$, so we have $r_a r_b r_c \neq 0$. In this case we say:

Publication Date: December 5, 2012. Communicating Editor: Paul Yiu.

with respect to Δ, R is of type $\begin{cases} 0, & \text{if } \operatorname{sgn}(r_a) = \operatorname{sgn}(r_b) = \operatorname{sgn}(r_c), \\ a, & \text{if } \operatorname{sgn}(r_b) = \operatorname{sgn}(r_c) \neq \operatorname{sgn}(r_a), \\ b, & \text{if } \operatorname{sgn}(r_c) = \operatorname{sgn}(r_a) \neq \operatorname{sgn}(r_b), \\ c, & \text{if } \operatorname{sgn}(r_a) = \operatorname{sgn}(r_b) \neq \operatorname{sgn}(r_c). \end{cases}$

In the plane of the original triangle ABC we use $\mathcal{L}_\infty$ for the line at infinity (instead of $\mathcal{L}_{ABC}(G)$ where G is the centroid of ABC), and we denote $\mathcal{E} - \mathcal{L}_\infty$ by $\mathcal{E}^-$. By d we denote the euclidean distance function. As usual, we do not define $\mathrm{d}(P,Q)$ for two points P and Q on the line $\mathcal{L}_\infty$, and we put $\mathrm{d}(P,Q) = \infty$ if exactly one of the points is infinite.

1.3. *Q^*-correspondent point and calculation of its coordinates.*
Let $P = (p_a : p_b : p_c)_{ABC}$ be a point in the plane of the triangle ABC, lying neither on a sideline of this triangle nor on $\mathcal{L}_\infty$. Let $A^*B^*C^*$ be the polar triangle of ABC with respect to a circle $\mathcal{S}$ with center P. For every point $Q^* = (q_a^* : q_b^* : q_c^*)_{A^*B^*C^*}$, we call the line $\mathcal{L}_\mathcal{S}(Q^*)$ the *Q^*-transversal of P* and its tripole with respect to ABC the *Q^*-correspondent of P*. The tripole we denote by $P\sharp Q^*$.

Remark. While the triangle $A^*B^*C^*$ and the point Q^* depend on the radius $r > 0$ of $\mathcal{S}$, the Q^*-transversal and the Q^*-correspondent of P do not.

Proposition. (1) *The Q^*-transversal of P has the equation*

$$(q_a^* p_b p_c)x + (q_b^* p_c p_a)y + (q_c^* p_a p_b)z = \Sigma_{cyclic}(q_a^* p_b p_c)x = 0.$$

(2) *If Q^* is not a vertex of the triangle $A^*B^*C^*$, then*

$$P\sharp Q^* = (p_a q_b^* q_c^* : p_b q_c^* q_a^* : p_c q_a^* q_b^*)_{ABC} = (p_a/q_a^* : \cdots : \cdots)_{ABC}.$$

Proof. (A) First, we calculate lengths a^*, b^*, c^* of the sides of $A^*B^*C^*$ for a finite point P not lying on any sideline of the triangle ABC. Let $(p_a, p_b, p_c) = (p_a, \cdots)$, $p_a + p_b + p_c = 1$, be the exact barycentric coordinates of P with respect to the triangle ABC and let a, b, c be the lengths of the sides and S be twice the area of ABC [1]. For a simpler calculation, we set the radius of the circle $\mathcal{S}$ to 1.

We then get $A^* = P + (B-C)^\perp / p'_a$ with $p'_a := p_a S = a \cdot \operatorname{sgn}(p_a) \cdot \mathrm{d}(P, BC)$. The difference of two points is interpreted as a vector of the two-dimensional vector space $\mathsf{V} = \mathbb{R}^2$ with euclidean norm $\|\cdots\|$, and $^\perp$ indicates a rotation of a vector by $+90°$: $(v_1, v_2)^\perp = (-v_2, v_1)$.

For a^* we get

$$\begin{aligned} (a^*)^2 &= \|B^* - C^*\|^2 = \|(C-A)/p'_b - (A-B)/p'_c\|^2 \\ &= (b/p'_b)^2 + 2S_A/(p'_b p'_c) + (c/p'_c)^2 \\ &= [(b/p_b)^2 + 2S_A/(p_b p_c) + (c/p_c)^2]/S^2. \end{aligned}$$

Note: We want to point out the following connection between the sidelengths a^*, b^*, c^* of the triangle $A^*B^*C^*$, the exact barycentric coordinates (p_a, p_b, p_c)

[1] We use Conway's triangle notation: $S = bc\sin A$, $S_A = (b^2 + c^2 - a^2)/2 = bc\cos A$, *etc.*

of the point P and the (exact) tripolar coordinates $(\mathrm{d}(P,A),\mathrm{d}(P,B),\mathrm{d}(P,C))$ of P (with respect to ABC):

$$\mathrm{d}(P,A)=\sqrt{(cp_b)^2+2S_Ap_bp_c+(bp_c)^2}=Sa^*|p_bp_c|. \quad (*)$$

We also mention that the vertices A^*,B^*,C^* are finite points in the plane of triangle ABC as long as P is a finite point in this plane with $p_ap_bp_c\neq 0$.

(B) Calculation of the coordinates of the Q^*-correspondent $P\sharp Q^*$. Given a point Q^* with exact barycentric coordinates (q_a^*,q_b^*,q_c^*) with respect to $A^*B^*C^*$, we want to find an equation of the line $\mathcal{L}_{\mathcal{S}}(Q^*)$ as well as the coordinates of its tripole with respect to ABC. To achieve the results easily, we borrow a method from the theory of vector spaces which - in case of the two-dimensional vector space $\mathsf{V}=\mathbb{R}^2$ - considers an element of the dual space V^* of linear forms (often such a linear form is called a covector) as a one-dimensional affine subspace (a line) of V, see for example [2, Chapter I]. This method is not essential for the calculation of the polar line but will simplify it. We do not even have to know the coordinates of Q^* with respect to ABC, which are in fact

$$(p_a^2p_bp_cS^2+p_ap_bq_c^*S_B+p_ap_cq_b^*S_C-p_bp_cq_a^*a^2:\ \cdots:\ \cdots).$$

Given a vector $\vec{v}=(v_1,v_2)\in\mathbb{R}^2$, the dual vector is a 1-form $v^*=v_1x+v_2y$. To visualize this object, we identify v^* with the line $v_1x+v_2y=v_1^2+v_2^2$, which is the polar line of $\vec{v}$ with respect to the unit circle $\{\vec{w}\in\mathbb{R}^2|\ w_1^2+w_2^2=1\}$. Within this interpretation, V^* is formed by all the lines of V that do not contain the zero vector, and additionally we have to include the line at infinity which represents $o^*=0x+0y$.

Obviously, the mapping Λ: $\mathsf{V}\mathsf{x}\mathsf{V}^*\to\mathbb{R},(\vec{v},w^*)=((v_1,v_2),w_1x+w_2y)\mapsto v_1w_1+v_2w_2$ is a bilinear pairing. The mapping $\chi_P:\mathcal{E}^-\to\mathbb{R}^2,R\mapsto R-P$, is an affine chart with $\chi_P(P)=\vec{o}$ and $\chi_P(\mathcal{S})=\{\vec{w}\in\mathbb{R}^2|\ w_1^2+w_2^2=1\}$. By means of this chart, we get a bilinear mapping

$$\Lambda_P:\mathcal{E}^-\mathsf{x}\,\{\text{lines in }\mathcal{E}\text{ not passing through }P\}\to\mathbb{R}$$

with

$$\begin{cases}\Lambda_P(R,l)=0, & \text{if } R=P \text{ or } l=\mathcal{L}_\infty \text{ or } l\parallel PR,\\ \Lambda_P(R,l)=1/t, & \text{if } P+t(R-P) \text{ is a point on } l.\end{cases}$$

For every line l not passing through P, we get a linear form $\lambda=\Lambda_P(\cdots,l)$. Starting with a linear form λ, we find the corresponding line by $l=\{R\mid\lambda(R)=1\}$.

Since we assume that P is not a point on any of the lines $\mathcal{L}_\infty,BC,CA,AB$, we have well defined 1-forms $\alpha:=\Lambda_P(\cdots,BC),\beta:=\Lambda_P(\cdots,CA),\gamma:=\Lambda_P(\cdots,AB)$. For every point $R\in\mathcal{E}-P$, we can calculate the values $\alpha(R)$, $\beta(R)$, $\gamma(R)$ quite quickly once we know the values $\alpha(A)$, $\alpha(B)$, ..., $\gamma(C)$. But we already know that $\alpha(B)=\alpha(C)=1$ and can easily calculate $\alpha(A)=1-1/p_a$. Figure 1 gives an illustration of the mapping Λ_P.

Because A^*, B^*, C^* are the poles with respect to $\mathcal{S}$ of the lines $\alpha=1,\beta=1,\gamma=1$, the point $Q^*=q_a^*A^*+q_b^*B^*+q_c^*C^*$ has a polar line $\mathcal{L}_{\mathcal{S}}(Q^*)$ with the equation $q_a^*\alpha+q_b^*\beta+q_c^*\gamma=1$.

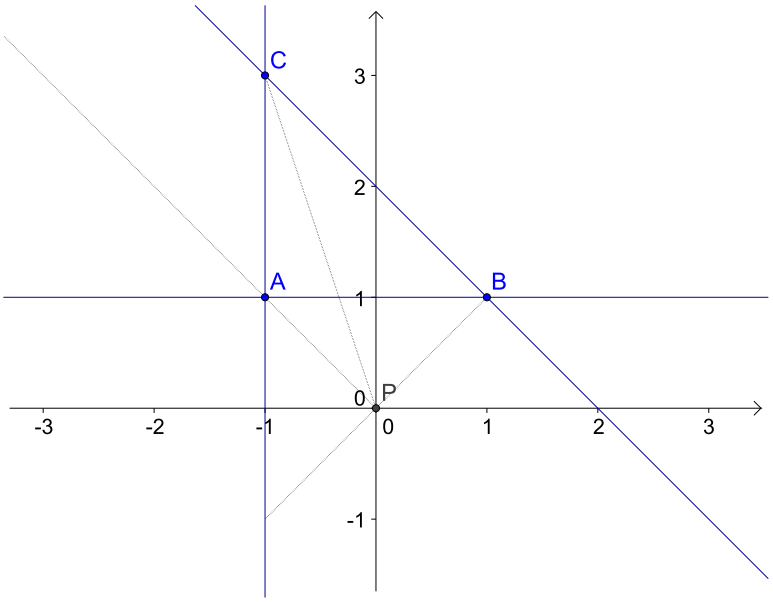

Figure 1. For the constellation shown here, we have $\Lambda_P(A, BC) = 0$, $\Lambda_P(B, CA) = -1$, $\Lambda_P(C, AB) = 1/3$.

We can now calculate the coordinates of the points of intersection of this Q^*-transversal with the sidelines of the triangle ABC. For example, the Q^*-transversal and the line BC intersect at $(0 : p_b q_c^* : -p_c q_b^*)_{ABC}$. Having calculated the three intersection points, the statements (1) and (2) of the proposition follow immediately. □

We introduce the point $Q^{[P]} := (q_a^* : \cdots : \cdots)_{ABC}$, so we can write the point $P\sharp Q^* = P/Q^{[P]}$ as a barycentric quotient of two points.

1.4. *A first example.* For Q^* we choose the centroid $G^* = X_2{}^*$ of the triangle $A^*B^*C^*$.[2] For every finite point P not lying on any side line of the triangle ABC, we have the equations $G^{[P]} = G$ and $P\sharp G^* = P$. Of course, we like to extend the domain of the correspondence mapping to points on ∂ABC and on $\mathcal{L}_\infty$. For $Q^* = G^*$ we can get a continuous extension $\sharp G^* = \mathrm{id}_{\mathcal{E}}$.

Before investigating Q^*-correspondence for different triangle centers Q*, we contribute some

1.5. *Basic properties of Q^*-correspondence.*

1.5.1. If we take the cevian triangle of Q^* with respect to $A^*B^*C^*$ und construct its polar triangle with respect to $\mathcal{S}$ then we get the anticevian triangle of $P\sharp Q^*$ with respect to ABC, see Figure 2. The polar triangle of the anticevian triangle of Q^* with respect to $A^*B^*C^*$ is the cevian triangle of $P\sharp Q^*$ with respect to ABC.

[2] We adopt the notation X_n of [7] for triangle centers.

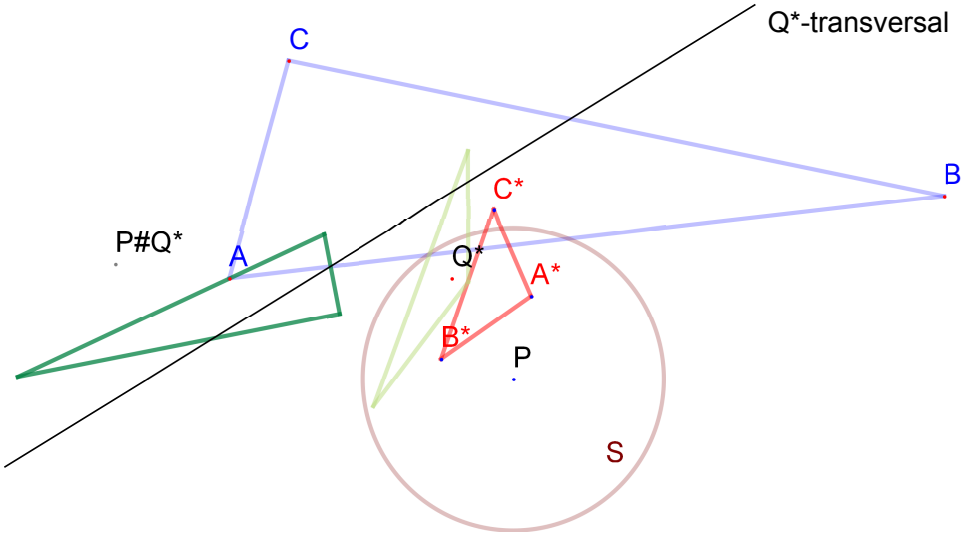

Figure 2. Besides the triangles ABC and $A^*B^*C^*$, the picture shows the cevian triangle of P with respect to $A^*B^*C^*$ (light green) and the anticevian triangle of $P\sharp Q^*$ with respect to ABC (green).

1.5.2. The polar triangle of the pedal resp. antipedal triangle of Q^* with respect to $A^*B^*C^*$ is the antipedal resp. pedal triangle of $P\sharp Q^*$ with respect to ABC.

1.5.3. If Q^* is a point on B^*C^* different from B^* and C^* then $P\sharp Q^* = A$.

1.5.4. Suppose $Q^* = (q_a^* : q_b^* : q_c^*)_{A^*B^*C^*}$ is a point satisfying the equation $P\sharp Q^* = G = X_2$, then we have $Q^* = Q^{[P]} = P$.

In the following we denote the tripolar line of Q^* with respect to $A^*B^*C^*$ by q^*.

1.5.5. In 1.2 the point $P\sharp Q^*$ was defined as the tripole with respect to ABC of the line $\mathcal{L}_{\mathcal{S}}(Q^*)$. But we can get $P\sharp Q^*$ as the pole of q^* with respect to $\mathcal{S}$, as well.

1.5.6. The set $P\sharp q^* := \{P\sharp R^* \mid R^* \in q^*\}$ is the circumconic of ABC with perspector $P\sharp Q^*$, so we can write

$$P\sharp q^* = \mathcal{C}_{ABC}(P\sharp Q^*) = \mathcal{C}_{ABC}(P/Q^{[P]}).$$

Two examples:

- For $q^* = \mathcal{L}_{A^*B^*C^*}(G^*) = L_\infty$ we get $P\sharp q* = \mathcal{C}_{ABC}(P)$.
- If $q^* = \mathcal{L}_{A^*B^*C^*}(X_{648}^*)$ is the Euler line of $A^*B^*C^*$, we get $P\sharp q^* = \mathcal{C}_{ABC}(P\sharp X_{648}^*)$. For special cases, see 3.1 and 3.2.

1.5.7. The polar lines with respect to $\mathcal{S}$ of points on $\mathcal{C}_{A^*B^*C^*}(Q^*)$ agree with the tangent lines of $\mathcal{J}_{ABC}(P\sharp Q^*)$. In other words: The $\mathcal{S}$-dual of $\mathcal{C}_{A^*B^*C^*}(Q^*)$ is $\mathcal{J}_{ABC}(P\sharp Q^*)$.

Example: The $\mathcal{S}$-dual of the Steiner circumellipse $\mathcal{C}_{A^*B^*C^*}(G^*)$ is $\mathcal{J}_{ABC}(P)$.

As special cases we get

- for $P = G$ the Steiner inellipse with center G ,
- for $P = Ge$ (Gergonne point) the incircle with center I (incenter),
- for $P = Na$ (Nagel point) the Mandart inellipse with center M (Mittenpunkt),
- for $P = K$ (symmedian point) the Brocard inellipse with center X_{39}.

1.5.8. The $\mathcal{S}$-dual of the inconic $\mathcal{J}_{A^*B^*C^*}(Q^*)$ of $A^*B^*C^*$ with perspector Q^* is $\mathcal{C}_{ABC}(P\sharp Q^*)$.

Examples:

- $\mathcal{J}_{A^*B^*C^*}(K^*)$ is the Brocard inellipse of $A^*B^*C^*$. Its $\mathcal{S}$-dual is $\mathcal{C}_{ABC}(P\sharp K^*)$, with $P\sharp K^* = (1/(p_a(p_b^2c^2 + 2p_bp_cS_A + p_c^2b^2)) : \cdots : \cdots)_{ABC}$. For the special case $P = O$, we get $P\sharp K^* = K$; the $\mathcal{S}$-dual of the Brocard inellipse of $A^*B^*C^*$ is the circumcircle of ABC.
- The $\mathcal{S}$-dual of the Steiner inellipse $\mathcal{J}_{A^*B^*C^*}(G^*)$ is $\mathcal{C}_{ABC}(P)$. As special cases we get
  - the circumellipse which is shown in Figure 5 for $P = I$,
  - the Steiner circumellipse for $P = G$,
  - the circumcircle for $P = K$,
  - the Kiepert hyperbola for $P = X_{523}$,
  - the Jerabek hyperbola for $P = X_{647}$.

1.6. *The I^*-correspondence (first part).* As mentioned above, we are mainly interested in the special case of Q^* being a triangle center of $A^*B^*C^*$. For further definitions we orient ourselves on the mapping $P \mapsto P\sharp I^*$ because I^* is the most important weak center of $A^*B^*C^*$, and it is a center for which the anticevians agree with extraversions: ${}_\tau I^* = I^*_\tau,\ \tau = 0, a, b, c$.

$(\mathrm{d}(P, A)\Delta|p_a| : \cdots : \cdots)$ are the homogeneous barycentric coordinates of I^* with respect to $A^*B^*C^*$ and of $I^{[P]}$ with respect to ABC. It can be easily seen that the mapping $\mathcal{E}^- - \partial ABC \to E, P \mapsto P/I^{[P]} = (\mathrm{sgn}(p_a)\mathrm{d}(P, B)\mathrm{d}(P, C) : \cdots : \cdots)_{ABC}$, cannot be extended to a continuous mapping with domain $\mathcal{E}^- - \{A, B, C\}$. But if we introduce the point

$$\begin{aligned} I^{[P,0]} &:= (a^P : b^P : c^P)_{ABC} \\ &:= (\mathrm{sgn}(p_a)a^* : \mathrm{sgn}(p_b)b^* : \mathrm{sgn}(p_c)c^*)_{ABC} \\ &= (p_a\mathrm{d}(P, A) : p_b\mathrm{d}(P, B) : p_c\mathrm{d}(P, C))_{ABC} \end{aligned}$$

and its anticevians $I^{[P,a]} := (-a^P : b^P : c^P)_{ABC}, \cdots$, all the mappings $\mathcal{E}^- - \{A, B, C\} \to E, P \mapsto P/I^{[P,\tau]} =: (P\sharp I^*)^\tau, \tau = 0, a, b, c$, are continuous. We get $(P\sharp I^*)^0 = (\mathrm{d}(P, B)\mathrm{d}(P, C) : \cdots : \cdots)_{ABC}$, which is a point of type 0, and the points $(P\sharp I^*)^\tau,\ \tau = a, b, c$, are the anticevians of $(P\sharp I^*)^0$.

We can see here that the same way the weak triangle center I^* comes in four versions (a main center I_0 and its three mates I_a, I_b, I_c), I^*-correspondence splits into four parts.

For $P \in \{A, B, C\}$ we have the equations $(P\sharp I^*)^\tau = P$, $\tau = 0, a, b, c$; the vertices are fixed points of all four I^*-correspondences.

Let us suppose now that the point P is a point on $\mathcal{L}_\infty$. Since we have $\lim_{R\to P}(a^R : b^R : c^R) = \lim_{R\to P}(p_a\mathrm{d}(R,A) : p_b\mathrm{d}(R,B) : p_c\mathrm{d}(R;C))) = (p_a : p_b : p_c)$, we put $(a^P : b^P : c^P) := (p_a : p_b : p_c)$ and define $I^{[P,0]} := (a^P : b^P : c^P)_{ABC}, \cdots$
We get $(P\sharp I^*)^\tau := P/I^{[P,\tau]} = {}_\tau G,\ \tau = 0, a, b, c.$
Conclusion: All four mappings $\mathcal{E}^- - \{A, B, C\} \to \mathcal{E}, P \mapsto (P\sharp I^*)^\tau,\ \tau = 0, a, b, c$, can be extended to continuous mappings $\mathcal{E} \to \mathcal{E}$.

1.6.1. *Special cases.*

- $P = I = X_1 : (I\sharp I^*)^0 = X_{174}$ (Yff-center of congruence).
- $P = G = X_2 : (G\sharp I^*)^0 = (1/\sqrt{2b^2 + 2c^2 - a^2} : \cdots : \cdots)_{ABC} = \sqrt{X_{598}}$.
- $P = O = X_3$, and suppose O is of type τ: $(O\sharp I^*)^\tau = {}_\tau G$.
- $P = H = X_4$, and suppose H is of type τ: $(H\sharp I^*)^\tau = {}_\tau X_{52}$.
- $(L_\infty\sharp I^*)^\tau = {}_\tau G$. (More accurately, we should write: $(L_\infty\sharp I^*)^\tau = \{{}_\tau G\}$.)

1.7. *The Definition of Q^*-correspondence for other centers of $A^*B^*C^*$.*
Let $Q^* = (q_a^* : q_b^* : q_c^*)_{A^*B^*C^*}$ be any triangle center of $A^*B^*C^*$ and let f^* be a barycentric center function, homogeneous in its arguments, with
$Q^* = ((f^*(a^* : b^* : c^*) : f^*(b^* : c^* : a^*) : f^*(c^* : a^* : b^*))_{A^*B^*C^*}$.
We take the definition of $(a^P : b^P : c^P)$ from the last subsection, introduce the points

$$\begin{cases} Q^{[P,0]} := (f^*(a^P : b^P : c^P) : f^*(b^P : c^P : a^P) : f^*(c^P : a^P : b^P))_{ABC}, \\ Q^{[P,a]} := (f^*(-a^P : b^P : c^P) : f^*(b^P : c^P : -a^P) : f^*(c^P : -a^P : b^P))_{ABC}, \\ \textit{etc}. \end{cases}$$

and put $(P\sharp Q^*)^\tau := P/Q^{[P,\tau]},\ \tau = 0, a, b, c.$

The Q^*-correspondent $(P\sharp Q^*)^\tau$ of P is well defined if and only if at least one of the three coordinates in the definition is not zero. We denote the set of points P where all the points $(P\sharp Q^*)^\tau,\ \tau = 0, a, b, c$, are defined by $\mathrm{dom}(Q^*)$.

The mappings $(\cdots\sharp Q^*)^\tau : \mathrm{dom}(Q^*) \to \mathcal{E},\ \tau = 0, a, b, c$, are continuous.

If Q^* is a strong center of $A^*B^*C^*$ then for every point P in $\mathrm{dom}(Q^*)$ the set $\{(P\sharp Q^*)^\tau \mid \tau = 0, a, b, c\}$ consists of only one point, $P\sharp Q^*$.

Examples.

1.7.1. Taking $P = H$, we have $(a^P : b^P : c^P) = (a : b : c)$. So we get $I^{[H,0]} = I,\ G^{[H,0]} = G^{[H]} = G,\ O^{[H,0]} = O^{[H]} = O, \cdots$ (see also 3.2.)

1.7.2. Let P be a point on $\mathcal{L}_\infty$. We get $P\sharp G^* = P,\ P\sharp O^* = P\sharp H^* = G$. The points G^*, O^*, H^* are points on the Euler line of the (degenerate) triangle $A^*B^*C^*$. If Q^* is any point on this line, $P\sharp Q^*$ is a point on the circumconic of ABC through G and P. The perspector of this conic is $P\sharp(X_{648})^*$.

Two special cases:

- Taking $P = X_{30}$ (Euler infinity point), we get $X_{648}^{[P]} = X_{648}$ and $P\sharp X_{648}^* = X_{30}/X_{648}$.

- If P is one of the two infinite points of the Kiepert hyperbola $\mathcal{C}_{ABC}(X_{523})$, we get $P\sharp X_{648}^* = X_{523}$.

1.7.3. If we take $Q^* = K^* = {X_6}^*$, we get

- $K^{[P]} = ({p_a}^2(c^2\,{p_b}^2 + 2S_A\,p_b\,p_c + b^2\,{p_c}^2) : \cdots : \cdots)_{ABC}$.
- $P\sharp K^* = (p_b p_c\,\mathrm{d}^2(P,B)\,\mathrm{d}^2(P,C) : \cdots : \cdots)_{ABC}$
  $= (1/(p_a(c^2{p_b}^2 + 2S_A p_b p_c + b^2{p_c}^2)) : \cdots : \cdots)_{ABC}$.
- $\mathrm{dom}(K^*) = \mathcal{E} - \{A, B, C\}$.

Special cases:

- $K^{[I]} = M = X_9$; $I\sharp K^* = Ge = X_7$.
- $K^{[G]} = X_{599}$; $G\sharp K^* = X_{598}$.
- $K^{[O]} = X_{577}$; $O\sharp K^* = X_{264} = G/O$.
- $K^{[H]} = K$; $H\sharp K^* = X_{264}$.
- $K^{[K]} = X_{574}$; $K\sharp K^* = X_{598}$.
- If P is not a point on a sideline of ABC then we have $\lim_{t\to 0}(A + tP)/K^{[A+tP]} = A$.
- If P is a point on a sideline of ABC but not a triangle vertex then $P\sharp K^*$ is the vertex opposite this sideline. For a point P on AB, different from A, we therefore get $\lim_{t\to 0}(A + tP)/K^{[A+tP]} = C$. This shows that K^*-correspondence $\sharp K^* : \mathrm{dom}(K^*) \to \mathcal{E}, P \mapsto P\sharp K^*$, does not have any extension that is continuous in A, B, C.
- $\mathcal{L}_\infty\sharp K^* = \mathcal{C}_{ABC}(G)$ (Steiner circumellipse).

If instead of P we take its isogonal conjugate K/P, we get
$K^{[K/P]} = (a^2(c^2{p_b}^2 + 2S_A p_b p_c + b^2{p_c}^2) : \cdots : \cdots)_{ABC}$ and $(K/P)\sharp K^* = P\sharp K^*$.

1.7.4. We take $Q^* = Ge^* = X_7^*$ and get

$$\begin{aligned}(P\sharp Ge^*)^0 &= (p_a(-a^P + b^P + c^P) : p_b(a^P - b^P + c^P) : p_c(a^P + b^P - c^P)),\\ (P\sharp Ge^*)^a &= (p_a(a^P + b^P + c^P) : p_b(-a^P - b^P + c^P) : p_c(-a^P + b^P - c^P)),\\ &\vdots\end{aligned}$$

A careful analysis shows that $\mathrm{dom}(Ge^*) = \mathcal{E}$.

Special cases:

- The vertices A, B, C are fixed points of all four Ge^*-correspondences.
- If $P = (0 : t : 1-t)_{ABC}$ is a point on BC and $t(1-t) > 0$ then
$$(P\sharp Ge^*)^\tau = \begin{cases} (\,2t(1-t)a : tg(t) : (1-t)g(t))_{ABC} \text{ for } \tau = 0,\\ (-2t(1-t)a : tg(t) : (1-t)g(t))_{ABC} \text{ for } \tau = a,\\ (0 : -t : 1-t)_{ABC} \text{ for } \tau = b, c,\end{cases}$$
where the polynomial function g is defined by
$$g(t) := \sqrt{-t(1-t)a^2 + (1-t)b^2 + tc^2}.$$

- If $P = (0 : t : 1-t)_{ABC}$ is a point on BC and $t(1-t) < 0$ then
$$(P\sharp Ge^*)^\tau = \begin{cases} (0 : -t : 1-t)_{ABC} \text{ for } \tau = 0, a \\ (\ 2|t|(1-t)a : tg(t) : (1-t)g(t))_{ABC} \text{ for } \tau = b, \\ (-2|t|(1-t)a : tg(t) : (1-t)g(t))_{ABC} \text{ for } \tau = c. \end{cases}$$
- For a point $P = (p_a : p_b : p_c)_{ABC}$ on $\mathcal{L}_\infty$ we get
$(P\sharp Ge^*)^0 = (p_a^2 : p_b^2 : p_c^2)_{ABC}$ (this is a point on the Steiner inellipse of ABC),
$(P\sharp Ge^*)^a = (0 : 1 : 1)_{ABC}$ *etc.*

1.8. *Fixed points of Q^*-correspondence.*

(A) Fixed points on a sideline of ABC. For different centers Q^* the situation can be quite different: For $Q^* = H^*$ (see [7]), $Q^* = I^*$ (see 1.6), $Q^* = Ge^*$ (see 1.7.3), the vertices of ABC are the only edgepoints which are fixed points of the correspondence mapping. (In case of the weak center $Q^* = I^*$, the vertices are fixed points for all four correspondences $(\cdots \sharp I^*)^\tau,\ \tau = 0, a, b, c$.) The correspondence of $Q^* = (X_{110})^* = (a^2/(b^2-c^2) : \cdots : \cdots)_{ABC}$ has exactly six fixed points on the sidelines, the vertices of ABC and the vertices of the orthic triangle. For some centers, as for $Q^* = (X_{76})^* = G^*/K^*$, every point on a sideline of ABC is a fixed point. In contrast, K^*-correspondence has no proper fixed point on a sideline of ABC (see 1.7.2).

(B) Fixed points not lying on a sideline of ABC. If we assume P is a finite point not lying on any side line of the triangle ABC, the equation $P\sharp Q^* = P$ is true if and only if $Q^* = G^*$ or $A^*B^*C^*$ is equilateral. $A^*B^*C^*$ is equilateral if and only if P is one of the two Fermat points X_{13}, X_{14}.

Suppose that F is a Fermat point and that Q^* is a weak center of $A^*B^*C^*$. If F is of type 0 then $(F\sharp Q^*)^0 = F$, $(F\sharp Q^*)^a$ is a point on the line AF, *etc.* If $P = F$ is of type a then $((F\sharp Q^*)^a = F$ and $(F\sharp Q^*)^0$ is a point on the line AF, $(F\sharp Q^*)^b$ is a point on the line BF, *etc.* We give a proof of the last statement: If $P = F$ is of type a then ${}_aQ^*$ is identical with the center G^* of the equilateral triangle $A^*B^*C^*$ and the points ${}_0Q^*,\ {}_bQ^*,\ {}_cQ^*$ lie on the lines G^*A^*, G^*B^*, G^*C^*, respectively. The polar line of ${}_0Q^*$ with respect to $\mathcal{S}$ passes through the pole of G^*A^* which is the point $(0 : -p_b : p_c)_{ABC}$. Therefore, $(F\sharp Q^*)^0$ is a point on the line through A and $(0 : p_b : p_c)_{ABC}$. But this line also goes through $P = F$. The same way follows that $(F\sharp Q^*)^b$, $(F\sharp Q^*)^c$ are points on BF resp. CF.

1.9. *Points P with an isosceles triangle $A^*B^*C^*$.* We assume that $A^*B^*C^*$ is an isosceles triangle with $b^* = c^*$. The last equation leads to the following condition for the exact coordinates (p_a, p_b, p_c) of the point P:

$$p_b^2((p_b-1)c^2 + p_c(b^2-c^2)) = p_c^2((p_c-1)b^2 + p_b(c^2-a^2)).$$

The locus of points P satisfying the last equation is (after completion) a cubic which passes through the points A, B, C, A being a dubble point. We denote this algebraic curve (a strophoide) by $\mathcal{K}(A; B, C)$. Since A is a dubble point of this curve, one can find a rational parametrisation for it. $\mathcal{K}(A; B, C)$ also passes

through the vertex H_A of the orthic triangle $H_AH_BH_C$, the two Fermat points and the infinite point $(-2:1:1)_{ABC}$ on the triangle median AG (see Figure 3).

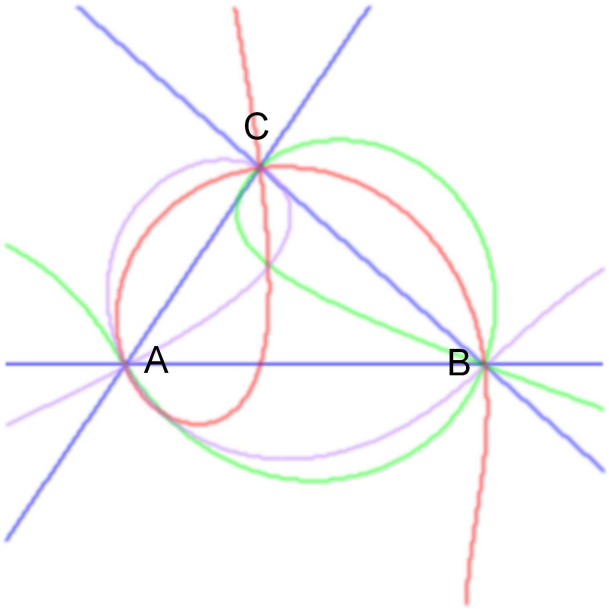

Figure 3. Here are shown the cubics $\mathcal{K}(A;B,C)$, $\mathcal{K}(B;C,A)$, $\mathcal{K}(C;A,B)$. See 1.9 for a definition of these curves.

1.10. *The image of the circumcircle of ABC under Q^*-correspondence.* If P is a point on this circle but not a triangle vertex then ABC and $A^*B^*C^*$ are similar triangles: $a^* : b^* : c^* = a : b : c$. Therefore, if Q^* is a center of $A^*B^*C^*$ with a center function f^*, we get $Q^{[P]} = (f^*(a,b,c) : \cdots : \cdots)_{ABC}$ and $P\sharp Q^*$ is a point on the circumconic $\mathcal{C}_{ABC}(K/Q^{[P]})$.

Examples.

- $\mathcal{C}_{ABC}(K)\sharp G^* := \{P/G^{[P]} \mid P \in \mathcal{C}_{ABC}(K)\} = \mathcal{C}_{ABC}(K/G) = \mathcal{C}_{ABC}(K)$.
- $\mathcal{C}_{ABC}(K)\sharp I_\tau^* = \mathcal{C}_{ABC}(K/I_\tau) = \mathcal{C}_{ABC}(I_\tau)$ for $\tau = 0, a, b, c$ (see Figure 4.)
- $\mathcal{C}_{ABC}(K)\sharp O^* = \mathcal{C}_{ABC}(K/O) = \mathcal{C}_{ABC}(H)$.
- $\mathcal{C}_{ABC}(K)\sharp H^* = \mathcal{C}_{ABC}(K/H) = \mathcal{C}_{ABC}(O)$, see [7].
- If we put $P\sharp K^* = P$ for $P = A, B, C$ (see 1.7.3) then $\mathcal{C}_{ABC}(K)\sharp K^* = \mathcal{C}_{ABC}(G)$.

We also look at the isotomic conjugates of these circumconics:

- $\{G^{[P]}/P \mid P \in \mathcal{C}_{ABC}(K)\} = \mathcal{L}_{ABC}(K)$.
- $\{I_\tau^{[P]}/P \mid P \in \mathcal{C}_{ABC}(K)\} = \mathcal{L}_{ABC}(I_\tau), \tau = 0, a, b, c$.
- $\{O^{[P]}/P \mid P \in \mathcal{C}_{ABC}(K)\} = \mathcal{L}_{ABC}(H)$.
- $\{H^{[P]}/P \mid P \in \mathcal{C}_{ABC}(K)\} = \mathcal{L}_{ABC}(O)$.
- $\{K^{[P]}/P \mid P \in \mathcal{C}_{ABC}(K)\} = \mathcal{L}_\infty$.

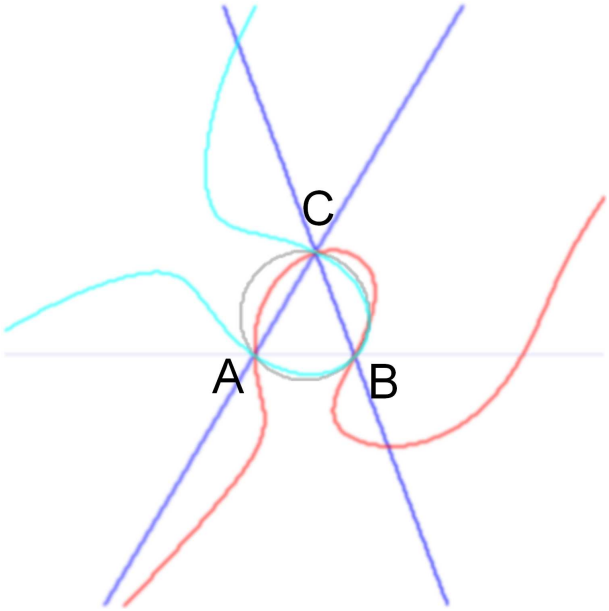

Figure 4. This shows the circumcircle (grey) and the cubics $\mathcal{V}(K^*, O)$ (cyan) and $\mathcal{V}(K^*, H)$ (red) for the triangle ABC, see 1.11.1.

1.11. *The preimage under Q^*-correspondence / Q^*-associates.* The mapping $\sharp G^* : \mathcal{E} \to \mathcal{E}$ is bijective. But in general, Q^*-correspondence is neither injective nor surjective. Gibert proved (see [3]) that for $Q^* = H^*$ there are up to two points having the same correspondent[3]. Points having the same correspondent he calls *associates*. We shall take this terminus here. As we could see in 1.7.3, a point P is a K^*-associate of its isogonal conjugate. There are centers Q^* with more than two Q^*-associates, $Q^* = O^*$ for example (see in 2.3.4). Q^*-correspondence doesn't have to be surjective, either. For example, for $Q^* = K^*$ there is no point $P\sharp Q^*$ on a sideline of the triangle ABC except for the vertices of this triangle.

We now describe a way of constructing the preimage of a point $R = (r_a : r_b : r_c)_{ABC}$ under Q^*-correspondence. We want to determine all points P with $P\sharp Q^* = R$ and omit all the special cases $(P\sharp Q^*)^\tau$, $\tau = 0, a, b, c$. (These can be easily adapted.)

We start with a point P and choose a point Q^* which is a triangle center of $A^*B^*C^*$ with barycentric center function $f^*(a^*, b^*, c^*)$. The Q^*-transversal of P, $\mathcal{L}_\mathcal{S}(Q^*)$, is the set of points $(x : y : z)_{ABC}$ satisfying the equation

$$\Sigma_{cyclic} p_b p_c f^*(a^*, b^*, c^*)\, x = 0.$$

Given a point T, we denote the set of points P with T a point on $\mathcal{L}_\mathcal{S}(Q^*)$ by $\mathcal{V}(Q^*, T)$. If T is not an edgepoint, the set $\mathrm{dom}(Q^*) \cap \mathcal{V}(Q^*, T)$ is the preimage of the circumconic $\mathcal{C}_{ABC}(T)$. If $T = (0 : t : 1-t)_{ABC}$, $t(1-t) \neq 0$, is a

[3]Gibert proved in fact that - using proper multiplicity - there are exactly two real or two complex points having the same correspondent.

point on BC but not a vertex then $\mathrm{dom}(Q^*) \cap \mathcal{V}(Q^*, T)$ is the preimage of the line through the points A and $(0 : t : t-1)_{ABC}$. Finally, if T is a triangle vertex then $\mathrm{dom}(Q^*) \cap \mathcal{V}(Q^*, T)$ is the preimage of this vertex.

Now we can present the preimage of a point R which is not a vertex of ABC: It is the set $\mathcal{V}(Q^*, T_1) \cap \mathcal{V}(Q^*, T_2) \cap \mathrm{dom}(Q^*)$ for any two different points T_1, T_2 on $\mathcal{L}_{ABC}(R)$.

1.11.1. Example. We want to determine the preimage of the point X_{648}, the tripole of the Euler line, under K^*-correspondence. So we choose two different points on $\mathcal{L}_{ABC}(X_{648})$, G and O for instance. For every point T, the set $\mathcal{V}(K^*, T)$ is a cubic curve. For $T = G$, this cubic is the union of the line at infinity and the circumcircle of ABC. We now look at $\mathcal{V}(K^*, O)$. There is exactly one infinite point, let us say P_1, on this curve, so this point is mapped to X_{648} by K^*-correspondence. In general, $\mathcal{V}(K^*, O)$ and the circumcircle have four common points. Three of them are the points A, B, C; the fourth common point is a the finite point, P_2, which is mapped to X_{648} by K^*-correspondence. For an isosceles but not equilateral triangle ABC, the point X_{648} agrees with one of the edges A, B, C, and so does the point P_2. See Figure 4 for a picture. For more examples, see 2.1.4 and 2.3.4.

1.12. *Pivotal curves.* In [3] Gibert introduces algebraic curves consisting of all points P for which the line through P and its orthocorrespondent $P\sharp H^*$ passes through a given point R. Such a curve Gibert calls *orthopivotal*, the point R being the *orthopivot*. We transfer Gibert's concept to other correspondences. Given a point $R = (r_a : r_b : r_c)_{ABC}$, the set of points P such that the points $R, P, P\sharp Q^*$ are collinear is

$$\{P = (p_a : p_b : p_c)_{ABC} \in \mathrm{dom}(Q^*) \mid \Sigma_{cyclic} r_a q_a^*(q_b^* - q_c^*)p_b p_c \ = \ 0\ \}.$$

We call this set *Q^*-pivotal set with pivot point R*. For a triangle center Q^* the coordinates q_a^*, q_b^*, q_c^* depend on P, of course.

For a strong center Q^*, the Q^*-pivotal set is an open set (with respect to the Zariski topology) of an algebraic curve which we denote by $\mathcal{P}(Q^*, R)$. For most strong centers, these curves are of high degree (> 4) and rather complicated. Thus, we do not go into an analysis of these. But for all of the curves $\mathcal{P}(Q^*, R)$, one can state that if R is not an edgepoint, they pass through the vertices A, B, C, the two Fermat points and the point R. Gibert gives a detailed description of the orthopivotal curves $\mathcal{P}(H^*, R)$. These are cubics. The question arises: What are the other pivotal curves of degree 3? The answer is: There aren't any! *Proof:* If $\mathcal{P}(Q^*, R)$ has degree 3 then the correspondent center Q^* must have a (homogeneous and bisymmetric) barycentric centerfunction $f^*(a^*, b^*, c^*) = 1/(ma^{*2} + n(b^{*2} + c^{*2}))$ with two different real numbers n, m. (For $i < 100$ there are just three such centers X_i, namely, X_4, X_{76} and X_{83}.) For all of these centers Q^* one gets $\mathcal{P}(Q^*, R)$ = $\mathcal{P}(H^*, R)$ because the points $P, P\sharp Q^*, P\sharp H^*$ are always collinear, as one can verify by simple calculation.

For a weak center Q^*, the set of points P so that for some $\tau \in \{0, a, b, c\}$ the three points $P, (P\sharp Q^*)^\tau$ and R are collinear is an open set of an algebraic curve which we denote by $\mathcal{P}(Q^*, R)$. In 3.1 we present a picture of $\mathcal{P}(I^*, R)$.

2. Q^*-correspondence for "classical" triangle centers Q^*.

2.1. I^*-correspondence (second part).

2.1.1. Geometric construction of the image and preimage points. For each point $P \in \mathcal{E}^- - \{A, B, C\}$ we define six points $P_A, P_A^{'}, P_B, P_B^{'}, P_C, P_C^{'}$ by: P_A is the intersection of BC with the internal bisector of the angle $\angle BPC$, and $P_A^{'}$ is the intersection of BC with the external bisector of this angle. Similarly we define the points $P_B, P_B^{'}, P_C, P_C^{'}$.

P. Yiu [10] shows the following properties of these six points: The triangle $P_A P_B P_C$ is the cevian triangle of some point that lies inside the triangle and that we call ${}_0R$. The tripolar line $\mathcal{L}_{ABC}({}_0R)$ of ${}_0R$ intersects the side lines BC, CA, AB in $P_A^{'}, P_B^{'}, P_B^{'}$, respectivly. The points $P_A^{'}, P_B, P_C$ are collinear with the line $\mathcal{L}_{ABC}({}_aR)$, the points $P_B{}', P_C, P_A$ collinear with the line $\mathcal{L}_{ABC}({}_bR)$ and the points $P_C^{'}, P_A, P_B$ collinear with the line $\mathcal{L}_{ABC}({}_cR)$. Further more, Yiu shows: The circles with diameters $P_A P_A^{'}, P_B P_B^{'}, P_C P_C^{'}$ - they are called *generalized Apollonian circles* [9], [10] [4] - have their centers on the line $\mathcal{L}_{ABC}(R^2)$, $R^2 = ({r_a}^2 : {r_b}^2 : {r_c}^2)_{ABC}$, and they are in the same pencil of circles through the point P and its image P' under the reflection in the circumcircle of ABC. (If P is a point on the circumcircle then all three circles are mutually tangent to each other and P is the point of tangency.)

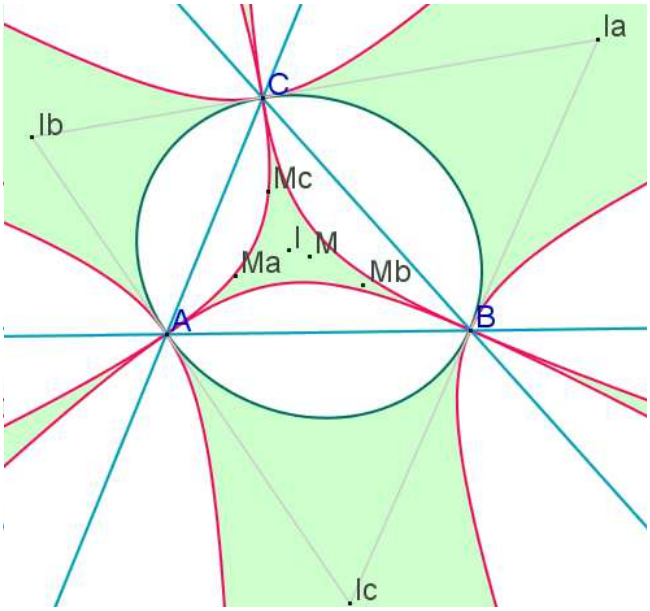

Figure 5.

[4] The original Apollonian circles we get for $P = I$.

Since ${}_0R = (\mathrm{d}(P,B)\mathrm{d}(P,C) : \cdots : \cdots)_{ABC}$, this point agrees with $(P\sharp I)^0$, and ${}_\tau R$ agrees with $(P\sharp I)^\tau$ for $\tau = a, b, c$. P' is the I^*-associate of P. A routine calculation gives its coordinates: $P' = (p_a^2a^2b^2c^2 + p_ap_ba^2c^2(a^2 - c^2) + p_ap_ca^2b^2(a^2 - b^2) + p_bp_ca^4 \cdot (a^2 - b^2 - c^2) : \cdots : \cdots)_{ABC}$.

Question: Given a point R, what is the number n_R of (real) points P with $R = (P\sharp I^*)^\tau$ for some $\tau \in \{0, a, b, c\}$? In [10] Yiu gives the following answer: The number n_R is 2, 1, or 0 according as the line $\mathcal{L}_{ABC}(R^2)$ intersects the circumcircle of ABC in 0, 1, or 2 points. Additionally, one could ask for a partition of $\mathcal{E}$ illustrating the domains of points R with $n_R = 0$ resp. 1 resp. 2. The set of points R with $n_R = 1$ is the union of circumconics $\mathcal{C}_{ABC}(I_\tau), \tau = 0, a, b, c$. The set of points R with $n_R = 2$ is the union of the open green domains shown in Figure 5. We also can get a partition of the plane by lines showing the domains of points $R^{-1} = G/R$ with $n_R = 0, 1, 2$ (see Figure 6).

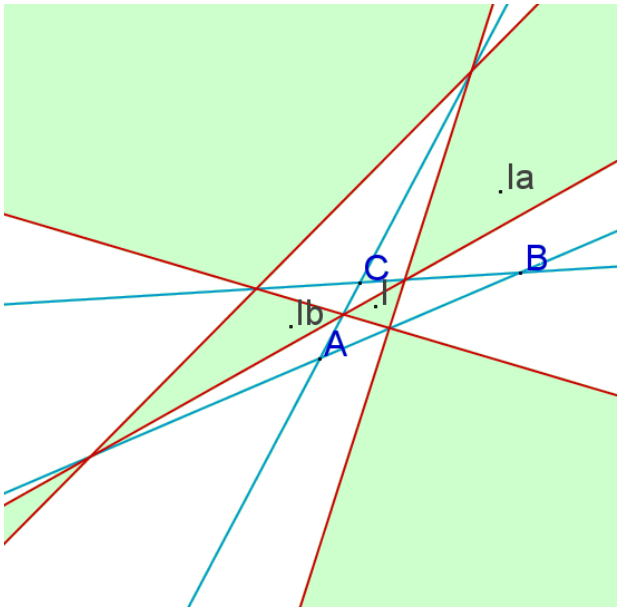

Figure 6.

The set of points R^{-1} with $n_R = 1$ is the union of lines $\mathcal{L}_{ABC}(I_\tau)$. The set of points R^{-1} with $n_R = 2$ is the union of the green areas. This way we can link Yiu's [10] and Weaver's [9] work to a problem that was put and solved by Bottema in [1]: Given a triplet (r_a, r_b, r_c) of real numbers, what is the number of points P satisfying $(r_a : r_b : r_c) = (\mathrm{d}(P,A) : \mathrm{d}(P,B) : \mathrm{d}(P,C))$? Identifying $(r_a : r_b : r_c)$ with the point $R = (r_a : r_b : r_c)_{ABC}$, Bottema's answer can be formulated as follows: The number of points depends on $\mathrm{d}(R, BC), \mathrm{d}(R, CA)$ and $\mathrm{d}(R, AB)$ being the sidelengths of a triangle (two points), a degenerate triangle (one point) or not a triangle (zero points).

Given a point $R = (r_a, r_b, r_c)_{ABC}$ of type τ, the points P and P' with $(P\sharp I^*)^\tau = (P'\sharp I^*)^\tau = R$ have coordinates

$$((b^2+c^2+({r_b}^2-{r_c}^2))\sqrt{a^4+b^4+c^4-2a^2b^2-2b^2c^2-2c^2a^2}$$
$$\pm[(c^2+a^2-b^2)\sqrt{c^4-2c^2({r_a}^2+{r_b}^2)+({r_a}^2-{r_b}^2)^2}$$
$$+(a^2+b^2-c^2)\sqrt{b^4-2b^2({r_c}^2+{r_a}^2)+({r_c}^2-{r_a}^2)^2}]$$
$$:\cdots:\cdots)_{ABC}.$$

We get real values for points R with $n_R \geq 1$.

2.1.2. There is a direct connection between I^*-correspondence and orthocorrespondence: The I^*-correspondent $P\sharp I^*$ agrees with the orthocorrespondent of P for the cevian triangle of $P\sharp I^*$. This is a consequence of the well known fact that the orthocenter H^* of the triangle $A^*B^*C^*$ is the incenter of its orthic triangle which we denote by Δ^*. Since the tripolar of any point with respect to a given triangle agrees with the tripolar of this point with respect to its cevian triangle, we have $\mathcal{L}_{A^*B^*C^*}(H^*) = \mathcal{L}_{\Delta^*}(H^*)$. The polar triangles of $A^*B^*C^*$ and Δ^* with respect to $\mathcal{S}$ are ABC and the cevian triangle of $P\sharp I^*$, respectivly.
Consequences: (1) P' is the orthoassociate of P with respect to the cevian triangle of $P\sharp I^*$.
(2) The circumcircle of ABC is identical with the polar circle of the cevian triangle of $P\sharp I^*$.
(3) The orthocorrespondent $P\sharp H^*$ of P with respect to ABC agrees with the I^*-correspondent of P for the anticevian triangle of $P\sharp H^*$.
(4) The polar circle of ABC is identical with the circumcircle of the anticevian triangle of $P\sharp H^*$.

2.1.3. The image of the sidelines. $\bigcup_{\tau=0,a,b,c}(AB\sharp I^*)^\tau$ is an analytic curve which is shown in Figure 7.

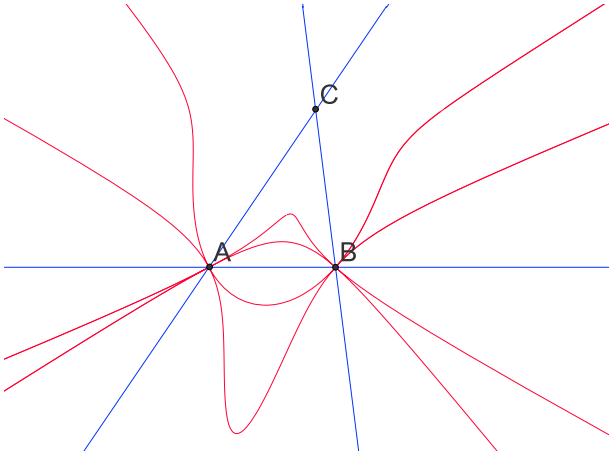

Figure 7. The red curve is the image of the sideline AB under the mappings $(I^*)^\tau,\ \tau = 0, a, b, c.$

2.1.4. *The preimage of $\mathcal{L}_\infty$ under I^*-correspondence.* A point P has the image point $(P\sharp I^*)^a$ on the line of infinity if and only if $1/\mathrm{d}(P,A) = 1/\mathrm{d}(P,B) + 1/\mathrm{d}(P,C)$. The set of points P satisfying the last equation is an analytic curve (an oval) $\mathcal{O}_a$ which is invariant under inversion with respect to the circumcircle $\mathcal{C}_{ABC}(K)$. The union of the three ovals $\mathcal{O}_\tau,\ \tau = a,b,c$, is the algebraic curve $\{P \mid \Sigma_{cyclic}\, \mathrm{d}^2(P,B)\mathrm{d}^2(P,C)(\mathrm{d}^2(P,B)\mathrm{d}^2(P,C) - 2\mathrm{d}^4(P,A)) = 0\}$ (see Figure 8).

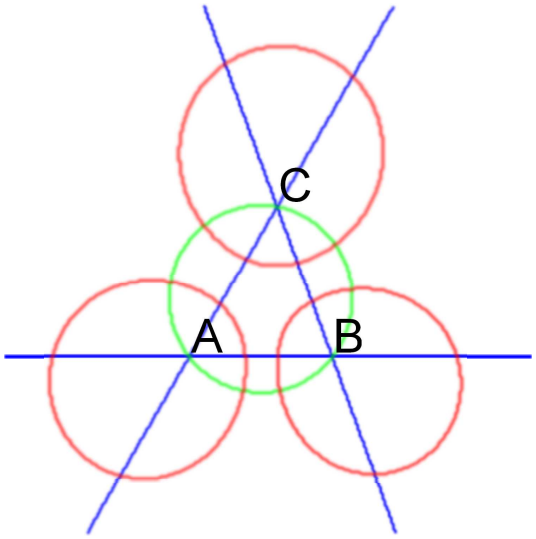

Figure 8. The set of points P with $(P\sharp Q^*)^\tau$ a point on $\mathcal{L}_\infty$, $\tau = a,b,c$, is an algebraic curve which is the union of the three (red) ovals.

2.1.5. *The $\mathcal{S}$-duals of the incircle and the excircles of the triangle $A^*B^*C^*$.* Because of the strong connection between the incenter and the incircle and the excenters and their correspondent excircles, we take a brief look at the incircle and the excircles of $A^*B^*C^*$, $J_{A^*B^*C^*}(Ge^*_\tau),\ \tau = 0,a,b,c$, and their $\mathcal{S}$-duals, $\mathcal{C}_{ABC}((P\sharp Ge^*)^\tau),\ \tau = 0,a,b,c$. The point P is a focus of each of these circumconics, and the lines $\mathcal{L}_{ABC}(P\sharp I^*)^\tau),\ \tau = a,b,c$, are the corresponding directrices. Figure 9 shows the situation for $P = O$.

2.1.6. *I^*-pivotal curves.* We take the notation $\mathcal{P}(Q^*,R)$ from 1.11. For the weak center $Q^* = I^*$, this set is an algebraic curve, given by the equation

$$\Sigma_{cyclic}\,(d_a^2d_b^2(xr_b - yr_a)^4 - 2d_a^2d_bd_c(xr_b - yr_a)^2(xr_c - zr_a)^2) = 0,$$

with $d_a := c^2y^2 + 2yzS_A + b^2z^2$, *etc.* For a picture, see Figure 10.

2.2. *G^*-correspondence.* In 1.4 we already saw that $P\sharp G^* = P$ for every point P in the triangle plane.

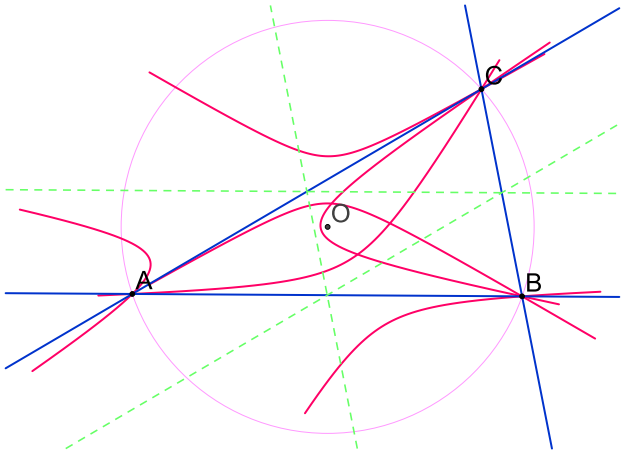

Figure 9. This shows the (pink) circumcircle $\mathcal{C}_{ABC}((O\sharp Ge^*_\tau)^0) = \mathcal{C}_{ABC}(K)$ and the (red) circumconics $C_{ABC}((O\sharp Ge^*)^\tau)$, $\tau = a, b, c$. The three (green) lines $\mathcal{L}_{ABC}((O\sharp I^*)^\tau)$, $\tau = a, b, c$, are the sidelines of the medial triangle.

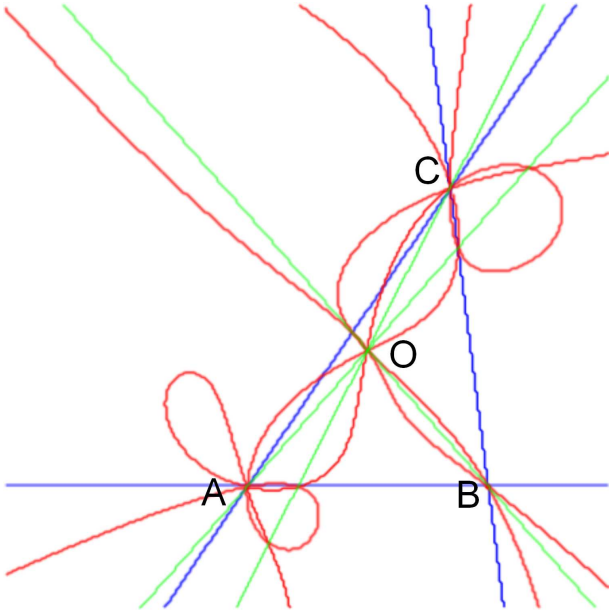

Figure 10. Besides the (red) algebraic curve $\mathcal{P}(I^*, O)$, the picture shows the lines AO, BO, CO (green). Without any proof, we state that all (ten) singular points of $\mathcal{P}(I^*, O)$ lie on these lines. Six singular points are points on ∂ABC. And for each $\tau = 0, a, b, c$, one is of type τ.

2.3. *O^*-correspondence.*

2.3.1. *Calculation of dom(O^*).* We have

$$O^{[P]} = ((p_b p_c(b^2 p_c^2 + 2p_b p_c S_A + c^2 p_b^2)(-p_a^2 S_A + p_a p_b S_B + p_a p_c S_C + p_b p_c a^2) : \cdots : \cdots)_{ABC}.$$

First, we look at the sets $\{(p_a : p_b : p_c)_{ABC} \mid b^2 p_c^2 + 2p_b p_c S_A + c^2 p_b^2 = 0\}$ and $\{(p_a : p_b : p_c)_{ABC} \mid -p_a^2 S_A + p_a p_b S_B + p_a p_c S_C + p_b p_c a^2 = 0\}$. The first set contains one real point, the vertex A. The second set is the circle with diameter BC. From this it follows that the first coordinate of $P\sharp O^*$ is zero if and only if P is a point of the line BC or a point on one of the circles with diameter AB resp. AC. This implies: $\mathrm{dom}(O^*) = \mathcal{E} - \{A, B, C, H_A, H_B, H_C\}$, where H_A, H_B, H_C are the vertices of the orthic triangle of ABC.

2.3.2. *Special images.* As special cases for $O^{[P]}$ and $P\sharp O^*$ we get

- for $P = I : O^{[I]} = I$ and $I\sharp O^* = G$,
- for $P = G : O^{[G]} = ((a^2 - 2b^2 - 2c^2)(5\Delta a^2 - b^2 - c^2) : \cdots : \cdots)_{ABC} = X_{1384}/X_{1383}$ and $G\sharp O^* = X_{1383}/X_{1384}$,
- for $P = O : O^{[O]} = X_{1147}$ and $O\sharp O^* = O/X_{1147}$,
- for $P = H : O^{[H]} = O$ and $H\sharp O^* = X_{2052}$.

2.3.3. *The image of the sidelines.* If $P = (0 : t : 1 - t)$ is a point on BC, different from B, C and H_A, then $P\sharp O^* = (t(t-1)(a^2(2t-1) - b^2 + c^2) : -2t(a^2 t(t-1) + b^2(1-t) + c^2 t) : 2(1-t)(a^2 t(t-1) + b^2(1-t) + c^2 t))_{ABC}$. The infinite point on BC is mapped to the point G. The image set $BC\sharp O^*$ can be extended to a connected analytic curve. This curve we denote by $\mathcal{A}(BC, O^*)$. See Figure 11 for a picture.

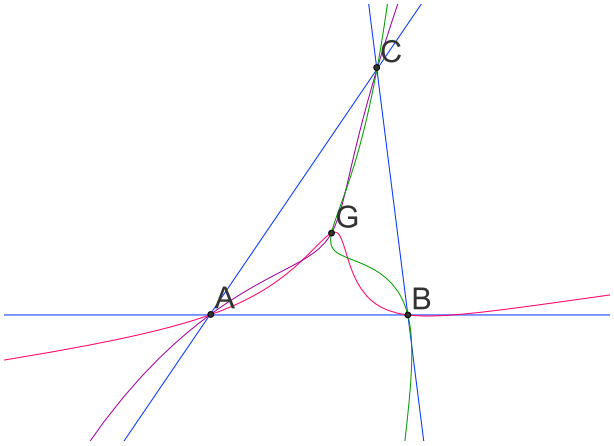

Figure 11. This picture shows the curves $\mathcal{A}(BC, O^*)$ (green), $\mathcal{A}(CA, O^*)$ (purple) and $\mathcal{A}(AB, O^*)$ (red).

2.3.4. *Connection between O^*- and H^*-correspondence.* The point O^* of the triangle $A^*B^*C^*$ is identical with the orthocenter of the pedal triangle of O^* which is the cevian triangle of G^*. Therefore, the O^*-transversal of P agrees with orthotransversal of P for the anticevian triangle of $P = P\sharp G^*$ (with respect to ABC).

2.3.5. *The $\mathcal{S}$-dual of the circumcircle of the triangle $A^*B^*C^*$.* The $\mathcal{S}$-dual of the circumcircle $\mathcal{C}_{A^*B^*C^*}(K^*)$ is the conic $\mathcal{J}_{ABC}(P\sharp K^*)$. The foci of this conic are P and its isogonal conjugate K/P. The line $\mathcal{L}_{ABC}(P\sharp O^*)$ is the polar line of P with respect to $\mathcal{J}_{ABC}(P\sharp K^*)$, so it is a directrix of the conic.

Two examples:

- For $P = O$, $\mathcal{J}_{ABC}(P\sharp K^*)$ is Brocard inellipse of ABC.
- For $P = I_\tau$, $\tau = 0, a, b, c$, we get $P\sharp O^* = G$. Therefore, $\mathcal{L}_{ABC}(P\sharp O^*)$ is the line at infinity, and the conic $\mathcal{J}_{ABC}(P\sharp K^*)$ is a circle. For $\tau = 0$ it is the incircle, for $\tau = a, b, c$ the corresponding excircle of ABC. O^*-correspondence maps the points I_τ , $\tau = 0, a, b, c$, to G. Let us determine the preimage of G under $\sharp O^*$. Obviously, the incenter and the excenters are the only finite points that are mapped to G by $\sharp O^*$. But the equation $P\sharp O^* = G$ is also correct for every point on $\mathcal{L}_\infty$, as can be easily checked.

2.3.6. *The preimage of a point under O^*-correspondence.* There are several possibilities to determine the preimage of a point R under O^*-correspondence. We describe two. Afterwards, we determine the preimage of $\mathcal{L}_\infty$.

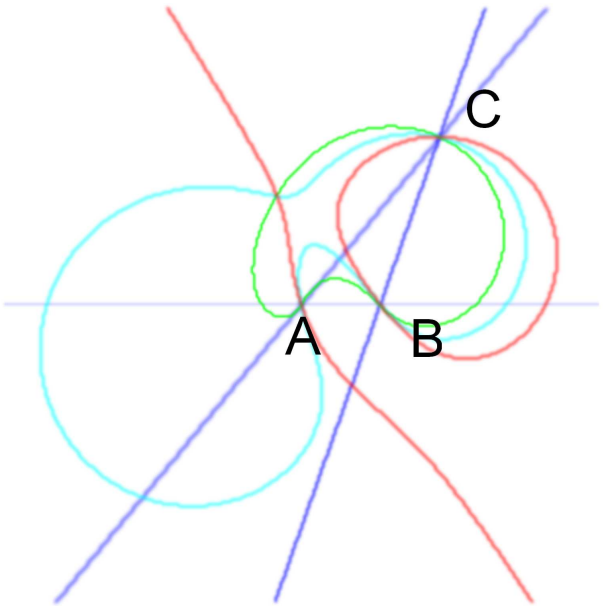

Figure 12. This "insect" consists of the triangle ABC, the (red) Neuberg cubic, the (green) quartic $\mathcal{V}(O^*, X_{647})$ and the (cyan) quartic $\mathcal{V}(O^*, X_{650})$. For the triangle shown here, one real point is (and four more complex points are) mapped to H by O^*-correspondence.

(A) First, we determine the preimages of G and H and the associates of the Gibert point X_{1141} using the way that was described in 1.11. We start with the quartic $\mathcal{V}(O^*, X_{523})$, given by the equation

$$\Sigma_{cyclic}(c^2y^2 + 2yzS_A + b^2z^2)(x(-xS_A + yS_B + zS_C) + yza^2)(b^2 - c^2) = 0.$$

$X_{523} = (b^2 - c^2 : \cdots : \cdots)_{ABC}$ is a point on $\mathcal{L}_\infty$ (the orthopoint of the Euler line). The quartic splits into the line at infinity and a cubic, which is called the Neuberg cubic and we denote by $\mathcal{K}_N$. Since $\mathcal{L}_\infty \sharp O^* = G$, $\sharp O^*$ maps the Neuberg cubic onto the Kiepert hyperbola.

- There are five points on $\mathcal{K}_N$ which are mapped to G by O^*-correspondence, the in- and excenters and the Euler infinity point X_{30}.
- The orthocenter H is the fourth (the non trivial) common point of the Kiepert hyperbola and the Jarabek hyperbola $\mathcal{C}_{ABC}(X_{647})$. Hence, the preimage of H under O^*-correspondence is the intersection of $\mathcal{K}_N$ with the quartic $\mathcal{V}(O^*, X_{647})$. See Figure 12.
- The orthocenter H is the fourth common point of the Kiepert hyperbola and the Feuerbach hyperbola $\mathcal{C}_{ABC}(X_{650})$. Therefore, we can get the preimage of H under O^*- correspondence as the intersection of the Neuberg cubic with the quartic $\mathcal{V}(O^*, X_{650})$. See Figure 12.

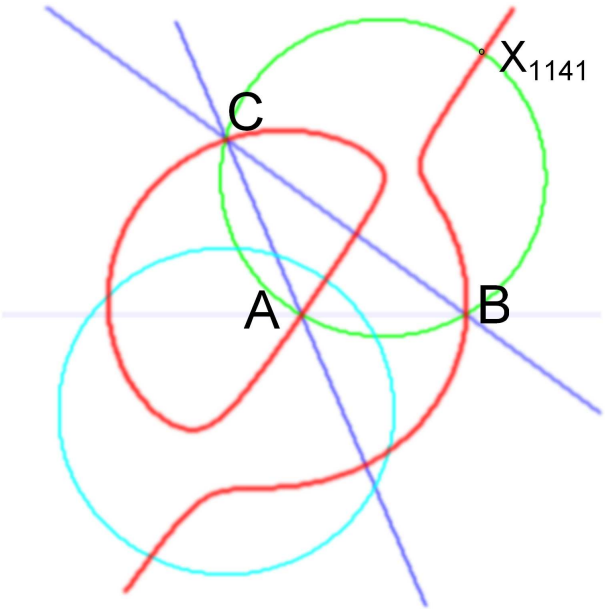

Figure 13. For an obtuse triangle ABC, the quartic $\mathcal{V}(O^*, H)$ splits into two circles, the circum circle (green) and the polar circle (cyan) of the triangle. The red curve is the Neuberg cubic. For the triangle presented here, there are four O^*-associates of X_{1141}, all lying on the polar circle.

- Apart from A, B, C, the Gibert point X_{1141} is the only common point of the circumcircle and the Neuberg cubic $\mathcal{K}_N$, see [3]. The O^*-correspondence

maps the circumcircle to the circumconic $\mathcal{C}_{ABC}(H)$ (see 1.10) and the Neuberg cubic to $\mathcal{C}_{ABC}(X_{523})$. Therefore, $X_{1141}\sharp O^*$ is the fourth common point of $\mathcal{C}_{ABC}(H)$ and $\mathcal{C}_{ABC}(X_{523})$. The line $\mathcal{L}_{ABC}(X_{1141}\sharp O^*)$ is a line trough H, perpendicular to the Euler line. (The point $X_{1141}\sharp O^*$ is not in the current edition of [7].) The quartic $\mathcal{V}(O^*, H)$ is the union of the circumcircle and the algebraic set $\{(p_a : \cdots : \cdots)_{ABC} | S_A p_a^2 + S_B p_b^2 + S_C p_c^2 = 0\}$. This set is the polar circle of ABC (the circle with center H and radius $\rho = \sqrt{-S_A S_B S_C}/(\sqrt{8}S)$ if ABC is obtuse, the set $\{H\}$ if ABC is right-angled, and the empty set (set without any real point) if ABC is acute. See Figure 13.

Another example: The preimage of the vertices A, B, C. The quartic $\mathcal{V}(Q^*, A)$ consists of the circle with diameter BC and the point A. Therefore, the preimage of A consists of all points lying on the circle with diameter BC but not on a sideline of ABC.

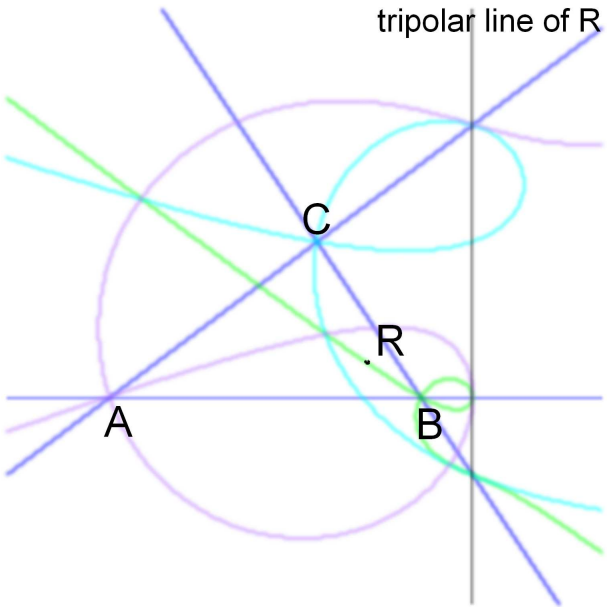

Figure 14. This shows the curves $\mathcal{K}(A; R_B, R_C)$ (purple), $\mathcal{K}(B; R_C, R_A)$ (green) and $\mathcal{K}(C; R_A, R_A)$ (light blue) and the (black) line $\mathcal{L}_{\mathcal{S}}(R)$. For the triangle ABC drawn here, the preimage of R under O^*-correspondence consists of three (real and two nonreal/complex) points. See 2.3.6.(B).

(B) A second way to determine the preimage of a point. The tripolar line $\mathcal{L}_{ABC}(R)$ of a point R intersects the triangle lines BC, CA, AB in $R_A := (0 : -r_b : r_c)_{ABC}$, $R_B := (r_a : 0 : -r_c)_{ABC}$, $R_C := (-r_a : r_b : 0)_{ABC}$, respectivly. Supposing that a point P is neither an edge-point nor a point on the line of infinity, this point P can be in the preimage of R only if the corresponding polar triangle $B^*C^*Q^*$ of $R_B R_C A$ is an isosceles triangle with $\mathrm{d}(Q^*, B^*) = \mathrm{d}(Q^*, C^*)$. Here, $Q^* = (pa/ra : \cdots : \cdots)_{ABC}$ is the pole of $\mathcal{L}_{ABC}(R)$ with respect to $\mathcal{S}$.

The locus of points P satisfying the last equation is (after completion) the cubic $\mathcal{K}(A; R_B, R_C)$. See 1.9 for a definition of the cubics $\mathcal{K}$ and Figure 14 for a picture.

(C) The preimage of $\mathcal{L}_\infty$. The points P whose coordinates satisfy the equation

$$\Sigma_{cyclic}\, p_a/[(a^{*2}(b^{*2}+c^{*2}-a^{*2})] = 0,\ a^* = a^*(p_a, p_b, p_c),\ \cdots,$$

are points on one of the sidelines of ABC or points on an octic which passes twice through each of the vertices A, B, C and also passes through the vertices of the orthic triangle, see Figure 15.

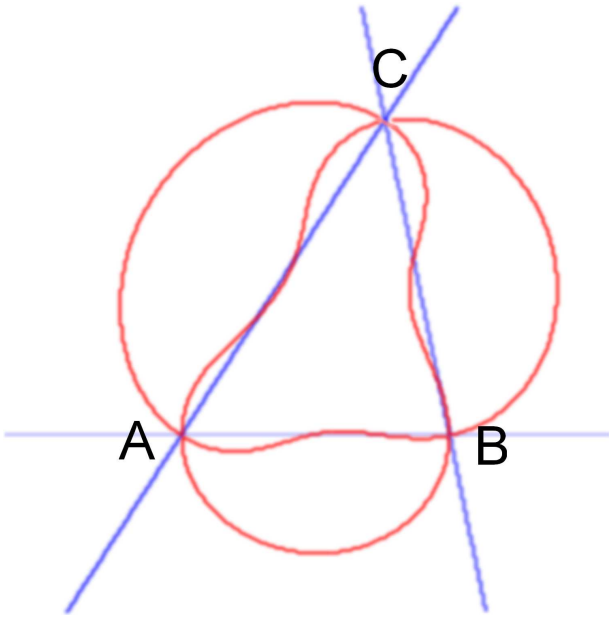

Figure 15. The preimage of $\mathcal{L}_\infty$ under $\sharp O^*$ consists of all points of $\mathrm{dom}(O^*)$ lying on the (red) octic, see 2.3.6.(C).

2.4. *H^*-correspondence.* For a nearly complete analysis of orthocorrespondence, see [3] and [4].

2.5. *N^*-correspondence.*

2.5.1. *Calculation of dom(N^*).* $N^{[P]} = (a^{*2}(b^{*2}+c^{*2}) - (b^{*2}-c^{*2})^2) : \cdots : \cdots)_{ABC},\ a^* = a^*(p_a, p_b, p_c), \cdots$. The algebraic set $\{(p_a : p_b : p_c)_{ABC} \mid a^{*2}(b^{*2}+c^{*2}) - (b^{*2}-c^{*2})^2) = 0\}$ splits into the line BC and the quartic $\mathcal{V}(N^*, A)$ which passes through all the vertices of ABC (A being a dubble point) and the vertices H_B and H_C of the orthic triangle. H_B and H_C are the only intersection points of $\mathcal{V}(N^*, A)$ with AC resp. AB. The two quartics $\mathcal{V}(N^*, B)$ and $\mathcal{V}(N^*, C)$ meet at six points, the vertices A, B, C, the point H_A and two more points, one of type 0 and one of type a, see Figure 15. If the triangle ABC is neither perpendicular nor equilateral, we have $\mathrm{dom}(N^*) = \mathcal{E} - 12$ points.

Special images

- $N^{[I]} = X_{10},\ I\sharp N^* = X_{81}$.

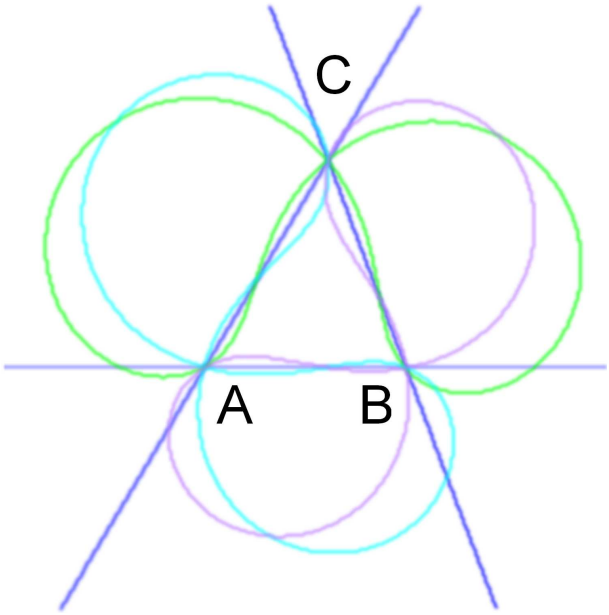

Figure 16. The picture shows the curves $\mathcal{V}(N^*, A)$ (light blue), $\mathcal{V}(N^*, B)$ (purple) and $\mathcal{V}(N^*, C)$ (green).

- $O\sharp N^* = (1/(S_A((a^2(b^2+c^2)-(b+c)^2(b-c)^2)^2 - 2a^4b^2c^2) : \cdots : \cdots)_{ABC}$.
- $G\sharp N^* = (1/(2a^4 - 18b^2c^2 + 7S_A(b^2+c^2)^2) : \cdots : \cdots)_{ABC}$.
- $N^{[H]} = H$, $H\sharp N^* = H/N = X_{275}$.
- $\mathcal{L}_\infty\sharp N^* = G$.
- $\sharp N^*$ maps a point $P = (0 : p_b : p_c)_{ABC}$, $p_bp_c \neq 0$ onto the point $(p_bp_c((p_b-p_c)a^2 - (b^2-c^2)) : p_bf_a(p_a,p_b,p_c) : p_cf_a(p_a,p_b,p_c))_{ABC}$, with $f_a(p_a,p_b,p_c) = ((p_b^2+p_c^2)a^4 - 2(p_bb^2+p_cc^2) - (b^2-c^2)^2)$.

2.5.2. *The $\mathcal{S}$-dual of the nine-point-circle of the triangle $A^*B^*C^*$.* We start from the well known fact that for any two different points P and Q in the plane of a triangle Δ, both not lying on $\partial\Delta$, there exists a conic which passes through the vertices of the cevian triangles of P and of Q, see [5] (for instance). This conic is uniquely determined by P and Q and we denote it by $\mathcal{C}_\Delta(P,Q)$.

Of course, the dual of this statement is also true: Given two different points P and Q, both not lying on $\partial\Delta$, there exists exactly one conic which is an inconic of the anticevian triangles of P and of Q. This conic we denote by $\mathcal{J}_\Delta(P,Q)$. We now specialize in the nine-point-circle $\mathcal{C}_{A^*B^*C^*}(G^*,H^*)$ and its $\mathcal{S}$-dual $\mathcal{J}_{ABC}(P,P\sharp H^*)$. Figure 17 shows a picture of this conic.

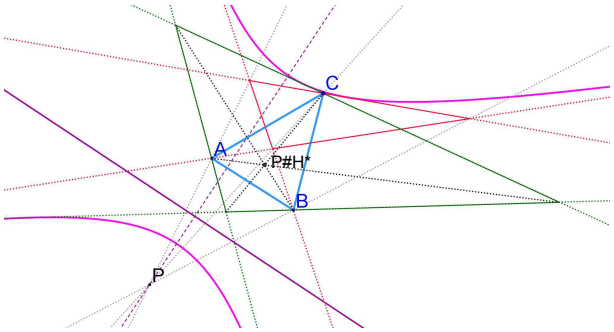

Figure 17. For the triangle ABC and the point P, the picture shows the (purple) conic $\mathcal{J}_{ABC}(P, P\sharp H^*)$, which is an inconic of the (red) anticevian triangle of $P\sharp G^* = P$ and of the (green) anticevian triangle of $P\sharp H^*$. The point P is a focus of this conic, and the purple line is the corresponding directrix which is also the tripolar line of the point $P\sharp N^*$.

3. Description of the algebraic set $P\sharp q*$ for $q^* = G^*O^*$.

We refer to results given in 1.5.5 and look at two special cases for P, $P = I$ and $P = H$.

3.1. $P = I$. We take $P = I$. Let $G^*O^* = \mathcal{L}_{A^*B^*C^*}(X^*_{648})$ be the Euler line of the triangle $A^*B^*C^*$. The lines $G^*O^* = \mathcal{L}_{A^*B^*C^*}(X^*_{648})$ and $IO = \mathcal{L}_{ABC}(X_{651})$ are identical lines because we have $O^* = I$ and the orthopoint X^*_{523} of G^*O^* agrees with the orthopoint X_{513} of IO. The $\mathcal{S}$-dual of the line G^*O^* is the point X_{513}, so the lines $\mathcal{L}_{\mathcal{S}}(Q^*)$ with Q^* a point on G^*O^* form a pencil through X_{513}. The $\mathcal{S}$-dual of O^* is the line at infinity, and for a point on G^*O^*, different from O^*, the $\mathcal{S}$-dual $\mathcal{L}_{\mathcal{S}}(Q^*)$ is perpendicular to IO. As a special case we have the line $\mathcal{L}_{\mathcal{S}}(X^*_{30})$ which passes through $I = O^*$. Because of the equation $\mathrm{d}(O^*, N^*) = \mathrm{d}(N^*, H^*)$, the quadruplet $(O^*, H^*; N^*, X^*_{30})$ is an harmonic range of points. Therefore, $(\mathcal{L}_{\mathcal{S}}(X^*_{30}), \mathcal{L}_{\mathcal{S}}(N^*); \mathcal{L}_{\mathcal{S}}(H^*), \mathcal{L}_{\mathcal{S}}(O^*))$ is an harmonic range of lines, and we get $\mathrm{d}(I, \mathcal{L}_{\mathcal{S}}(H^*)) = d(\mathcal{L}_{\mathcal{S}}(H^*), \mathcal{L}_{\mathcal{S}}(N^*))$. We also have an harmonic range $(O^*, N^*; G^*, H^*)$ which implies that the quadruplet $(\mathcal{L}_{\mathcal{S}}(H^*), \mathcal{L}_{\mathcal{S}}(G^*); \mathcal{L}_{\mathcal{S}}(N^*), \mathcal{L}_{\mathcal{S}}(O^*))$ is harmonic and we have equal distances between the lines $\mathcal{L}_{\mathcal{S}}(H^*), \mathcal{L}_{\mathcal{S}}(N^*)$ and the lines $\mathcal{L}_{\mathcal{S}}(N^*), \mathcal{L}_{\mathcal{S}}(G^*)$. After all, we involve the DeLongchamps point L. Because of the harmonic range $(H^*, L^*; O^*, X^*_{30})$, we have equal distances between the lines $\mathcal{L}_{\mathcal{S}}(H^*)$, $\mathcal{L}_{\mathcal{S}}(X^*_{30})$ and the lines $\mathcal{L}_{\mathcal{S}}(X^*_{30})$, $\mathcal{L}_{\mathcal{S}}(L^*)$. The constellation of these lines is shown in Figure 18.

IO intersects

- $\mathcal{L}_{\mathcal{S}}(H^*)$ in X_{1319} (Bevan-Schröder-Point, midpoint of I and X_{36} , see [6], [7], [8],
- $\mathcal{L}_{\mathcal{S}}(N^*)$ in X_{36} (inverse in circumcircle of the incenter; midpoint of I and X_{484}, see [7]) ,
- $\mathcal{L}_{\mathcal{S}}(G^*)$ in X_{1155} (Schröder-Point; midpoint of X_{36} and X_{484} and intersection of $\mathcal{L}_{ABC}(I)$ with IO, see [6], [7]),

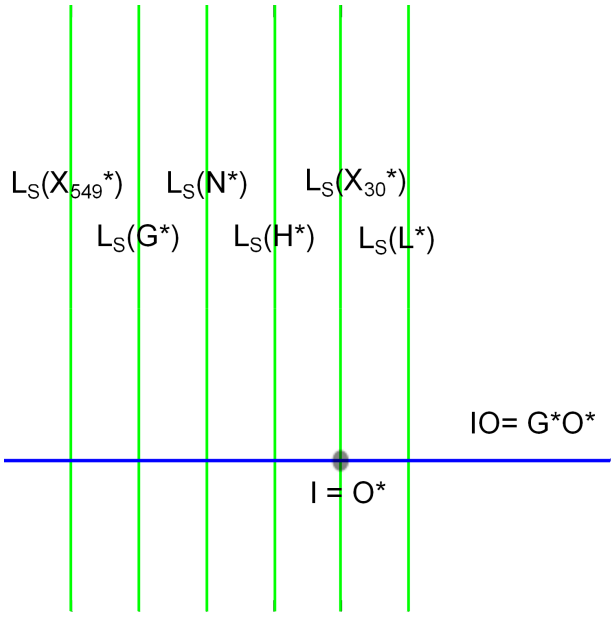

Figure 18. This shows the constellation of the lines $\mathcal{L}_{\mathcal{S}}(Q^*),\ Q^* = H^*, N^*, G^*, L^*, X_{30}{}^*, X^*_{549}$, in case of $P = I$.

- $\mathcal{L}_{\mathcal{S}}(L^*)$ in $(3a^4(b+c)+2a^3(b^2-13bc+c^2)+4a^2(-b^3+4b^2c+4bc^2-c^3)+2a(-b^4+5b^3c-12b^2c^2+5bc^3-c^4)+(b+c)(b-c)^4 : \cdots : \cdots)_{ABC}$,
- $\mathcal{L}_{\mathcal{S}}(X^*_{549})$ in X_{3245} (X^*_{549} is the midpoint of I* and O*; X_{3245} is the reflection of I in X_{1155}, see [7]).

I propose to call the point I/Q the *I-conjugate* of Q. The set of I-conjugates of points on IO is the circumconic $\mathcal{C}_{ABC}(X_{513})$, for short: The I-conjugate of IO is $\mathcal{C}_{ABC}(X_{513})$. This conic passes through the points $I = I\sharp G^*$ and $G = I\sharp O^*$, so it is a hyperbola. It also passes through the points $I\sharp H^* = X_{57}, I\sharp N^* = X_{81}$ and $I\sharp L^* = X_{145}$. The center of the circumconic is the point $X_{1015} = X^2_{513}$. It should not be too difficult (but quite a bit of work) to calculate the center functions of $I\sharp Q^*$ for all known centers Q^* on the Euler line q^*. A few of the points $I\sharp Q^*$ are listed in [7], many are not, even though some of them have relatively simple center functions.

The circle $\mathcal{S}$ is concentric with the incircle $\mathcal{J}_{ABC}(Ge)$ of ABC, so we can choose $\mathcal{S} = \mathcal{J}_{ABC}(Ge)$. In this case, the triangle $A^*B^*C^*$ is the intouch triangle of ABC. The line IO intersects the incircle in X_{2446} and in X_{2447}, see [7]. In [7] we also can find $X_{30}{}^* = X_{517}$, $H^* = X_{65}$, $N^* = X_{942}$, $G^* = X_{354}$ (Weill-point), $L^* = X_{3057}$.

Note. Choosing $P = {}_\tau I$ for $\tau \in \{a, b, c\}$, the Euler line of the triangle $A^*B^*C^*$ is identical with the line ${}_\tau IO$ of ABC.

3.2. $P = H$. We assume that ABC is an oblique triangle. Taking $P = H$, the triangles ABC and $A^*B^*C^*$ are homothetic with center H, and we have $(a^* : b^* : c^*) = (a : b : c)$. The point H is an inner center if ABC is acute, and it is an

outer center if ABC is obtuse. If we put the radius of $\mathcal{S}$ to $\sqrt{|S_A S_B S_C|}/(\sqrt{8}S)$, the triangle $A^*B^*C^*$ agrees with ABC in case of an obtuse triangle ABC ($\mathcal{S}$ is the polar circle of ABC), while for an acute triangle we get $A^*B^*C^*$ by reflecting ABC in H.

We can state the following

Lemma. Real version: For every point Q in the plane of an obtuse triangle ABC, the line $\mathcal{L}_{ABC}(H/Q)$ agrees with the polar line of Q with respect to the polar circle S. For every point Q in the plane of an acute triangle ABC, one gets the line $\mathcal{L}_{ABC}(H/Q)$ by reflecting the polar line of Q (with respect to the circle $\mathcal{S}$) in H. Complex version: For every point Q in the plane of an oblique triangle ABC, the line $\mathcal{L}_{ABC}(H/Q)$ agrees with the polar line of Q with respect to the quadric $S_A x^2 + S_B y^2 + S_C z^2 = 0$.

I propose to call the point H/Q the *H-conjugate of Q*. The H-conjugate of the Euler line is the Kiepert hyperbola.

The constellation of the lines $\mathcal{L}_{\mathcal{S}}(Q^*),\ Q^* = N^*, G^*, O^*, L^*, X_{30}^*$, is shown in Figure 19. The proof of this is quite similar to the proof of the constellation of lines given in the previous subsection.

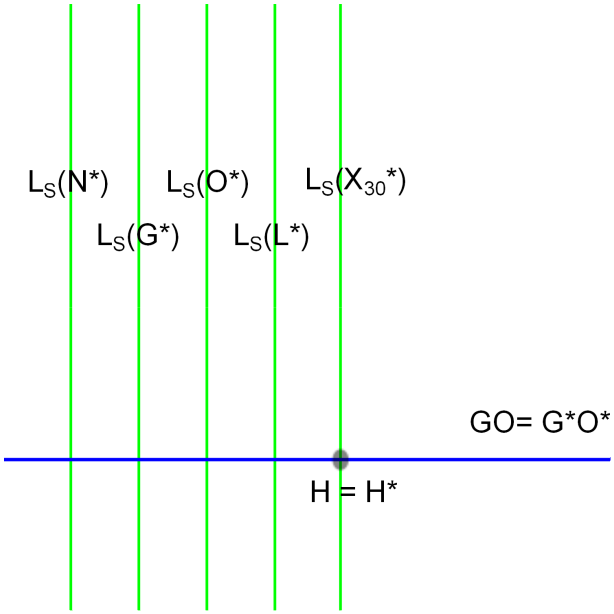

Figure 19.

GO intersects

- $\mathcal{L}_{\mathcal{S}}(G^*) = \mathcal{L}_{ABC}(H)$ in X_{486} (inner Vecten point),
- $\mathcal{L}_{\mathcal{S}}(O^*) = \mathcal{L}_{ABC}(X_{2052})$ in X_{403} (X_{403} is the point X_{36} of the orthic triangle, see [7]),
- $\mathcal{L}_{\mathcal{S}}(N^*) = \mathcal{L}_{ABC}(X_{275})$ in X_{186} (inverse in circumcircle of H, see [7]),
- $\mathcal{L}_{\mathcal{S}}(L^*) = \mathcal{L}_{ABC}(K/L)$ in $((2a^6 - a^4(b^2+c^2) - 4a^2(b^2-c^2)^2 + 3(b^2-c^2)^2(b^2+c^2))/S_A : \cdots : \cdots)_{ABC}$.

References

[1] O. Bottema, *Hoofdstukken uit de Elementaire Meetkunde*, 2nd ed., Utrecht: Epsilon, 33–38, 1987.
[2] W. L. Burke, *Applied Differential Geometry*, Cambridge University Press, Cambridge, 1985.
[3] B. Gibert, Orthocorrespondence and Orthopivotal Cubics, *Forum Geom.*, 3 (2003) 21–27.
[4] B. Gibert and F. M. van Lamoen, The Parasix Configuration and Orthocorrespondence, *Forum Geom.*, **3** (2003) 169-180.
[5] B. Gibert, Bicevian Conics and CPCC Cubics, March 11 2006 edition, available at `http://bernard.gibert.pagesperso-orange.fr/files/bicevian.html`.
[6] D. Grinberg, Schröder Points Database, Jul 4 2004 edition, available at `http://www.cip.ifi.lmu.de/ grinberg/Schroeder/Schroeder.html`.
[7] C. Kimberling, *Encyclopedia of Triangle Centers (ETC)*, March 20 2011 edition, available at `http://faculty.evansville.edu/ck6/encyclopedia/ETC.html`.
[8] H. Schröder, Die Inversion und ihre Anwendung im Unterricht der Oberstufe, *Der Mathematikunterricht*, **1** (1957) 59-80.
[9] J. H. Weaver, A generalization of the circles of Apollonius, *Amer. Math. Monthly*, 45 (1938) 17–21.
[10] P. Yiu, Generalized Apollonian circles, *Journal for Geometry and Graphics*, 8 (2004) 225–230.

Manfred Evers: Bendenkamp 21, Ratingen, 40880 Germany
E-mail address: `manfred_evers@yahoo.com`

Forum Geometricorum
Volume 12 (2012) 283–286.

FORUM GEOM
ISSN 1534-1178

An Elementary View on Gromov Hyperbolic Spaces

Wladimir G. Boskoff, Lucy H. Odom, and Bogdan D. Suceavă

Abstract. In the most recent decades, metric spaces have been studied from a variety of viewpoints. One of the important characterizations developed in the study of distances is Gromov hyperbolicity. Our goal here is to provide two approachable, but also intuitive examples of Gromov hyperbolic metric spaces. The authors believe that such examples could be of interest to readers interested in advanced Euclidean geometry; such examples are in fact a familiar introduction into coarse geometries. They are both elementary and fundamental. A scholar familiar with concepts like Ptolemy's cyclicity theorem or various geometric loci in the Euclidean plane could find a familiar environment by working with the concepts presented here.

1. Motivation

The reader familiar with the advanced Euclidean geometry will already have a major advantage when she/he pursues the study of specialized themes in metric geometry. On certain topics, the insight into some ideas developed historically within the triangle geometry or alongside classes of fundamental inequalities serves as a great aid in understanding the profound phenomena in metric spaces. Additionally, from a mathematical standpoint, it is of particular interest to find connections of advanced Euclidean geometry with other areas of mathematics.

One of the most accessible introductions into metric geometry is D. Burago, Y. Burago, and S. Ivanov's monograph [2]. In this well-written monograph, section 8.4 (pp. 284–288) is dedicated to the study of Gromov hyperbolic spaces. The chapter is particularly detailed, but we feel that some more elementary examples would serve the exposition well.

Our motivation in writing this note is to provide the reader who is familiar with advanced Euclidean geometry with an idea of a possible research topic in a more advanced context.

2. Gromov hyperbolic spaces: definition, notations, brief guidelines among references

Following M. Gromov's influential work [5], in recent years several investigators have been interested in showing that metrics, particularly in the area of geometric function theory, are Gromov hyperbolic (to mention here with a few examples,

Publication Date: December 11, 2012. Communicating Editor: Paul Yiu.

see [1, 7, 8, 9]). In the classical theory, an important class of examples of Gromov hyperbolic spaces are the CAT(κ) spaces, with $\kappa < 0$ (see [4], p.106). The reader's ultimate goal is to understand the fundamental monograph [6], which serves as guidelines to many researchers and attracts major interest.

For a formal definition, consider a metric space (M, d) where d satisfies the usual definition of a distance. Given $X, Y, Z \in M$, the quantity $(X|Y)_Z = \frac{1}{2}[d(X, Z) + d(Y, Z) - d(X, Y)]$ is called the *Gromov product* of X and Y with respect to Z. Denote $a \wedge b = \min\{a, b\}$. The metric space (M, d) is called *Gromov hyperbolic* (see Definition 8.4.6, p. 287 in [2]) if there exists some constant $\delta \geq 0$ such that

$$(X|Y)_W \geq (X|Z)_W \wedge (Z|Y)_W - \delta,$$

for all $X, Y, W, Z \in M$.

Sometimes it is more convenient to study the pointwise characterization of Gromov hyperbolic spaces. Using the fact that $a \vee b = \max\{a, b\}$, the Gromov hyperbolic condition can be rewritten in the following way:

(M, d) is a Gromov hyperbolic metric space if there exists a constant $\delta \geq 0$ such that

$$d(X, Z) + d(Y, W) \leq [d(Z, W) + d(Y, Z)] \vee [d(X, Y) + d(Z, W)] + 2\delta, \quad \forall X, Y, W, Z \in M.$$

The geometric idea is best captured in Mikhail Gromov's description from [6, p.19], where he writes: "It is hardly possible to find a convincing definition of the curvature (tensor) for an arbitrary metric space X, but one can distinguish certain classes of metric spaces corresponding to Riemannian manifolds with curvatures of a given type. This can be done, for example, by imposing inequalities between mutual distances of finite configurations of points in X".

3. Examples of Gromov hyperbolic spaces

In this section we present two examples of Gromov hyperbolic spaces.

Proposition 1. *Let $A(-1, 0), B(0, 1)$, and $D(0, -1)$ be points in the Cartesian plane endowed with the Euclidean distance d. Let $M \subset \mathbb{R}^2$ be the set*

$$M = \{A, B, D\} \cup \{C | C(x, 0), x \geq 0\}.$$

Then the metric space (M, d) is Gromov hyperbolic with $\delta \in \left[\frac{3-\sqrt{2}}{2}, \frac{4-\sqrt{2}}{2}\right]$.

Proof. We check that there exists a constant $\delta \geq 0$ such that

$$d(X, Z) + d(Y, W) \leq [d(Z, W) + d(Y, Z)] \vee [d(X, Y) + d(Z, W)] + 2\delta,$$

for all X, Y, $Z \in M$. Note that $d(B, D) = 2$, $d(A, C) = x + 1$, $d(A, B) = d(A, D) = \sqrt{2}$, and

$$d(C, D) = d(C, B) = \sqrt{x^2 + 1}.$$

In order to determine our constant $\delta > 0$, we require the following condition:

$$d(A,C) + d(B,D) \leq [d(A,B) + d(C,D)] \vee [d(A,D) + d(C,B)] + 2\delta.$$

However, $d(A,B) + d(C,D) = d(A,D) + d(C,B)$, thus finding δ reduces to the following:

$$x + (3 - \sqrt{2}) - 2\delta \leq \sqrt{x^2+1}, \qquad \forall x \geq 0.$$

An inequality such as $x + b \leq \sqrt{x^2+1}$, for all $x \geq 0$ leads to $\delta \geq \frac{3-\sqrt{2}}{2}$ when $b \leq 0$ and $\delta \leq \frac{4-\sqrt{2}}{2}$ when $b \geq -1$. In all the other cases, the basic inequality holds for $\delta \geq 0$. That is, the metric space (M,d) is Gromov hyperbolic with $\delta \in \left[\frac{3-\sqrt{2}}{2}, \frac{4-\sqrt{2}}{2}\right]$. □

Proposition 2. *Let $A(0,1)$, $B(-1,0)$, $C(0,-1)$ $D(a,0)$, with $a \in (0,2)$ be points in the interior of the disk centered at the origin of radius 2, endowed with the Cayley distance (see* [3]*)*

$$d(X,Y) = \frac{1}{2} \ln \frac{SX}{SY} : \frac{sX}{sY}, \tag{1}$$

where $\{s,S\} = \overline{XY} \cap C((0,0),2)$. Then the set

$$M = \{A,B,C\} \cup \{D | D(a,0), a \in (0,2)\}$$

endowed with the metric space induced by Cayley's distance is a Gromov hyperbolic metric space if

$$\delta > \frac{1}{4} \cdot \ln 27\sqrt{3} \left(\frac{\sqrt{7}+1}{\sqrt{7}-1} \right)^2.$$

Proof. A direct computation shows that

$$d(A,D) = d(C,D) = \frac{1}{2} \ln \left[\frac{\sqrt{3a^2+4}+1}{\sqrt{3a^2+4}-1} \cdot \frac{\sqrt{3a^2+4}+a^2}{\sqrt{3a^2+4}-a^2} \right]$$

$$d(A,B) = d(B,C) = \frac{1}{2} \ln \left[\frac{\sqrt{7}+1}{\sqrt{7}-1} \right]^2$$

$$d(A,C) = \frac{1}{2} \ln 9, \quad d(B,D) = \frac{1}{2} \ln \frac{3(2+a)}{2-a}.$$

In order to determine $\delta > 0$, we require the condition:

$$d(A,C) + d(B,D) \leq [d(A,B) + d(C,D)] \vee [(d(A,D) + d(C,B)] + 2\delta.$$

On the other hand, $d(A,B) + d(C,D) = d(A,D) + d(C,B)$, thus determining δ reduces to

$$\ln \frac{27(2+a)}{2-a} \leq \ln \left[\left(\frac{\sqrt{7}+1}{\sqrt{7}-1} \right)^2 \cdot \frac{\sqrt{3a^2+4}+1}{\sqrt{3a^2+4}-1} \cdot \frac{\sqrt{3a^2+4}+a^2}{\sqrt{3a^2+4}-a^2} \cdot e^{4\delta} \right]$$

for any $a \in (0, 2)$. In fact, the inequality

$$\frac{27(2+a)}{2-a} \leq \left(\frac{\sqrt{7}+1}{\sqrt{7}-1}\right)^2 \cdot \frac{\sqrt{3a^2+4}+1}{\sqrt{3a^2+4}-1} \cdot e^{4\delta}$$

holds exactly when

$$\left(\frac{\sqrt{7}+1}{\sqrt{7}-1}\right)^2 \cdot e^{4\delta} > 27\sqrt{3}.$$

Therefore

$$\delta > \frac{1}{4} \cdot \ln 27\sqrt{3} \left(\frac{\sqrt{7}+1}{\sqrt{7}-1}\right)^2.$$

□

In all the other cases one should consider in this proof, we obtain similar computations; these computations have not been included here, to preserve the quality of our presentation. Our goal is to underline the fundamental geometric core of Gromov hyperbolic metric spaces by the use of these examples.

Note that in the second example, the order of the points in the Cayley distance in (1) is chosen so that the cross-ratio yields a value greater than 1.

References

[1] M. Bonk, J. Heinonen and P. Koskela, Uniformizing Gromov hyperbolic spaces, *Astérisque*, 270 (2001) 266–3-6.

[2] D. Burago, Y. Burago, and S. Ivanov, *A Course in Metric Geometry*, Amer. Math. Society, 2001.

[3] A. Cayley, A sixth memoir upon quantics, *Philosophical Transactions of the Royal Society of London*, 149 (1859) 61–90.

[4] M. M. Deza and E. Deza, *Encyclopedia of Distances*, Springer-Verlag, 2009.

[5] M. Gromov, Hyperbolic groups, in *Essays in group theory* (S. M. Gersten, ed.), MSRI Publ. 8 (1987) 75–263.

[6] M. Gromov, *Metric Structures for Riemannian and Non-Riemannian Spaces*, Birkhäuser, second printing with corrections, 2001.

[7] P. A. Hästö, Gromov Hyperbolicity of the j_G and $\tilde{j}_G$ metrics, *Proc. Amer. Math. Soc.*, 134 (2005) 1137–1142.

[8] Z. Ibragimov, Hyperbolizing metric spaces, *Proc. Amer. Math. Soc.*, 139 (2011) 4401–4407.

[9] A. Karlsson and G. A. Noskov, The Hilbert metric and Gromov hyperbolicity, *Enseign.Math.*, 48 (2002) 73–89.

Wladimir G. Boskoff: Department of Mathematics and Computer Sciences, Ovidius University, Constanţa, Romania.

Lucy H. Odom and Bogdan D. Suceavă: Department of Mathematics, P. O. Box 6850, California State University at Fullerton, Fullerton, CA 92834-6850.

Forum Geometricorum
Volume 12 (2012) 287–300.

FORUM GEOM
ISSN 1534-1178

On Tripolars and Parabolas

Paris Pamfilos

Abstract. Starting with an analysis of the configuration of chords of contact points with two lines, defined on conics circumscribing a triangle and tangent to these lines, we prove properties relating to the case the conics are parabolas and a resulting method to construct the parabola tangent to four lines.

1. Introduction

It is well known ([3, p. 42], [10, p. 184], [7, II, p. 256]), that given three points A, B, C and two lines in general position, there are either none or four conics passing through the points and tangent to the given lines. A light simplification of Chasles notation ([2, p. 304]) for these curves is $3p2t$ *conics*. The conics exist if either the two lines do not intersect the interior of the triangle ABC or the two lines intersect the interior of the same two sides of ABC. In all other cases there are no conics satisfying the above requirements. In this article, we obtain a formal condition (Theorem 6) for the existence of these conics, relating to the geometry of the triangle ABC. In addition we study the configuration of a triangle and two lines satisfying certain conditions. In §2 we introduce the *middle-tripolar*, which plays a key role in the study. In §3 we review the properties of generalized quadratic transforms, which are relevant for our discussion. In §§4, 5 we relate the classical result of existence of $3p2t$ conics to the geometry of the triangle ABC. In the two last sections we prove related properties and construction methods for parabolas.

2. The middle-tripolar

If a parabola circumscribes a triangle ABC and is tangent to a line l (at a point different from the vertices), then l does not intersect the interior of ABC. In this section we obtain a characterization of such lines. For this, we start with a point P on the plane of triangle ABC and consider its traces A_1, B_1, C_1 and their harmonic conjugates A_2, B_2, C_2, with respect to the sides BC, CA, AB, later lying on the tripolar $tr(P)$ of P (See Figure 1). By applying Newton's theorem ([5, p. 62]) on the diagonals of the quadrilateral $A_1B_1B_2A_2$ we see that the middles A', B', C' respectively of the segments A_1A_2, B_1B_2, C_1C_2 are on a line, which I call the *middle-tripolar* of the point P and denote by m_P. In the following discussion a crucial role plays a certain symmetry among the four lines defined by the sides of the cevian $A_1B_1C_1$ of P and the tripolar $tr(P)$, in relation to the *harmonic associates* ([13, p. 100]) P_1, P_2, P_3 of P. It is, namely, readily seen that for each of these four points the corresponding sides of cevian triangle and tripolar define the same set of four lines. A consequence of this fact is that all four points P, P_1, P_2, P_3 define the same middle-tripolar, which lies totally in the exterior of

Publication Date: December 17, 2012. Communicating Editor: Paul Yiu.

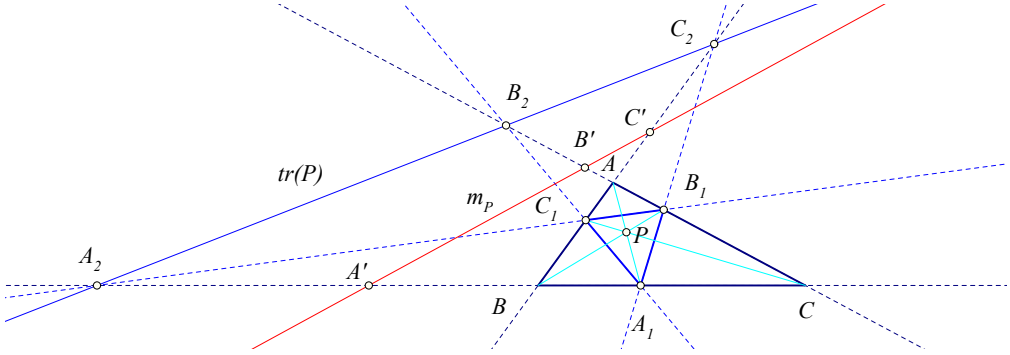

Figure 1. The middle-tripolar m_P of P

the triangle ABC. Combining these two properties, we see that for every point P of the plane, not coinciding with the side-lines or the vertices of the triangle, the corresponding middle-tripolar m_P lies always outside the triangle. It is easy to see that all these properties are also consequences of the following algebraic relation, which is proved by a trivial calculation.

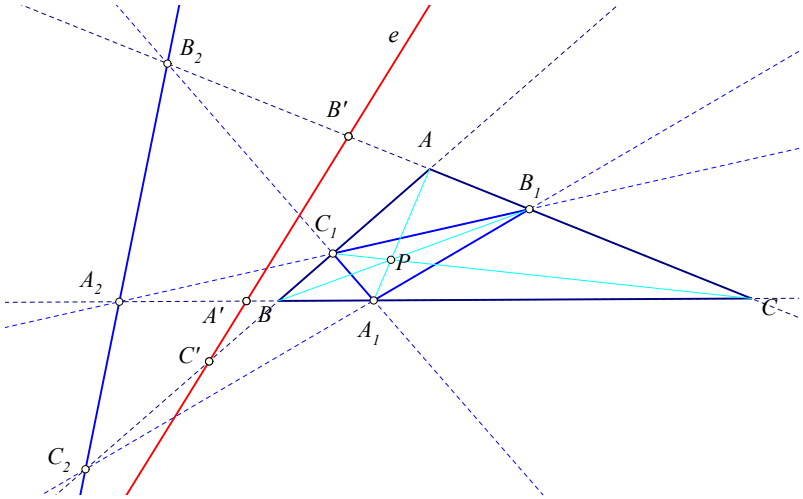

Figure 2. Given e find P such that $e = m_P$

Lemma 1. *If the point P defines through its trace A_1 the ratio $\frac{A_1B}{A_1C} = k$, then the corresponding middle-tripolar m_P defines on the same side of the triangle ABC the ratio $\frac{A'B}{A'C} = k^2$.*

Using this lemma, we can see that every line e exterior to the triangle and not coinciding with a side-line or vertex, defines a point P, interior to the triangle, such that $e = m_P$. It suffices for this to take the ratios defined by e on the side lines

$$k_1 = \frac{A'B}{A'C}, \qquad k_2 = \frac{B'C}{B'A}, \qquad k_3 = \frac{C'A}{C'B}$$

and define the points A_1, B_1, C_1 with corresponding ratios

$$\frac{A_1B}{A_1C} = -\sqrt{k_1}, \qquad \frac{B_1C}{B_1A} = -\sqrt{k_2}, \qquad \frac{C_1A}{C_1B} = -\sqrt{k_3}.$$

A simple application of Ceva's theorem implies that these points define cevians through the required point P, and proves the following lemma.

Lemma 2. *Every line e not intersecting the interior of the triangle ABC and not coinciding with a side-line or vertex of the triangle is the middle-tripolar m_P of a unique point P in the interior of the triangle ABC.*

3. Quadratic transform associated to a base

If a conic circumscribes a triangle ABC and is tangent to two lines l, l' (at points different from the vertices), then it is easily seen that either the lines do not intersect the interior of the triangle or they intersect the interior of the same couple of sides of the triangle. In this section we obtain a characterization of such lines. For this we start with a *base* $A(1,0,0), B(0,1,0), C(0,0,1), D(1,1,1)$ of the projective plane ([1, I, p. 95]). To this base is associated a quadratic transform f, described in the corresponding coordinates through the formulas

$$x' = \frac{1}{x}, \qquad y' = \frac{1}{y}, \qquad z' = \frac{1}{z}.$$

This generalizes the *Isogonal* and the *Isotomic* transformations of a given triangle ABC and has analogous to them properties ([9]). The most simple of them are, that f is involutive $(f^2 = I)$, fixes D and its three harmonic associates, and maps lines to conics through the vertices of ABC. In addition, the harmonic associates of D define analogously the same transformation. Of interest in our study is also the induced transformation f^* of the dual space $(P^2)^*$, consisting of all lines of the projective plane P^2. The transformation f^* can be defined by the requirement of making the following diagram of maps commutative $(f^* \circ tr = tr \circ f)$.

$$\begin{array}{ccc} P^2 & \xrightarrow{\ f\ } & P^2 \\ {\scriptstyle tr}\downarrow & & \downarrow{\scriptstyle tr} \\ (P^2)^* & \xrightarrow[\ f^*\ ]{} & (P^2)^* \end{array}$$

Here tr denotes the operation $l_P = tr(P)$ of taking the tripolar line of a point with respect to ABC. For every line l the line $l' = f^*(l)$ is found by first taking the tripole P_l of l, then taking $P' = f(P_l)$ and finally defining $l' = tr(P')$. It is easily seen that $(f^*)^2 = I$ and that f^* fixes the sides of the cevian triangle and the tripolar of P. The next lemma follows from a simple computation, which I omit (See Figure 3).

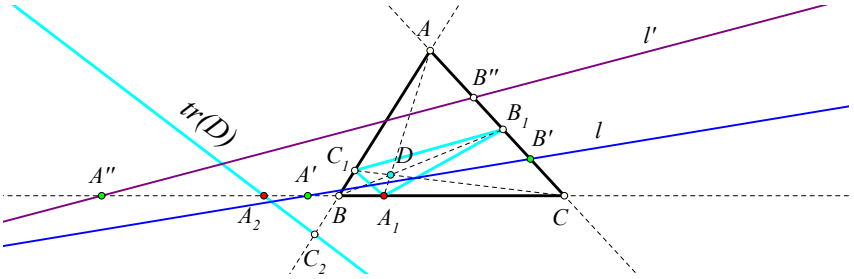

Figure 3. $l' = f^*(l)$ intersects BC on $A'' = A'(A_1A_2)$

Lemma 3. *Let A_1, B_1, C_1 be the traces of D on BC, CA, AB and A_2, B_2, C_2 their harmonic conjugates with respect to these side-endpoints. For every line l intersecting these sides, correspondingly, at A', B', C', the line $l' = f^*(l)$ intersects these sides at the corresponding harmonic conjugates $A'' = A'(A_1A_2), B'' = B'(B_1B_2), C'' = C'(C_1C_2)$.*

Lemma 4. *Let A, B, C, D be a projective base and f the corresponding quadratic transform. For every line l not coinciding with a side-line or vertex of ABC, the lines $l, l' = f^*(l)$ satisfy the following property: either both do not intersect the interior of ABC or both intersect the interior of the same pair of sides of ABC.*

The proof is again an easy calculation in coordinates, which I omit. The next theorem, a sort of converse of the preceding one, shows that this construction characetrizes the lines tangent to a conic circumscribing a triangle.

Theorem 5. *Let ABC be a triangle and l, l' be a pair of lines having the property of the previous lemma. Then there is a point D, such that A, B, C, D is a projective base with quadratic transformation f and such that $l' = f^*(l)$.*

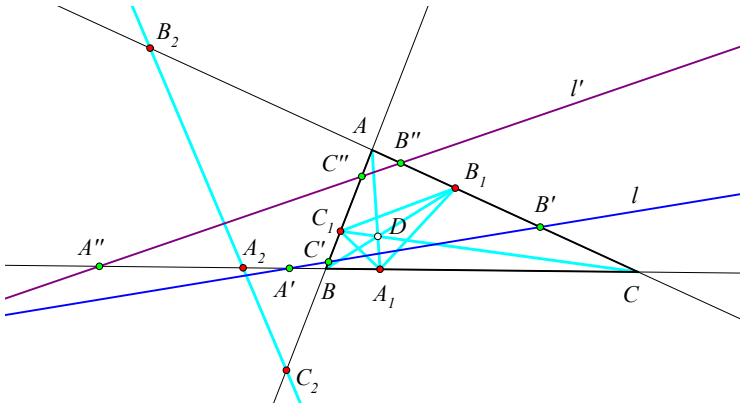

Figure 4. The common harmonics defined by ABC and the two lines

To prove the theorem consider first the intersection points A', B', C' of l, and A'', B'', C'' of l' correspondingly with the sides BC, CA, AB of the triangle. By

the hypothesis follows that the pairs of segments $A'A'', BC$ either do not intersect or one of them contains the other. The same is true for the pairs $B'B'', CA$ and $C'C'', AB$. It follows that there are exactly two real points A_1, A_2 on line BC, which are common harmonics with respect to (B, C) and (A', A'') i.e. (A_1, A_2) are simultaneously harmonic conjugate with respect to (B, C) and (A', A''). Analogously there are defined the common harmonics (B_1, B_2) of (C, A) and (B', B'') and the common harmonics (C_1, C_2) of (A, B) and (C', C'') (See Figure 4). To prove the theorem, it is sufficient to show that three points out of the six A_1, A_2, B_1, B_2, C_1, C_2 are on a line. This can be done by a calculation or, more conveniently, by reducing it to lemma 2 (see also [6, p. 232]). In fact, consider the projecitvity g fixing A, B, C and sending line l' to the line at infinity $m' = g(l')$. Then line l maps to a line $m = g(l)$. Since projectivities preserve cross ratios, the common harmonic points of l, l' map to corresponding common harmonic points of m, m'. By Lemma 2 line m is the middle-tripolar of some point and three of these harmonic points are on a line. Consequently, their images under g^{-1} are also on a line.

4. $3p2t$ conics

The structure of a triangle ABC and two lines l, l', studied in the preceding section, is precisely the one for which we have four solutions to the problem of constructing a conic passing through three points and tangent to two lines (a $3p2t$ conic). The standard proof of this classical theorem ([3, p. 42], [10, p. 184], [7, II, p. 256], [4], [12]) relies on a consequence of the theorem of Desargues ([11, p. 127]).

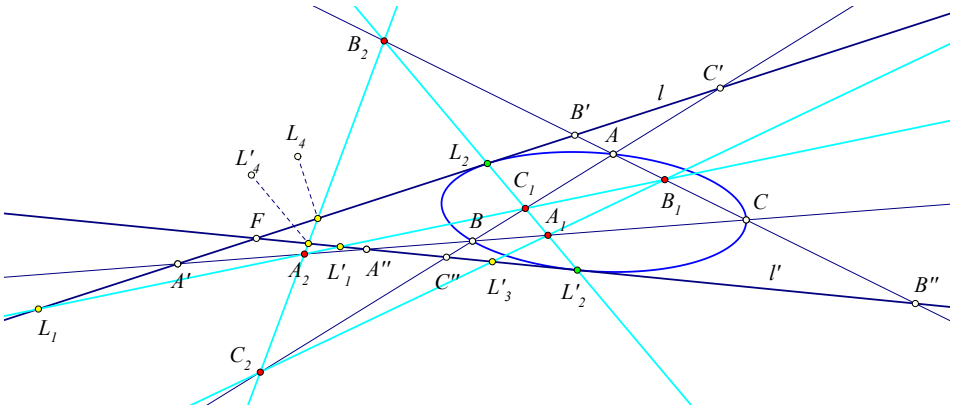

Figure 5. A_1, A_2 fixed points of the involution interchanging $(B, C), (A', A'')$

By this, all conics, tangent to two fixed lines l, l' at two fixed points, determine through their intersections with a fixed line an involution ([11, p. 102]) on the points of this line. Such an involution is completely defined by giving two pairs of corresponding points, such as (B, C) and (A', A'') in Figure 5. The chord of contact points contains the fixed points of the involution, characterized by the fact

to be simultaneous harmonic conjugate with respect to the two pairs defining the involution. In Figure 5, the fixed points of the involution on line BC are A_1, A_2. Analogously are defined the fixed points of the involutions operating on the two other sides of the triangle ABC. Thus, there are obtained three pairs of points $(A_1, A_2), (B_1, B_2), (C_1, C_2)$ on respective sides of the given triangle.

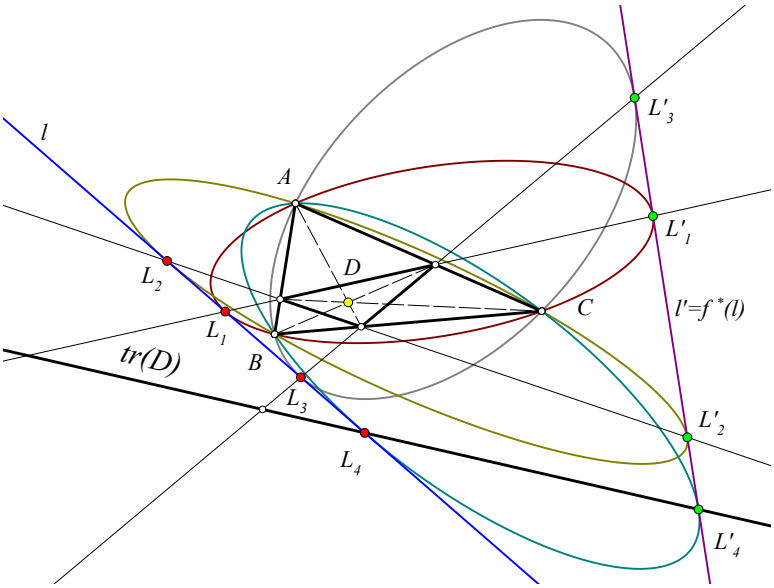

Figure 6. The four circumconics of ABC tangent to $l, l' = f^*(l)$

By the analysis made in the previous sections we see that these six points lie, by three, on four lines, whose intersections with l, l' define the contact points with the conics. The ingredient added to this proof by our remarks is that these four lines are the sides of a cevian triangle and the associated tripolar of a certain point D, defined directly by the triangle ABC and the two lines l, l' (See Figure 6). Thus, the theorem can be formulated in the following way, which brings into the play the geometry of the triangle involved.

Theorem 6. *Let A, B, C, D be a projective base and l a line not coinciding with the side-lines or vertices of triangle ABC. Let also $L_i, L'_i, (i = 1, 2, 3, 4)$ be the intersections of lines $l, l' = f^*(l)$ with the side-lines of the cevian triangle of D and the tripolar $tr(D)$. The four conics, passing, each, through $(A, B, C, L_i, L'_i$ $(i = 1, 2, 3, 4))$, are tangent to l and l'. Conversely, every conic circumscribing ABC and tangent to two lines l, l' is part of such a configuration for an appropriate point D.*

Remarks. (1) The transformation f^* is a sort of *dual* of f and operates in $(P^2)^*$ in the same way f operates in P^2. As noticed in §3, f^* is an involutive quadratic transformation, which fixes the sides of the cevian triangle of D and the tripolar $tr(D)$. Analogously to f, which maps lines to circumconics of ABC, f^* maps

the lines of the pencil through a fixed point Q, representing a *line* of $(P^2)^*$, to the tangents of the conic inscribed in ABC, whose perspector ([13, p. 115]) is $f(Q)$. The theorem identifies points (L_i, L_i') with the *lines* of $(P^2)^*$ joining the *fixed points* of this transformation, correspondingly, with the *points* l, l' of $(P^2)^*$.

(2) In the converse part of the theorem the point D is not unique. The structures, though, defined by it and which are relevent for the problem at hand, are indeed unique. Any one of the harmonic associates D_1, D_2, D_3 of D will define the same f and f^* and the same four lines, intersecting the lines l, l' in the same pairs of points (L_i, L_i'). In each case, three of the lines will be the side-lines of the associated cevian triangle and the fourth will be the associated tripolar. Thus, in the last theorem, one can always select the point D in the interior of the triangle ABC, and this choice makes it unique.

Corollary 7. *Given the triangle ABC, the pairs of lines l, l' for which there is a corresponding $3p2t$ conic, are precisely the pairs $l, l' = f^*(l)$, where l is any line not coinciding with the side-lines or vertices of ABC and f^* is defined by a point D lying in the interior of the triangle.*

5. Four parabolas and a hyperbola

If one of the two lines of the last theorem, l' say, is the line at infinity, then it is easily seen that the other line can be identified with the middle-tripolar of some point D. This leads to the following theorem.

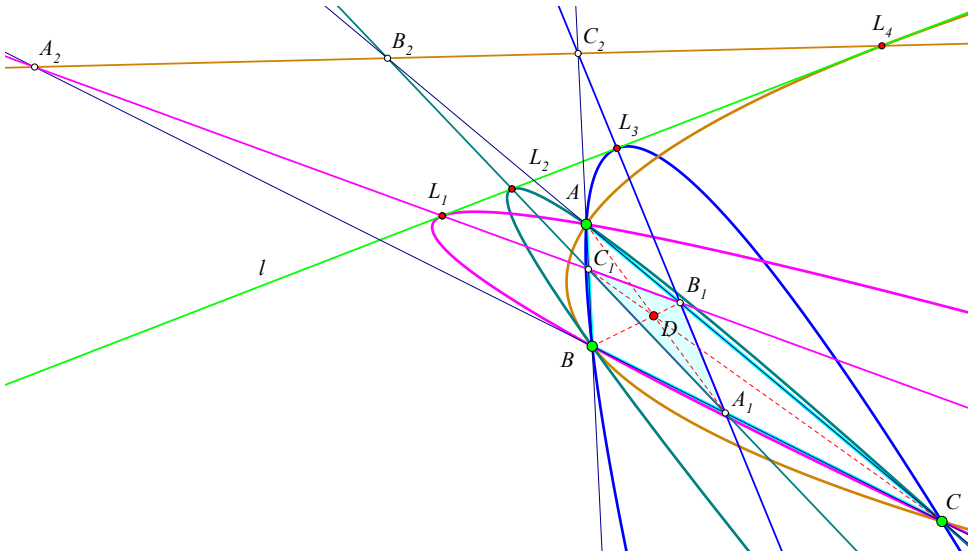

Figure 7. The four parabolas through A, B, C tangent to line $l = m_D$

Theorem 8. *For every point D in the interior of the triangle ABC the sides of its cevian triangle and its tripolar are parallel to the axes of the four parabolas circumscribing the triangle and tangent to its middle-tripolar m_D. The intersections*

of these four lines with m_D are the contact points of the parabolas with m_D. Conversely, every parabola through the vertices of a triangle ABC, touching a line l is member of a quadruple of parabolas constructed in this way.

Figure 7 shows a complete configuration of three points A, B, C, a line $l = m_D$ and the four parabolas passing through the points and tangent to the line. By the analysis made in §2, line l contains the middles of segments A_1A_2, B_1B_2 and C_1C_2.

The theorem implies that if a parabola c circumscribes a triangle ABC, then for each tangent l to the parabola, at a point different from the vertices, there are precisely three other parabolas circumscribing the same triangle and tangent to the same line. These three parabolas can be then determined by first locating the corresponding point D. The possibility to have D lying in the interior of the triangle, shows that one of the lines drawn parallel to the axes of these parabolas from the corresponding contact point does not intersect the interior of the triangle, whereas the other three do intersect the interior, defining the cevian triangle of point D. Point D is the tripole of that parallel, which does not intersect the interior. This rises the interest for finding the locus of D in dependence of the tangent to the parabola. The next theorem lists some of the properties of this locus and its relations to the parabola.

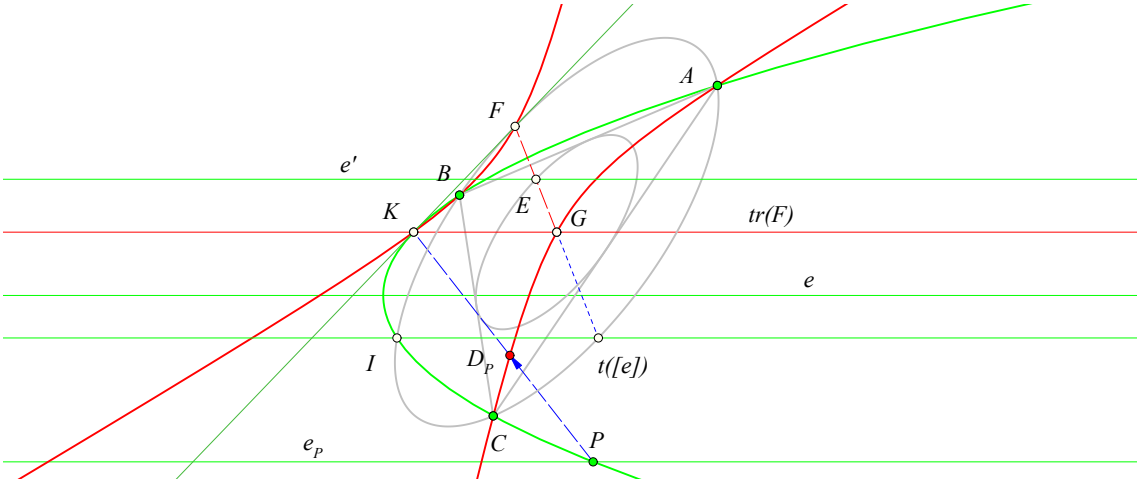

Figure 8. The hyperbola locus

Theorem 9. *Let c be a parabola with axis e circumscribing the triangle ABC. The locus of tripoles D_P of lines e_p, which are the parallels to the axis from the points P of the parabola, is a hyperbola circumscribing the triangle and has, among others, the properties:*

(1) *The hyperbola passes through the centroid G and has its perspector at the point at infinity $[e]$ determined by the direction of e. The perspector E of the parabola is on the inner Steiner ellipse of ABC and coincides with the center of the hyperbola.*

(2) *Line EG passes through the fourth intersection point F of the hyperbola with the outer Steiner ellipse. This line contains also the isotomic conjugate $t([e])$ of $[e]$. The tripole of this line is the fourth intersection point I of the parabola with the outer Steiner ellipse.*
(3) *The fourth intersection point K of the parabola and the hyperbola is the tripole of e', where e' the parallel to e through E. Line KG is parallel to the axis e and is also the tripolar of F. It is also $D_K = F$ and line FK is a common tangent to the parabola and the outer Steiner ellipse. The tangents to the hyperbola at F, K intersect on the parabola at its intersection point with line e'.*
(4) *The hyperbola is the image $g(c)$ of the parabola under the homography g, which fixes A, B, C and sends K to F.*
(5) *All lines joining P to D_P pass through K.*

Most of the properties result by applying theorems on general conics circumscribing a triangle, adapted to the case of the parabola.

In (1) the result follows from the general property of circumconics to be generated by the tripoles of lines rotating about a fixed point (the *perspector* of the conic). In our case the fixed point is the point at infinity $[e]$, determined by the direction of the axis of the parabola, and the lines passing through $[e]$ are all lines parallel to e. That the conic is a hyperbola follows from the existence of two tangents to the inner Steiner ellipse, which are parallel to the axis e. These two parallels have their tripoles at infinity, as do all tangents to the inner Steiner ellipse, implying that the conic is a hyperbola. That this hyperbola passes through the centroid G results from its definition, since G is the tripole of the line at infinity, which is a line of the pencil generating the conic. The claim on the perspector E follows also from a well known property for circumscribed conics, according to which the center C and the perspector P of a circumconic are *cevian quotients* ($C = G/P$, [13, p. 109]). This is a reflexive relation, and since the perspector $[e]$ of the hyperbola coincides with the center of the parabola, their quotients will be also identical.

In (2) point F is the symmetric of G w.r. to E. It belongs to the outer Steiner ellipse, which is homothetic to the inner one and lies also to the hyperbola, since E is its center. That points $E = G/[e], G$ and $t([e])$ are collinear follows by the vanishing of a simple determinant in barycentrics. The tripole I of line EG is the claimed intersection, since E, G are the respective perspectors of these conics.

In (3) line e' contains both the perspector of the parabola and the perspector of the hyperbola, so its tripole belongs to both corresponding conics.

In $(4, 5)$ and the rest of (3) the statements follow by an easy computation, and the fact, that the matrix of g^{-1} in barycentrics is

$$\begin{pmatrix} a & 0 & 0 \\ 0 & b & 0 \\ 0 & 0 & c \end{pmatrix},$$

where (a, b, c) are the coordinates of the point at infinity of line e. This is a homography mapping the outer Steiner ellipse to the hyperbola, by fixing A, B, C and sending F to K.

6. Relations to parabolas tangent to four lines

The two next theorems explore some properties of the parabolas tangent to four lines, which are the sides of a triangle together with the tripolar of a point with respect to that triangle. The focus is on the role of the middle tripolar m_D.

Theorem 10. *Let $A_1B_1C_1$ be the cevian triangle of point D with respect to triangle ABC. The parabola tangent to the sides of $A_1B_1C_1$ and the tripolar of D has its axis parallel to line $l = m_D$. In addition, the triangle ABC is self-polar with respect to the parabola.*

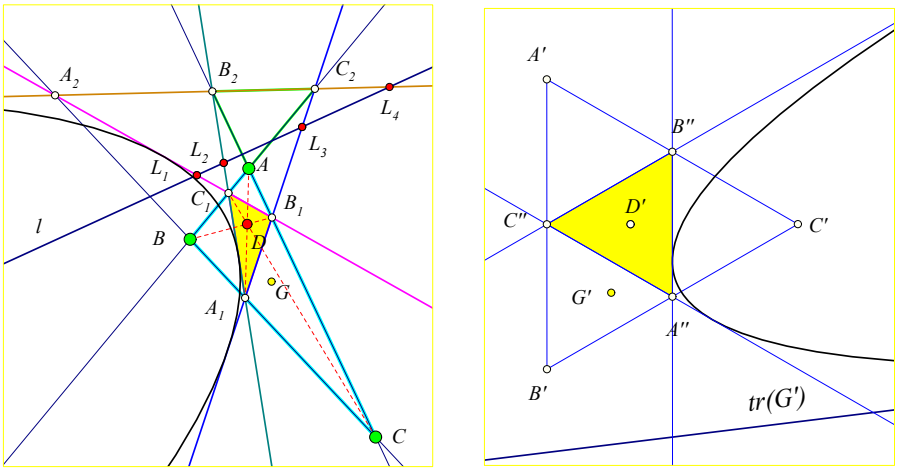

Figure 9. Reduction to the equilateral

The proof of the first part is a consequence of the theorem of Newton ([3, p. 208]), according to which, the centers of the conics which are tangent to four given lines is the line through the middles of the segments joining the diagonal points of the quadrilateral defined by the four lines (the *Newton line* of the quadrilateral [5, p. 62]). The parabola c tangent to the four lines has its center at infinity, thus later coincides with the point at infinity of this line and this proves the first part of the theorem. The second part results from a manageable calculation, but it can be given also a proof, by reducing it to a special configuration via an appropriate homography. In fact, consider the homography f, which maps the vertices of the triangle ABC and point D, correspondingly, to the vertices of the equilateral $A'B'C'$ and its centroid D'. Since homographies preserve cross ratios, they preserve the relation of a line, to be the tripolar of a point. Thus, the line at infinity, which is the tripolar of the centroid G, maps to the tripolar $tr(G')$ of point $G' = f(G)$ (See Figure 9). It follows that the image conic $c' = f(c)$ of the parabola c is also a parabola, since it is tangent to five lines $A''B'', B''C'', C''A'', tr(G'), f(A_2B_2)$, one of which is the line at infinity ($f(A_2B_2)$). Here $A'' = f(A_1), B'' = f(B_1), C'' = f(C_1)$ denote the middles of the sides of the equilateral. The proof of the second part results then from the following lemma.

Lemma 11. *If a parabola is inscribed in a triangle, then the anticomplementary triangle is self-polar with respect to the parabola.*

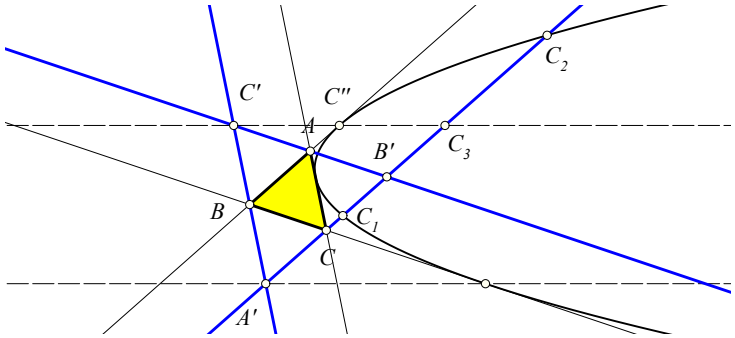

Figure 10. $A'B'C'$ is self-dual w.r. to the parabola inscribed in ABC

To prove the lemma consider a parabola c inscribed in a triangle ABC. Consider also its anticomplementary $A'B'C'$ and the point C'' of tangency with side AB (See Figure 10). The parallel to AB through C, which is a side of the anticomplementary, intersects the parabola at two points C_1, C_2 and by a well known property of parabolas ([8, p. 58]), the tangents at C_1, C_2 meet at the symmetric C' of the middle C_3 of C_1C_2 with respect to C''. Thus C' coincides with a vertex of the anticomplementary, being also the pol of line C_1C_2, as claimed.

Remark. The converse is also true: *If a conic is inscribed in a triangle, such that the anticomplementary is self-polar, then the conic is a parabola.*

Theorem 12. *Let the parabola c be tangent to the sides of the triangle ABC and to the tripolar $tr(D)$ of a point D. Then its contact point with $tr(D)$ is the intersection point of this line with the middle-tripolar $l = m_D$.*

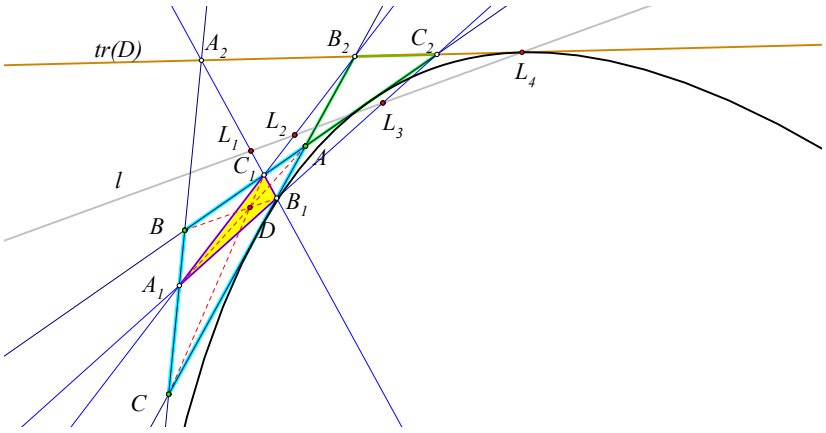

Figure 11. The contact point L_4 with the tripolar

This is proved by an argument similar to that, used in the preceding theorem. In fact, define the homography f mapping triangle ABC to an equilateral $A'B'C'$ and point D to the centroid of $A'B'C'$. Then, see, as in the preceding theorem, that the image conic $c' = f(c)$ of the parabola c is again a parabola. Let then P be the pole of line $l = m_D$ with respect to c. Since P is on line $A_2B_2 = tr(D)$ (See Figure 11), which maps under f to the line at infinity, its image $P' = f(P)$ is at infinity. Hence the image-line $l' = f(l)$ is parallel to the axis of c'. Thus, l' intersects the parabola c' at its point at infinity, which is the image $f(Q)$, where Q is the contact point of c with the line A_2B_2. From this follows that point Q coincides with the intersection point of lines l and A_2B_2, as claimed.

7. The points of tangency

Four lines in general position define a complete quadrilateral $ABCDEF$, four triangles ADE, ABF, BCE, CDF, the diagonal triangle HIJ and four points $ADEp, ABFp, BCEp$ and $CDFp$, which are correspondingly the tripoles of one of these lines with respect to the triangle of the remaining three (See Figure 11). The notation is such, that the tripolar of each of these four points, with respect to the triangle appearing in its label, is the remaining line out of the four, carrying the missing from the label letters (e.g. triangle ABF, tripole $ABFp$ and tripolar DCE). The harmonic associates of each of these points with respect to the corresponding triangle are the vertices of the diagonal triangle HIJ. It is easily seen that the harmonic associates of any of the four points $ADEp, ABFp, BCEp$ and $CDFp$, with respect to HIJ, are the remaining three points.

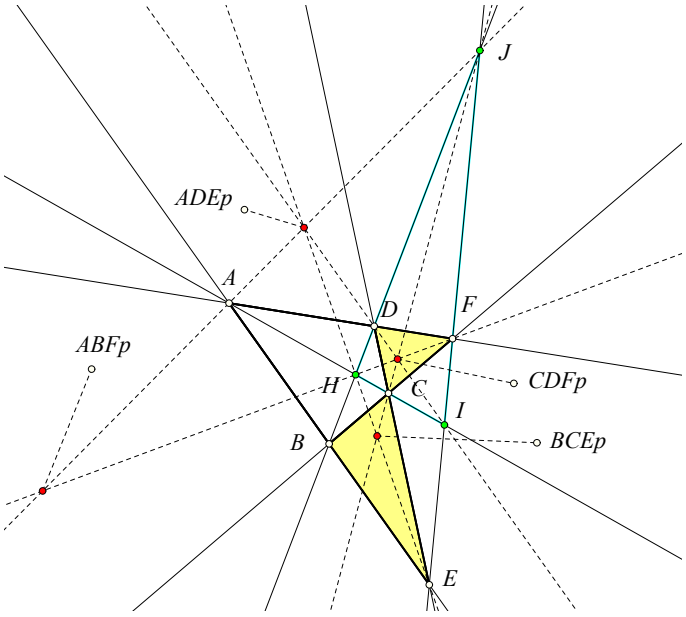

Figure 12. Four lines, four triangles, four points

Applying theorem-12 to each one of the four triangles and the corresponding tripole we obtain four middle-tripolars $ADEn, ABFn, BCEn, CDFn$, which intersect the corresponding lines BCF, CDE, ADF, ABE at corresponding points of tangency $ADEq, ABFq, BCEq, CDFq$ with the parabola tangent to the four given lines (See Figure 12). This remark leads to a construction method of the parabola tangent to four given lines. The method is not more complicated than the classical one ([8, p. 57]), which uses the circumcircles and orthocenters of the triangles defined by the four lines. In fact, once the middle-tripolars are found, the method uses only intersections of lines. The determination of the middle-tripolars, on the other side, requires either the construction of the harmonic conjugate of a point w.r. to two other points, or the construction of points on lines having a given ratio of distances to two other points of the same line. For example, referring to the last Figure 12, if the ratio $\frac{BA}{BE} = k$, then the corresponding ratio of the intersection point B' of lines $ADEn$ and ABE is $\frac{B'A}{B'E} = k^2$. Point B' is also the middle of segment $B''B$, where $B'' = B(A, E)$ is the harmonic conjugate of B w.r. to (A, E). Once the four contact points are found, one can easily construct a fifth point on the parabola and define it as a conic passing through five points. For this it suffices to find the middle M of a chord, e.g. the one joining $BCEq, CDFq$ and take the middle of MA.

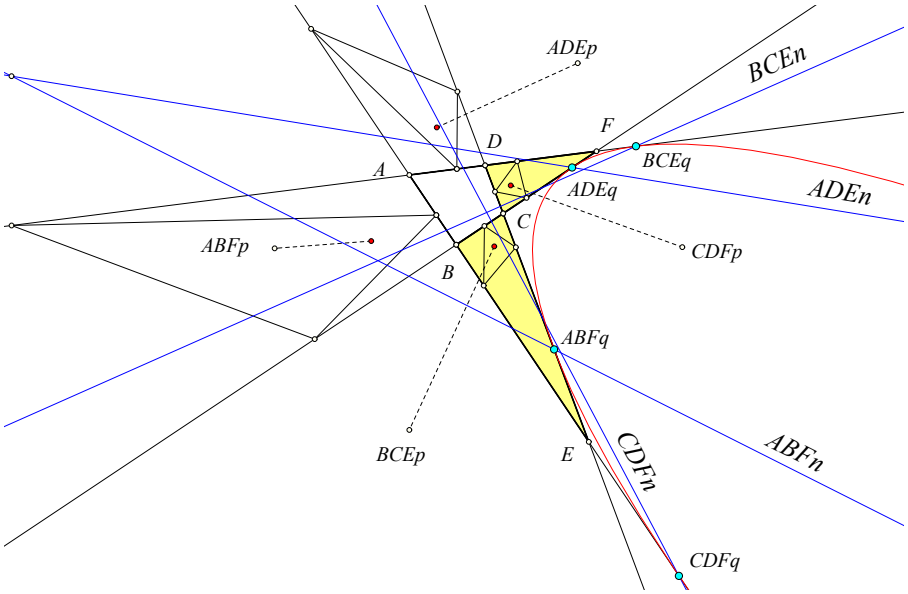

Figure 13. The contact points of the parabola tangent to four lines

References

[1] M. Berger, *Geometry*, vols I, II, Springer Verlag, Heidelberg, 1987.

[2] M. Chasles, Construction des coniques qui satisfont a cinq conditions, *Comptes rendues de l Academie des Sciences, Paris*, 58 (1864) 297–308.

[3] M. Chasles, *Traite de Sections Coniques*, Gauthier-Villars, Paris, 1865.
[4] M. W. Haskell, The construction of conics under given conditions, *Bull. Amer. Math. Soc.*, 11 (1905) 268–273.
[5] R. A. Johnson, *Advanced Euclidean Geometry*, Dover Publications, New York, 1960.
[6] J. W. Russell, *A treatise on Pure Geometry*, Clarendon Press, Oxford, 1893.
[7] J. Steiner, *Gesammelte Werke*, vol. I, II, Chelsea Publishing Company, New York, 1971.
[8] C. Taylor, *Geometry of Conics*, Deighton Bell and Co, Cambridge, 1881.
[9] J. Verdina, On point transformations, *Math. Mag.*, 42 (1969) 187–193.
[10] G. K. C. von Staudt, *Geometrie der Lage*, Bauer und Raspe, Nuernberg, 1847.
[11] O. Veblen and J. Young, *Projective Geometry*, vol. I, II, Ginn and Company, New York, 1910.
[12] B. M. Woods, The construction of conics under given conditions, *Amer. Math. Monthly*, 21 (1914) 173–180.
[13] P. Yiu, *Introduction to the Geometry of the Triangle*, Florida Atlantic University Lecture Notes, 2001.

Paris Pamfilos: Department of Mathematics, University of Crete, Greece
E-mail address: pamfilos@math.uoc.gr

Forum Geometricorum
Volume 12 (2012) 301–304.

FORUM GEOM
ISSN 1534-1178

The Butterfly Theorem Revisited

Nikolaos Dergiades and Sung Hyun Lim

Abstract. We start with a proof of the original butterfly theorem, give without proof Mackay's generalization, and finally prove a full generalization of these two versions of the butterfly theorem.

1. Introduction

We give the proof of the original version of the butterfly theorem (Theorem 2 below) with the aid of the following theorem concerning the intersection ratio of two chords in a circle.

Theorem 1. *If the chord BB' in a circle intersects the chord AA' at the point P, then the division ratio*

$$\frac{AP}{PA'} = \frac{AB \cdot AB'}{A'B \cdot A'B'}.$$

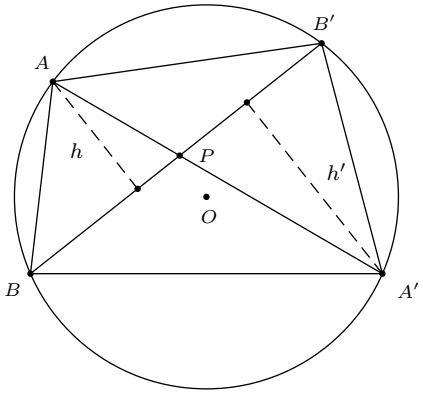

Figure 1

Proof. If R is the radius of the circle (see Figure 1) and h, h' are the heights of triangles ABB', $A'BB'$ from A and A' respectively, then

$$\frac{AP}{PA'} = \frac{h}{h'} = \frac{\frac{AB\cdot AB'}{2R}}{\frac{A'B\cdot A'B'}{2R}} = \frac{AB \cdot AB'}{A'B \cdot A'B'}.$$

□

Publication Date: December 17, 2012. Communicating Editor: Paul Yiu.

Theorem 2 (Butterfly theorem, original version)**.** *If three chords AA', BB', CC' in a circle are concurrent at the midpoint M of AA', then the lines BC and $B'C'$ intersect the line AA' at two points P, P' equidistant from M.*

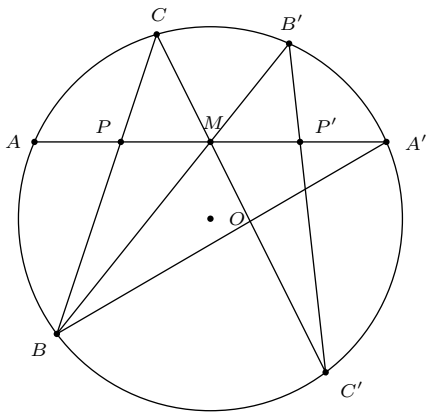

Figure 2

Proof. It is sufficient to prove that $\frac{AP}{PA'} = \frac{A'P'}{P'A'}$ (see Figure 2). From Theorem 1 we have

$$1 = \frac{AM}{MA'} = \frac{AB \cdot AB'}{A'B \cdot A'B'}$$

implying

$$\frac{A'B'}{AB'} = \frac{AB}{A'B}, \tag{1}$$

$$\frac{A'C'}{AC'} = \frac{AC}{A'C}. \tag{2}$$

Hence from Theorem 1 and (1), (2) we have

$$\frac{A'P'}{P'A} = \frac{A'B'}{AB'} \cdot \frac{A'C'}{AC'} = \frac{AB}{A'B} \cdot \frac{AC}{A'C} = \frac{AP}{PA'}.$$

□

Remark. Since $BCB'C'$ with the lines BC, $B'C'$, BC', $B'C$ is a complete quadrangle inscribed in a circle, we may consider AA' as a line that cuts the pair BB', CC' not at M but at two equidistant points from M or from O. So we have the following generalization of the butterfly theorem.

Theorem 3 (Butterfly theorem, Mackay's version)**.** *Given a complete quadrangle inscribed in a circle; if any line cuts two opposite sides at equal distances from the center of the circle, it cuts each pair at equal distances from the center.*

For a proof, see [1, p.105, Theorem 105].

2. A complete generalization of the Butterfly theorem

Since the pairs $(BC,\ B'C')$, $(BB',\ CC')$ and $(BC',\ B'C)$ can be thought of as conics that pass through the four concyclic points B, C, B', C', Theorem 3 and the butterfly theorem can be generalized as in Theorem 5. We first establish a lemma.

Lemma 4. *Two points P and P' are conjugate relative to a circumconic of triangle ABC if and only if the conic passes through the cevian product of P and P'.*

Proof. Let $P = (u : v : w)$ and $P' = (u' : v' : w')$ in barycentric coordinates with respect to triangle ABC. Their cevian product is the point

$$S = \left(\frac{1}{vw' + v'w} : \frac{1}{wu' + w'u} : \frac{1}{uv' + u'v} \right).$$

The two points P and P' are conjugate relative to the circumconic $pyz + qzx + rxy = 0$ with matrix

$$M = \begin{pmatrix} 0 & r & q \\ r & 0 & p \\ q & p & 0 \end{pmatrix}$$

if and only if $PMP'^{\mathrm{t}} = 0$ (see [2, §10.6.1]). This amounts to

$$p(vw' + v'w) + q(wu' + w'u) + r(uv' + u'v) = 0.$$

Equivalently, the conic passes through S. □

Theorem 5. *Let $ABCD$ be a cyclic quadrilateral, and M be the orthogonal projection of circumcenter O on a line $\mathscr{L}$. If a conic passing through A, B, C, D intersects $\mathscr{L}$ at two points P and Q equidistant from M, then for every conic passing through A, B, C, D and intersecting $\mathscr{L}$, the two intersections are equidistant from M.*

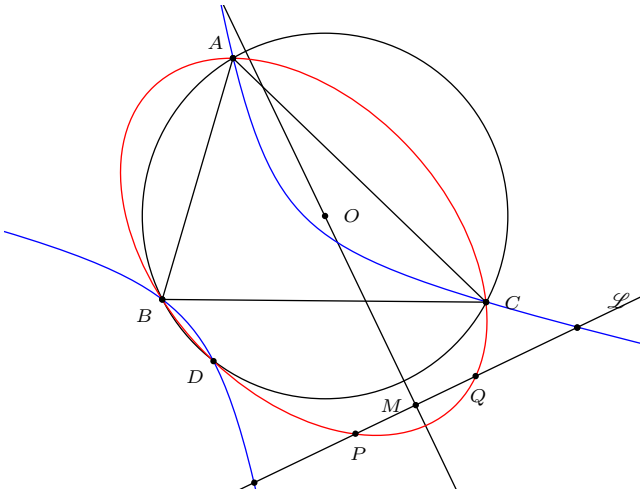

Figure 3

Proof. Let N be the infinite point of the line $\mathscr{L}$, which intersects the conic at P and Q (Figure 3). Since M and N are harmonic conjugate with respect to P and Q, the points M and N are conjugate relative to the conic. The polar of N relative to the circumcircle of ABC is a line perpendicular to NO at O. This is the line OM. So the points M and N are also conjugate relative to the circumcircle of ABC. Hence from Lemma 4 we conclude that D must be the cevian product of M and N relative to ABC. By Lemma 4 again, they must be conjugate relative to every conic that passes through A, B, C, D. If this conic meets $\mathscr{L}$, it must intersect the line at two points equidistant from M. □

References

[1] R. A. Johnson, *Advanced Euclidean Geometry*, Dover reprint, 2007.
[2] P. Yiu, *Introduction to the Geometry of the Triangle*, Florida Atlantic University Lecture Notes, 2001.

Nikolaos Dergiades: I. Zanna 27, Thessaloniki 54643, Greece
E-mail address: ndergiades@yahoo.gr

Sung Hyun Lim: Kolon APT 102-404, Bang-yi 1 Dong, Song-pa Gu, Seoul, 138-772 Korea.
E-mail address: progressiveforest@gmail.com

Forum Geometricorum
Volume 12 (2012) 305–306.

FORUM GEOM
ISSN 1534-1178

Author Index